

Advances in Material Research and Technology

Md Saquib Hasnain
Amit Kumar Nayak
Saad Alkahtani *Editors*

Polymeric and Natural Composites

Materials, Manufacturing and
Biomedical Applications

 Springer

Advances in Material Research and Technology

Series Editor

Shadia Jamil Ikhmayies, Physics Department, Isra University, Amman, Jordan

This Series covers the advances and developments in a wide range of materials such as energy materials, optoelectronic materials, minerals, composites, alloys and compounds, polymers, green materials, semiconductors, polymers, glasses, nanomaterials, magnetic materials, superconducting materials, high temperature materials, environmental materials, Piezoelectric Materials, ceramics, and fibers.

More information about this series at <http://www.springer.com/series/16426>


Md Saquib Hasnain · Amit Kumar Nayak ·
Saad Alkahtani
Editors


Polymeric and Natural Composites

Materials, Manufacturing and Biomedical
Applications

 Springer

Editors

Md Saquib Hasnain 
Department of Pharmacy
Palamau Institute of Pharmacy
Daltonganj, Jharkhand, India

Amit Kumar Nayak 
Department of Pharmaceutics, Seemanta
Institute of Pharmaceutical Sciences
Mayurbhanj, Odisha, India

Saad Alkahtani 
Department of Zoology, College
of Science, King Saud University
Riyadh, Saudi Arabia

ISSN 2662-4761

ISSN 2662-477X (electronic)

Advances in Material Research and Technology

ISBN 978-3-030-70265-6

ISBN 978-3-030-70266-3 (eBook)

<https://doi.org/10.1007/978-3-030-70266-3>

© The Editor(s) (if applicable) and The Author(s), under exclusive license to Springer Nature Switzerland AG 2022

This work is subject to copyright. All rights are solely and exclusively licensed by the Publisher, whether the whole or part of the material is concerned, specifically the rights of translation, reprinting, reuse of illustrations, recitation, broadcasting, reproduction on microfilms or in any other physical way, and transmission or information storage and retrieval, electronic adaptation, computer software, or by similar or dissimilar methodology now known or hereafter developed.

The use of general descriptive names, registered names, trademarks, service marks, etc. in this publication does not imply, even in the absence of a specific statement, that such names are exempt from the relevant protective laws and regulations and therefore free for general use.

The publisher, the authors and the editors are safe to assume that the advice and information in this book are believed to be true and accurate at the date of publication. Neither the publisher nor the authors or the editors give a warranty, expressed or implied, with respect to the material contained herein or for any errors or omissions that may have been made. The publisher remains neutral with regard to jurisdictional claims in published maps and institutional affiliations.

This Springer imprint is published by the registered company Springer Nature Switzerland AG
The registered company address is: Gewerbestrasse 11, 6330 Cham, Switzerland

Preface

Polymeric composites are known as engineered materials of high performance and versatility. In general, polymeric composites are designed by employing a combination of materials containing different phases, at least one of which, normally the matrix, is a polymer and the resultant composites possess advantageous mechanical and thermal characteristics, which are insufficient to be accomplished by a single polymer. In addition, polymeric composites are capable to facilitate excellent friction and wear performances after being modified with functional fillers and reinforcements. The recent trend is to explore naturally derived raw materials from various renewable resources because of growing environmental concerns over the sustainability of raw materials extracted from synthetic resources for the threat to the ecosystem and well-being. Various naturally derived raw materials are also becoming more commercialized due to their biodegradability and sustainable production/extraction from the renewable natural resources. Recently, these natural materials are employed as useful raw materials for the manufacturing of polymeric composites, which makes these more flexible for the uses in many industrial applications including biomedical uses. In this context, raw materials, their manufacturing and biomedical applications (i.e. in drug delivery, growth factor delivery, orthopaedics, dentistry, wound dressing, etc.) of different polymeric and natural composites need to be thoroughly understood.

The current book highlights the overview and extensive knowledge of the up-to-date research and developments of various types of polymeric and natural composites. Exclusively, it covers the different aspects of raw materials, manufacturing and biomedical applications of polymeric and natural composites by prominent researchers in academia and industry as well as government/private research laboratories across the world. Overall, this book *Polymeric and Natural Composites—Materials, Manufacturing and Biomedical Applications* will serve as a holistic reference source suitable for professionals, students and researchers from different disciplines.

The current book is a collection of totally 14 chapters presenting different key topics by the academicians and researchers across the world. A concise account on the contents of each chapter has been described to provide a glimpse of the book to the readers.

The first chapter entitled “[Natural Polymers-Based Biocomposites: State of Art, New Challenges, and Opportunities](#)” describes the role of different carbohydrates and protein-based natural polymers along with their physical, chemical and biological properties.

The second chapter entitled “[Natural Fibre-Reinforced Polymer Composites: Manufacturing and Biomedical Applications](#)” presents the most relevant and more recent advances in natural fibre-reinforced polymer composites, their manufacturing and uses in biomedical applications.

The third chapter entitled “[Polymeric Biocomposites from Renewable and Sustainable Natural Resources](#)” focuses on the use of biocomposites in tissue engineering and analytical applications. The studied materials include polysaccharides such as chitosan, cellulose and alginate, as well as polyhydroxyalcanoates as matrixes, and fillers like nanoparticles, carbon nanotubes or polymers, among other combinations.

The fourth chapter entitled “[Polymer/Carbon Nanocomposites for Biomedical Applications](#)” presents a comprehensive survey of the existing and current literature on different aspects of CNTs, their NCs with polymeric materials and their biomedical applications. This chapter also highlights a variety of methods used to produce CNT polymer nanocomposites, along with their characterization techniques. Polymer nanocomposites (PNCs) based on CNTs offer remarkably improved mechanical, electrical and sensing properties. All this justifies the emergent interest in both academia and industrial development. Likewise, the present status and upcoming possibilities of CNT/PNCs are examined in general along with appropriate examples drawn from the existing literature.

The fifth chapter entitled “[Molecularly Imprinted Polymer—Carbon Dot Composites for Biomedical Application](#)” deals with the biomedical application of molecularly imprinted polymer functionalized carbon dots. The brief characterization of carbon dot synthetic approaches together with summarized overview of imprinting process and its limitations followed by detailed discussion of the current state of the art of the carbon dot molecularly imprinted polymer conjugates for biomedicine will provide insight into the future prospects of those advanced materials.

The sixth chapter entitled “[Magnetic Polymer Nanocomposites: Manufacturing and Biomedical Applications](#)” discusses the current explanation of magnetic nanocomposites from basic science to the latest innovations as given. Starting with the introduction of magnetism and magnetic materials, characterization of magnetic biomaterials, synthesis techniques, production methods and application areas were studied. An easy way to understand new techniques emerging in this field is presented to the reader. In addition, more current processes and practices are briefly mentioned.

The seventh chapter entitled “[Jackfruit Seed Starch-Based Composite Beads for Controlled Drug Release](#)” presents a comprehensive review of various JSS-based composite beads for controlled sustained releasing of encapsulated drugs.

The eighth chapter entitled “[Polymeric Nanocomposites for Cancer-Targeted Drug Delivery](#)” deals with the polymeric nanocomposites for cancer-targeted drug delivery, their efficacy and impact on cancer therapy and multiscale molecular simulation studies for nanostructured polymer systems.

The ninth chapter entitled “[Biopolymeric-Inorganic Composites for Drug Delivery Applications](#)” focuses on the use of biopolymeric–inorganic composites in the preparation of drug delivery systems. The types of biopolymeric and inorganic materials that can be combined into composite materials and their characteristics are summarized herein. The given materials are just examples for the composite materials of interest, and many other composites can be synthesized from different types of inorganic and biopolymeric materials.

The tenth chapter entitled “[Natural Polymeric-Based Composites for Delivery of Growth Factors](#)” deals with the different natural polymer-based composites for growth factor delivery.

The eleventh chapter entitled “[Biopolymers/Ceramic-Based Nanocomposite Scaffolds for Drug Delivery in Bone Tissue Engineering](#)” presents a distinct variety of biopolymer–ceramic-based nanocomposite scaffolds for drug delivery in bone tissue engineering.

The twelfth chapter entitled “[Biopolymeric Nanocomposites for Orthopedic Applications](#)” summarizes the recent research results on the development and applications of various types of biopolymeric nanocomposites utilized in prosthetic devices to bone grafts, for cell delivery, with a special focus on material type, formulations, current design and performance in bone tissue engineering. Important challenges related to the degradation of biopolymeric nanocomposite scaffolds, wide range of properties and benefits for bone healing are addressed.

The thirteenth chapter entitled “[Natural Polymer-Based Composite Wound Dressings](#)” scrutinizes the evolution of natural polymers in wound dressing from traditional to modern-day treatment methods. The major property of a natural polymer which is widely utilized as biomaterials is presented. Properties of composite material with peculiar heed on their applications in the skin tissue repair field are discussed. Finally, the unmet needs and developmental prospectives of the new generations of environmentally friendly, naturally derived, smart wound dressings are addressed in the light of future research.

The fourteenth chapter entitled “[A View on Polymer-Based Composite Materials for Smart Wound Dressings](#)” presents an overview on the challenges and complexity of a chronic wound, exploring the event of a wound infection and discussing the large range of polymer-based composite materials and products in use for each specific wound condition, taking into account the key decision aspects defined by the clinicians. Different tissue engineering strategies are also herein addressed with varied reported clinical success, ranging from non-cellularized to considerably sophisticated cellularized products, reproducing the compositional complexity of both dermis and epidermis. Recent advances in smart dressings and sensors are also brought to discussion as sensing the wound can give us new insights about the series of complex biochemical events related to the healing and regeneration process, while contributing for a better wound assessment.

We would like to convey our sincere thanks to all the authors of the chapters for providing timely and valuable contributions. We thank the publisher—Springer Nature. We specially thank Dr. Shadia Jamil Ikhmayies (Series Editor, *Advances in Material Research and Technology*, Springer Nature), Mayra Castro and

Boopalan Renu for their invaluable support in organization of the editing process right through the beginning to finishing point of this book. We gratefully acknowledge the permissions to reproduce copyright materials from various sources. Finally, we would like to thank our family members, all respected teachers, friends, colleagues and dear students for their continuous encouragements, inspirations and moral supports during the preparation of the current book. Together with our contributing authors and the publishers, we will be extremely pleased if our endeavour fulfils the needs of academicians, researchers, students, biomedical experts, pharmaceutical students and drug delivery formulators. In a nutshell, it will also help the health professionals in academia as well as in the industries.

Jharpokharia, India
Daltonganj, India
Riyadh, Saudi Arabia

Dr. Amit Kumar Nayak
Dr. Md Saquib Hasnain
Dr. Saad Alkahtani

Contents

Natural Polymers-Based Biocomposites: State of Art, New Challenges, and Opportunities	1
Laxmikant Gautam, Anamika Jain, Priya Shrivastava, Sonal Vyas, and Suresh P. Vyas	
Natural Fibre-Reinforced Polymer Composites: Manufacturing and Biomedical Applications	25
Tielidy A. de M. de Lima, Gabriel Goetten de Lima, and Michael J. D. Nugent	
Polymeric Biocomposites from Renewable and Sustainable Natural Resources	65
Daniela M. Fidalgo, Mario D. Contin, Adriana A. Kolender, and Norma D'Accorso	
Polymer/Carbon Nanocomposites for Biomedical Applications	109
Jyotendra Nath, Kashma Sharma, Shashikant Kumar, Vijay Kumar, and Rakesh Sehgal	
Molecularly Imprinted Polymer—Carbon Dot Composites for Biomedical Application	151
Monika Sobiech and Piotr Luliński	
Magnetic Polymer Nanocomposites: Manufacturing and Biomedical Applications	187
Hüsünügül Yılmaz Atay	
Jackfruit Seed Starch-Based Composite Beads for Controlled Drug Release	213
Amit Kumar Nayak, Saad Alkahtani, and Md Saquib Hasnain	

Polymeric Nanocomposites for Cancer-Targeted Drug Delivery	241
Luiza Steffens Reinhardt, Mabilly Cox Holanda de Barros Dias, Jussania Gnoatto, Anna Wawruszak, Marta Halasa, Pablo Ricardo Arantes, Neil J. Rowan, and Dinara Jaqueline Moura	
Biopolymeric-Inorganic Composites for Drug Delivery	
Applications	271
Shaimaa A. Khalid, Ahmed S. Abo Dena, and Ibrahim M. El-Sherbiny	
Natural Polymeric-Based Composites for Delivery of Growth	
Factors	299
M. D. Figueroa-Pizano and E. Carvajal-Millan	
Biopolymers/Ceramic-Based Nanocomposite Scaffolds for Drug	
Delivery in Bone Tissue Engineering	337
K. Lavanya, S. Swetha, and N. Selvamurugan	
Biopolymeric Nanocomposites for Orthopedic Applications	377
Maria Râpă, Raluca Nicoleta Darie-Nița, and Cornelia Vasile	
Natural Polymer-Based Composite Wound Dressings	401
Shreya Sharma, Bhasha Sharma, Shashank Shekhar, and Purnima Jain	
A View on Polymer-Based Composite Materials for Smart Wound	
Dressings	425
S. Baptista-Silva, P. Alves, I. Guimarães, S. Borges, F. Tavaría, P. Granja, M. Pintado, and A. L. Oliveira	
Index	457

About the Editors

Dr. Md Saquib Hasnain is currently working as Professor in the Department of Pharmacy, Palamau Institute of Pharmacy, Jharkhand, India. He has over 9 years of research experience in the field of drug delivery and pharmaceutical formulation analyses, especially systematic development and characterization of diverse nanostructured drug delivery systems, controlled release drug delivery systems, bioenhanced drug delivery systems, nanomaterials and nanocomposites employing quality by design approaches and many more. Till date, he has authored over 50 publications in various high-impact peer-reviewed journals and 100 chapters to his credit. In addition, he has authored 2 books and edited 9 books published by International Publisher(s). He is also serving as Reviewer of several prestigious journals. Overall, he has earned highly impressive publishing and cited record in Google Scholar (H-Index: 26). He has also participated and presented his research work at over ten conferences in India and abroad. He was also Member of scientific societies, i.e. Royal Society of Chemistry, Great Britain; International Association of Environmental and Analytical Chemistry, Switzerland; and Swiss Chemical Society, Switzerland.

Dr. Amit Kumar Nayak is currently working as Associate Professor at Seemanta Institute of Pharmaceutical Sciences, Odisha, India. He earned his Ph.D. in pharmaceutical sciences from IFTM University, India. He worked as Senior Research Associate at IIT Kanpur in a CSIR-sponsored project. He has over 12 years of research experiences in the field of pharmaceuticals, especially in the development and characterization of novel biopolymeric and nanostructured drug delivery systems made of natural biopolymers. He has authored over 130 research and review articles in various high-impact peer-reviewed journals and 102 chapters in various international books. In addition, he has authored 2 books and edited 10 books published by International Publisher(s). He has received University Foundation Day Research Award-2019 by Biju Patnaik University of Technology, Odisha. He serves as Reviewer for several reputed journals and is Life Member of Association of Pharmaceutical Teachers of India (APTI).

Dr. Saad Alkahtani has over 26 years of research and teaching experience in the field of cell biology and genetics, especially isolation and cDNA synthesis, isolation, purification, cloning, sequencing, electrophoresis and RFLP analysis, conventional drug delivery systems and nanostructured drug delivery systems, controlled release drug delivery systems, bioenhanced drug delivery systems, nanomaterials and nanocomposites and many more. Till date, he has authored over 187 publications in various high-impact peer-reviewed journals and 3 books to his credit. He is also serving as Reviewer of several prestigious journals. Overall, he has earned highly impressive publishing and cited record in Google Scholar (*H*-index: 20). He has also participated and presented his research work at over 25 conferences.

Natural Polymers-Based Biocomposites: State of Art, New Challenges, and Opportunities



Laxmikant Gautam, Anamika Jain, Priya Shrivastava, Sonal Vyas, and Suresh P. Vyas

Abstract In the present scenario, in the development of the novel drug delivery system, the role of the natural polymer will be more preferential as compared to the other derivative. The biocompatible and biodegradable nature of the natural polymer is the aim of current research. Along with that natural polymer can be worked as a site-directed ligand that can specifically bind with the cell receptor and target the diseased cell/tissues. The role of different carbohydrates and protein-based natural polymers were incorporated in this chapter along with their physical, chemical, and biological properties. The role of these natural polymers in the pharmaceutical and biomedical applications also are incorporated.

Keywords Carbohydrates · Protein · Drug delivery system · Ligand

1 Introduction

Natural polymers are obtained from animals and plant sources. Chitin, starch, cellulose, casein, alginates, soy protein, polyhydroxyalkanoates, hemicelluloses alginates, and polylactic acid are some of the examples of natural polymers. Various attractive features of natural polymers have drawn the attention of many researchers for their pharmaceutical application. They are natural, biodegradable, renewable, abundant, and biocompatible. Nowadays research is focused on the development of advanced polymeric materials such as nanocomposites, blends, and composites by combining natural polymers with other polymers and fillers [1]. Natural polymers have been explored for the delivery of drugs and bioactive molecules. They can be easily modified for drug delivery; exhibit specific interaction with biomolecules and undergo controlled enzyme degradation. Natural polymers can be used for the delivery of

L. Gautam · A. Jain · P. Shrivastava · S. P. Vyas (✉)
Drug Delivery Research Laboratory, Department of Pharmaceutical Sciences, Dr. Harisingh Gour Vishwavidyalaya, Sagar 470003, India

S. Vyas
Bundelkhand Medical College, Sagar 470002, India

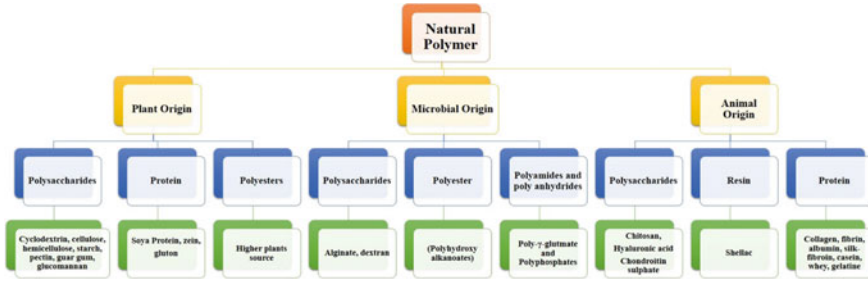


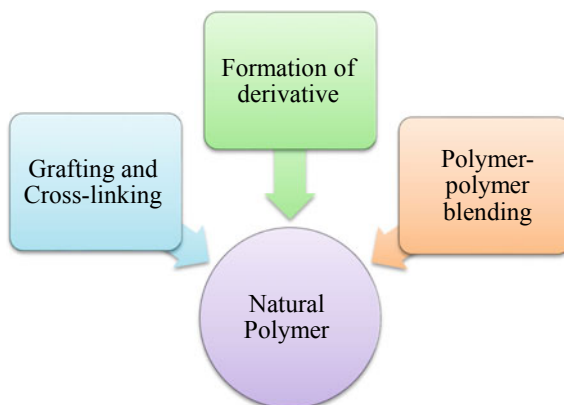
Fig. 1 Biodegradable natural polymer applied in drug delivery

proteins, DNA, as well as tissue engineering, apart from small molecular weight drugs, wound healing, , and anticancer drugs. Various chemical and morphological modifications are also carried out to enable them target orientation, stimuli sensitive etc. As compared to other synthetic polymers, natural polymers offer various advantages including accessibility, modification, and biocompatibility. Natural polymers possess various reactive groups, thus activity-specific functional groups can be introduced, with various altered however desirable physico-chemical properties [2] (Fig. 1).

1.1 Natural Polymers: An Insight

Natural polymers have been extensively explored as a carrier for the delivery of various bioactives. Most of the natural polymers are used as an excipient in pharmaceutical preparations because they are generally considered safe in vivo. Polysaccharides exhibit various superior characteristics such as biocompatibility, enzyme degradation characteristics, non-toxic, highly stable, harmless, gel-forming ability, and as per need can be altered chemically and biochemically [3]. Natural polymers largely include polysaccharides such as dextran, chitosan, agarose, hyaluronic acid, alginate, cyclodextrin, and carrageenan and protein-based polymers which include collagen, albumin, soy, gelatin, etc. These polymers exhibit broad molecular distribution and batch-to-batch variability, which impose various challenges. Chitosan is one of the most widely used polymers due to its easy surface modification, non-immunogenic properties, lower toxicity, and blending property with other polymers. Chitosan and alginate have widely been explored as compared to other polymers. Several preclinical trials suggest successful use of some biodegradable polymers, however, only a few have been accepted for further clinical trials and none of them enter the post clinical trials. Thus there is a scope to explore new polymers for the targeted delivery and sustained drug release [4].

Fig. 2 Modifications in natural polymers



1.2 Modifications of Natural Polymers

Modification of natural polymers imparts versatility and drug release and delivery properties. Other properties such as solubility, viscosity, and microbial degradation can be further modified to overcome the drawbacks. The modification should not alter their biological properties. Various modification methods include polymer–polymer blending, grafting, crosslinking, and formation of derivative [5] (Fig. 2).

1.3 Grafting and Cross-Linking

Mittal and coworkers chemically grafted Barley husk (BH) following its copolymerization with palmitic acid. Urea formaldehyde cross-linked PVA/Starch composite films, along with natural BH, poly vinyl alcohol/starch and, grafted BH were used to prepare a blend grafted film. The effect of content of BH, urea/starch ratio, and grafted BH on the water uptake (%), mechanical properties and biodegradability of composite films was studied. Tensile strength of cross-linked film was increased by 40.23% as compared to the PVA/St film, when urea starch ratio increases from 0 to 0.5 in blend. Whilst the tensile strength was recorded to be enhanced by 72.4% as compared to PVA/St film in a grafted BH composite film. The degradation rate of PVA/St film was shorter than natural BH composite film. Nevertheless, film properties can be modulated by varying the degree of cross-linking polymer network [6]. Astrain and coworkers designed some bionanocomposite hydrogels from furan modified gelatin by using maleimide-functionalized cellulose nanocrystals (CNCs) as multifunctional cross linkers. Functionalization of the nanocrystals with maleimide component was confirmed by X-ray photoelectron spectroscopy. Functionalized cellulose nanocrystals were used as cross-linkers using Diels–Alder “click” reaction to furan modified gelatin. Swelling and rheological parameters were assessed to ascertain the role of CNCs as cross-linkers for gelatin. Changes in the swelling properties of the

hybrid hydrogels clearly depict the additional cross-linking points resulted due to the presence of functionalized CNCs. Thus synthetic strategies seem to be of potential applications in the material design for use in pharmaceuticals [7].

1.4 Formation of Derivative

Physiochemical properties of the natural polymers such as solubility, drug release, hydrophilicity, swellability, targeting, film coating and stimuli-responsiveness can be ameliorated by polymers derivatization. Various derivatives are based on acetylation, phosphorylation, carboxymethylation, esterification, cyanoethylation etc. Koliada and coworkers synthesized collagen derivatives of porcine skin with polyvinyl acetate (PVAc) and polyvinyl alcohol (PVA) and studied the morphology of the prepared fibers. The distance between collector and syringe needle was 9–12 cm. Material obtained from the PVAc and PVA with the addition of gelatin and collage were the derivative fibers of diameter within the range of 0.502–0.894 μm for PVAc:CD and PVA:CD, respectively [8]. Chitosan is used as a polymer for concentration, recovery, and separation of metal ions as well as formation of a range of functional materials. Unmodified chitosan possesses unique complexing properties for various metal ions, although its selectivity and sorption capacity can be enhanced by means of chemical modification. Lewis basicity and chelating ability of chitosan can be adjusted through introduction of functional groups apart from the hydroxyl and amino groups [9].

1.5 Polymer–polymer Blending

Polymer–polymer blending is a convenient way to modify polymers without application of any chemical reaction or synthesis of new polymer. Van der Waals forces, London dispersion forces, and hydrogen bonding play an important role in polymer–polymer blending. Although some sort of chemical bonding also gets involved in some blending. Blending of xanthan gum, alginate and locust bean gum in the formation of microspheres increases the drug entrapment efficiency and reduces drug release as compared to locust bean, alginate and xanthan gum [5].

2 Recent Application of Natural Polymers in Nano-Drug Delivery

Nanomedicines are the new generation medicines unique due to their nano size features. After oral delivery, various drugs in macro or micro formulations exhibit poor pharmacokinetics and lesser bioavailability. Thus, formulation based on natural

or synthetic biodegradable polymers have gained attention in the field of controlled and targeted drug delivery to enhance safety, biocompatibility, enhanced permeability, bioavailability, lesser toxicity, and greater retention time. Suitable biodegradable polymers can be chosen as drug carrier for sustained as well as targeted delivery [4]. Polymeric amphiphiles have a great potential to deliver anticancer drugs, possess minimum side effects, thus gained attention over the past decade. These polymers can be self-assembled in the micelles, with a hydrophilic corona and hydrophobic core. This structure possesses great potential in anticancer drug targeting including prolonged circulation. The hydrophilic outer layer act as a barrier, which decreases interaction with the other cells and hence results in prolonged circulation. The hydrophobic core is responsible for the pharmacokinetic properties, such as drug release and drug entrapment. Enhanced permeation and retention (EPR) effect can be achieved with a polymeric nanosized drug carrier, thus enhances localization of drug within tumor site [10]. Apart from the pharmaceutical application, natural polymers also exhibit great potential in the bio nanotechnology and nanomedical field. Biodegradable natural polymers possess great potential for targeted and site-specific drug delivery, especially for the development of artificial limbs, biosensing application and tissue engineering. Various natural polymers are suitable for bio nano technological applications, when blended, cross-linked, and functionalized for the designing of nano scaffolds. Several natural polymers are used as a scaffold for corneal repair including chitosan, alginate, cellulose, heparin, gelatin, silk fibroin etc. Chitosan promotes corneal wound healing, alginate improves viability of the corneal epithelial cells, cellulose improves mechanical and chemical properties of the ophthalmic formulation, gelatin provides transparency to the formulation and silk fibroin is compatible with limbal stem cell and promotes epithelial formation [11]. Polymeric drug delivery is also used for biomimetic, targeting polymeric drug delivery drug and also as free macromolecular therapeutics. Polymeric gene delivery systems, non-viral vectors, and viral vectors for gene delivery have extensively been studied in the past decade. The systems for viral vectors are RNA conjugates and DNA conjugates for gene delivery and for non-viral vectors are polyethyleneimine copolymers, polyethyleneimine derivative, and polyethyleneimine conjugated bioreducible polymers. Polymeric drug carriers that are based on the pathogen like viruses and bacteria are potentially immunogenic. Although they also have adjuvant ability, thus certain degree of immunogenicity can be expected from polymeric drug carriers. The polymeric drug delivery systems thus possess great potential in near future by combining biological and synthetic fields [12]. In Table 1 different carbohydrates and protein- based natural polymer are listed along with their properties and application.

Table 1 Different types of carbohydrates-protein-based natural polymer and their properties and pharmaceutical applications

S. No.	Polysaccharide	Monomer unit	Properties	Pharmaceutical application	References
1	Chitosan	Linear copolymer of β -(1 \rightarrow 4)-linked 2-acetamido-2-deoxy- β -D-glucopyranose and 2-amino-2-deoxy- β -D-glucopyranose	Chitosan is less toxic, non-immunogenic, simplicity of modification, biocompatible, degradable by enzymes, high bioavailability	Chitosan act as a stabilizing agent, reducing agent	[12, 13]
2	Cellulose	Glucose linked via β -(1 \rightarrow 4) glycosidic linkage	Excellent film forming nature, Conventional softener, low conductivity, and high resistivity	Mucoadhesive and bio-adhesive drug delivery system, ether and ester derivatives in solid dosages form coating process, osmotic drug delivery	[14]
3	Alginate	Linear copolymer composed of 2 monomeric units (D-mannuronic acid and L-guluronic acid)	Low toxic, biocompatible, mild gelation by addition of Ca^{2+}	Binder, disintegrant, taste masking agent, stabilizer, thickener, emulsifier, surface active agent, suspending and viscosity increasing agent	[15, 16]
4	Heparinara>	Sulfate repeating disaccharides units	Linear anionic polysaccharides having 2-O-sulfo- α -iduronic acid and 2-deoxy-2-sulfamino-6-O-sulfo- α -d-glucose unit	Anticoagulant, antithrombic	[17]
5	Guar Gum	Galactose and mannose units	high molecular weight polysaccharides composed of galactomannans consisting of a (1 \rightarrow 4)-linked β -D-mannopyranose backbone with branch points from their 6-positopns linked to α -D-galactose (i.e. 1 \rightarrow 6-linked α -D-galactopyranose)	Thickener, stabilizer, emulsifier, disintegrant, binder, bulking gent in laxatives	[18]

(continued)

Table 1 (continued)

S. No.	Polysaccharide	Monomer unit	Properties	Pharmaceutical application	References
6	Pectin	Galacturonic acid monomer units are linked via α -(1 \rightarrow 4)-glycosidic bond	Exists as solid, freely soluble in water, and a weakly acidic compound	Biodegradable polymer, possess gelling properties, used as a matrix for the entrapment and/or delivery of a variety of drugs, proteins and cells	[19, 20]
7	Alginates	D-mannuronic acid and L-guluronic acid	Anionic polymer obtained from brown seaweed	Biocompatibility, relatively low toxicity, and cost-effective	[15]
9	Hyaluronic acid	D-glucuronic acid and N-acetyl-D-glucosamine, linked via alternating β -(1 \rightarrow 4) and β -(1 \rightarrow 3) glycosidic bonds	Anionic polymer	Biodegradability, and non-immunogenicity	[21]
10	Carrageenan	D-galactose-2-sulfate (1, 3-linkage) and D-galactose-2,6-disulfate (1, 4-linkage)	Anionic polysaccharides	Used as gelling, thickening, emulsifying, and stabilizing agent in pharmaceutical formulations	[22]
11	Gelatin	18 different amino acids joined together in a chain	Cationic by character	Biodegradable, biocompatible, could be used in sustained and controlled release formulations	[23]
12	Collagen	3 proteins arranged in a triple helix with non-helical ends	Fibrous protein, great tensile strength, and elasticity	Sustained and controlled drug delivery, as controlling material for transdermal drug delivery	[24]

(continued)

Table 1 (continued)

S. No.	Polysaccharide	Monomer unit	Properties	Pharmaceutical application	References
13	Albumin	It is monomeric in nature	Globular protein	Plasma expander, drug delivery, pulmonary-based vaccines	[25]
14	Silk fiber	Sericin and fibroin	Smooth natural fiber, good moisture regains property	Nanocrystal and nanoparticle stabilization, solubility enhancement, and sustained and controlled release formulations	[26]
15	Chitin	β -(1-4)-linked D-glucosamine (deacetylated unit) and N-acetyl-D-glucosamine (acetylated unit)	Mucopolysaccharides, biodegradability, inert in nature and low toxicity	Used in mucoadhesive formulations, antioxidant, anticancer, antimicrobial activity, and immune-stimulating characteristics	[27, 28]

2.1 Polysaccharides Based Drug Delivery Systems

2.1.1 Chitosan-Based Nanocomposites

Environmental pollution such as water pollution has become a global concern in recent years. Various pollutants include dyes, phosphate, biodegradable waste, metals, nitrate, toxic chemicals, pharmaceuticals and radioactive pollutants. Among them, dyes are of main concern, especially crystal violet (CV), which belongs to basic dyes. Massoudinejad et al. have recovered CV dye using magnetic chitosan nano-composites (MCNCs) and studied process variables which effects dye recovery. These variables include CV concentration, pH, contact time, adsorbent dose, etc. via response surface methodology (RSM). Modeling-based results suggest that MCNCs dosage and contact time were effective process variables which showed their effect on adsorption efficiency. pH played an insignificant role in the adsorption uptake. Maximum adsorption efficiency (72%) of MCNCs was obtained, when adsorbent dosage, contact time, and initial concentration of CV were 1 g, 140 min, and 77 mg/L, respectively. Freundlich, Langmuir, and Temkin model has been used to evaluate the qualitative uptake of CV. Freundlich isotherm was well fitted with experimental results. Kinetic studies reveal the pseudo-first-order model fitted the experimental data, which shows adsorption rate of CV onto MCNC was time-dependent. Thus chitosan nanocomposite proves to be a potential adsorbent for dye-containing waste water treatment [29]. Ciprofloxacin (CIP) is widely used 2nd generation fluoroquinolone antibiotics. Although CIP possesses various benefits, but CIP residues can cause some serious health hazards. Thus, there is a need of developing effective and sensitive methodologies for the detection and management of CIP residues in food products. Hu et al. have developed novel electrochemical aptasensing transducer platform, which is based on the carbon nanotube (CNT)-V₂O₅-chitosan (CS) nanocomposites with modified screen-printed carbon electrode (SPCE) for measurement of CIP. Single-stranded DNA aptamer was immobilized within CNT-V₂O₅-CS/SPCE as basal electrode transducer platform. Electrochemical impedance spectroscopy (EIS) is used for the quantitative detection of CIP. This formulation combines film forming strength of CS, efficient electron transfer capacity of multiwalled CNTs, biocompatibility of V₂O₅, and portability of SPCE. The aptasensor possesses a dynamic range from 0.5 to 64.0 ng mL⁻¹, limit of detection was 0.5 ng mL⁻¹ and linearity were obtained between 0.5 to 8.0 ng mL⁻¹. Thus these results show good selectivity to CIP [30] (Fig. 3).

2.1.2 Alginates-Based Nanocomposites

Alginate is obtained from the brown seaweeds including *Laminaria japonica*, *Laminaria hyperborea*, *Ascophyllum nodosum*, *Laminaria digitata*, and *Macrocystis pyrifera*. It is made up of two (1N4)-linked α -L-guluronate and β -D-mannuronate monomer. The proportion of monomers was from different sources. Alginate exhibits

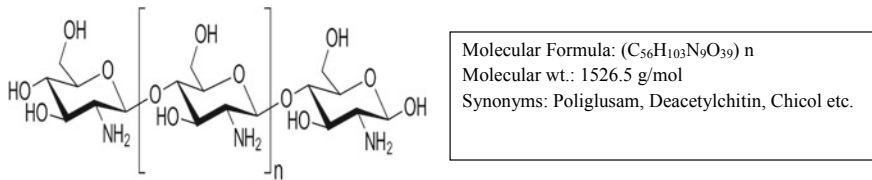


Fig. 3 Chemical structure of chitosan

high availability, biocompatible and low toxicity, which impart alginates widest biomedical applicability. Alginate is mainly used as a stabilizer in pharmaceutical formulation [31]. Alginate- based nanocomposites have been extensively studied drug delivery systems due to their good biocompatibility and biodegradability. Alginate is used to produce particles with various applications due to properties such as easy availability, cheap, natural origin, sol-gel transition, and versatility [32,33]. Auriemma et al. have prepared alginate--based gastro-retentive delivery system bearing piroxicam with a bimodal release profile in the gastrointestinal tract (GIT). Higher oral absorption and prolonged half-life shown by piroxicam, however its elimination is inconsistent in old age patients. Thus, to overcome these limitations floating gastro-retentive gel beads with sustained release profile were prepared using prilling techniques. Matrix of the beads prepared as a hollow/multipolymeric system, which is based on the alginate, hydroxypropyl methylcellulose. Various parameters such as floating properties, particle micromeritics, drug release profile, hollow inner structure in the GIT tract were studied. Thus, formulation provides desired bimodal drug release pattern with the controlled and delayed in vitro piroxicam drug release. As compared to standard piroxicam, in vivo anti-inflammatory activity of the floating beads achieved up to 48 h. Hence desired characteristics can be achieved in the elderly patient with chronic inflammatory disease, which required rapid onset of action followed by maintenance dose [34]. Ligin et al. have prepared alginate- based hydrogel as an oral drug carrier for the colon targeting. Hydrogel exhibited immense potential for clinical application owing to their antibacterial and pH-sensitive properties. Hydrogel was characterized by using Scanning electron microscopy (SEM), Fourier transform-infrared spectroscopy (FT-IR), and thermogravimetric analysis (TGA) analysis. Water absorption capacity of the hydrogel of various monomer compositions and effect of salt, temperature and pH was studied. Diclofenac sodium was used as a model drug to study in vitro drug release in gastric fluid and simulated intestinal fluid. Disc diffusion method was used to study antibacterial effects of hydrogels against gram-positive and gram-negative bacteria. The results of studies demonstrated that produced hydrogels could exhibit potential for developing pH-controlled drug delivery devices [35] (Fig. 4).

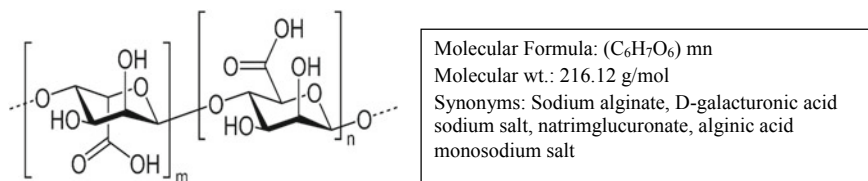


Fig. 4 Chemical structure of alginates

2.1.3 Cellulose Based Nanocomposites

Cellulose is produced from the photosynthesis and is the most abundant polymer on earth. Cellulose nanomaterials are produced from the lignocellulos's biomass and inturn used to develop new materials for use in nanotechnology. Cellulose- based hydrogels have gain attention during the last decade due to their biodegradability, low toxicity, biocompatibility, and excellent mechanical stability. Hydrogels represent three-dimensional polymeric network, which has the capacity to absorb greater amount of water or biological fluid. Their ability to retain water confers similar properties as shown by natural living tissues. Du et al. have prepared cellulose nanofibrils (CNFs) and cellulose nanocrystals- (CNCs) based hydrogel. CNFs and CNCs based hydrogels are used for wound dressings, drug delivery and tissue engineering scaffolds. Thus cellulose- based nanocomposites possess great potential in various biomedical applications [36]. Self-healing hydrogels, which mimic human skin's function, have been studied in recent years. There is still a challenge to prepare an integrative conductive gel which exhibits self-healing as well as offers mechanical properties. Shao et al. have developed self-healing, tough and self-adhesive ionic gel by forming synergistic multiple coordination bonds between tannic acid-coated cellulose nanocrystals., poly (acrylic acid) chains, and metal ions within a covalent polymeric network. Excellent mechanical performance was obtained by the dynamic connected bridge within the porous network, in which multiple coordination bonds are present. Reversible coordination interactions are responsible for superior recovery property as well as reliable electrical and mechanical self-healing property without any aid of external stimuli. Catechol group of the tannic acid is responsible for the durable and reproducible adhesiveness, which could be adhered on skin without any irritation or inflammatory response. Apart from these ionic gels show a larger strain sensitivity, through which flexible strain sensors can be employed to monitor large motions (joint bending) and subtle motion (pulse and breath). Thus, data can be analyzed via programmable wireless transmission on the user interfaced with a smart phone. Thus this work provides a hope in near future to design biocompatible cellulose-based hydrogels, exhibiting self-adhesive, stretchable, self-healing, and strain-sensitive properties for wearable electronic sensors and healthcare monitoring [37] (Fig. 5).

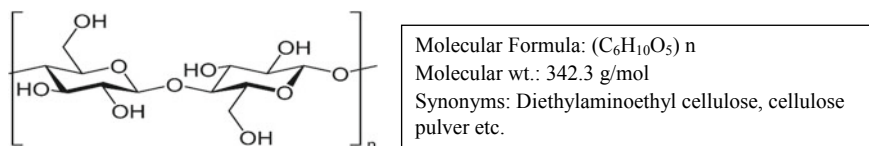


Fig. 5 Chemical structure of cellulose

2.1.4 Heparin Based Nanocomposites

Shi et al. have prepared Graphene based nanomaterials for drug delivery and photothermal therapy due to their unique physiochemical properties. However, biocompatibility issues and limited water solubility limit their further applications. Shi et al. have prepared smaller and uniform size grapheme oxide (GO) nanosheets (approx. 85 nm) using modified Hummers' method. They grafted unfractionated heparin (UFH) on GO covalently using adipic acid dihydrazide (ADH) as a linker to developed nanocomposites for the delivery of curcumin (Cur). The novel nanocomposites exhibit stronger photothermal effect. They were of small size (42 nm) and lateral dimension as compared to GO nanosheets. In vitro experiments conducted on cell lines revealed combined i.e., chemotherapeutic and photothermal effect of Cur-loaded vehicles. They exhibited cytotoxicity of Rgo-ufh/Cur against A549 and MCF-7 cell line. Retention time of Cur was enhanced in nanocomposites as compared to the free Cur solution. Thus it has a immense potential as drug delivery vehicles [38]. Ataei et al. have developed plasma-treated polyurethane/heparinized carbon nanotube (PU/HCNT) nanocomposite based thin films as polymeric heart valve. The nanocomposite films (PU/HCNT) were developed by solvent casting technique. Carbon nanotube was heparinized to overcome the dispersal and calcification resistance of CNTs and the polyurethane matrix. The dispersal of CNTs within matrix of produced films was analyzed by Transmission Electron Microscopy (TEM). Greater calcification resistance and storage modules were observed for nanocomposites. The nanocomposites were exposed to O_2 plasma treatment. The nanocomposites film surface was characterized by using SEM, ATR-FTIR, and EDXA, and water drop contact angle measurements. Cytotoxicity studies were performed on L929 fibroblast cells, wherein no cytotoxicity was observed. Platelets adhesion test revealed that the modified film was more blood compatible as compared to unmodified film [39] (Fig. 6).

2.1.5 Hyaluronic acid (HA) Based Nanocomposites

HA found in many tissues and fluids but abundantly present in articular cartilages and synovial fluids. HA is a naturally occurring non-sulfated glycosaminoglycan (GAG) with repeating units of β -1, 4-D-glucuronic acid and β -1, 3-N-acetylglucosamine units. The HA has binding affinity basically for receptors: (A) Intercellular adhesion molecule 1 (ICAM-1), (B) Hyaluronate mediated mobility receptors, and (C) most

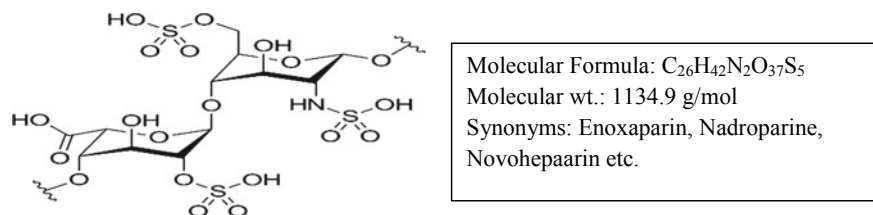


Fig. 6 Chemical structure of heparin sulfate

importantly membrane proteoglycans (CD44) which interact with the other ligands including osteopontin, collagen and matrix metalloproteinase (MMPs) [40]. Some of the formulation conjugated with the HA are described here with their different targetability and approaches in drug delivery system. Makvandi et al. have developed thermo sensitive and injectable hydrogels, which are composed of hyaluronic acid, β -tricalcium phosphate and corn silk extract nano silver for bone tissue regeneration engineering. Microwave-assisted green approach using CSE is used to synthesize spherical nanoparticles of silver. Rheological studies reveal that thermo sensitive hydrogels have edification temperature (T_{gel}), which is closed to the body temperature. The formulation exhibited antibacterial activity against gram-positive and gram-negative bacteria, without any cytotoxicity. Mesenchymal stem cells seeded within nanocomposites showed greater bone differentiation, which clearly depicts that they could be an ideal candidate for bone tissue regeneration [41]. Pandey and his co-worker synthesized novel pH responsive hyaluronic acid (HA)-lenalidomide nanoconjugates for glioblastoma. They prepared a HA modified drug delivery system by using carbodiimide chemistry of lenalidomide and characterized using different spectroscopic methods, i.e., FTIR, PXRD, SEM, TEM, AFM, etc. The Functionalization of HA result in the CD-44 mediated cellular uptake inside the tumor cells. The size and surface charge reported 128.5 ± 3.2 nm and 131.1 ± 2.5 nm, 20.5 ± 2.2 mV and 19.3 ± 2.1 mV respectively. The result showed that systems were cationic in nature having high efficiency of cell interaction and internalization. The expression of CD44 on blood-brain barrier (brain microvascular endothelial cells) involved into transport the conjugated systems. The cytokine assay showed reduced level of IL-6 and increased level of TNF α . The outcome of the research concluded that dual drug delivery can effectively work in the brain tumor [42]. In another research for the dermal treatment Faccendini and his group, synthesized the hyaluronic acid or chondroitin sulfate conjugated, norfloxacin loaded pullulan and chitosan nanocomposites by using electro spanning with fiber range of 500 nm. This system is shown affinity to decrease the bio-burden up to 100 folds and due to this the resultant drug loading effect showed that there is no effect on biological activity of norfloxacin. The formulation showed minimal swelling in aqueous environment and controlled release of norfloxacin [43]. The treatment of cancer the chemo photo-thermal therapy, based on gold nanorods functionalized with hyaluronic acid containing doxorubicin were reported by Geo et al. They synthesized a system with responsive action to pH/ thermal sensitive release, EPR effect, deep tumor penetration

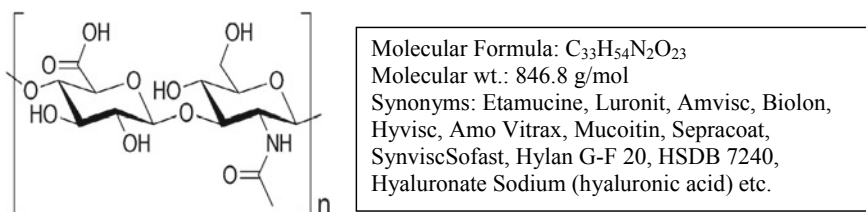


Fig. 7 Chemical structure of hyaluronic acid

affinity, targeting through receptor-mediated endocytosis, and synergistic therapeutic effects [44] (Fig. 7).

2.1.6 Carrageenan Based Nanocomposites

Carrageenan is extracted from natural polysaccharides red sea woods of Rhodophyceae class. It is a gelling (viscosity \uparrow) agent used in different drug delivery system, tissue engineering, and wound dressing. Carrageenan based silver nanoparticles/clay nanocomposites film developed by using solution casting method. The effect of Plasmonic on these particles was analyzed by UV spectroscopy at 420 nm, tensile strength of the composites increases 14–26 folds due to the nanofillers and water vapor permeability decreased up to 12–27 folds due to the carrageenan film. The result showed the characteristic gram-negative anti-microbial activity [45]. Tavakoli et al. developed the nanocomposites based hydrogel with Kappa carrageenan coated cellulose/starch nanofibers for the hemostatic application. Comparative research of different formulations showed 2 times higher mechanical strength of Kappa carrageenan coated hydrogels. The above results conclude the synergistic effects, good blood clotting ability, adjustable degradation rate, and good mechanical properties of Kappa carrageenan coated hydrogel formulations [46]. Currently, the use of carrageenan in the development of ecofriendly drug delivery system has been reported. Polat et al. prepared the formulation of triethylene glycol divinyl ether cross-linked agar/Kappa-carrageenan/montmorillonite hydrogel. Swelling properties were found to be 2523% under at 70 °C. Non-Fickian behavior of each formulation showed controlled swelling behavior of the hydrogel, thus suggests an effective carrier potential for the biomedical applications [47] (Fig. 8).

2.1.7 Pectin Based Nanocomposites

Pectin, is a polysaccharide of esterified D-galacturonic acid that resides in α -(1–4) chain. It is also known as methoxy pectin/D-lyxose as a derivative of glucuronic acid derivative. Pectin is water soluble, physically solid by nature, on the basis of pKa it is a component with acidic characteristics. The presence of pectin is reported in all human tissues, specifically located in lysosomes. The role of pectin is reported

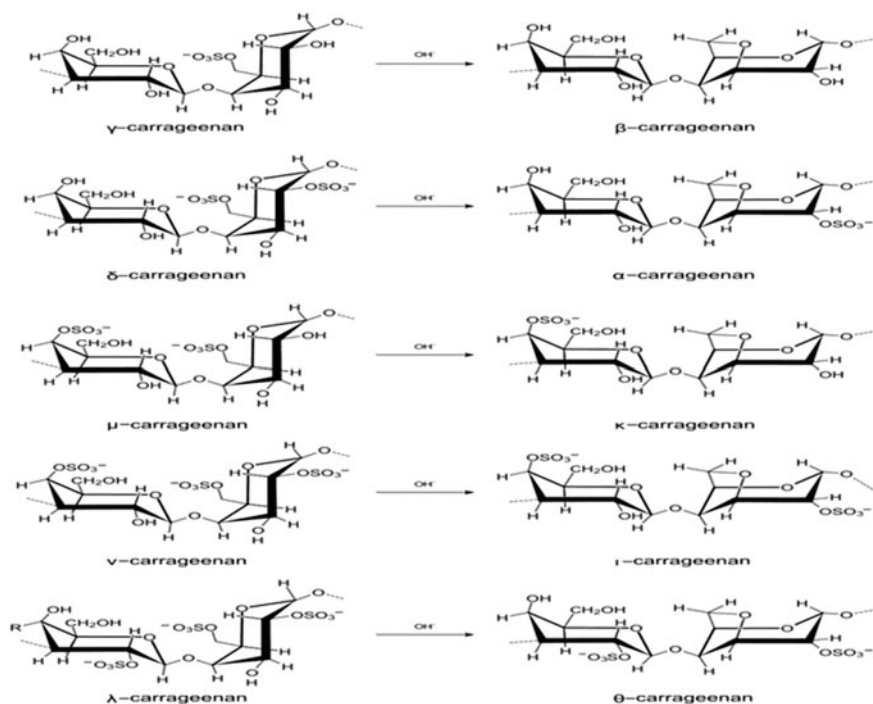


Fig. 8 Chemical structure and different types of Carrageenan structure

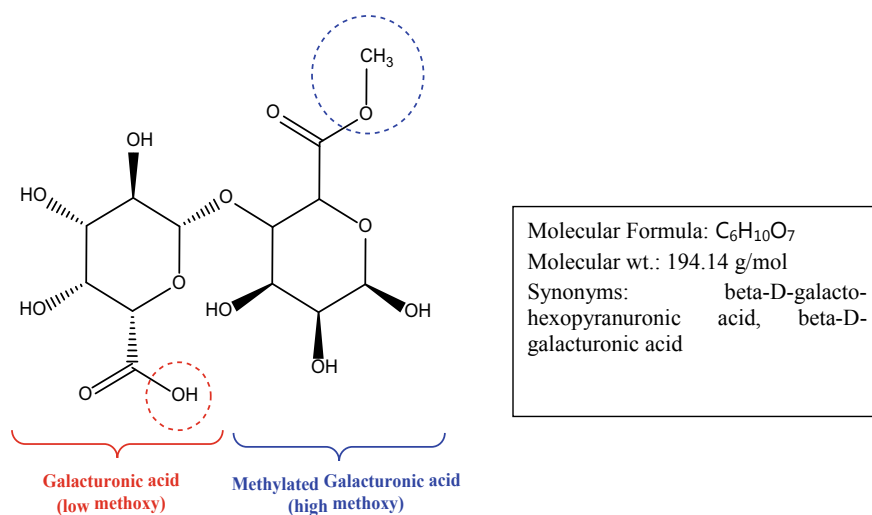
in colon specific drug delivery system. Wang et al. reported that pectin modified nano-carbon nanocomposites based gel films effectively worked in oral/colonic-specific delivery of the 5-fluorouracil. The entrapment efficiency was found to be 30.1–52.6%. The release pattern was better in comparison to the single pectin based system. The MTT assay was performed on A549 (Lung cancer), HeLa (Cervical cancer) and L 929 (Murine fibroblast) cell lines, A549 and HeLa effective cytotoxic effect were recorded [48]. In another scientific report, pH-responsive film based on pectin containing curcumin and sulfur nanoparticle exhibited effective antibacterial and antioxidant activity. The solution casting method was used for the development of formulation. The resultant film showed thermal stability as well as higher water contact angle. The antibacterial activity was checked on *E. Coli* and *L. monocytogenes* [49]. In Table 2 different extraction methods are reported (Fig. 9).

2.1.8 Guar Gum-Basednanocomposites

Galactomannan (galactose + mannose) is a polysaccharide extracted from guar beans also known as guaran. Pharmaceutically it is a viscosity enhancer, and stabilizing agent, also used in feed, food industries. In the drug delivery system guar gum grafted

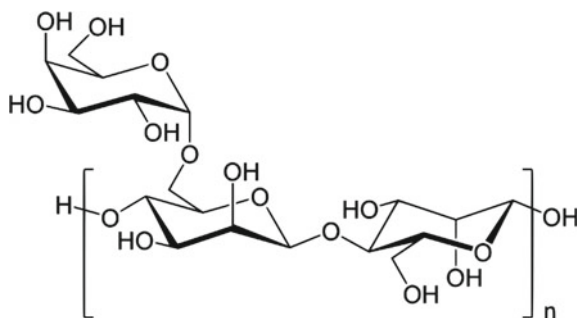
Table 2 Natural pectin obtained from different raw materials using various extraction procedures [50]

Extraction method	Raw Materials
Hydrothermal-assisted extraction	Potato peel, orange peel, pomegranate peel, apple peel, cashew apple pulp, chamomile, durian rind, jackfruit peel, hibiscus, banana peel, passion fruit, tomato husk (All waste material)
Hydrodynamic cavitation	Orange peel waste
Enzyme-assisted extraction	Sisal waste, Artichoke
Microwave-assisted extraction	Tobacco waste
Ultrasound-assisted extraction	Mango peel waste, Sisal waste, Passion fruit, Custard apple peel waste
Subcritical water extraction	Cocoa pod husk waste

**Fig. 9** Chemical structure of low and high methoxy pectin

nanoparticles were developed for the biomedical application. Palem et al., prepared silver nanocomposite hydrogel grid of grafted polymer of guar gum (polyacrylamidoglycolic acid) for the delivery of 5-fluorouracil. The designed system displayed effective antimicrobial activity against *B. Subtilis* and *S. ebony*. Thermal analysis confirm the higher stability of the formulation [51]. Another hydrogel formulation of guar gum/ Al_2O_3 used as effective photocatalyst prepared by sol-gel method. The formulation in the presence of solar irradiation responds to 80 and 90% degradation of malachite green dye followed by coupled adsorption and photocatalysis [52] (Fig. 10).

Fig. 10 Chemical structure of Guar gum



2.2 Protein Based Drug Delivery Systems

Besides carbohydrate based nanocomposites, protein-based drug delivery modules are also used as vehicles for the bioactive(s) delivery. In addition to the characteristics like biodegradability and biocompatibility, the surface of this protein based nanocomposites or nanoparticles could be easily functionalized owing functional groups into their primary structure. Moreover, charged proteins allow the facilitation of the loading of the bioactive(s) via electrostatic interactions [53, 54]. The nanoparticles which are based on natural polymers could be prepared under mild or aqueous conditions. The process of fabricating these nanoparticles is easy and safe as compared to those that are prepared by using synthetic polymers. Natural proteins possess the ability to uplift the cell retention and the toxicity caused by byproducts during degradation. Among proteins, core zein is generally employed to fabricate nanoparticles for the bioactive(s) delivery. This protein holds the potential for controlled and prolonged release of the bioactive(s) due to their hydrophobic nature [55]. Lai et al., formulated 5-fluorouracil loaded nanoparticles by using core zein protein. A standard phase separation procedure was employed to synthesize these nanoparticles. The size and % bioactive entrapment of these nanoparticles was measured to be 115 nm in diameter and 56.7% respectively. The author reported an initial burst release of the drug from the nanoparticles i.e., 22.4%. Animal studies revealed that the nanoparticles remained in systemic circulation for up to 24 h that is attributed to their high molecular weight prior to their localization in the liver [56]. Previously in literatures, it is reported that the core zein nanoparticles are also being employed for the sustained release of therapeutic proteins such as catalase and superoxide dismutase [57] and vitamin D3 [58]. In another study, Xu et al., fabricated hollow zein based nanoparticles. The manufacturing technique involves the blending of the protein i.e., core zein and sodium citrate based solutions. The core zein polymer is then deposited or collected in the vicinity of the sodium citrate crystals. It has resulted in the development of the nanoconstructs in which the core contains sodium citrate and the shell contains zein protein. These core-shell particles were then added to the aqueous phase i.e., water to produce hollow particles resulted in sodium citrate core dissolution. The size and % bioactive entrapment of these nanocomposites was measured to be < 100 nm and 30% respectively. Ex

vivo studies revealed that these nanoconstructs were also successfully internalized by the cells upon incubation with 3T3 fibroblast cells [59]. Several other protein based drug delivery modules are also discussed here.

2.2.1 Gelatin Based Nanocomposites

Gelatin is generally procured from bones and skins of animals, connective tissues, and by breakdown and hydrolysis of collagen. In drug delivery, it is commonly referred to as a matrixing agent. Gautam et al., in their scientific research synthesized the mannosylated gelatin mesosphere's for the effective delivery of doxorubicin to the lung cancer. They were using steric stabilization process for the synthesis and prepared the insufflation formulation with the size range of 8.7 μm , zeta-potential 1.74 mV. The lung accumulation study of different system(s) have been performed and better result was found in the gelatin conjugated system. The report showed better target ability, effective drug release pattern, and effective cell viability [60]. Das et al., reported paclitaxel loaded nanoparticles consisted of gelatin mixed with montmorillonite (MMT). The solvent evaporation method was employed to produce these nanoparticles. The author reported that swelling was increased on increasing glutaraldehyde concentration and subsequently drug release up to a certain point. The further increase in the crosslinker concentration has resulted in enhanced swelling and bioactive release. The cumulative release of the bioactive was observed to be enhanced at higher pH. At pH 7.4, the release of the bioactive was observed to be 80% within 8 h whereas at pH 1.2 the drug release was less than 44% within 4 h. Drug release was enhanced by increasing the concentration of the loaded bioactive [61]. The protein based nanocomposites are often used in gene therapy. Both viral and non-viral vectors are frequently employed for the transfection of DNA into the cells. It is because, in the living tissues, the injection of naked DNA leads to the degradation of enzymes and decreased cell uptake because of the repulsion between the negatively charged DNA and cell membrane. Zwiorek et al., worked on gelatin nanoparticles and demonstrated its potential for effective and safe non-viral gene delivery. The nanoparticles were manufactured by using the two-step desolvation method. The cationized particles showed homogenous size distribution with a low polydispersity index, efficient in enabling gene expression, and possess less toxicity [62]. These gelatin based nanocomposites are promising and hold the potential in gene therapy and tissue engineering.

2.2.2 Collagen Based Nanocomposites

Collagen is another natural protein of animal origin that is extensively employed in the formulation of nanocomposites. The collagen possesses a triple helix structure comprising of amino acids like proline, hydroxyproline, and glycine molecules [63]. They are considered suitable materials and are largely employed in multiple sectors like pharmaceuticals, cosmetics, and medical sectors. In one of the studies,

Thanikaivelan et al., developed collagen-SPION (superparamagnetic iron oxide nanoparticles) nanobiocomposites. The nanobiocomposites were fabricated by a simple method by using protein wastes from the leather industry. The nanobiocomposites showed magnetic tracking ability and selective oil absorption. Moreover, the author has also reported its oil removal applications. This strategy paves the new ways of converting bio-wastes into functional and effective nanocomposites [64]. Zhang et al., worked on nanocomposite hydrogel based on collagen to revitalize articular cartilage via stem cell therapy. The author developed aldehyde functionalized surface-modified cellulose nanocrystals by using facile one-pot oxidation. A nanocomposite was developed from the cellulose based nanocrystals and collagen hydrogel by applying Schiff base chemistry. The results demonstrated self-healing attributes of nanocomposites with fast shear thinning and increased elastic modulus. The author also reported the potential of developed nanocomposite in mesenchymal stem cell (MSC) delivery. MSCs loaded surface-modified cellulose nanocrystals/collagen hydrogel nanocomposite exhibited increased cell viability, higher cell retention, and enhanced implant integrity. In addition to cell protection during injection, the developed collagen based hydrogel would also fit into the inconsistent cartilage defect [65]. Therefore, the developed nanocomposite appears to be promising and holds enormous potential for the MSCs delivery for cartilage regeneration by using minimally invasive procedures.

2.2.3 Albumin Based Nanocomposites

Albumin as a natural carrier has been largely exploited in the design and development of drug delivery modules in cancer therapy. It is because it possesses and assures several advantages such as biocompatibility, easy availability, low toxicity, and other versatile characteristics. Therefore, for the diagnosis of cancer and its treatment, several kinds of albumin based nanoconstructs are being fabricated for the purpose of multiple imaging and therapeutic effectiveness [66]. Xu et al., fabricated albumin stabilized nanoconstructs which are based on manganese for the effective delivery of siRNA to brain tumors. In this study, bovine serum albumin functionalized with Arg-Gly-Asp (RGD) peptide was employed as a stabilizer to produce nanocomposites. The author reported that the developed nanocomposite improves tumor oxygenation and decreases endogenous H₂O₂ and acidity in the tumor microenvironment. Apart from these characteristics, nanocomposite showed good stability and excellent biocompatibility. In a glioblastoma (U87MG) orthotopic model, the developed nanocomposite exhibited strong contrast improvement at pH 6.5–6.9. In addition to this, imaging performance was enhanced inside the tumor region due to the disproportionation reaction of manganese in the weakly acidic environment [67]. Zhao et al., reported gold nanocomposite that is based on albumin. A moderate one-pot reduction route was employed to develop bovine serum albumin based gold nanoparticles using hydrazine hydrate as a reducer. The developed nanoconstruct was functionalized with hyaluronic acid. The mean diameter of the nanocomposites was 13.82 nm. The nanocomposites were reported to exhibit good colloidal

stability, water dispersibility, low cytotoxicity, and hemocompatibility. Moreover, the nanocomplex exhibited enhanced contrast in CT scanning [68]. Therefore these albumin based nanoplatforms could be explored as a contrast agent in MRI and CT scanning and in other biomedical applications.

2.2.4 Silk-Fibres Based Nanocomposites

Recently, silk proteins or silk fibers are being widely exploited in the fabrication of biomaterials. By processing these nanobiomaterials such as nanoparticles, hydrogels, microspheres, nanofibres, nano devices into a diverse set of morphologies, the utilization of these silk protein based biomaterials have increased for future biomedical applications. Silk proteins/fibers are versatile by a character in terms of biocompatibility, controllable in vivo biodegradation rate, exceptionally robust mechanical characteristics, etc. These versatile properties of silk proteins have triggered a prompt interest of the scientists in the biomaterial field [69]. Kishimoto et al., developed silk fibroin based nanocomposites. Montmorillonite (MMT) was incorporated into silk fibers to improve its physical properties. High-resolution Transmission electron microscopy micrographs exhibited 1.2 nm thick MMT layers have interacted with spun silk nanofibres in an unknown way. The developed nanocomposite exhibited a circular cross-section and a three-dimensional high porosity structure. The silk fiber-based nanocomposites may be employed as a scaffold for several biomedical applications and tissue engineering like bone regeneration. It is because the nanocomposites consist of biocompatible and biodegradable silk protein and osteoinductive MMT. Additionally, these nanocomposites can be useful in cell culture owing to the especially high surface area [70].

3 Challenges and Opportunities of Using Natural Polymers in Nanodrug Delivery

Natural polymer based nanocomposites serve as frontier areas in the bioactive(s) delivery that has gained huge attention from both academia and industry. From the pharmaceutical standpoint, natural polymers are commonly employed as binders, diluents, disintegrant, and matrixing agents in solid oral dosage forms. Over the last few years, these polymers are being used in the development of nanotechnology based nanocomposites. By virtue of their versatile characteristics like biodegradability, biocompatibility, easy availability, low immunogenicity, sustained and targeted drug release, these polymers are effectively and extensively utilized in the drug and vaccine delivery. These polymers are also being studied for gene therapy and tissue engineering. Despite promising trends and huge potential for applicability, these

biodegradable polymers of natural origin are also associated with some disadvantages. The disadvantages include such as poor mechanical properties, rapid degradation rate, and high hydrophilic capacity. Moreover, in some cases, some polymers exhibit poor mechanical properties in the presence of humid environments making their application unprofitable/unviable.

4 Conclusion

Conclusively, natural polymers play a pivotal role in advanced bioactive delivery because of their biodegradability, compatibility, and less toxicity. They are selected according to the pharmaceutical dosage form. So by understanding the chemical, physical, and pharmacological properties, one can select a particular polymer for a drug delivery system. Additionally, the use of natural polymer has increased in the present scenario. These natural polymers are also used as surface modifying agents (as a ligand) in different drug delivery systems such as solid lipid nanoparticles, nanorods, liposomal formulations, microspheres, mesospheres, immunological preparations, etc. Moreover, they are widely employed as drug delivery modules for the treatment of various diseases such as cancer, rheumatoid arthritis, infectious diseases, and so on. The natural polymer-based research now has reached the preclinical/clinical levels.

Acknowledgements This work was supported by the Indian Council of Medical Research (ICMR, New Delhi), India (Grant Number: For Laxmikant Gautam 45/16/2018-Nan/BMS, dated 11/05/2018, Anamika Jain 45/38/2018-PHA/BMS, dated 24/07/2018) and Department of Science and Technology (DST, New Delhi), India (Grant Number: For Priya Shrivastava DST/INSPIRE Fellowship 2017/ IF170447, dated 01/16/2018).

References

1. Visakh PM, Mathew AP, Thomas S (2013) Natural polymers: their blends, composites and nanocomposites: state of art, new challenges and opportunities. 18:1–20
2. Tong X, Pan W, Su T, Zhang M, Dong W, Qi X (2020) Recent advances in natural polymer-based drug delivery systems. *React Funct Polym* 148:104501
3. Nur M, Vasiljevic T (2017) Can natural polymers assist in delivering insulin orally? *Int J Biol Macromol* 103:889–901
4. George A, Shah PA, Shrivastav PS (2019) Natural biodegradable polymers based nanoformulations for drug delivery: a review. *Int J Pharm* 561:244–264
5. Ngwuluka NC, Ocheke NA, Aruoma OI (2014) Naturapolyceutics: the science of utilizing natural polymers for drug delivery. *Polymers* 6(5):1312–1332
6. Mittal A, Garg S, Kohli D, Maiti M, Jana AK, Bajpai S (2016) Effect of cross linking of PVA/starch and reinforcement of modified barley husk on the properties of composite films. *Carbohydr Polym* 151:926–938

7. García-Astrain C, González K, Gurrea T, Guaresti O, Algar I, Eceiza A et al (2016) Maleimide-grafted cellulose nanocrystals as cross-linkers for bionanocomposite hydrogels. *Carbohydr Polym* 149:94–101
8. Koliada M, Ishchenko O, Plavan V, Bessarabov V (2018) Characterisation of electrospun fibers made of PVA or PVAc and collagen derivative. *Fibres Text*
9. Pestov A, Bratskaya S (2016) Chitosan and its derivatives as highly efficient polymer ligands. *Molecules* 21(3):330
10. Sabra S, Abdelmoneem M, Abdelwakil M, Mabrouk MT, Anwar D, Mohamed R et al (2017) Self-assembled nanocarriers based on amphiphilic natural polymers for anti-cancer drug delivery applications. *Curr Pharm Des* 23(35):5213–5229
11. Raveendran S, Rochani AK, Maekawa T, Kumar DS (2017) Smart carriers and nanohealers: a nanomedical insight on natural polymers. *Materials* 10(8):929
12. Katas H, Moden NZ, Lim CS, Celesistinus T, Chan JY, Ganasan P et al (2018) Biosynthesis and potential applications of silver and gold nanoparticles and their chitosan-based nanocomposites in nanomedicine. *J Nanotechnol*
13. Shariatinia Z (2019) Pharmaceutical applications of chitosan. *Adv Coll Interface Sci* 263:131–194
14. Shokri J, Adibkia K (2013) Application of cellulose and cellulose derivatives in pharmaceutical industries. In: *Cellulose-medical, pharmaceutical and electronic applications*, 29 August 2013. IntechOpen
15. Lee KY, Mooney DJ (2012) Alginate: properties and biomedical applications. *Prog Polym Sci* 37(1):106–126
16. Szekalska M, Puciłowska A, Szymańska E, Ciosek P, Winnicka K (2016) Alginate: current use and future perspectives in pharmaceutical and biomedical applications. *Int J Polym Sci*
17. Mallik AK, Shahrzaman M, Zaman A, Biswas S, Ahmed T, Sakib MN, Haque P, Rahman MM (2019) Fabrication of polysaccharide-based materials using ionic liquids and scope for biomedical use. In: *Functional polysaccharides for biomedical applications*, 1 January 2019. Woodhead Publishing, pp 131–171
18. Mudgil D, Barak S, Khatkar BS (2014) Guar gum: processing, properties and food applications—a review. *J Food Sci Technol* 51(3):409–418
19. Sriamornsak P (2003) Chemistry of pectin and its pharmaceutical uses: a review. *Silpakorn Univ Int J* 3(1–2):206–228
20. Srivastava P, Malviya R (2011) Sources of pectin, extraction and its applications in pharmaceutical industry—an overview. *2(1):10–18*
21. Huang G, Huang H (2018) Application of hyaluronic acid as carriers in drug delivery. *Drug Deliv* 25(1):766–772
22. Kalsoom Khan A, Saba AU, Nawazish S, Akhtar F, Rashid R, Mir S, Nasir B, Iqbal F, Afzal S, Pervaiz F, Murtaza G (2017) Carrageenan based bionanocomposites as drug delivery tool with special emphasis on the influence of ferromagnetic nanoparticles. *Oxidative Med Cell Longevity* 2017
23. Zhang Z, Ortiz O, Goyal R, Kohn J Chapter 23-biodegradable polymers A2-Lanza. In: Langer R, Vacanti J (eds) *Robert in principles of tissue engineering*
24. Lee CH, Singla A, Lee Y (2001) Biomedical applications of collagen. *Int J Pharm* 221(1–2):1–22
25. Sleep D (2015) Albumin and its application in drug delivery. *Expert Opin Drug Deliv* 12(5):793–812
26. Shitole M, Dugam S, Tade R, Nangare S (2020) Pharmaceutical applications of silk sericin. In: *Annales pharmaceutiques francaises*, 20 June 2020. Elsevier Masson
27. Islam S, Bhuiyan MR, Islam MN (2017) Chitin and chitosan: structure, properties and applications in biomedical engineering. *J Polym Environ* 25(3):854–866
28. Park BK, Kim MM (2010) Applications of chitin and its derivatives in biological medicine. *Int J Mol Sci* 11(12):5152–5164
29. Sung YK, Kim SW (2020) Recent advances in polymeric drug delivery systems. *Biomater Res* 24(1):1–12

30. Massoudinejad M, Rasoulzadeh H, Ghaderpoori M (2019) Magnetic chitosan nanocomposite: fabrication, properties, and optimization for adsorptive removal of crystal violet from aqueous solutions. *Carbohydr Polym* 206:844–853
31. Hu X, Goud KY, Kumar VS, Catanante G, Li Z, Zhu Z et al (2018) Disposable electrochemical aptasensor based on carbon nanotubes-V₂O₅-chitosan nanocomposite for detection of ciprofloxacin. *Sens Actuators B Chem* 268:278–286
32. Cardoso MJ, Costa RR, Mano JF (2016) Marine origin polysaccharides in drug delivery systems. *Marine Drugs* 14(2):34
33. Lopes M, Abraham B, Veiga F, Seica R, Cabral LM, Arnaud P et al (2017) Preparation methods and applications behind alginate-based particles. *Exp Opin Drug Deliv* 14(6):769–782
34. Auriemma G, Cerciello A, Sansone F, Pinto A, Morello S, Aquino RP (2018) Polysaccharides based gastroretentive system to sustain piroxicam release: development and in vivo prolonged anti-inflammatory effect. *Int J Biol Macromol* 120:2303–2312
35. Ilgin P, Ozay H, Ozay O (2020) Synthesis and characterization of pH responsive alginate based-hydrogels as oral drug delivery carrier. *J Polym Res* 27(9):1–11
36. Du H, Liu W, Zhang M, Si C, Zhang X, Li B (2019) Cellulose nanocrystals and cellulose nanofibrils based hydrogels for biomedical applications. *Carbohydr Polym* 209:130–144
37. Shao C, Wang M, Meng L, Chang H, Wang B, Xu F et al (2018) Mussel-inspired cellulose nanocomposite tough hydrogels with synergistic self-healing, adhesive, and strain-sensitive properties. *Chem Mater* 30(9):3110–3121
38. Shi X, Wang Y, Sun H, Chen Y, Zhang X, Xu J et al (2019) Heparin-reduced graphene oxide nanocomposites for curcumin delivery: in vitro, in vivo and molecular dynamics simulation study. *Biomater Sci* 7(3):1011–1027
39. Ataei B, Khorasani MT, Karimi M, Daliri-Joupari M Plasma modification of heparinised CNT/PU nanocomposite and measuring of mechanical, calcification and platelet adhesion properties for application in heart valve. *Plast Rubber Compos* 2020:1–11
40. Makvandi P, Ali GW, Della Sala F, Abdel-Fattah WI, Borzacchiello A (2020) Hyaluronic acid/corn silk extract based injectable nanocomposite: a biomimetic antibacterial scaffold for bone tissue regeneration. *Mater Sci Eng C* 107:110195.
41. Gupta RC, Lall R, Srivastava A, Sinha A (2019) Hyaluronic acid: molecular mechanisms and therapeutic trajectory. *Frontiers Vet Sci* 6:192
42. Pandey A, Kulkarni S, Vincent AP, Nannuri SH, George SD, Mutalik S. Hyaluronic acid-drug conjugate modified core-shell MOFs as pH responsive nanoplatforam for multimodal therapy of glioblastoma. *Int J Pharm* 119735
43. Faccendini A, Ruggeri M, Miele D, Rossi S, Bonferoni MC, Aguzzi C, Grisoli P, Viseras C, Vigani B, Sandri G, Ferrari F (2020) Norfloxacin-loaded electrospun scaffolds: montmorillonite nanocomposite versus free drug. *Pharmaceutics* 12(4):325
44. Gao L, Zhang L, Zhu X, Chen J, Zhao M, Li S, Yu C, Hu L, Qiao H, Guo Z (2020) Hyaluronic acid functionalized gold nanorods combined with copper-based therapeutic agents for chemophotothermal cancer therapy. *J Mater Chem B*
45. Rhim JW, Wang LF (2014) Preparation and characterization of carrageenan-based nanocomposite films reinforced with clay mineral and silver nanoparticles. *Appl Clay Sci* 1(97):174–181
46. Tavakoli S, Kharaziha M, Nemati S, Kalateh A (2020) Nanocomposite hydrogel based on carrageenan-coated starch/cellulose nanofibers as a hemorrhage control material. *Carbohydr Polym* 117013
47. Polat TG, Duman O, Tunç S (2020) Preparation and characterization of environmentally friendly agar/κ-carrageenan/montmorillonite nanocomposite hydrogels. *Colloids Surf A Physicochem Eng Aspects* 124987
48. Wang SY, Meng YJ, Li J, Liu JP, Liu ZQ, Li DQ (2020) A novel and simple oral colon-specific drug delivery system based on the pectin/modified nano-carbon sphere nanocomposite gel films. *Int J Biol Macromol*
49. Ezati P, Rhim JW (2020) pH-responsive pectin-based multifunctional films incorporated with curcumin and sulfur nanoparticles. *Carbohydr Polym* 230:115638

50. Mellinas C, Ramos M, Jiménez A, Garrigós MC (2020) Recent trends in the use of pectin from agro-waste residues as a natural-based biopolymer for food packaging applications. *Materials* 13(3):673
51. Palem RR, Shimoga G, Rao KK, Lee SH, Kang TJ (2020) Guar gum graft polymer-based silver nanocomposite hydrogels: synthesis, characterization and its biomedical applications. *J Polym Res* 27(3):1–20
52. Pathania D, Katwal R, Sharma G, Naushad M, Khan MR, Ala'a H. Novel guar gum/Al₂O₃ nanocomposite as an effective photocatalyst for the degradation of malachite green dye. *Int J Biol Macromol* 87:366–74
53. DeFrates K, Markiewicz T, Gallo P, Rack A, Weyhmiller A, Jarmusik B, Hu X (2018) Protein polymer-based nanoparticles: fabrication and medical applications. *Int J Mol Sci* 19(6):1717
54. Tarhini M, Greige-Gerges H, Elaissari A (2017) Protein-based nanoparticles: from preparation to encapsulation of active molecules. *Int J Pharm* 522(1–2):172–197
55. Jao D, Xue Y, Medina J, Hu X (2017) Protein-based drug-delivery materials. *Materials* 10(5):517
56. Lai LF, Guo HX (2011) Preparation of new 5-fluorouracil-loaded zein nanoparticles for liver targeting. *Int J Pharm* 404(1–2):317–323
57. Lee S, Alwahab NS, Moazzam ZM (2013) Zein-based oral drug delivery system targeting activated macrophages. *Int J Pharm* 454(1):388–393
58. Luo Y, Teng Z, Wang Q (2012) Development of zein nanoparticles coated with carboxymethyl chitosan for encapsulation and controlled release of vitamin D₃. *J Agric Food Chem* 60(3):836–843
59. Xu H, Jiang Q, Reddy N, Yang Y (2011) Hollow nanoparticles from zein for potential medical applications. *J Mater Chem* 21(45):18227–18235
60. Gautam L, Sharma R, Shrivastava P, Vyas S, Vyas SP (2020) Development and characterization of biocompatible mannose functionalized mesospheres: an effective chemotherapeutic approach for lung cancer targeting. *AAPS PharmSciTech* 21(5):1–3
61. Das PR, Nanda RM, Behara A, Nayak PL (2011) Gelatin blended with nanoparticle cloisite30B (MMT) for control drug delivery of anticancer drug paclitaxel. *Int Res J Biochem Bioinform* 1:35–42
62. Zwirok K, Kloeckner J, Wagner E, Coester C (2004) Gelatin nanoparticles as a new and simple gene delivery system. *J Pharm Pharm Sci* 7(4):22–28
63. Sionkowska A (2011) Current research on the blends of natural and synthetic polymers as new biomaterials. *Prog Polym Sci* 36(9):1254–1276
64. Thanikaivelan P, Narayanan NT, Pradhan BK, Ajayan PM (2012) Collagen based magnetic nanocomposites for oil removal applications. *Sci Rep* 2(2):230
65. Zhang S, Huang D, Lin H, Xiao Y, Zhang X (2020) Cellulose nanocrystal reinforced collagen-based nanocomposite hydrogel with self-healing and stress-relaxation properties for cell delivery. *Biomacromol* 21(6):2400–2408
66. Li C, Wang X, Song H, Deng S, Li W, Li J, Sun J (2020) Current multifunctional albumin-based nanoplatforams for cancer multi-mode therapy. *Asian J Pharm Sci* 15(1):1–2
67. Xu K, Zhao Z, Zhang J, Xue W, Tong H, Liu H, Zhang W (2020) Albumin-stabilized manganese-based nanocomposites with sensitive tumor microenvironment responsivity and their application for efficient siRNA delivery in brain tumors. *J Mater Chem B* 8(7):1507–1515
68. Zhao W, Chen L, Wang Z, Huang Y, Jia N (2018) An albumin-based gold nanocomposites as potential dual mode CT/MRI contrast agent. *J Nanopart Res* 20(2):40
69. Vepari C, Kaplan DL (2007) Silk as a biomaterial. *Prog Polym Sci* 32(8–9):991–1007
70. Kishimoto Y, Ito F, Usami H, Togawa E, Tsukada M, Morikawa H, Yamanaka S (2013) Nanocomposite of silk fibroin nanofiber and montmorillonite: fabrication and morphology. *Int J Biol Macromol* 1(57):124–128

Natural Fibre-Reinforced Polymer Composites: Manufacturing and Biomedical Applications



Tielidy A. de M. de Lima, Gabriel Goetten de Lima,
and Michael J. D. Nugent

Currently, the use of natural fibres as a reinforcement in composites presents many attractive benefits, including the reduction of materials from non-renewable sources and reduction of environmental impact. Intensive research is being carried out to develop biocomposites which combine natural fibres with biodegradable polymers. One major advantages of these biocomposites is that they are totally degradable and sustainable. Additionally, such compounds exhibit a wide variety of properties and can compete with non-biodegradable polymers in different industrial fields.

One major aspect in the use of natural fibres is the reduction in the amount of polymeric material in the end application. The scope for using natural fibres is wide, ranging from traditional applications, in the textile industry, to the reinforcement of thermoplastic and thermoset polymer matrices. Natural fibres are less abrasive than inorganic fibres, are usually used as reinforcement, and thus, generate less wear on the equipment involved in their processing [1]. Natural fibres offer the possibility of delivering greater added value to the final product, due to the lower costs of manufacture, sustainability, and recyclability, especially in the automotive industry.

When selecting fibres for reinforcement in composites, it is essential to consider several factors such as: cost and availability, effect on the viscosity characteristics of the polymer, physical properties, thermal stability, chemical resistance, abrasiveness or wear, biodegradability, toxicity, recyclability, wettability, and compatibility with the polymer matrix [2–4]. A particularly important aspect, one should also consider is the possibility of incompatibility between the polymeric matrix and the fibre, given that the interfacial interaction is, in many cases, very weak. In this case, a third

T. A. de M. de Lima · G. G. de Lima · M. J. D. Nugent (✉)
Materials Research Institute, Athlone Institute of Technology, Athlone, Ireland
e-mail: MNugent@AIT.IE

G. G. de Lima
Programa de Pós-Graduação em Engenharia e Ciência dos Materiais – PIPE, Universidade
Federal do Paraná, Curitiba, Paraná, Brazil

component is used in the composite, reducing the interfacial tension and increasing the adhesion between the phases of the polymer blend: the compatibilizing agent. There are several compounds that have this function, such as copolymers, glycidyl methacrylate, maleic anhydride, and among others [5].

Natural fibres are the most widely used for fabrication of biocomposites and can be applied in several areas such as railway sleepers[6], automotive[1, 7, 8], for wind turbine blades[9], building/construction industry [10–12], and biomedical applications [13–17]. The focus of this chapter is the study of natural fibre-reinforced polymer composites, their manufacturing and biomedical applications.

The demand for new materials for cell therapy, regenerative medicine, and drug release is increasing due to the decrease in recovery time and the improvement in the quality of life of patients benefited by such systems. Systems for carrying and releasing drugs for permanent or temporary replacement of injured tissues are examples of growing applications in the biomedical area; in such cases, natural degradable polymers are shown potential in temporary tissue replacement. The development of new materials for applications in these areas has undergone major changes in recent decades; however, there is much to be explored in optimizing the end properties [18].

1 Natural Fibre

Natural fibres can be found in plants, animals, and minerals; occurring spontaneously in nature and/or grown in agricultural activities. Within these fibres, there are three main divisions namely,

1. Minerals—formed by elongated crystalline chains can be further categorized as amosite, crocidolite, tremolite, actinolite, and anthophyllite.
2. Vegetable fibres which have a cellulosic nature [19]. Plant-derived natural fibres can be classified according to the part, or type, of the plant from which they are extracted, as shown in Fig. 1. These fibres include lignocellulose fibres because the majority contains lignin in their structure, a natural polyphenol polymer [5–7, 20, 21].
3. Animal Fibres—generally comprise proteins; examples include silk, wool, horse hair, and alpaca hair.

1.1 *Advantages and Disadvantages of Biocomposites*

Biocomposites from natural fibres have multiple advantages and disadvantages as a reinforcement in conjugated materials (composites) and these are listed in Table 1 [6, 7, 22, 23].

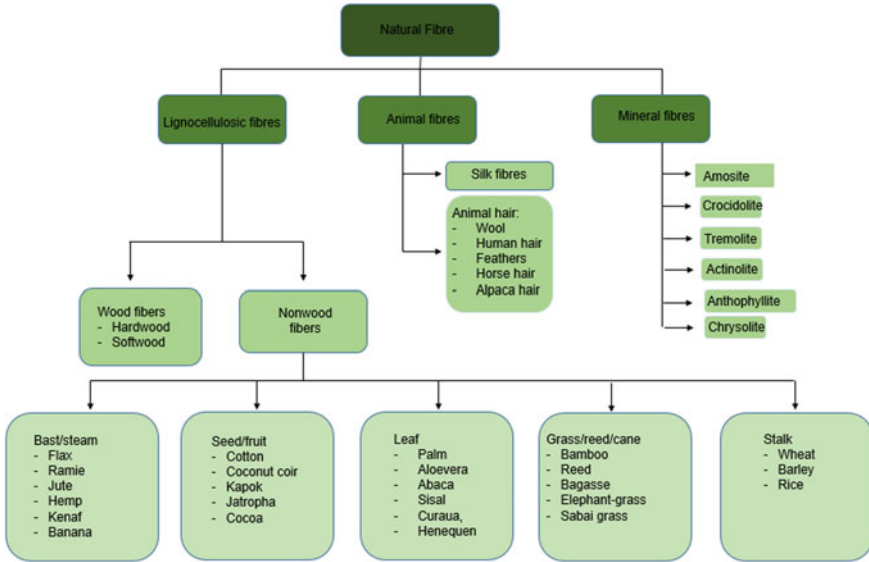


Fig. 1 Classification of the natural fibres

1.2 Chemical Compositions and Physical Properties of Natural Fibres

A natural fibre is a composite material consisting of cellulose, hemicelluloses, lignin, and further components. In this chapter, the focus will be concentrating on cellulose; however, we will briefly discuss each component present in natural fibre.

The chemical properties depend mainly on the content of cellulose and can vary; therefore, it is important to analyse each component present in the structure [6]. The physical properties of vegetable fibres are mainly determined by their chemical and physical composition, such as the fibre structure, cellulose, and degree of polymerization.

1.2.1 Cellulose

Cellulose is the essential component of all plants and this polymer exists abundantly in nature. Due to its chemical nature, it is capable of forming hydrogen bonds and is very hydrophilic. Between 40 and 50% of wood dry weight is in the form of cellulose [24]. Chemically, cellulose is a polysaccharide of molecular formula $(C_6H_{10}O_5)_n$ and composed from the union of β -D-glucopyranose molecules through β -1,4-glycosidic bonds. Due to its high degree of crystallinity and polymerization, cellulose is usually more stable to degradation, be it mechanical, chemical, or thermal, when compared to non-cellulosic components co-forming these fibres.

Table 1 Advantages and disadvantages for natural fibres in biocomposites

<i>Advantages</i>
• Resources from renewable sources
• Abundant
• Desirable mechanical properties
• High specific strength
• Flexible behaviour
• Biodegradable
• Non-abrasive
• Low thermal conductivity
• Nonmagnetic and nonconductive
• Lightweight
• Environmentally safe and non-toxic
• Unique acoustic and thermal insulating properties
• Low cost
<i>Disadvantages</i>
• Low biological resistance—attacked by fungus and bacteria
• Usually requires low processing temperature in order to be shaped into desirable materials
• High thermal expansion coefficient
• Inconsistent physical properties for natural fibres vary with harvesting season and region
• Properties are dependent on the harvesting process, locality, and maturity of the plant

1.2.2 Hemicellulose

In addition to cellulose, hemicellulose also exists in natural fibres where 25–40% of the wood dry weight is in the form of hemicellulose [24]. The differences observed between cellulose and hemicellulose are associated with the chemical structure. Hemicelluloses are formed from various sugars with several branches that binds to cellulose microfibrils. The low crystallinity may be related to the branched and random structure of the hemicelluloses. In comparison with cellulose, hemicelluloses have shorter polymer chains and, therefore, low molecular weight. Hemicellulose is composed of pentoses, hexoses and is more susceptible to hydrolysis when compared to cellulose, since it has a lower degree of polymerization[24]. It occurs mainly in the primary cell wall with branched polymers containing five to six carbon sugars of varied chemical structures.

1.2.3 Lignin

Lignin is the third component fundamental to natural fibres, comprising between 15 and 35% of the wood dry weight. Lignin is a highly complex non-crystalline molecule comprised of a large number of phenyl-propane units [24]. Lignin is amorphous and has an aromatic structure with a high molecular weight.

1.2.4 Further Components

In addition to cellulose, hemicellulose, and lignin, we can find several other components in the structure of natural fibres. These compounds are in lesser quantity and can be turpines, waxes, acids, alcohols, proteins, inorganic material, among others. Chemical modification is usually required for natural fibres in order to remove surface impurities, and to eliminate the hydrophilic hydroxyl groups and, along with physical treatments, are widely used to modify its surface and structure to increase its performance [25, 26].

1.3 *Modifications in the Surfaces of Natural Fibres*

The interfacial bonding between both materials (matrix/fibre) in a biocomposite defines many of the composite properties. If the interface is clean, there will be a good bond between matrix and fibre which will help in effective load transfer. In the case of a lack of compatibility and adhesion between fibres and matrix, it could cause problem in processing and material performance [27]. Therefore, in order to achieve a better interaction, and to enhance the fibre/matrix compatibility, fibres are usually subjected to physical and chemical modifications [28]. Chemical and physical methods treat the surface of the fibre and optimize this interaction [29].

In chemical treatments, a variety of chemicals can be used, such as alkali treatments or coupling agents. These treatments can influence the cellulosic fibril, the degree of polymerization, the extraction of lignin and hemicellulose compounds, reduce the number of cellulose hydroxyl groups in the fibre-matrix interface, improve fibre-matrix adhesion, increase the strength of composite, decrease its water absorption and improve thermal stability [25, 30]. Abaca, coir, aspen, flax, hemp, ramie, sisal, and jute fibres have been studied using chemical treatments and the mechanical properties such as tensile strength, flexural modulus, and Young's modulus of the composites were increased significantly as well as the storage modulus [31–37].

Physical treatments can improve thermal stability, crystallinity, physical and mechanical properties, modification of the surface, polarity, and compatibility between hydrophilic fibres and the hydrophobic matrix [27, 38, 39]. As an example, thermal treatment (autoclave) as shown by Tavares et al. (2019) on açai seeds (*Euterpe oleracea*) fibre were performed in order to use it as a composite reinforcement with

a polypropylene (PP) matrix; which contributed to an increase of the fibre crystallinity and an increase in the fibre surface roughness, without compromising the thermal stability of the fibres. In addition, this treatment improved tensile strength but with a reduction in the tensile modulus [40]. Another useful treatment is the plasma treatment in which Sun (2016) demonstrated that surface modification of natural fibres can produce rougher and smoother surfaces. The treatment can provide many advantages, including altering surface properties of textiles and reducing the use of environmentally hazardous chemicals [41].

Recent works report the combined usage of using both chemical and physical methods in order to obtain materials with improved properties [42–45].

2 Composites/Biocomposites

Different combinations of metals, ceramics, and polymers can form composite materials. The composites can be classified on the basis of their structural components [3]:

1. Scale: nano-composites;
2. Reinforcement geometry: Fibre reinforced, particles reinforced, and sheet moulded;
3. Matrix material: Polymer matrix composites (PMCs), ceramic matrix composites (CMCs), and metal matrix composites (MMCs);
4. Biocomposites.

The focus of this chapter will be on the effect of natural fibres processed under various manufacturing processes in order to produce composites within various common polymeric matrices.

Natural fibres have been garnering considerable attention in composite applications because of advantages like reasonable mechanical properties, low density, renewability, resources from renewable sources, abundance, and economic feasibility [45]. The performance of natural fibre composites depends on numerous factors such as composition, structure, length, treatment of fibres, and fibre/matrix interface [29].

2.1 Composites Reinforced with Natural Fibres

Several studies incorporating natural fibres such as hemp [46–48], jute [48–50], banana [48, 51, 52], kenaf [48, 53–55], ramie [48], sisal [48, 56], coir [57], bamboo [52, 58–60], flax [61, 62], and Abaca [36, 49] have been reported, exploring their potential as a reinforcement into different polymer matrices.

2.2 *Polymer Matrix Composites (PMCs)*

A matrix is a binder material that is used to hold fibres and transfer external loads to internal reinforcements. A wide variety of thermoset and thermoplastic resins are used in polymer composites which have different chemical structures and undergo different reactions.

The polymeric matrix reinforced with natural fibres has higher resistance and this enables the interfacial bonding to maintain their chemical and mechanical identities. Fibres are the main members of the charge carriers, while the matrix retains them in place, and at a desired orientation [63]. In these composites, two types of matrices are commonly used, thermoplastic and thermoset, as shown in Table 2. A thermoset resin is cured by the application of heat and often by the addition of chemicals labelled as curing agents.

The mechanical properties of bast, fibrous material from a specific part of a plant—phloem—depend on the cellulose content and the angle of the microfibrils. Banana fibres have a complex structure with a high cellulose content (60–65%) and low microfibrillar angle. As such, banana fibre is emerging as one of the most important reinforcements due to its good specific strength and rotting resistance [28].

2.3 *Advantages in Using Composites with Natural Fibres*

Natural fibres are used as reinforcement in polymeric composites and depend on factors such as plant fibre structure, thermal stability, length, loading and orientation, presence of voids and moisture absorption of fibres [64]. The thermal behaviour is always affected by the moisture, additives, and other factors [137].

Varying the composite matrix, it is possible to have significant variations in the values of tensile strength and Young's modulus as seen in Fig. 2. Depending on the interfacial bonds and surface tension, it is possible that increasing the concentration of fibre will increase the mechanical properties values and make it stiffer. In addition, if more than one fibre is added and if they have similar polyvalences and charges, it is possible that these properties remains even more strong and a more resistant material is obtained. Finally, if these fibres are aligned towards the desired load, the resistance is also increased. Such behaviour has been reported extensively in the literature [138].

However, natural fibres may present different mechanical properties depending on the interfacial bond between the polymer, for example, the tensile modulus of jowar fibre composite is reported to be 11% greater than those of bamboo composites and 45% greater than those of sisal composites, respectively, at 0.40 volume fraction of fibre. The flexural strength of jowar composite is greater 4% than those of bamboo composites and also 35% greater than those of sisal composites with a flexural modulus 1.12 times and 2.16 times greater than those of bamboo and sisal composites, respectively. Jowar fibres as reinforcement in polyester matrix can be

Table 2 Thermoplastic and thermoset polymeric composites reinforced with different natural fibres [63, 64]

Thermoplastic	Characteristics	Vegetal fibres
Polypropylene (PP)	Lightweight material, good insulation properties, non-toxic, low moisture absorption, and low cost	Curaua [65], flax [66, 67], hemp [68], jute [69], palm, sisal [67], wheat straw [67], banana [70]
Polyethylene (PE)	Non-toxic, low moisture absorption, low cost, rigid, and moisture resistant	Banana [71], green coconut husks [72], rice husk [73], sisal
Nylon	High stability and adaptability	Kenaf, flax, hemp [74]
Cellulose acetate	Low toxicity, good stability, high permeability, high glass transition temperature (T _g), production of resistant films, biocompatibility with a series of additive agents, and ability to form micro and nanoparticles	Kenaf [75, 76], curauá [77], sisal [78]
Polystyrene (PS)	High resistance to alkalis and acids, low density and moisture absorption, low resistance to organic solvents, and heat	Agave [79], banana [80], hemp [80], sisal [80]
Polycarbonate (PC)	Excellent electrical insulating characteristics, strong, and rigid	Pineapple [81]
Polyvinyl chloride (PVC)	Resistant, waterproof, durable, innocuous, non-toxic	Areca [82], bamboo [83], straw [84], rice [85]
Acrylonitrille-butadiene-styrene (ABS)	Outstanding impact strength and high mechanical strength	Palm [86], kenaf [87]
High-density polyethylene (HDPE)	Good low-temperature impact resistance and excellent chemical resistance	Banana [88], curaua [89], sisal [90]
High impact polystyrene (HIPS)	Flexibility, impact resistance, easy machinability, and low cost	Green coconut husks [91], sisal [92], sugar cane bagasse [93]
<i>Thermoset</i>	<i>Characteristics</i>	<i>Vegetable fibres</i>
Polyester	Strong, flexible, dries quickly, resists wrinkles and shrinking	Bamboo [94], banana [95, 96], coconut [97, 98], curaua [99], flax [100],hemp [101, 102], jute [103, 104], pineapple [105], sisal [106–108]

(continued)

Table 2 (continued)

Thermoplastic	Characteristics	Vegetal fibres
Polyurethane (PU)	High abrasion resistance, good low-temperature capability, wide molecular structural variability, ambient curing possible, and low cost	Banana [109], coir [110], sisal [110–112], curaua [113]
Epoxy	Virtually no post-mould shrinkage, resistance to high impact and high temperatures, chemical resistant and fungus resistant	Banana [114–116], coir [117], cotton [118], flax [119, 120], hemp[120], Jute [121, 122], pineapple [123], sisal [116, 124–127]
Phenolic	Excellent dielectric strength, great mechanical strength and dimensional stability, resistant to high heat, wear resistant, low moisture absorption	Banana [128, 129], cotton [130] flax [131], jute [130], sisal [112, 132]
Urea–Formaldehyde	Very hard, scratch-resistant material with good chemical resistance, electrical qualities, and heat resistance	Allo [133], cotton [133], sisal [134], coir [135], straw [136]

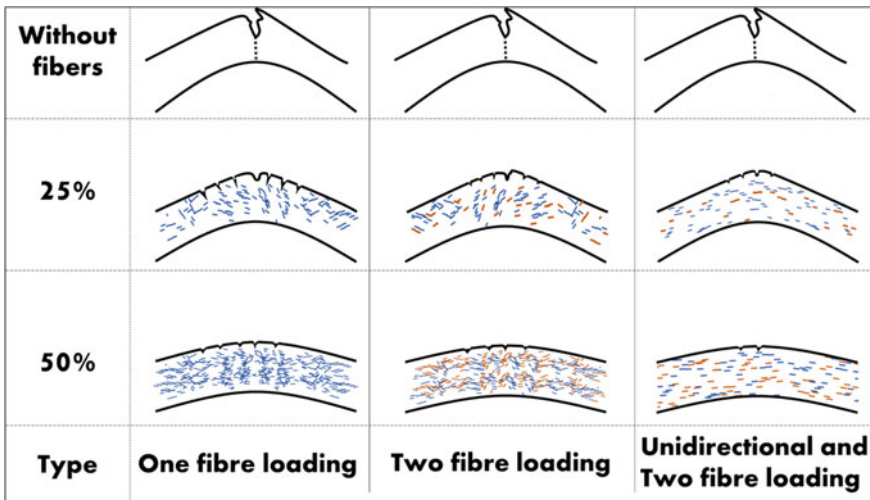


Fig. 2 Schematic representing the effect of adding different fibres, direction, and concentration in the resistance of the material

successfully developed as a composite material containing high strength and rigidity, with lightweight applications compared to conventional sisal and bamboo composites [139].

In the case of jute fibres, its usage can also improve the mechanical properties of composites, for example, the tensile strength obtained for PP laminate prepared from its own filaments was 23.24 MPa. However, when this same PP filament is synthesized with jute yarns, with a jute content of 19.34%, its tensile strength increased up to 31.21 MPa. On further increase the jute content to 37.1% and 55.89%, the tensile strength increased to 38.27 MPa and 53.06 MPa, respectively. Tensile modulus of composite containing jute yarn with matrix PP resulted, with fibre contents of 19.34%, 37.1%, and 55.89%, exhibits a tensile modulus increase in 23.7%, 50.42%, and 79.31%, respectively, compared with pure PP [69], as shown in Fig. 2.

The maximum tensile strength and tensile modulus of banana fibres incorporated into polypropylene composites (50%wt) are 70.82% and 67.60% higher than PP pure, respectively [70]. Using the same matrix, the variation in mechanical properties occurs by using different natural fibres, using flax fibre with epoxy resin increased 81.95% the tensile strength compared with banana fibre in the same matrix [116, 140]. In addition, hybrid composite with two or more fibre in the same matrix presents an improvement in tensile strength. Hemp composites with epoxy resin present a tensile strength of 36.48 MPa, a hybrid composites with Hemp/flax had 44.17 MPa and hybrids composites with hemp/flax/jute this value increased to 58.59 MPa. An increase of 21.08% and 60.60%, respectively [140].

3 Manufacturing Techniques

From ancient civilizations through to future innovation, composites have an important role. These materials offer many advantages such as: corrosion resistance, design flexibility, durability, lightweight ratios, and strength. Composites have been used for thousands of years in different areas. The first record was in 1500 BC when early Egyptians and Mesopotamian settlers used a mixture of mud and straw to create strong and durable buildings. This combination of mud and straw gives it a strong property against compression, torsion or bending [45]. In 1200 AD, the Mongols combined “animal glue”, bone, and wood in order to produce the first composite bow. In 1945, more than 3 million kg of glass fibres were used for various products, primarily for military applications. Composite materials continued to take off after the war and grew rapidly through the 1950s. In the following years, many records of the use of composites can be found in the most diverse areas. With the advance in the use of composites, processing techniques have been improved, and today, it is possible to develop diverse materials for applications ranging from aircraft turbines or advanced products in the biomedical field. Indeed, the composite industry is still developing, with much of the growth now focused on renewable energy and new manufacturing techniques. The following sections will discuss the main manufacturing techniques

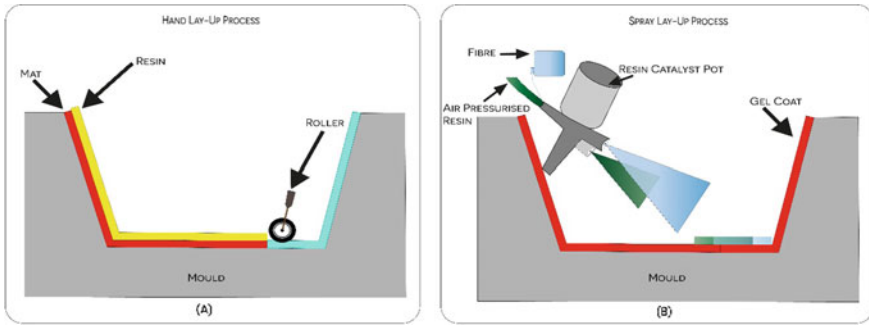


Fig. 3 a Hand lay-up process; b spray lay-up process

in the production of composites like hand lay-up, filament winding, compression moulding, injection moulding, and among others [141].

3.1 Open Moulding Technique

In this process, resin and fibres are cured in an open mould.

3.1.1 Hand Lay-up or Spray Lay-up

This technique is the simplest method of composite processing requiring minimal infrastructure [142]. Fibre reinforcements are placed by hand in a mould and resin is applied with a brush, roller, or spray, as shown in Fig. 3. There is no requirement of heat for the curing process.

However, there are quality issues using this technique, such as air entrapment can create a weak matrix and low-strength parts; the resin and catalyst should be accurately metered and thoroughly mixed for correct curing times; its toxicity and flammability of resin is an important safety issue, especially because of its high manual handling and the final application product; in addition, the surface roughness and surface detail could be acceptable on a moulded surface, but very poor in the opposite surface and shrinkage increases with higher resin volume fraction [143].

3.1.2 Filament Winding

Filament winding is an automated open moulding process that uses a rotating mandrel as the mould. The mould configuration produces a finished inner surface and a laminate surface on the outside diameter of the product as shown in Fig. 4. Various

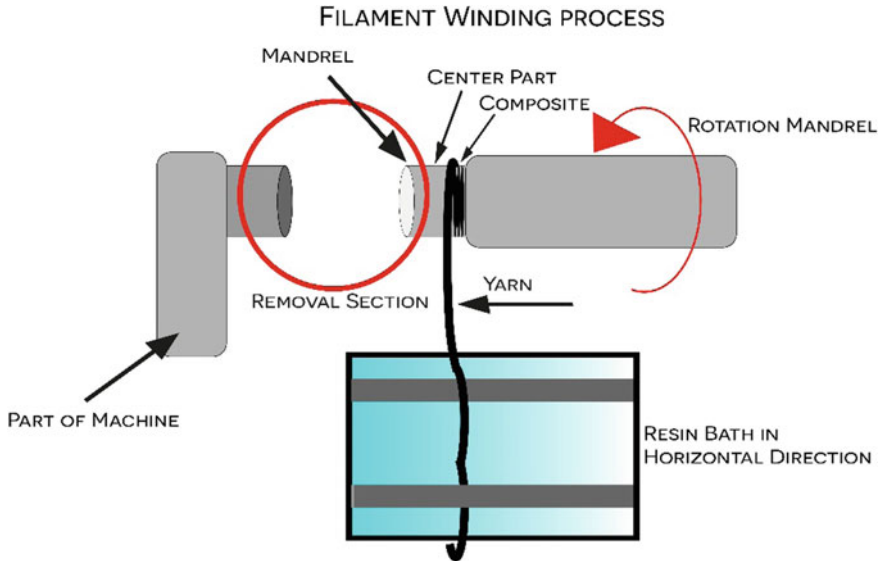


Fig. 4 Filament winding process

benefits to filament winding are evident such as short winding because of simplified tooling concept; short mandrel preparation time; availability of raw materials; relatively low cost of raw materials (matrices and reinforcements); relatively low tooling costs; polymers can easily be formulated, and the formulation can easily be changed according to individuals' needs; the process is reproducible or repetitive; continuous fibres can be used for the entire components; high fibre volume is achievable; fibres can be oriented in the loading direction; part size is not limited by oven-size; and process can be automated with cost savings. The main drawbacks of this process are that component must facilitate removal of mandrel; high cost of mandrel and complex; winding reverse curvature is not possible; difficulty in placing fibres parallel to the mandrel axis and need for external mandrel surface treatment for surface evenness [144, 145].

Ansari et al. (2019) studied the effect of winding speed on the mechanical properties of kenaf fibre reinforcement as geopolymer composites via filament winding technique. In this study, four speed winding (very low, low, high, very high) were used. The kenaf fibre was impregnated with resin by the means of a homemade impregnation machine. Compression tests in vertical axis results in values of 3.022, 7.328, 10.705, and 14.278 MPa for windings speeds from low to very high. The highest winding speed also resulted in highest strain, 9.69 mm/mm, while the lowest strain was for the lowest winding speed, 2.4 mm/mm. The maximum load to increase as well when increasing the speed, from 1.54 kN to 10.19 kN. Results of testing for the horizontal position were similar to vertical position. The speed of winding had

affected the pattern of winding, additionally, it will also affect the thickness of filament wound product and the mechanical properties of the filament wound product [146].

3.2 Closed Moulding

In this process, resin and fibres are cured inside the mould.

3.2.1 Centrifugal Casting

Centrifugal casting, also called rotational moulding, rotomoulding, rotational casting, or corotational moulding. Fibre-reinforced composites can be produced by rotating a mixture of chopped strand and catalyzed resin inside a hollow mandrel as shown in Fig. 5. These composites can be less homogeneous than those produced by other techniques, because of differences in specific gravity [147]. Advantages of centrifugal casting include its ability to produce hollow parts with complex shapes; both mould and machine are simple and low cost; low-pressure process allows thin-walled low-strength moulds to be used; different sizes of parts can be produced simultaneously on the same machine; large metal inserts, graphics, surfaces, and textures can be moulded directly into parts with, usually, very low scrap as all the materials are consumed to make the part. On the other hand, this process has some disadvantages like the process is not suited for very large production runs of smaller parts; there is limited selection of material available for this process [141, 147]; cycle times are comparatively longer as the mould needs to be heated and then cooled, loading, and unloading of the mould could be labour intensive and large flat surfaces, bosses, ribs, and dimensional tolerances can be difficult to produce [141].

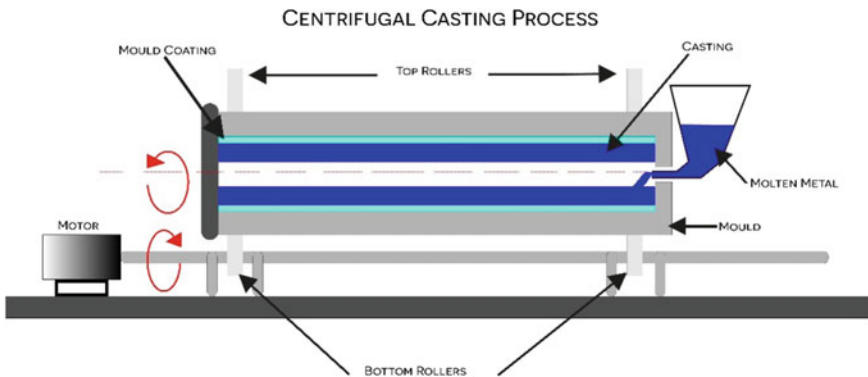


Fig. 5 Centrifugal casting process

Jamaludin et al. (2019) fabricated cylindrical tubes of functionally graded natural fibre-reinforced polymer (FGNF/epoxy) composite using horizontal centrifugal casting method. In this work, a coconut coir was mixed with epoxy; obtaining four different compositions 0%, 5%, 10%, and 15%. The fibres were chemically treated (NaOH solution) for 24 h and were mixed with epoxy using the centrifugal casting. When more natural fibre is added, decreases the material density from 1.1782 to 1.1656 (g/cm^3) at maximum load. The hardness and compression strength increased with natural fibres reinforcement from 66,25HD to 84HD 5% for hardness and 15 to 33,631 MPa, but it was slightly decreased with additional fibres load which was attributed to the porosity increase [147].

3.2.2 Pultrusion

Pultruded material has a constant cross section, manufactured through a mould (or mandrel). The matrix consists of mixing homogeneous resin and mineral fillers, whereas the reinforcement is a continuous filament (roving), as shown in Fig. 6 [141]. Fibre content varies between 50 and 80% by weight, depending on strength requirements; vinyl ester and epoxy resins provides up to 30% more strength than polyester resins; residual stresses and distortions can be minimized by specifying constant wall thicknesses, which cools more uniformly; approximately, 2–3% shrinkage can occur on the cross section when fully cured [143]. The range of the temperature for the pultruded composite profile is generally between 100 and 200 °C. The temperature setting for the pultruded fibre composites has to be carefully chosen to prevent the loss in their properties [148]. The main advantages of using pultrusion can be related to its high stiffness-to-weight ratio; ability to make tubes and sheets with precision

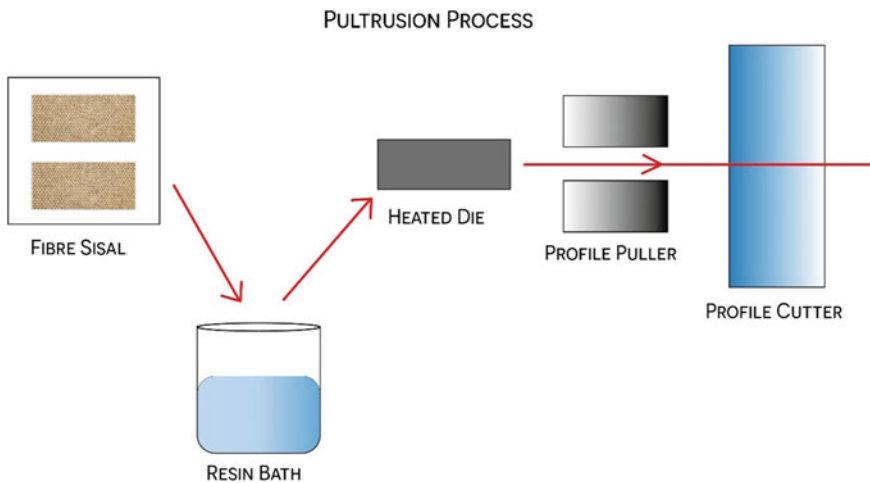


Fig. 6 Pultrusion process

wall thickness; high strength-to-weight ratio; low cost; high efficiency, durability, and noncorrosive character traits [141]. However, limited work has been reported on the processing parameters of pultruded natural fibre composites.

Chang et al. (2019) investigated the mechanical and wear properties of heat-treated pultruded kenaf fibre-reinforced polyester composites (PKFPCs) using pultrusion technique. The results showed that PKFPC with a 140 °C heat treatment exhibited better wear performance than untreated PKFPC and PKFPC using 120 and 170 °C heat treatments. The temperature of 120 °C had the best results regarding its flexural strength and modulus of PKFPC compared with untreated samples with an increase of 37% and 16%, respectively. The kenaf fibre in PKFPC was damaged when the heating temperature reached about 170 °C and led to the reduction in flexural properties. Physical modification by heat treatment, on the natural fibre, can be an effective way to improve the mechanical and wear properties of natural fibre-reinforced polymer composites [149].

Fairuz et al. (2016) studied the effect of filler loading on mechanical properties of pultruded kenaf fibre-reinforced vinyl ester composites. The tensile strength and tensile modulus showed an increase in the filler loading, improved the mechanical properties of the composites. The tensile strength had an increase of 20% when the percentage of the filler loading was increased from 20 to 50%. The tensile modulus increases 25% from 20 to 50% of filler loading, as in the case of tensile strength [150].

3.2.3 Compression Moulding

A measured quantity of raw, unpolymerized plastic material is introduced into a heated mould, which is subsequently closed under pressure, forcing the material into all areas of the cavity as it melts, this is shown in Fig. 7. Variation in raw material charge weight results in variation of part thickness and scrap; air entrapment is possible; internal stresses are minimal; dimensions in the direction of the mould opening and the product density will tend to vary more than those perpendicular to the mould opening. Surface detail is good and the surface roughness is a function of the die condition, in which typically, 0.8 µm is obtained [143].

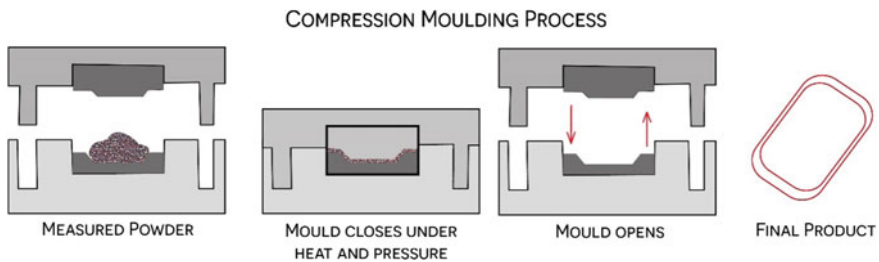


Fig. 7 Compression moulding process

Halim et al. (2019) studied the fabrication of unidirectional coir fibre as reinforcement for nonwoven melt-blown glass fabric using compression moulding. In this work, the fibres were chemically treated with NaOH and silane coupling agent, and the fibres were immersed in the materials which were oriented to achieve unidirectional preforms. A sandwich of preform with glass sheet in the middle was compacted in 5 MPa for 8 min at 170 °C. The tensile strengths were improved in samples with chemical modification, in addition to their storage modulus. The higher value indicates the higher stiffness and load bearing capacity of coir fibres in the reinforcement system. The chemical treatment of coir fibres acting as reinforcement to the nonwoven glass fabric increased the thermal resistance of the composite [151].

Yang et al. (2019) studied thermal and mechanical performance of unidirectional composites from Bamboo fibres reinforced with epoxy resin by the hand lay-up technique followed by compression moulding using various fibre volume fractions (0%-70%). Bamboo fibre-epoxy-based composites have a better thermal stability when compared with neat resin. The resin storage modulus is 2.5 GPa but when reinforced it increases from up to 9.7 GPa at the maximum filler addition. This increase in storage modulus with an increase in fibre content indicated that the composite stiffness is improved. The loss modulus of composites is much higher than that of neat resin, and the peak value of loss modulus increases with the increase of fibre content. In addition, the tensile strength increases from 21.0 to 134.3 MPa when increasing the fibre content from 0 and 70%. The improvement of mechanical performance makes it possible for epoxy-based composites to be widely used in certain practical applications [137].

3.2.4 Vacuum Bag Moulding

The vacuum bag moulding is one of the most versatile processes used for manufacture composite parts. This process combines a manual method using hand lay-up, or spray-up, on an open mould to produce a laminated component with a vacuum process and covering using a polymeric sheet. A vacuum is applied between the mould and the bag to squeeze the resin/reinforcement together, removing any trapped air, as shown in Fig. 8. Curing is normally performed in an oven [3, 152]. Some advantages of vacuum bag moulding are higher fibre content, laminates are easily produced with this technique; lower void contents and resin flow throughout structural fibres, with excess into bagging materials; the vacuum bag reduces the amount of volatiles emitted during cure, in addition to high-quality moulds, with complete elimination of voids and air bubbles.

Manjunath and Krishnamurthy (2019) studied the mechanical properties of hybrid composites using jute and e-glass by the hand lay-up and vacuum bagging technique. Tensile test results for hand lay-up technique resulted in 60.40 MPa and Young's modulus of 4306.6 MPa with flexural and hardness test of 159.47Mpa and 92 MPa, respectively. When the vacuum bagging technique was performed tensile strength and Young's modulus were 116.04 MPa and 8721.67 Mpa with flexural and hardness test of 450.50 MPa and 96 MPa, respectively. Mechanical and physical properties are

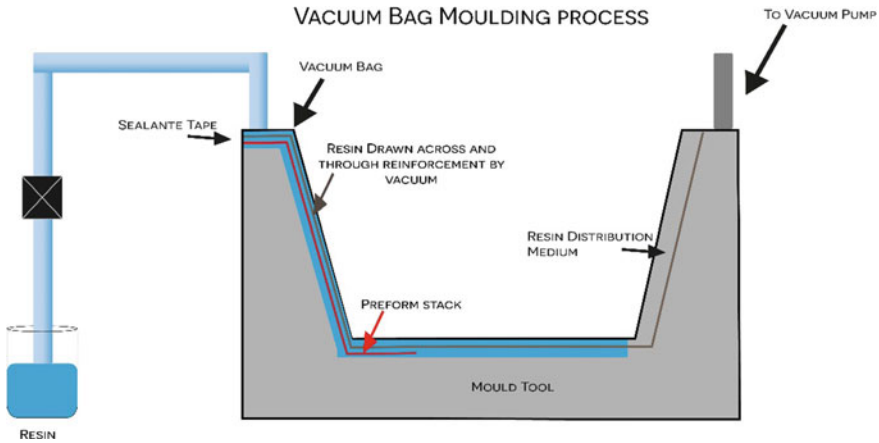


Fig. 8 Vacuum bag moulding process

greatly affected by fibre type and orientation. Vacuum bagging technique was found to be more suitable as compared to hand lay-up technique since vacuum bagging has yielded considerable better results [153].

Fajrin (2016) studied mechanical properties of natural fibre composite made of Indonesian grown sisal by vacuum bag process. In this work, Fajrin compared sisal fibre prepared using randomly orientation (RSO) and unidirectional oriented fibre (UOS). For UOS, the values of tensile, flexural, shear, and compressive stress were 40.25 MPa, 62.16 MPa, 23.26 MPa, and 60.88 MPa, respectively. Regarding the RSO, the values of tensile, flexural, shear, and compressive stress were 22.52 MPa, 51.5 MPa, 22.34 MPa and 49.12 MPa, respectively. This study shows that the orientation of sisal fibre alters the mechanical properties and unidirectional oriented provides laminates with higher mechanical properties [154].

Sanjay et al. (2018) studied the impact and inter-laminar strength of e-glass with jute/kenaf woven fabric epoxy composites, with the aim of evaluating the hybridization effects on different laminate stacking sequences made by these materials by the vacuum bagging method. The hybrid composite laminates with kenaf and jute containing e-glass fabrics demonstrated better results than composites laminates without the e-glass fibres. Laminate composites containing only natural fibre (jute, kenaf, or jute + kenaf) had impact strength ranging from 122.5 to 171.5 J/m. Nonetheless, the hybrids composites laminate exhibited values between 792.4 to 1078.4 J/m on impact strength. Therefore, the impact strength of composites depends on the inter-laminar and interfacial adhesion between the fibre and the matrix and also depends on the properties of individual fibres—fibre length, fibre loading and fibre orientation, for example, jute with e-glass composite the impact strength was 792.4 and kenaf with e-glass had 897.4 J/m [155].

3.2.5 Vacuum Infusion

Vacuum infusion is also known as the resin film infusion process. This technique consists of absorption of the matrix through a vacuum inside of a mould with the reinforcements, natural fibres, already arranged, and pre-oriented as shown in Fig. 9. The vacuum infusion process is widely used to manufacture large pieces [3, 143, 152] since it promotes better interfacial bonding between fibres and matrix phases that, consequently, produces a composite material with outstanding mechanical properties.

Bosquetti et al. (2019) studied the evaluation of the mechanical strength of sisal fibre reinforced with polyurethane composites panels using the vacuum infusion processing method. The tensile strength of the panels resulted in values of 146.34 MPa, 9.19 MPa, and 15.87 MPa for aligned, one-layer, and three-layered panels, respectively. When fibres were aligned to the load, they were responsible for bearing the applied load resulting in an improved resistance. When fibres were placed opposite direction to the load direction, the composite panel loses the resistance capability lowering its ultimate strength. Composites with one-layer of fabric and three-layers presented tensile strength of 9.19 MPa to one-layer and 15.87 for three-layered [156].

Yusuff and Ahmad (2019) studied the mechanical performances of a hybrid composites from kenaf/carbon with epoxy resin, which were fabricated via vacuum infusion technique in order to investigate the effect of various load of these natural fibres into the matrix. The kenaf fibre addition to the composite material improves the elongation at break, presenting highest elongation at break at 25 vol.% of kenaf fibre contents. The kenaf fibre exhibits good stiffness, which affects the elongation at break compared to carbon fibre [157].

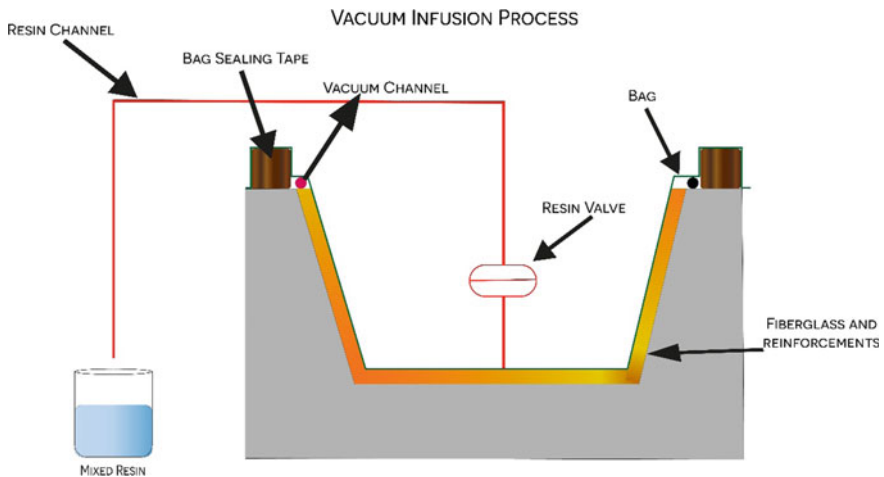


Fig. 9 Vacuum infusion process

Aisyah et al. (2019) studied the effects of carbon fibre hybridization on the thermal properties of woven kenaf-reinforced epoxy composites using vacuum infusion technique. In this work, a hybrid composite with higher kenaf fibre content had better thermal stability by presenting higher decomposition temperature, which was presented by the DSC, leading to a higher thermal stability was in pure carbon fibre composite [158].

3.2.6 Resin Transfer Moulding (RTM)

The resin transfer moulding (RTM) injects resin under pressure using an injection equipment into the mould cavity, in which the dry reinforcement materials are already arranged and pre-oriented. RTM is performed at room temperature with fast cycle times. A characteristic of the RTM is its low injection pressure. [3, 143, 152]. Some benefits of RTM are the possibility of producing large pieces; good dimensional tolerance; low cost of equipment for production; ability to produce parts with inserts; short production time cycles; possibility of automating the process; can operate with different types of resin; ability to vary the volumetric fraction of the composites; low solvent emission (operates within a closed mould), causing low environmental impact. Figure 10 shows a schematic of the RTM process.

Pinto et al. (2019) evaluated the impact resistance of hybrid jute-cotton fabric composites by the RTM process. A comparative study of the mechanical properties on impact of composites with four and six layers of jute/cotton fabric was carried out. Non-ageing specimens proved to be more resistant to impact than aged specimens. This behaviour was already expected, as the absorption of water makes it difficult for the matrix to adhere due to the fact that water lodges between the fibre/matrix interface and degrades both materials. The impact strength increased with the amount of the fabric layers that reinforces the composite.

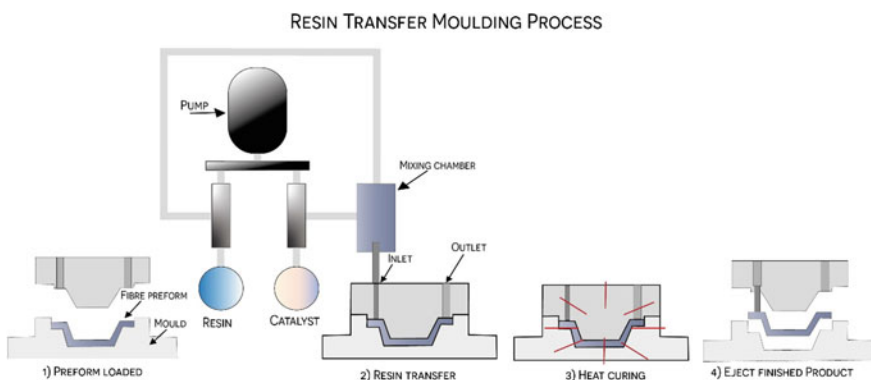


Fig. 10 Resin transfer moulding process

Mbakop et al. (2019) studied the effect of compacting parameters on preform permeability and mechanical properties of unidirectional flax fibre composites by RTM. In these reinforcements, the unidirectional fibre yarns were held together by a thin mat layer of short flax fibres. Reinforcements were compacted in dry or wet conditions at ambient or high temperature prior to permeability testing. Hot and wet compaction does not alter the permeability of the UD flax/mat reinforcement. The samples non-compacted and compacted followed by drying in ambient temperature exhibited the lowest value of tensile strength in 280 MPa and 290 MPa, respectively. Samples compacted without humidity using temperature of 100 °C and wet compacted at 23 °C and 100 °C exhibited the highest values of tensile strength as 340, 350, and 360 MPa, respectively [159].

3.2.7 Injection Moulding

This process can be performed using thermoplastic and thermosetting polymers. Composites are fed into a heated barrel, mixed, and forced into a mould cavity, where it cools and hardens to the configuration of the mould cavity, Fig. 11 [143, 152].

The main advantages of injection moulding are high production rates; repeatable high tolerances; ability to use a wide range of materials; excellent surface detail; low labour cost, minimal scrap losses, and little need to finish parts after moulding.

Correa-Aguirre et al. (2020) explored the reprocessing behaviour of polypropylene-sugar cane bagasse biocomposites, using neat and chemically treated cane bagasse fibres. These biocomposites were reprocessed five times using the extrusion process, followed by injection moulding after each reprocessing cycle. The mechanical properties indicate that microfibers bagasse fibres addition and chemical treatments generate improvements in the mechanical properties. The first processing

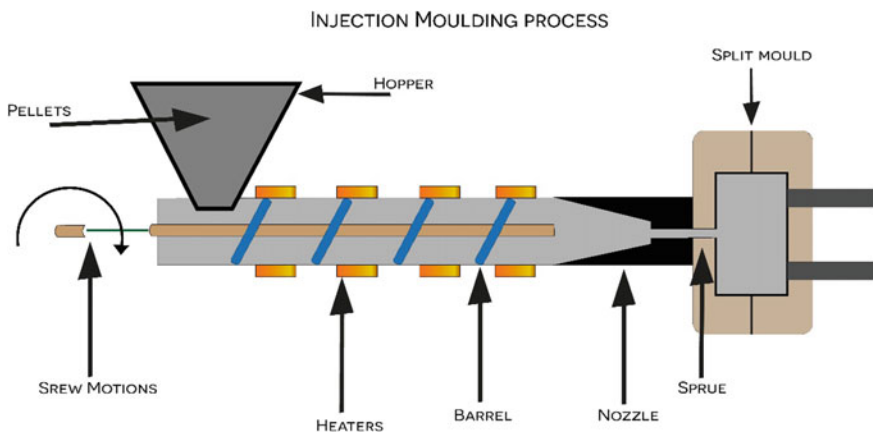


Fig. 11 Injection moulding process

cycle presented a flexural modulus of biocomposites PP-Bagasse (2069 MPa) and PP-Bagasse + alkali (1847 MPa), increased by 60% and 42% compared to neat PP (1296 MPa). Additionally, the flexural strength values increased for PP-Bagasse (48 MPa) and PP-Bagasse + alkali (43.3 MPa), increased by 20% and 8% compared to neat PP (40 MPa). For the third processing cycle, all flexural modulus and flexural strength values of the biocomposites presented significant differences compared to the flexural modulus value of the pure PP matrix. These increments were 57% and 48% for PP-Bag., PP-Bag. + alkali, respectively; also, flexural strength values increased by 11% and 7%, respectively. The last cycle had no significant differences were detected among the biocomposites in regard to flexural modulus and flexural strength. This could be related to the higher thermal stability of chemically modified fibres and a better interaction fibre–matrix, generated by the reprocessing cycles. Reprocessing and chemical modifications induced a better adhesion on the interface between bagasse fibres and PP matrix, while also increased the PP capacity to absorb energy perceived by the DMA.

3.2.8 Extrusion

Extrusion as a single- or twin-screw is the main industrial process to incorporate lignocellulose fibres into polymers [160]. In this process, plastics are continuously melted and pressed as a viscous mass from a pressure chamber through a shaping die. The moulding compound is granulated or powder, which is plasticized and compacted. The finished compressed part is cooled in the next step by water or air so that hardens, as shown in Fig. 12 [161]. Low cost per part; flexibility of

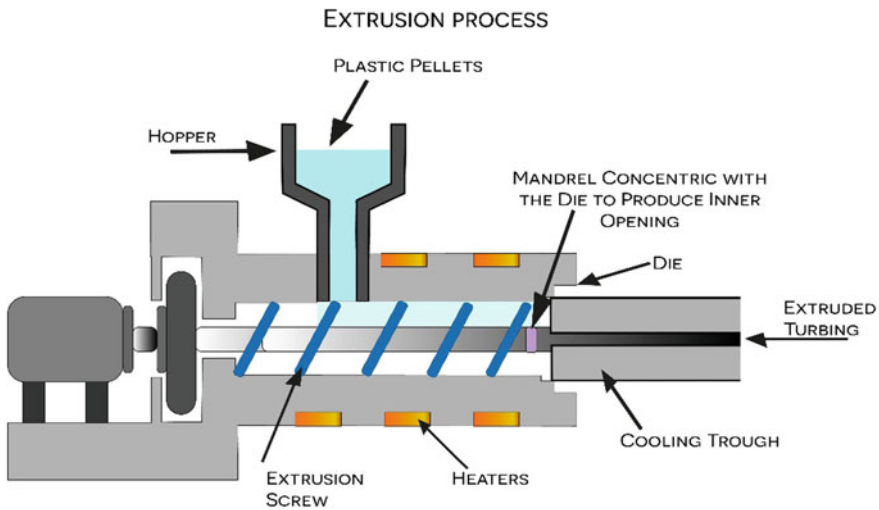


Fig. 12 Extrusion process

operation; in hot extrusion, post-execution alterations are easy because the product is still heated, continuous operation; high production volumes; many types of raw materials can be used; good mixing (compounding); surface finish obtained is good and good mechanical properties obtained in cold extrusion are some benefits of extrusion process.

Munde et al. (2019) studied the effect of sisal fibre loading on mechanical, morphological, and thermal properties of extruded polypropylene composites. The tensile modulus increases from 760.5 MPa to 1009 MPa for 10 wt% fibre loading, compared with neat PP, showing 33% improvement. Further addition of fibre at 20 wt% and 30 wt%, tensile modulus increases by 105% and 153%, respectively, due to the stronger interfacial interaction between the fibre and polymer. Thermal analysis shows a considerable improvement in thermal stability of composite compared to pure PP. The maximum 15.38% improvement in decomposition temperature is observed for 20% weight fraction of sisal fibre [162].

Miyahara et al. (2018) prepared and characterized composite materials using plastic waste from hydropulper (PWH) obtained from paper industries and extruded with sugar cane fibre (SCF) residues from ethanol industries. Higher fibre proportion in the composite presented positive effects, mainly in the compression and impact tests. Thermal analysis showed that between 250 °C and 450 °C the composite with 40% fibre loses lower mass and degrades more slowly than the sample with 30% fibre, this is because natural fibre compounds have higher heat resistance and consequently high resistance to decomposition [163].

Teixeira et al. (2019) studied the impact of content and length of curauá fibres on mechanical behaviour of extruded cementations composites. The fibre content directly influenced the mechanical performance and fibres with greater lengths which presented better mechanical results for the modulus of rupture and fracture energy. These results demonstrated that curauá fibres after 200 accelerated ageing cycles were better in comparison with composites at 7 days, because of the cement hydration, which filled the pores, densified its structure, and improved the transition zone fibre matrix [164].

4 Biomaterials

Biomaterials are defined as devices that works within biological systems (including biological fluids) and may consist of compounds of synthetic or natural origin, as well as chemically modified natural materials. They can also consist as solids, gels, pastes, or even liquids, not necessarily being manufactured, such as pig heart valves and human skin flaps treated for use as implants [18, 165, 166]. These biomaterials comprise all, or part, of a living structure or biomedical device that performs, augments, or replaces a natural function to improve patients' quality of life. The scope of biomaterials includes simple implants like intraocular lenses, sutures, wound dressings, cell matrices, bone plates, joint replacements to more complex materials

like biosensors, catheters, pacemakers, blood vessels, and artificial hearts. Biocompatibility means that the biomaterials must not form thrombi in the blood system, resulting in tumours in the surrounding tissues, or be immediately attacked, encapsulated, or rejected by the body [167]. The term biocompatibility was redefined in 1987 by Williams as the ability of a material to perform with an appropriate tissue response in a specific application. There are some factors that impact negatively in biocompatibility such as toxicology; reactions related to products from extrinsic microbiologic organisms colonizing the biomaterial; mechanical effects (rubbing, irritation, compression, and modulus mismatch) and also a broad range of interactions with surrounding proteins, and cells, inducing cell–biomaterials interactions (and tissue–biomaterials interactions) that might direct longer-term in vivo bioreaction.

The properties of biomaterials are classified into chemical, physical, mechanical, and biological in relation to the bulk and surface of the material. Figure 13 shows the different factors involved in biomaterials properties [168].

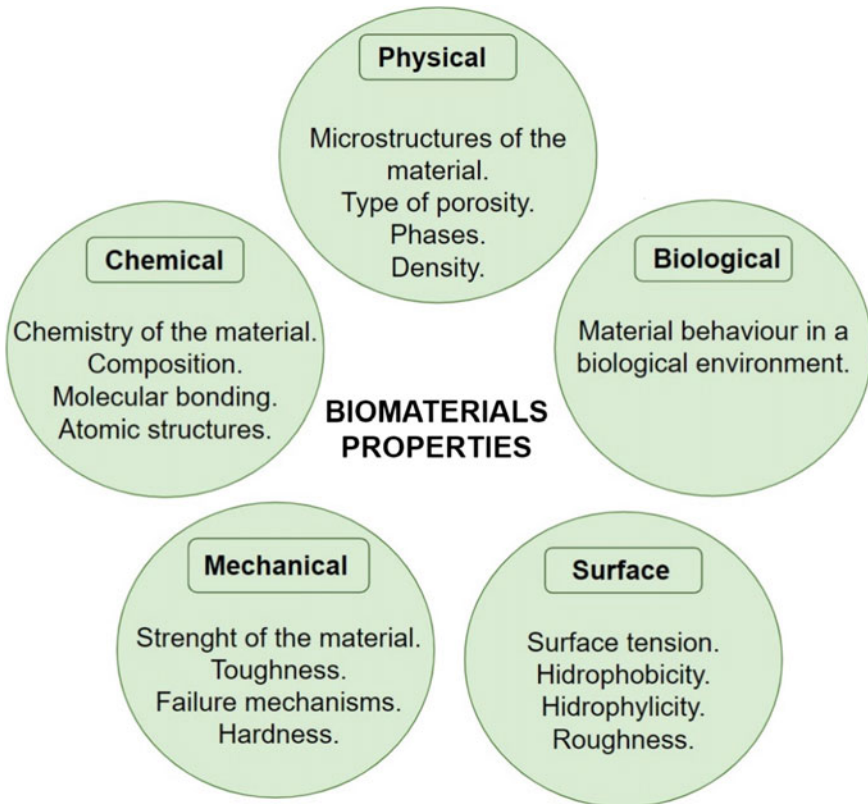


Fig. 13 Biomaterials properties

The properties and biocompatibility are important factors when choosing biomaterials; related with performance and success of implants and medical device to accomplish specific functions in the human body. Besides, these properties have been shown to have an important influence in their dynamic interactions with the biological surroundings when used as medical implants and organ or tissue replacements. Biomaterials are used in diagnostics (gene arrays and biosensors), medical supplies (blood bags and surgical tools), therapeutic treatments (medical implants and devices), and emerging regenerative medicine (tissue-engineered skin and cartilage) [18, 168].

A large number of polymers are used in multiple applications. Polymers are available in the most varied compositions, properties, and forms (solids, fibres, films, and gel), and they can be produced in diverse shapes and structures.

In addition, the success of the biomaterial in the body depends on several factors; Table 3 summarizes these in the selection of materials for biomedical applications.

The detailed analysis of the categories for chemical compounds used in the constitution of biomaterials, properties, advantages, limitations, and applicability are of great importance. Many materials can be used in biomedical application and they may be grouped into metals, ceramics, polymers, and composites. In this section, we will focus on polymers and composites.

Polymers are well suited for biomedical applications because of their diverse properties. The main advantages of polymeric biomaterials compared to ceramic or metallic materials includes the ease of manufacture to produce, varied shapes (particles, films, wires, among others), secondary processing, reasonable cost, and availability in finding materials with mechanical and physical properties desired for specific applications [170, 171]. Polymers can be obtained from polymerization reactions or by means of living organisms, thus, being classified, respectively, as synthetic and natural, which can also be chemically modified.

Natural polymers can include proteins (such as collagen, elastin, and silk fibroin) and polysaccharides (such as chitosan, alginate, xanthan gum, hyaluronic acid, and pectin).

Synthetic polymers can include polyamides, polyethylene, polypropylene, polyacrylates, fluorocarbons, polyesters, polyethers, polyurethanes, and among others. Table 4 can be observed some natural polymers and synthetic polymers and their application.

Natural Materials:

Composite materials consist of two or more distinct parts. The formation of composite biomaterials can occur by various methodologies, and the main associations being of the polymer-ceramic and metal-ceramic type [29, 170].

Table 3 Various factors of importance in material selection for biomedical applications [169]

Factors	Description		
First-level material properties	Chemical/biological characteristics Chemical composition (bulk and surface)	Physical characteristics Density	Mechanical/structural characteristics Elastic modulus Poisson's ratio Yield strength Tensile strength Compressive strength
Second-level material properties	Adhesion	Surface topology (texture and roughness)	Hardness Shear modulus Shear strength Flexural modulus Flexural strength
Specific functional requirements (based on application)	Biofunctionality (non-thrombogenic, etc.) Bioinert (non-toxic, non-irritant, non-allergic, non-carcinogenic, etc.) Bioactive Biostability (resistant to corrosion, hydrolysis, oxidation, etc.) Biodegradation	Form (solid, porous, coating, film, fibre, mesh, powder) Geometry Coefficient of thermal expansion Electrical conductivity Colour, aesthetics Refractive index Opacity or translucency	Stiffness or rigidity Fracture toughness Fatigue strength Creep resistance Friction and wear resistance Adhesion strength Impact strength Proof stress Abrasion resistance
Processing and fabrication	Reproducibility, quality, sterilizability, packaging, secondary processability		
Characteristics of host: tissue, organ, species, age, sex, race, health condition, activity, systemic response			
Medical/surgical procedure, period of application/usage			
Cost			

4.1 Biomedical Applications of Natural Fibres

Several studies in the literature incorporating natural fibres such as aloe vera, hemp, jute, banana, kenaf, ramie, sisal, coir, bamboo, flax, and abaca have been reported for biomedical applications. This section will describe recent works that have been published using natural fibres for biomedical applications.

Rodrigues et al. (2019) used the acemannan (ACE), which is a phytocompounds from aloe vera, which is reported to have beneficial biomedical properties such as cytocompatibility, wound healing inducing capability, as it promotes the release of several growth factors, antibacterial and immunomodulatory activities. In this work, ACE-based films were prepared through the combination of ACE with chitosan

Table 4 Polymeric biomaterials and application [18, 165, 170–172]

Natural polymers	Application
Proteins: Collagen, gelatine, elastin, silk, albumin, fibrin, keratin	Tissue regeneration and engineering, scaffold materials, drug delivery vehicles, and wound healing
Polysaccharides: Chitosan, alginic acid, hyaluronic acid, cellulose, chondroitin sulphate	Wound dressing, regenerative medicine (sponges, hydrogels, fibres, and membranes), tissue engineering, regeneration of bone, adipose-derived stem cell treatment, cartilage regeneration, surgical tools, dialysis membranes, biosensors, and drug delivery. Postoperative adhesion prevention, ophthalmic and orthopaedic lubricant, and cell scaffold
<i>Synthetic polymers</i>	
Poly(α -Esters): Poly (glycolic acid), polylactic acid, poly(lactide-co-glycolide), bacterial polyesters, polydioxanone and polycaprolactone	Load bearing, scaffolds, biocomposite materials, prostheses, tissue engineering, orthopaedic, bone pins and plates, suture, a drug/vaccine carrier, and a long-term contraceptive with zero-order drug release
Polyurethanes	Use in long-term implants such as cardiac pacemakers, vascular grafts, and tissue replacements
Polyphosphazenes	Scaffolds for tissue engineering, microencapsulating agents, biodegradable materials, biocompatible coatings, and carriers for gene delivery
Polyanhydrides	Drug delivery, eye disorder, local anaesthetics, and anticoagulants and used for treating brain tumours
Poly(propylene fumarate)	Bone tissue, ocular drugs, and estrogenic tissue engineering
Poly(ethylene glycol)	Hip and knee implants, artificial tendons and ligaments, synthetic vascular grafts, dentures, and facial implants
Poly(ortho esters)	Drug delivery, ocular delivery, periodontal disease treatment, and applications in veterinary medicine
Poly(ester amide)s	Tissue engineering, controlled drug release systems, hydrogels, adhesives and smart materials

or alginate at various concentrations. Blended films had a good homogeneity and mechanical stability. Films containing alginate and ACE had large storage modulus which indicates higher resistance to deformation. Films containing chitosan had lower values when ACE was incorporated; a significant weakening of the strength of the formed networks with the increase of ACE content was seen. The films produced

by the authors revealed a very promising alternative to further biomedical applications; especially considering the polymeric blends of alginate containing higher ratios of acemannan, showing an improved resistance and stable structure[173].

Atmakuri et al. (2019) investigated the mechanical properties of hemp and flax fibres within an epoxy resin hardener. From the contact angle measurements, pure flax shows the maximum contact angle of 65.98° and a mixture of 20% hemp and flax show a decrease in the contact angle of 10 degrees. The materials presented a maximum flexural strength at 84.80 MPa to hemp/flax composites with a weight fraction of 25/15 and 3.30 GPa of flexural modulus. Because of its low density, high strength, and availability, they can be used in biomedical applications[174].

Furlan et al. (2019) used sisal cellulose and magnetite nanoparticles in order to obtain a magnetic hybrid film. A sisal cellulose film was prepared by a solvent casting evaporation method. The SEM images of the hybrid films exhibited a fibrous structure. The films presented higher tensile strengths (14.3 MPa and 12.1 MPa, respectively) than the neat cellulose film (9.9 MPa). The elastic modulus of cellulose film (1860 MPa) is higher than of hybrid films 1500–1650 MPa and 780 for a higher dosage, indicating that the incorporation of nanoparticles in the cellulosic matrix decreased the films' stiffness[175].

Tejero et al. (2019) investigated suitable agronomical approaches for industrial hemp (*Cannabis sativa* L.) cultivation for biomedical applications. This work evaluated the agronomical response of two industrial hemp cultivars (Carma and Ermes) subjected to different management practices [176].

5 Conclusion

Natural fibre-reinforced polymer composites show a great deal of promise as biomaterials in medical applications. They can be used for high-tech applications, and in comparison, to certain fibre-reinforced composites, have particular advantages such as low density and improved thermal insulation. Composites reinforced with natural fibres are an area attractive to researchers and industries in creating effective and low-cost alternative materials that are environmentally friendly. These aspects are becoming more pertinent with the present ecological crisis that is occurring throughout the world.

Several manufacturing techniques are used in the manufacture of composites. Processing mediums are chosen according to the fibre used and according to the desired final product. These product characteristics will define the type of resin used and the most suitable technique for processing. The polymeric matrix is responsible for distributing the stress applied to the composite; however, the choice of polymer is limited mainly by the temperature required for processing, so, it is necessary to choose a polymeric matrix and a type of natural fibre that does not degrade in its processing phase. *Aloe vera*, hemp, jute, banana, kenaf, ramie, sisal, coir, bamboo, flax, and abaca are some of the possible materials for use in biomaterial applications.

The use of biomaterials is already well established in the most diverse applications. However, the development of innovative composite materials has potential in the area of tissue engineering and stem cell cultures and other novel biomedical applications. In addition, there are few reports in the literature that have focused on the application of natural fibres in the production of composites for biomedical applications. There is extensive work necessary in the future to fully realize the potential of natural fibre-reinforced composites for biomedical applications, in particular, studies on the processing, characteristics, and end-of-life implications. However, there is a renewed emphasis on natural alternatives and as such the future looks promising.

References

1. Ramli N, Mazlan N, Ando Y, Leman Z, Abdan K, Aziz AA et al (2018) Natural fiber for green technology in automotive industry: a brief review. *IOP Conf Ser Mater Sci Eng* [Internet]. 2018 Jun; 368:012012. Available from: <https://iopscience.iop.org/article/https://doi.org/10.1088/1757-899X/368/1/012012>
2. Rohan T, Tushar BGTM (2018) Review of natural fiber composites. *IOP Conf Ser Mater Sci Eng* [Internet]. 2018 Feb; 314:012020. Available from: <https://iopscience.iop.org/article/https://doi.org/10.1088/1757-899X/314/1/012020>
3. Rajak DK, Pagar DD, Kumar R, Pruncu CI (2019) Recent progress of reinforcement materials: a comprehensive overview of composite materials. *J Mater Res Technol* [Internet]. 2019 Nov; 8(6):6354–6374. Available from: <https://linkinghub.elsevier.com/retrieve/pii/S2238785419312086>
4. Balla VK, Kate KH, Satyavolu J, Singh P, Tadimeti JGD (2019) Additive manufacturing of natural fiber reinforced polymer composites: processing and prospects. *Compos Part B Eng* [Internet]. 2019 Oct; 174:106956. Available from: <https://linkinghub.elsevier.com/retrieve/pii/S1359836819310017>
5. Jones D, Ormondroyd GO, Curling SF, Popescu C-M, Popescu M-C (2017) Chemical compositions of natural fibres. In: *Advanced high strength natural fibre composites in construction* [Internet]. Elsevier, pp 23–58. Available from: <https://linkinghub.elsevier.com/retrieve/pii/B9780081004111000029>
6. Santulli C (2019) Natural fiber-reinforced composites. In: *Biomass, biopolymer-based materials, and bioenergy* [Internet]. Elsevier, pp 225–238. Available from: <https://linkinghub.elsevier.com/retrieve/pii/B9780081024263000126>
7. Peijs T (2000) Natural fiber based composites. *Mater Technol* [Internet]. 2000 Jan 25; 15(4):281–285. Available from: <https://www.tandfonline.com/doi/full/https://doi.org/10.1080/10667857.2000.11752892>
8. Huda MS, Drzal LT, Ray D, Mohanty AK, Mishra M (2008) Natural-fiber composites in the automotive sector. In: *Properties and performance of natural-fibre composites* [Internet]. Elsevier, pp 221–268. Available from: <https://linkinghub.elsevier.com/retrieve/pii/B9781845692674500077>
9. Mishnaevsky L, Branner K, Petersen H, Beauson J, McGugan M, Sørensen B (2017) Materials for wind turbine blades: an overview. *Materials (Basel)* [Internet]. 2017 Nov 9; 10(11):1285. Available from: <http://www.mdpi.com/1996-1944/10/11/1285>
10. Singh Rajeshwar, Gupta M (2005) Natural fiber composites for building applications. In: *Natural fibers, biopolymers, and biocomposites* [Internet], CRC Press. Available from: <http://www.crcnetbase.com/doi/https://doi.org/10.1201/9780203508206.ch8>
11. Pacheco-Torgal F, Jalali S (2011) Cementitious building materials reinforced with vegetable fibres: a review. *Constr Build Mater* [Internet]. 2011 Feb; 25(2):575–581. Available from: <https://linkinghub.elsevier.com/retrieve/pii/S0950061810004095>

12. Galan-Marin C, Rivera-Gomez C, Garcia-Martinez A (2016) Use of natural-fiber biocomposites in construction versus traditional solutions: operational and embodied energy assessment. *Materials* (Basel) [Internet]. 2016 Jun 13; 9(6):465. Available from: <http://www.mdpi.com/1996-1944/9/6/465>
13. Maan AA, Nazir A, Khan MKI, Ahmad T, Zia R, Murid M et al (2018) The therapeutic properties and applications of Aloe vera : a review. *J Herb Med* [Internet]. 2018 Jun; 12:1–10. Available from: <https://linkinghub.elsevier.com/retrieve/pii/S2210803318300022>
14. Singhvi MS, Zinjarde SS, Gokhale DV (2019) Polylactic acid: synthesis and biomedical applications. *J Appl Microbiol* [Internet]. 2019 Dec 17; 127(6):1612–1626. Available from: <https://onlinelibrary.wiley.com/doi/abs/10.1111/jam.14290>
15. Khan BA, Wang J, Warner P, Wang H (2015) Antibacterial properties of hemp hurd powder against *E. coli*. *J Appl Polym Sci* [Internet]. 2015 Mar 10; 132(10):n/a-n/a. Available from: <http://doi.wiley.com/10.1002/app.41588>
16. Moghaddam AB, Shirvani B, Aroon MA, Nazari T (2018) Physico-chemical properties of hybrid electrospun nanofibers containing polyvinylpyrrolidone (PVP), propolis and aloe vera. *Mater Res Express* [Internet]. 2018 Sep 26; 5(12):125404. Available from: <https://iopscience.iop.org/article/10.1088/2053-1591/aae0bf>
17. Nazarzadeh Zare E, Makvandi P, Tay FR (2019) Recent progress in the industrial and biomedical applications of tragacanth gum: a review. *Carbohydr Polym* [Internet]. 2019 May; 212:450–467. Available from: <https://linkinghub.elsevier.com/retrieve/pii/S0144861719302188>
18. He W, Benson R (2014) Polymeric biomaterials. In: *Handbook of polymer applications in medicine and medical devices* [Internet]. Elsevier, pp 55–76. Available from: <https://linkinghub.elsevier.com/retrieve/pii/B9780323228053000049>
19. Bledzki A (1999) Composites reinforced with cellulose based fibres. *Prog Polym Sci* [Internet]. 1999 May; 24(2):221–274. Available from: <https://linkinghub.elsevier.com/retrieve/pii/S0079670098000185>
20. Djafari Petroudy SR (2017) Physical and mechanical properties of natural fibers. In: *Advanced high strength natural fibre composites in construction* [Internet]. Elsevier, pp 59–83. Available from: <https://linkinghub.elsevier.com/retrieve/pii/B9780081004111000030>
21. Chaitanya S, Singh I (2016) Novel Aloe Vera fiber reinforced biodegradable composites—development and characterization. *J Reinf Plast Compos* [Internet]. 2016 Oct 5; 35(19):1411–1423. Available from: <http://journals.sagepub.com/doi/10.1177/0731684416652739>
22. Ramezani Kakroodi A, Cheng S, Sain M, Asiri A (2014) Mechanical, thermal, and morphological properties of nanocomposites based on polyvinyl alcohol and cellulose nanofiber from aloe vera rind. *J Nanomater* [Internet]. 2014; 2014:1–7. Available from: <http://www.hindawi.com/journals/jnm/2014/903498/>
23. Keya KN, Kona NA, Koly FA, Maraz KM, Islam MN, Khan RA (2019) Natural fiber reinforced polymer composites: history, types, advantages, and applications. *Mater Eng Res* [Internet] 1(2):69–87. Available from: <https://www.syncsci.com/journal/index.php/MER/article/view/267>
24. Desch HE, Dinwoodie JM (2016) *Timber: structure, properties, conversion and use*. Macmillan International Higher Education
25. Li X, Tabil LG, Panigrahi S (2007) Chemical treatments of natural fiber for use in natural fiber-reinforced composites: a review. *J Polym Environ* [Internet] 15(1):25–33. Available from: <http://link.springer.com/10.1007/s10924-006-0042-3>
26. Komuriah A, Kumar NS, Prasad BD (2014) Chemical composition of natural fibers and its influence on their mechanical properties. *Mech Compos Mater* [Internet] 50(3):359–376. Available from: <http://link.springer.com/10.1007/s11029-014-9422-2>
27. Cruz J, Fanguero R (2016) Surface modification of natural fibers: a review. *Procedia Eng* [Internet] 155: 285–288. Available from: <https://linkinghub.elsevier.com/retrieve/pii/S187705816321713>
28. Gunge A, Koppad PG, Nagamadhu M, Kivade SB, Murthy KVS (2019) Study on mechanical properties of alkali treated plain woven banana fabric reinforced biodegradable composites.

- Compos Commun [Internet] 13:47–51. Available from: <https://linkinghub.elsevier.com/retrieve/pii/S2452213918302377>
29. Tavares TD, Antunes JC, Ferreira F, Felgueiras HP (2020) Biofunctionalization of natural fiber-reinforced biocomposites for biomedical applications. *Biomolecules* [Internet] 10(1):148. Available from: <https://www.mdpi.com/2218-273X/10/1/148>
 30. Karthi N, Kumaresan K, Sathish S, Gokulkumar S, Prabhu L, Vigneshkumar N (2020) An overview: natural fiber reinforced hybrid composites, chemical treatments and application areas. *Mater Today Proc* [Internet] 27: 2828–2834. Available from: <https://linkinghub.elsevier.com/retrieve/pii/S2214785320300511>
 31. Rahman MM, Khan MA (2007) Surface treatment of coir (*Cocos nucifera*) fibers and its influence on the fibers' physico-mechanical properties. *Compos Sci Technol* [Internet] 67(11–12): 2369–2376. Available from: <https://linkinghub.elsevier.com/retrieve/pii/S026635380700449>
 32. Xue Y, Veazie DR, Glinsey C, Horstemeyer MF, Rowell RM (2007) Environmental effects on the mechanical and thermomechanical properties of aspen fiber–polypropylene composites. *Compos Part B Eng* [Internet] 38(2):152–158. Available from: <https://linkinghub.elsevier.com/retrieve/pii/S1359836806001119>
 33. Bledzki AK, Fink H-P, Specht K (2004) Unidirectional hemp and flax EP- and PP-composites: influence of defined fiber treatments. *J Appl Polym Sci* [Internet] 93(5):2150–2156. Available from: <http://doi.wiley.com/10.1002/app.20712>
 34. Goda K, Sreekala MS, Gomes A, Kaji T, Ohgi J (2006) Improvement of plant based natural fibers for toughening green composites—effect of load application during mercerization of ramie fibers. *Compos Part A Appl Sci Manuf* [Internet] 37(12): 2213–2220. Available from: <https://linkinghub.elsevier.com/retrieve/pii/S1359835X05004422>
 35. Manikandan Nair K, Thomas S, Groeninckx G (2001) Thermal and dynamic mechanical analysis of polystyrene composites reinforced with short sisal fibres. *Compos Sci Technol* [Internet] 61(16):2519–2529. Available from: <https://linkinghub.elsevier.com/retrieve/pii/S0266353801001701>
 36. Shibata M, Ozawa K, Teramoto N, Yosomiya R, Takeishi H (2003) Biocomposites made from short abaca fiber and biodegradable polyesters. *Macromol Mater Eng* [Internet] 288(1):35–43. Available from: <http://doi.wiley.com/10.1002/mame.200290031>
 37. Salem TF, Tirkas S, Akar AO, Tayfun U (2020) Enhancement of mechanical, thermal and water uptake performance of TPU/jute fiber green composites via chemical treatments on fiber surface. *e-Polymers* [Internet] 20(1):133–143. Available from: <https://www.degruyter.com/view/journals/epoly/20/1/article-p133.xml>
 38. Ahmad R, Hamid R, Osman SA (2019) Physical and chemical modifications of plant fibres for reinforcement in cementitious composites. *Adv Civ Eng* [Internet] 2019:1–18. Available from: <https://www.hindawi.com/journals/ace/2019/5185806/>
 39. Mukhopadhyay S, Figueiro R (2009) Physical modification of natural fibers and thermoplastic films for composites—a review. *J Thermoplast Compos Mater* [Internet] 22(2):135–162. Available from: <http://journals.sagepub.com/doi/10.1177/0892705708091860>
 40. da Tavares FF C, de Almeida MDC, da Silva JAP, Araújo LL, Cardozo NSM, Santana RMC (2020) Thermal treatment of açaí (*Euterpe oleracea*) fiber for composite reinforcement. *Polímeros* [Internet] 30(1). Available from: http://www.scielo.br/scielo.php?script=sci_arttext&pid=S0104-14282020000100408&tng=en
 41. Sun D (2016) Surface modification of natural fibers using plasma treatment. In: *Biodegradable green composites* [Internet]. Wiley, Hoboken, NJ, pp 18–39. Available from: <http://doi.wiley.com/10.1002/9781118911068.ch2>
 42. Huda MS, Drzal LT, Mohanty AK, Misra M (2008) Effect of fiber surface-treatments on the properties of laminated biocomposites from poly(lactic acid) (PLA) and kenaf fibers. *Compos Sci Technol* [Internet] 68(2):424–432. Available from: <https://linkinghub.elsevier.com/retrieve/pii/S0266353807002643>
 43. Kushwaha PK, Kumar R (2010) Studies on water absorption of bamboo–epoxy composites: effect of silane treatment of mercerized bamboo. *J Appl Polym Sci* [Internet] 115(3):1846–1852. Available from: <http://doi.wiley.com/10.1002/app.31317>

44. Puglia D, Monti M, Santulli C, Sarasini F, De Rosa IM, Kenny JM (2013) Effect of alkali and silane treatments on mechanical and thermal behavior of Phormium tenax fibers. *Fibers Polym* [Internet] 14(3):423–427. Available from: <http://link.springer.com/10.1007/s12221-013-0423-x>
45. Ngo T-D (2020) Introduction to composite materials. In: *Composite and nanocomposite materials—from knowledge to industrial applications* [Internet]. IntechOpen. Available from: <https://www.intechopen.com/books/composite-and-nanocomposite-materials-from-knowledge-to-industrial-applications/introduction-to-composite-materials>
46. Gong Y, Niu P, Wang X, Long S, Yang J (2012) Influence of processing temperatures on fiber dimensions and microstructure of polypropylene/hemp fiber composites. *J Reinf Plast Compos* [Internet] 31(19):1282–1290. Available from: <http://journals.sagepub.com/doi/10.1177/0731684412457887>
47. Sawpan MA, Pickering KL, Fernyhough A (2011) Improvement of mechanical performance of industrial hemp fibre reinforced polylactide biocomposites. *Compos Part A Appl Sci Manuf* [Internet] 42(3):310–319. Available from: <https://linkinghub.elsevier.com/retrieve/pii/S1359835X1000312X>
48. Ramesh M (2018) Hemp, jute, banana, kenaf, ramie, sisal fibers. In: *Handbook of properties of textile and technical fibres* [Internet]. Elsevier, pp 301–325. Available from: <https://linkinghub.elsevier.com/retrieve/pii/B9780081012727000092>
49. Bledzki AK, Jaszkiwicz A (2010) Mechanical performance of biocomposites based on PLA and PHBV reinforced with natural fibres—a comparative study to PP. *Compos Sci Technol* [Internet] 70(12):1687–1696. Available from: <https://linkinghub.elsevier.com/retrieve/pii/S0266353810002319>
50. Plackett D, Løgstrup Andersen T, Batsberg Pedersen W, Nielsen L (2003) Biodegradable composites based on l-poly lactide and jute fibres. *Compos Sci Technol* [Internet] 63(9):1287–1296. Available from: <https://linkinghub.elsevier.com/retrieve/pii/S0266353803001003>
51. Shih Y-F, Huang C-C (2011) Poly lactic acid (PLA)/banana fiber (BF) biodegradable green composites. *J Polym Res* [Internet] 18(6):2335–2340. Available from: <http://link.springer.com/10.1007/s10965-011-9646-y>
52. Sailesh A, Shanjeevi C, Arputhabalan JJ (2014) Tensile strength of Banana–Bamboo–Glass fiber reinforced natural fiber composites. *Appl Mech Mater* [Internet] 592–594:1195–1199. Available from: <https://www.scientific.net/AMM.592-594.1195>
53. Serizawa S, Inoue K, Iji M (2006) Kenaf-fiber-reinforced poly(lactic acid) used for electronic products. *J Appl Polym Sci* [Internet] 100(1):618–624. Available from: <http://doi.wiley.com/https://doi.org/10.1002/app.23377>
54. Saba N, Paridah MT, Jawaid M (2015) Mechanical properties of kenaf fibre reinforced polymer composite: a review. *Constr Build Mater* [Internet] 76: 87–96. Available from: <https://linkinghub.elsevier.com/retrieve/pii/S0950061814012628>
55. Joshi A, Shivakumar Gouda PS, Savanur S, Uppin V, Veereshkumar GB (2019) Influence of Kenaf on mechanical properties of glass epoxy composites. *IOP Conf Ser Mater Sci Eng* [Internet] 577: 012161. Available from: <https://iopscience.iop.org/article/10.1088/1757-899X/577/1/012161>
56. Phiri G, Khoathane M, Sadiku E (2014) Effect of fibre loading on mechanical and thermal properties of sisal and kenaf fibre-reinforced injection moulded composites. *J Reinf Plast Compos* [Internet] 33(3): 283–293. Available from: <http://journals.sagepub.com/doi/10.1177/0731684413511548>
57. Yousif BF, Ku H (2012) Suitability of using coir fiber/polymeric composite for the design of liquid storage tanks. *Mater Des* [Internet] 36: 847–853. Available from: <https://linkinghub.elsevier.com/retrieve/pii/S0261306911001841>
58. Wang G, Chen F (2017) Development of bamboo fiber-based composites. In: *Advanced high strength natural fibre composites in construction* [Internet]. Elsevier, pp 235–255. Available from: <https://linkinghub.elsevier.com/retrieve/pii/B9780081004111000108>
59. Bansal A, Zoolagud (2002) Bamboo composites: Material of the future. *J Bamboo Ratt* [Internet] 1(2):119–30. Available from: <http://booksandjournals.brillonline.com/content/journals/10.1163/156915902760181595>

60. Goh LD, Zulkornain AS (2019) Influence of bamboo in concrete and beam applications. *J Phys Conf Ser* [Internet] 1349:012127. Available from: <https://iopscience.iop.org/article/10.1088/1742-6596/1349/1/012127>
61. Bos HL, Müssig J, van den Oever MJA (2006) Mechanical properties of short-flax-fibre reinforced compounds. *Compos Part A Appl Sci Manuf* [Internet] 37(10): 1591–1604. Available from: <https://linkinghub.elsevier.com/retrieve/pii/S1359835X05003982>
62. Bodros E, Pillin I, Montrelay N, Baley C (2007) Could biopolymers reinforced by randomly scattered flax fibre be used in structural applications? *Compos Sci Technol* [Internet] 67(3–4): 462–470. Available from: <https://linkinghub.elsevier.com/retrieve/pii/S0266353806003356>
63. Yashas Gowda TG, Sanjay MR, Subrahmanya Bhat K, Madhu P, Senthamaraiannan P, Yogesha B (2018) Polymer matrix–natural fiber composites: an overview. In: Pham D (ed) *Cogent Eng* [Internet]. 2018 Mar 2; 5(1). Available from: <https://www.cogentia.com/article/10.1080/23311916.2018.1446667>
64. Pereira PHF, Rosa M de F, Cioffi MOH, Benini KCC de C, Milanese AC, Voorwald HJC et al (2015) Vegetal fibers in polymeric composites: a review. *Polímeros* [Internet] 25(1): 9–22. Available from: http://www.scielo.br/scielo.php?script=sci_arttext&pid=S0104-14282015000100002&lng=en&tlng=en
65. Mano B, Araújo JR, Spinacé MAS, De Paoli M-A (2010) Polyolefin composites with curaua fibres: effect of the processing conditions on mechanical properties, morphology and fibres dimensions. *Compos Sci Technol* [Internet] 70(1):29–35. Available from: <https://linkinghub.elsevier.com/retrieve/pii/S026635380900311X>
66. Duc A Le, Vergnes B, Budtova T (2011) Polypropylene/natural fibres composites: Analysis of fibre dimensions after compounding and observations of fibre rupture by rheo-optics. *Compos Part A Appl Sci Manuf* [Internet] 42(11):1727–1737. Available from: <https://linkinghub.elsevier.com/retrieve/pii/S1359835X11002338>
67. Moigne N Le, Oever M van den, Budtova T (2011) A statistical analysis of fibre size and shape distribution after compounding in composites reinforced by natural fibres. *Compos Part A Appl Sci Manuf* [Internet] 42(10):1542–50. Available from: <https://linkinghub.elsevier.com/retrieve/pii/S1359835X11002181>
68. Yan ZL, Wang H, Lau KT, Pather S, Zhang JC, Lin G et al (2013) Reinforcement of polypropylene with hemp fibres. *Compos Part B Eng* [Internet] 46: 221–226. Available from: <https://linkinghub.elsevier.com/retrieve/pii/S1359836812005756>
69. George G, Tomlal Jose E, Jayanarayanan K, Nagarajan ER, Skrifvars M, Joseph K (2012) Novel bio-commingled composites based on jute/polypropylene yarns: Effect of chemical treatments on the mechanical properties. *Compos Part A Appl Sci Manuf* [Internet] 43(1): 219–230. Available from: <https://linkinghub.elsevier.com/retrieve/pii/S1359835X11003502>
70. Mahesh D, Kowshigha KR, Raju NV, Aggarwal PK (2020) Characterization of banana fiber-reinforced polypropylene composites. *J Indian Acad Wood Sci* [Internet] 17(1): 1–8. Available from: <http://link.springer.com/10.1007/s13196-019-00244-x>
71. Ibrahim MM, Dufresne A, El-Zawawy WK, Agblevor FA (2010) Banana fibers and microfibrils as lignocellulosic reinforcements in polymer composites. *Carbohydr Polym* [Internet] 81(4): 811–819. Available from: <https://linkinghub.elsevier.com/retrieve/pii/S014486171002377>
72. Brahmakumar M, Pavithran C, Pillai R (2005) Coconut fibre reinforced polyethylene composites: effect of natural waxy surface layer of the fibre on fibre/matrix interfacial bonding and strength of composites. *Compos Sci Technol* [Internet] 65(3–4): 563–569. Available from: <https://linkinghub.elsevier.com/retrieve/pii/S026635380400243X>
73. (2005) Effect of chemical treatment on rice husk (RH) reinforced polyethylene (PE) composites. *BioResources* 5(2):854–869
74. Ozen E, Kiziltas A, Kiziltas EE, Gardner DJ (2013) Natural fiber blend-nylon 6 composites. *Polym Compos* [Internet] 34(4): 544–553. Available from: <http://doi.wiley.com/10.1002/pc.22463>
75. Pang C, Shanks R, Ing K, Daver F (2013) Plasticised cellulose acetate–natural fibre composite. *World J Eng* [Internet] 10(5): 405–410. Available from: <http://multi-science.atypon.com/doi/10.1260/1708-5284.10.5.405>

76. Pang C, Shanks RA, Daver F (2014) Bio-composites based on cellulose acetate and kenaf fibers: processing and properties, pp 350–353. Available from: <http://aip.scitation.org/doi/abs/10.1063/1.4873798>
77. Gutiérrez MC, De Paoli M-A, Felisberti MI (2012) Biocomposites based on cellulose acetate and short curauá fibers: effect of plasticizers and chemical treatments of the fibers. *Compos Part A Appl Sci Manuf* [Internet] 43(8): 1338–1346. Available from: <https://linkinghub.elsevier.com/retrieve/pii/S1359835X12000991>
78. Lima PRL, Santos HM, Camilloto GP, Cruz RS (2017) Effect of surface biopolymeric treatment on sisal fiber properties and fiber-cement bond. *J Eng Fiber Fabr* [Internet] 12(2):155892501701200. Available from: <http://journals.sagepub.com/doi/10.1177/155892501701200207>
79. Singha AS, Rana RK (2012) Natural fiber reinforced polystyrene composites: effect of fiber loading, fiber dimensions and surface modification on mechanical properties. *Mater Des* [Internet] 41: 289–297. Available from: <https://linkinghub.elsevier.com/retrieve/pii/S0261306912003019>
80. Mishra S, Naik JB (2005) Effect of treatment of maleic anhydride on mechanical properties of natural fiber: polystyrene composites. *Polym Plast Technol Eng* [Internet] 44(4): 663–675. Available from: <http://www.tandfonline.com/doi/abs/10.1081/PTE-200057814>
81. Threepopnatkul P, Kaerkitcha N, Athipongarporn N (2009) Effect of surface treatment on performance of pineapple leaf fiber–polycarbonate composites. *Compos Part B Eng* [Internet] 40(7): 628–632. Available from: <https://linkinghub.elsevier.com/retrieve/pii/S1359836809000687>
82. Nayak S, Mohanty JR, Samal PR, Nanda BK (2020) Polyvinyl chloride reinforced with areca sheath fiber composites—an experimental study. *J Nat Fibers* [Internet] 17(6): 781–792. Available from: <https://www.tandfonline.com/doi/full/10.1080/15440478.2018.1534186>
83. Shi SQ, Cai L, Weng Y, Wang D, Sun Y (2019) Comparative life-cycle assessment of water supply pipes made from bamboo vs. polyvinyl chloride. *J Clean Prod* [Internet] 240: 118172. Available from: <https://linkinghub.elsevier.com/retrieve/pii/S0959652619330422>
84. Jiang L, He C, Fu J, Li X (2018) Wear behavior of alkali-treated sorghum straw fiber reinforced polyvinyl chloride composites in corrosive water conditions. *BioResources* 13(2):3362–3376
85. Wang L, He C, Yang X (2019) Effects of pretreatment on the soil aging behavior of rice husk fibers/polyvinyl chloride composites. *BioResources* 14(1):59–69
86. Neher B, Bhuiyan MMR, Kabir H, Qadir MR, Gafur MA, Ahmed F (2014) Study of mechanical and physical properties of palm fiber reinforced acrylonitrile butadiene styrene composite. *Mater Sci Appl* [Internet] 05(01): 39–45. Available from: <http://www.scirp.org/journal/doi.aspx?DOI=10.4236/msa.2014.51006>
87. Lufti MTM, Majid DL, Faizal ARM, Norkhairunnisa M (2015) Biocomposite from acrylonitrile-butadiene-styrene polymer and Kenaf whole stem fibre: mechanical properties. *Adv Mater Res* [Internet] 1119: 263–267. Available from: <https://www.scientific.net/AMR.1119.263>
88. Liu H, Wu Q, Zhang Q (2009) Preparation and properties of banana fiber-reinforced composites based on high density polyethylene (HDPE)/Nylon-6 blends. *Bioresour Technol* [Internet] 100(23): 6088–6097. Available from: <https://linkinghub.elsevier.com/retrieve/pii/S0960852409006658>
89. Araujo JR, Mano B, Teixeira GM, Spinacé MAS, De Paoli M-A (2010) Biomicrofibrillar composites of high density polyethylene reinforced with curauá fibers: Mechanical, interfacial and morphological properties. *Compos Sci Technol* [Internet] 70(11): 1637–1644. Available from: <https://linkinghub.elsevier.com/retrieve/pii/S0266353810002320>
90. Choudhury A (2008) Isothermal crystallization and mechanical behavior of ionomer treated sisal/HDPE composites. *Mater Sci Eng A* [Internet] 491(1–2): 492–500. Available from: <https://linkinghub.elsevier.com/retrieve/pii/S0921509308002906>
91. Carvalho KCC, Mulinari DR, Voorwald HJC, Cioffi MOH (2010) Chemical modification effect on the mechanical properties of hips/coconut fiber composites. *BioResources* 5(2):1143–1155

92. Antich P, Vázquez A, Mondragon I, Bernal C (2006) Mechanical behavior of high impact polystyrene reinforced with short sisal fibers. *Compos Part A Appl Sci Manuf* [Internet] 37(1):139–150. Available from: <https://linkinghub.elsevier.com/retrieve/pii/S1359835X04003124>
93. Beninia KCCC, Voorwald HJC, Cioffi MOH (2011) Mechanical properties of HIPS/sugarcane bagasse fiber composites after accelerated weathering. *Proc Eng* [Internet] 10: 3246–3251. Available from: <https://linkinghub.elsevier.com/retrieve/pii/S1877705811007247>
94. Wong KJ, Zahi S, Low KO, Lim CC (2010) Fracture characterisation of short bamboo fibre reinforced polyester composites. *Mater Des* [Internet] 31(9):4147–4154. Available from: <https://linkinghub.elsevier.com/retrieve/pii/S0261306910002402>
95. Sreekumar PA, Albert P, Unnikrishnan G, Joseph K, Thomas S (2008) Mechanical and water sorption studies of ecofriendly banana fiber-reinforced polyester composites fabricated by RTM. *J Appl Polym Sci* [Internet] 109(3):1547–1555. Available from: <http://doi.wiley.com/10.1002/app.28155>
96. Mariatti M, Jannah M, Abu Bakar A, Khalil HPSA (2008) Properties of Banana and Pandanus Woven fabric reinforced unsaturated polyester composites. *J Compos Mater* [Internet] 42(9): 931–941. Available from: <http://journals.sagepub.com/doi/10.1177/0021998308090452>
97. Monteiro SN, Terrones LAH, D'Almeida JRM (2008) Mechanical performance of coir fiber/polyester composites. *Polym Test* [Internet] 27(5):591–595. Available from: <https://linkinghub.elsevier.com/retrieve/pii/S014294180800041X>
98. Mulinari DR, Baptista CARP, Souza JVC, Voorwald HJC (2011) Mechanical properties of coconut fibers reinforced polyester composites. *Procedia Eng* [Internet] 10: 2074–2079. Available from: <https://linkinghub.elsevier.com/retrieve/pii/S1877705811005315>
99. Monteiro SN, Aquino RCMP, Lopes FPD (2008) Performance of curaua fibers in pullout tests. *J Mater Sci* [Internet] 43(2): 489–493. Available from: <http://link.springer.com/10.1007/s10853-007-1874-5>
100. Charlet K, Jernot J-P, Gomina M, Bizet L, Bréard J (2010) Mechanical properties of flax fibers and of the derived unidirectional composites. *J Compos Mater* [Internet] 44(24): 2887–2896. Available from: <http://journals.sagepub.com/doi/10.1177/0021998310369579>
101. Sawpan MA, Pickering KL, Fernyhough A (2011) Effect of fibre treatments on interfacial shear strength of hemp fibre reinforced polylactide and unsaturated polyester composites. *Compos Part A Appl Sci Manuf* [Internet] 42(9):1189–1196. Available from: <https://linkinghub.elsevier.com/retrieve/pii/S1359835X11001382>
102. Rouison D, Sain M, Couturier M (2006) Resin transfer molding of hemp fiber composites: optimization of the process and mechanical properties of the materials. *Compos Sci Technol* [Internet] 66(7–8): 895–906. Available from: <https://linkinghub.elsevier.com/retrieve/pii/S026635805003234>
103. Sever K, Sarikanat M, Seki Y, Erkan G, Erdoğan ÜH, Erden S (2012) Surface treatments of jute fabric: The influence of surface characteristics on jute fabrics and mechanical properties of jute/polyester composites. *Ind Crops Prod* [Internet] 35(1): 22–30. Available from: <https://linkinghub.elsevier.com/retrieve/pii/S0926669011001877>
104. Akil HM, Cheng LW, Mohd Ishak ZA, Abu Bakar A, Abd Rahman MA (2009) Water absorption study on pultruded jute fibre reinforced unsaturated polyester composites. *Compos Sci Technol* [Internet] 69(11–12):1942–1948. Available from: <https://linkinghub.elsevier.com/retrieve/pii/S0266358090001638>
105. Devi LU, Bhagawan SS, Thomas S (2011) Dynamic mechanical properties of pineapple leaf fiber polyester composites. *Polym Compos* [Internet] 32(11):1741–1750. Available from: <http://doi.wiley.com/10.1002/pc.21197>
106. Dicuila M, Boudenne A, Umadevi L, Ibos L, Candau Y, Thomas S (2006) Thermophysical properties of natural fibre reinforced polyester composites. *Compos Sci Technol* [Internet] 66(15):2719–2725. Available from: <https://linkinghub.elsevier.com/retrieve/pii/S026635806001084>

107. Sreekumar PA, Saiah R, Saiter JM, Leblanc N, Joseph K, Unnikrishnan G et al (2009) Dynamic mechanical properties of sisal fiber reinforced polyester composites fabricated by resin transfer molding. *Polym Compos* [Internet] 30(6):768–775. Available from: <http://doi.wiley.com/10.1002/pc.20611>
108. Sreekumar PA, Thomas SP, Saiter J marc, Joseph K, Unnikrishnan G, Thomas S (2009) Effect of fiber surface modification on the mechanical and water absorption characteristics of sisal/polyester composites fabricated by resin transfer molding. *Compos Part A Appl Sci Manuf* [Internet] 40(11):1777–1784. Available from: <https://linkinghub.elsevier.com/retrieve/pii/S1359835X0900253X>
109. Merlini C, Soldi V, Barra GMO (2011) Influence of fiber surface treatment and length on physico-chemical properties of short random banana fiber-reinforced castor oil polyurethane composites. *Polym Test* [Internet] 30(8):833–840. Available from: <https://linkinghub.elsevier.com/retrieve/pii/S0142941811001401>
110. Mothé C, de Araújo C (2000) Properties of polyurethane elastomers and composites by thermal analysis. *Thermochim Acta* [Internet] 357–358:321–325. Available from: <https://linkinghub.elsevier.com/retrieve/pii/S0040603100004032>
111. Bakare IO, Okieimen FE, Pavithran C, Abdul Khalil HPS, Brahmakumar M (2010) Mechanical and thermal properties of sisal fiber-reinforced rubber seed oil-based polyurethane composites. *Mater Des* [Internet] 31(9):4274–4280. Available from: <https://linkinghub.elsevier.com/retrieve/pii/S0261306910002244>
112. Milanese AC, Cioffi MOH, Voorwald HJC (2011) Mechanical behavior of natural fiber composites. *Procedia Eng* [Internet] 10:2022–2027. Available from: <https://linkinghub.elsevier.com/retrieve/pii/S1877705811005236>
113. Mothé CG, de Araújo CR (2004) Caracterização térmica e mecânica de compósitos de poliuretano com fibras de Curauá. *Polímeros* [Internet] 14(4):274–278. Available from: http://www.scielo.br/scielo.php?script=sci_arttext&pid=S0104-14282004000400014&lng=pt&tlng=pt
114. Sapuan SM, Leenie A, Harimi M, Beng YK (2006) Mechanical properties of woven banana fibre reinforced epoxy composites. *Mater Des* [Internet] 27(8):689–693. Available from: <https://linkinghub.elsevier.com/retrieve/pii/S0261306905000257>
115. Irawan AP, Sukania IW (2015) Tensile strength of Banana fiber reinforced epoxy composites materials. *Appl Mech Mater* [Internet] 776: 260–263. Available from: <https://www.scientific.net/AMM.776.260>
116. Venkateshwaran N, ElayaPerumal A, Alavudeen A, Thiruchitrabalam M (2011) Mechanical and water absorption behaviour of banana/sisal reinforced hybrid composites. *Mater Des* [Internet] 32(7):4017–4021. Available from: <https://linkinghub.elsevier.com/retrieve/pii/S0261306911001579>
117. Biswas S, Kindo S, Patnaik A (2011) Effect of fiber length on mechanical behavior of coir fiber reinforced epoxy composites. *Fibers Polym* [Internet] 12(1):73–78. Available from: <http://link.springer.com/10.1007/s12221-011-0073-9>
118. Gohil PP, Shaikh AA (2011) Cotton-epoxy composites: development and mechanical characterization. *Key Eng Mater* [Internet] 471–472:291–296. Available from: <https://www.scientific.net/KEM.471-472.291>
119. Gning PB, Liang S, Guillaumat L, Pui WJ (2011) Influence of process and test parameters on the mechanical properties of flax/epoxy composites using response surface methodology. *J Mater Sci* [Internet] 46(21): 6801–6811. Available from: <http://link.springer.com/10.1007/s10853-011-5639-9>
120. Buksnowitz C, Adusumalli R, Pahler A, Sixta H, Gindl W (2010) Acoustical properties of Lyocell, hemp, and flax composites. *J Reinf Plast Compos* [Internet] 29(20): 3149–3154. Available from: <http://journals.sagepub.com/doi/10.1177/0731684410367533>
121. Karaduman Y, Onal L (2011) Water absorption behavior of carpet waste jute-reinforced polymer composites. *J Compos Mater* [Internet] 45(15):1559–71. Available from: <http://journals.sagepub.com/doi/10.1177/0021998310385021>
122. MIR A, Zitoune R, Collombet F, Bezzazi B (2010) Study of mechanical and thermomechanical properties of jute/epoxy composite laminate. *J Reinf Plast Compos* [Internet] 29(11):1669–1680. Available from: <http://journals.sagepub.com/doi/10.1177/0731684409341672>

123. Lopattananon N, Payae Y, Seadan M (2008) Influence of fiber modification on interfacial adhesion and mechanical properties of pineapple leaf fiber-epoxy composites. *J Appl Polym Sci* [Internet] 110(1):433–443. Available from: <http://doi.wiley.com/10.1002/app.28496>
124. Mohan TP, Kanny K (2011) Water barrier properties of nanoclay filled sisal fibre reinforced epoxy composites. *Compos Part A Appl Sci Manuf* [Internet] 42(4):385–393. Available from: <https://linkinghub.elsevier.com/retrieve/pii/S1359835X1000326X>
125. Abera Betelie A, Nicholas Sinclair A, Kortschot M, Li Y, Tilahun Redda D (2019) Mechanical properties of sisal-epoxy composites as functions of fiber-to-epoxy ratio. *AIMS Mater Sci* [Internet] 6(6):985–996. Available from: <http://www.aimspress.com/article/10.3934/mat ersci.2019.6.985>
126. Francklin HM, Motta LAC, Cunha J, Santos AC, Landim MV (2019) Study of epoxy composites and sisal fibers as reinforcement of reinforced concrete structure. *Rev IBRACON Estruturas e Mater* [Internet] 12(2): 255–287. Available from: http://www.scielo.br/scielo.php?script=sci_arttext&pid=S1983-41952019000200255&tlng=en
127. Di Landro L, Janszen G (2014) Composites with hemp reinforcement and bio-based epoxy matrix. *Compos Part B Eng* [Internet] 67:220–226. Available from: <https://linkinghub.elsevier.com/retrieve/pii/S1359836814003011>
128. Joseph S, Thomas S (2008) Electrical properties of banana fiber-reinforced phenol formaldehyde composites. *J Appl Polym Sci* [Internet] 109(1):256–263. Available from: <http://doi.wiley.com/10.1002/app.27452>
129. Joseph S, Sreekala MS, Thomas S (2008) Effect of chemical modifications on the thermal stability and degradation of banana fiber and banana fiber-reinforced phenol formaldehyde composites. *J Appl Polym Sci* [Internet] 110(4): 2305–2314. Available from: <http://doi.wiley.com/10.1002/app.27648>
130. de Medeiros ES, Agnelli JAM, Joseph K, de Carvalho LH, Mattoso LHC (2005) Mechanical properties of phenolic composites reinforced with jute/cotton hybrid fabrics. *Polym Compos* [Internet] 26(1):1–11. Available from: <http://doi.wiley.com/10.1002/pc.20063>
131. Kalia S, Kaith BS, Sharma S, Bhardwaj B (2008) Mechanical properties of flax-g-poly(methyl acrylate) reinforced phenolic composites. *Fibers Polym* [Internet] 9(4):416–422. Available from: <http://link.springer.com/10.1007/s12221-008-0067-4>
132. Peng X, Zhong L, Ren J, Sun R (2010) Laccase and alkali treatments of cellulose fibre: Surface lignin and its influences on fibre surface properties and interfacial behaviour of sisal fibre/phenolic resin composites. *Compos Part A Appl Sci Manuf* [Internet] 41(12):1848–1856. Available from: <https://linkinghub.elsevier.com/retrieve/pii/S1359835X10002526>
133. Bhandari NL, Dhungana BR, Lach R, Henning S, Adhikari R (2019) Synthesis and characterization of urea–formaldehyde eco-friendly composite based on natural fibers. *J Inst Sci Technol* [Internet] 24(1):19–25. Available from: <https://www.nepjol.info/index.php/JIST/article/view/24623>
134. Zhong JB, Lv J, Wei C (2007) Mechanical properties of sisal fibre reinforced urea-formaldehyde resin composites. *Express Polym Lett* [Internet] 1(10):681–687. Available from: <http://www.expresspolymlett.com/letolt.php?file=EPL-0000363&mi=c>
135. Milawarni, Yassir (2019) Properties of composite boards from coconut coir, plastic waste and urea formaldehyde adhesives. *IOP Conf Ser Mater Sci Eng* [Internet] 536:012110. Available from: <https://iopscience.iop.org/article/10.1088/1757-899X/536/1/012110>
136. Sun E, Liao G, Zhang Q, Qu P, Wu G, Xu Y et al (2018) Green preparation of straw fiber reinforced hydrolyzed soy protein isolate/urea/formaldehyde composites for biocomposite flower pots application. *Materials* (Basel) [Internet] 11(9):1695. Available from: <http://www.mdpi.com/1996-1944/11/9/1695>
137. Yang M, Wang F, Zhou S, Lu Z, Ran S, Li L et al (2019) Thermal and mechanical performance of unidirectional composites from bamboo fibers with varying volume fractions. *Polym Compos* [Internet] 40(10):3929–37. Available from: <https://onlinelibrary.wiley.com/doi/abs/10.1002/pc.25253>

138. Song Y, Gandhi U, Koziel A, Vallury S, Yang A (2018) Effect of the initial fiber alignment on the mechanical properties for GMT composite materials. *J Thermoplast Compos Mater* [Internet] 31(1): 91–109. Available from: <http://journals.sagepub.com/doi/10.1177/0892705716681400>
139. Ratna Prasad AV, Mohana Rao K (2011) Mechanical properties of natural fibre reinforced polyester composites: Jowar, sisal and bamboo. *Mater Des* [Internet] 32(8–9): 4658–4663. Available from: <https://linkinghub.elsevier.com/retrieve/pii/S0261306911001713>
140. Chaudhary V, Bajpai PK, Maheshwari S (2018) Studies on mechanical and morphological characterization of developed jute/hemp/flax reinforced hybrid composites for structural applications. *J Nat Fibers* [Internet] 15(1):80–97. Available from: <https://www.tandfonline.com/doi/full/10.1080/15440478.2017.1320260>
141. Shrivastava A (2018) Plastics processing. In: *Introduction to plastics engineering* [Internet]. Elsevier, pp 143–177. Available from: <https://linkinghub.elsevier.com/retrieve/pii/B978032395007000058>
142. Abdurrohman K, Satrio T, Muzayadah NL, Teten (2018) A comparison process between hand lay-up, vacuum infusion and vacuum bagging method toward e-glass EW 185/lycal composites. *J Phys Conf Ser* [Internet] 1130: 012018. Available from: <https://iopscience.iop.org/article/10.1088/1742-6596/1130/1/012018>
143. Swift KG, Booker JD (2013) Plastics and composites processing. In: *Manufacturing process selection handbook* [Internet]. Elsevier, pp 141–174. Available from: <https://linkinghub.elsevier.com/retrieve/pii/B9780080993607000057>
144. Misri S, Ishak MR, Sapuan SM, Leman Z (2015) Filament winding process for Kenaf fibre reinforced polymer composites. In: *Manufacturing of natural fibre reinforced polymer composites* [Internet]. Springer International Publishing, Cham, pp 369–383. Available from: http://link.springer.com/10.1007/978-3-319-07944-8_18
145. (2001) Filament Winding. In: *Composites* [Internet]. ASM International, pp 536–549. Available from: <https://dl.asminternational.org/books/book/60/chapter/704683/filament-winding>
146. Ansari SM, Ghazali CMR, Othman NS (2019) The effect of winding speed on the mechanical properties of Kenaf fiber reinforced geopolymer composites via filament winding technique
147. Jamaludin MIH, Jamian S, Awang MK, Kamarudin KA, Nor MKM, Ismail AE (2020) Characterization of continuous gradient functionally graded natural fiber reinforced polymer composites. *IOP Conf Ser Mater Sci Eng* [Internet] 824:012019. Available from: <https://iopscience.iop.org/article/10.1088/1757-899X/824/1/012019>
148. Fairuz AM, Sapuan SM, Zainudin ES, Jaafar CAN (2015) Pultrusion Process of Natural Fibre-Reinforced Polymer Composites. In: *Manufacturing of Natural Fibre Reinforced Polymer Composites* [Internet]. Springer International Publishing, Cham, pp 217–231. Available from: http://link.springer.com/10.1007/978-3-319-07944-8_11
149. Chang BP, Chan WH, Zamri MH, Md Akil H, Chuah HG (2019) Investigating the effects of operational factors on wear properties of heat-Treated Pultruded Kenaf fiber-reinforced polyester composites using Taguchi method. *J Nat Fibers* [Internet] 16(5):702–717. Available from: <https://www.tandfonline.com/doi/full/10.1080/15440478.2018.1432001>
150. Fairuz AM, Sapuan SM, Zainudin ES, Jaafar CAN (2016) Effect of filler loading on mechanical properties of pultruded kenaf fibre reinforced vinyl ester composites. *J Mech Eng Sci* [Internet] 10(1):1931–1942. Available from: http://jmes.ump.edu.my/images/VOLUME_10_Issue_1_June_2016/16_Fairuz_et_al.pdf
151. Fahad Halim AFM (2019) Fabrication of unidirectional coir fiber reinforced nonwoven melt-blown glass fabric composite by compression molding. *J Text Sci Fash Technol* [Internet] 4(2). Available from: <https://irispublishers.com/jtsft/fulltext/fabrication-of-unidirectional-coir-fiber-reinforced-nonwoven-melt-blown-glass-fabric-composite.ID.000582.php>
152. Khayal O (2019) Advancements in polymer composite structures
153. Krishnamurthy (2019) N2 KVM&. Studies on mechanical properties of hybrid composites using jute and e-glass by hand layup and vacuum bagging technique. *Glob J Eng Sci Res* 135–140

154. Fajrin J (2016) Mechanical properties of natural fiber composite made of Indonesian grown sisal. *Jurn[1] J Fajrin, Mech Prop Nat Fiber Compos Made Indones Grown Sisal, J Info Tek* 17 69–84. *al Info Tek*. 2016 Jun 1; 17: 69–84
155. Sanjay MR, Arpitha GR, Senthamaikannan P, Kathiresan M, Saibalaji MA, Yogesha B (2019) The hybrid effect of Jute/Kenaf/E-Glass woven fabric epoxy composites for medium load applications: impact, inter-laminar strength, and failure surface characterization. *J Nat Fibers* [Internet] 16(4):600–612. Available from: <https://www.tandfonline.com/doi/full/10.1080/15440478.2018.1431828>
156. Bosquetti M, da Silva AL, Azevedo EC, Berti LF (2019) Analysis of the mechanical strength of polymeric composites reinforced with sisal fibers. *J Nat Fibers* [Internet] 1–6. Available from: <https://www.tandfonline.com/doi/full/10.1080/15440478.2019.1612310>
157. Sarifuddin N, Ahmad Z, Yusuff MI (2019) Mechanical properties of woven carbon Fiber/Kenaf Fabric reinforced epoxy matrix hybrid composites. *Malaysian J Microsc* 2(15):10–16
158. Aisyah HA, Paridah MT, Sapuan SM, Khalina A, Berkalp OB, Lee SH et al (2019) Thermal properties of Woven Kenaf/Carbon fibre-reinforced epoxy hybrid composite panels. *Int J Polym Sci* [Internet] 2019:1–8. Available from: <https://www.hindawi.com/journals/ijps/2019/5258621/>
159. Mbakop RS, Lebrun G, Brouillette F (2019) Effect of compaction parameters on preform permeability and mechanical properties of unidirectional flax fiber composites. *Compos Part B Eng* [Internet] 176: 107083. Available from: <https://linkinghub.elsevier.com/retrieve/pii/S1359836818344445>
160. Gallos A, Paës G, Allais F, Beaugrand J (2017) Lignocellulosic fibers: a critical review of the extrusion process for enhancement of the properties of natural fiber composites. *RSC Adv* [Internet] 7(55):34638–34654. Available from: <http://xlink.rsc.org/?DOI=C7RA05240E>
161. Torres FG, Ochoa B, Machicao E (2003) Single screw extrusion of natural fibre reinforced thermoplastics (NFRT). *Int Polym Process* [Internet] 18(1):33–40. Available from: <http://www.hanser-elibrary.com/doi/abs/10.3139/217.1727>
162. Munde YS, Ingle RB, Siva I (2019) Effect of sisal fiber loading on mechanical, morphological and thermal properties of extruded polypropylene composites. *Mater Res Express* [Internet] 6(8):085307. Available from: <https://iopscience.iop.org/article/10.1088/2053-1591/ab1dd1>
163. Miyahara RY, Melquiades FL, Ligowski E, Santos A do, Fávoro SL, Antunes Junior O dos R (2018) Preparation and characterization of composites from plastic waste and sugar cane fiber. *Polímeros* [Internet] 28(2):147–154. Available from: http://www.scielo.br/scielo.php?script=sci_arttext&pid=S0104-14282018000200147&lng=en&tlng=en
164. Teixeira RS, Santos SF, Christoforo AL, Payá J, Savastano H, Lahr FAR (2019) Impact of content and length of curauá fibers on mechanical behavior of extruded cementitious composites: analysis of variance. *Cem Concr Compos* [Internet] 102: 134–144. Available from: <https://linkinghub.elsevier.com/retrieve/pii/S0958946518308308>
165. Wang X (2013) Overview on biocompatibilities of implantable biomaterials. In: *Advances in biomaterials science and biomedical applications* [Internet]. InTech. Available from: <http://www.intechopen.com/books/advances-in-biomaterials-science-and-biomedical-applications/overview-on-biocompatibilities-of-implantable-biomaterials>
166. Love B (2017) Polymeric biomaterials. In: *Biomaterials* [Internet]. Elsevier, pp 205–238. Available from: <https://linkinghub.elsevier.com/retrieve/pii/B9780128094785000092>
167. Jiao M, Zhang P, Meng J, Li Y, Liu C, Luo X et al (2018) Recent advancements in biocompatible inorganic nanoparticles towards biomedical applications. *Biomater Sci* [Internet] 6(4):726–45. Available from: <http://xlink.rsc.org/?DOI=C7BM01020F>
168. Dahman Y (2019) *Biomaterials science and technology* [Internet]. Taylor & Francis, Boca Raton, CRC Press. Available from: <https://www.taylorfrancis.com/books/9780429878350>
169. Ramakrishna S, Mayer J, Wintermantel E, Leong KW (2001) *Biomedical applications of polymer-composite materials: a review*. *Compos Sci Technol* [Internet] 61(9):1189–1224. Available from: <https://linkinghub.elsevier.com/retrieve/pii/S0266353800002414>

170. Kuhn LT (2012) Biomaterials. In: Introduction to biomedical engineering [Internet]. Elsevier, pp 219–271. Available from: <https://linkinghub.elsevier.com/retrieve/pii/B9780123749796000058>
171. Loureiro dos Santos LA (2017) Natural polymeric biomaterials: processing and properties ☆. In: Reference module in materials science and materials engineering [Internet], Elsevier. Available from: <https://linkinghub.elsevier.com/retrieve/pii/B9780128035818022530>
172. Tang X, Thankappan SK, Lee P, Fard SE, Harmon MD, Tran K et al (2014) Polymeric biomaterials in tissue engineering and regenerative medicine. In: Natural and synthetic biomedical polymers [Internet]. Elsevier, pp 351–371. Available from: <https://linkinghub.elsevier.com/retrieve/pii/B9780123969835000223>
173. Rodrigues LC, Silva SS, Reis RL (2019) Acemannan-based films: an improved approach envisioning biomedical applications. Mater Res Express [Internet] 6(9):095406. Available from: <https://iopscience.iop.org/article/10.1088/2053-1591/ab2f66>
174. Atmakuri A, Palevicius A, Griskevicius P, Janusas G (2019) Investigation of mechanical properties of hemp and flax fibers hybrid composites for biomedical applications. Mechanics [Internet] 25(2). Available from: <http://mechanika.ktu.lt/index.php/Mech/article/view/22712>
175. Furlan DM, Morgado DL, Oliveira AJA de, Faceto ÂD, Moraes DA de, Varanda LC et al (2019) Sisal cellulose and magnetite nanoparticles: formation and properties of magnetic hybrid films. J Mater Res Technol [Internet] 8(2):2170–2179. Available from: <https://linkinghub.elsevier.com/retrieve/pii/S2238785418308998>
176. García-Tejero IF, Durán Zuazo VH, Sánchez-Carnenero C, Hernández A, Ferreiro-Vera C, Casano S (2019) Seeking suitable agronomical practices for industrial hemp (*Cannabis sativa* L.) cultivation for biomedical applications. Ind Crops Prod [Internet] 139:111524. Available from: <https://linkinghub.elsevier.com/retrieve/pii/S0926669019305369>

Polymeric Biocomposites from Renewable and Sustainable Natural Resources



Daniela M. Fidalgo, Mario D. Contin, Adriana A. Kolender,
and Norma D'Accorso

Abstract The use of polymeric composite materials from renewable biomass has acquired great importance in different and varied fields. Moreover, its application in the biomedical applications has found a fast development in recent years. In this context, this chapter is focused on the use of biocomposites in tissue engineering and analytical applications. The studied materials include polysaccharides such as chitosan, cellulose, and alginate, as well as polyhydroxyalcanoates as matrixes, and fillers like nanoparticles, carbon nanotubes or polymers, among other combinations.

Keywords Chitosan · Nanocellulose · Gelatin · Polyhydroxyalcanoates · Analytical applications · Tissue engineering

D. M. Fidalgo · A. A. Kolender (✉) · N. D'Accorso (✉)
Facultad de Ciencias Exactas y Naturales, Departamento de Química Orgánica, Universidad de Buenos Aires, Buenos Aires, Argentina
e-mail: adrianak@qo.fcen.uba.ar

N. D'Accorso
e-mail: norma@qo.fcen.uba.ar

D. M. Fidalgo
CONICET- Centro de Investigaciones en Bionanociencias (CIBION), Buenos Aires, Argentina

M. D. Contin
Facultad de Farmacia y Bioquímica, Departamento de Química Analítica, Universidad de Buenos Aires, Buenos Aires, Argentina

Consejo Nacional de Investigaciones Científicas y Tecnológicas, CONICET, Buenos Aires, Argentina

A. A. Kolender · N. D'Accorso
CONICET- Universidad de Buenos Aires. Centro de Investigaciones en Hidratos de Carbono (CIHIDECAR), Buenos Aires, Argentina

Abbreviations and Acronyms

ALP	Alkaline phosphatase
BTE	Bone tissue engineering
CCNWs	Carboxymethylcellulose nanowhiskers
CPAs	Chlorophenoxy acids
CNCs	Cellulose nanocrystals
CQ	<i>Cissus quadrangularis</i>
CS	Chitosan
DSPE	Dispersive solid phase extraction
EDS	Energy –dispersive X-ray spectroscopy
ECHNN	Electrospun cellulose/nano-HA nanocomposite nanofibers
GC-MS	Gas chromatography–mass spectrometry
Gel	Gelatin
GO	Grapheme oxide
HAp	Hydroxyapatite
hASCs	Human adipose derived stem cells
HECA	Hydroxyethyl cellulose acetate
IgG	Immunoglobulin
MCNPs	Magnetic cellulose nanoparticles
MNPs	Magnetic nanoparticles
MOFs	Magnetic organic frameworks
mcl-PHAs	Medium chain length PHAs
MNPs@X	Modified magnetic nanoparticles
MSPE	Magnetic solid phase extraction
MWCNTs	Multi-walled carbon nanotubes
NBGC	Bioactive glass ceramic nanoparticles
NC	Nanocellulose
NHAp	Nanohydroxyapatite
PAHs	Polycyclic aromatic hydrocarbons
PAEs	Phthalate esters
PCBs	Polychlorinated biphenyls
PCL	Poly(ϵ -caprolactone)
PDA	Polydopamine
PEG	Poly(ethylene glycol)
PHAs	Polyhydroxyalkanoates
P3HB	Poly(3-hydroxybutyrate)
P4HO	Poly(4-hydroxyoctanoate)
P3HHx	Poly(3-hydroxyhexanoate)
P(LcG)	Poly(lactic- <i>co</i> -glycolic acid)
PPD	poly(<i>m</i> -phenylenediamine)
PP	Polypropylene
PVA	Poly(vinyl alcohol)
SBF	Simulated body fluid

SWCNT	Single-walled carbon nanotubes
SBSDME	Stir bar-sorptive dispersive microextraction
SPE	Solid phase extraction
TE	Tissue engineering
XRD	X-ray diffraction

1 Introduction

A composite can be defined as the arrangement of two or more different compounds, one of them plays the role of filler and the other one is the matrix in which the filler is dispersed. This combination leads to a new material with improved performance over the individual constituent materials [1]. The nature of both components may differ depending on the proposed application, thus composites can be classified into different categories.

In the last years, it was observed a renaissance of renewable polymers and development of bio-based macromolecular materials. There are several reasons that promote a gradual shift from oil-based materials to bio-based materials, from economical to environmental awareness. The last one is due to global demand for sustainable and “green” products, as well as new environmental legislation and regulations that encourage the development of environmentally friendly products with low carbon footprint [2].

In the case of biocomposites, the matrix is a polymer where the monomers are entirely or partially derived from biomass, and thus, the matrix can be classified as natural polymers or biopolymers. Natural polymers include only materials synthesized as such in nature like cellulose or starch, in opposition to biopolymers. Thus, all natural polymers can be considered as biopolymers, but not all biopolymers are natural polymers [3]. It is worth mentioning, the term “biodegradable biocomposites” where the matrix can be obtained either from biomass or petroleum-based, but it is degraded by anaerobic or aerobic biological processes, leading to the formation of carbon dioxide, water, methane, biomass, and mineral salts.

The other component of a composite is the filler, which is added to a polymeric matrix in order to reduce cost, improve processing, or modify some property. In the case of biocomposites, the nature of the fillers may differ from silicates, carbonates, magnetite, active pharmaceutical compounds, or other polymers [4].

Regarding the “green” nature of biocomposites, it may be expected that some of them would be biocompatible and useful for biomedical proposes. For example, several commercially natural polymer-ceramic composites are currently available for bone reconstruction [5]. However, there are many other fields where biocomposites can be useful as it is further described in this chapter.

The aim of this chapter is to summarize the usefulness of biocomposites in two well-established fields like tissue engineering and stationary phases for analytical applications, as well as other miscellaneous and not widely used applications.

2 Application of Polymeric Biocomposites in Analytical Chemistry

Polymeric biocomposites have been extensively used as sorbent for contaminant removal in waste eluents or in downstream procedures to recover valuable products [6]. However, only recently sorbents based on polymeric biocomposites have been used for analytical purposes.

A classical analytical procedure can be divided into three mayor steps: sample preparation, measurement, and data analysis. Despite there is not always a clear limit, sample preparation concerns the procedures that take place after sampling and before the introduction in the measurement system. The aim of sample preparation may differ depending on the type of compounds to be analyzed, the nature of the sample, and the purpose of the analysis. However, usual goals of sample preparation are to isolate the analytes from a complex matrix, to remove interferences from the sample and to concentrate the analytes in order to reach proper limits for detection [7, 8].

In the wide field of sample preparation, polymeric biocomposites have been used as sorbents in solid phase extraction (SPE). In traditional and miniaturized SPE devices, the solid phase (sorbent) is held on different supports which lead to different types of SPE techniques. Abundant examples and description of SPE techniques can be found in more specific literature [7]. However, a brief summary of the most relevant SPE techniques is given herein.

Conventional solid phase extraction is largely known as SPE, where basically a sample solution is forced to pass through a column filled with a sorbent. Then, the retained analytes are subsequently eluted with a proper solvent. In order to overcome some disadvantages of conventional SPE, different miniaturized solid phase extraction techniques were developed. The starting point was the development of solid phase microextraction (SPME) in 1990, by using a solid inert fiber covered with an active phase layer where actual extraction takes place. On the other hand in dispersive solid phase extraction (DSPE), the sorbent is dispersed through a sample solution and recovered by centrifugation together with the adsorbed analytes. Similarly, dispersive micro-solid phase extraction (DMSPE) takes advantage of nanomaterials as sorbent material. Magnetic solid phase extraction (MSPE) is a variation of DSPE; but in this case, an external magnetic field is used to recover the sorbent with magnetic properties. In stir bar-sorptive extraction (SBSE), the sorbent covers a magnetic stirrer. While stirring, the bar adsorbs the analytes to be extracted. Stir bar-sorptive dispersive microextraction (SBSDME) combine SBSE and DSPE by using a magnetic stir bar without any sorption property and magnetic nanoparticles (MNPs) that act as sorbent; while the stir bar is moving, the MNPs are dispersed but when it stops the MNPs and the adsorbed analytes come back to the stir bar surface.

In general, biocomposites meant to serve as solid phases are designed with a native or grafted natural polymer and a filler. The main natural polymers in this field are alginate, chitosan, and cellulose, among others. Fillers may be metal organic

frameworks (MOFs) [9], graphene oxide (GO) [10], MNPs, or modified magnetic nanoparticles (MNPs@X) [11].

Barium alginate was employed by Zhang et al. to overcome the low dispersion capacity of hydrophobic octadecyl (C-18) functionalized MNPs in aqueous solution. Basically, Fe_3O_4 @C-18 was dispersed in a sodium alginate solution under sonication and vigorous stirring, while a barium chloride solution was dropped. The morphological analysis revealed a core shell structure based on Ba^{2+} -alginate vesicles as a light area surrounding a dark core of Fe_3O_4 @C-18. Normally, that kind of hydrogel displays porous surfaces, and the swelling properties allow the free movement of water and solutes through the inner cavities [11]. The developed MSPE was successfully employed for the preconcentration of polycyclic aromatic hydrocarbons (PAHs) and phthalate esters (PAEs) from environmental water samples.

Usually MNPs, especially Fe_3O_4 , are added to natural polymers. In some cases, MNPs do not play a primordial role as sorptive material but allow a simple material removal procedure by using an external magnetic field due to its magnetism.

Bunkoed et al. incorporated MNPs (Fe_3O_4) into alginate beads which were subsequently decorated with a layer of polypyrrole as sorbent material (Fig. 1) The authors evaluated the extraction efficiency of estriol, bisphenol A, β -estradiol employing alginate, alginate/ Fe_3O_4 , and alginate/ Fe_3O_4 /polypyrrole as sorbent materials. Alginate/ Fe_3O_4 /polypyrrole was the optimal sorbent due to the hydrophobic and π - π interaction established between the analytes and polypyrrole [12].

Graphene oxide (GO) is another interesting sorbent material due to its large surface area and functional groups. It is composed of carbon atoms in a sp^2 single-atom layer of a hybrid connection [13]. The presence of functional groups such as epoxy, hydroxyl, and carboxyl groups in GO promotes its dispersion in water, although that could obstruct its separation from aqueous media. Thus, the incorporation of MNPs onto the GO sheets makes the separation easier with an external magnet. Tasmia et al. took advantage of magnetic graphene oxide and included it into an alginate-Fe matrix to extract endocrine disrupting compounds from water compounds [10]. In

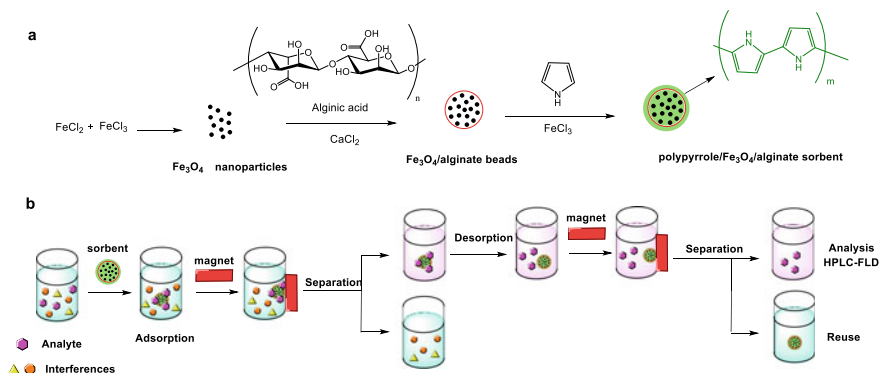


Fig. 1 a Synthesis of polypyrrole/ Fe_3O_4 /alginate sorbent. b Schematic illustration of SPE magnetic procedure. Adapted from Bunkoed et al. [12]

this case, the addition of alginate in the system reduced the magnetic-GO toxicity and enhanced the material biocompatibility.

Beyond magnetic materials, many other materials have been incorporated in natural polymers composites. Zirconia nanoparticles have been used as stationary phases due to its behavior as Lewis acid that can interact with Lewis-based functional groups, like $R-PO_3^-$, present in organophosphorus pesticides (OPPs). Zirconia nanoparticle/calcium alginate hydrogel fiber was employed by Zare et al. [14] for OPPs extraction from water and juice samples. An interesting point of this development was to perform the extraction without the need of centrifugation, filtration, or employing an external magnetic field as with usual magnetic adsorbents, because the obtained composite was a floating, fibrous solid phase that can be removed from the solution using forceps.

Metal organic frameworks (MOFs) also filled alginate hydrogels mutually benefiting for solid phase extraction. MOFs were found to be exceptionally stable and highly porous frameworks, first reported in 1999 [15], constructed from inorganic metal ions (node) and organic linkers. MOFs are characterized by a high porosity, crystallinity, large internal surface area, thermal stability, discrete order, and low density that render them interesting for sorptive material [16]. Tan et al. combined a hydrophobic MOF like MIL-101(Cr)- NH_2 , (a supertetrahedral building unit constructed with terephthalate ligands and trimeric chromium octahedral clusters) with magnetite nanoparticles and alginate to yield an effective material for chlorophenoxy acids (CPAs) extraction from aqueous media [9]. The interaction experiment revealed that alginate polymer provided a polar hydrophilic surface that helped to draw the analytes closer toward MIL-101(Cr)- NH_2 . On the other hand, magnetite provided magnetism for an easy separation. According to the performed extraction assays, neither magnetite nor alginate had a major impact over direct CPAs interaction, remarking the importance of MIL-101(Cr)- NH_2 as sorptive material.

It is worth to mention that alginates can directly interact with different analytes and work directly as a sorbent material. A novel alginate/zein hydrogel supported in a polypropylene (PP) fiber was developed by Castilhos et al. (Fig. 2) [17] to be used in a SPME procedure for hormones, pharmaceuticals, and detergents of different polarities. Zein is a four fraction protein (α , β , γ , and δ) obtained from maize, with a particularly important fraction α due to its hydrophobic characteristic. The authors studied the effect of the zein addition over the hydrogel structure by performing loss of water, swelling, and methylene blue migration assays as well as the extraction performance. The results indicated that a more compact network with smaller pores and more plastic character is obtained when zein is incorporated to the alginate hydrogel, possibly due to the effect of the zein as an additional cross-linking agent, beside Ca^{2+} ions. In terms of analyte extraction, less polar analytes were more efficiently extracted when alginate/zein was employed compared to simple alginate hydrogel as sorption material. Conversely, more polar analytes were preferably extracted with alginate hydrogels. Zein modification produced a hydrophobic character in the sorption phase, decreasing the initial hydrogel water uptake and allowing for a better interaction between the analytes and the sorption phase through the functional groups of the alginate and zein. In conclusion, the solid phase based on alginate and zein was able

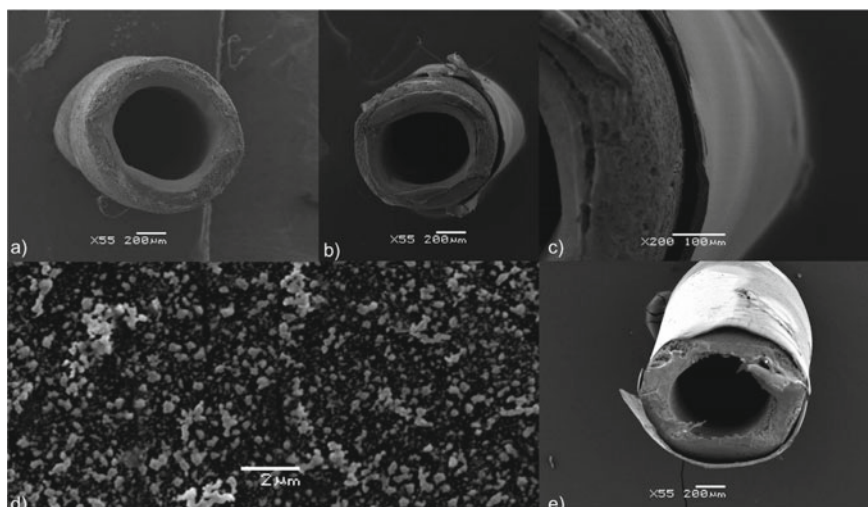


Fig. 2 Scanning electron microscopy of: **a** bare PP fiber, **b** PP fiber with alginate/zein hydrogel, **c** higher magnification of **b**, **d** alginate/zein film, and **e** PP fiber with alginate/zein hydrogel after extraction procedure. Reprinted from Castilhos et al. [17] Copyright 2017, with permission of Elsevier

to extract both polar and nonpolar compounds in water samples, due to its amphiphilic sorption behavior.

Nanocellulose (NC) is another biopolymer that has been studied as a sorbent material for analytical purposes. An excellent review from Ruiz-Palomero regarding NC as an analyte and analytical tool is highly recommended [18]. NC is characterized for a large superficial area, chemical reactivity, stiffness, and lightness that have been exploited for analytical goals.

A wide number of analytical applications is described in literature, but only cellulose in composites will be considered in this chapter.

Chemical modification of cellulose by oxolane, sulfonate, and amine groups allows the solid phase extraction of different metal ions, dyes, and silver nanoparticles [18]. β -Cyclodextrin moieties have also been incorporated into NC surface promoting the complexation with danofloxacin [19] with high recoveries.

Anirudhan et al. [20] developed a poly(methacrylic acid-co-vinyl sulfonic acid)-grafted-magnetite/nanocellulose composite for extraction of immunoglobulin (IgG). The authors extracted NC from saw dust and mixed it with iron salts producing magnetite nanoparticles in situ by co-precipitation. Finally, vinyl monomers methacrylic acid and vinyl sulfonic acid and ethyleneglycoldimethacrylate as cross-linker were added with the radical initiator ammonium peroxodisulfate to induce polymerization over the magnetic NC (Fig. 3). The composite material was physically characterized with special attention on swelling properties and pH dependence. The swelling percentage was higher than 450%. The material was applied to fully recover IgG from a protein mixture through five adsorption–desorption cycles.

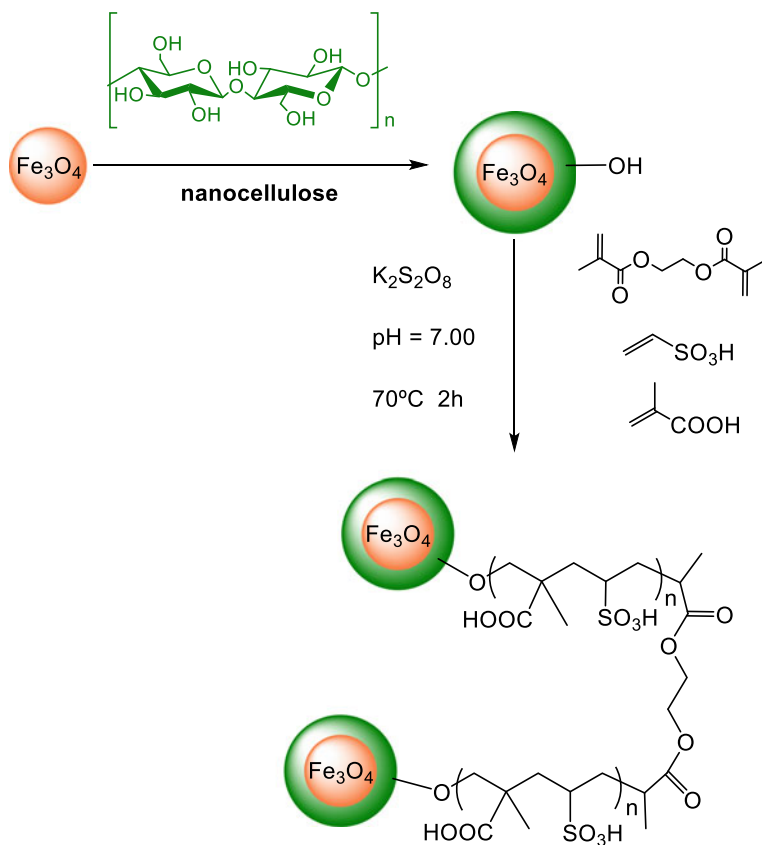


Fig. 3 Synthesis of poly(methacrylic acid-co-vinyl sulfonic acid)-grafted-magnetite/nanocellulose. Adapted from Anirudhan et al. [20]

Magnetic cellulose nanoparticles (MCNPs), without any further modification, were also employed as sorbent, although this is a vacant area. Abujaber et al., proposed a novel approach for MCNPs solid phase extraction based on SBS DME [21]. The methodology was employed for the determination of nine polychlorinated biphenyls (PCBs) in fruit juice samples by gas chromatography–mass spectrometry (GC–MS). MCNPs were able to be reused at least five times without significant loss in recovery.

Nurek et al. employed cellulose acetate as scaffold due to its porosity and high surface area, and coated cellulose acetate fibers (CFs) with calixarene-functionalized GO and polydopamine (PDA) [22]. Polydopamine had multifunctional groups, and GO was satisfactory proven as sorbent material, meanwhile calixarene provided π - π interactions due to the phenol units linked via methylene bridges. Polydopamine was prepared by auto-polymerization adding cellulose acetate fibers to a dopamine solution at pH 8.00. On the other hand, GO and 4-*t*-butylcalixarene were treated

with hydrazine and ammonia solution, and the combined material was physically adsorbed and entrapped in the as-prepared porous PDA-CFs adsorbent. The final material was placed into a SPE polypropylene tube to yield a SPE device for the extraction of aflatoxins from corn samples.

Chitosan (CS) due to its biocompatibility, no toxicity, biodegradability, easy modification, and free amino groups is another biopolymer that has been widely studied as sorbent material. Chitosan as a sorbent material for analytical proposes has promising prospects as showed by Xu et al. [23] by developing a DMSPE for flavonol extraction using ultramicro chitosan. Definitely, composites based on CS can enhance or modify its own properties.

Guo et al. trapped MNPs into a chitosan matrix and modified its amino surface groups with rhein acid ($\text{Fe}_3\text{O}_4@CS$ -rhenic acid), a dihydroxyanthraquinone with polar functional groups such as hydroxyl and carboxyl groups and a plane structure with a great conjugated system (Fig. 4) [24]. Thus, rhenic acid can form hydrogen bonds and $\pi-\pi$ or $n-\pi$ transfer interaction with aromatic polar compounds like isoflavones. The authors also developed magnetite NPs with surface amine groups ($\text{Fe}_3\text{O}_4@APTES$) later modified with rhenic acid following the same procedure to yield $\text{Fe}_3\text{O}_4@APTES$ -rhenic acid. Both materials were evaluated in the MSPE of isoflavones on soymilk. It is interesting to point out that the adsorption of polymeric microparticles coated by chitosan was higher than those ones prepared by APTES, because the surface of chitosan contains a large number of amino groups, so more

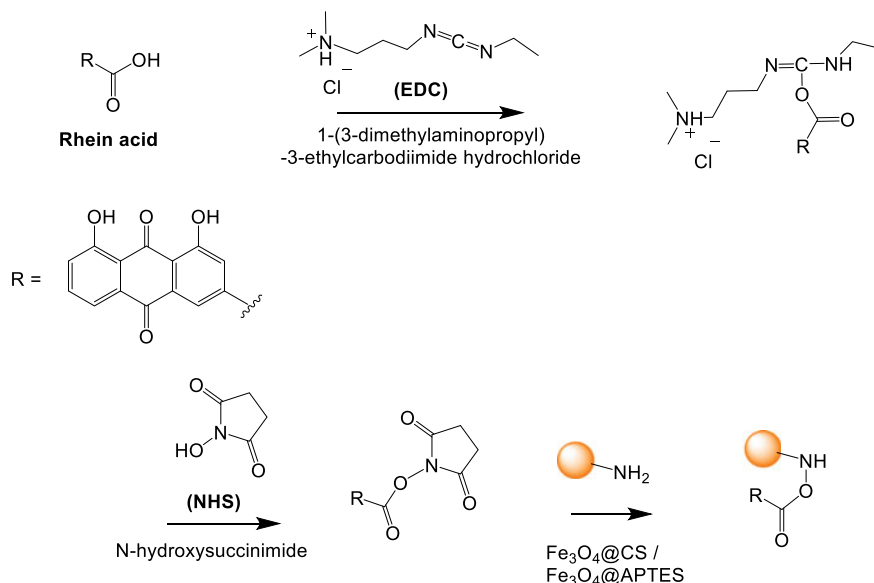


Fig. 4 Synthetic route of $\text{Fe}_3\text{O}_4@CS$ -rhenic acid or $\text{Fe}_3\text{O}_4@APTES$ -rhenic acid. Adapted from Guo et al. [24]

rhein acid can be connected via the amide formation to the magnetic particle. Thus, the importance of chitosan for this material was demonstrated.

Following a standard procedure to yield $\text{Fe}_3\text{O}_4@\text{CTS}$, Liao et al. covered this magnetic material with poly (*m*-phenylenediamine) (PPD) following a self-assembly approach. According to the authors, $\text{Fe}_3\text{O}_4@\text{CTS}$ has hydrophobic and hydrophilic moieties that could facilitate the dissolution of *m*-phenylenediamine monomers before its polymerization by adding ammonium peroxydisulfate as initiator. The final material, $\text{Fe}_3\text{O}_4@\text{CTS}$ -PPD, was employed for MSPE of polychlorinated biphenyls from water samples [25].

Chitosan-grafted polyaniline as sorbent material was developed in order to improve chitosan sorption properties. Razavi et al. applied a chitosan-grafted polyaniline for the preconcentration of phthalate esters in DSPE coupled to HPLC–UV detection. Basically, chitosan was dissolved in aqueous acetic acid with aniline as monomer and ammonium persulfate as initiator to yield the final composite after aniline polymerization [26].

3 Application of Polymeric Biocomposites in Tissue Engineering

It is important to remark the role of carbohydrates in many different and relevant applications. They are products obtained from renewable biomass have high functionality, low cost, and offer interesting chemical possibilities of functionalization. For example, cotton fibers modified with citric acid, sodium lignin sulfonate, and boric acid gave fabrics with flame retardancy, antioxidant activity, antibacterial activity, and UV protection properties [27]. Marine carbohydrates had found applications in pharmaceutical and cosmetic [28]; however, more recently, they have been used in the biomedical field.

On the other hand, Aparecida de Oliveira et al. [29] discussed the environmental impact derived from the exclusive use of thermoplastics, such as polylactic acid and their composites, in comparison with the use of products obtained from cotton fibers. The authors concluded that the products derived from natural polymers have less impact on the environment, despite its lower efficiency related to their mechanical properties. Therefore, it is important to emphasize the importance of the design of new materials that provide solutions and respect the environment simultaneously.

A scaffold for tissue engineering should fulfill some requirements including biocompatibility, biodegradability, mechanical durability, and porosity [30]. It is often necessary to make a combination of suitable biomaterials to achieve the necessary properties [31]. A 3D matrix-based scaffold system able to simulate the structure and function of a proposed tissue has become a main goal of biomaterials research [32].

4 Chitosan

Tissue engineering (TE) is an interdisciplinary field that aims to improve or replace biological tissues and involves the architecture of artificial cellular scaffolds which mimic extracellular matrix. Chitosan (CS) has been extensively used in the design of a variety of 3D scaffolds for its application in TE. Its physicochemical and biological properties make it an interesting material to apply as a base in the fabrication of scaffolds. CS is biocompatible, biodegradable, bioactive, and antibacterial; it is also endowed with a hydrophilic surface useful for wound healing properties. Besides, it has been reported that CS has an important role in enhanced cell adhesion and proliferation [25, 33–38]. However, CS scaffolds present low mechanical properties and fast degradation, undesired properties for materials meant to be applied in TE. Looking forward to achieving an optimal material for a specific TE application, the properties of CS scaffolds can be tuned by the development of CS-based biocomposite by addition of other polymers, ceramics, and/or nanoparticles [31, 39–41].

In bone tissue engineering (BTE), the scaffolds should satisfy various properties such as adequate porosity, biocompatibility, water retention, protein adsorption, biomineralization, biodegradability, and mechanical properties [42]. Additionally, scaffolds must possess important properties like osteointegration and osteoconduction [43]. Several scaffolds have been developed for bone tissue engineering with compositions that mimic the extracellular matrix of native bone. Human bone composition includes 30% organic matter, mainly type I collagen (Col)1 and 70% of hydroxyapatite (HAp, $\text{Ca}_{10}(\text{PO}_4)_6(\text{OH})_2$) depositing on the extracellular protein matrix. Collagen, a natural component of extracellular matrix protein, has been used as in scaffolds for a variety of tissues, including bone [44], skin [45], and cornea [46]. It has excellent biocompatibility, cell adhesion, and consequently enhanced tissue regeneration [47]. In addition, HAp has been applied as a reinforcement for scaffolds in bone tissue engineering, due to inherent biocompatibility and osteoconductivity properties combined with mechanical properties [48, 49].

The development of composites by combination of natural polymers with ceramics is one of the most used strategies to mimic the chemical composition of the tissue. Recently, a variety of CS/nanoceramic composite scaffolds were designed to obtain materials with enhanced biocompatibility, biodegradability, mechanical properties, and biological activity as a result of the combination of the individual advantages of each component [31]. The use of nanoceramics allows taking advantage of their known benefits compared to the bulk material. Moreover, they are structurally very similar to the inorganic component of the bone.

Nanoceramics could be incorporated into CS scaffolds by various methods. Depending on which one is used, different interactions will be observed between the polymer matrix and the ceramics. Considering what properties are sought for the material, the type and conditions of the method can be chosen. CS has been combined with nanohydroxyapatite (NHAp), bioactive glass ceramic nanoparticles (NBGC), nSiO_2 , nTiO_2 , and nZrO_2 bioceramics to obtain a variety of nanocomposites with potential application in the TE field [31]. Among them, NHAp is one of the

most utilized biomaterials, especially in BTE. In addition to its relationship with the natural bond composition, NHAp is biocompatible and stimulates osteoconduction. Nevertheless, its crystalline nature confers poor mechanical properties, so it needs to be combined with polymers to be applied in TE. The structural characteristics of CS have been exploited in a variety of CS-NHAp or CS-HAp composites that were produced by different methods [50].

Yamaguchi et al. [51] prepared a CS/HAp composites by one of the most used methods, the co-precipitation. A CS/ H_3PO_4 solution was gradually dropped into a $Ca(OH)_2$ suspension. Then, the pH was slowly changed up to 9 until CS became insoluble and precipitated with small HAp crystals. The ratio of CS/ H_3PO_4 was adjusted to obtain composites with different weight ratio content of CS/HAp. The formation of the nanocomposites was a result of the interaction between the amino groups in CS and the Ca^{2+} ions of the HAp. It was observed that the CS content affected the ζ -potential of the solutions, and it had a consequence in the size of the formed particles. The maximum size observed by TEM (17 μm) was using a CS content of 25 wt.%, where the ζ -potential was closed to zero. All these results suggested that the size of the precipitate was affected by the surface charge, with an electrostatic repulsive force being minimal around the isoelectric point. Furthermore, a small amount of citric acid was added to a CS/HAp suspension after the formation of the composite. Citric acid is a multivalent negative ion that can participate in ionic interactions with positively charged ions and eliminate surface hydration water of particles. This could allow the formation of lower surface charged layers or shorter distances between charged particles. As it was expected, the addition of citric acid enlarged the precipitate size of the nanocomposites, probably due the formation of an ionic complex between the carboxyl groups of the acid and the NH_3^+ of the CS. Additionally, the incorporation of citric acid influenced the mechanical properties, since the compressive strength and Young's modulus were increased. This suggested that the bonding strength between particles was enhanced by the citric acid.

CS/HAp composites can also be obtained by the mineralization biomimetic method. When CS comes into contact with a simulated body fluid (SBF) solution, formation and precipitation of HAp occurs slowly. This process can occur directly on the CS surface or the surface can be modified somehow. Fraga et al. [52] synthesized CS/HAp composites by mineralization of HAp over CS membranes with and without previous treatment with a sodium silicate (SS) solution, where SS acted as a nucleation agent. The free primary hydroxyl group of C-6 in CS can interact with silanol groups of the SS solution promoting the activation of the membrane surface. This way, the silicate ions were observed on the CS membrane until the nucleation of HAp began over the silicate ions. Finally, the HA crystals grow because of the saturated SBF solution to develop a HAp layer over the CS surface (Fig. 5). The characterization of the coated membranes by SEM, XRD, and FTIR demonstrated that the use of SS in the mineralization method and the exposure time to SBF affected the phase formation of HAp. The HAp layer homogeneously covered the entire surface of CS, and it had a semi-crystalline structure similar to the mineral phase of human bone.

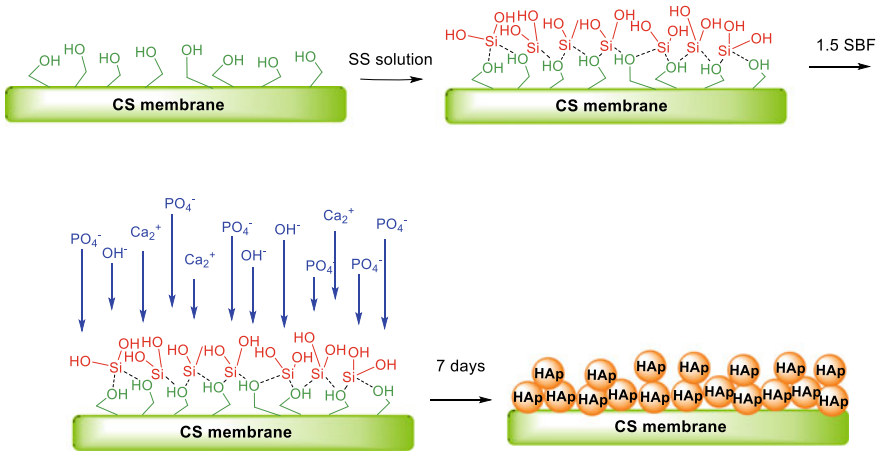


Fig. 5 Schematic illustration of the proposed coating mechanisms of CS membranes with HAP using the mineralization biomimetic method. Adapted from Fraga et al. [52]

CS can be chemically modified to enhance its physicochemical properties and cellular response. D. Depan et al. [53] created an organic/inorganic hybrid network structure nanocomposite based on grafted CS. First, CS was modified by reaction of the amino groups with propylene oxide to obtain hydroxypropylated CS which was subsequently linked with ethylene glycol functionalized NHAp (Fig. 6). Finally, the 3D-network of the nanocomposite (CS-g-NHAp) was prepared by lyophilization. Thus, NHAp was included as part of the network instead of being a filler. The SEM

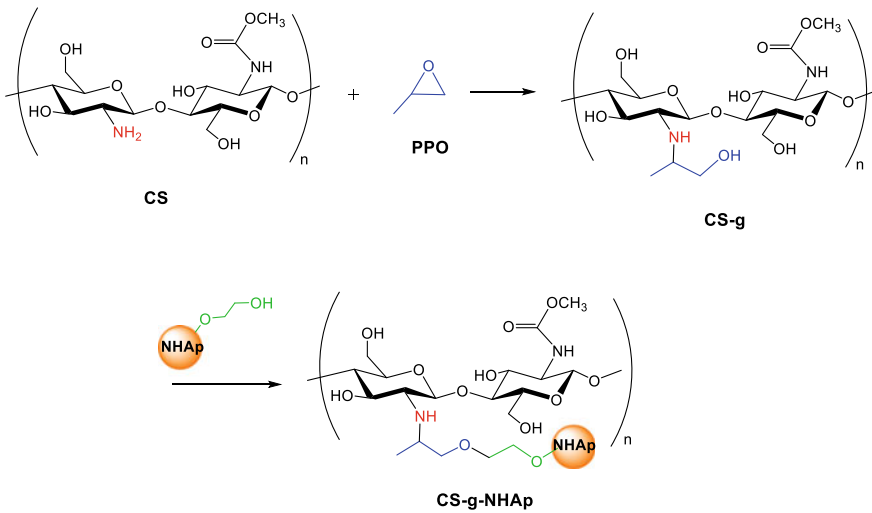


Fig. 6 Synthesis of CS-g-NHAp. Adapted from Depan et al. [53]

micrographs analysis showed that CS-g-NHAp was highly porous. The pore size was slightly larger than that of the unmodified CS scaffold (CS-NHAp), probably due to the grafting of propylene oxide onto CS. The modification of CS led to a more cross-linked matrix with more homogeneously distributed and interconnected pores than the pure CS. Consequently, CS-g-NHAp exhibited greater Young's modulus, controlled degradation rate, and higher affinity toward pre-osteoblast compared to CS-NHAp.

Another strategy to improve the properties of CS scaffolds was the use of cross-linking reagents. Aiming to modulate the hydrophobic/hydrophilic balance and mechanical properties of CS films, Li et al. [54] used genipin as a water-soluble bifunctional cross-linking reagent to develop a NHAp/chitosan cross-linking composite film (Fig. 7a). The NHAp was dispersed into a CS–genipin solution by ultrasound, and then, the suspension was dried at 37 °C for 2 days. The formation of a cross-linked matrix made the entrapment of NHAp more efficient. FTIR and TGA analysis demonstrated that part of the amino groups in CS had reacted with genipin and evidenced a hydrogen bond and electronic interaction between the positively charged amino groups of CS and PO_4^{3-} . The cross-linked composite films showed well cytocompatibility, water adsorption, and appropriate tensile strength.

In order to increase the cell attachment onto a scaffold, Atack et al. [55] used glutaraldehyde as a cross-linking agent (Fig. 7b) and modified NHAp nanoparticles to generate a CS-NHAp-NH₂ biocomposite for BTE. The NHAp nanoparticles were modified by reaction with 3-aminopropyltriethoxysilane (APTES) to incorporate NH₂ groups with cross-linking ability in their surface. CS was mixed with the NHAp-NH₂ nanoparticles, and then, glutaraldehyde was added to cross-link the CS matrix.

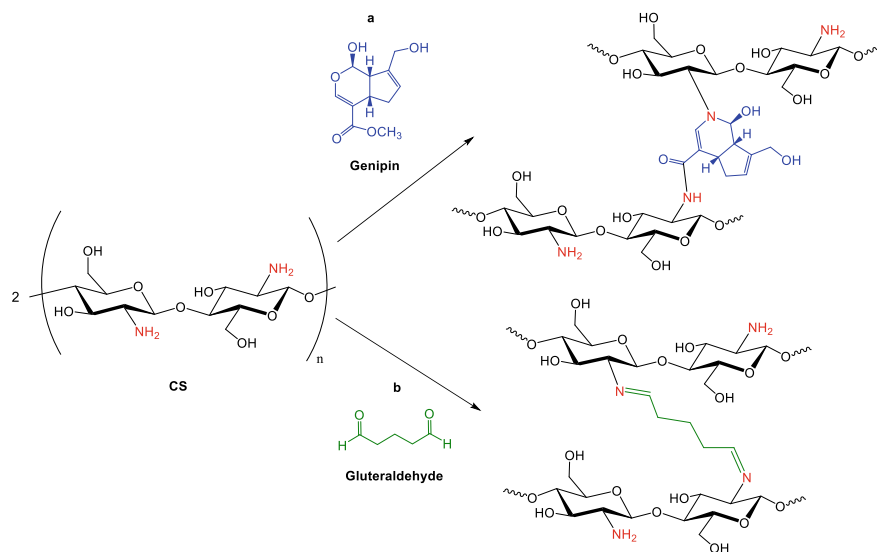


Fig. 7 Cross-linking reactions between CS and **a.** genipin or **b.** glutaraldehyde

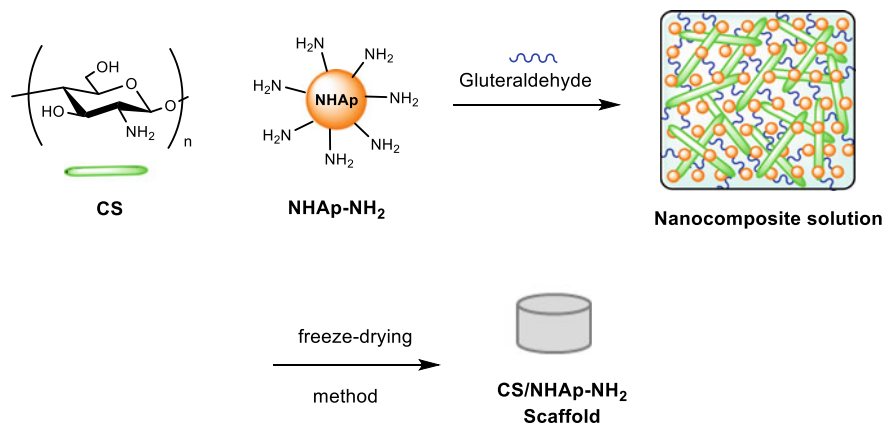


Fig. 8 Synthesis of the CS/NHAp-NH₂ scaffold. Adapted from Atak et al. [55]

Finally, the scaffold was prepared via a freeze-drying method (Fig. 8). The FTIR analysis of the scaffold confirmed that NHAp-NH₂ nanoparticles were cross-linked in the polymer matrix, and the SEM images showed an increase of the distribution behavior of the nanoparticles in the surface of the biocomposite. Comparing with other scaffolds (CS and CS-NHAp), the CS-NHAp-NH₂ revealed a better degradation rate, cell attachment, survival, and proliferations of human bone mesenchymal stem cells and osteogenic differentiation.

Even though chitosan-NHAp composite biomaterials have demonstrated their importance as potential scaffolds, more complex composite systems can also be prepared. The incorporation of other biopolymers, synthetic polymers, or metals to the biocomposites can further enhance their properties. Because of their biocompatibility and potential biodegradability, other polysaccharides can be assembled with CS to develop biocomposites. Furthermore, the hydroxyl groups of their framework can interact with the amino groups of the chitosan to form cross-linked networks with enhanced mechanical properties. They can additionally incorporate more centers of interaction with the Ca²⁺ ions of HAp facilitating the crystallization process of NHAp. Taking this into account, tamarind seed polysaccharide (TSP, Fig. 9a) and starch (ST, Fig. 9b) were combined with CS to obtain NHAp/CS/TSP [56] and NHAp/CS/ST [57] nanocomposites by the co-precipitation method. A comparative assessment of their properties and NHAp/CS nanocomposite was done. In both cases, it was observed increased thermal stability, compressive strength, and Young's modulus. This was probably due to the strong intermolecular interactions between the three components that were observed by FTIR analysis. Also, the SEM images demonstrated that the presence of the polysaccharides influenced the surface morphology of the scaffolds and that the NHAp nanoparticles were more homogeneously dispersed and could mimic natural bone apatite in terms of morphology and size. The biological properties were also improved suggesting that the nanocomposites are promising materials for applications in BTE.

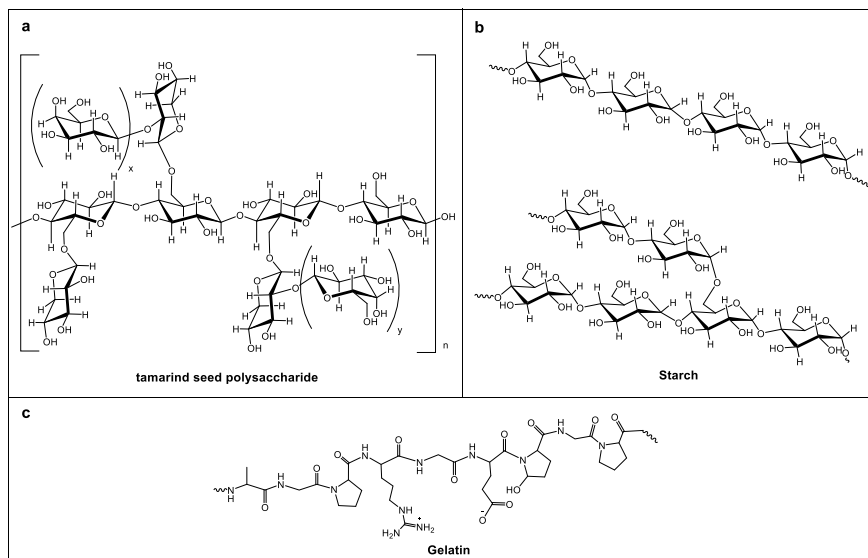


Fig. 9 Representative structures of **a.** tamarind seed polysaccharide; **b.** starch; and **c.** gelatin

Gelatin (Gel), a biocompatible and biodegradable biopolymer which can promote the adherence of cells because of the Arg-Gly-Asp sequences included in its structure (Fig. 9c), was also blended with CS to design more complex biocomposites [58, 59]. Neacsu et al. [60] mixed CS and Gel with a biomimetic HAp synthesized by microwave using an interwoven hierarchical structure of eggshell membrane (ESM). Also bone ash (BA), a natural source of both HAp and tricalcium phosphate (TCP), was added aiming to produce an even higher degree of biocompatibility [61, 62] and to obtain a scaffold more similar to natural bone, since its nonstoichiometric structure can contain other elements in addition to Ca and P (Na, Zn, Mg, K; Si, BA, F) [63, 64]. After using glutaraldehyde as a cross-linking agent, the sample was subjected to the freeze-drying process to obtain a porous HAp/BA/CS/Gel composite material with uniform distribution of the inorganic powder. The *in vitro* studies proved that the scaffold was biocompatible and non-cytotoxic and allowed cellular proliferation, stem cells adhesion, and multiplication. The biological properties observed for the new composite suggested that it might accelerate the bone healing process.

Saravanan et al. [65] used silver nanoparticles (NAg) to prepare a CS/NHAp/NAg scaffold. The authors compared the swelling and biodegradation rate of the composites with and without the incorporation of NAg. The presence of silver in the composite decreased the swelling percentage, which is important to ensure good mechanical strength and avoid loosening of the scaffold from the implanted site. Moreover, CS/NHAp/NAg biodegradation rate decreased compared to CS/NHAp scaffold suggesting that the material will be accessible for a longer time until bone tissue ingrowth. The NAg also increased the antibacterial activity of the new biocomposite. Although CS/NHAp scaffold exhibited antibacterial activity due to the presence of

CS which possesses this natural characteristic, the activity was considerably lower than that observed for CS/NHAp/nAg.

Another approach to keep the stiffness of chitosan would be to blend it with synthetic polymers with high mechanical properties. Poly(vinyl alcohol) (PVA) is useful for this purpose since it is a biodegradable, biocompatible, water-soluble polymer, and miscible with chitosan. Wu et al. [66] prepared films from PVA/CS blends and suggested that they were physically cross-linked by the formation of intermolecular hydrogen bonds. The use of PVA/CS blends could also be used to optimize the fabrication of nanofibers scaffolds by electrospinning, since the sufficient chain entanglement necessary for electrospinning was not achieved in the medium in which CS is soluble (aqueous acetic acid). This was probably due to the repulsive interaction between the chains generated by the amino groups of CS. The addition of PVA helped to reduce the repulsive interaction between the CS chains by forming hydrogen bonds with CS and thus facilitated the electrospinning process of the CS-PVA blend solution. Shen et al. [67] used CS/PVA blends to test the influence of different parameters (content of PVA, applied voltage, and flow rate) on the morphology of the nanofibers and determined the optimal conditions to produce a uniform and ultrafine nanofibrous CS bicomponent. Figure 10 shows that as the content of the PVA solution increased, the finer and more consistent nanofibers could

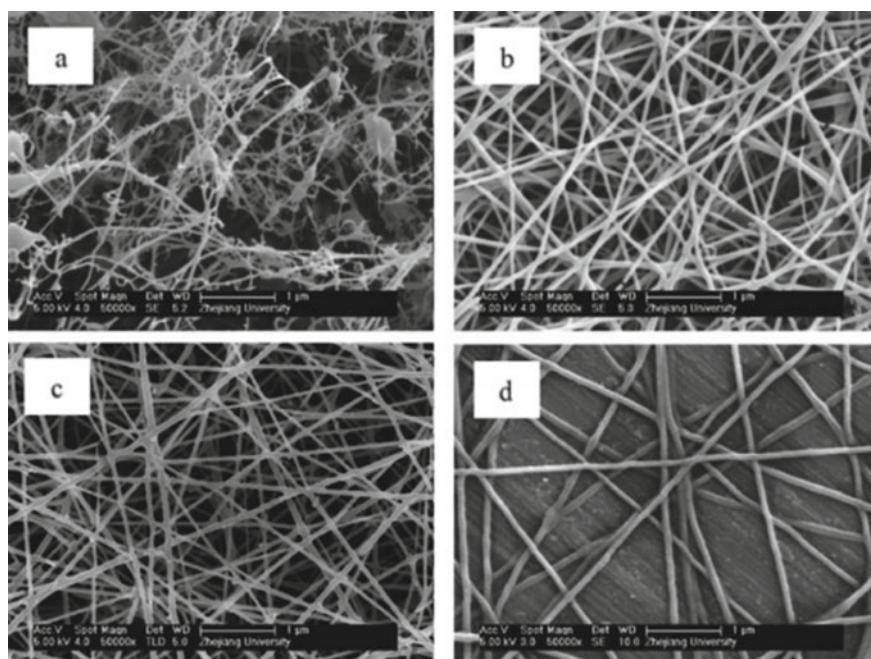


Fig. 10 SEM images of CS/PVA nanofibers electrospun under different volume ratios **a** 90/10; **b** 80/20; **c** 70/30; **d** 50/50. Reprinted from Journal of Applied Polymer Science © 2019, with permission of John Wiley & Sons, Ltd. [67]

be electrospun. The CS/PVA bicomponent mats were filled with HAp nanoparticles to development new materials that have potential application in BTE.

As already mentioned, CS or its derivatives are fragile. Also, it has been proved that unplasticized CS cast films were very brittle when stored at low relative humidity [68]. Thus, the need of using a plasticizer, such as glycerol, became evident [69]. A plasticizer decreases the intermolecular interactions, increases the free volume, and enhances the molecular motions, but it decreases the barrier properties of the polymer films [70, 71]. Besides, the plasticizer may migrate to the polymer surface and give undesired effects on the performance of the polymer films [72, 73]. This issue may be overcome by the use a plasticizer with higher molecular weight with a hampered migration to the bulk of the matrix. Poly(ethylene glycol) (PEG) is a water soluble, biodegradable, and biocompatible polymer with a flexible backbone. It is available in a wide range of molecular weights and may be an efficient plasticizer for chitosan. A blend of CS with increased amounts of PEG can give higher swelling ratios and *in vitro* biodegradation [74]. In opposition, the addition of a plasticizer to CS decreases its mechanical strength and thermal stability [69]. Jiang et al. [75] dissolved CS in aqueous $\text{AlCl}_3 \cdot 6\text{H}_2\text{O}$ and prepared PVA/chitosan blend films with glycerol as plasticizer. The combined use of glycerol and $\text{AlCl}_3 \cdot 6\text{H}_2\text{O}$ had a synergistic effect on the film properties. Chen et al. concluded that chitosan crystallinity can be decreased by the combination with PEG in blends [74]. Recently, PVA/CS blends, plasticized with PEG and glycerol, were prepared, and their physical and mechanical properties were investigated [76]. The plasticization efficiency and the compatibility of glycerol, PEG, and combinations with PVA/CS blends were evaluated using different characterization methods. A set of plasticizers including glycerol, PEG400, PEG1000 and the combination of glycerol and PEG1000 were used. The results from different analytical methods revealed that the optimum PEG: PVA ratio should be 1:9. Higher concentration of PEG would give phase separation and affect the performance of the film. For PVA/CS blends, PEG was also a compatibilizer, due to its ability to act as a hydrogen bond acceptor with the blend components. However, the high interaction affinity of glycerol with PVA and CS decreased the linkage through hydrogen bonds between PVA and the polysaccharide. On the other hand, glycerol enhanced the crystallinity of PVA/CS blends, whereas PEG reduced it (Fig. 11). Therefore, a combination of both plasticizers, glycerol, and PEG was employed and led to the highest level of compatibility. The antibacterial properties of the blends were investigated in order to analyze their potential for biomedical or food industry applications. The antibacterial activity of the blend plasticized with PEG/glycerol was notably decreased compared to the use of any single plasticizer. This was attributed a lower number of free amino groups in chitosan, as a consequence of the interactions between PVA and chitosan. In addition, the migration of PEG from the blend was much lower than that of glycerol, and the mixture of glycerol with PEG reduced the plasticizer migration.

Some biomolecules, growth factors, or stimulating agents have been added to the scaffolds to promote bone cell growth and to enhance the biological properties of the biocomposites. Considering that *Cissus quadrangularis* (CQ) extract was reported as beneficial for bone fracture healing [77–81], Tamburaci et al. [82] proposed a blend of

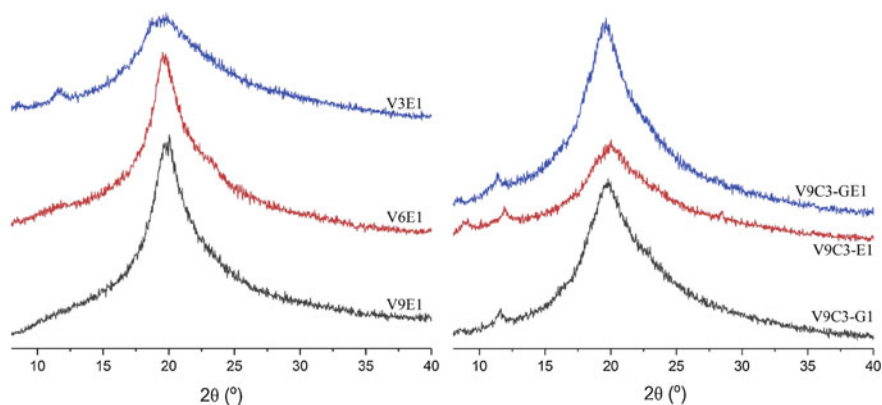


Fig. 11 XRD diffractions for PVA/PEG, PVA/chitosan/glycerol, PVA/chitosan/PEG, and PVA/chitosan/glycerol/PEG. To compare all the spectra, the y-axis was kept constant. The samples were coded as V_xE_1 in which V and E represent PVA and PEG; V9C3-G1 and V9C3-E1 where C and G account for chitosan and glycerol, respectively, sample V9C3-GE1 was prepared using a combination of glycerol and PEG. Reprinted from Sofla et al. [76] © 2020, with permission from Elsevier

CQ extract with CS/Na-carboxymethyl cellulose, in scaffolds to enhance the alkaline phosphatase (ALP) activity of Saos-2 osteosarcoma. Soumya et al. [83] included CQ extract in alginate/O-carboxymethyl CS scaffolds to promote osteoblast proliferation and ALP activity. The resulting biocomposite scaffolds had different porosity and swelling properties. Recently, Thongtham et al. [84] proposed a controlled release of the bioactive compounds from CQ extract, included in nanoparticles, in scaffolds made of Col, CS, and HAp. An ethanolic extract of CQ was encapsulated in polymer nanoparticles, instead of using a direct blend with the biopolymers. As a hydrophilic component, CQ was encapsulated by the double emulsion technique [85]. Poly(lactic-co-glycolic acid) (PLcG) and PEG are commonly used to form the first emulsion, while PVA and pluronic are utilized for the second emulsion formation to give nanoparticles (CQ-PCL NPs) with homogeneous size distribution [86, 87]. The CQ-PCL NPs were included in the CS/Col/HAp scaffolds. The scaffolds with and without CQ-PCL NPs were studied in terms of morphology, chemical composition, compressive modulus, water swelling, weight loss, and biocompatibility. The results showed that 20 mg/mL PCL and 0.5% (w/v) PVA were suitable for CQ-PCL NPs preparation, which were then included into the porous CS/Col/HAp scaffolds (Fig. 12). The surface of the nanoparticles was modified as a consequence of the blend, giving a slow release rate of CQ. The loaded CS/Col/HAp scaffolds showed similar properties to those of pristine CS/Col/HAp scaffolds. In addition, the CQ-PCL NPs-loaded CS/Col/HAp scaffolds were nontoxic to MC3T3-E1 murine osteoblasts (Fig. 13).

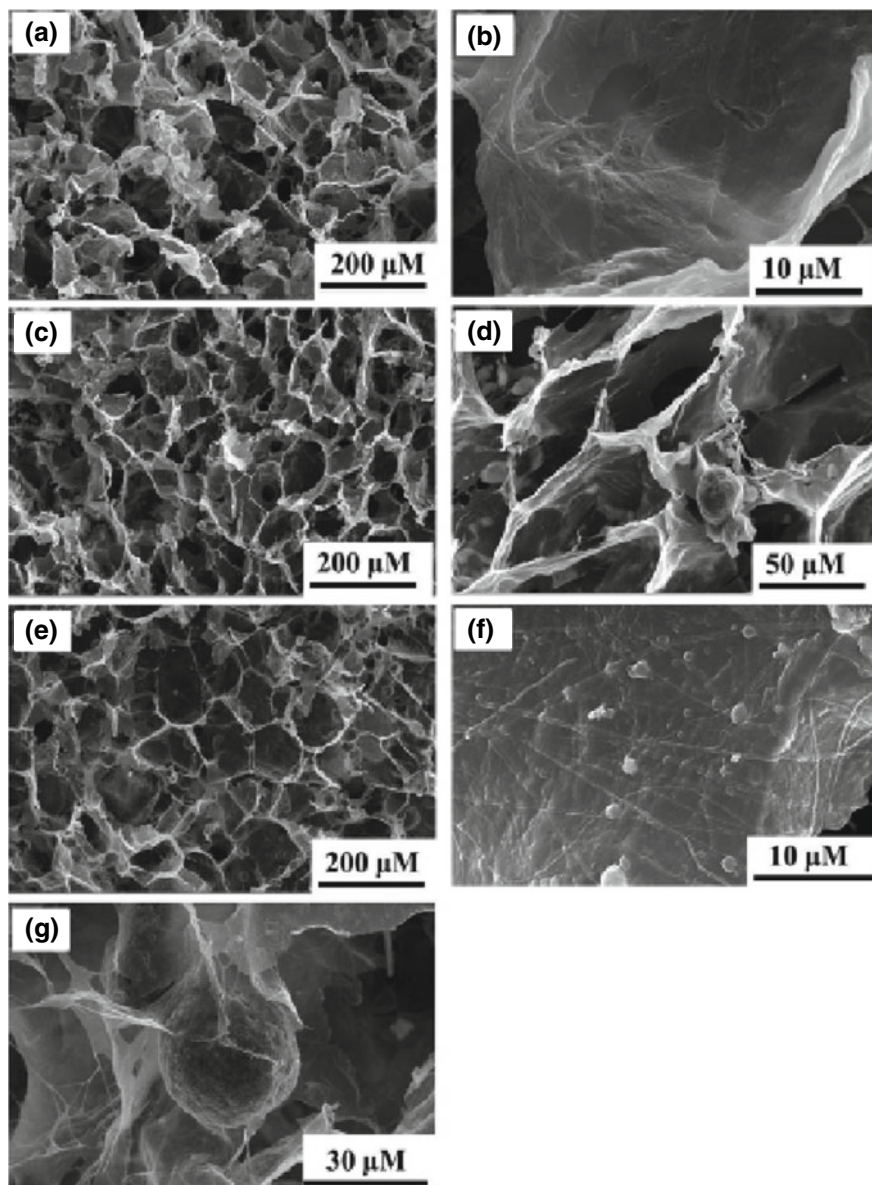
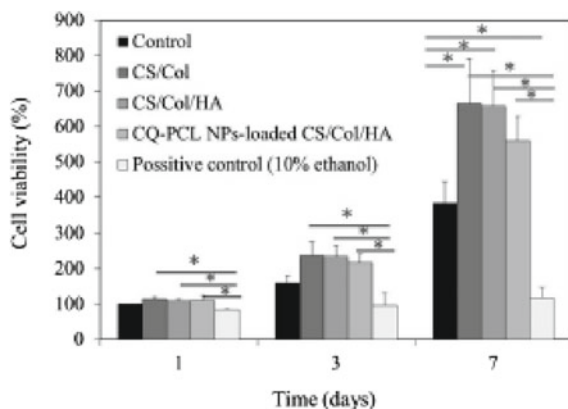


Fig. 12 SEM images of cross-sections of (a, b) CS/Col scaffolds, (c, d) CS/Col/HA scaffolds, (e, f, g) CQ-PLC-NPs-loaded CS/Col/HA scaffolds. Reprinted from *Polymers for Advanced Technologies* © 2019, with permission of John Wiley & Sons, Ltd. [84]

Fig. 13 Cell viability of MC3T3-E1 cells cultured with different scaffolds at 1, 3 and 7 days. $*p < 0.05$. Reprinted from *Polymers for Advanced Technologies* © 2019, with permission of John Wiley & Sons, Ltd. [84]



5 Cellulose

Cellulose is one of the most abundant natural renewable materials of the world. It is a diverse material with tunable chemical, physical, and mechanical properties [88]. Additionally, it has excellent biodegradability and biocompatibility. All these qualities make it an ideal candidate to be applied in the development of cellulose-based biomaterials for TE. In order to achieve materials with excellent performance in terms of their mechanical and biological properties [89, 90], cellulose could be modified, used in its nanoscale form, and combined with other polymers or ceramics to design composites. As in the case of CS, many research groups have reported recently its use in combination with HAp to enhance their mechanical and biological properties and produce scaffolds that could mimic bone tissue.

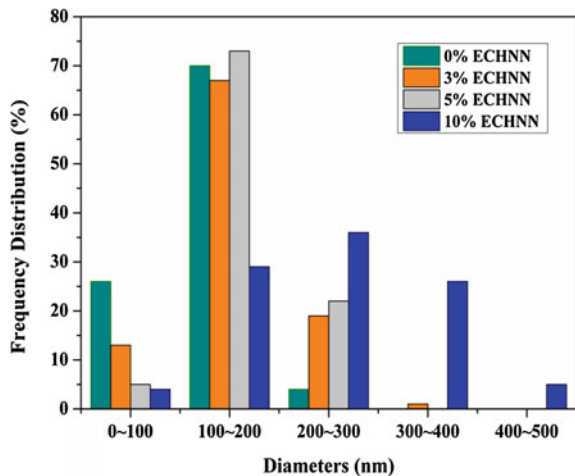
The chemical modification of cellulose is a widely used strategy to improve the solubility, the ability to fuse with the other materials that are part of the composite, and to modify the final biological and mechanical properties of the new material. Azzaoui et al. [91] synthesized hydroxyethyl cellulose acetate (HECA) and obtained an inorganic-organic film with potential application in BTE by evaporating the solvent of a solution of HECA and HAp in DMF. The structure and properties of the films were characterized with SEM, TGA, DTA, FTIR, and NMR. The cellulose modification allowed the improvement of the material workability and the formation of a specific interaction between the carbonyl groups in HECA and the HAp which probably contributes to the formation of uniform films. The HAp particles were well dispersed and immobilized throughout the formed films.

Nanocellulose (NC) properties (high surface area and crystallinity, low thermal expansion and cost, high specific strength and modulus, good biodegradability, and environmentally friendly) made it attractive to use in the design of composites. In the TE field, the electrospinning of biopolymers results an efficient procedure to obtain nanofibers. These kinds of polymers could easily form 2D or 3D nano-scaled systems with the ability of mimic the nanofibrillar components of the extracellular matrix (ECM) that surrounds cells within tissues. Thus, the use of biopolymers-based

composites with a nanoscale matrix has been widely investigated for the application in TE. Ao et al. [92] fabricated electrospun cellulose/NHAp nanocomposite nanofibers (ECHNN) based on native cotton cellulose and different NHAp concentration. The authors studied the physical properties of ECHNN and their potential application in BTE. The morphological analysis by SEM demonstrated that the nanofibers in scaffolds had a diameter distribution comparable to the natural ECM fibers (50–500 nm) (Fig. 14). The mechanical properties were enhanced with the addition of NHAp, especially when the NHAp loading was 5%. In this case, the SEM images proved that the nanoparticles were well dispersed. The 5% ECHNN showed distinctively higher values for tensile strength and Young's modulus (70.6 MPa and 3.12 GPa, respectively) than those of neat cellulose nanofiber mat (52.9 MPa, 1.64 GPa). The observed mechanical properties are promising for the ECHNN to be applied in BTE due to their similarity with those of natural bone.

NC can be blended with other polymers by the electrospun method to develop bio-nanocomposites. Turng et al. [93] incorporated cellulose nanocrystals (CNCs) functionalized with PEG (CNC-g-PEGs) into a PLA matrix by electrospinning. The PLA/CNC-g-PEG composite nanofibers were characterized in terms of morphology, thermal behavior, contact angle, wettability, and biocompatibility in human mesenchymal stem cells (hMSC). The use of CNC grafted with PEG enhanced the dispersion of cellulose nanocrystals in the PLA matrix. Consequently, it was demonstrated an enhanced mechanical strength and improved cell viability and proliferation. Therefore, they could be efficiently applied in TE. Si et al. [94] designed an electrospun poly(ϵ -caprolactone) PCL/NC scaffold with HAp mineralized on the surface. In this study, the authors decided to incorporate NC to improve the hydrophilicity and mechanical properties of the scaffold and to take advantage of the hydroxyl groups in the NC to generate nucleation sites to form mineral crystals over the polymer surface. It is known that during mineralization, the hydroxyl

Fig. 14 Fiber diameter distributions of ECHNN. Reprinted from Ao et al. [92] © 2017, with permission from Elsevier



groups can form ionic bonds with Ca^{2+} and hydrogen bonds with PO_4^{3-} generating local supersaturation and then nucleation of the crystals [95]. The scaffold was prepared starting from a fibrous PCL/NC matrix produced by an electrospun methodology. Then, this matrix was mineralized by immersion in SBF solution, which contained different salts of sodium, potassium, magnesium, and calcium to simulate body corporal medium (Fig. 15). An interesting conclusion was the influence of the NC content in the nanofibers to induce the HAp nucleus deposition and its efficient subsequent growth. SEM, energy-dispersive X-ray spectroscopy (EDS), and X-ray diffraction (XRD) analysis revealed that HAp crystal layers were formed after few days and that this was only possible on the composite fiber surfaces that included NC. The higher content of NC not only favored formation of crystals on the surface of the electrospun fibers, but also increased the hydrophilicity and the mechanical properties of the fiber mats.

Another way to improve nucleation and locally control the growth of HAp crystals is to use chemically functionalized NC [96]. Fragal et al. [97, 98] introduced sulfate, phosphate, carboxylate, and amino groups on the surface of cellulose nanowhiskers (CNWs) obtained through acid hydrolysis of the cellulose extracted from sugarcane bagasse. The functionalization of the primary hydroxyl groups of the CNWs is important because it might enhance the reactivity of the nucleation sites to promote homogeneous growth of HAp crystals [99]. The crystallization of the HAp layer at

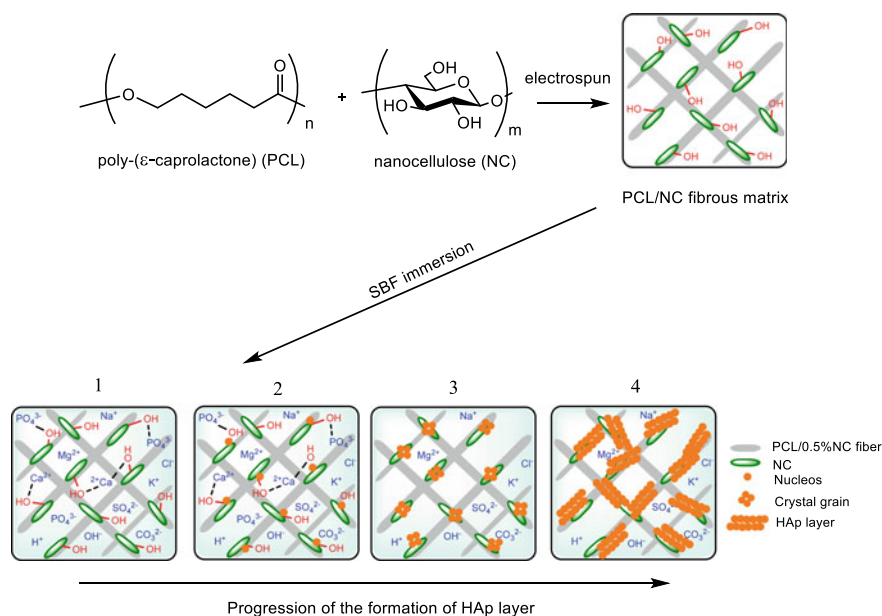


Fig. 15 Methodology used for the preparation of PCL/NC scaffold and schematic illustration showing the influence of NC content in the nanofibers to induce the HAp nucleus deposition and the progression of the HAp layer mineralization over its surface. Adapted from Si et al. [94]

the CNWs bearing carboxylate and amino groups was achieved by the interaction of these groups with Ca^{2+} using the biomimetic method under SBF for 14 and 28 days (Fig. 16). The stable nuclei, necessary to achieve the growth of the HAp layer over the CNWs surface, were formed through ionic and hydrogen interactions between the carboxylate, amino, and hydroxyl groups of the CNWs and Ca^{2+} and PO_4^{3-} ions. Moreover, it was revealed that the functionalized cellulose nanowhiskers could promote cell viability for the pre-osteoblasts (MC3T3-E1) comparable to HAp itself.

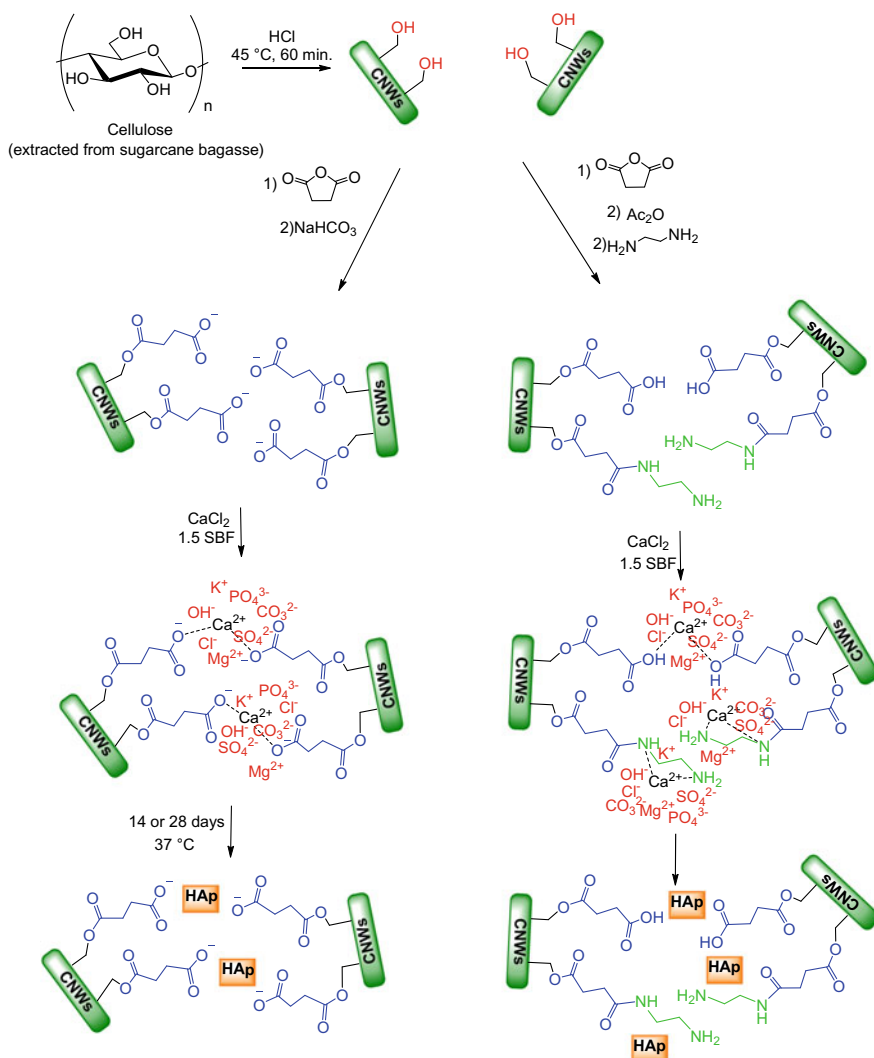


Fig. 16 Schematic illustration for the synthesis of modify CNWs and HAp crystal growth in the biomimetic method for 14 or 28 days. Adapted from Fragal et al. [98]

NC can also be used in the design of functional film bone scaffolds that are very interesting due to their tuneable surface structure, chemical and biological properties, and diverse functions. As already mentioned, there is a great interest in incorporating HAp to biocomposites due to the properties that it provides to the material [100]. However, it has been showed that combining HAp and thin films lead to development of materials with mechanical instability and susceptible to the surrounding environment [101]. Looking to solve this problem, Ragauskas group [102] described a methodology of layer-by-layer coating to produce a bone film scaffold. First, they prepared a CAN/HAp matrix by an in situ coating of HAp on the nanocrystal of cellulose (CNC). Then the CNC/HAp matrix was used as a template for building up the layer-by-layer assemblies with CS and hyaluronic acid (HA) (Fig. 17). The authors described that the HAp coating produced an increase in Young's modulus and matrix hardness. The incorporation of CS and HA layers increased the hydrophilicity of the material, identified by the decrease in the contact angle. Although the authors reported a decrease in the composite mechanical resistance with the layer-by-layer assembly, it was higher than CNCs, and therefore, it could be used as a bone scaffold.

6 Polyhydroxyalkanoates

In the field of biopolymers, the polyhydroxyalkanoates (PHAs) play an important role. The discovery of these biopolymers is due to the Maurice Lemoigne [103–107], who reported that their chemical structures depended of the bacterial species as well as the substrates present in the culture media. PHAs are biodegradable and biocompatible polyesters, synthesized by several microorganisms as intracellular carbon and energy storage compounds [108–110]. The repetitive unit of these polyesters consists of a 3-hydroxyacid with an alkyl substituent on C-3. A relevant representative of these biopolymers is the poly(3-hydroxybutyrate) (P3HB), which is a biodegradable thermoplastic derived from [*R*]-3-hydroxybutyric acid (Fig. 18). This chiral monomer may generate an optically active polymer. PHAs can be divided into two main groups depending on the number of carbon atoms in the monomeric units: short chain length PHAs (scl-PHAs), that contain between 3 and 5 carbon atoms (e.g., P3HB), poly(4-hydroxybutyrate) [P4HB], etc.) and medium chain length PHAs (mcl-PHAs) containing 6–14 carbon atoms (e.g., poly(3-hydroxyhexanoate) [P3HHx], poly(3-hydroxyoctanoate) [P3HO], etc.)

Lenz and Marchessault [111] reported an interesting work describing the biosynthesis and biotechnology of these polyesters, while Sudesh et al. [112] described their biochemistry and physicochemistry. Considering the biodegradability of these biopolymers, they have found different and varied applications. Since they are biocompatible as well, they are widely applied in the medicinal field in drug delivery, tissue engineering, scaffolds supporting regrowth of damaged tissues, and biodegradable implants biocontrol [113, 114]

Despite the interesting properties of PHAs, they are often combined with other polymers for several applications. The blending is prone to the generation of surface

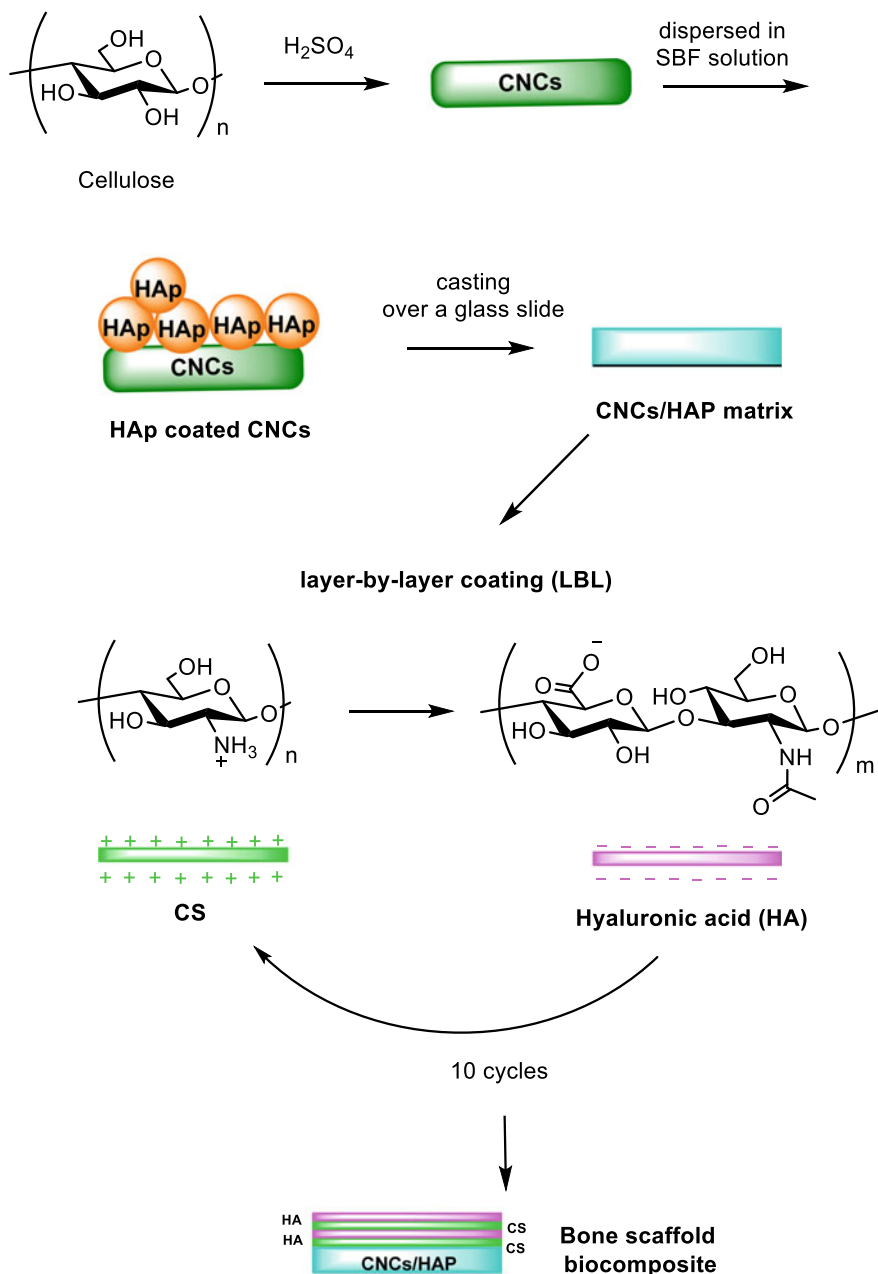
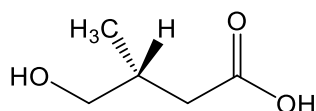


Fig. 17 Nanocomposite synthesis by layer-by-layer coating of CS/HA multilayers on a hard CNAs/HAp matrix

Fig. 18 Chemical structure of [*R*]-3-hydroxybutyric acid



separation, with the consequent fragility of the material. In this sense, Dufresne and Vincendon [115] studied polymeric blends with different thermomechanical properties, such as P3HB with P3HO using casting methodology and chloroform as solvent, and have determined the physical behavior and morphology of the biphasic mixtures.

A challenge for materials science is the development of biocompatible materials able to mimic neural tissue characteristics, maintain functionality in chronic devices, with minimal inflammation and neuronal cell loss. Soft electrically conducting polymers or elastomers have been proposed as alternatives to metallic implants [116–119] considering that biomaterial-tissue interface is a dynamic region where chronic inflammation may take place from incompatibilities between elastic modulus and relative micromotion of the implanted materials [120]. Usually, a threshold material stiffness must be kept to ensure the implant to penetrate the neural tissue to reach the final insertion point. However, the tissue would give a glial scar formation and electrode encapsulation, contributing to a chronic peri-electrode inflammatory response in vivo [120, 121]. Elastomeric polymers may be helpful to decrease the mechanical gap between the brain tissue and soft polymers at the neuroelectrode interface [122] and to improve the integration of the electrode with the tissue [123]. Relative micromotion of the device may be solved by the use of flexible materials, improving the electrode charge transfer capability [124].

Medium chain length PHAs (mcl-PHAs), containing 6–14 carbon atoms, are relevant due to their low crystallinity (T_m 45–60 °C), low T_g (in the range –25 to –50 °C), Young's modulus (3–70 MPa), and up to 500% elongation at break. Besides, they may be easily processed via traditional thermoplastic techniques, and their properties can be improved by their use in composite systems [125, 126].

On the other hand, nanocomposites incorporating multi-walled carbon nanotubes (MWCNTs) have been successfully employed in compliant electrode technologies to yield materials with interesting neuronal adhesion, survival, and support neurite elongation [27]. Carbon nanotube interfaces also stimulate spontaneous synaptic and can be applied to distribute electrical stimulation to neuronal pathways in vitro [128, 129].

MWCNTs were included in a mcl-PHA copolymer based on 3-hydroxyoctanoate and 3-hydroxyhexanoate to give a conductive elastomeric composite that could be interesting as a neuroelectrode material (Fig. 19) [123].

The thermoplastic elastomer behavior of the mcl-PHA was modified by the incorporation of MWCNTs, with the aim of applying the new material as a neurointerface-specific biomaterial. The stiffness of mcl-PHA gradually increased with the amount of MWCNTs from approximately 8 MPa (pristine mcl-PHA) to approximately 50 MPa (1 wt.% MWCNTs). The inclusion of the stiff nanofillers would promote the

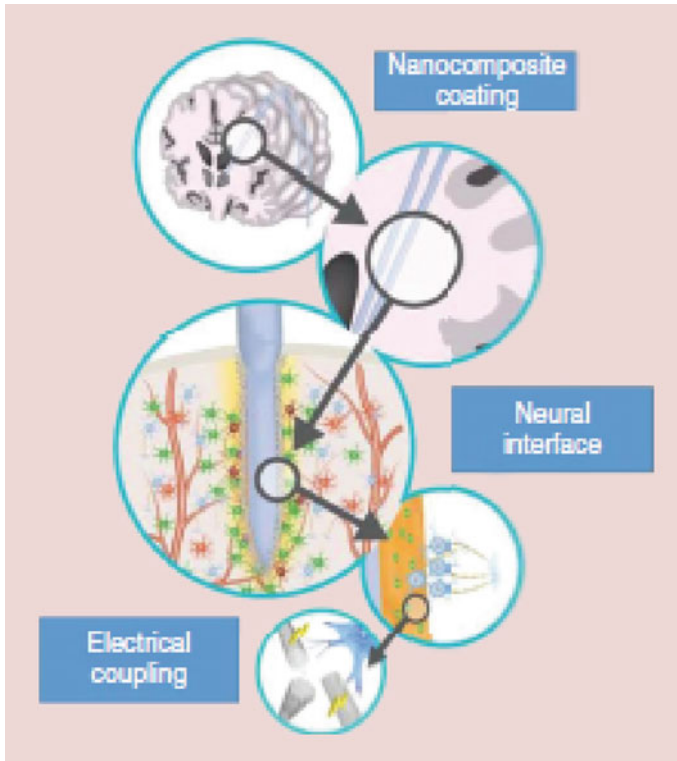


Fig. 19 Schematic overview of the challenges associated with neural interfacing technologies republished with permission of Future Medicine Ltd., from Vallejo-Giraldo et al. [123]

entanglement of the polymeric chains, thus the material had an enhanced stiffness. Incorporation of MWCNTs also promoted the conductivity of the composite. Incorporation of 0.5 wt.% of MWCNTs changed the behavior of the samples from resistive to capacitors. Both mechanical and electrical properties would have impact on the biological response. The mcl-PHA/0.5 wt.% MWCNTs composite was particularly interesting since it promoted neuron maintenance without any detrimental modification to neurite length (with respect to platinum control). Furthermore, this material produced a characteristic neural physiological type response in electrically stimulated VM neuronal populations (Fig. 20).

Hore and Laradji [130] performed theoretical studies using dynamics simulations, and they have proposed the introduction of nanorods, as emulsifying agents. Russell et al. [131] reported on the blending of poly(3-hydroxybutyrate) (PHB) and poly(3-hydroxyoctanoate) (PHO) with different thermomechanical properties and the effect of single wall carbon nanotubes (SWCNT) on their miscibility, electrical conductivity, and thermomechanical performance. Miscibility of scl-/mcl-PHA solvent

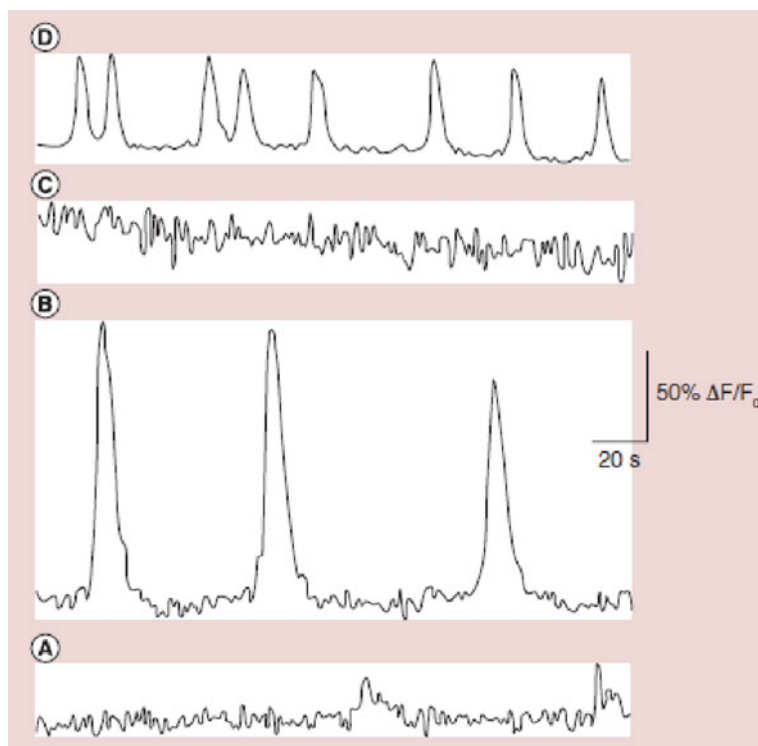


Fig. 20 Representative traces showing responses of selected regions of interest (single neurons) to stimulation induced changes in intracellular calcium. Stimulation was delivered to the films as biphasic voltage pulses (900 mV/cm^2 , 0.003 s pulse, 0.2 Hz). Cells were grown on **a** pristine mcl-PHA, **b** mcl-PHA/ $0.5 \text{ wt.}\%$ MWCNTs, and **c** mcl-PHA/ $1.0 \text{ wt.}\%$ MWCNTs. **d** Control stimulation experiments were conducted on Pt coated glass. Republished with permission of Future Medicine Ltd., from Vallejo-Giraldo et al. [123]

cast blends had been probed by scanning electron microscopy (SEM) and thermomechanical analysis [115]. The chemical imaging of deuterium-labeled poly(3-hydroxyoctanoate) (D-PHO) using infrared microspectroscopy (IRM) revealed phase separation in films containing PHB and P3HO [115, 132]. The addition of SWCNT to these polymer blends was expected to enhance miscibility of the components and therefore yield a biomaterial with improved thermomechanical properties. Moreover, a good dispersion of the SWCNT would increase the electrical conductivity of the films that could be applied for electrical stimulation through the material. The results suggested improved phase miscibility due to nanoparticle addition. The electrical percolation threshold in nanocomposite films was observed at $0.5\text{--}1 \text{ wt}\%$ SWCNT. At these levels, the surface resistivity was eight orders of magnitude lower than the insulating polymer blend. In addition, a SWCNT content up to $2.5 \text{ wt}\%$ did not affect significantly on mechanical properties of films. A solvent cast bionanocomposite film with $1 \text{ wt}\%$ SWCNT gave a material with enhanced electrical conductivity

compared to the SWCNT-free blend. This optimized blend held the growth of olfactory ensheathing cells and established a basis for developing biopolymer scaffolds able to conduct electrical stimulation. A biomaterial to support nerve repair should be stiff enough to allow implantation without tissue compression, but also flexible to tolerate movement, and give a stable electrode-tissue interface [133].

Many natural materials have been proposed for biomedical, biotechnological, and tissue engineering applications, and among them, protein-derived biomaterials are interesting potential candidates [134]. Keratin-based biomaterials have been considered due to their biocompatibility, biodegradability, mechanical properties, and natural abundance [135, 136]. *In vitro* biocompatibility studies of keratin-based scaffolds have been shown good swelling, attachment, and proliferation of mice fibroblast cells on the surface of the scaffolds [137]. Other cell lines have been tested, and the *in vitro* biocompatibility was validated for keratin biomaterials [138, 139]. Moreover, promising results were obtained for *in vivo* evaluation of keratin biomaterials in different animal models [140, 141].

Several research groups have described P(3HB)-based scaffolds with suitable structure and biocompatibility for tissue engineering applications [142–144]. Hydroxyapatite, bioglass, chitosan, silk, and carbon nanotubes have been blended with P(3HB) to promote biomedical applications [144]. Nanofibers can be easily obtained by electrospinning [145]; they allow cell migration and proliferation, may replace the extracellular matrix [146, 147], and find application as scaffolds in tissue engineering [148]. Zarei et al. [149] used chicken feather-derived keratin and P(3HB) to prepare porous structure scaffolds for tissue engineering. These scaffolds were able to mimic the extracellular matrix environment as they showed good uniformity, structural integrity, enhanced mechanical strength, and bioactivity. The results implied a high potential for these electrospun scaffolds in tissue regeneration or tissue repair applications. In addition, the simple and cost-effective methods used may lead to an easy scale-up. The approach of blending and spinning protein-based polymer with other biocompatible polymers may be extended to give a variety of biocomposites to mimic natural ECM for various tissue engineering applications.

7 Miscellaneous Applications

Most of the materials used in the construction industry derive from non-renewable resources or resources that require considerable time to be renewed [150]. Biopolymers and natural fibers (NF) may have interesting applications in this area [151, 152]. Some biocomposites have been considered in construction applications [153–155]. In particular, the application of NFs and biocomposites in construction was studied [156–161]. The effect of foam core density on the behavior of sandwich panels was studied by CoDyre et al. [159]. In this work, novel biocomposite unidirectional flax fiber-reinforced polymer skins were compared with panels of conventional glass-FRP skins. Structural sandwich panels were developed as replacement of conventional glass fiber-reinforced polymer (GFRP) skins [160]. This panels were made

with bio-based skins that were prepared with unidirectional flax fibers and a resin blend of epoxidized pine oil.

The use of cellulose fibers as reinforcement in green composites has been recommended, as an alternative to petroleum-based plastics [162], petrochemicals, and minerals [163, 164]. Inherently, green or biocomposites made from renewable resources are biodegradable and degraded into substances harmless to the environment [165, 166]. In biocomposite formulations, NFs are stronger and stiffer than polymeric matrix [167, 168]; however, a fundamental role is the binding between fibers and matrix, which contributes to stress distribution. When biopolymers are used as matrices, they can protect the fibers, and the overall behavior of the biocomposite depends on: type of fiber, matrix, distribution pattern of the fibers in matrix, etc.

Biopolymers may be obtained from renewable resources, synthesized microbially, or synthesized from petroleum-based chemicals [169]. Polyhydroxybutyrate (PHB) has mechanical properties equal or even better than traditional thermoplastics [170]. Additionally, the replacement of synthetic fibers by biofibers has been considered [171, 172]. Bast fibers, as majority of NFs, have several advantages as replacements for classic glass fibers in composites [173], namely they may lead to materials with reduced weight, less abrasive than glass particles, thus inducing less damage to machinery and personnel during the manufacturing process [174]. Kenaf bast fiber (KBF) has high strength-to-weight/stiffness-to-weight ratio in comparison to other fibers. Additionally, it has a very high carbon dioxide absorption capacity, which is valuable in the prevention of global warming [175]. Hybrid composites composed by two or more types of fibers together with a matrix would overcome the deficiencies of one fiber with another one [176, 177]. Among the NFs, oil palm empty fruit bunches (EFB) is hard and tough and found to be a potential reinforcement in composite applications [178]. The main advantages of EFB hybrid composite are low density, non-abrasiveness, and biodegradability. Hybridization of EFB with jute fibers [179, 180], sisal [179, 180], and glass [181, 182] led to enhancement of physical and mechanical properties of the hybrid composites. Therefore, a hybrid composite of two fibers may include the beneficial properties of the constituents. Tensile strength (TS) is one interesting feature of the NFs, and it is defined as the greatest longitudinal stress that a material can bear without tearing apart. Kenaf fibers have high TS, and thus, they could be employed as a reinforcing component in structural composites for construction industry. In contrast, kenaf fibers have low toughness leading to low impact resistance of the composite. Therefore, kenaf fibers were combined EFB, due to its toughness. A KBFw/EFB hybrid reinforced with PHB biocomposite was developed for application in building material [183]. The KBFw/EFB hybrid reinforced PHB biocomposite was made from polymer films and kenaf together with EFB fabric by lamination and compression molding. PHB is stiff and brittle, so triethyl citrate (TEC) was chosen as a plasticizer [184] in order to improve the mechanical properties and handling of PHB films [185, 186]. Also, a silane coupling agent was chosen to promote interfacial adhesion between reinforcements and matrix of the biocomposite [187]. Figure 21 shows the sample arrangements of the KBFw/EFB hybrid

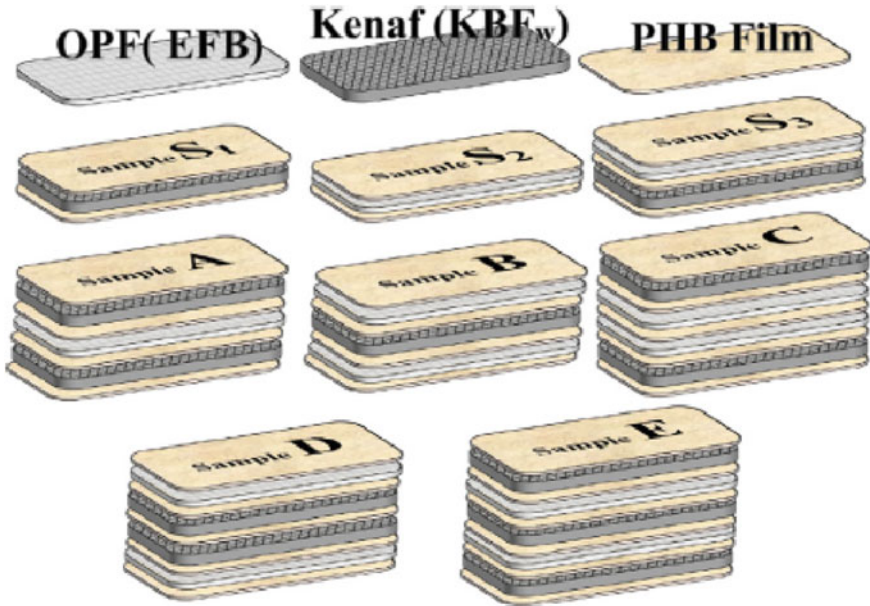


Fig. 21 Sample arrangement of KBFw/EFB hybrid reinforced PHB biocomposite. Reprinted from *Construction and Building Materials* © 2017, with permission from Elsevier [183]

reinforced PHB biocomposites. The results showed that the tensile and flexural properties would be increased when NFs with higher TS were used. The flexural stiffness of the biocomposite increased with a EFB reinforcement. The sample composed by 11 layers (sample E) might replace some wood and woody production in some applications.

Hasan et al. [188] described nano-biocomposite scaffolds with interesting antimicrobial activity as well as mechanical strength. The synthesis, described in Fig. 22, started with the acid hydrolysis of cellulose to produce cellulose nanowhiskers (CNWs), which were treated with TEMPO to produce the oxidation of primary hydroxyl groups yielding carboxymethylcellulose nanowhiskers (CCNWs). Then, silver nitrate (AgNO_3) was added to an aqueous dispersion of the nanowhiskers to give CCNWs/ Ag^+ . The reduction of silver cations was accomplished by addition of sodium borohydride, according to the methodology described by Liu et al. [189, 190]. Finally, the composites were lyophilized and kept at 4 °C.

Bacterial cellulose BC is synthesized by different species of bacteria, being *Gluconacetobacter xylinum* the most common. It presents chemical purity, high crystallinity, high porosity, high thermal stability, high hydrophilicity, high surface area, and Young's modulus. In addition, it forms well-organized 3D structures with different sizes and shapes. These unique properties allowed it to be used in the development of a variety of composites with possible applications in the TE field.

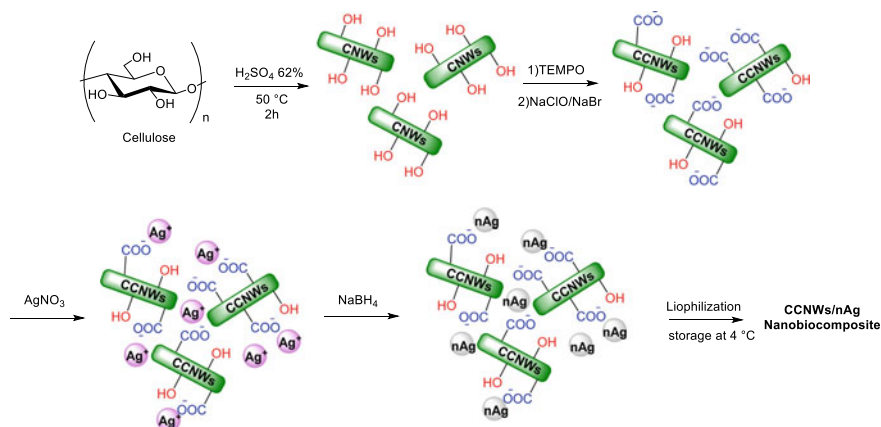


Fig. 22 Synthesis of CCNWs/nAg. Adapted from Hasan et al. [188]

The structural properties of the bacterial cellulose can be modified by election of the growth medium and the environmental conditions during the production of the cellulose. Costa et al. [191] demonstrated by SEM and AFM analysis that the surface morphology of BC biocomposites could be altered by changes in the fermentation medium incorporating some additives such as sugar cane, honey, and dates paste. Also, DSC and TGA analysis showed a change in the crystallinity and higher thermal properties of the new biocomposites. Another common way of interfering with the production rates and the overall properties of biocellulose is the incorporation of carboxymethylcellulose (CMC) in the BC culture medium. The changes in either the cross-linking density or overall network porosity of the biocomposite can be modulated using CMC with different degree of substitution (DS, the average number of carboxymethyl groups per monomeric unit). Thus, De Lima Fontes et al. [192] prepared BC/CMC biocomposites by in situ modification of a static culture medium using *Gluconacetobacter* bacteria and examined the effect of the incorporation of different DS-CMC (Fig. 23). The addition of the cellulose derivative did not generate chemical changes in the biocomposite structure, but a slight decrease in the crystallinity was observed. The FEG-SEM micrographs of the composites revealed that the CMC incorporation into BC nanofibers promoted the reduction of the material porosity. Also, the average elastic modulus decreased with the incorporation of CMC and the increase of the DS, probably due to low elastic modulus of the CMC phase and the decreasing inter/intra hydrogen bonds interaction between the chains of the CMC as a result of the substitution of hydroxyl groups in the glycopyranose molecule. Finally, the authors tested the in vitro release of methotrexate (MTX), a poorly water-soluble drug used in the treatment of cancer, inflammatory, and autoimmune diseases. It is well known that the highly porous structure of BC does not constitute a barrier against the drug molecules diffusion, but the addition CMC demonstrated to reduce the MTX release rate. These results suggested that this kind of biomaterials could be promising for the application through the cutaneous route in different pathologies.

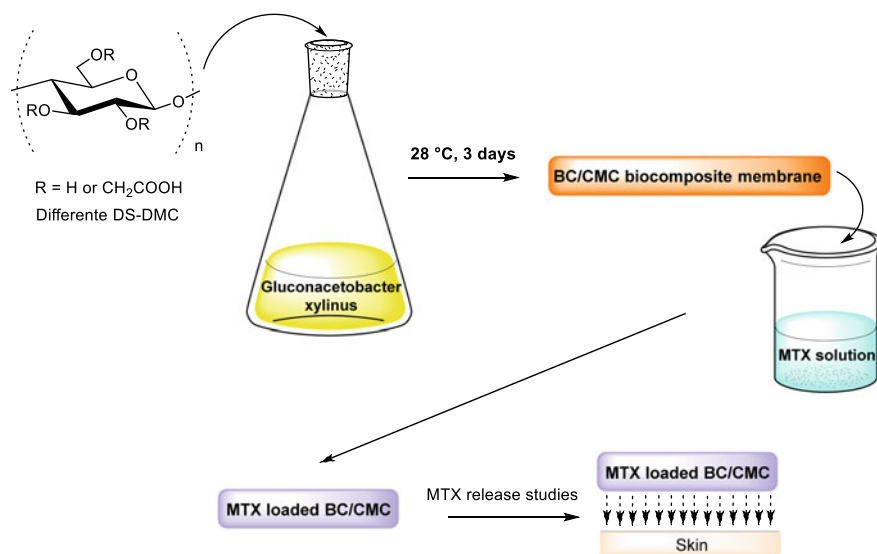


Fig. 23 Schematic representation of the synthesis of BC/CMC biocomposites, MTX loading, and release studies for topical applications. Adapted from Lima Fontes et al. [192]

According to the intended application of a biomaterial, its properties could be adapted by the incorporation of nanoparticles to a BC matrix. In order to give cellulose nanofibers antibacterials properties, Jalili Tabaii et al. [193] developed a silver nanoparticles (AgNPs)/BC composite to consider its application as infectious wound dressing. The AgNPs were successfully impregnated in the BC matrix through in situ reduction of silver nitrate in the presence of sodium tripolyphosphate (TPP) or sodium hydroxide (NaOH). High transparent nano sheets were obtained with the AgNPs firmly and uniformly attached to BC nanofibers. This is very important to ensure a control release of Ag ions which can minimize the potential cytotoxicity and prolonged the antibacterial activity. The (AgNPs)/BC composite exhibited high swelling ability, strong antibacterial activity against both Gram-negative and Gram-positive bacteria, biocompatibility, and no cytotoxicity. The showed characteristics of the biocomposited were a consequence of taking advantage of the individual properties of the materials that constituted it and gives it a promising potential application as antibacterial wound dressing. Galateanu et al. [194] fabricated bio-nanocomposites based on BC and magnetic nanoparticles (Fe₃O₄) for efficient chronic wounds healing. In this case, the composites were obtained directly during the biosynthesis process of BC by dispersing various amounts of magnetite nanoparticles (MNPs) in the culture medium. The biocompatibility of these innovative materials was studied in relation to human adipose derived stem cells (hASCs) in terms of cellular morphology, viability, and proliferation as well as scaffolds cytotoxic potential. The hASCs have an important role in stimulate recovery into injured or diseased tissue by promoting the recruitment of endogenous stem cells to the site of injury. All

the BC-based nanocomposites promote hASCs proliferation but the one with highest percentage of MNPs (BC/MNPs 5%) exhibited the greater cell density, viability, and adhesion over its surface.

8 Conclusions

Biocomposites are a hot spot area in material science according to the novel advances and current developments. Despite bio or natural polymers have several useful properties, such as biocompatibility, biodegradability, and abundance in nature, the incorporation of different fillers into the polymeric matrix or a chemical modification can enhance those properties or even add new ones.

Tissue engineering seems to be one of the most promising as well as the best established area for biocomposites, mainly due to the high demand of safe and compatible biomedical devices. It is expected that in future, the use of biocomposites for bone replacement will replace the use of autografts (patients own tissue) which is the current standard treatment.

On the other hand, there are several developments involving biocomposites, from glass production for construction to analytical processes. Regarding this last issue, considering that one of the principles of green analytical chemistry stipule that: "reagents obtained from renewable source should be preferred" [195] biocomposites involved in any kind of analytical procedure will be more than welcomed and will be increasingly found in future analytical developments.

Acknowledgements MDC, AAK and NBD are research members of the National Council of Research and Technology (CONICET, Argentina). DMF is a postdoctoral fellow from CONICET. Financial support was received UBA (UBACyT projects 20020130100021BA and 20020170100403BA), CONICET (PIP 112-201101-00370CO, PIP 112-2015-0100443CO). The authors would like to thank John Wiley & Sons, Ltd. for permission granted for Figs. 10, 12, and 13. The authors would like to thank Elsevier for permission granted for Figs. 2, 11, 14, and 21.

References

1. Wei L, McDonald AG (2016) A review on grafting of biofibers for biocomposites. *Materials (Basel)* 9:303–326
2. Mühlaupt R (2013) Green polymer chemistry and bio-based plastics: Dreams and reality. *Macromol Chem Phys* 214:159–174
3. Vilaplana F, Strömberg E, Karlsson S (2010) Environmental and resource aspects of sustainable biocomposites. *Polym Degrad Stab* 95:2147–2161
4. Rothon R (2017) Fillers for polymer applications. Rothon R (ed). Springer International Publishing, 489 p
5. Yunus Basha R, Sampath SK, Doble M (2015) Design of biocomposite materials for bone tissue regeneration. *Mater Sci Eng C* 57:452–463

6. Quesada HB, de Araújo TP, Vareschini DT, de Barros MASD, Gomes RG, Bergamasco R (2020) Chitosan, alginate and other macromolecules as activated carbon immobilizing agents: a review on composite adsorbents for the removal of water contaminants. *Int J Biol Macromol* 164:2535–2549
7. Płotka-Wasyłka J, Szczepańska N, de la Guardia M, Namieśnik J (2015) Miniaturized solid-phase extraction techniques. *TrAC—Trends Anal Chem* 73:19–38
8. Dimpe KM, Nomngongo PN (2016) Current sample preparation methodologies for analysis of emerging pollutants in different environmental matrices. *TrAC—Trends Anal Chem* 82:199–207
9. Tan SC, Lee HK (2019) A hydrogel composite prepared from alginate, an amino-functionalized metal-organic framework of type MIL-101(Cr), and magnetite nanoparticles for magnetic solid-phase extraction and UHPLC-MS/MS analysis of polar chlorophenoxy acid herbicides. *Microchim Acta* 186:545–556
10. Tasmia Shah J, Jan MR (2020) Eco-friendly alginate encapsulated magnetic graphene oxide beads for solid phase microextraction of endocrine disrupting compounds from water samples. *Ecotoxicol Environ Saf* 190: 110099
11. Zhang S, Niu H, Cai Y, Shi Y (2010) Barium alginate caged Fe₃O₄@C18 magnetic nanoparticles for the pre-concentration of polycyclic aromatic hydrocarbons and phthalate esters from environmental water samples. *Anal Chim Acta* 665:167–175
12. Bunkoed O, Nurerk P, Wannapob R, Kanatharana P (2016) Polypyrrole-coated alginate/magnetite nanoparticles composite sorbent for the extraction of endocrine-disrupting compounds. *J Sep Sci* 39:3602–3609
13. Manousi N, Rosenberg E, Deliyanni EA, Zachariadis GA (2020) Sample preparation using graphene-oxide-derived nanomaterials for the extraction of metals. *Molecules* 25:2411–2436
14. Zare M, Ramezani Z, Rahbar N (2016) Development of zirconia nanoparticles-decorated calcium alginate hydrogel fibers for extraction of organophosphorous pesticides from water and juice samples: facile synthesis and application with elimination of matrix effects. *J Chromatogr A* 1473:28–37
15. Li H, Eddaoudi M, O’Keeffe M, Yaghi OM (1999) Design and synthesis of an exceptionally stable and highly porous metal-organic framework. *Nature* 402:276–279
16. Gangu KK, Maddila S, Mukkamala SB, Jonnalagadda SB (2016) A review on contemporary metal-organic framework materials. *Inorganica Chim Acta* 446:61–74
17. Castilhos NDB, Sampaio NMF, da Silva BC, Riegel-Vidotti IC, Grassi MT, Silva BJG (2017) Physical-chemical characteristics and potential use of a novel alginate/zein hydrogel as the sorption phase for polar organic compounds. *Carbohydr Polym* 174:507–516
18. Ruiz-Palomero C, Soriano ML, Valcárcel M (2017) Nanocellulose as analyte and analytical tool: opportunities and challenges. *TrAC Trends Anal Chem* 87:1–18
19. Ruiz-Palomero C, Soriano ML, Valcárcel M (2015) β -Cyclodextrin decorated nanocellulose: a smart approach towards the selective fluorimetric determination of danofloxacin in milk samples. *Analyst* 140:3431–3438
20. Anirudhan TS, Rejeena SR (2013) Poly(methacrylic acid-co-vinyl sulfonic acid)-grafted-magnetite/ nanocellulose superabsorbent composite for the selective recovery and separation of immunoglobulin from aqueous solutions. *Sep Purif Technol* 119:82–93
21. Abujaber F, Guzmán Bernardo FJ, Rodríguez Martín-Doimeadros RC (2019) Magnetic cellulose nanoparticles as sorbents for stir bar-sorptive dispersive microextraction of polychlorinated biphenyls in juice samples. *Talanta* 201:266–270
22. Nurerk P, Bunkoed W, Kanatharana P, Bunkoed O (2018) A miniaturized solid-phase extraction adsorbent of calix[4]arene-functionalized graphene oxide/polydopamine-coated cellulose acetate for the analysis of aflatoxins in corn. *J Sep Sci* 41:3892–3901
23. Xu JJ, Ye LH, Cao J, Cao W, Zhang QY (2015) Ultramicro chitosan-assisted in-syringe dispersive micro-solid-phase extraction for flavonols from healthcare tea by ultra-high performance liquid chromatography. *J Chromatogr A* 1409:11–18
24. Guo H, Xue L, Yao S, Cai X, Qian J (2017) Rhein functionalized magnetic chitosan as a selective solid phase extraction for determination isoflavones in soymilk. *Carbohydr Polym* 165:96–102

25. Seol Y-J, Lee J-Y, Park Y-J, Lee Y-M, Ku Y, Rhyu I-C et al (2004) Chitosan sponges as tissue engineering scaffolds for bone formation. *Biotechnol Lett* 26: 1037–1041
26. Razavi N, Sarafrax YA (2017) New application of chitosan-grafted polyaniline in dispersive solid-phase extraction for the separation and determination of phthalate esters in milk using high-performance liquid chromatography. *J Sep Sci* 40:1739–1746
27. Safi K, Kant K, Bramhecha I, Mathur P, Sheikh J (2020) Multifunctional modification of cotton using layer-by-layer finishing with chitosan, sodium lignin sulphonate and boric acid. *Int J Biol Macromol* 158:903–910
28. Ahmed ABA, Adel M, Karimi P, Peidayesh M (2014) Pharmaceutical, cosmeceutical, and traditional applications of marine carbohydrates. In: Kim S-K (ed) *Advances in food and nutrition research*. Academic Press, pp 197–220
29. de Oliveira SA, Nunes de Macedo JR, Rosa D dos S (2019) Eco-efficiency of poly (lactic acid)-Starch-Cotton composite with high natural cotton fiber content: environmental and functional value. *J Clean Prod* 217: 32–41
30. Hollister SJ (2005) Porous scaffold design for tissue engineering. *Nat Mater* 4:518–524
31. Deepthi S, Venkatesan J, Kim S-K, Bumgardner JD, Jayakumar R (2016) An overview of chitin or chitosan/nano ceramic composite scaffolds for bone tissue engineering. *Int J Biol Macromol* 93:1338–1353
32. Chen F-M, Liu X (2016) Advancing biomaterials of human origin for tissue engineering. *Prog Polym Sci* 53:86–168
33. Aranaz I, Mengibar M, Harris R, Panos I, Miralles B, Acosta N et al (2009) Functional characterization of chitin and chitosan. *Curr Chem Biol* 3:203–230
34. Di Martino A, Sittinger M, Risbud MV (2005) Chitosan: a versatile biopolymer for orthopaedic tissue-engineering. *Biomaterials* 26:5983–5990
35. Bano I, Arshad M, Yasin T, Ghauri MA, Younus M (2017) Chitosan: a potential biopolymer for wound management. *Int J Biol Macromol* 102:380–383
36. Lu Z, Gao J, He Q, Wu J, Liang D, Yang H et al (2017) Enhanced antibacterial and wound healing activities of microporous chitosan-Ag/ZnO composite dressing. *Carbohydr Polym* 156:460–469
37. Nehra P, Chauhan R, Garg N, Verma K (2018) Antibacterial and antifungal activity of chitosan coated iron oxide nanoparticles. *Br J Biomed Sci* 75:13–18
38. Singh R, Shitiz K, Singh A (2017) Chitin and chitosan: biopolymers for wound management. *Int Wound J* 14:1276–1289
39. Cano L, Pollet E, Avérous L, Tercjak A (2017) Effect of TiO₂ nanoparticles on the properties of thermoplastic chitosan-based nano-biocomposites obtained by mechanical kneading. *Compos Part A Appl Sci Manuf* 93:33–40
40. Chen J, Pan P, Zhang Y, Zhong S, Zhang Q (2015) Preparation of chitosan/nano hydroxyapatite organic–inorganic hybrid microspheres for bone repair. *Colloids Surf B Biointerfaces* 134:401–407
41. Kassem A, Ayoub GM, Malaeb L (2019) Antibacterial activity of chitosan nano-composites and carbon nanotubes: a review. *Sci Total Environ* 668:566–576
42. Saravanan S, Leena RS, Selvamurugan N (2016) Chitosan based biocomposite scaffolds for bone tissue engineering. *Int J Biol Macromol* 93:1354–1365
43. Wang W, Yeung KWK (2017) Bone grafts and biomaterials substitutes for bone defect repair: a review. *Bioact Mater* 2:224–247
44. Zhang D, Wu X, Chen J, Lin K (2018) The development of collagen based composite scaffolds for bone regeneration. *Bioact Mater* 3:129–138
45. Gaspar A, Moldovan L, Constantin D, Stanciuc AM, Sarbu Boeti PM, Efrimescu IC (2011) Collagen-based scaffolds for skin tissue engineering. *J Med Life* 4:172–177
46. Doillon CJ, Watsky MA, Hakim M, Wang J, Munger R, Laycock N et al (2003) A collagen-based scaffold for a tissue engineered human cornea: physical and physiological properties. *Int J Artif Organs* 26:764–773
47. Davis GE (1992) Affinity of integrins for damaged extracellular matrix: $\alpha\upsilon\beta 3$ binds to denatured collagen type I through RGD sites. *Biochem Biophys Res Commun* 182:1025–1031

48. Kaczmarek B, Sionkowska A, Osyczka AM (2018) Physicochemical properties of scaffolds based on mixtures of chitosan, collagen and glycosaminoglycans with nano-hydroxyapatite addition. *Int J Biol Macromol* 118:1880–1883
49. Sionkowska A, Kaczmarek B (2017) Preparation and characterization of composites based on the blends of collagen, chitosan and hyaluronic acid with nano-hydroxyapatite. *Int J Biol Macromol* 102:658–666
50. Venkatesan J, Kim S-K (2010) Chitosan composites for bone tissue engineering—an overview. *Mar Drugs* 8:2252–2266
51. Yamaguchi I, Iizuka S, Osaka A, Monma H, Tanaka J (2003) The effect of citric acid addition on chitosan/hydroxyapatite composites. *Colloids Surf A Physicochem Eng Asp* 214:111–118
52. Fraga AF, Filho E de A, Rigo EC da S, Boschi AO (2011) Synthesis of chitosan/hydroxyapatite membranes coated with hydroxycarbonate apatite for guided tissue regeneration purposes. *Appl Surf Sci* 257: 3888–3892
53. Depan D, Venkata Surya PKC, Girase B, Misra RDK (2011) Organic/inorganic hybrid network structure nanocomposite scaffolds based on grafted chitosan for tissue engineering. *Acta Biomater* 7:2163–2175
54. Li X, Nan K, Shi S, Chen H (2012) Preparation and characterization of nano-hydroxyapatite/chitosan cross-linking composite membrane intended for tissue engineering. *Int J Biol Macromol* 50:43–49
55. Atak BH, Buyuk B, Huysal M, Isik S, Senel M, Metzger W et al (2017) Preparation and characterization of amine functional nano-hydroxyapatite/chitosan bionanocomposite for bone tissue engineering applications. *Carbohydr Polym* 164:200–213
56. Shakir M, Zia I, Rehman A, Ullah R (2018) Fabrication and characterization of nanoengineered biocompatible n-HA/chitosan-tamarind seed polysaccharide: bio-inspired nanocomposites for bone tissue engineering. *Int J Biol Macromol* 111:903–916
57. Shakir M, Jolly R, Khan MS, Iram N, Khan HM (2015) Nano-hydroxyapatite/chitosan–starch nanocomposite as a novel bone construct: synthesis and in vitro studies. *Int J Biol Macromol* 80: 282–292
58. Ranganathan S, Balangadhara K, Selvamurugan N (2019) Chitosan and gelatin-based electrospun fibers for bone tissue engineering. *Int J Biol Macromol* 133:354–364
59. Christy PN, Basha SK, Kumari VS, Bashir AKH, Maaza M, Kaviyarasu K et al (2020) Biopolymeric nanocomposite scaffolds for bone tissue engineering applications—a review. *J Drug Deliv Sci Technol* 55: 101452
60. Neacsu IA, Serban AP, Nicoara AI, Trusca R, Ene VL, Iordache F (2020) Biomimetic composite scaffold based on naturally derived biomaterials. *Polymers (Basel)* 12:1161–1180
61. Aycan D, Alemdar N (2018) Development of pH-responsive chitosan-based hydrogel modified with bone ash for controlled release of amoxicillin. *Carbohydr Polym* 184:401–407
62. Galeano S, García-Lorenzo ML (2014) Bone mineral change during experimental calcination: an X-ray diffraction study. *J Forensic Sci* 59:1602–1606
63. Mohd Pu'ad NAS, Koshy P, Abdullah HZ, Idris MI, Lee TC (2019) Syntheses of hydroxyapatite from natural sources. *Heliyon* 5: e01588
64. Gelli R, Ridi F, Baglioni P (2019) The importance of being amorphous: calcium and magnesium phosphates in the human body. *Adv Colloid Interface Sci* 269:219–235
65. Saravanan S, Nethala S, Pattnaik S, Tripathi A, Moorthi A, Selvamurugan N (2011) Preparation, characterization and antimicrobial activity of a bio-composite scaffold containing chitosan/nano-hydroxyapatite/nano-silver for bone tissue engineering. *Int J Biol Macromol* 49:188–193
66. Wu Y, Ying Y, Liu Y, Zhang H, Huang J (2018) Preparation of chitosan/poly vinyl alcohol films and their inhibition of biofilm formation against *Pseudomonas aeruginosa* PAO1. *Int J Biol Macromol* 118:2131–2137
67. Shen K, Hu Q, Chen L, Shen J (2010) Preparation of chitosan bicomponent nanofibers filled with hydroxyapatite nanoparticles via electrospinning. *J Appl Polym Sci* 115:2683–2690
68. Epure V, Griffon M, Pollet E, Avérous L (2011) Structure and properties of glycerol-plasticized chitosan obtained by mechanical kneading. *Carbohydr Polym* 83:947–952

69. Suyatma NE, Tighzert L, Copinet A, Coma V (2005) Effects of hydrophilic plasticizers on mechanical, thermal, and surface properties of chitosan films. *J Agric Food Chem* 53:3950–3957
70. Fundo JF, Carvalho A, Feio G, Silva CLM, Quintas MAC (2015) Relationship between molecular mobility, microstructure and functional properties in chitosan/glycerol films. *Innov Food Sci Emerg Technol* 28: 81–85
71. Sanyang M, Sapuan S, Jawaid M, Ishak M, Sahari J (2015) Effect of Plasticizer type and concentration on tensile, thermal and barrier properties of biodegradable films based on sugar palm (*Arenga pinnata*) Starch. *Polymers (Basel)* 7:1106–1124
72. Huang C, Zhu J, Chen L, Li L, Li X (2014) Structural changes and plasticizer migration of starch-based food packaging material contacting with milk during microwave heating. *Food Control* 36:55–62
73. Li X, He Y, Huang C, Zhu J, Lin AH-M, Chen L et al (2016) Inhibition of plasticizer migration from packaging to foods during microwave heating by controlling the esterified starch film structure. *Food Control* 66: 130–136
74. Chen S-H, Tsao C-T, Chang C-H, Lai Y-T, Wu M-F, Liu Z-W et al (2013) Synthesis and characterization of reinforced poly(ethylene glycol)/chitosan hydrogel as wound dressing materials. *Macromol Mater Eng* 298:429–438
75. Jiang X, Zhao Y, Hou L (2016) The effect of glycerol on properties of chitosan/poly(vinyl alcohol) films with $AlCl_3 \cdot 6H_2O$ aqueous solution as the solvent for chitosan. *Carbohydr Polym* 135:191–198
76. Shojaee Kang Sofla M, Mortazavi S, Seyfi J (2020) Preparation and characterization of polyvinyl alcohol/chitosan blends plasticized and compatibilized by glycerol/polyethylene glycol. *Carbohydr Polym* 232: 115784
77. Shirwaikar A, Khan S, Malini S (2003) Antiosteoporotic effect of ethanol extract of *Cissus quadrangularis* Linn. on ovariectomized rat. *J Ethnopharmacol* 89: 245–250
78. Kumar TS, Jegadeesan M (2006) Physico-chemical profile of *cissus quadrangularis* L. Var-I in different soils. *Anc Sci Life* 26:50–58
79. Madan CLNSL (1859) A pharmacognostical study of the stem of *Cissus quadrangularis* Linn. *J Sci Ind Res (India)* 18:253–255
80. Mehta M, Kaur N, Bhutani KK (2001) Determination of marker constituents from *Cissus quadrangularis* Linn. and their quantitation by HPTLC and HPLC. *Phytochem Anal* 12: 91–95
81. Potu BK, Bhat KM, Rao MS, Nampurath GK, Chamallamudi MR, Nayak SR et al (2009) Petroleum ether extract of *Cissus quadrangularis* (Linn.) enhances bone marrow mesenchymal stem cell proliferation and facilitates osteoblastogenesis. *Clinics* 64: 993–998s
82. Tamburaci S, Kimna C, Tihminlioglu F (2018) Novel phytochemical *Cissus quadrangularis* extract-loaded chitosan/Na-carboxymethyl cellulose-based scaffolds for bone regeneration. *J Bioact Compat Polym* 33:629–646
83. Soumya S, Sajesh KM, Jayakumar R, Nair SV, Chennazhi KP (2012) Development of a phytochemical scaffold for bone tissue engineering using *Cissus quadrangularis* extract. *Carbohydr Polym* 87:1787–1795
84. Thongtham N, Chai-in P, Unger O, Boonrungsiman S, Suwanton O (2020) Fabrication of chitosan/collagen/hydroxyapatite scaffolds with encapsulated *Cissus quadrangularis* extract. *Polym Adv Technol* 31:1496–1507
85. Iqbal M, Zafar N, Fessi H, Elaissari A (2015) Double emulsion solvent evaporation techniques used for drug encapsulation. *Int J Pharm* 496:173–190
86. Teekamp N, Duque LF, Frijlink HW, Hinrichs WL, Olinga P (2015) Production methods and stabilization strategies for polymer-based nanoparticles and microparticles for parenteral delivery of peptides and proteins. *Expert Opin Drug Deliv* 12:1311–1331
87. Giovino C, Ayensu I, Tetteh J, Boateng JS (2012) Development and characterisation of chitosan films impregnated with insulin loaded PEG-b-PLA nanoparticles (NPs): a potential approach for buccal delivery of macromolecules. *Int J Pharm* 428:143–151
88. Domingues RMA, Gomes ME, Reis RL (2014) The potential of cellulose nanocrystals in tissue engineering strategies. *Biomacromol* 15:2327–2346

89. Armiento AR, Stoddart MJ, Alini M, Eglin D (2018) Biomaterials for articular cartilage tissue engineering: learning from biology. *Acta Biomater* 65:1–20
90. Ciardelli G, Chiono V, Vozzi G, Pracella M, Ahluwalia A, Barbani N et al (2005) Blends of poly-(ϵ -caprolactone) and polysaccharides in tissue engineering applications. *Biomacromol* 6:1961–1976
91. Azaoui K, Mejdoubi E, Lamhamdi A, Zaoui S, Berrabah M, Elidrissi A et al (2015) Structure and properties of hydroxyapatite/hydroxyethyl cellulose acetate composite films. *Carbohydr Polym* 115:170–176
92. Ao C, Niu Y, Zhang X, He X, Zhang W, Lu C (2017) Fabrication and characterization of electrospun cellulose/nano-hydroxyapatite nanofibers for bone tissue engineering. *Int J Biol Macromol* 97:568–573
93. Zhang C, Salick MR, Cordie TM, Ellingham T, Dan Y, Turng L-S (2015) Incorporation of poly(ethylene glycol) grafted cellulose nanocrystals in poly(lactic acid) electrospun nanocomposite fibers as potential scaffolds for bone tissue engineering. *Mater Sci Eng C* 49:463–471
94. Si J, Cui Z, Wang Q, Liu Q, Liu C (2016) Biomimetic composite scaffolds based on mineralization of hydroxyapatite on electrospun poly(ϵ -caprolactone)/nanocellulose fibers. *Carbohydr Polym* 143:270–278
95. Heinemann S, Heinemann C, Bernhardt R, Reinstorf A, Nies B, Meyer M et al (2009) Bioactive silica–collagen composite xerogels modified by calcium phosphate phases with adjustable mechanical properties for bone replacement. *Acta Biomater* 5:1979–1990
96. Wan YZ, Huang Y, Yuan CD, Raman S, Zhu Y, Jiang HJ et al (2007) Biomimetic synthesis of hydroxyapatite/bacterial cellulose nanocomposites for biomedical applications. *Mater Sci Eng C* 27:855–864
97. Fragal EH, Cellet TSP, Fragal VH, Witt MA, Companhoni MVP, Ueda-Nakamura T et al (2019) Biomimetic nanocomposite based on hydroxyapatite mineralization over chemically modified cellulose nanowhiskers: An active platform for osteoblast proliferation. *Int J Biol Macromol* 125:133–142
98. Fragal EH, Cellet TSP, Fragal VH, Companhoni MVP, Ueda-Nakamura T, Muniz EC et al (2016) Hybrid materials for bone tissue engineering from biomimetic growth of hydroxyapatite on cellulose nanowhiskers. *Carbohydr Polym* 152:734–746
99. González M, Hernández E, Ascencio JA, Pacheco F, Pacheco S, Rodríguez R (2003) Hydroxyapatite crystals grown on a cellulose matrix using titanium alkoxide as a coupling agent. *J Mater Chem* 13:2948–2951
100. Wei G, Ma PX (2004) Structure and properties of nano-hydroxyapatite/polymer composite scaffolds for bone tissue engineering. *Biomaterials* 25:4749–4757
101. Sato K, Nakajima T, Anzai J (2012) Preparation of poly(methyl methacrylate) microcapsules by in situ polymerization on the surface of calcium carbonate particles. *J Colloid Interface Sci* 387:123–126
102. Huang C, Fang G, Zhao Y, Bhagia S, Meng X, Yong Q et al (2019) Bio-inspired nanocomposite by layer-by-layer coating of chitosan/hyaluronic acid multilayers on a hard nanocellulose-hydroxyapatite matrix. *Carbohydr Polym* 222: 115036
103. Lemoigne M (1923) Production of β -hydroxybutyric acid by certain bacteria of the *B. subtilis* group. *Comptes rendus l'Académie des Sci* 176: 1761–1763
104. Lemoigne M (1924) Production of β -hydroxybutyric acid by a bacterial process. *Comptes rendus l'Académie des Sci* 178:253–256
105. Lemoigne M (1925) The origin of β -hydroxybutyric acid obtained by bacterial process. *Comptes rendus l'Académie des Sci* 180:1539–1541
106. Lemoigne M (1926) Products of dehydration and of polymerization of β -hydroxybutyric acid. *Bull Soc Chim Biol (Paris)* 8:770–782
107. Lemoigne M (1927) Chemical origin of the products of dehydration and of polymerization of β -hydroxybutyric acid. *Hydroxybutyric fermentation. Bull Soc Chim Biol (Paris)* 9: 446–453
108. Shabina M, Afzal M, Hameed S (2015) Bacterial polyhydroxyalkanoates-eco-friendly next generation plastic: production, biocompatibility, biodegradation, physical properties and applications. *Green Chem Lett Rev* 8: 56–77

109. Lee SY (2000) Bacterial polyhydroxyalkanoates. *Biotechnol Bioeng* 49:1–14
110. Lee SY (1996) Plastic bacteria? Progress and prospects for polyhydroxyalkanoate production in bacteria. *Trends Biotechnol* 14:431–438
111. Lenz RW, Marchessault RH (2005) Bacterial polyesters: biosynthesis, biodegradable plastics and biotechnology. *Biomacromol* 6:1–8
112. Sudesh K, Abe H, Doi Y (2000) Synthesis, structure and properties of polyhydroxyalkanoates: biological polyesters. *Prog Polym Sci* 25:1503–1555
113. Ray S, Kalia VC (2017) Biomedical applications of polyhydroxyalkanoates. *Indian J Microbiol* 57:261–269
114. Zinn M, Witholt B, Egli T (2001) Occurrence, synthesis and medical application of bacterial polyhydroxyalkanoate. *Adv Drug Deliv Rev* 53:5–21
115. Dufresne A, Vincendon M (2000) Poly(3-hydroxybutyrate) and poly(3-hydroxyoctanoate) blends: morphology and mechanical behavior. *Macromolecules* 33:2998–3008
116. McClain MA, Clements IP, Shafer RH, Bellamkonda RV, LaPlaca MC, Allen MG (2011) Highly-compliant, microcable neuroelectrodes fabricated from thin-film gold and PDMS. *Biomed Microdevices* 13:361–373
117. Biran R, Martin DC, Tresco PA (2007) The brain tissue response to implanted silicon micro-electrode arrays is increased when the device is tethered to the skull. *J Biomed Mater Res Part A* 82A:169–178
118. Asplund M, Nyberg T, Inganäs O (2010) Electroactive polymers for neural interfaces. *Polym Chem* 1:1374
119. Apollo NV, Maturana MI, Tong W, Nayagam DAX, Shivdasani MN, Foroughi J et al (2015) Soft, flexible freestanding neural stimulation and recording electrodes fabricated from reduced graphene oxide. *Adv Funct Mater* 25:3551–3559
120. Vallejo-Giraldo C, Kelly A, Biggs MJP (2014) Biofunctionalisation of electrically conducting polymers. *Drug Discov Today* 19:88–94
121. Thelin J, Jörentell H, Psouni E, Garwicz M, Schouenborg J, Danielsen N et al (2011) Implant size and fixation mode strongly influence tissue reactions in the CNS. *PLoS One* 6: e16267
122. Keohan F, Wei XF, Wongsarnpigoon A, Lazaro E, Darga JE, Grill WM (2007) Fabrication and evaluation of conductive elastomer electrodes for neural stimulation. *J Biomater Sci Polym Ed* 18:1057–1073
123. Vallejo-Giraldo C, Pugliese E, Larrañaga A, Fernandez-Yague MA, Britton JJ, Trotier A et al (2016) Polyhydroxyalkanoate/carbon nanotube nanocomposites: flexible electrically conducting elastomers for neural applications. *Nanomedicine* 11:2547–2563
124. Khodagholy D, Doublet T, Gurfinkel M, Quilichini P, Ismailova E, Leleux P et al (2011) Highly conformable conducting polymer electrodes for in vivo recordings. *Adv Mater* 23:H268–H272
125. Misra SK, Valappil SP, Roy I, Boccaccini AR (2006) Polyhydroxyalkanoate (PHA)/inorganic phase composites for tissue engineering applications. *Biomacromol* 7:2249–2258
126. Barrett JSF, Abdala AA, Srienc F (2014) Poly(hydroxyalkanoate) elastomers and their graphene nanocomposites. *Macromolecules* 47:3926–3941
127. Cellot G, Toma FM, Kasap Varley Z, Laishram J, Villari A, Quintana M et al (2011) Carbon nanotube scaffolds tune synaptic strength in cultured neural circuits: novel frontiers in nanomaterial-tissue interactions. *J Neurosci* 31:12945–12953
128. Lovat V, Pantarotto D, Lagostena L, Cacciari B, Grandolfo M, Righi M et al (2005) Carbon nanotube substrates boost neuronal electrical signaling. *Nano Lett* 5:1107–1110
129. Mazzatenta A, Giugliano M, Campidelli S, Gambazzi L, Businaro L, Markram H et al (2007) Interfacing neurons with carbon nanotubes: electrical signal transfer and synaptic stimulation in cultured brain circuits. *J Neurosci* 27:6931–6936
130. Hore MJA, Laradji M (2008) Prospects of nanorods as an emulsifying agent of immiscible blends. *J Chem Phys* 128: 054901
131. Russell RA, Foster LJR, Holden PJ (2018) Carbon nanotube mediated miscibility of polyhydroxyalkanoate blends and chemical imaging using deuterium-labelled poly(3-hydroxyoctanoate). *Eur Polym J* 105:150–157

132. Russell RA, Darwish TA, Puskar L, Martin DE, Holden PJ, Foster LJR (2014) Deuterated polymers for probing phase separation using infrared microspectroscopy. *Biomacromol* 15:644–649
133. Hassarati RT, Foster LJR, Green RA (2016) Influence of biphasic stimulation on olfactory ensheathing cells for neuroprosthetic devices. *Front Neurosci* 10:article 432
134. Gentile P, Chiono V, Carmagnola I, Hatton P (2014) An overview of poly(lactic-co-glycolic acid (PLGA)-based biomaterials for bone tissue engineering. *Int J Mol Sci* 15:3640–3659
135. Baliga A, Borkar S (2016) A review of the 3D designing of scaffolds for tissue engineering with a focus on keratin protein. Preprints 2016090091
136. Rouse JG, Van Dyke ME (2010) A review of Keratin-based biomaterials for biomedical applications. *Materials (Basel)* 3:999–1014
137. Verma V, Verma P, Ray P, Ray AR (2008) Preparation of scaffolds from human hair proteins for tissue-engineering applications. *Biomed Mater* 3: 025007
138. Reichl S (2009) Films based on human hair keratin as substrates for cell culture and tissue engineering. *Biomaterials* 30:6854–6866
139. Hartrianti P, Ling L, Goh LMM, Ow KSA, Samsonraj RM, Sow WT et al (2015) Modulating mesenchymal stem cell behavior using human hair Keratin-coated surfaces. *Stem Cells Int* Article ID 752424
140. Borrelli M, Joepen N, Reichl S, Finis D, Schoppe M, Geerling G et al (2015) Keratin films for ocular surface reconstruction: evaluation of biocompatibility in an in-vivo model. *Biomaterials* 42:112–120
141. Passipieri JA, Baker HB, Siriwardane M, Ellenburg MD, Vadhavkar M, Saul JM et al (2017) Keratin hydrogel enhances In Vivo skeletal muscle function in a rat model of volumetric muscle loss. *Tissue Eng Part A* 23:556–571
142. Hajiali H, Karbasi S, Hosseinalipour M, Rezaie HR (2010) Preparation of a novel biodegradable nanocomposite scaffold based on poly (3-hydroxybutyrate)/bioglass nanoparticles for bone tissue engineering. *J Mater Sci Mater Med* 21:2125–2132
143. Sadeghi D, Karbasi S, Razavi S, Mohammadi S, Shokrgozar MA, Bonakdar S (2016) Electrospun poly(hydroxybutyrate)/chitosan blend fibrous scaffolds for cartilage tissue engineering. *J Appl Polym Sci* 133:44171
144. Karbasi MZS (2018) Evaluation of the effects of multiwalled carbon nanotubes on electrospun poly(3-hydroxybutyrate) scaffold for tissue engineering applications. *J Porous Mater* 25: 259–272
145. Haider A, Haider S, Kang I-K (2018) A comprehensive review summarizing the effect of electrospinning parameters and potential applications of nanofibers in biomedical and biotechnology. *Arab J Chem* 11:1165–1188
146. Cheng Y, Ramos D, Lee P, Liang D, Yu X, Kumbar SG (2014) Collagen functionalized bioactive nanofiber matrices for osteogenic differentiation of mesenchymal stem cells: bone tissue engineering. *J Biomed Nanotechnol* 10:287–298
147. Ahmed FE, Lalia BS, Hashaikh R (2015) A review on electrospinning for membrane fabrication: challenges and applications. *Desalination* 356:15–30
148. Khorshidi S, Solouk A, Mirzadeh H, Mazinani S, Lagaron JM, Sharifi S et al (2016) A review of key challenges of electrospun scaffolds for tissue-engineering applications. *J Tissue Eng Regen Med* 10:715–738
149. Zarei M, Tanideh N, Zare S, Aslani FS, Koohi-Hosseinabadi O, Rowshanghias A et al (2020) Electrospun poly(3-hydroxybutyrate)/chicken feather-derived keratin scaffolds: Fabrication, in vitro and in vivo biocompatibility evaluation. *J Biomater Appl* 34:741–752
150. Pheng Low S, Ying Liu J, Wu P (2009) Sustainable facilities: Institutional compliance and the Sino-Singapore Tianjin Eco-city Project. *Facilities* 27:368–386
151. Christian SJ, Billington SL (2011) Mechanical response of PHB- and cellulose acetate natural fiber-reinforced composites for construction applications. *Compos Part B Eng* 42:1920–1928
152. Abdul Khalil HPS, Bhat AH, Ireana Yusra AF (2012) Green composites from sustainable cellulose nanofibrils: a review. *Carbohydr Polym* 87:963–979

153. Mohanty AK, Misra M, Drzal LT (2005) Natural fibers, biopolymers, and biocomposites. In: Mohanty AK, Misra M, Drzal LT (eds). CRC Press, Boca Raton, FL, 896 p
154. Jonh M, Thomas S (2008) Biofibres and biocomposites. *Carbohydr Polym* 71:343–364
155. Dicker MPM, Duckworth PF, Baker AB, Francois G, Hazzard MK, Weaver PM (2014) Green composites: a review of material attributes and complementary applications. *Compos Part A Appl Sci Manuf* 56:280–289
156. Yan L, Chouw N (2013) Experimental study of flax FRP tube encased coir fibre reinforced concrete composite column. *Constr Build Mater* 40:1118–1127
157. Yan L, Chouw N, Jayaraman K (2014) Effect of column parameters on flax FRP confined coir fibre reinforced concrete. *Constr Build Mater* 55:299–312
158. Yan L, Su S, Chouw N (2015) Microstructure, flexural properties and durability of coir fibre reinforced concrete beams externally strengthened with flax FRP composites. *Compos Part B Eng* 80:343–354
159. CoDyre L, Mak K, Fam A (2018) Flexural and axial behaviour of sandwich panels with bio-based flax fibre-reinforced polymer skins and various foam core densities. *J Sandw Struct Mater* 20:595–616
160. Mak K, Fam A, MacDougall C (2015) Flexural behavior of sandwich panels with bio-FRP skins made of flax fibers and epoxidized pine-oil resin. *J Compos Constr* 19:04015005
161. Yan L, Chouw N, Huang L, Kasal B (2016) Effect of alkali treatment on microstructure and mechanical properties of coir fibres, coir fibre reinforced-polymer composites and reinforced-cementitious composites. *Constr Build Mater* 112:168–182
162. Sealy C (2015) How green are cellulose-reinforced composites? *Mater Today* 18:531
163. Abdul HPS, Jawaid M, Hassan A, Paridah MT, Zaido A (2012) Oil palm biomass fibres and recent advancement in oil palm biomass fibres based hybrid biocomposites. In: Hu N (ed) *Composites and their applications*. InTech
164. Hervy M, Evangelisti S, Lettieri P, Lee K-Y (2015) Life cycle assessment of nanocellulose-reinforced advanced fibre composites. *Compos Sci Technol* 118:154–162
165. Wool RP (2005) Polymers and composite resins from plan oils. In: Wool R, Sun XS (eds) *Bio-based polymers and composites*. Elsevier, pp 56–113
166. Faruk O, Bledzki AK, Fink H-P, Sain M (2012) Biocomposites reinforced with natural fibers: 2000–2010. *Prog Polym Sci* 37:1552–1596
167. Fowler PA, Hughes JM, Elias RM (2006) Biocomposites: technology, environmental credentials and market forces. *J Sci Food Agric* 86:1781–1789
168. Terzopoulou ZN, Papageorgiou GZ, Papadopoulou E, Athanassiadou E, Alexopoulou E, Bikiaris DN (2015) Green composites prepared from aliphatic polyesters and bast fibers. *Ind Crops Prod* 68:60–79
169. Mohanty AK, Misra M, Drzal LT (2002) Sustainable bio-composites from renewable resources: opportunities and challenges in the green materials world. *J Polym Environ* 10:19–26
170. Wong S, Shanks R, Hodzic A (2002) Properties of poly(3-hydroxybutyric acid) composites with flax fibres modified by plasticiser absorption. *Macromol Mater Eng* 287:647–655
171. Yan L, Chouw N (2014) Natural FRP tube confined fibre reinforced concrete under pure axial compression: a comparison with glass/carbon FRP. *Thin-Walled Struct* 82:159–169
172. Yan L, Chouw N, Jayaraman K (2014) Effect of triggering and polyurethane foam-filler on axial crushing of natural flax/epoxy composite tubes. *Mater Des* 56:528–541
173. Foulk J, Akin D, Dodd R, Ulven C (2011) Production of flax fibers for biocomposites. In: Kalia S, Kaith BS, Kaur I (eds) *Cellulose fibers: bio- and nano-polymer composites*. Springer, Berlin, pp 61–95
174. Foulk JA, Rho D, Alcock MM, Ulven CA, Huo S (2011) Modifications caused by enzyme-retting and their effect on composite performance. *Adv Mater Sci Eng Article ID* 179023
175. Akil HM, Omar MF, Mazuki AAM, Safiee S, Ishak ZAM, Abu BA (2011) Kenaf fiber reinforced composites: a review. *Mater Des* 32:4107–4121
176. Karger-Kocsis J (2000) Reinforced polymer blends. In: Paul DR CBB (eds) *Polymer blends*. Wiley, NY, USA, pp 395–428

177. Fu S-Y, Xu G, Mai Y-W (2002) On the elastic modulus of hybrid particle/short-fiber/polymer composites. *Compos Part B Eng* 33:291–299
178. Jawaid M, Abdul Khalil HPS (2011) Cellulosic/synthetic fibre reinforced polymer hybrid composites: a review. *Carbohydr Polym* 86:1–18
179. Jawaid M, Abdul Khalil HPS, Abu BA (2011) Woven hybrid composites: tensile and flexural properties of oil palm-woven jute fibres based epoxy composites. *Mater Sci Eng A* 528:5190–5195
180. Zainudin ES, Yan LH, Haniffah WH, Jawaid M, Alothman OY (2014) Effect of coir fiber loading on mechanical and morphological properties of oil palm fibers reinforced polypropylene composites. *Polym Compos* 35:1418–1425
181. Hariharan ABA, Khalil HPSA (2004) Influence of oil palm fibre loading on the mechanical and physical properties of glass fibre reinforced epoxy bi-layer hybrid laminated composite. In: *Proceeding of 3rd USM-JIRCAS joint international symposium*. Penang, Malaysia, pp 230–233
182. Hariharan ABA, Khalil HPSA (2005) Lignocellulose-based Hybrid bilayer laminate composite: Part I—studies on tensile and impact behavior of oil palm fiber-glass fiber-reinforced epoxy resin. *J Compos Mater* 39:663–684
183. Khoshnava SM, Rostami R, Ismail M, Rahmat AR, Ogunbode BE (2017) Woven hybrid Biocomposite: mechanical properties of Woven Kenaf bast fibre/oil palm empty fruit bunches hybrid reinforced poly hydroxybutyrate biocomposite as non-structural building materials. *Constr Build Mater* 154:155–166
184. Wang L, Zhu W, Wang X, Chen X, Chen G-Q, Xu K (2008) Processability modifications of poly(3-hydroxybutyrate) by plasticizing, blending, and stabilizing. *J Appl Polym Sci* 107:166–173
185. Garcia MA, Martino MN, Zaritzky NE (2000) Lipid addition to improve barrier properties of edible starch-based films and coatings. *J Food Sci* 65:941–944
186. Choi JS, Park WH (2004) Effect of biodegradable plasticizers on thermal and mechanical properties of poly(3-hydroxybutyrate). *Polym Test* 23:455–460
187. Agrawal R, Saxena N, Sharma K, Thomas S, Sreekala M (2000) Activation energy and crystallization kinetics of untreated and treated oil palm fibre reinforced phenol formaldehyde composites. *Mater Sci Eng A* 277:77–82
188. Hasan A, Waibhaw G, Saxena V, Pandey LM (2018) Nano-biocomposite scaffolds of chitosan, carboxymethyl cellulose and silver XE “Silver” nanoparticle modified cellulose nanowhiskers for bone tissue engineering applications. *Int J Biol Macromol* 111:923–934
189. Liu H, Wang D, Song Z, Shang S (2011) Preparation of silver nanoparticles on cellulose nanocrystals and the application in electrochemical detection of DNA hybridization. *Cellulose* 18:67–74
190. Liu H, Song J, Shang S, Song Z, Wang D (2012) Cellulose nanocrystal/silver nanoparticle composites as bifunctional nanofillers within waterborne polyurethane. *ACS Appl Mater Interfaces* 4:2413–2419
191. Costa LMM, de Olyveira GM, Basmaji P, Filho LX (2011) Bacterial cellulose towards functional green composites materials. *J Bionanosci* 5:167–172
192. de Lima FM, Meneguín AB, Tercjak A, Gutierrez J, Cury BSF, dos Santos AM et al (2018) Effect of in situ modification of bacterial cellulose with carboxymethylcellulose on its nano/microstructure and methotrexate release properties. *Carbohydr Polym* 179:126–134
193. Jalili Tabaii M, Emtiazi G (2018) Transparent nontoxic antibacterial wound dressing based on silver nano particle/bacterial cellulose nano composite synthesized in the presence of tripolyphosphate. *J Drug Deliv Sci Technol* 44:244–253
194. Galateanu B, Bunea M-C, Stanescu P, Vasile E, Casarica A, Iovu H et al (2015) In Vitro studies of bacterial cellulose and magnetic nanoparticles smart nanocomposites for efficient chronic wounds healing. *Stem Cells Int Article ID* 195096
195. Gałuszka A, Migaszewski Z, Namieśnik J (2013) The 12 principles of green analytical chemistry and the SIGNIFICANCE mnemonic of green analytical practices. *TrAC—Trends Anal Chem* 50:78–84

Polymer/Carbon Nanocomposites for Biomedical Applications



Jyotendra Nath, Kashma Sharma, Shashikant Kumar, Vijay Kumar,
and Rakesh Sehgal

Abstract The technological need for novel and intelligent materials as well as the drive for basic understanding has led to noteworthy progress in the field of polymer science. The current interest in polymer matrix-based nanocomposites (NCs) has materialized mainly due to research including exfoliated clay, carbon nanotubes (CNTs), carbon nanofillers, graphene, nanocrystalline metals, and a host of additional nanoscale inorganic fillers. This chapter presents a comprehensive survey of the existing and current literature on different aspects of CNTs, their NCs with polymeric materials and their biomedical applications. This chapter also highlights a variety of methods used to produce CNTs polymer nanocomposites, along with their characterization techniques. Polymer nanocomposites (PNCs) based on CNTs offer remarkably improved mechanical, electrical, and sensing properties. All this justifies the emergent interest in both academia and industrial development. Likewise, the present status and upcoming possibilities of CNT/PNCs are examined in general along with appropriate examples drawn from existing literature.

Keywords Carbon nanotubes · Polymers · Nanocomposites · Drug delivery · Tissue engineering · Biomedical

J. Nath · S. Kumar

Department of Chemical Engineering, National Institute of Technology Srinagar, Srinagar, Jammu and Kashmir 190006, India

K. Sharma

Department of Chemistry, DAV College, Sector-10, Chandigarh 160014, India

V. Kumar (✉)

Department of Physics, National Institute of Technology Srinagar, Srinagar, Jammu and Kashmir 190006, India

R. Sehgal (✉)

Department of Mechanical Engineering, National Institute of Technology Srinagar, Srinagar, Jammu and Kashmir 190006, India

1 Introduction

As cutting-edge innovations keep on developing every day, there is a consistent need for novel materials such as polymers, ceramics, glasses, nanomaterials, hybrid materials, and colloidal materials with unusual properties and/or combinations of distinctive properties. In the pursuit of modified and improved properties of polymers, numerous endeavors have been made for the last few decades utilizing novel nanotechnology and nanoscience information to get novel materials with improved properties which in turn may be used in various applications including energy generation and storage [1], engineering and construction [2], electronics [3, 4], display technologies [5], food packaging [6, 7], and environmental and biomedical applications [8], etc. In the sector of nanoscience and nanotechnology, polymer matrix-based nanocomposites (NCs) have created noteworthy attention in recent years. Polymer nanocomposites (PNCs) have revolutionized the research attempt in the field of composites as they lead to the realization of synergistic properties from the organic and inorganic components of the system and have led to the growth of the spectrum of application of the commodity polymers to innovative end products [9, 10]. These NCs offer the prospect of significant enhancements in materials properties. Nanoscience and nanotechnology are widely seen as having vast prospects in various fields of science and technology (viz, chemical, physical, and biological, to medicine, engineering, and electronics) [11, 12]. The prefix “nano” is denoted to a Greek prefix meaning “dwarf” or something very small and is equal to one-billionth of a meter, 10⁻⁹ m [11, 12]. As a correlation, one must understand that a single human hair is 60,000 nm thickness and the DNA double helix has a radius of 1 nm (Fig. 1) [12].

Nanotechnology is the study and fine-tuning of materials at molecular, atomic, and macromolecular scales, where properties change much from those at the micro-scale. As researchers use more advanced control over the molecular level organization, the morphology of materials is a very important factor. Hence, the evolution from micro-

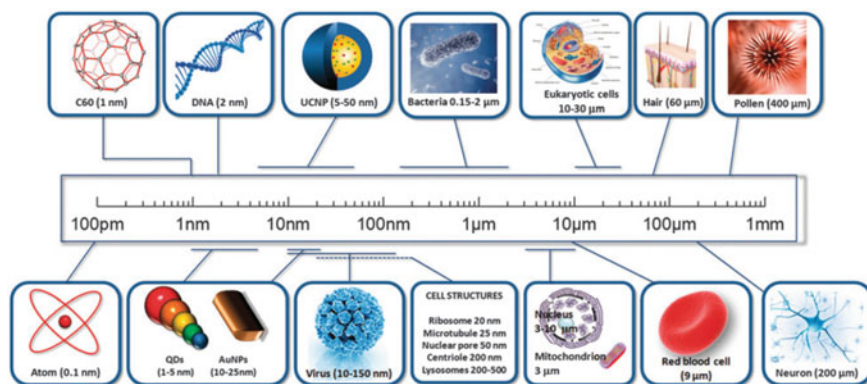
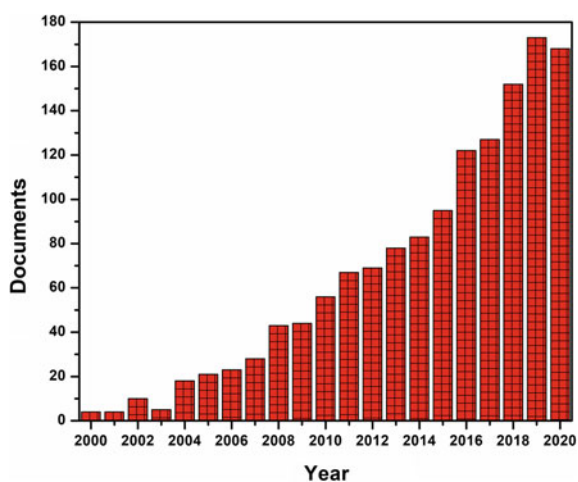


Fig. 1 The size of lanthanide-doped nanoparticles referenced to other, biologically. [Reprinted with permission from Ref. [1]. Copyright (2011) The Royal Society of Chemistry

to nanoparticles led to a desirable alteration in its physical and chemical properties. The properties of nanoparticles can arise from two important factors: first the increase in the ratio of the surface area to volume (S/V) and second, the size of the particle. The higher surface to volume ratio decreases the particle size thereby affects the overall material properties and this higher S/V ratio of nanoparticles also enhances the reactivity with the other particles which results in the increases in strength, heat resistance, etc. K. Eric Drexler was the first person to popularize this technology in the early 1980s [13]. Thereafter, nanotechnology becomes a key thrust area to enable new science and exploration of new technologies. Recently, NCs emerged as a new field of research and maturity in the physical as well as in medical sciences which intended the foundation of new and smart materials for use in advanced technological applications. NCs material has categorized appreciably to include a number of systems such as 1-D, 2-D, 3-D, and amorphous materials, made of clearly different components and blended at the nanometer scale. The noteworthy attempt is centered around the ability to deal with the nanoscale structures via novel synthesis methods. The properties of NCs depend not just on the properties of their every counterpart but also on their morphology and interfacial features. This fast-growing field is creating many fascinating novel materials. There is also the prospect of interesting properties that are unidentified in their parent counterparts. Polymer-based NCs have been a sign of a new paradigm for materials since the 1960s [14].

To date, a large number of published papers on polymer-based NCs have increased progressively since 2000 (Fig. 2) [15–34]. However, PNCs based on carbon nanotubes (CNTs) have been the subject of many types of research for decades. Now a day's these are the most widely used nanofillers in various matrices. Numerous studies on NCs elaboration and characterization have been observed with all polymer families. CNTs-reinforced PNCs have good attraction properties, but this depends on their fabrication method. The shape, size, interaction, dispersion, and orientation of CNTs play an important role in the production of CNTs-reinforced PNCs [35].

Fig. 2 Number of research papers available on the use of various PNCs for wide range of applications per year from 2000 to 2020 extracted from Scopus with the keywords “Polymer-based nanocomposites”



The extensive use of polymers benefits from their excellent blending properties, lightweight, and ease of handling. In any case, many substances are added to the polymer matrix and polymer compounds are formed to develop specific properties, such as heat resistance and mechanical resistance. The NCs are characterized by a blend of at least two materials with different physical and chemical properties and a recognizable interface. Compared to many metallic compounds, important concerns of composites are high specific stiffness and strength, high hardness, corrosion resistance, low density, and thermal insulation properties [36–38]. Thus, the focus of this chapter is to describe the recent progress in polymer (viz. polystyrene, polyethylene, and polyvinyl) NCs based on CNTs. In this section, a meticulous discussion of the developments made in the polymer/CNTs NCs is presented. A portion of the properties of these materials that have specific importance in the utilization of these materials in the biomedical fields is also summed up. The motive of the introduction part is to give adequate information to comprehend the importance of CNTs and their NCs with polymeric materials. The aim of this chapter is not to cover all the documented literature, but rather to check some of the most important accomplishments in this direction. The second part deals with the structure and properties of CNTs. In the third section, various synthesis methods of CNTs such as arc discharge, laser ablation, and chemical vapor deposition are included. The fourth part comprises brief information about polymer matrix and the related properties suitable for the synthesis of NCs with various nanomaterials. In the fifth section, the preparation of CNTs-based PNCs is discussed. The sixth section will incorporate the biomedical applications (viz. drug delivery and tissue engineering) of polymer/CNTs nanocomposites. Conclusion and opportunities for the future improvement of polymer/CNTs-based NCs are presented at the end.

2 Structure and Properties of Carbon Nano Tubes (CNTs)

CNTs have drawn the attention of many scientists due to their important physical, chemical, and biological properties [39]. CNTs consist of a moving graphite sheet covered with a hemispherical structure whose curves are formed by pentagonal and hexagonal rings. CNTs have a hollow cylindrical one-dimensional structure. CNTs immobilize carbon molecules within the ring, which gives them high strength and mechanical properties. Nanotubes have excellent electrical conductivity. Due to the dislocation of electrons in the hexagonal structure of the carbon ring, the charge of electrons in the nanotubes can develop freely. CNTs also have tremendous thermal conductivity due to the vibration of the carbon atoms in the CNTs, which allow them to conduct heat [40]. CNTs can be classified into two types based on the number of carbon layers they contain. CNTs are also classified as single-walled nanotubes (SWNTs) and multi-walled nanotubes (MWNTs). Single-walled carbon nanotubes (SWCNTs) consist of a single-walled graphite layer with a diameter of 0.4–2 nm, usually in the form of a hexagonal bundle. In 1960, Roger Bacon first discovered micron-sized carbon tubes that were structurally equivalent to the

new multi-walled carbon nanotubes (MWCNTs). The first nanotubes observed were multilayer MWCNTs consisting of circular hollow graphite sheets of at least two concentric shells arranged coaxially around a hollow core, with graphitic (0.34 nm) spacing between the layers. MWCNTs consist of two or more cylindrical graphite flakes. Their diameters range from 1 to 3 nm [41] and as a result, they have a high aspect ratio (132 000 000:1). This makes them excellent candidates for various applications. There are three unique geometries of CNTs and these are also called flavors [40]. The three flavors are armchair, zigzag, and chiral. Because nanotubes can be both semiconductors and metallic subject to the diameter and “twist” they exhibit extremely fascinating characteristics. CNTs are classified into three categories: zigzag, armchair, and chiral, depending on the arrangement of the contained carbon and the properties of CNTs differ according to these arrangements [40].

CNTs have outstanding chemical and physical properties such as tensile strength, ultra-lightweight, special electronic structure, and high chemical and thermal stability. Researchers have shown great interest in these nanomaterials due to some special properties [42]. CNTs have excellent electrical, mechanical, and thermal properties due to their high S/V ratio. Theoretical and experimental results show that CNTs has Young’s modulus of up to 1500 GPa/1.5 TPa and very high tensile strength of 50–500 Gpa unusual mechanical properties of CNTs [43, 44]. Experimental techniques such as SEM, TEM, AFM, and Raman spectroscopy, as well as theoretical models such as ab initio models, molecular dynamics, and continuum models were used to explain the various properties of CNTs [45–50]. The young modules of SWNTs and MWNTs were measured by micro-Raman spectroscopy in the temperature range of 2.8–3.6 TPa and 1.7–2.4 TPa by various authors [45, 46]. They found to have high stiffness, high modules, very low density of 1.3 gm/cm³, higher strength than iron, and at the same time lighter weight [45, 46]. Besides their mechanical properties, the theoretical electrical properties of the SWNTs were also studied. It was concluded that the diameter and chiralities of the tubes and SWNTs can be metallic or semiconducting [51, 52]. CNTs can be semiconductors or metals depending on their shape. It has been shown that about 66% of them are semiconductors and the rest are metals; the conductivity of CNTs depends on the shape of the tube [51–55], and the conductivity of each CNTs ranges from 10⁴ to 10⁷ s/m [56, 57], and the conductivity of MWNTs has been measured with four probes in the 10⁷–10⁸ s/m range [53]. The resistivity of metal CNTs is usually in the range of 10⁻⁸–10⁻⁷ Ωm [58]. SWCNTs form a network of contact blocks [59–61]. The formation of the contact block depends on the length, diameter, and structural configuration of the nanotube. Connecting molecules within the framework of the medium or matrix increase the adhesion of the molecular center. In both cases, the electrical tunneling effect leads to a stronger grounded shell and decreases the electrical conductivity of the material. Nanotube corrugations play a vital role in controlling the electrical conductivity of CNTs [54], and they have some benefits over other carbon materials in terms of electrical and thermal properties.

3 Synthesis of CNTs

CNTs are mostly fabricated by three primary techniques: arc discharge, laser ablation, and chemical vapor deposition [62]. However, researchers are exploring more cost-effective ways to synthesize these structures. A brief overview of each synthesis method is given below.

3.1 Arc-Discharge Method

The arc-discharge technique is the one by which CNTs were first synthesized and documented [63]. The historical backdrop of CNTs is firmly identified with the large-scale manufacturing of fullerenes produced by Krätschmer and coworkers [64]. This method uses two carbon electrodes connected to an energy source of roughly 50–100 A and a potential difference of approximately 20 V. The best results were obtained in the presence of an inert gas, which is probably due to the high ionization potential of helium (He). In the presence of the inert gas, the helium accelerates the deposition of carbon and once the pressure is adjusted, the current is switched on. The positive electrode near the negative anode fills the electrical curve. This causes the electrode to turn red and hot, producing plasma. As the arc settles, the rods remain slightly apart and the carbon nanotubes gather at the negative electrode. When a certain distance is touched, the current is cut off and the discharge is cooled. The process allows the formation of MWCNTs and SWCNTs. The resulting MWCNTs are measured over a wide range of different microns. At the preferred position, the framework MWCNTs crystallize anomalously and are surrounded by van der Waals forces [65–68].

3.2 Laser Ablation Method

The synthesis of SWNT by laser ablation method was described for the first time by Smalley and his colleagues in 1995 [69]. Laser ablation is the vaporization of graphite containing a few metal catalysts (Co, Ni) in an electric laser furnace at an extremely high temperature of 1200 °C and the constant pressure of 500 Torr in the presence of inert gas. The resulting SWCNTs were formed in uniform strands or bundles with diameters of 10–20 nm, while the length of the tubes was about 100 μm and evolved into multilayered thin films using a high vacuum ablation layer. The properties of the formed CNTs depend on the catalyst, laser power, inert gas, temperature, and pressure; the byproducts formed during the synthesis are fullerenes and graphite polyhedron [70, 71].

3.3 Chemical Vapor Deposition Method (CVD)

CVD is normally used for large-scale production of CNTs [63]. The disintegration of hydrocarbons into CNTs requires high temperatures at atmospheric pressure (500–750 °C) and enough energy, but with the use of hydrocarbons such as CH₄, C₂H₂, and CO as carbon sources, CNTs can be obtained [53]. The chemical deposition of C₂H₂ using cobalt or iron as catalysts and silica as support allows the synthesis of many CNTs. A mixture of hydrogen and CH₄ dispersed in a metal catalyst with MgO as solid support was used to produce CNTs in high yields. This synthesis was carried out by CVD using microwave energy [72]. Subsequently, other changes were made to this method. Plasma-enhanced chemical vapor deposition (PECVD) is a commonly used technique for the synthesis of CNTs [73].

4 Polymer Matrix

A “composite material” is a mixture of materials with unique physical and chemical properties at the macroscopic level [74]. The resulting materials generally have properties that are not identical to those of the individual components. Through the use of composites, properties such as mass, resistance to high temperatures, consumption, extreme temperature conditions, and the required coefficient of thermal expansion can be achieved. Composites consist of two phases, the matrix is usually a continuous phase, and the different phases incorporated into this matrix are called “reinforcements”. Several interesting mixtures of these meshes (e.g., polymers, carbon, metals, and ceramics) and reinforcements (e.g., particles, wires, and laminates) have been used to combine different composites and NCs [75]. Polymers are generally reinforced with different dosing levels to ease the expansion of applications to include specific polymers. The use of nanofillers to improve the mechanical and physical properties of polymers has led to the extreme neglect of traditional polymer composites. In any case, nanoscale fillers are characterized by the desired size at the nanoscale, which is fundamentally different from isotropic and planar or highly anisotropic needle-like forms. Nanoscience and nanotechnology have generated special opportunity costs for the production of progressive mixtures of nanocomposite fillers and polymers to get attractive PNCs [76, 77].

The establishment of PNCs as nanotechnology has generated extraordinary logical interest and found widespread applications from toys to aircraft. By definition, PNCs are polymers that are reinforced with nanomaterials, such as nanofillers. In the case of polymer nanocomposites, the most important consideration is the dispersion of the nanofillers in the polymer matrix. The uniform cycling of the nanofillers improves the properties of the resulting polymer nanocomposites. However, the solid van der Waals forces between the particles tend to agglomerate the nanomaterials, which lead

to degradation of the polymer nanocomposites. It has been established that nanomaterials can be functionally modified on the surface to improve the dispersion of nanomaterials in the polymer matrix. Surface modification and functionality of nanomaterials improve the interfacial cooperation or similarity between the polymer matrix and the filler, resulting in better dispersion and thus producing high-performance nanocomposite applications [78]. Polymer nanoscience is the field of research and use of nanoscience's identified by polymeric nanoparticle matrices. These types of compounds consist of polymers dispersed in a polymer matrix with nanofillers. The development from a small scale to the nanoscale has proved to be one of the properties due to the extreme changes in the physical and composite structure of each molecule. When these particles react with other molecules, this has an extraordinary effect on their properties. Since nanoparticles have a large surface area, they are more likely to cooperate with different types of particles within them. This increases their mechanical resistance, thermal resistivity, and many other confounding factors [79]. Nanoparticles such as graphene, CNTs, MoS₂, and WS₂ are increasingly being employed as reinforcement agents for the synthesis of biodegradable and mechanically strong polymeric NCs for bone tissue engineering [80, 81]. The study of CNTs has unlocked new spaces for the development of polymer matrix compounds with innovative properties and applications. The most commonly reported nanofibers for the fire resistance of polymers are CNTs. The very small diameter and high aspect ratio of CNTs make them ideal for improving the properties of polymer matrices. CNTs have been used to improve the properties of traditional flame retardants and nanoclay. It has gained a lot of consideration as an alternative. It has been documented to enhance the flammability of a large number of polymers by incorporating it at a low loading ratio (<3% by weight) [82, 83]. The fillers are used to reinforce the polymer matrix in a range of sizes. The degree of reinforcement is clear in the molecular size range below 100 nm [84]. Reinforcement materials used to form PNCs can be ranked according to their shape and size [85–88]. The second type of reinforcement consists of a framework of nanotubes with two-dimensional massive shapes and nanoscale elongated structures. Nanoclay, graphene, and cellulose wastes also constitute the second type. The third type of reinforcement is described by a single dimension of nano-regions [89–92]. These nanometers contain extended one-dimensional structures and are reinforced with nanofibers or nanotubes, such as carbon nanofibers and CNTs, or halogen nanotubes as reinforced nanofillers, to make sure excellent properties of the material [93, 94].

5 Preparation of CNTs-Based Polymer Nanocomposites

Polymeric compounds are in high demand in many modern applications, such as electrical protection materials, insulating materials, and high-performance compounds in the automotive and aerospace sectors, although these compounds have certain limitations. CNTs in polymer compounds can achieve better reinforcement when the total amount of CNTs is not compatible, and in general, CNTs need to be well

dispersed in the polymer matrix. Several techniques are available to increase the distribution of CNTs in the polymer matrix, such as solution blending, melting and in situ polymerization.

5.1 Solution Mixing

Solution mixing or solvent molding is a process for producing composite materials such as graphite, nanotubes, and polymers. It is the simplest and most widely used process for CNT/PNCs, where CNTs and polymers are mixed with an appropriate solvent, and the solvent is evaporated to a controlled state after forming an NC film on the substrate surface. Thermoplastic and thermoset materials have been produced; a variety of polymers processed in this way include PMMA, polyethylene (PE), polyhydroxy amino ether (PHAE), polyvinyl alcohol (PVA), polystyrene (PS), PEO, and epoxy resins with CNT added [95–99]. It is well documented that it is hard to completely disperse intact CNTs in solvents by simple agitation, and high-power ultrasonic methods are more effective in forming CNT dispersions. Ultrasonic irradiation is widely used for dispersion, emulsification, comminution, and activation of particles. Investigating the multiple effects of ultrasound is effective in decomposing aggregated and entangled CNTs [100]. CNTs in polystyrene matrix were dispersed after ultrasonic stirring at 300 W for 30 min and ultrasonic treatment can be used to get a uniform dispersion of CNTs in PS [97, 101]. Some studies have shown that the surface modification of CNTs is achieved by adding functional groups to obtain the correct dispersion. However, there may be compatibility issues between the functional groups and the polymer matrix. Another approach is electrospinning, which involves treating polymer fibers in the presence of an electric field [102–105].

5.2 Melt Mixing

Solvent blending is one of the most efficient and eco-friendly techniques in the production of composites. The composition is usually performed in a single-screw or twin-screw extruder, where a mixture of polymer and nanoparticles is heated to form a solution. Compounds are subjected to cutting and tensile stresses during processing to help decompose some of the filler aggregates and offer uniform dispersion in the polymer matrix; MWCNTs and SWCNTs provide better dispersion. When mixing solutions, it is always better to use a dissolved polymer matrix. Melting is a general and simple technique that is mainly suitable for thermoplastic polymers such as polystyrene, polypropylene, polycarbonate, thick polyethylene, polyamide, polyoxyethylene, and polyesters [106–111]. This technique involves dissolving the polymers into a viscous liquid, which is then mixed with CNTs. The shear mixture obtained by extrusion or injection improves the dispersion of the CNTs [106, 112, 113]. During softening, a high temperature shear mixer is used to mechanically

disperse the CNTs into the polymer matrix [114]. Polymers with suitable sleeves can react with useful sleeves in the nanotubes to improve the dispersion [115]. Tension flow is preferred over shear flow to disperse the nanotubes [116]. One of the obstacles to this technique is that the dispersion of CNTs in the polymer matrix is very low compared to the dispersion that may be obtained by mixing solutions. Due to the high viscosity of the compounds, stacking the CNTs higher should result in lower CNTs [56].

5.3 *In Situ Polymerization*

Several polymerized CNT compounds have been synthesized by in situ polymerization method. This method can be used for both thermoplastic and thermosetting materials. In this method, the CNTs are dispersed in the presence or absence of solvent and then polymerized. Monomers and non-polymers are used as raw materials in this process. The higher content of CNTs is effectively dispersed by this method and can form a strong bond with the polymer matrix. One of the advantages of this method is that the polymer molecules can be grafted onto the walls of the cylinder, resulting in better dispersion coefficients and better coordination between the CNTs and the polymer matrix. This method is useful, such as for placing compounds with polymers that cannot be treated by the matrix or polymers with mixtures of insoluble and thermally unstable polymers that soften the polymer that cannot be treated by the matrix. Several studies have been performed on polystyrene, polyurethane, polyethylene, PMMA, PU, PCL, nylon, and epoxy [117–127].

6 Polymer/Carbon Nanotube Nanocomposites

6.1 *Polystyrene/CNT*

Hill et al. [106] reported the functionalization of SWCNTs and MWCNTs with a polystyrene copolymer. The functionalized CNTs are soluble in various organic solvents, which help to characterize these functionalized CNTs not only by solid-state but also by solution-based techniques. The homogeneous dispersion of CNTs within the PS network provides a model for the general expectation that the dissolution of nanotubes can lead to the desired alignment of CNTs-based PNC [106]. The effect of PS-CNT enhancement on the tribological properties of the NCs was investigated [127]. The improvement of the friction mechanism and wear of the NCs during dry-slip compared to carbon steel alone is also discussed. The CNTs used in this paper were combined with chemically catalyzed vapor deposition. The results show that when the CNT content is less than 1.5 wt%, the microhardness of the NCs is significantly improved; when the CNT content is more than 1.5 wt%,

the microhardness value slightly decreases; CNTs significantly improve the wear resistance of the NCs and reduce the coefficient of friction. It is well known that PS-CNT NCs containing 1.5% by weight of CNTs have the lowest wear rate and the lowest coefficient of friction. The decisive improvement in the tribological properties of PS-CNT NCs is due to the excellent mechanical properties of CNTs and the unique cylindrical topology. Due to the structure; the higher strength and durability of CNTs also improve the wear resistance of the NCs [127]. In the year 2005, Zhang and coworkers also reported in situ polymerization of styrene (PS) in the visible region of MWCNTs [128]. Polystyrene and MWCNTs were mixed in different solutions to prepare different types of conductive polymers. The permeation behavior and resistance to natural vapors of the compounds were investigated, focusing on their structures and test conditions to explore the feasibility of MWCNT compounds as chemical vapor recognition sensors. The polymeric filler compounds exhibited significant sensitivity to organic vapors of suitable solvents in the matrix in a short period, and the resistance was quickly restored when the examples were taken to the air and to their unique stimuli. The polymer fillers were more sensitive to organic vapors over a range of MWCNTs than compounds arranged in mixed solutions. However, changes in soluble compound/composition and solvent partial pressure by local temperature to form the most extreme electrical sensitivity of the compound reduce the rate of increase of the reaction; MWCNT/PS compounds could be candidates for gas sensors, and current research is focused on carbon nanotubes. It has the potential to create new applications [128].

The conductivity and mechanical properties of well-dispersed SWNT/PS composite were studied by Chang et al. [129]. They have used a simple technique that gives good dispersion of SWNT in a polymer matrix and studied the effect of SWNT dispersion on conductivity and mechanical properties of composites. The mechanical moduli of the annealed SWNT/PS composites are just expanded marginally and the explanation behind this discrepancy remains unclear [129]. Zhang et al. [130] reported the effect of molten blends on the interaction of MWNTs with PS matrix and discussed the mechanism of the interaction between the polymer and MWNTs. Preparation and characterization of styrene grafted SWCNT and its polystyrene nanocomposite was reported by Nayak and coworkers [131]. They have concluded that the flexural modulus, tensile strength, and electrical properties of the PS/functionalized SWCNTs composite increase by the addition of functionalized SWCNTs. This increase suggests the enhanced compatibility and dispersibility between the SWCNT and PS matrix owing to the existence of 4-vinylaniline on the surface.

The multi-step production of carbon/PS composites by using latex technology is shown schematically in Fig. 3 [132]. The MWCNTs were first ultrasonically dispersed in an aqueous solution of sodium dodecyl sulfate (SDS) sequence and then mixed with different amounts of PS latex. MWCNT/PS compounds were produced from these mixtures by freeze drying and compression molding. The aqueous solutions of MWCNT and SDS were mixed in a bottle and the resulting mixture was rung several times under mild conditions to prepare the dispersions. As SDS is enriched, the maximum absorption plateau increases, the dispersion of MWCNTs at the onset

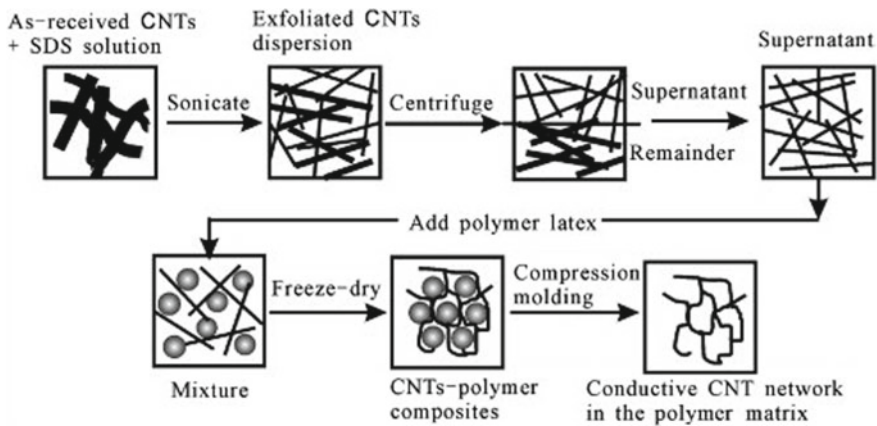


Fig. 3 Schematic description of the multi-step process for preparation of CNT/polymer composites by using latex technology. [Reproduced by permission of Elsevier from Ref. [132]]

of sonication increases, and the total energy required obtaining the most extreme dispersion of MWCNTs decreases; an organized MWCNT conductor is placed in the PS network and the amount of MWCNTs decreases. When the percolation threshold is reached, the conductivity of the compound increases extremely [114]. A grafting method was used for the functionalization of CNTs with PS [133]. The polymers were synthesized using a high vacuum anionic polymerization method, which ensures both the subatomic properties of the polymer and the presence of active carbon at the end of the polymer chain. This functionalization has been demonstrated by the reaction of the anion with carbon molecules stretched on the CNT sidewalls. The current approach is based on anionic high vacuum polymerization, which optimally controls the atomic properties of the polymer chains grafted onto the CNTs compared to the near-controlled radical polymerization. All process media were used in a high vacuum to make sure the reliability of the anions and the consistency of the bound polymer chains during the reaction. The separation and dispersion of CNTs are important in the design of PNCs/CNTs [134]. This is the main report to increase the dispersion of CNTs in aqueous arrays using Gemini cationic surfactants. It has been reported in Ref. [134] that in the prepared nanocomposites, individual MWNTs were dispersed homogeneously in the PS matrix as shown in Fig. 4. Strong van der Waals interactions are found to result in a dominant population of huge MWNTs. Here, the dispersion of the twin surfactants from toluene is remarkable, indicating that neither precipitation nor aggregation can be observed. In addition, the PS/MWNT NCs have comparable extended thermal stability to PS without failure by TEM. For the NCs with low MWNT content, an undeniable increase in modulus of 0.25% by weight was observed, which is about 12% more than the full PS at that MWNT content. This study may open up new ways for the dispersion of CNTs, including monolayer CNTs (SWNTs), in various natural solvents and could be extended to the design

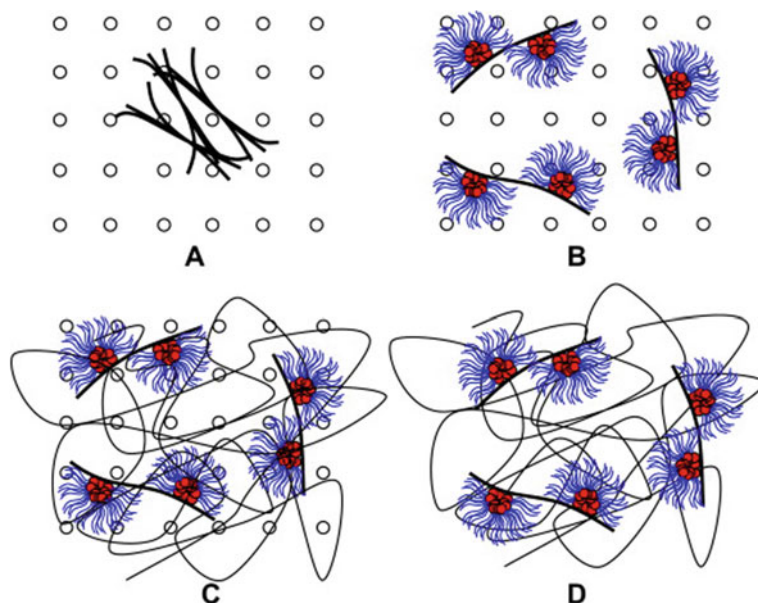


Fig. 4 Schematic representation of the preparation process of the PS/MWNT nanocomposites. [Reproduced by permission of Elsevier from Ref. [134]]

of other polymeric nanocomposites/CNTs loaded by Gemini surfactants with ideal atomic structure [134].

In another study, Sun and coworkers reported a homogeneous dispersion of MWCNTs in syndiotactic polystyrene (SPS) by a simple layering technique [135]. The reported SPS/MWCNT composites exhibit significant crystallization behavior and significantly improved thermal and electrical properties. The reported method does not involve surface modifications such as reactive oxidation, fluorination, surfactant coating, and covalent bonding, which can improve the properties, especially the thermal stability and electrical conductivity. This method can be applied to a variety of structures, including monolayer CNTs and other polymeric materials [135]. Martins and coworkers considered the effect of greater flexibility on the flow behavior of polymers and molten compounds [136]. To assess this, shear tests were performed at different temperatures on compounds with different molten polymer and nanotube concentrations. The plastic deformation rate hypothesis was applied to the flow activation in polystyrene castings and compounds with different polyvalent carbon nanotube concentrations. Perturbations induced by varying the shear rate of the monotonic test to bring the melt thickness close to homogeneity were investigated. The response of the material to the perturbation allows assessment of the amount of flow activation. In the case of pure polymers, the volume of the flow trigger is compared to the volume of the tube to which the flow is attached to confirm the validity of the cylinder model. The amount of flow activation was assessed by transient experiments with test flows of polymers and compounds fused

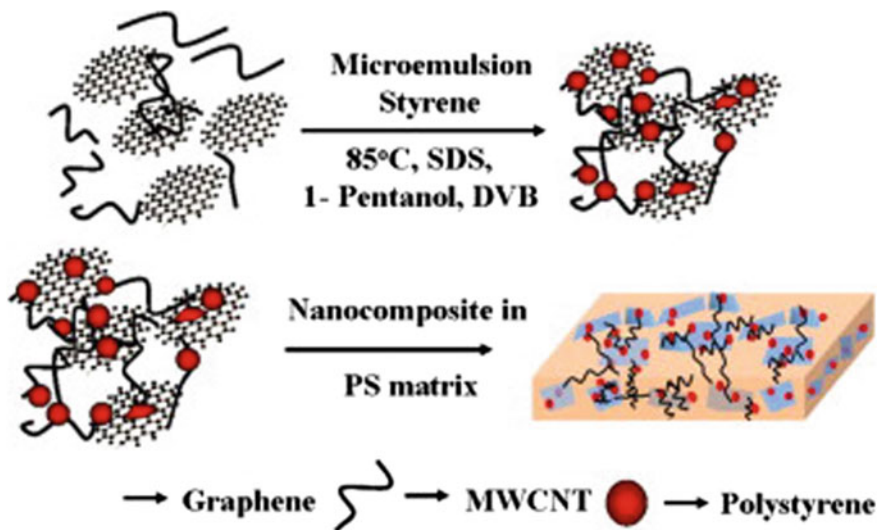


Fig. 5 Multi-step synthesis process for making the conducting graphene/MWCNT/PS films. [Reproduced by permission of Elsevier from Ref. [137]]

to carbon nanotubes. Self-assembled graphene/CNT/PS hybrid nanocomposite by in situ microemulsion polymerization was reported [137]. The complete synthesis and thin film formation are shown in Fig. 5. This new hybrid nanostructure has many prospective applications in various fields.

Raman spectroscopic study of PS nanofibers filled with MWCNTs of different sizes was reported [138]. This study focuses on embedding CNTs into electrospun polymer nanofibers to get better thermal, mechanical and electrical properties. The addition of polyaniline coated MWCNTs and uncoated MWCNTs into the PS matrix were reported by using the solution and melt mixing techniques [139]. PANi-coated MWCNTs have a lower conductivity limit (0.4 wt%) than uncoated MWCNTs (0.7 wt%) because of the better dispersion of PANi-coated MWCNTs in the PS framework. Due to the lower interfacial viability of PANI with PS, the coating resulted in better dispersion of MWCNTs in the PS framework compared to the interfacial viability of MWCNTs with PS. The gel alignment of MWCNT is smoother and rheologically permeable than that of uncoated MWCNT, characterized by interconnected rheological boundaries, such as the ratio (G/G) corresponding to the electroosmotic line [139]. Suemori and coworkers reported the in-plane and out-of-plane thermoelectric characteristics of thick CNT-PS composites prepared by the solution process [140]. They have concluded that the performance of devices that work by thermal flows along the out-of-plane direction is directly related to the orientation of the CNTs in the polymer matrix. Synthesis and mechanical properties of graphene oxide/CNTs aerogel-polystyrene composites were reported [141]. They have concluded that the current preparation technique not only solves the problem of dispersion of graphene oxide in a polymer matrix but also helps in the synthesis of

the mechanically strong composite. Conductive polymer composites (CPCs) based on polycarbonate/PS/MWCNT blends with various blend ratios were investigated and evaluated for their morphological and electrical properties [142].

6.2 Polyethylene/CNT

In recent years, CNTs offered exciting opportunities for new materials due to their excellent properties. In particular, one possible application that has attracted a great deal of attention in the materials engineering community is the incorporation of CNTs as nanofiller mainly within a polymeric matrix to form CNTs-based nanocomposites. These materials are expected to show outstanding mechanical, surface, and multifunctional, electrical, and optical properties suited for different applications [143–151]. These properties make CNTs the promising material of the twenty-first century for various applications [31–34]. In 1994, Ajayan and coworkers reported the synthesis of first PNCs using CNTs as fillers [152]. Several methods have already been developed over the last years to achieve an efficient dispersion of CNTs and some of them are already discussed in earlier sections [152–155]. This section mainly deals with polyethylene/CNTs-based nanocomposites. In this regard, McNally and coworkers reported the synthesis of polyethylene (PE) MWCNTs with various ratios of MWCNTs ranging from 0.1 to 10 wt% by melt blending using a mini twin-screw extruder [156]. Subsequently, Zhang and coworkers developed a new method for producing compounds in which CNTs were sprayed on the surface of polymer powders in the form of a suspension [157]. They have used HDPE materials containing SWCNTs. At very low SWCNTs concentrations (< 3.4 wt%), the rheological behavior of SWCNTs increases, and the electrical conductivity is improved with a load of only 0.5 wt%. The tensile strength and initial modulus strongly rise with increasing SWNTs content in the polymer matrix. The electrical and thermal conductivity of SWCNT/PE NCs were investigated by considering three factors that enhance thermal conductivity [158]. Kanagaraj and his group reported the use of CNTs to study the mechanical properties of high-density polymeric materials and the use of CNT/HDPE composites to determine the tensile strength of injection molding machines with different volume fractions [159]. The mechanical properties of the nanocomposites, with elastic modulus as tensile strength, hardness, elongation at break, and wear rate, increased proportionally with the addition of CNTs. The temperature was not affected by the addition of CNTs, but the crystallinity increases. The effect of processing parameters on the mechanical and thermophysical behavior of MWNT-reinforced PE compounds was studied [160]. The effect of SWCNTs and MWCNTs on the main melt flow instability of various PE was investigated in detail [161]. A dry state dispersion in linear arrays of LDPE at room temperature without chemical or physical treatment of the nanotubes using a high energy ball milling (HEBM) technique is reported [162]. The mechanical properties showed a significant increase in strength with increasing resistance ratio for all compositional ranges studied. The improvement was most pronounced at low nanotube loading

(i.e., 1–3% w/w), reaching a platform value of 10% w/w. The electrical properties are very low at all drag speeds for nanotube loading, and the percolation threshold for solid entrainment due to network failure tends to decrease with increasing drag speed, resulting in an increase in the conductivity of the LDPE insulating substrate by about 9 orders of magnitude [162]. The mechanical properties and oxidation stability of irradiated HDPE reinforced by various concentrations of MWCNTs are studied by Sreekanth and coworkers [163]. They have concluded that the presence of MWCNTs in the PE matrix could successfully confine the loss of mechanical properties because of irradiation. This behavior is observed at high irradiation dose. Various authors investigated the effects of CNTs on the various properties of PE [164–168]. For the first time, a simple and cost-effective surface treatment method was developed to modify the surface roughness of carbon fibers (CFs) by spraying CNTs [169]. CNTs were deposited on the surface of CFs using a spraying technique and then compounded into NTC/CF/HDPE compounds by extrusion and injection molding. The tensile test results of pure HDPE, CF/PEAD compounds, and layered CNT-CF/PEAD compounds with different CF contents showed a significant upward trend in the tensile strength of the CF/PEAD compounds compared to the pure HDPE polymers. This result can be attributed to the high strength and high modulus of CF since higher stiffness loading than the matrix generally improves the mechanical properties of the compounds. They have concluded that spraying CNTs in CF is a promising surface modification method to produce CNT-CF/HDPE compounds with better interfacial properties and it is proved to be an effective method to increase the mechanical properties of hierarchical compounds [169]. A simple and effective method to modify MWCNTs with aqueous cationic epoxy emulsions to improve the dispersion of MWCNTs and increase the interfacial interaction between the substrate and the filler material is reported by Peng and coworkers [170]. Kurup and coworkers developed an LMDPE/EVA-based shape memory NC with improved shape recovery performance by incorporating MWCNTs [171]. They have inferred that the formulation optimization to meet the stability of properties for the development of LMDPE/EVA/MWCNT shape memory NCs in an industry-friendly point of view and could be used in a number of applications from high-performance systems to smart devices.

6.3 Polyvinyl Chloride/CNT

The properties of polymer/CNT NCs are influenced by different components comprising surface contacts, adhesion power, preparation technique, and dispersion of CNT in the polymer matrix. Poor interfacial attachment and un-even dispersion of CNT in polymer structure have become the difficulties for the treatment of polymer/CNT nanocomposite. Broza and coworkers reported the production of NCs of polyvinyl chloride (PVC) with CNTs to investigate the effect of CNTs on electrical and mechanical properties [172]. PVC is a product with various applications, which is rich in natural and chemical resistance, and which has more diverse mechanical

properties due to the expansion of plasticizers. The effect of Kevlar coated CNTs for reinforcement of PVC on the mechanical properties was reported by O'Connor and coworkers [173]. These functionalized Kevlar nanotubes can serve as an additional promising material to support PVC. Significant improvements in the stiffness (up to half) and modulus (up to 70%) of the functionalized nanotubes have been observed compared to pure polymer compounds and nanotube-polymer compounds. These nanotube compounds have incredible potential as additives for the production of new ultra-high-strength polymer materials [173]. The influence of CNTs on glass transition temperature, thermal, mechanical, antibacterial, electrical, charge transport, and magnetic properties of PVC was studied by various authors [174–181]. The various property improvements for polymer/carbon nanotube NCs are reviewed in Table 1.

7 Biomedical Applications of Carbon-Based Polymer Nanocomposites

CNTs, discovered by Japanese scientist Iijima in 1991 [209], are now viewed as a cutting-edge research topic in various sectors of science and technology. Since the start of the twenty-first century, CNTs have been used in pharmacies and therapeutic drug delivery systems for pharmaceuticals [41]. The exceptional blend of mechanical, optical, and electrical properties possessed by CNTs has cultivated research for their utilization in various types of applications [210]. The various biological applications of CNTs are shown schematically in Fig. 6 [211–215].

7.1 Drug and Gene Delivery

Several studies have been done in past to demonstrate the use of CNTs in a range of biomedical applications, including drug delivery/quality therapy, biosensors, bioimaging, and therapeutics. The combination of the excellent mechanical, electrical, and thermal properties of CNTs with the properties of polymers makes them suitable for a lot of applications. The blend of gene therapy and chemotherapy has as of late got extensive consideration for cancer treatment [216]. On the other hand, low transfection efficiency and poor endosomal escape of genes from nanocarriers intensely inhibit the realization of the clinical use of small interfering RNA (siRNA). A new pH-responsive, surface-modified SWCNT was developed for the codelivery of doxorubicin (DOX) and survivin siRNA [216]. It was concluded that DOX-functional SWCNTs and survival siRNAs show potent antitumor effects in vitro and in vivo, and thus may represent a substitute approach for the joint use of antitumor drugs and genes. Some of the unique properties of CNTs such as high drug loading limit, huge surface area, high mechanical properties, and chemical stability make them excellent

Table 1 Property improvements for Polymer/carbon nanotube nanocomposites

S. No.	CNT type	CNT wt%	Matrix	Synthesis method	Approach	Properties	Percentage/improvement	References
1	MWCNTs	0.08–0.32	PS	Irradiation	Mechanical	Tensile strength	250%	[182]
2	MWCNTs	0–1	PS	Solution casting	Mechanical	Tensile strength	25%	[56]
3	SWCNTs	0.1–2	PS	Solution mixing	Mechanical, Electrical	Tensile strength, conductivity	Improve M.S and increase E.C	[129]
4	MWCNTs	1–5	PS	Solution mixing, spin casting	Mechanical, Electrical	Tensile strength, conductivity	40% Highly conductivity	[97]
5	MWCNTs	0.2–10	PS	Noncovalent grafting	Mechanical, Electrical	Young's modulus	160%	[183]
6	CNTs	0–4	PS	In situ polymerization	Mechanical	Wear resistance, Tribological	Improve W.R and increase Tribological	[127]
7	MWCNT/graphene	Various conc.	PS	In situ microemulsion polymerization	Mechanical, Thermal	Tensile strength, stability	Increase T.S and Thermal stability	[137]
8	MWCNTs	0–10	PS	Solution mixing/Electro spinning	Thermal	Thermal stability	Improve Thermal stability	[138]
9	MWCNTs	Diff. conc.	PS/PANI	Solution/Melt mixing	Electrical, Rheological	Dispersion	Good dispersion for both at low E/R percolation.	[139]

(continued)

Table 1 (continued)

S. No.	CNT type	CNT wt%	Matrix	Synthesis method	Approach	Properties	Percentage/improvement	References
10	GOCA	Variou conc.	PS	Self-assembly/Freeze drying/In situ polymerization	Mechanical	Porous, Mechanical, Hardness, Modulus	High porosity, high microhardness/compression modulus, Excellent M.P	[141]
11	MWCNTs	40	PS	Melt mixing	Mechanical	Tensile strength	10%	[114]
12	MWCNTs	40–50	PC/PS	Melt Processing	Electrical	Conductivity	Highest electrical conductivity	[142]
13	MWCNTs	0–5	HDPE	Melt mixing	Mechanical/Punch test	Tensile	12%	[110]
14	MWCNTs	1–10	LLDPE	High energy ball mill	Mechanical, Thermal, Electrical	Strength, Stability, Conductivity	Improved M.S, T.S, E.C	[162]
15	MWCNTs	0.25–1	HDPE	Injection modeling	Mechanical	Mechanical, Irradiation oxidative	Loss of M.P, Oxidation index (–56%)	[163]
16	SWCNT	–	PE	First principal method	Mechanical	Young's modulus	70%	[184]
17	MWCNT	1–18	HDPE	Melt Mixing	Electrical	Conductivity, EMI-SE	Improve with increase MWCNT	[164]
18	CNTs	Diff. CNT	PE	Finite element method	Electrical	Conductivity, EPT	Improve conductivity and current density	[165]

(continued)

Table 1 (continued)

S. No.	CNT type	CNT wt%	Matrix	Synthesis method	Approach	Properties	Percentage/improvement	References
19	MWCNT	1–10	LDPE	Solvent mixing process	Mechanical	Strength	High strength	[166]
20	MWCNT	0.1	LDPE	Screw extruder	Mechanical	Tensile test	Ultimate tensile strength	[167]
21	CNT/CF	–	HDPE	Extrusion and injection molding	Mechanical, Morphological	Tensile, Flexural	70.62 and 40.38%	[169]
22	MWCNTs	–	PE	Solution mixing	Mechanical, Electrical	Tensile, conductivity	Increased tensile and tremendous conductivity	[170]
23	MWCNT	1–3	LMDPE/EVA	Melt mixing	Electrical, Mechanical, Thermal	Conductivity, Strain, Shape memory	High conductivity, >98% excellent S.M	[171]
24	SNWNT/MWCNT	0.1–0.2/5–20	PVC	Solution mixing	Electrical	Conductivity	Increase electrical conductivity	[172]
25	CNT	–	PVC	In situ purification	Mechanical	Tensile, Young's modulus	T.S—50% Y.M—70%	[173]
26	MWCNT	0.2–2	PVC	Pressing method	Mechanical	Microhardness	Microhardness increased	[185]
27	MWCNT	0.5	PVC	Melt mixing	Mechanical, Thermal	Modulus, Tensile strength, Stability,	Modulus increases T.S reduced, increase stability	[175]
28	SWCNTs	–	PVC	Wet phase inversion process	–	Flux, Surface, Antibacterial	Surface/flux Slightly improve, no bacterial	[176]

(continued)

Table 1 (continued)

S. No.	CNT type	CNT wt%	Matrix	Synthesis method	Approach	Properties	Percentage/improvement	References
29	SWCNTs	0–20	PVC	Homogenous solution	Thermal	Stability, Spectroscopic	Increase T.S, Poor spectroscopic result	[186]
30	MWCNT	0–15	PVC	HSBM/HEBM	Electrical, Mechanical	Conductivity, Tensile strength	Improve conductivity and T.S	[177]
31	SWCNT	0.25–1	PVC	Plastisol curing method	Mechanical, Thermal	Tensile, Young's, toughness, elongation, stability	All are high and greatly improve	[179]
32	SWCNT	0.01–0.06	PVC/PU	Homogenous solution	Mechanical, Thermal	Tensile, Modulus, Stability	Increase tensile, elastic modulus and stability	[180]
33	MWCNTs	0.1–2	PVC	Acid ultrasonic method	Mechanical, Thermal	Tensile, Toughness, Stability	Enhance T.S and toughness, Excellent stability	[181]
34	SWCNTs	1.8	PP	Solution mixing	Dynamic mechanical analysis	Composite modulus	15% increase	[187]
35	SWCNT	Varying level	PP	Solution process	Mechanical	Tensile, Modulus, Fiber density	All are increase	[188]

(continued)

Table 1 (continued)

S. No.	CNT type	CNT wt%	Matrix	Synthesis method	Approach	Properties	Percentage/improvement	References
36	MWCNT	–	PP	Melt blending	Morphology, Mechanical, Thermal	Strength, Toughness, Stability	Disperse well, all properties are improve	[189]
37	SWCNT	5–20	PP	Solution mixing	Mechanical	Tensile, Young's	Low conc. Both are increase, High conc. decrease	[190]
38	MWCNT	0.1–8	PP	In situ polymerization	Mechanical	Tensile, Young's	Both are increase	[191]
39	MWCNT	0–1 vol. %	PP	Melt mixing	Electrical	Conductivity	Improve E.C	[192]
40	MWCNTs	0.1–3.5	PP	In situ polymerization	Mechanical, Thermal	Young's, Stability	22–37% Increase stability	[193]
41	CNTs	–	PP	In situ graft method	Mechanical	Tensile, Young's	T–110% Y–113%	[194]
42	MWCNTs	0–5	PP	Melt mixing	Mechanical	Tensile, Young's	T–39% Y–69%	[195]
43	CNTs	0–5	PP	Melt mixing	Mechanical, Thermal	Tensile, Elongation, Stability	T and E max. increase at 3% Improve stability	[196]
44	MWCNTs	–	PP	Melt mixing	Electrical	Conductivity	Improve E.C	[197]
45	MWCNT	0–5	PP	In situ polymerization	Mechanical, Thermal	Modulus, Stability	High modulus, T.S–Sharply increase	[198]
46	MWCNTs	0.001–1	PP	Melt processing	Mechanical	Impact strength	Increase 152%	[199]

(continued)

Table 1 (continued)

S. No.	CNT type	CNT wt%	Matrix	Synthesis method	Approach	Properties	Percentage/improvement	References
47	MWCNT	0.1–1	PP	Melt blending	Fracture mechanism	Shear strength (2.2 MPa)	Improve (17.8 MPa)	[200]
48	MWCNT	0.5	PA6	In situ polymerization	Mechanical	Tensile, Modulus	Slightly improve T.S and modulus	[201]
49	MWCNT	–	PA6	Melt mixing	Mechanical	Scratch, Tribological	Both are increase	[202]
50	MWCNT	0.5	PA6	Solution mixing	Thermal	Stability	Better T.S and mechanical, structural	[203]
51	MWCNT	0.1–2	PA6	Melt mixing	Thermal	Stability	Increase T.S	[204]
52	MWCNT	–	PA	Melt mixing	Electrical, Thermal	Van der waals Stability,	Strong van der waals forces and better stability, conductivity	[205]
51	MWCNT	–	PA	Interfacial polymerization	–	Flux, Rejection	Water flux increase and salt rejection decrease	[206]
52	CNT	1–4.5	PA	Melt mixing	Mechanical, Electrical	Tensile, Elongation, modulus, Conductivity	All properties are significantly improved	[207]
53	MWCNT	2.5–20	PA6	Melt mixing	Mechanical	Modulus	Improve modulus	[208]
54	CNT	20	PO	Melt mixing	Mechanical, Electrical	Tensile strength, modulus, conductivity	T.S/T.M are decreases and E.C are High	[182]



Fig. 6 Carbon nanotubes applications in bio world. [Reproduced by permission of Elsevier from Ref. [211]]

materials to be used in drug delivery devices [217–219]. Improvements in peptide-modified SWCNTs have identified the main enemy of tumor action and improved tumor localization [220]; PH dependent efflux also allows drug delivery near tumor tissue [221, 222]. Due to the multi-walled nature of CNTs, there is a force between carbon molecules that forms a cylindrical partition, known as the van der Waals force [223]. The distance between van der Waals forces, static electricity, communication, and nanotubes has been shown to be associated with the encapsulation of drug particles. These compounds play an important pharmacological role in the case of CNT intoxication. MWCNTs and PH-responsive gels pose challenges for the availability of doxorubicin, a nano-hybrid scaffold. The created nano-hybrid structures were designed to deliver drugs to cells with glioblastoma U-87 and it was found that drug delivery with nano-hybrid structures could limit cancer growth [224]. Percutaneous immobilization of electrical properties using multi-walled carbon polymer nanotubes allows the creators to take advantage of the high electrical properties of CNTs; it accelerates drug organization by subjecting it to heat [225]. Cross-linked polymer hydrogels-MWCNTs generate electrolytic reactions through pulsed discharges to sucrose; the discharge curves are evaluated using radioactive sucrose as an electric

field as a model for hydrophilic drugs [226]. CNTs were also used as carriers for the inoculation of antigens [227]. Multilayered CNTs are employed for binding to neural tissue cells and are valuable for creating competent drug transport and mass structures [228]. The limitations of SWCNTs in drug binding are more obvious. Exocytosis and enzymatic disruption are two components of CNTs release from the cell [229]. The low cytotoxicity and enhanced anti-Lishman motility of cisplatin MWCNTs show that it enhances low-binding CNTs, highlighting the great ability of CNTs as nano-drug carriers [230]. Due to the unique physicochemical properties of CNT loading on several small drug particles, ciprofloxacin, methotrexate, temozolomide, oxaliplatin, doxorubicin, docetaxel, gemcitabine, cisplatin, epirubicin, amantadine, and lamivudine were studied [231–233]. Sustained release and biodegradation of multilayer carbon nanotubes and biocompatibility the presentation of multilayer carbon nanotubes diclofenac has been improved in enabling the release of diclofenac sodium with an economical release profile [234]. Lofi and coworkers [235] analyzed the noncovalent interactions and various covalent functionalization mechanisms of the anticancer drug cladribine (CDA) with CNTs using quantum computational studies. A group of researchers from the Chinese Academy of Medical Sciences & Peking Union Medical College, PR China reported a concurrent fluorescence imaging monitoring of the programmed release of doxorubicin (DOX) and rhodamine B (RB) as the model drugs from a hydrogel-CNT delivery system (Fig. 7) [236].

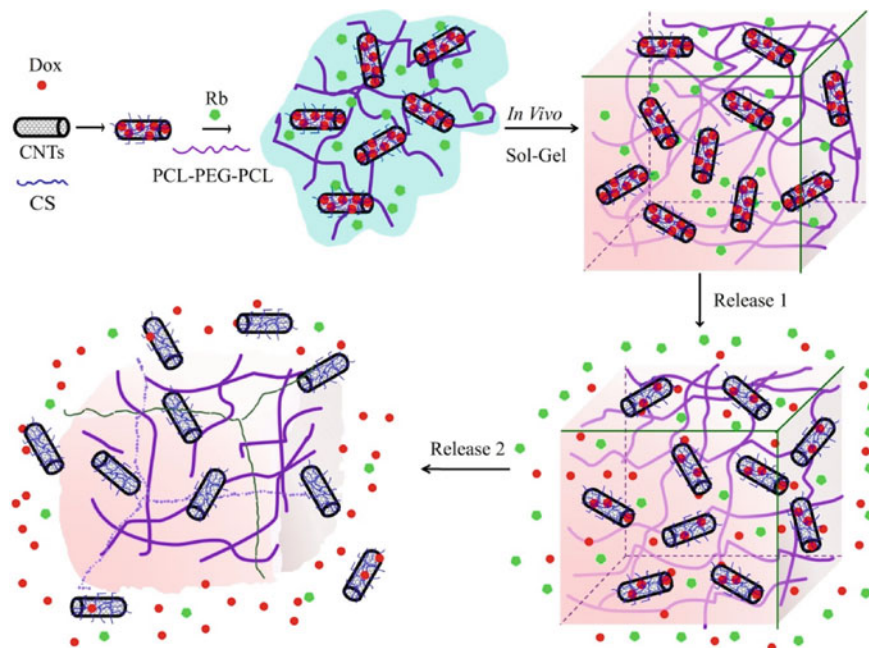


Fig. 7 Scheme of the programmed release of dual fluorescent drugs from hydrogel-carbon nanotubes delivery system. [Reproduced by permission of Elsevier from Ref. [236]]

The decoration of MWCNTs with gold TiO_2 nanoparticles to improve their biocompatibility for DOX delivery was reported [237]. They have concluded that this is an effective method for the preparation of carbon-based NCs for practical applications in nanobiomedicine [237]. Mazzagira and coworkers [238] developed a new platform of MWCNTs-cyclodextrin modified with branched polyethyleneimine (PEI) and alloyed rhodium and investigated as a drug delivery system. Mallakpour and coworkers [239] reported the ability to deliver drugs in a hydrophobic model of starch/CNT NCs. The results suggest that MWCNT-G1 plays two important roles: as a stabilizer for nanoparticle production and as a carrier for nanodrugs. Lavado-Gonzalez and coworkers examined several surface oxidative pretreatments to enhance the removal of MWCNTs by macrophages that support biomimetic properties with microtubules and ultimately exert anti-proliferative, anti-migratory, and cytotoxic effects on cancer cells [240]. The biodegradation of these nanotubes could be demonstrated after several days of therapeutic effects. Hesabi and coworkers [241] investigated the interactions between the anticancer drug hydroxyurea and functional zigzag carbon carboxylate (CNT) at the B3LYP and CAM-B3LYP levels in the gas and solvent phases using the functional density theory (FDT) approach. The results showed that all the complexes were favorable, especially in the aqueous phase. In a similar study, Kamel and coworkers [242] investigated the structural and electronic effects of interactions between f-CNTs and FLT molecules in the gas phase and aqueous solution using functional density theory. The results obtained show that the drug adsorption process on the outer surface of functionalized nanotubes is exothermic and all configurations are stable. They have also been observed that the intermolecular hydrogen bonding between FLT drugs and functionalized nanotubes plays an important role in the stability of the physically adsorbed structures. Various authors studied Li and coworkers [243] successfully fabricated the compound FA-CS-CNT(Fe)/HA as a magnetic targeted drug carrier to achieve controlled release of anti-cancer drugs (DOX) by catalyzing in situ CVD of CH_4 in HA nanodot-dorders. The synthesized CNTs, Fe, and HA form CNT(Fe)/HA compound structures, which can be used as carriers of targeted magnetic drugs based on acidification, the addition of CS, and AF graft functionalization. The addition of CNTs to hydrogels improved the swelling behavior of mixed hydrogels [244]. Biagiotti and colleagues [245] investigated the formation of metformin salts using oxidized CNTs and their viability testing in three different cell lines with met and ox-MWCNTs with dose-dependent inhibitory activity against PC3 and MCF7 cell cultures. The effect of iron-filled CNTs on the adsorption capacity and sustained release of drugs is reported by Sukhodub and coworkers [246]. They have also studied the mechanical properties of HA-based composite biomaterials formed to create model regions of bone tissue, where the material can resist mechanical stress. This material can be used to model in 3D the regions of bone tissue that need to resist mechanical stress. Rafi and coworkers [247] studied the introduction of pH-sensitive polymer chains into the walls of CNTs to prepare pH-sensitive CNT nano-hybrid polymer systems. The release rate of naproxen was insignificant due to the hydrogen bonding between the polar group and the polymer chain; at pH 7.4, the polar group was deprotonated and

the hydrogen bonding was replaced by repulsive electrostatic interactions, resulting in an increased release rate.

Due to their physicochemical properties, CNTs have been developed as transport scaffolds for the treatment of cancer growth [248]. Due to various problems (toxicity, low resistance to excipients, and multidrug resistance, limited cell penetration), the effectiveness of common drug transport systems is limited. Therefore, it is intended to structure an efficient transport system with better cellular development of effective drugs. CNTs can dispense with a large number of cross-linked cell-stretching membranes, and in this sense, the anticancer drugs administered by CNTs are administered in situ at full concentration and, as needed, will be more successful in tumor cells than drugs modulated by standard therapy [248, 249]. Cancer is represented by the uncontrolled development of cells that cause damage to common tissues and organs. Harmful development leads to inadequate cell expansion. Especially in the treatment of cancer growth, the use of conventional chemotherapeutic drugs carries the risk of excessive baseline effects, just as they are less effective in completely destroying cancer cells. Carbon nanotubes comprise a high percentage, have a large surface area, and have a needle-like structure, thus allowing them to bind to drug molecules [250–252]. CNTs are beneficial as nanocarriers in the treatment of cancer [252–254]. Photothermal therapy with CNTs can lead to the cure of tumors [255–258].

7.2 *Tissue Engineering*

Tissue engineering (TE) is a multidisciplinary discipline that focuses on reincarnation events and uses information from science, materials science, design, life science, and clinical science to solve fundamental medical issues such as tissue loss and organ failure [259]. Tissue design, which originated from the field of biomaterial modification, is the combination of bioactive scaffolds, cells, and particles to create functional tissue [260–262]. The purpose of tissue design is to bring together practical entities that repair, support, or enhance damaged tissues and entire organs. CNTs can be used for tissue engineering, cell tracking, and nomenclature, and to improve their performance [263–265]. Advances in tissue engineering have demonstrated new methods for unprecedented evaluation of cultured tissues; CNTs can improve cell screening, biosensors, transfection experts, and platform placement. Also, CNTs can be fused to scaffolds to help structural reinforcement and provide platforms with new properties, such as electrical conductivity, to promote cell development [266]. Recently, the carbon nanotube method has been used for tissue engineering and regenerative medicine culture [267]. In this technique, cells are encapsulated in appropriate biomaterials to allow the continued development of new tissues [267–269]. Carbon nanotubes are valuable in improving the mechanics and electrical aspects of scaffolds, allowing cells to feel microscopic sensations and responses of intracellular substances. Tissue engineering applications are twofold, such as the repair of damaged tissues and the development of in vitro human models. In vitro 3D

models, however, could change the way we understand cancer. Lovat and coworkers [270] investigated the use of CNTs as a possible device to improve the transmission of neural signals while promoting dendritic outgrowth and cell adhesion. The results strongly suggest that the growth of neural circuits in CNT networks is associated with a significant increase in network activity. The improved efficiency of neural signal transmission may be linked to the particular properties of CNT materials, such as high electrical conductivity.

It was reported that poly(2-hydroxyethyl methacrylate) pHEMA/mWCNTs lead to the increased electrical conductivity of the material, which activates SHSY5Y cells as neurotransmitter channels when transferring electrical potentials [271]. mWCNTs seem to contribute to improved cell adhesion and conductive nerve potentials. It may be preferable to align the mWCNTs on the membrane before seeding the cells and then applying lower potentials than the alignment used in this study. Armentano and coworkers [272] provided an overview of current research trends in tissue engineering-related nanocomposites: including biodegradable polymers, organic/inorganic nanostructures, matrix interactions between nanostructures, and strategies for fabricating interconnected pore nanocomposite scaffolds. The combination of biodegradable polymers with nanostructures opens up new perspectives in the field of NCs for biomedical applications with tunable mechanical, thermal, morphological, and electrical properties [272]. The preparation and characterization of the collagen/CNT matrix and the cellular response of PC12 cells when cultured in this composite membrane in the absence and the presence of electrical stimulation was studied [273]. Compared to collagen membranes, the electrical conductivity and electroactivity of the composites were greatly improved by the deposition of CNTs, even at less than 1% charge. It was also found that the concentration of CNTs added to composite membranes altered cellular activities such as adhesion, metabolic activity, and neuronal expansion. Cells grown on SWCNT were damaged, chromatin concentrated, and apoptosis occurred after SWCNT acid treatment [274]. The hypothesis that CNT-based electrospun PLA scaffolds that could be produced for tissue engineering applications were tested by Mackle et al. [275]. Ogihara and coworkers [276] were the first to investigate the biocompatibility and bone tissue compatibility of CNT/alumina composites with alumina ceramics *in vivo* and *in vitro*. The results showed that the compound exhibited good bone histocompatibility in bone grafting studies and was directly transformed into new bone. The production of unidirectional bioglass fibers (BGF) (13–93) and reinforced polylactic acid (PLA) compounds that have improved the mechanical properties of bone plates for healing weight fractures of tubular bone were reported by Mehboob et al. [277]. The mechanical and microscopic properties, *in vitro* degradation, and bioactivity of the BGF/PLA compounds, were also evaluated. Badhe et al. [278] studied a bilayer macroporous vascular scaffold based on a chitosan-gel compound with many desirable properties that accurately mimic the morphology and mechanical properties of biological blood vessels. The macroporous layer offers a huge surface with strong cell adhesion and proliferation properties. The non-porous outer layer delivers cell protection and gives extra flexibility and elasticity to the reinforcement. Biomedical applications of different CNTs polymer-based NCs are summarized in Table 2.

Table 2 Biomedical applications of CNTs/polymer-based nanocomposites

S. No.	Backbone	Drug	Application	Ref.
1	Hydrogel combine with CNTs	doxorubicin, rhodamine B	Release dual drug delivery system, demand on combination chemotherapy	[236]
2	CNT Fe/Hydroxyapatite [(CNT(Fe)/HA)]	Anticancer drug doxorubicin	Realizing magnetic targeted delivery	[243]
3	pH-responsive Polyethylenimine–betaine functionalized SWCNTs	siRNA and DOX	Effective antitumor effects in vitro and in vivo, codelivery of anticancer drugs and genes.	[216]
4	Antibody-conjugated CNTs	Anti-P-glycoprotein	P-glycoprotein-targeted photo thermal therapy	[278]
5	Starch nanocomposite films containing MWCNT	Zolpidem	Drug/gene delivery	[239]
6	Hydroxypropyl- β -cyclodextrin (HP- β -CD) modified carboxylated SWCNT	Formononetin	Drug delivery	[279]
7	Biodegradable MWCNTs	oxidized MWCNTs (o-MWCNTs)	Anti-tumoral effect	[240]
8	Carboxylation of CNT	Hydroxyurea	Improved drug loading	[241]
9	Functionalized SWCNT	Flutamide	Improved drug loading	[242]
10	MWCNTs modified with cyclodextrins and polyethylenimine	Cidofovir	Antiviral drug delivery	[238]

8 Conclusion

In this chapter, an attempt has been made to combine all the crucial information about CNTs, polymer matrix, CNTs-based PNCs including synthesis methods, properties, and biomedical applications. Arc discharge, laser ablation, and chemical vapor deposition techniques for CNTs have been briefly discussed. Biomedical applications of CNTs and their NCs with polymeric materials have also been discussed in detail. The remarkable properties of CNTs viz. mechanical, electrical, and thermal makes them ideal candidates as fillers in the various polymer matrix. The field of NCs has been one of the most encouraging and growing at a fast pace. They find exceptional consideration because of the novel properties, for example, lightweight, ease of synthesis, and flexibility. A characterizing highlight of PNCs is that the nano size of the fillers prompts an enormous increase in the interfacial area when contrasted with customary composites. CNTs-based NCs possess novel properties to use them in various applications. CNTs are a particularly alluring class of fillers for polymers on account of their high mechanical and thermal properties. They stand for one of the strongest and toughest materials known. In short the field of nanocomposites, developing mechanically strong, electrically conducting, and novel materials based on CNTs and the polymer is just the foundation and hoping to become a very charming sector in science and technology in near future.

References

1. Liu X-W, Sun X-F, Huang Y-X, Sheng G-P, Wang S-G, Yu H-Q (2011) Carbon nanotube/chitosan nanocomposite as a biocompatible biocathode material to enhance the electricity generation of a microbial fuel cell. *Energ Environ Sci* 4:1422–1427
2. Taha MA, El-Sabbagh AM, Taha IM (2010) Design, development and testing of rubber nanocomposites. *Key Eng Mater* 425:61–93
3. Karttunen M, Ruuskanen P, Pitkänen V, Albers WM (2008) Electrically conductive metal polymer nanocomposites for electronics applications. *J Electron Mater* 37(7):951–954
4. Wayne E, Jones Jr, Jasper C, Edwin J, Ashok P, Daryl S (2010) Electrically and thermally conducting nanocomposites for electronic applications. *Mater* 3(2):1478–1496
5. Miomandre F, Audebert P, Bonnett JP, Brosseau A, Perriat P, Weisbuch C, Wen W, Sheng P (2008) Silica-polypyrrole core-shell nanocomposites as active materials for dielectrophoretic displays. *J Nanosci Nanotechnol* 8(9):4353–4359
6. Henriette MC, de Azeredo (2009) Nanocomposites for food packaging applications. *Food Res Inter* 42:1240–1253
7. Arora A, Padua GW (2010) Review: nanocomposites in food packaging. *J Food Sci* 75(1):43–49
8. Meng ZX, Zheng W, Ding MH, Zhou HM, Chen XQ, Chen JC, Liu MK, Zheng YF (2011) Fabrication and characterization of elastomeric polyester/carbon nanotubes nanocomposites for biomedical application. *J Nanosci Nanotech* 11(4):3126–3133
9. Sanchez C, Julián B, Belleville P, Popall M (2005) Applications of hybrid organic–inorganic nanocomposites. *J Mater Chem* 15:3559–3592
10. Müller K, Bugnicourt E, Latorre M, Jorda M, Sanz YE, Lagaron JM, Miesbauer O, Bianchin A, Hankin S, Bölz U, Pérez G, Jesdinszki M, Lindner M, Scheuerer Z, Castelló S, Schmid M

- (2017) Review on the processing and properties of polymer nanocomposites and nanocoatings and their applications in the packaging. *Automot Solar Energy Fields Nanomater* 7(4):74
11. Bayda S, Adeel M, Tuccinardi T, Cordani M, Rizzolio F (2020) The history of nanoscience and nanotechnology from chemical-physical applications to nanomedicine. *Molecules* 25:112
 12. Gnach A, Lipinski T, Bednarkiewicz A, Rybka J, Capobianco JA (2015) Up converting nanoparticles assessing the toxicity. *Chem Soc Rev* 44:1561–1584
 13. Reynolds GH (2003) Nanotechnology and regulatory policy: three futures. *Harv J Law Technol* 17:179–209
 14. Ramanathan T, Abdala AA, Stankovich S, Dikin DA, Herrera-Alonso M, Piner RD, Adamson DH, Schniepp HC, Chen X, Ruoff RS, Nguyen ST, Aksay IA, Prud'Homme RK, Brinson LC (2008) Functionalized graphene sheets for polymer nanocomposites. *Nat Nanotech* 3:327–331
 15. Giannelis EP (1996) Polymer layered silicate nanocomposites. *Adv Mater* 8(1):29–35
 16. Sternitzke M (1997) Structural ceramic nanocomposites. *J Eur Ceram Soc* 17(9):1061–1082
 17. Peigney A, Laurent CH, Flahaut E, Rousset A (2000) Carbon nanotubes in novel ceramic matrix nanocomposites. *Ceram Int* 26(6):677–683
 18. Alexandre M, Dubois P (2000) Polymer-layered silicate nanocomposites: preparation, properties and uses of a new class of materials. *Mater Sci Eng* 28(1–2):1–63
 19. Gangopadhyay R, Amitabha D (2000) Conducting polymer nanocomposites: a brief overview. *Chem Mater* 12(7):608–622
 20. Thostenson ET, Ren Z, Chou TW (2001) Advances in the science and technology of carbon nanotubes and their composites: a review. *Compos Sci Technol* 61(13):1899–1912
 21. Gall K, Dunn ML, Liu Y, Finch D, Lake M, Munshi NA (2002) Shape memory polymer nanocomposites. *Acta Mater* 50(20):5115–5126
 22. Kickelbick G (2003) Concepts for the incorporation of inorganic building blocks into organic polymers on a nanoscale. *Prog Polym Sci* 28(1):83–114
 23. Fischer H (2003) Polymer nanocomposites: from fundamental research to specific applications. *Mater Sci Eng C* 23(6–8):763–772
 24. Ray SS, Okamoto M (2003) Polymer—layered silicate nanocomposites: a review from preparation to processing. *Prog Polym Sci* 28(11):1539–1641
 25. Andrews R, Weisenberger MC (2004) Carbon nanotube polymer composites. *Curr Opin Solid State Mater Sci* 8(1):31–37
 26. Wang C, Guo ZX, Fu S, Wu W, Zhu D (2004) Polymers containing fullerene or carbon nanotube structures. *Prog Polym Sci* 29(11):1079–1141
 27. Pandey JK, Reddy KR, Kumar AP, Singh RP (2005) An overview on the degradability of polymer nanocomposites. *Polym Degrad Stab* 88(2):234–250
 28. Thostenson ET, Li C, Chou TW (2005) Nanocomposites in context. *Compos Sci Technol* 65(3–4):491–516
 29. Jordan J, Jacob KI, Tannenbaum R, Sharaf MA, Jasiuk I (2005) Experimental trends in polymer nanocomposites: a review. *Mater Sci Eng A* 393(1–2):1–11
 30. Choi SM, Awaji H (2005) Nanocomposites: a new material design concept. *Sci Technol Adv Mater* 6(1):2–10
 31. Xie XL, Mai YW, Zhou XP (2005) Dispersion and alignment of carbon nanotubes in polymer matrix: a review. *Mater Sci Eng R* 49(4):89–112
 32. Ray SS, Bousmina M (2005) Biodegradable polymers and their layered silicate nanocomposites: in greening the 21st century materials world. *Prog Mater Sci* 50(8):962–1079
 33. Pandey JK, Kumar AP, Misra M, Mohanty AK, Drzal LT, Singh RP (2005) Recent advances in biodegradable nanocomposites. *J Nanosci Nanotechnol* 5(4):497–526
 34. Camargo PHC, Satyanarayana KG, Wypych F (2009) Nanocomposites: synthesis, structure, properties and new application opportunities. *Mater Res* 12(1):1–39
 35. Endo M, Hayashi T, Kim YA, Terrones M, Dresselhaus MS (2004) Applications of carbon nanotubes in the twenty-first century. *Royal Soc* 362:2223–2238
 36. Mouritz AP, Gibson AG (2006) Fire Properties of polymer composite materials. Springer, p 143

37. Askeland DR (1996) Composite materials. In: *The science and engineering of materials*. Springer, Boston, MA. https://doi.org/10.1007/978-1-4899-2895-5_16
38. Rajak DK, Pagar DD, Menezes PL, Linul E (2019) Fiber-reinforced polymer composites: manufacturing. *Prop Appl Polym* 11:1667
39. Ruoff RS, Lorents DC (1995) Mechanical and thermal properties of carbon nanotubes. 33:925-930
40. Zhang Y (2015) Blends of cyclic poly (butylene terephthalate)/multiwalled carbon nanotube nanocomposites prepared by in situ polymerization. Diss. University of Birmingham
41. He H, Pham-huy LA, Dramou P, Xiao D, Zuo P, Pham-huy C (2013) Carbon nanotubes: applications in pharmacy and medicine. *BioMed Res Int* 1-13
42. Che J, Cagin T, Goddard WA (2000) Thermal conductivity of carbon nanotubes. *Nanotechnology* 11:65-69
43. Thostenson ET, Ren Z, Chou TW (2001) Advances in the science and technology of carbon nanotubes and their composites: a review. *Compos Sci Technol* 61:1899-1912
44. Lau AKT, Hui D (2002) The revolutionary creation of new advanced materials—carbon nanotube composites. *Compos B Eng* 33:263-277
45. Treacy MMJ, Ebbesen TW, Gibson JM (1996) Exceptionally high Young's modulus observed for individual carbon nanotubes. *Nature* 381:678
46. Lourie O, Wagner HD (1998) Evaluation of Young's modulus of carbon nanotubes by micro-Raman spectroscopy. *J Mater Res* 13:2418
47. Yu MF, Lourie O, Dyer MJ, Moloni K, Kelly TF, Ruoff RS (2000) Strength and breaking mechanism of multiwalled carbon nanotubes under tensile load. *Science* 287:637
48. Yu MF, Files BS, Arepalli S, Ruoff RS (2000) Tensile loading of ropes of single wall carbon nanotubes and their mechanical properties. *Phys Rev Lett* 84:5552
49. Yakobson BI, Brabec CJ, Bernholc J (1996) Nanomechanics of carbon tubes: instabilities beyond linear response. *Phys Rev Lett* 76:2511
50. Overney G, Zhong W, Tomanek D (1993) Structural rigidity and low frequency vibrational modes of long carbon tubules. *Zeitschrift für Physik D Atoms, Molecules and Clusters* 27:93-96
51. Mintmire JW, Dunlap BI, White CT (1992) Are fullereue tubules metallic? *Phys Rev Lett* 68:631
52. Hamada N, Sawada SI, Oshiyama A (1992) New one-dimensional conductors: graphitic microtubules. *Phys Rev Lett* 10:1579
53. Ebbesen TW, Lezec HJ, Hiura H, Bennett JW, Ghaemi HF, Thio T (1996) Electrical conductivity of individual carbon nanotubes. *Nature* 382:54
54. Pop E, Mann D, Wang Q, Goodson K, Dai H (2006) Thermal conductance of an individual single-wall carbon nanotube above room temperature. *Nano Lett* 6(1):96-100
55. Tiwari SK, Kumar V, Huczko A, Oraon R, Adhikari AD, Nayak GC (2016) Magical allotropes of carbon: prospects and applications. *Crit Rev Solid State Mater Sci* 41(4):257-317
56. Qian D, Dickey EC (2000) Load transfer and deformation mechanisms in carbon nanotube-polystyrene composites. *Appl Phys Lett* 76(20):2868
57. Schadler LS, Giannaris SC, Ajayan PM (1998) Load transfer in carbon nanotube epoxy composites. *Appl Phys Lett* 73(26):3842-3844
58. Charlier JC, Issi JP (1996) Electrical conductivity of novel forms of carbon. *J Phys Chem Solids* 57:957
59. Stadermann M, Papadakis SJ, Falvo MR, Novak J, Snow E, Fu Q, Liu J, Fridman Y, Boland JJ, Superfine R, Washburn S (2004) Nanoscale study of conduction through carbon nanotube networks. *Phys Rev B* 69:10-12
60. Hecht D, Hu L, Grüner G (2006) Conductivity scaling with bundle length and diameter in single walled carbon nanotube networks. *Appl Phys Lett* 89:133112-133113
61. Li C, Thostenson ET, Chou TW (2007) Dominant role of tunneling resistance in the electrical conductivity of carbon nanotube-based composites. *Appl Phys Lett* 91:
62. Ahmad A, Kholoud MM, El-Nour A, Reda AA, Al-Warthan AA (2012) Carbon nanotubes, science and technology part (I) structure, synthesis and characterization. *Arab J Chem* 5:1-23

63. Ando Y, Zhao X, Sugai T, Kumar M (2004) Growing carbon nanotubes, *materialstoday. Appl Phys Lett* 7:22–29
64. Krätschmer W, Lamb LD, Fostiropoulos K, Huffman DR (1990) Solid C60: a new form of carbon. *Nature* 347:354–358
65. Vanderwal RL, Berger G, Ticich TM (2003) Carbon nanotube synthesis in a flame using laser ablation for in situ catalyst generation. *Appl Phys A* 77:885–889
66. Ebbesen TW, Ajayan PM (1992) Large-scale synthesis of carbon nanotubes. *Nature* 358:220
67. Bethune DS, Klang CH, Devries MS, Gorman G, Savoy R, Vazquez J, Beyers R (1993) Cobalt-catalysed growth of carbon nanotubes with single-atomic-layer wall. *Nature* 363:605
68. Hutchison JL, Kiselev NA, Krinichnaya EP, Krestinin AV, Loutfy RO, Morawsky AP, Muradyan VE, Obraztsova ED, Sloan J, Terekhov SV, Zakharov DN (2001) Double-walled carbon nanotubes fabricated by a hydrogen arc discharge method. *Carbon* 39:761–770
69. Guo T, Nikolaev P, Thess A, Colbert DT, Smalley RE (1995) Catalytic growth of single-walled nanotubes by laser vaporization. *Chem Phys Lett* 243:49–54
70. Thess A, Lee R, Nikolaev P, Dai H, Petit P, Robert J, Xu C, Lee YH, Kim SG, Rinzler AG, Colbert DT, Scuseria GE, Tomanek D, Fischer JE, Smalley RE (1996) Crystalline ropes of metallic carbon nanotubes. *Science* 273:483–487
71. Dai H (2002) Carbon nanotubes: opportunities and challenges. *Surf Sci* 500:218–241
72. Cassell AM, Raymakers JA, Kong J, Dai H (1999) Large scale CVD synthesis of single-walled carbon nanotubes. *J Phys Chem B* 103:6484–6492
73. Ren ZF, Huang ZP, Xu JW, Wang JH, Bush P, Siegal MP, Provencio PN (1998) Synthesis of large arrays of well-aligned carbon nanotubes on glass. *Science* 298:1105
74. Fadiran OO, Girouard N, Meredith JC (2018) Pollen fillers for reinforcing and strengthening of epoxy composites. *Emergent Mater* 1:95–103
75. Ajayan PM, Schadler LS, Braun PV (2003) Nanocomposite science and technology. 3-527-30359-6
76. Young RJ, Kinloch IA, Gong L, Novoselov KS (2012) The mechanics of graphene nanocomposites: a review. *Compos Sci Technol* 72:1459–1476
77. Reynaud E, Gauthier C, Perez J (1999) Nanophases in polymers. *Revue De Metallurgie* 98:169–176
78. Ajayan PM, Stephan O, Colliex C, Trauth D (1994) Aligned carbon nanotube arrays formed by cutting a polymer resin-nanotube composite. *Science* 265:1212–1214
79. Manias E (2007) Nanocomposites: stiffer by design. *Nat Mater* 6(1):9–11
80. Fayyad EM, Abdullah AM, Hassan MK, Mohamed AM, Jarjoura G, Farhat Z (2018) Recent advances in electroless-plated Ni-P and its composites for erosion and corrosion applications: a review. *Emergent Mater* 1:1–22
81. Paul DR, Robeson LM (2008) Polymer nanotechnology: nanocomposites. *Polymer* 49:3187–3204
82. Friedrich K, Fakirov S, Zhang Z (2005) Polymer composite from nano-scale to macro-scale. Springer
83. Gabbott P (2008) Principles and applications of thermal analysis. Wiley
84. Edwards DC (1990) Polymer-filler interactions in rubber reinforcement. *J Mater Sci* 25:4175–4185
85. Kargarzadeh H, Mariano M, Huang J, Lin N, Ahmad I, Dufresne A, Thomas S (2017) Recent developments on nanocellulose reinforced polymer nanocomposites: a review. *Polymer* 132:368–393
86. Herron N, Thron DL (1998) Nanoparticles: uses and relationships to molecular cluster compounds. *Adv Mater* 10:1173–1184
87. Liu Y, Wang A, Claus R (1997) Molecular Self-Assembly of TiO₂/polymer nanocomposite films. *J Phys Chem* 101:1385–1388
88. Huang JC, He CB, Xiao Y, Mya KY, Dai J, Siow YP (2003) Polyimide/POSS nanocomposites: interfacial interaction, thermal properties and mechanical properties. *Polymer* 44:4491–4499
89. Fasolino A, Los JH, Katsnelson MI (2007) Intrinsic ripples in graphene. *Nat Mater* 6:858–861

90. Favier V, Canova GR, Shrivastava SC, Cavaille JY (1997) Mechanical percolation in cellulose whisker nanocomposites. *Polym Eng Sci* 37:1732–1739
91. Chazeau L, Cavaille JY, Dendievel R, Bouterin B (1999) Viscoelastic properties of plasticized PVC reinforced with cellulose whiskers. *J Appl Polym Sci* 71:1797–1808
92. Ogawa M, Kuroda K (1997) Preparation of inorganic-organic nanocomposites through intercalation of organoammonium ions into layered silicates. *Bull Chem Soc Japan* 70:2593–2618
93. Calvert P (1999) Nanotube composites—a recipe for strength. *Nature* 399:210–211
94. Liu M, Jia Z, Jia D, Zhou C (2014) Recent advance in research on halloysite nanotubes-polymer nanocomposite. *Prog Polym Sci* 39:1498–1525
95. Du F, Fischer JE, Winey KI (2003) Coagulation method for preparing single-walled carbon nanotube/poly(methyl methacrylate) composites and their modulus, electrical conductivity, and thermal stability. *J Polym Science Part B* 41:3333
96. Shaffer MSP, Windle AH (1999) Fabrication and characterization of carbon nanotube/poly(vinyl alcohol) composites. *Adv Mater* 11:937
97. Safadi B, Andrews R, Grulke EA (2002) Multiwalled carbon nanotube polymer composites: synthesis and characterization of thin films. *J Appl Polym Sci* 84:2660
98. Jin L, Bower C, Zhou O (1998) Alignment of carbon nanotubes in a polymer matrix by mechanical stretching. *Appl Phys Lett* 73:1197–1199
99. Geng H, Rosen R, Zheng B, Shimoda H, Fleming L, Jie L, Zhou O (2002) Fabrication of properties of composites of poly(ethylene oxide) and functionalized carbon nanotubes. *Adv Mater* 14:1387–1390
100. Chen L, Pang XJ, Qu MZ, Zhang QT, Wang B, Zhang BL, Yu ZL (2005) Fabrication and characterization of polycarbonate/carbon nanotubes composites. *Compos A Appl Sci Manuf* 37:1485–1489
101. Sahoo NG, Jung YC, Yoo HJ, Cho JW (2006) Effect of functionalized carbon nanotubes on molecular interaction and properties of polyurethane composites. *Macromol Chem Phys* 207:1773–1780
102. Cui S, Scharff P, Siegmund C, Schneider D, Risch K, Klotzer S, Spiess L, Romanus H, Schawohl J (2004) Investigation on preparation of multiwalled carbon nanotubes by DC arc discharge under N₂ atmosphere. *Carbon* 42:931–939
103. Sen R, Zhao B, Perea D, Itkis ME, Hu H, Love J, Bekyarova E, Haddon RC (2004) Preparation of single-walled carbon nanotube reinforced polystyrene and polyurethane nanofibers and membranes by electrospinning. *Nano Lett* 4:459–464
104. Dror Y, Salaha W, Khalifin RL, Cohen Y, Yarin AL, Zussman E (2003) Carbon nanotubes embedded in oriented polymer nanofibers by electrospinning. *Langmuir* 19:7012–7020
105. Andrews R, Jacques D, Qian D, Rantell T (2002) Multiwall carbon nanotubes: synthesis and application. *Acc Chem Res* 35:1008–1017
106. Hill DE, Lin Y, Rao AM, Allard LF, Sun YP (2002) Functionalization of carbon nanotubes with polystyrene. *Macromolecules* 35:9466–9471
107. Potschke P, Bhattacharyya AR, Janke A (2004) Melt mixing of polycarbonate with multiwalled carbon nanotubes: microscopic studies on the state of dispersion. *Eur Polym J* 40:137–148
108. Kim JY, Kim SH (2006) Influence of multiwall carbon nanotube on physical properties of poly(ethylene 2,6-naphthalate) nanocomposites. *J Polym Sci Part B Polym Phys* 44:1062–1071
109. Haggenueller R, Zhou W, Fischer JE, Winey KI (2003) Production and characterization of polymer nanocomposites with highly aligned single-walled carbon nanotubes. *J Nanosci Nanotechnol* 3:105–110
110. Tang W, Santare MH, Advani SG (2003) Melt processing and mechanical property characterization of multi-walled carbon nanotube/high density polyethylene (MWNT/HDPE) composite films. *Carbon* 41:2779–2785
111. Zeng Y, Ying Z, Du J, Cheng HM (2007) Effects of carbon nanotubes on processing stability of polyoxymethylene in melt-mixing process. *J Phys Chem C* 111:13945–13950
112. Cooper CA, Ravich D, Lips D, Mayer J, Wagner HD (2002) Distribution and alignment of carbon nanotubes and nanofibrils in a polymer matrix. *Compos Sci Technol* 62:1105–1112

113. Moniruzzaman M, Winey KI (2006) Polymer nanocomposites containing carbon nanotubes. *Macromolecules* 39:5194–5205
114. Andrews R, Jacques D, Minot M, Rantell T (2002) Fabrication of carbon multiwall nanotube/polymer composites by shear mixing. *Macromol Mater Eng* 287:395–403
115. Wu D, Sun Y, Zhang M (2009) Kinetics study on melt compounding of carbon nanotube/polypropylene nanocomposites. *J Polym Sci Part B Polym Phys* 47:608–618
116. Hong JS, Kim C (2007) Extension-induced dispersion of multi-walled carbon nanotube in non-Newtonian fluid. *J Rheol* 51:833–850
117. Kim ST, Choi HJ, Hong SM (2007) Bulk polymerized polystyrene in the presence of multiwalled carbon nanotubes. *Colloid Polym Sci* 285:593–598
118. Yoo HJ, Jung YC, Sahoo NG, Cho JW (2006) Polyurethane-carbon nanotube nanocomposites prepared by in-situ polymerization with electroactive shape memory. *J Macromol Sci Part B* 45:441–451
119. Wu TM, Lin SH (2006) Synthesis, characterization, and electrical properties of polypyrrole/multiwalled carbon nanotube composites. *J Polym Sci Part A Polym Chem* 44:6449–6457
120. Kang M, Myung SJ, Jin HJ (2006) Nylon 610 and carbon nanotube composite by in situ interfacial polymerization. *Polymer* 47:3961–3966
121. Haggemueller R, Fischer JE, Winey KI (2006) Single wall carbon nanotube/polyethylene nanocomposites: nucleating and templating polyethylene crystallites. *Macromolecules* 39:2964–2971
122. Hu N, Zhou H, Dang G, Rao X, Chen C, Zhang W (2007) Efficient dispersion of multi-walled carbon nanotubes by in situ polymerization. *Polym Int* 56:655–659
123. Geng Y, Liu MY, Li J, Shi XM, Kim JK (2008) Effects of surfactant treatment on mechanical and electrical properties of CNT/epoxy nanocomposites. *Compos A Appl Sci Manuf* 39:1876–1883
124. Chowdhury SR, Chen Y, Wang Y, Mitra S (2009) Microwave-induced rapid nanocomposite synthesis using dispersed single-wall carbon nanotubes as the nuclei. *J Mater Sci* 44:1245–1250
125. Moaisala A, Li Q, Kinloch IA, Windle AH (2006) Thermal and electrical conductivity of single-walled and multi-walled carbon nanotube-epoxy composites. *Compos Sci Technol* 66:1285–1288
126. Ma PC, Tang BZ, Kim JK (2008) Effect of CNT decoration with silver nanoparticles on electrical conductivity of CNT-polymer composites. *Carbon* 46:1497–1505
127. Yang Z, Dong B, Huang Y, Liu L, Yan FY, Li HL (2005) Enhanced wear resistance and microhardness of polystyrene nanocomposites by carbon nanotubes. *Mater Chem Phys* 94:109–113
128. Zhang B, Fu RW, Zhang MQ, Dong XM, Lan PL, Qiu JS (2005) Preparation and characterization of gas-sensitive composites from multi-walled carbon nanotubes/polystyrene. *Sens Actuators B Chem* 109:323–328
129. Chang TE, Kisliuk A, Rhodes SM, Brittain WJ, Sokolov AP (2006) Conductivity and mechanical properties of well-dispersed single-wall carbon nanotube/polystyrene composite. *Polymer* 47:7740–7746
130. Zhang Z, Zhang J, Chen P, Zhang B, He J, Hu GH (2006) Enhanced interactions between multi-walled carbon nanotubes and polystyrene induced by melt mixing. *Carbon* 44:692–698
131. Nayak RR, Lee KY, Shanmugaraj AM, Ryu SH (2007) Synthesis and characterization of styrene grafted carbon nanotube and its polystyrene nanocomposite. *Eur Polym J* 43:4916–4923
132. Yu J, Lu K, Sourty E, Grossiord N, Koning CE, Loos J (2007) Characterization of conductive multiwall carbon nanotube/polystyrene composites prepared by latex technology. *Carbon* 45:2897–2903
133. Mountrichas G, Pispas S, Tagmatarchis N (2008) Grafting-to approach for the functionalization of carbon nanotubes with polystyrene. *Mater Sci Eng B* 152:40–43
134. Sun G, Chen G, Liu J, Yang J, Xie J, Liu Z, Li R, Li X (2009) A facile gemini surfactant-improved dispersion of carbon nanotubes in polystyrene. *Polymer* 50:5787–5793

135. Sun G, Chen G, Liu Z, Chen M (2010) Preparation, crystallization, electrical conductivity and thermal stability of syndiotactic polystyrene/carbon nanotube composites. *Carbon* 48:1434–1440
136. Martins JA, Cruz VS (2011) Flow activation volume of polystyrene/multiwall carbon nanotubes composites. *Polymer* 52:5149–5155
137. Patole AS, Patole SP, Jung SO, Yoo JB, An JH, Kim TH (2012) Self assembled graphene/carbon nanotube/polystyrene hybrid nanocomposite by in situ microemulsion polymerization. *Eur Polym J* 48:252–259
138. Chipara DM, Macossay J, Ybarra AVR, Chipara AC, Eubanks TM (2013) Raman spectroscopy of polystyrene nanofibers Multiwalled carbon nanotubes composites. *Appl Surf Sci* 275:23–27
139. Sarvi A, Sundararaj U (2014) Rheological percolation in polystyrene composites filled with polyaniline-coated multiwall carbon nanotubes. *Synth Met* 194:109–117
140. Suemori K, Kamata T (2017) Thermoelectric characteristics in out-of plane direction of thick carbon nanotube-polystyrene composites fabricated by the solution process. *227:177–181*
141. Cong L, Li X, Ma L, Peng Z, Yang C, Han P, Wang G, Li H, Song W, Song G (2018) High-performance graphene oxide/carbon nanotubes aerogel/polystyrene composites: preparation and mechanical properties. *Mater Lett* 214:190–193
142. Li Y, Pionteck J, Potschke P, Voit B (2019) Organic vapor sensing behavior of polycarbonate/polystyrene/ multi-walled carbon nanotube blend composites with different microstructures. *Mater Des* 179:
143. Joulazadeha M, Navarchian AH (2010) Study on elastic modulus of cross linked polyurethane/organoclay nanocomposites. *Polym Adv, Technol*
144. Yung KC, Wang J, Yue TM (2006) Modeling Young's modulus of polymer-layered silicate nanocomposites using a modified Halpin—Tsai micromechanical model. *J Reinf Plast Compos* 25:8847–8861
145. Kojima Y, Usuki A, Kawasumi M, Okada A, Kurauchi T, Kamigaito OJ (1993) *J Polym Sci Part A Polym Chem* 31:983
146. Yano K, Usuki A, Kurauchi T, Kamigaito O (1993) *J Polym Sci Part A Polym Chem* 31:2493
147. Vaia RA, Ishii H, Giannelis EP (1993) Synthesis and properties of two-dimensional nanostructures by direct intercalation of polymer melts in layered silicates. *Chem Mater* 5:1694–1696
148. Koo CM, Ham HT, Choi MH, Kim SO, Chung IJ (2003) Characteristics of polyvinylpyrrolidone-layered silicate nanocomposites prepared by attrition ball milling. *Polymer* 44:681–689
149. Kojima Y, Usuki A, Kawasumi M, Okada A, Fukushima Y, Kurauchi T, Kamigaito O (1993) *J Mater Res* 8:1185
150. Kojima Y, Usuki A, Kawasumi M, Okada A, Kurauchi T, Kamigaito O (1993) *J Appl Polym Sci* 8:1185
151. Charitos I, Georgousis G, Kontou E (2019) Preparation and thermomechanical characterization of metallocene linear low-density polyethylene/carbon nanotube nanocomposite. *Polym Compos* 40:1263–1273
152. Bae J, Jang J, Yoon SH (2002) *Macromol. Chem Phys* 203:2196–2204
153. Kearns JC, Shambaugh RL (2002) Polypropylene fibers reinforced with carbon nanotubes. *J Appl Polym Sci* 86:2079–2084
154. Pirlot C, Willems I, Fonseca A (2002) Preparation and characterization of carbon nanotube/polyacrylonitrile composites. *Adv Eng Mater* 4:109–114
155. Musa I, Baxendale M, Amaratunga GAJ, Eccleston W (1999) Properties of regioregular poly (3-octylthiophene)/multi-wall carbon nanotube composites. *Synth Met* 102:1250
156. McNally T, Potschke P, Halley P, Murphy M, Martin D, Bell SEJ, Brennan GP, Bein D, Lemoine P, Quinn JP (2005) Polyethylene multiwalled carbon nanotube composites. *Polymer* 46:8222–8232
157. Zhang Q, Rastogi S, Chen D, Lippits D, Lemstra PJ (2006) Low percolation threshold in single-walled carbon nanotube/high density polyethylene composites prepared by melt processing technique. *Carbon* 44:778–785

158. Haggenueller R, Guthy C, Lukes JR, Fischer JE, Winey KI (2007) Single wall carbon nanotube/polyethylene nanocomposites: thermal and electrical conductivity. *Macromolecules* 40:2417–2421
159. Kanagaraj S, Varanda FR, Zhil'tsova TV, Oliveira MSA, Simoes JAO (2007) Mechanical properties of high density polyethylene/carbon nanotube composites. *Compos Sci Technol* 67:3071–3077
160. Adhikari AR, Chipara M, Lozano K (2009) Processing effects on the thermo-physical properties of carbon nanotube polyethylene composite. *Mater Sci Eng A* 526:123–127
161. Palza H, Reznik B, Kappes M, Hennrich F, Naue IFC, Wilhelm M (2010) Characterization of melt flow instabilities in polyethylene/carbon nanotube composites. *Polymer* 51:3753–3761
162. Gorrasi G, Lieto RD, Patimo G, Pasquale SD, Sorrentino A (2011) Structure property relationships on uniaxially oriented carbon nanotube/polyethylene composites. *Polymer* 52:1124–1132
163. Sreekant PSR, Kumar NN, Kanagaraj S (2012) Improving post irradiation stability of high density polyethylene by multi walled carbon nanotubes. *Compos Sci Technol* 72:390–396
164. Yim YJ, Park SJ (2015) Electromagnetic interference shielding effectiveness of high-density polyethylene composites reinforced with multi-walled carbon nanotubes. *J Ind Eng Chem* 21:155–157
165. Malekie S, Ziaie F (2015) Study on a novel dosimeter based on polyethylene–carbon nanotube composite. *Nucl Instrum Methods Phys Res Sect A* 791:1–5
166. Goyal M, Goyal N, Kaur H, Gera A, Minocha K, Jindal P (2016) Fabrication and characterisation of low density polyethylene (LDPE)/multi walled carbon nanotubes (MWCNTs) nano-composites. *Persp Sci* 8:403–405
167. Yang J, Zhang X, Liu C, Li X, Li H, Ma G, Tian F (2017) Effects of 1 MeV electrons on the deformation mechanisms of polyethylene/carbon nanotube composites. *Nucl Instrum Methods Phys Res Sect B* 409:2–8
168. Kazakova MA, Selyutin AG, Semikolenova NV, Ishchenko AV, Moseenkov SI, Matsko MA et al (2018) Structure of the in situ produced polyethylene based composites modified with multi-walled carbon nanotubes: in situ synchrotron X-ray diffraction and differential scanning calorimetry study. *Compos Sci Technol* 167:148–154
169. Hu C, Liao X, Qin QH, Wang G (2019) The fabrication and characterization of high density polyethylene composites reinforced by carbon nanotube coated carbon fibers. *Compos A Appl Sci Manuf* 121:149–156
170. Peng B, Jiang Y, Zhu A (2019) A novel modification of carbon nanotubes for improving the electrical and mechanical properties of polyethylene composites. *Polym Test* 74:72–76
171. Kurup SN, Ellingford C, Wan C (2020) Shape memory properties of polyethylene/ethylene vinyl acetate/carbon nanotube composites. *Polym Test* 81:
172. Broza G, Piszczek K, Schulte K, Sterzynski T (2007) Nanocomposites of poly(vinyl chloride) with carbon nanotubes (CNT). *Compos Sci Technol* 67:890–894
173. O'connor I, Hayden H, O'connor S, Coleman JN, Gun'ko YK (2008) Kevlar coated carbon nanotubes for reinforcement of polyvinylchloride. *J Mater Chem* 18:5585–5588
174. Sterzynski T, Tomaszewska J, Piszczek K, Skorczewska K (2010) The influence of carbon nanotubes on the PVC glass transition temperature. *Compos Sci Technol* 70:966–969
175. Mkhabela VJ, Mishra AK, Mbianda XY (2011) Thermal and mechanical properties of phosphorylated multiwalled carbon nanotube/polyvinyl chloride composites. *Carbon* 49:610–617
176. Zaho F, Qiu F, Zhang X, Yu S, Kim SH, Park HD, Takizawa S, Wang P (2012) Preparation of single-walled carbon nanotubes/ polyvinylchloride membrane and its antibacterial property. *Water Sci Technol* 66:2275–2283
177. Song BJ, Ahn JW, Cho KK, Roh JS, Lee DY, Yang YS et al (2013) Electrical and mechanical properties as a processing condition in polyvinylchloride multi walled carbon nanotube composites. *J Nanosci Nanotechnol* 13:7723–7727
178. Vasanthkumar MS, Bhatia R, Arya VP, Sameera I, Prasad V, Jayanna HS (2014) Characterization, charge transport and magnetic properties of multi-walled carbon nanotube–polyvinyl chloride nanocomposites. *Physica E* 56:10–16

179. Zanjanijam AR, Bahrami M, Hajian M (2016) Poly(vinyl chloride)/single wall carbon nanotubes composites: investigation of mechanical and thermal characteristics. *J Vinyl Add Tech* 22:128–133
180. Hezma AM, Elashmawi IS, Abdelrezek EM, Rajesh A, Kamal M (2017) Enhancement of the thermal and mechanical properties of polyurethane/polyvinyl chloride blend by loading single walled carbon nanotubes. *Prog Natl Sci Mater Int* 27:338–343
181. Jiashun T, Yujun Q, Pu Z, Zhixin G (2019) Preparation and properties of polyvinyl chloride/carbon nanotubes composite. *J Wuhan Univ Technol Mater Sci Ed* 34(3):516–520
182. Daver F, Baez E, Shanks RA, Brandt M (2016) Conductive polyolefin–rubber nanocomposites with carbon nanotubes. *Compos A Appl Sci Manuf* 80:13–20
183. Lee SH, Park JS, Lim BK, Kim SO (2008) Polymer/carbon nanotube nanocomposites via noncovalent grafting with end-functionalized polymers. *J Appl Polym Sci* 110:2345–2351
184. Haghghatpanah S, Bolton K (2013) Molecular-level computational studies of single wall carbon nanotube–polyethylene composites. *Comput Mater Sci* 69:443–454
185. Ritter U, Scharff P, Pinchuk TM (2010) Radiation modification of polyvinyl chloride nanocomposites with multi-walled carbon nanotubes. *Mater Sci Eng Technol* 41:675–681
186. Chipara M, Cruz J, Vega ER, Alarcon J, Mion T, Chipara DM, Ibrahim E, Tidrow SC, Hui D (2012) Polyvinylchloride-single-walled carbon nanotube composites: thermal and spectroscopic properties. *J Nanomater* 1–6
187. Grady BP, Pompeo F, Shambaugh RL, Resasco DE (2002) Nucleation of polypropylene crystallization by single-walled carbon nanotubes. *J Phys Chem B* 106:5852–5858
188. Moore EM, Ortiz DL, Marla VT, Shambaugh RL, Grady BP (2004) Enhancing the strength of polypropylene fibers with carbon nanotubes. *J Appl Polym Sci* 93:2926–2933
189. Yang J, Lin Y, Wang J, Lai M, Li J, Liu J, Tong X, Chen H (2005) Morphology, thermal stability, and dynamic mechanical properties of atactic polypropylene/carbon nanotube composites. *J Appl Polym Sci* 98:1087–1091
190. Manchado MAL, Valentini L, Biagiotti J, Kenny JM (2005) Thermal and mechanical properties of single-walled carbon nanotubes–polypropylene composites prepared by melt processing. *Carbon* 43:1499–1505
191. Funck A, Kaminsky W (2007) Polypropylene carbon nanotube composites by in situ polymerization. *Compos Sci Technol* 67:906–915
192. Tjong SC, Liang GD, Bao SP (2007) Electrical behavior of polypropylene/multiwalled carbon nanotube nanocomposites with low percolation threshold. *Scripta Mater* 57:461–464
193. Koval'chuk AA, Shchegolikhin AN, Shevchenko VG, Nedorezova PM, Klyamkina AN, Aladyshev AM (2008) Synthesis and properties of polypropylene/multiwall carbon nanotube composites. *Macromolecules* 41:3149–3156
194. Li WH, Chen XH, Yang Z, Xu LS (2009) Structure and properties of polypropylene-wrapped carbon nanotubes composite. *J Appl Polym Sci* 113:3809–3814
195. Soitong T, Pumchusak J (2011) Morphology and tensile properties of polypropylenemulti-walled carbon nanotubes composite fibers. *J Appl Polym Sci* 119:962–967
196. Long GJ, Hui LY, Ming LD (2011) Preparation and properties of recycled polypropylene/carbon nanotube composites. *Adv Mater Res* 279:106–111
197. Tambe PB, Bhattacharyya AR, Kulkarni AJ (2012) The influence of melt-mixing process conditions on electrical conductivity of polypropylene/multiwall carbon nanotubes composites. *J Appl Polym Sci* 1–10
198. Araujo RS, Oliveira RJB, Marques MDFV (2014) Preparation of nanocomposites of polypropylene with carbon nanotubes via masterbatches produced by in situ polymerization and by melt extrusion. *Macromol React Eng* 8:747–754
199. Ghoshal S, Wang PH, Gulgunje P, Verghese N, Kumar S (2016) High impact strength polypropylene containing carbon nanotubes. *Polymer* 100:259–274
200. Wang PH, Sarkar S, Gulgunje P, Verghese N, Kumar S (2018) Fracture mechanism of high impact strength polypropylene containing carbon nanotubes. *Polymer* 151:287–298
201. Zhao C, Hu G, Justice R, Schaefer DW, Zhang S, Yang M, Han CC (2005) Synthesis and characterization of multi-walled carbon nanotubes reinforced polyamide 6 via in situ polymerization. *Polymer* 46:5125–5132

202. Giraldo LF, Lopez BL, Brostow W. Effect of the Type of Carbon Nanotubes on Tribological Properties of Polyamide 6. *Polymer Engineering & Science*. 2009; 896–902
203. Mahmood, N., Islam, M., Hameed, A., Saeed, S., Polyamide 6/Multiwalled Carbon Nanotubes Nanocomposites with Modified Morphology and Thermal Properties 2013, 5, 1380–1391
204. Li J, Tong L, Fang Z, Gu A, Xu Z (2006) Thermal degradation behavior of multi-walled carbon nanotubes/polyamide 6 composites. *Polym Degrad Stab* 91:2046–2052
205. Ha H, Kim SC (2010) Morphology and Properties of Polyamide/Multi-walled Carbon Nanotube Composites. *Macromol Res* 18:660–667
206. Zhao H, Qiu S, Wu L, Zhang L, Chen H, Gao C (2014) Improving the performance of polyamide reverse osmosis membrane by incorporation of modified multi-walled carbon nanotubes. *J Membr Sci* 450:249–256
207. Ferreira T, Paiva MC, Pontes AJ (2013) Dispersion of carbon nanotubes in polyamide 6 for microinjection moulding. *J Polym Res* 301:1–9
208. Logakis E, Pandis C, Peogols V, Pissis P, Stergiou C, Pionteck J, Potschke P, Micusik M, Omastova M (2009) Structure-Property Relationships in Polyamide 6/Multi-Walled Carbon Nanotubes Nanocomposites. *Journal of Polymer Science*. 47:764–774
209. Iijima S (1991) Helical microtubules of graphitic carbon. *Nature* 354(6348):56–58
210. Simon J, Flahaut E, Golzio M (2019) Overview of Carbon Nanotubes for Biomedical Applications. *Materials*. 12:624
211. Sireesha M, Babu VJ, Ramakrishna S (2017) Functionalized carbon nanotubes in bio-world: Applications, limitations and future directions. *Mater Sci Eng, B* 223:43–63
212. Hirlekar R, Yamagar M, Garse H, Vij M, Kadam V (2009) Carbon nanotubes and its applications: a review. *Asian Journal*. 2:17–27
213. Kunzmann A, Andersson B, Thurnherr T, Krug H, Scheynius A, Fadeel B. Toxicology of engineered nanomaterials: Focus on biocompatibility, biodistribution and biodegradation. *Biochimica et Biophysica Acta (BBA) - General Subjects*. 2011; 1810:361–373
214. Smart SK, Cassidy AI, Lu GQ, Martin DJ (2006) The biocompatibility of carbon nanotubes. *Carbon* 44:1034–1047
215. Dey P, Das N (2013) Carbon nanotubes: it's role in modern health care. *International Journal of Pharmacy and Pharmaceutical Sciences*. 5:9–13
216. Cao Y, Huang H-Y, Chen L-Q, Du H-H, Cui J-H, Zhang LW, Lee B-J, Cao Q-R (2019) Enhanced lysosomal escape of pH-responsive PEI-betaine functionalized carbon nanotube for the co-delivery of survivin siRNA and doxorubicin. *ACS Appl Mater Interfaces* 11:9763–9776
217. Chou CC, Hsiao HY, Hong QS, Chen CH, Peng YW, Chen HW, Yang PC (2008) Single-Walled Carbon Nanotubes Can Induce Pulmonary Injury in Mouse Model. *Nano Lett* 8:437–445
218. Khan MU, Reddy KR, Snguanwongchai T, Haque E, Gomes VG (2016) Polymer brush synthesis on surface modified carbon nanotubes via in situ emulsion polymerization. *Colloid Polym Sci* 294:1599–1610
219. Che J, Cagin T, Goddard WA III (2000) Thermal conductivity of carbon nanotubes. *Nanotechnology*. 11:65–69
220. Song C, Yun J, Lee H, Park H, Jeong YR, Lee G, Kim MU, Ha JS. A Shape Memory High-Voltage Supercapacitor with Asymmetric Organic Electrolytes for Driving an Integrated NO₂ Gas Sensor. *Advanced Functional Materials*. 2019; 1–12
221. Liu Z, Sun X, Ratchford NN, Dai H (2007) Supramolecular Chemistry on Water Soluble Carbon Nanotubes for Drug Loading and Delivery. *ACS Nano* 1:50–56
222. Liu Z, Fan AC, Rakhra K, Sherlock S, Goodwin A, Chen X et al (2009) Supramolecular Stacking of Doxorubicin on Carbon Nanotubes for In Vivo Cancer Therapy. *Angew Chem* 48:7668–7672
223. Miyawaki J, Yudasaka M, Imai H, Yorimitsu H, Isobe H, Nakamura E, Iijima S (2006) Synthesis of Ultrafine Gd₂O₃ Nanoparticles Inside Single-Wall Carbon Nanohorns. *J. Phys. Chem. B*. 110:5179–5181
224. Kim J, Yoo H, Ba VAP, Shin N, Hong S (2018) Dye-functionalized Sol-gel Matrix on Carbon Nanotubes for Refreshable and Flexible Gas Sensors. *Scientific reports*. 8:11958

225. Im JS, Bai BC, Lee YS (2010) The effect of carbon nanotubes on drug delivery in an electro-sensitive transdermal drug delivery system. *Biomaterials* 31:1414–1419
226. Servant A, Methven L, Williams RP, Kostarelou K (2013) Electroresponsive polymer-carbon nanotube hydrogel hybrids for pulsatile drug delivery in vivo. *Adv Healthcare Mater* 2:806–811
227. Foldvari M, Bagonluri M (2008) Carbon nanotubes as functional excipients for nanomedicines: II. Drug delivery and biocompatibility issues. *Nanomed Nanotechnol Biol Med* 4:183–200
228. Wang JTW, Fabbro C, Venturini E, Methven L, Ros TD, Robinson MK (2014) The relationship between the diameter of chemically-functionalized multi-walled carbon nanotubes and their organ biodistribution profiles in vivo. *Biomaterials* 35:9517–9528
229. Costa PM, Bourgognon M, Wang JTW, Jamal KTA (2016) Functionalised carbon nanotubes: from intracellular uptake and cell-related toxicity to systemic brain delivery. *J Controlled Release* 241:200–219
230. Akhtari J, Faridnia R, Kalani H, Bastani R, Fakhari M, Rezvan H, Beydokhti AK (2019) Potent in vitro antileishmanial activity of a nanoformulation of cisplatin with carbon nanotubes against *Leishmania major*. *J Glob Antimicrob Resist* 16:11–16
231. Loos LR, Coelho LAF, Pezzin SH, Amico SC (2008) Effect of carbon nanotubes addition on the mechanical and thermal properties of epoxy matrices. *Mater Res* 11:347
232. Lam CW, James JT, McCluskey R, Hunter RL (2004) Pulmonary toxicity of single-wall carbon nanotubes in mice 7 and 90 days after intratracheal instillation. *Toxicol Sci* 77:126–134
233. Fang L, Zhao C, Chen Y, Sheng L, An K, Yu L, Ren W, Zhao X (2015) Single-chirality separation of ultra-thin semiconducting arc discharge single-walled carbon nanotubes. *Carbon* 91:408–415
234. Khazaei A, Rad MNS, Borazjani MK (2010) Organic functionalization of single-walled carbon nanotubes (SWCNTs) with some chemotherapeutic agents as a potential method for drug delivery. *Int J Nanomed* 5:639–645
235. Lotfi M, Morsali A, Bozorgmehr MR (2018) Comprehensive quantum chemical insight into the mechanistic understanding of the surface functionalization of carbon nanotube as a nanocarrier with cladribine anticancer drug. *Appl Surf Sci* 462:720–729
236. Wei C, Dong X, Zhang Y, Liang J, Yang A, Zhu D, Liu T (2018) Simultaneous fluorescence imaging monitoring of the programmed release of dual drugs from a hydrogel-carbon nanotube delivery system. *Sens Actuators B Chem* 273:264–275
237. Karthika V, Kaleeswaran P, Gopinath K, Arumugam A, Govindarajan M, Alharbi NS, Khaled JM, Al-anbr MN, Benelli G (2018) Biocompatible properties of nano-drug carriers using TiO₂-Au embedded on multiwall carbon nanotubes for targeted drug delivery. *Mater Sci Eng C* 90:589–601
238. Mazzaglia A, Scala A, Sortinao G, Zagami R, Zhu Y, Pizzo MM, Piperno A (2018) Intracellular trafficking and therapeutic outcome of multiwalled carbon nanotubes modified with cyclodextrins and polyethylenimine. *Colloids Surf B* 163:55–63
239. Mallakpour S, Khodadadzadeh L (2018) Ultrasonic-assisted fabrication of starch/MWCNT-glucose nanocomposites for drug delivery. *Ultrason Sonochem* 40:402–409
240. Gonzalez-Lavado E, Iturrioz-Rodriguez N, Padin-Gonzalez E, Gonzalez J, Villegas JC, Valiente R, Fanarraga ML Biodegradable multi-walled carbon nanotubes trigger antitumoral effects. *Nanoscale* 1–8
241. Hesabi M, Behjatmanesh-Ardakani R (2018) Investigation of carboxylation of carbon nanotube in the adsorption of anti-cancer drug: a theoretical approach. *Appl Surf Sci* 427:112–125
242. Kamel M, Raissi H, Morsali A, Shahabi M (2017) Assessment of the adsorption mechanism of flutamide anticancer drug on the functionalized single-walled carbon nanotube surface as a drug delivery vehicle: an alternative theoretical approach based on DFT and MD. In: *APSUSC* 2017
243. Li H, Sun X, Li Y, Liang C, Wang H (2018) Preparation and properties of carbon nanotube (Fe)/hydroxyapatite composite as magnetic targeted drug delivery carrier. *Mater Sci Eng*

244. Saeednia L, Yao L, Cluff K, Asmatulu R (2019) Sustained releasing of methotrexate from injectable and thermosensitive chitosan-carbon nanotube hybrid hydrogels effectively controls tumor cell growth. *ACS Omega* 4:4040–4048
245. Biagitto G, Ligi MC, Fedeli S, Pranzini E, Gamberi T, Cicchi S, Paoli P (2018) Metformin salts with oxidized multiwalled carbon nanotubes: in vitro biological activity and inhibition of CNT internalization. *J Drug Delivery Sci Technol* 254–258
246. Sukhodub LB, Sukhodub LF, Prylutsky YI, Strutynska NY, Vovchenko LL, Soroca VM, Slobodyanik NS, Tsierkezos NG, Ritter U (2018) Composite material based on hydroxyapatite and multi-walled carbon nanotubes filled by iron: preparation, properties and drug release ability. *Mater Sci Eng C*
247. Rafi AA, Jeedi MK, Hashemi AB, Mahkam M (2017) Synthesis of multiwalled carbon nanotubes–poly(Methacrylic Acid) nanohybrid systems: characterization, thermal properties, and in vitro release studies of naproxen as a model drug. *Polym Plast Technol Eng* 1–8
248. Saito N, Haniu H, Usui Y, Aoki K, Hara K, Takanashi S et al (2014) Safe clinical use of carbon nanotubes as innovative biomaterials. *Chem Rev* 114(11):6040–6079
249. Serpell CJ, Kostarelos K, Davis BG (2016) Can carbon nanotubes deliver on their promise in biology? Harnessing unique properties for unparalleled applications. *ACS Cent Sci* 2:190–200
250. Kuche K, Maheshwari R, Tambe V, Mak K-K, Jogi H, Raval N et al (2018) Carbon nanotubes (CNTs) based advanced dermal therapeutics: current trends and future potential. *Nanoscale* 10:8911–8937
251. Zuru DU (2019) Theoretical model for the design and preparation of a CNT–ursonic acid drug matrix as HIV-gp120 entry inhibitor. *Sci Afr* 6:00177
252. Elhissi AMA, Ahmed W, Hassan IU, Dhanak VR, D’Emanuele A (2012) Carbon nanotubes in cancer therapy and drug delivery. *J Drug Delivery* 837327:10
253. Madani SY, Naderi N, Dissanayake O, Tan A, Seifalian AM (2011) A new era of cancer treatment: carbon nanotubes as drug delivery tools. *Int J Nanomed* 6:2963–2979
254. Sanginario A, Miccoli B, Demarchi D (2017) Carbon nanotubes as an effective opportunity for cancer diagnosis and treatment. *Biosensors* 7:9
255. Jaque D, Maestro LM, Rosal BD, Haro-Gonzalez P, Benayas A, Plaza JL, Rodríguez EM, Solé JG (2014) Nanoparticles for photothermal therapies. *Nanoscale* 6:9494–9530
256. Liu Z, Robinson JT, Tabakman SM, Yang M, Dai H (2011) Carbon materials for drug delivery and cancer therapy. *Materialstoday* 14:316–323
257. Zhou F, Xing D, Ou Z, Wu B, Resasco DE, Chen WR (2009) Cancer photothermal therapy in the near-infrared region by using single-walled carbon nanotubes. *J Biomed Opt* 14(2):
258. Sobhani Z, Behnam MA, Emami F, Dehghanian A, Jamhiri I (2017) Photothermal therapy of melanoma tumor using multiwalled carbon nanotubes. *Int J Nanomed* 12:4509–4517
259. Langer R, Vacanti JP (1993) *Tissue Eng* 260:920–926
260. Chen F-M, Liu X (2016) Advancing biomaterials of human origin for tissue engineering. *Prog Polym Sci* 53:86–168
261. Ma PX (2004) Scaffolds for tissue fabrication. *Materialstoday* 7:30–40
262. Nikolova MP, Chavali MS (2019) Recent advances in biomaterials for 3D scaffolds: a review. *Bioactive Mater* 4:271–292
263. Stout DA, Webster TJ (2012) Carbon nanotubes for stem cell control. *Materialstoday* 15:312–318
264. Veetil JV, Ye K (2009) Tailored carbon nanotubes for tissue engineering applications. *Biotechnol Prog* 25(3):709–721
265. Eivazzadeh-Keihan R, Maleki A, Guardia MDL, Bani MS, Chenab KK, Pashazadeh-Panahi P et al (2009) Carbon based nanomaterials for tissue engineering of bone: building new bone on small black scaffolds: a review. *J Adv Res* 18:185–201
266. Gurjar PN, Chouksey S, Patil G, Naik N, Agrawal S (2013) Carbon nanotubes: pharmaceutical applications. *Asian Biomed Pharm* 3:8–13
267. Paul A, Hasan A, Al KH, Gaharwar K, Rao VTS, Nikkhah M et al (2014) Injectable graphene oxide/hydrogel-based angiogenic gene delivery system for vasculogenesis and cardiac repair. *ACS Nano* 8:8050–8062

268. Hasan A, Ragaert K, Swieszkowski W, Selimovic S, Paul A, Camci-unal G, Mofrad MRK, Khademhosseini A (2014) Biomechanical properties of native and tissue engineered heart valve constructs. *J Biomech* 47:1949–1963
269. Bosi S, Ballerini L, Prato M (2013) Carbon nanotubes in tissue engineering. *Making Exploit Fullerenes Graphene Carbon Nanotubes* 348:181–204
270. Lovat V, Pantarotto D, Lagostena L, Cacciari B, Grandolfo M, Righi M, Spalluto G, Prato M, Ballerini L (2005) Carbon nanotube substrates boost neuronal electrical signaling. *Nano Lett* 5(6):1107–1110
271. Arslantunali D, Budak G, Hasirci V (2013) Multiwalled CNT-pHEMA composite conduit for peripheral nerve repair. *J Biomed Mater Res Part A*
272. Armentano I, Dottori M, Fortunati E, Mattioli S, Kenny JM (2010) Biodegradable polymer matrix nanocomposites for tissue engineering: a review. *Polym Degrad Stab* 95:2126–2146
273. Cho Y, Borgens RB (2010) The effect of an electrically conductive carbon nanotube/collagen composite on neurite outgrowth of PC12 cells. *Wiley Online Library*, pp 1–8
274. Zhang X, Wang X, Lu Q, Fu C (2008) Influence of carbon nanotube scaffolds on human cervical carcinoma HeLa cell viability and focal adhesion kinase expression. *Carbon* 46:453–460
275. Mackle JN, Blond DJ-P, Mooney E, McDonnell Blau WJ, Shaw G, Barry FP, Murphy JM, Barron V (2011) In vitro characterization of an electroactive carbon-nanotube-based nanofiber scaffold for tissue engineering. *Macromol Biosci* 11:1272–1282
276. Ogihara N, Usui Y, Aoki K, Shimizu M, Narita N, Hara K, Taruta S, Saito N (2012) Biocompatibility and bone tissue compatibility of alumina ceramics reinforced with carbon nanotubes. *Nanomedicine* 7(7):981–993
277. Badhe RV, Bijukumar D, Chejara DR, Mabrouk M, Choonara YE, Kumar P, Toit LCD, Kondiah PPD (2016) A composite chitosan-gelatin bi-layered, biomimetic macroporous scaffold for blood vessel tissue engineering. *Carbohydr Polym* 1–10
278. Suo X, Eldridge BN, Zhang H, Mao C, Min Y, Sun Y, Singh R, Ming X (2018) P-Glycoprotein-Targeted photothermal therapy of drug-resistant cancer cells using antibody-conjugated carbon nanotubes. *ACS Appl Mater Interfaces* 10:33464–33473
279. Liu X, Xu D, Liao C, Fang Y, Guo B (2018) Development of a promising drug delivery for formononetin: cyclodextrin modified single-walled carbon nanotubes. *J Drug Delivery Sci Technol* 43:461–468

Molecularly Imprinted Polymer—Carbon Dot Composites for Biomedical Application



Monika Sobiech and Piotr Luliński 

Abstract Carbon dots, a kind of materials discovered nearly two decades ago, have attracted attention due to unique properties such as bright fluorescence emission, facile synthetic ways, high chemical and photostability, low cytotoxicity, good biocompatibility and environmental friendliness. The tunable fluorescence features caused widespread applicability in different scientific fields but mainly in biomedicine. However, the analytical methods that based on carbon dot fluorescence measurements are characterized by insufficient selectivity, weak anti-interference ability and moderate sensitivity. Thus, prior to utilization to highly complex biomedical samples, those materials have to be functionalized. Here, molecularly imprinted polymers are the class of materials, synthesized in the presence of template molecules, that provide sufficient selectivity, high cleanup capabilities as well as satisfactory enrichment potential. In this chapter, the biomedical application of molecularly imprinted polymer-functionalized carbon dots will be presented. The brief characterization of carbon dot synthetic approaches together with summarized overview of imprinting process and its limitations followed by detailed discussion of the current state of the art of the carbon dot molecularly imprinted polymer conjugates for biomedicine will provide insight into the future prospects of those advanced materials.

Keywords Carbon dot · Molecularly imprinted polymer · Biomedical application · Biomolecules · Material characterization

1 Introduction

Molecular imprinting technology enables production of materials called molecularly imprinting polymers (MIPs) with unique, desirable properties of specific recognition of target molecules or similar objects. MIPs are paying researchers' attention

M. Sobiech · P. Luliński (✉)
Department of Organic Chemistry, Faculty of Pharmacy,
Medical University of Warsaw, Banacha 1, 02-097 Warsaw, Poland
e-mail: piotr.lulinski@wum.edu.pl

© The Author(s), under exclusive license to Springer Nature Switzerland AG 2022
M. S. Hasnain et al. (eds.), *Polymeric and Natural Composites*,
Advances in Material Research and Technology,
https://doi.org/10.1007/978-3-030-70266-3_5

151

due to high selectivity and specificity toward the chosen analytes. Additionally, the MIPs are characterized by satisfactory stability and resistance to chemicals and mechanical treatment as well as simpler and less expansive preparation process when compared to the biological selectively recognized systems such as enzymes or antibodies [1]. Described advantageous qualities of MIPs paved the way for application in various fields including: extraction [2], chromatography [3] and electrophoresis [4] as stationary phases, different types of sensors (electrochemical, optical, mass-sensitive, etc.) as recognizing elements [5], drug delivery systems [6], catalysis [7], synthesis [8] (Fig. 1).

The wide spectrum of MIPs applications imposes defined structural format of the material suitable to the chosen purpose from monoliths and membranes to beads and films. The most common way of MIPs synthesis is bulk polymerization as a simple and low-cost method. However, obtained product possesses some drawbacks such as the template leakage, mass transfer limitation and wide range of particle size [9]. To overcome the problems, the production of nano-sized MIPs that enables their application in biomedical areas such as diagnostics, imaging and drug delivery is an alternative. Among nano-sized MIPs, the core-shell nanoparticles can be distinguished. The above-mentioned MIP form includes the imprinted shell and the core built from different kinds of materials that could affect MIP core-shell optical, magnetic, electronic or mechanical properties.

One of the core materials utilized for MIPs core-shell production is carbon dots (CDs). Due to their optical properties, CDs enable to execute fluorescence measurements. The advantages of the fluorescence analysis such as cost-effectiveness,

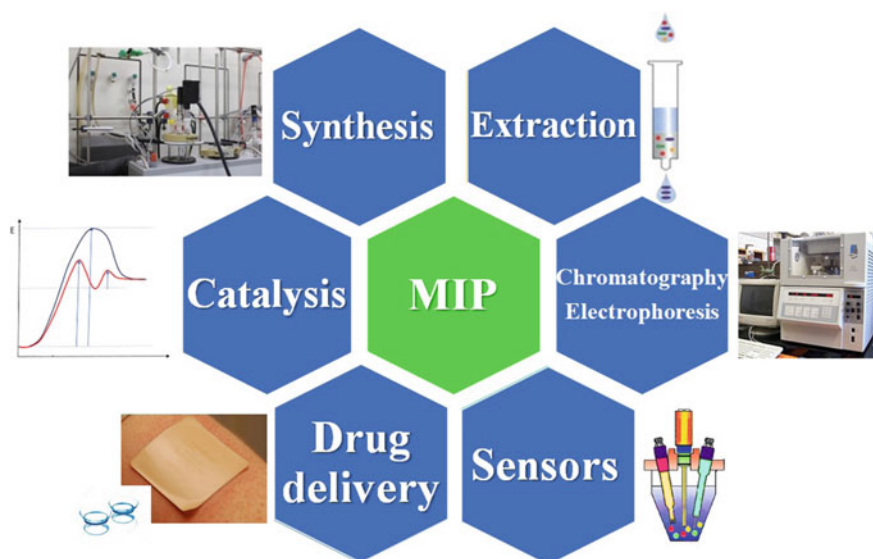


Fig. 1 Application of MIPs

simplicity and satisfactory sensitivity made this instrumental technique highly attractive. Nevertheless, the direct fluorescence analysis of target analytes is not frequently proceeded because of the limited group of compounds, possessing fluorescence properties. For that reason, CDs could be a valuable alternative. Additionally, CDs possess satisfactory chemical stability and controllable optical properties. The designability and functionality of the fluorescent CDs resulted with unprecedented biomedical applicability. However, taking into account biomedical applications of such devices, the complicated sample matrix could affect the measurements. Thus, the fabrication of materials that possess ability to reduce the sample matrix effect or to enhance the cleanup capabilities is highly required. Here, merging CDs with MIPs could result with selective and sensitive fluorescence probes that can be utilized in the biomedical analysis.

In this chapter, we will focus on CDs synthesis and functionalization processes with the use of specific precursors and we will highlight principles and limitations of MIPs prior to discussion of recent advances in the fabrication and the biomedical application of CD–MIPs conjugates. Finally, the current limits and future prospects for the CD–MIPs conjugates will be pointed out.

2 Carbon Dot (CD)—Synthetic Approaches

The CDs are new fascinating zero-dimensional carbon-built nanomaterials with the size less than 20 nm [11, 12]. The structure of CDs is composed of the core, consisting of the sp^2 -hybridized carbon embedded in the sp^3 carbon matrix or graphene nanosheets consisting of stabilized shell of functionalized groups such as carboxyl, hydroxyl, amine, ether, carbonyl or polymeric aggregates [13, 14]. The core provides fluorescence properties of CDs, and the shell is responsible for control of optical properties, water solubility, biocompatibility and the capability for compositing with other materials [14–16]. The term of CDs ranges four carbon nanostructures: carbon quantum dots (CQDs), carbon nanodots (CNDs), graphene quantum dots (GQDs) and carbon polymeric nanodots (CPDs) which are classified according to the crystal core structure, properties and surface groups. The CQDs are spherical nanoparticles composed of the multilayered crystalline graphitic structures with chemical groups on the surface, the CNDs do not possess crystal lattice structure, the core of GQDs is built from small graphene sheets, and the CPDs possess polymer/carbon hybrid structure including multiple functional groups and/or polymer chains on the surface and a carbon core [14, 15, 17].

The discovery of CDs in 2000 was related to the observation of green luminescence of polymer-bound carbon nanotubes in the solution [18]. The phenomenon was explained, concerning the presence of luminescent impurities or small aromatic species from the solubilization reactions. The first synthesis of CDs was performed accidentally in 2004 during the purification process of single-walled carbon nanotubes derived from arc-discharge soot [19]. However, the term of CDs was used for the first time in 2006 by Sun et al. [20] during the studies that aimed to explain

the impact of the surface passivation on the luminescence properties of CDs. Ever since, there has been growing interest in the preparation of fluorescent CDs as an attraction for toxic quantum dots because of desirable properties of CDs, including superior optical properties (e.g., strong absorption, bright photoluminescence, excellent light stability and resistance to light bleaching) [21, 22], low toxicity [23, 24], eco-friendliness [25, 26], good biocompatibility [27, 28], high water solubility [29, 30], easy synthesis [31], and functionalization processes [32, 33] or tunable fluorescence and quantum yield (QY) [34, 35]. The syntheses of CDs were performed, showing wide spectrum of possible CDs application fields such as bioimaging [36, 37], disease therapy [38, 39], gene and drug delivery [40, 41], energy conversion (e.g., light-emitting diodes) [42], photovoltaic solar cells [43], sensing [44, 45] and catalysis [46, 47] (Fig. 2).

Taking into account the kind of starting carbon source, the synthetic strategies of CDs could be divided into two main types, so-called top-down and bottom-up. In the “top-down” strategy, a large-sized carbon material is destroyed or dispersed into nano-sized CDs by chemical or physical treatment. On the other hand, in the “bottom-up” method, the small molecular structures are converted into CDs, mainly by the chemical reaction [33, 48, 49].

During the CDs formation by the “top-down” method, the bulky or sheet carbon sources such as graphene [50], graphene oxide [51], carbon soot [52], carbon fibers [53], carbon nanotubes [54], activated carbon [55], graphite [56], oxidized graphite [57], carbohydrates [58], fullerene [59] and coal [60] are breaking down, using mainly arc discharge, laser ablation/passivation, chemical oxidation or electrochemical methods [33, 61, 62]. In the green synthesis as carbon precursor candle, tire or natural gas soot could be used as well [44].



Fig. 2 Application of CDs

In the first report that documented the synthesis of CDs in 2004, the **arc-discharge** method was applied. Xu et al. [19] obtained water-soluble, green–blue, yellow and orange fluorescent CDs from arc-discharged single-walled carbon nanotube soot. Unfortunately, the product possessed wide size distribution. In another example, Dey et al. [63] prepared undoped and B-doped GQDs from graphite in two-step process. Firstly, gas-phase arc-discharge method with carbon and boron sources was applied followed by the chemical cutting. Resultant particles had average diameter of 5–6 nm and strong blue emission related to the excitation wave. The B-doped CDs were prepared because the heteroatom doping is a preferable way to improve the performance of CDs.

In the pioneering study in which the name “carbon dots” in 2006 was used for the first time, Sun et al. [20] obtained CDs from appropriately prepared mixture of graphite powder and cement via **laser ablation** method. In the presence of water vapor in an argon atmosphere and acidic treatment, the CDs were produced prior to passivation by organic and polymeric agents. Resultant products had the average diameter of about 5 nm and the QY between 4 and 10% that depended on the effectiveness of passivation process. Yu et al. [64] formed CDs by laser irradiation with the use of toluene as the carbon source. Nguyen et al. [65] applied double-pulse femtosecond laser ablation for synthesis of ultra-small CDs from graphite powder dispersed in ethanol. The size of CDs varied between 0.5 and 2.0 nm, and it was smaller than the size of CDs obtained by single-pulse ablation.

The **chemical oxidation** method treats the carbon material with the use of strong oxidants such as nitric and sulphuric acids, potassium permanganate or hydrogen peroxide. This easy, fast and repeatable technique gives the possibility of large-scale production and enables to introduce hydrophilic groups (such as carboxyl or hydroxyl) on the surface [33, 49]. Liu et al. [66] applied acidic oxidation during the synthesis of multicolor fluorescent CDs from candle soot. Obtained products were small with the size under 2 nm and were characterized by water solubility but possessed relatively low QY value of 0.8 or 1.9%. In another example, Zhou et al. [59] produced yellow-emissive CDs from fullerene soot with the use of oxidizing mixture of nitric and sulphuric acids. The structures had a diameter of 2–3 nm. The QY of the co-produced CDs was in the range of 3–5% which is relatively satisfactory value, considering the CDs obtained by “top-down” methods. Coal was used as a carbon source to produce CDs by “top-down” method which combined carbonization and acidic oxidation techniques [67]. The size and QY value of resultant CDs were dependent on the carbonization temperature and varied between 2 and 3.1 nm and 0.55 and 1.1%, respectively. After the CDs reduction, the QY increased to 8.8%. The product was successfully applied for Cu^{2+} ion sensing in water samples.

The **electrochemical method** is a simple operation carried out under the normal pressure and in room temperature. Together with readily available setup, this method is the most frequently used among “top-down” approaches. Zhou et al. [68] demonstrated the first electrochemical synthesis of blue fluorescent CDs from multi-walled carbon nanotubes that covered carbon paper. Obtained product had the size of about 2.8 nm and QY of 6.4%. Li et al. [69] prepared CDs from graphite rods with the use of aqueous salt solution as electrolyte. The addition of salt to distilled water

used as electrolyte shortened operation time from 7 days to 20 min only, giving the product with comparable size (1–3 nm) and easy access for the scale-up production. In another example, the GQDs were produced from graphite rods with the use of sodium hydroxide and citric acid mixture as the electrolyte in the electrochemical exfoliation process [70]. The average size of blue to green fluorescent GQDs was ranged between 2 and 3 nm. Other methods that could be used during cutting process of carbon materials into CDs include: nanolithography [71], hydrothermal [72], solvothermal [73], microwave-assisted [74], sonication-assisted [75] or photo-fenton reaction [76, 77]. The “top-down” methods were applied preferably in the early stage of CDs investigations. However, the high cost of carbon sources, harsh reaction condition, long reaction time, uncontrollable CDs parameters (size and optical properties), sophisticated equipment, complicated post-processing treatment and low QY hampered the application of “top-down” methods for CDs production [32, 62, 77, 78].

In the “bottom-up” strategy, small molecular or oligomeric carbon precursors are aggregated in four-step synthetic process which includes: condensation, polymerization, carbonization and passivation. The small precursors are condensed to form intermediate polymeric chain prior to aggregating using covalent or non-covalent interactions. In the next step, the polymers are carbonized in high temperature to create CDs core. Finally, the surface passivation process is performed to improve CDs optical properties [44, 79].

The most common method used during CDs synthesis is **hydrothermal/solvothermal** approach. It is a simple, low-cost, eco-friendly strategy with non-complicated setup. Additionally, resultant products are uniform in size and are characterized by high QY [49, 62, 80]. During hydrothermal/solvothermal process, a carbon source is dissolved in an appropriate solvent and heat up to the temperature between 100 and 200 °C in autoclave, forming nano-sized CDs [13]. This method was firstly applied for CDs synthesis in 2010. Zhang et al. [81] obtained CDs with the size of 2 nm and QY of 6.75% from L-ascorbic acid as a carbon source. Carbon sources used in the hydrothermal procedure could provide other elements such as N or S atoms that are doped to regulate fluorescence behavior of CDs. Guo and Zhao [82], in one-pot synthesis, prepared blue-emissive N-doped CDs with a size of about 3 nm and a high QY equal to 84.8%. Citric acid was applied as a carbon source and diethylenetriamine, as a source of nitrogen. Resultant product was successfully utilized to detect ellagic acid in urine samples. Yu et al. [83] used dopamine as carbon precursor to synthesize CDs with the size of 3–5 nm and QY of 6.4%, which showed broad emission spectra. The material was applied for the determination of Fe³⁺ ions in real water samples and dopamine in human urine and serum samples. In the CDs hydrothermal synthesis, different organic small molecules such as glucosamine [84], glucose [85], sucrose [86], ampicillin [87], amino acids: serine, histidine and cysteine [88], tryptophan [89], alanine [90], lysine and glutathione [91], folic acid [92], glycerol [93], organic acids and their salts: succinic acid [93], maleic acid [94], perfluorooctanoic sulfonate [95], phenols: catechol [96], p-hydroquinone [97], hexadecylpyridinium chloride [98], carbamaldehyde [99], ethanediamine [100] as well as the polymeric compounds (hyaluronic acid [101] and polyacrylic acid [102]) could be applied as

carbon precursors. In order to make CDs synthetic process environmentally benign, the renewable natural products are used in hydrothermal/solvothermal method, as carbon sources, including tragacanth [103], gardenia fruit [104], lemon and grape fruits [105], Seville orange [106], fungi of *Thelephora ganbajun* [107], seeds of *Lens culinaris* [108], seeds of *Azadirachta indica* [109], seeds of *Nigella sativa* [110], leaves of grass [111], ginkgo [112] or guava [113], *Hibiscus sabdariffa* leaves [114], wheat straw [115], flowers of *Magnolia liliiflora* [116], water hyacinth [117], potatoes [118], green alga of *Dunaliella salina* [119], fungi of *Cryptococcus* [120], chocolate [121], cornflour [122], apple juice [123], chitosan [124], human urine [125], chicken blood [126] and others [44, 61, 79, 127, 128].

The general rules and types of carbon precursors that are applied in **microwave-assisted** “bottom-up” CDs synthesis are similar to the hydrothermal method, but heating process is replaced by the microwave irradiation. This method is popular according to cleanness, easiness, short time of reaction and low cost. Zhou et al. [129] prepared fluorescent CDs via 2–10-min microwave pyrolysis of polyethylene glycol and saccharide solution. The QY of resultant product ranged from 3.1 to 6.3%, and the diameter was from 2.65 to 3.75 nm. Recently, Pajewska-Szmyt et al. [130] synthesized N- and S-doped CDs from citric acid and glutathione or urea with microwave-assisted method set for 5 min. The average diameter and QY of CDs was equal to 14.6 nm and 26%, respectively. The product was used for the mercury ion detection in river and wastewater samples. Fast (3 min only) microwave-assisted method was developed for preparing CDs with strong solid-state fluorescence, using phthalic acid and piperazine as precursors [131]. The powdered CDs with the diameter of 1.5 nm were characterized by high QY equal to 48.7% and emission of bright yellow-green solid-state fluorescence. The CDs were successfully used in rapid latent fingerprint detection. In the microwave-assisted methods, natural renewable carbon sources such as linter [132], kelp [133], eggshells [134], sewage sludge [135], human fingernails [136] and others [44, 61, 79, 127, 128] were also utilized.

Another group of the “bottom-up” methods for CDs production is the **thermal** routes such as thermolysis/pyrolysis/carbonization or combustion. Thermal pyrolysis route of CDs obtained was firstly described by Bourlinos et al. [137] who used ammonium citrate salts and 4-aminoantipyrine as the carbon source. Fabricated CDs were characterized by QY of 3% and size of 5–9 nm. Carbonization process is oftenly employed in the CDs synthetic process with the use of natural products as carbon sources. Sha et al. [138] described the CDs synthesis by a single-step pyrolytic treatment of chia seeds. The CDs had the size of 2–6 nm and were applied to form platinum nanoflower CDs composite. In the next example, the photoluminescent carbon nanoparticles were prepared by a simple confined combustion of aromatic compounds (benzene, toluene, xylene) or their mixture in air [139]. The size and QY were 50 nm and 12–13%, respectively.

Apart from the “bottom-up” synthetic methods that were mentioned above, other examples include: ultrasound-assisted method [140], anchor/supported methods [141], microplasma process [142] or fullerene cage opening [143]. The “bottom-up” approach is usually low cost and efficient, the operation is simple, and the conditions are easily controllable, giving the possibility for producing fluorescent CDs on

a large scale. Those materials are characterized by excellent optical properties and high QY—the properties highly required for the production of novel materials for biomedical applications [32, 72].

The pristine CDs do not have any specific groups which can interact with the analytes. Thus, the detection process is not sensitive in the presence of interferences. Moreover, the emission of only blue fluorescence, low QYs (less than 5%) and unsatisfactory interactions with biological systems hamper potential application of CDs. Thus, the functionalization of CDs is a powerful tool to improve photophysical and photochemical properties of CDs as well as broaden their application potential [12, 144]. Two main approaches of CDs functionalization include heteroatom doping and surface modification [12]. Heteroatom doping is achieved through the application of appropriate synthetic method and precursors during CDs fabrication. This process modifies inner structure and electron distribution of CDs, resulting in the change of optical, electronic and chemical properties of CDs as well as moderates QY, emission spectra shifting, charge transfer ratio, orbital structures, surface and local chemical features, and others. The CDs doping could be realized using nonmetals and metals [12, 145]. The most often nonmetal-doping includes N- [146], S- [147], P- [148], Si- [149], B- [150], F- [151], Cl- [152], I- [153] and Te-doping [154]. Additionally, the examples of co-doping were described such as: N,S- [155], N,P- [156], N,B- [157], N,Si- [158], N,Cl- [159], N,F- [160], S,Cl- [161] and N,I-doping [162]. It provides significant improvement of the QY of CDs. Metal atom doping can be used to modulate the band structure of CDs; therefore, moderate color-emitting QY could decay CDs lifetime [12, 35]. Different examples of metal-doping were reported: Au- [163], Cu- [164], Al- [165], Ga- [165], Sn- [166], Zn- [166], Ag- [166], Ca- [167], Mo- [168], Hf- [169], Er- [170], Zn- [171], Mn- [172], Co- [173], K- [174] and Fe-doping [175]. Also, the examples of co-doping of metal and nonmetal were reported such as N,Cu- [176], N,Fe- [177], N,Mg- [178], N,Gd- [179], N,Mn- [180], N,Zn- [181], N,Tb- [182] and S,Gd-doping [183] as well as tri-doping of different atoms: Se,N,Cl- [184], N,S,I- [185], N,S,P- [186], N,Zn,Cu- [187], S,N,F- [188] and B,N,S-doping [189].

The surface modification functionalizes CDs to vary the surface states and to increase the number of active sites. The typical functional ligands include ions, organic molecules, polymers, DNA or proteins. Those could be combined to CDs via covalent or non-covalent interactions with the functional group that is present in the CDs shell. The whole process is more complicated than doping but provides unique properties to CDs as well as significantly improves QY (i.e., surface passivation) [12]. Ions attached to CDs give the new reactive sites in CDs, changing the physical and chemical properties such as catalytic ability as well as could enhance fluorescence properties. Here, metal ions, e.g., Fe^{3+} [190], Cu^{2+} [191], Ca^{2+} [192] or lanthanides [193], could be applied in the surface modification of CDs [12]. Small organic molecules linked to the CDs surface improve the QY, supporting unique properties, enhancing hydrophilic properties and making recognition functional group. Many examples of small molecules modifying CDs surface were reported, including: imidazole [194], 4-aminoantipyrine [195], 3,4-hydroxypyridinone [196], L-cysteine [197], β -cyclodextrin [198], 4-naphthalenyl-3-thiosemicarbazide [199], hexadecyl

trimethyl ammonium bromide [200] and triphenylphosphonium [201]. The CDs could be conjugated with biological molecules to create the possibility of CDs application in the field of biomedicine. Biomolecules that were attached to the CDs surface or were conjugated during synthetic process include: ribonuclease A [202], DNA fragments (aptamers) [203] or antibodies [204]. However, the most common surface passivation agents are polymers, enhancing QY dramatically due to the cutoff of other non-emitting ways and amplification of the emission intensity caused by irradiation [205]. Among the polymers commonly used in the passivation process are: polyethylene glycol [206], polyethylene imine [207], poly(diphenylbutadiene) [208], a four-arm star polymer [209], polyvinylpyrrolidone [210], polydopamine [211] and polyacrylic acid [212]. Table 1 summarized exemplary methods of synthesis, precursors and application of CDs.

Here, the MIPs could be considered as attractive candidates for surface-modified agents [213].

3 Molecular Imprinting Process

The MIPs are characterized by the high level of selectivity and specificity because of the presence of specific recognition sites in the polymer network formed by the template-tailored synthesis. In the MIPs synthetic process, three main stages could be determined. Firstly, the prepolymerization structure, often named as the prepolymerization complex, is formed from functional monomers and the template molecules in the presence of appropriate solvent. It is a crucial stage, because it determines creation of specific sites responsible for MIPs selectivity and specificity. This step could be realized by the covalent or non-covalent approaches. Two above-mentioned methodologies differ from the type of interactions formed between the template and monomers. The covalent approach is executed via creation of chemical bonds, and as a result new prepolymerization compound is obtained [214]. In the non-covalently created prepolymerization complex, weak molecular interactions, such as hydrogen bonds, ionic forces, π -type interactions or van der Waals forces, are responsible for stability of the system [215]. In the next step of imprinting process, the polymerization reaction is performed, mostly with the addition of chosen cross-linker and the initiator to fix the prepolymerization structure and to form polymeric matrix with recognition sites and the template bound inside of them. In the last stage, the template is removed from the polymer by appropriate reaction (in covalent approach) or with the use of eluting solution (in the non-covalent approach). As a final product, highly cross-linked polymeric matrix is obtained with three-dimensional recognition sites complementary in terms of the size, shape and chemical functionalities to the template molecule. Preferably, the MIPs are synthesized using the non-covalent approach because of the simplicity and reversible interactions with the template and analytes. In the covalent strategy, the template removal is mostly a time-consuming process carried out as the chemical reaction. Nevertheless, the footprint of template

Table 1 Exemplary methods of synthesis, precursors and application of CDs

	Precursors	Method	QY	Size	Application	References
Top-down methods	Carbon nanotube	Arc discharge	1.6%	–	–	[19]
	Hot-pressed graphite powder and cement	Laser ablation and HNO ₃ treatment	4–10%	5 nm	–	[20]
	Toluene	Laser ablation	18%	4 nm	–	[64]
	Graphite	Laser ablation	–	1 nm	–	[65]
	Natural gas soot	Acid treatment	0.4%	5 nm	–	[52]
	Carbon nanotubes and graphite	Acidic oxidation	3–6%	3–4 nm	In vivo imaging	[54]
	Activated carbon	Acidic oxidation	12.6%	4.5 nm	Cell imaging	[55]
	Fullerene carbon soot	Acidic oxidation	3–5%	40–50 nm	–	[59]
	Candle soot	Acidic oxidation	1.9%	1 nm	–	[66]
	Coal	Carbonization and acidic oxidation	5–30%	2–3 nm	Cu ²⁺ detection in water	[67]
	Graphite rods	Electrochemical	–	2 nm	–	[69]
	Polyamide resin	Ultrasonic-assisted	28.3%	3 nm	Light-emitting diode	[75]
	Bottom-up methods	Citric acid and phenylalanine	Hydrothermal	–	2–3 nm	Fe ³⁺ detection in tap water
<i>Piper betel</i> leaf		Hydrothermal	12%	3–6 nm	Cell imaging; writing/drawing on the filter paper	[22]
Tapioca		Hydrothermal	–	3–4 nm	Adsorption of Pb ²⁺ ions from aqueous solution	[26]
Duck breast		Hydrothermal	38%	2–3 nm	Cell imaging	[27]
						(continued)

Table 1 (continued)

Precursors	Method	QY	Size	Application	References
Sorbic acid and proline	Hydrothermal	8.5 and 4.5%	2 nm	Cr(VI) detection in water samples; cell imaging	[30]
Ascorbic acid	Hydrothermal	6%	2 nm	—	[81]
Citric acid and diethylenetriamine	Hydrothermal	85%	3 nm	Ellagic acid detection in urine	[82]
Dopamine	Hydrothermal	6.4%	4 nm	Fe ³⁺ detection in real water samples; dopamine detection in human urine/serum samples	[83]
Citric acid, glucosamine, polyethylenimine, urea	Hydrothermal	13%	1–15 nm	Cell imaging and Cu ²⁺ detection in drinking water	[84]
Seville orange	Hydrothermal	13.3%	5 nm	Fe ³⁺ detection in tap and ground water	[106]
N-methyl-1,2-phenylenediamine hydrochloride	Solvothermal	18%	1–2 nm	Lysosome imaging in cells	[24]
Citric acid, 1-(2-pyridylazo)-2-naphthol	Solvothermal	46.7%	3 nm	Light-emitting diode	[34]
<i>m</i> -Phenylenediamine, maleic acid	Dehydration and condensation reaction at room temperature	42% (blue) 35% (green)	3 nm (green) 5 nm (blue)	Tetracycline detection in urine; cell imaging; light-emitting diode	[23]
Glucose	Microwave-assisted	-	2 nm	Photocatalyst	[28]

(continued)

Table 1 (continued)

Precursors	Method	QY	Size	Application	References
Polyethylene glycol and saccharides	Microwave-assisted	3.1–6.3%	3–4 nm	–	[129]
Citric acid, glutathione, thiourea	Microwave-assisted	26%	14 nm	Hg(II) detection in tap water and wastewater	[130]
Phthalic acid and piperazine	Microwave-assisted	48.7%	1–2 nm	Latent fingerprint detection	[131]
Waste cotton linter	Microwave-assisted	-	10 nm	Cell imaging	[132]
Sewage sludge	Microwave-assisted	21.7%	4 nm	p-Nitrophenol detection in river/tap water	[135]
Albumin	Alkaline hydrolysis	16.8%	3 nm	Cell imaging	[31]
Citrate salts	Thermolysis	–	7 nm	–	[137]
4-Aminoantipyrine	Pyrolysis	–	5–9 nm	–	
Glucose	Alkali/acid-assisted ultrasonic treatment	7%	5 nm	–	[140]
Resols	Silica-supported method	14.7%	1.5–2.5 nm	Cell imaging	[141]
Citric acid and ethylenediamine	Microplasma-assisted	9.9%	6 nm	–	[142]

molecule is better defined. Historically, it was the pioneering methodology of MIPs obtaining [214].

Despite the advantages derived from the template-tailored synthesis, the heterogeneity in the population of specific adsorption sites on the MIPs surface remains the main problem. The origins of MIPs heterogeneity could be related to the diversity of the functional monomer and cross-linker interactions with the template, while the non-covalent approach is considered. Moreover, additional aspects should be considered in order to identify the factors affecting the recognition behavior of polymers: the conformational stability of the template, the dimerization or self-complexation of templates, and the chemical stability of the template.

In an excellent paper published by Karlsson et al. [216], it was stated that despite being weak, the cross-linker forms interactions with template molecule which becomes a significant factor during the formation of shape-specific recognition sites in the imprinted polymer. It was underlined that the change in the population of template conformations could be driven by the changes in the local microenvironment of the template governed by the presence of the cross-linker molecules. This hypothesis explains the fact that more functionalized cross-linking agents can be successfully used to provide highly specific MIPs. The problem was also investigated by other groups [217–219]. Finally, it should also be pointed out that the polymerization reaction is under kinetic control, making the nature of template complexation of great importance for the recognition process and distribution of binding sites in the resulting MIPs.

The problem of template conformational stability was also discussed by Olsson et al. [220]. The template–template complexation could occur, resulting with the heterogeneity of the MIP because of the population of highly specific binding sites for two molecule complexes in the specific adsorption site. In such a site, the adsorption does not rely only on the interactions with positioned residual functional groups from monomers but also from template–template contacts. Moreover, additional complexes were postulated such as those involving two molecules of templates interacting with one molecule of the functional monomer acting as a bridge between them.

Another reason underlying the formation of the heterogeneous population of adsorption sites was also identified. Martin et al. [221] revealed unexpected selectivity of a propranolol imprinted polymer toward a compound of tamoxifen. The mechanism, explaining the behavior of MIP, was not discussed, but it was concluded that a rigorous screen of MIPs should be conducted in order to determine fitting to their targeted analyte. In another example, Klejn et al. [222] investigated the structural transformations of the template during the imprinting process of 3,3-diindolylmethane, resulting in the MIP, providing high binding capacity toward a structurally related compound, indole-3-methanol. A cascade of free radical reactions promoted the transformation of the template molecule of 3,3-diindolylmethane to indole-3-methanol, the compound that was subsequently present in the prepolymerization system and was imprinted into the resulting polymer matrix. In the consequence, a highly heterogeneous population of adsorption sites was formed. It was

concluded that the presence of a free radical initiator and elevated temperature could be responsible for the structural changes of the template. However, it should be underlined that most of the template molecules are stable enough to survive the polymerization conditions notably when the free radical thermal process is carried out.

The main parameter, showing the efficacy of imprinting process, is the imprinting factor (IF). The IF is commonly defined as a ratio of the binding capacity of the template on the MIP to the binding capacity of the template on the reference non-imprinted polymer (NIP). Hence, the conditions of NIP synthesis have to be identical as MIP production with omitting the addition of the template molecule [223].

4 Molecularly Imprinted Carbon Dot Conjugates—Biomedical Application

In the subsequent part of the chapter, the most valuable and interesting papers devoted to CD–MIP conjugates will be discussed, emphasizing the fabrication process of MIP layer as well as the analytical performance of the material and the application in biomedical field. In order to systemize the section, firstly CD conjugated with inorganic MIP shell obtained by ionic mechanism of the reaction will be described followed by the CD–MIP organic materials prepared by the free radical polymerization. Those latter materials were fabricated, for instance, for cell targeting and imaging, making their biomedical purpose highly attractive.

4.1 CD–Inorganic MIP Shell Conjugates

The solgel hydrolysis and condensation approach to fabricate CD–inorganic MIP shell conjugates proceeds in mild and controllable synthetic condition, even at room temperature. The mild polymerization conditions are advantageous during MIP synthesis because elevated temperature could diminish the prepolymerization complex between the template and the functional monomer, affecting the efficacy of the imprinting process. However, the excessive amount of the functional monomer or cross-linker could result with thick MIP layer, deteriorating both, the efficiency and the responsive time of fluorescent probe. In contrary, the insufficient amount of functional monomer and cross-linker leads to decrease of sensitivity and selectivity of the material.

Xu et al. [224] developed a new and sensitive method for fluorescent determination of caffeic acid, using the silane-functionalized CDs coated with MIP. The target analyte of caffeic acid is characterized by unique antioxidant properties responsible for anti-inflammatory, anti-tumor or immunomodulatory actions. Caffeic acid

is used in the therapy of leucopenia, thrombocytopenia and hemostasis. Nevertheless, the compound could be also responsible for carcinogenic effects. Thus, the monitoring of caffeic acid levels is necessary in order to make the therapy safe. For that purpose, the new method was proposed. The material was composed of CD synthesized in the presence of 3-aminopropyltriethoxysilane and tetraethoxysilane as well as caffeic acid acting as the template molecule. The post-synthetic process was optimized, aiming to remove entirely the template. The process of template removal is crucial because it results with the formation of spatial geometries on the MIPs surface commonly described as the three-dimensional cavities. Here, different eluents, including methanol, methanol–acetic acid (90:10 v/v), methanol–water (90:10 v/v), ethanol, ethanol–acetic acid (90:10 v/v) and ethanol–water (90:10 v/v), were analyzed to wash out the template effectively. The highest fluorescence of CD–MIP conjugates was revealed when methanol–acetic acid (90:10 v/v) was used as the eluent. It means that the template was efficiently removed, resulting with only limited quenching of fluorescence. The comprehensive characterization of resulted material is compulsory to prove its morphology and structure. Here, transmission electron microscopy revealed the appearance of CD–MIP conjugates as the spherical structures with a mean diameter of about 140 nm. The Fourier transformation infrared spectroscopy could confirm the presence of characteristic vibrations derived from specific bonds in the material, such as absorption peak at 1667 cm^{-1} assigned to the stretching vibration of amide carbonyl group and peak at 1576 cm^{-1} , attributing to secondary amine R–NH–R bending vibration. These two different signals confirmed the formation of amide type of bonding, demonstrating the successful acylation reaction of 3-aminopropyltriethoxysilane. The peaks at 1061 cm^{-1} and at 792 cm^{-1} were ascribed to Si–O–Si asymmetric stretching and Si–O vibrations, and the peak at 1488 cm^{-1} was assigned to the aromatic ring stretching vibration of template molecules of caffeic acid. This latter peak disappeared in the spectrum of the material after the template extraction process, confirming the effectiveness of the template removal step. The X-ray photoelectron spectroscopy is another versatile technique to confirm the structure of conjugates. The elemental composition revealed four peaks at 101.62, 398.65, 283.94 and 531.43 eV, which were assigned to Si2p, N1s, C1s and O1s, respectively. Finally, the most important is the spectroscopic analysis of optical properties of CD–MIPs conjugates. The fluorescence excitation and emission spectra of conjugates revealed symmetric fluorescence emission peak at $\lambda_{em} = 450\text{ nm}$ obtained after excitation at $\lambda_{ex} = 360\text{ nm}$. It indicated that the silica coating at the surface did not restrict the photoluminescence properties of CD since the silica layer was optically transparent and inert. The photoluminescence stability is also a very important parameter that should be taken into account when the material is considered for practical application. Here, the results showed that the relative standard deviation of the material fluorescence intensity changes within six hours was equal to 3.1% only. It confirmed great stability of CD–MIPs conjugates against photobleaching. In order to confirm the specificity of the material, the adsorption of caffeic acid from standard solutions was carried out and the fluorescence quenching was quantitatively determined employing the Stern–Volmer equation. The linear relationship was studied in the concentration range between 0.5 and $200\text{ }\mu\text{mol L}^{-1}$. The

calculated limits of detection and quantification were equal to 0.11 and 0.34 $\mu\text{mol L}^{-1}$, respectively. The selectivity of the material is another important parameter that should be analyzed before application because it allows to assess cleanup capabilities in the presence of competing components of the complex matrix. Here, various interfering components in plasma, including ions (Na^+ , Ca^{2+} , Mg^{2+}), hydrocarbons (glucose and galactose), amino acids (glycine and cysteine) and proteins (bovine serum albumin), were investigated to evaluate the practical applicability of proposed biosensor platform for caffeic acid detection. The results confirmed high selectivity of obtained material with very low non-selective adsorption of tested compounds. Finally, in order to prove the utility of new material, the analysis of caffeic acid in human plasma sample was carried out. The recoveries for spiked concentration between 5 and 150 $\mu\text{mol L}^{-1}$ varied from 98.4 to 107.6% with relative standard deviation between 3.6 and 10.2%. It was concluded that the probe was easy to synthesize and simple to operate, merging the virtue of the high sensitivity of CDs and the high selectivity of MIPs.

Shariati et al. [225] constructed CD–MIPs conjugates for determination of phenobarbital. This drug is used in the pharmacotherapy of epilepsy. However, if overdosed, it may cause sedation and hypnosis and may promote symptoms such as shallow breathing, drowsiness, decreased urination and level of consciousness. Thus, the monitoring of the drug levels in plasma during the pharmacotherapy is crucial not only to make therapy effective but also to avoid adverse effects. Authors used pulverized Cedrus as a source of CDs, obtaining the material characterized by relatively high QY of 18.6% when compared to CDs obtained by other ways (QY of ca. 5%). The QYs of the CDs are low when compared to QYs of semiconductor nanocrystals which are characterized by values of ca. 50–60%. Here, the main problem responsible for unsatisfactory QY is related to the presence of surface defects. The material was composed from CDs coated by 3-aminopropyltriethoxysilane and tetraethoxysilane in the presence of phenobarbital template. The transmission electron microscopy and Fourier transformation infrared spectroscopy were employed together with X-ray diffraction and dynamic light scattering. The X-ray diffraction measurements are valuable technique to reveal the crystalline structure of materials. Here, the X-ray diffraction pattern exhibited a broad peak at $2\Theta = 24.7^\circ$, corresponding to the (002) diffraction planes of carbon materials. It indicated the amorphous structure. The data obtained from the dynamic light scattering measurements revealed the average size of CDs equal to 5.5 nm. The zeta potential of CDs was calculated as -10.5 mV. It was underlined that the negative charge of nanoparticles prevented their accumulation and increased their stability. The adsorption process was optimized in terms of temperature and time of contact. It was found that the fluorescence intensity of the CD–MIP conjugates decreased with increasing temperature. The response time increased with time up to 10 min and then remained almost unchanged. The analytical performance of the sensor was evaluated in the concentration range between 0.4 and 34.5 nmol L^{-1} , and the limit of detection was equal to 0.1 nmol L^{-1} . The selectivity tests were carried out in order to measure the mutual competition of phenobarbital and other compounds (dopamine, tryptamine, tryptophan, cysteine, ascorbic acid, primidone or selected ions). The highest competing capability to phenobarbital was revealed

by biogenic amines and primidone, a structural analog of the template compound of phenobarbital. Among tested ions, the interfering capability of K^+ was recognized as the most important. Finally, the applicability of the sensor was confirmed by the analysis of human blood plasma samples. The recoveries of phenobarbital from spiked samples were between 96.5 and 109.5%. In conclusion, it was mentioned that new sensor had advantages of being simple, cost-effective, rapid, independent of organic solvents and easy to use.

Apart from the above solgel method, the reverse microemulsion is another approach to generate the silica-based CD–MIPs conjugates. The reverse microemulsion is an oil-in-water stable micelle system. The oil phase is a continuous phase, and the water phase is inside the reverse micelle formed by the surfactant. Usually, cyclohexane and Triton X-100 are selected as the oil phase and surfactant for the preparation of CD–MIPs conjugates. Thus, the Triton X-100 diffuses and stabilizes water droplets, containing CDs in cyclohexane.

Ensafi et al. [226] used above-mentioned technique to fabricate an optical sensor for selective fluorescent determination of promethazine. This compound is an anti-histamine drug that is used to treat allergy symptoms such as rash and itching or to prevent nausea and vomiting. However, the side effects include endocrinal, cardiac and reproductive alterations. The material was synthesized from CDs coated by 3-aminopropyltriethoxysilane and tetraethoxysilane in the presence of promethazine hydrochloride, acting as the template. Additionally to transmission electron microscopy, Fourier transformation infrared spectroscopy and X-ray diffraction analyses, the dynamic light scattering diagrams were studied to characterize the material. The results revealed that the average sizes of CD–MIPs and CDs–NIPs particles possess a diameter of 62.1 and 64.5 nm, respectively. The higher polydispersity indices for CD–MIPs and CD–NIPs conjugate (0.391 and 0.362, respectively) than to CDs (0.189) showed that both conjugates were characterized by the broader size distributions than CDs alone. The obtained material was also characterized by very fast adsorption kinetic and equilibrium time equal to 2 min. The regeneration capability of the sensor was analyzed. The recovery efficiency was remained almost unchanged after five sorption cycles. Therefore, the sensor could be used up to 5 times without loss of its sorption properties. The analytical performance for adsorption of promethazine was analyzed in the range between 2 and 250 $\mu\text{mol L}^{-1}$, and the limit of detection was calculated at 0.5 $\mu\text{mol L}^{-1}$. The selectivity tests were carried out toward a group of competitors such as cysteine, lysine, ascorbic acid, tryptamine or histamine and ions (K^+ , Mg^{2+} , Ca^{2+}). The interfering role of ions was most significant to affect the adsorption capabilities of new sensor toward promethazine. Finally, the recoveries from promethazine spiked human blood plasma were investigated in order to prove the utility of the material. The recoveries of promethazine from spiked samples were between 96.4 and 102.3%, showing that the proposed method was suitable for detection of promethazine in real samples.

In order to enhance the sorption properties of imprinted layer, Bhogal et al. [227] described the fabrication of CD–MIPs conjugate using N-(2-aminoethyl)-3-aminopropyltrimethoxysilane that acted as the coordinating solvent, providing passivation of the surface of CDs as well as the functional monomer for the polymerization

reaction. The presence of tetraethoxysilane ensured cross-linking of the ketoprofen, a template molecule. Ketoprofen is frequently used nonsteroidal anti-inflammatory drug. Prolonged administration of ketoprofen and overdosing could cause intestinal bleeding, ulceration and heart failures. Thus, due to widespread use of the drug, it is important to possess a rapid, simple and efficient method for analysis of ketoprofen. The Fourier transformation infrared spectroscopy was employed to analyze the composition of material. The spectrum of silane-functionalized CDs showed peaks at 1588 and at 1656 cm^{-1} that correspond to the amide N–H and C = O stretching vibrations, respectively. A broad peak at 3276 cm^{-1} was assigned to N–H stretching, confirming the formation of amide group during passivation reaction. The stretching vibration of Si–O–CH at 1080 cm^{-1} and the asymmetric stretch of Si–CH₂ at 747.9 cm^{-1} as well as the bands at 2933 cm^{-1} , corresponding to C–H stretching, were the evidence of the presence of aminoalkyl group derived from N-(2-aminoethyl)-3-aminopropyltrimethoxysilane. The spectra of CD–MIP and CD–NIP conjugates revealed strong peak at 1078 cm^{-1} from Si–O–Si asymmetric stretching and peaks at 755 cm^{-1} and 417 cm^{-1} from Si–O vibrations. The bands at 2922 and 2965 cm^{-1} were assigned to aliphatic C–H stretching, and the bands at 3452 and 1591 cm^{-1} were assigned to N–H stretching, indicating the presence of aminoalkyl groups. The detailed Fourier transformation infrared spectroscopy analysis proved the presence of MIP layer. The fluorescence stability of the sensor was obtained by twelve-repeated detections after every 5 min up to a total of one hour from 1.9 $\mu\text{mol L}^{-1}$ ketoprofen standard solution with relative standard deviation below 4%. The response time of the sensor was set for 5 min. The analytical characterization was as follows: the linear response of the sensor to ketoprofen was performed in the range of 0.039–3.9 $\mu\text{mol L}^{-1}$ with limit of detection equal to 0.01 $\mu\text{mol L}^{-1}$ and limit of quantification equal to 0.33 $\mu\text{mol L}^{-1}$. To validate the applicability of the sensor, the proposed method was employed for analysis of ketoprofen in real human urine samples. Recovery studies were carried out by spiking the samples with ketoprofen in the concentration range between 0.4 and 2 $\mu\text{mol L}^{-1}$, revealing the total recoveries between 96 and 104%. In conclusion, it was emphasized that the robust, inert and non-toxic CD–MIP conjugates were fabricated with high specificity and faster adsorption kinetics, enabling for development of a new highly sensitive and selective analytical method for ketoprofen determination in real samples.

The effective imprinted shell layer for the analysis of low molecular weight organic compounds is relatively easy to proceed. In contrast, the imprinting of macromolecular proteins is still challenging: firstly, because those molecules are fragile for usage of organic solvents, and secondly, due to conformational instability of these structures. Wang et al. [228] described the fluorescent nanosensor for determination of ovalbumin, applying imprinting process to form a silane MIP shell that was further conjugated with fluorescein isothiocyanate to enhance the fluorescence signal. Ovalbumin is a glycoprotein present in egg albumen but also in fetal bovine serum and human serum. Transmission and scanning electron microscopies were employed to analyze the surface of materials. The micrographs revealed that the surface of CD–silane nanoparticles was velvety and uniformly dispersed with an average particle size of 70 nm, but the size increased to 90 nm after MIP coating and conjugation

with fluorescein isothiocyanate, showing a highly rough imprinting layer. It was underlined that thin imprinted layer benefits from unique advantages such as better accessibility and facile mass transfer of the analyte. It also hinders stereo avoidance for the large target protein to enter MIPs' cavities. The working conditions of the sensor were optimized in terms of pH of adsorption and stability. The acidic pH significantly reduced the emission intensity of fluorescein isothiocyanate because of the dominant formation of neutral and cationic forms responsible for lower intensity fluorescence. However, the amine groups of 3-aminopropyltriethoxysilane at pH value below 6 adopt proton and change the charge to positive, leading to decrease of affinity toward ovalbumin. At pH above 7, the amine groups are in the neutral form, increasing the affinity of the material to ovalbumin. The stability of the nanosensor did not significantly change over 2 h, indicating that the system was characterized by acceptable fluorescence stability. The selectivity tests were carried out toward bovine serum albumin, phycocyanin, lysozyme and bovine hemoglobin. The adsorption of all tested compounds on CD–NIP material was very similar, but nearly double amount of ovalbumin was adsorbed on CD–MIP conjugates when compared to adsorption capacity of other competitors. Finally, the material was placed on the test papers, presenting the obvious color responses to the different concentrations of ovalbumin. The method was applied to human urine spiked with ovalbumin, revealing total recoveries between 92 and 104% with relative standard deviation between 3.3 and 3.9%. In summary, it was stated that the developed strategy was facile and convenient. The sensitive and selective detection of ovalbumin can be displayed on fluorescent test papers by unaided eye observation. Consequently, it should be expected that the work will pave the way for the growing sensing of biologically important macromolecules.

To sum up, the potential of CD–silane-based MIPs conjugates was revealed. The methods for CD surface modification were presented, showing the utility of new devices in the biomedical analyses. However, a few limits should be outlined here. Those are characterized by limited adhesive properties, moderate porosity and difficulties in controlling of the particle size, morphology and monodispersity. The limited number of silane precursors of modifiable chemical functionalities is another disadvantage. The commercially available silane functional monomers are strictly limited to several compounds, providing a scarce choice of functional groups to interact with the template molecules when compared to organic monomers that could be used in the synthesis of MIP layers.

4.2 CD–Polydopamine MIP Shell Conjugates

In order to overcome the above-mentioned problems, a polydopamine, an organic copolymer that is characterized by an excellent biocompatibility, hydrophobicity, biodegradability and the unique adhesive properties, could be considered for the formation of a film on a wide range of substrates such as CDs.

Jalili and Amjadi [229] described a novel fluorescent sensor for determination of 3-nitrotyrosine. The sensor consisted of green-emitting CDs as a signal transducer

conjugated to imprinted layer of polydopamine. The synthesis is based on previous observations that a simple immersion of semiconductor nanocrystals in a dopamine alkaline solution leads to spontaneous deposition of polydopamine layer. Here, the deposition was carried out in the presence of 3-nitrotyrosine, a template molecule. 3-Nitrotyrosine could indicate the elevated levels of reactive nitrogen species in cells. Those species lead to damage of cellular components, provoking pathological actions. In proteins, most of nitration reactions appear on a tyrosine aromatic ring which is easily nitrated to 3-nitrotyrosine, a compound characterized by higher acidity than tyrosine, affecting the conformational stability of protein. As a result, an accelerated degradation of modified proteins is observed and higher levels of free 3-nitrotyrosine are detected. The analysis of nitratively altered macromolecules in biological samples attracted attention due to their role in the pathogenesis of various diseases. Higher levels of 3-nitrotyrosine were reported in the pathogenesis of asthma, diabetes or neurological disorders. Here, the analytical performance of the sensor was comprehensively analyzed. The relative intensity after adsorption of 3-nitrotyrosine on CD-MIP polydopamine material increased up to 8 min, reaching equilibrium. Thus, the sensor was characterized by the extraordinary rapid response derived probably from the high porosity of imprinted polydopamine layer. The impact of pH on the effectiveness of the adsorption process was evaluated further, revealing the maximum fluorescence quenching between pH values of 6 and 7. This fact could be explained by the analysis of pK_a values of 3-nitrotyrosine that are equal to 2.2, 7.2 and 9.1, and pH value at the point of zero charged of polydopamine that is equal to 4. Polydopamine is negatively charged at pH values higher than 4, and 3-nitrotyrosine has also a net negative charge above pH 7. Therefore by increasing the pH of standard solution, the repulsion between polydopamine layer and 3-nitrotyrosine would prevent the latter compound from penetration to adsorption sites, resulting with the decrease of fluorescence quenching. The linear range of the regression line was between 0.050 and $1.85 \mu\text{mol L}^{-1}$. The limit of detection was equal to 17 nmol L^{-1} . The relative standard deviation for five replicate determinations of 3-nitrotyrosine at $0.45 \mu\text{mol L}^{-1}$ was 3.6%, indicating the good repeatability of the sensor. The stability tests proved that the CDs-MIP polydopamine material was stable for more than two weeks when stored at 4°C and that the fluorescence intensity was 95.1% of its initial value after three weeks. The selectivity tests revealed that glucose, lactose, uric acid, ascorbic acid, cysteine, glycine and creatinine as well as Na^+ , K^+ , NH_4^+ , Ag^+ , Ca^{2+} , Zn^{2+} , Mg^{2+} , Fe^{2+} , Cd^{2+} , Pb^{2+} , Ni^{2+} , Cu^{2+} , Fe^{3+} and Al^{3+} ions did not affected the fluorescence response significantly. The recovery studies were carried out on spiked human serum samples, revealing the values between 95.6 and 101.2% with relative standard deviation in the range of 1.4–3.9% for the concentration range between 0.4 and $1.0 \mu\text{mol L}^{-1}$. In summary, it was stated that the sensor showed a bright green emission which was selectively quenched by 3-nitrotyrosine adsorption probably via photoinduced electron transfer mechanism. The sensor was characterized by the comparable sensitivity to immunoassays and revealed increasing sensitivity when compared to selected chromatographic techniques.

Current challenges in biomedical analysis aimed to simplify the analytical process. New analytical methods should be elaborated in order to make them available for

complex matrices as well as to facilitate and to make them faster. One of the excellent tools to fulfill above-mentioned demands is to merge CDs–MIPs conjugates with magnetic susceptible materials. Those materials could be easily employed in the dispersive mode of solid phase extraction, resulting with the reduction of time and costs of the sample preparation process. For that purpose, Lv et al. [230] proposed magnetic CDs-based MIP system for fluorescent detection of hemoglobin. The synthetic approach involved hydrothermal method to obtain carbon–magnetite hybrid material. Then, the hemoglobin, the template, was immobilized on the surface of material which was subsequently coated with a polydopamine thin layer. The presence of magnetite core allowed for fast and easy separation of the material from sample environment by the simple application of external magnetic field. The characterization of material included Fourier transformation infrared spectroscopy, X-ray electron-dispersive spectroscopy and vibration sample magnetometry. The elemental analysis revealed the atomic percent of C, O and Fe in the magnetic CD–MIP equal to 45.80%, 34.87% and 18.43%, respectively. The saturation magnetization value of the magnetic CDs was equal to 56.4 emu g^{-1} but decreased to 44.1 emu g^{-1} for magnetic CD–MIP. It means that the magnetic properties of magnetic CD–MIP were decreased due to the additional presence of polydopamine layer. The analytical characterization was carried out, revealing linearity in the range of $0.05\text{--}16.0 \text{ }\mu\text{mol L}^{-1}$ and calculated limit of detection for hemoglobin equal to 17.3 nmol L^{-1} . The selectivity tests were performed toward the group of competing proteins such as ovalbumin, bovine serum albumin and human serum albumin. The results of adsorption of magnetic CDs–MIP revealed that only halved amounts of competitors were adsorbed when compared to the adsorption of hemoglobin. It means that the sensor was characterized by satisfactory selectivity. The recoveries from spiked bovine urine samples were in the range between 102.0 and 102.7% and from spiked bovine serum between 99.0 and 104.0%. It was concluded that the high selectivity and sensitivity of the material make new method promising for specific recognition and determination of proteins in biological fluids.

4.3 CD–Acrylate-/Methacrylate-Derived MIP Layer

In order to address the limits derived from silane-based MIPs such as moderate porosity and a lack of modifiable chemical functionalities, the organic acrylate- or methacrylate-based functional monomers are attractive alternative. Those compounds possess different functional groups that can interact via various types of non-covalent interactions with the templates, strengthening the stability of the prepolymerization complexes. Unsaturated double bonds from acrylate- or methacrylate-based functional monomers make possible free radical polymerization process after thermal or photo-initiation. The free radical process suffers from randomness and limited scale-up. Moreover, the thermal conditions could destabilize the prepolymerization complex resulting with heterogeneous population of adsorption sites. For that purpose, Li et al. [231] proposed additional component present in

the organic imprinted layer, viz. thiolated calix[6]arene to increase the stabilization of prepolymerization complex between methacrylic acids, acting as the functional monomer and L-DOPA, the template. The above-mentioned approach was called as dual recognition strategy, and it was recognized as very effective to provide MIPs for chiral resolution. L-DOPA is a prodrug, frequently used in the treatment of neurological disorders, which possesses ability to cross the blood–brain barrier to increase dopamine concentration. Here, the CDs composite with iridium–gold fluorescent nanoparticles was fabricated followed by addition of thiolated calix[6]arene with L-DOPA. Then, methacrylic acid and N,N'-methylenebisacrylamide were added to form, after polymerization, an organic MIP layer. The transmission electron microscopy, X-ray diffraction, X-ray photoelectron spectroscopy, porosity measurements and inductively coupled plasma atomic emission spectroscopy were used to characterize the material. The X-ray diffraction pattern revealed the peak at 25.8° attributed to the C atom, the diffraction peaks at 37.8° , 43.0° , 62.8° and 76.0° were assigned to the (111), (200), (220) and (311) planes, respectively, of the gold lattice, whereas the diffraction peaks at 40.5° , 47.8° and 69.2° were corresponded to the (111), (200) and (220) planes, respectively, of the iridium lattice. These results indicated that iridium and gold on the surface of CDs were characterized by good crystallinity. The X-ray photoelectron spectrum showed intense peaks assigned to Au (4f_{2/5}) at 84.08 eV and Au (4f_{2/7}) at 87.08 eV, the characteristic peaks for zero valence state of gold atom as well as peak assigned to Ir(4f) at 64.08 eV characteristic for zero valence state of iridium. The mass fractions of gold and iridium, determined by atomic absorption spectroscopy, were equal to 23.4% and 22.8%, respectively. The porosity measurement using Brunauer–Emmett–Teller isotherm revealed the specific surface area of CD–Au/Ir–MIP composite equal to $285.8 \text{ m}^2 \text{ g}^{-1}$ and the total pore volume equal to $0.32 \text{ cm}^3 \text{ g}^{-1}$. The analytical performance was analyzed in the range between 0.5 and 120 nmol L^{-1} . The limit of detection was set at $0.145 \text{ nmol L}^{-1}$. To study the chiral resolution of the material, the adsorption capabilities of both enantiomers, viz. L-DOPA and D-DOPA, were carried out. The results revealed that the fluorescence intensity of the imprinted material did not change significantly even after using a 100-fold excess D-DOPA. This observation confirmed high ability of MIPs to discriminate enantiomers. It could be explained by the spatial geometry of the specific adsorption site that was imprinted by the specific enantiomer. The selectivity tests were carried out toward selected biomolecules such as ascorbic acid, L-tyrosine, epinephrine, endorphins, phenylethylamine, pyrocatechin and amphetamine as well as ions such as Cl^- , NO_3^- , SO_4^{2-} , Na^+ , K^+ , Cu^{2+} , Hg^{2+} , Fe^{2+} , Mn^{2+} , Mg^{2+} , Co^{2+} , Zn^{2+} , Fe^{3+} , Ni^{2+} , Al^{3+} and Ca^{2+} , revealing minor impact on the L-DOPA adsorption. It was concluded that the combination of thiolated calix[6]arene and MIP provided more recognition sites for chiral recognition and, thus, effectively eliminated enantiomer interference. The integration of CDs with iridium–gold formed fluorescent nanoparticles that possessed potential to be a versatile sensor. However, the adsorption capacity and stability of the material needed further improvement, and the preparation process was relatively complicated.

Another interesting modification of the composition of CD–MIPs conjugate was presented by Zhao et al. [232] who described the synthesis of silanized CDs based on

thermo-sensitive MIP. The fluorescence sensor was dedicated to determine bovine hemoglobin in urine samples. The MIP layer was composed from methacrylic acid acting as the functional monomer, N-isopropylacrylamide, the monomer sensitive to temperature and N,N-methylenebisacrylamide, the cross-linker. Bovine hemoglobin was used as the template. The thermo-sensitive element was introduced into the material to increase the binding capacity and to improve the imprinting efficacy. In the lower temperature, the material was transformed into hydrophilic pellets, making the adsorption of hemoglobin more favorable and therefore increasing the fluorescence signal. The analytical performance was analyzed in the range between 0.31 and 15.5 $\mu\text{mol L}^{-1}$, revealing the limit of detection at 0.155 $\mu\text{mol L}^{-1}$. The determination of hemoglobin in real sample revealed the recoveries between 98.6 and 100.5% with the relative standard deviation between 0.85 and 2.6%. It was underlined that one could expect that the material would serve in the future as a promising sensor for special recognition and detection of hemoglobin, and this strategy could also be expended to the detection of other proteins in biological fluids. However, the non-specific adsorption still could be a problem, while the MIP organic hydrophobic layer was formed on the composite.

To overcome the problem, Liu et al. [233] proposed a fabrication of CD-restricted access MIP for selective detection of metronidazole in serum. Metronidazole is an antiprotozoal and antibacterial drug used frequently to treat pelvic inflammatory disease, endocarditis and bacterial vaginosis. The material containing CD-MIP conjugates was composed from acrylamide (the functional monomer), ethylene glycol dimethacrylate (the cross-linker) and glycidyl methacrylate, the monomer, possessing epoxy ring which could be used as the copolymerization functional monomer, providing dual surface configuration. After the polymerization, the epoxy ring is hydrolyzed to obtain hydroxyl groups which makes the materials hydrophilic and eliminates the interference of biological macromolecules. The characterization of material consisted of transmission electron microscopy, Fourier transformation infrared as well as the specific measurement of the water contact angles to prove the hydrophilic character. Those experiments were carried out of CD-MIP material without and with glycidyl methacrylate (after the hydrolysis). The results revealed that the static state contact angle was equal to 102.0° and 73.8°, respectively. It means that the latter material possessed more hydrophilic properties. Such material was ideal for protein exclusion, improving the selectivity of MIP. The selectivity tests toward ornidazole, dimetridazole (the structural analogs of metronidazole) as well as toward chloramphenicol confirmed satisfactory selectiveness. The analytical performance was carried out in the range between 50 and 1200 $\mu\text{g L}^{-1}$ with limit of detection at 17.4 $\mu\text{g L}^{-1}$. The applicability of material was studied by detecting the content of metronidazole in serum samples. The total recoveries from spiked samples varied between 93.5 and 102.7%, and relative standard deviations were between 1.9 and 3.6%. In conclusion, it was stated that the sensor possessed a capability to detect trace substances in the biological applications. However, the complicated synthetic process of CD-restricted access MIPs limits usage of the method.

Finally, fluorescent probes based on CD-MIP materials were used for cell targeting and imaging. Fang et al. [234] presented a novel fluorescent probe for

lysozyme detection and cell imaging. The material was constructed from acrylamide (functional monomer), N-isopropylacrylamide (thermo-sensitive monomer) and N,N-methylenebisacrylamide (cross-linker). The most important part of investigation was dedicated to assess the cytotoxicity of novel material since its application required direct contact with living cells. Thus, the MTT assays were carried out. It was revealed that the cell viability was at the level of 80% when the CD–MIP conjugates were applied to HepG-2 cells at test concentrations between 1.56 and 100 mg L⁻¹. It means that the material had a minor cytotoxic effect on HepG-2 cells. In conclusions, it was emphasized that combining the fascinating optical properties of CDs with the favorable selectivity of MIPs, a new type of fluorescent probe for lysozyme detection and cell imaging was constructed for the first time. The material was characterized by low cytotoxicity, providing a new way to detect lysozyme in vitro and to probe intracellular lysozyme in vivo.

To sum up, CDs exhibit unexpected advantages in fluorescence sensing and imaging because those materials are characterized by high chemical stability, biocompatibility and low toxicity. Merging CD with MIPs opens a way to selective adsorption of analytes and targeted cell therapy or imaging. Table 2 summarized biomedical application of CD–MIP conjugates.

Those profits make CD–MIP conjugates attractive materials for the biomedical and clinical applications as well as highly desirable tools in the field of nanomedicine.

Table 2 Exemplary biomedical application of CD–MIP conjugates

MIP type	CD functionalization	Analyte	Sample	LOD	References
Silane-based	Silane	Caffeic acid	Plasma	0.11 μM	[224]
	Silane	Phenobarbital	Plasma	0.1 nmol L ⁻¹	[225]
	–	Promethazine hydrochloride	Plasma	0.5 μmol L ⁻¹	[226]
	Silane	Ketoprofen	Serum/urine	0.01 μM	[227]
	-	Ovalbumin	Urine	15.4 nM	[228]
Polydopamine	-	3-Nitrotyrosine	Serum	17 nM	[229]
	Fe ₃ O ₄	Bovine hemoglobin	Bovine urine/blood	17.3 nM	[230]
Acrylate/methacrylate	Ir/Au	L-DOPA	Urine/chicken meat	0.145 nmol L ⁻¹	[231]
	Silane	Bovine hemoglobin	Urine	0.155 μM	[232]
	–	Metronidazole	Serum	17.4 μg L ⁻¹	[233]
	Silane	Lysozyme	Chicken egg	0.55 mg L ⁻¹	[234]

5 Current Status and Future Prospects

Carbon dots exhibit unexpected advantages in fluorescence sensing and imaging due to high chemical stability, biocompatibility and low toxicity. Merging carbon dot with molecularly imprinted polymer provides materials capable to selective adsorption of analytes for biomedical purposes because of high selectivity, sufficient cleanup and enrichment abilities of imprinted layer. It also opens a way to targeted cell therapy and tissue imaging. However, a few drawbacks shall be addressed at this point. Firstly, low quantum yields of carbon dots could limit their practical use. Thus, novel synthetic approaches for fabrication of carbon dots shall be developed to reduce surface imperfections and improve quantum yield of those nanoparticles. Secondly, the heterogeneity of imprinted layers shall be minimized in order to improve the selectivity of materials. Finally, the alternative ways to apply carbon dots—molecularly imprinted polymers for biotargeting and tissue imaging could result with progress in tumor identification and cancer therapy. To sum up, above-mentioned profits make carbon dot—molecularly imprinted polymer conjugates attractive materials for the biomedical and clinical application as well as highly desirable tools in the field of nanomedicine.

References

1. BelBruno JJ (2019) Molecularly imprinted polymers. *Chem Rev* 119:94–119
2. Madikizela LM, Tavengwa NT, Chimuka L (2018) Applications of molecularly imprinted polymers for solid-phase extraction of non-steroidal anti-inflammatory drugs and analgesics from environmental waters and biological samples. *J Pharm Biomed Anal* 147:624–633
3. Li P, Wang T, Lei F, Peng X, Wang H, Qin L, Jiang J (2017) Preparation and evaluation of paclitaxel-imprinted polymers with a rosin-based crosslinker as the stationary phase in high-performance liquid chromatography. *J Chromatogr A* 1502:30–37
4. Rutkowska M, Namieśnik J (2019) *Comprehensive analytical chemistry* (Chap 9). Elsevier, Amsterdam, Netherlands. Molecularly imprinted polymers applied in capillary electrochromatography and electrophoresis techniques 86:235–259
5. Romero M, Macchione MA, Mattea F, Strumia M (2020) The role of polymers in analytical medical applications: a review. *Microchem J* 159:105366
6. Luliński P (2017) Molecularly imprinted polymers based drug delivery devices: a way to application in modern pharmacotherapy: a review. *Mater Sci Eng C* 76:1344–1353
7. Li S, Zhu M, Whitcombe MJ, Piletsky SA, Turner APF (2015) *Molecularly imprinted catalysts, principles, syntheses, and applications*. Elsevier, Amsterdam, Netherlands
8. Bonomi P, Servant A, Resmini M (2012) Modulation of imprinting efficiency in nanogels with catalytic activity in the Kemp elimination. *J Mol Recognit* 25:352–360
9. Refaat D, Aggour MG, Farghali AA, Mahajan R, Wiklander JG, Nicholls IA, Piletsky SA (2019) Strategies for molecular imprinting and the evolution of MIP nanoparticles as plastic antibodies—synthesis and applications. *Int J Mol Sci* 20:6304
10. Rani UA, Ng LY, Ng CY, Mahmoudi E (2020) A review of carbon quantum dots and their applications in wastewater treatment. *Adv Colloid Interface Sci* 278:102124
11. Yao B, Huang H, Liu Y, Kang Z (2019) Carbon dots: a small conundrum. *Trends Chem* 1:235–246

12. Chen BB, Liu ML, Li CM, Huang CZ (2019) Fluorescent carbon dots functionalization. *Adv Colloid Interface Sci* 270:165–190
13. Anwar S, Ding H, Xu M, Hu X, Li Z, Wang J, Liu L, Jiang L, Wang D, Dong C, Yan M, Wang Q, Bi H (2019) Recent advances in synthesis, optical properties, and biomedical applications of carbon dots. *ACS Appl Bio Mater* 2:2317–2338
14. Chung YJ, Kim J, Park CB (2020) Photonic carbon dots as an emerging nanoagent for biomedical and healthcare applications. *ACS Nano* 14:6470–6497
15. Xia C, Zhu S, Feng T, Yang M, Yang B (2019) Evolution and synthesis of carbon dots: from carbon dots to carbonized polymer dots. *Adv Sci* 6:1901316
16. Zheng A, Guo T, Guan F, Chen X, Shu Y, Wang J (2019) Ionic liquid mediated carbon dots: preparations, properties and applications. *Trends Anal Chem* 119:115638
17. Cayuela A, Soriano ML, Carrillo-Carrión C, Valcárcel M (2016) Semiconductor and carbon-based fluorescent nanodots: the need for consistency. *Chem Commun* 52:1311–1326
18. Riggs JE, Guo Z, Carroll DL, Sun Y-P (2000) Strong luminescence of solubilized carbon nanotubes. *J Am Chem Soc* 122:5879–5880
19. Xu X, Ray R, Gu Y, Ploehn HJ, Gearheart L, Raker K, Scrivens WA (2004) Electrophoretic analysis and purification of fluorescent single-walled carbon nanotube fragments. *J Am Chem Soc* 126:12736–12737
20. Sun Y-P, Zhou B, Lin Y, Wang W, Fernando KAS, Pathak P, Mezziani MJ, Harruff BA, Wang X, Wang H, Luo PG, Yang H, Kose ME, Chen B, Veca LM, Xie S-Y (2006) Quantum-sized carbon dots for bright and colorful photoluminescence. *J Am Chem Soc* 128:7756–7757
21. Pu Z-F, Wen Q-L, Yang Y-J, Cui X-M, Ling J, Liu P, Cao Q-E (2020) Fluorescent carbon quantum dots synthesized using phenylalanine and citric acid for selective detection of Fe³⁺ ions. *Spectrochim Acta A* 229:117944
22. Atchudan R, Edison TNJI, Perumal S, Vinodh R, Lee YR (2019) Betel-derived nitrogen-doped multicolor carbon dots for environmental and biological applications. *J Mol Liq* 296:111817
23. Qiao G, Chen G, Wen Q, Liu W, Gao J, Yu Z, Wang Q (2020) Rapid conversion from common precursors to carbon dots in large scale: Spectral controls, optical sensing, cellular imaging and LEDs application. *J Colloid Interface Sci* 580:88–98
24. Qin H, Sun Y, Geng X, Zhao K, Meng H, Yang R, Qu L, Li Z (2020) A wash-free lysosome targeting carbon dots for ultrafast imaging and monitoring cell apoptosis status. *Anal Chim Acta* 1106:207–215
25. Ghadiri R, Saei P-S, Sabri A, Ghasemi Z, Kong F (2020) Enhanced phthalocyanine-sensitized solar cell efficiency via cooperation of nitrogen-doped carbon dots. *J Clean Prod* 268:122236
26. Pudza MY, Abidin ZZ, Rashid SA, Yasin FM, Noor ASM, Issa MA (2020) Eco-friendly sustainable fluorescent carbon dots for the adsorption of heavy metal ions in aqueous environment. *Nanomaterials* 10:315
27. Cong S, Liu K, Qiao F, Song Y, Tan M (2019) Biocompatible fluorescent carbon dots derived from roast duck for in vitro cellular and in vivo *C. elegans* bio-imaging. *Methods* 168:76–83
28. Zhang H, Wang H, Wang Y, Xin B (2020) Controlled synthesis and photocatalytic performance of biocompatible uniform carbon quantum dots with microwave absorption capacity. *Appl Surf Sci* 512:145751
29. Liu Y, Zhang J, Zhao X, Li W, Wang J, Gao Y, Cui Y, Xu S, Luo X (2020) Water-soluble carbon dots with blue, yellow and red emissions: mechanism investigation and array-based fast sensing application. *Chem Commun* 56:4074–4077
30. Li J, Li P, Wang D, Dong C (2019) One-pot synthesis of aqueous soluble and organic soluble carbon dots and their multi-functional applications. *Talanta* 202:375–383
31. Hu X, An X, Li L (2016) Easy synthesis of highly fluorescent carbon dots from albumin and their photoluminescent mechanism and biological imaging applications. *Mater Sci Eng C* 58:730–736
32. Pan M, Xie X, Liu K, Yang J, Hong L, Wang S (2020) Fluorescent carbon quantum dots—synthesis, functionalization and sensing application in food analysis. *Nanomaterials* 10:930
33. Pawar S, Togiti UK, Bhattacharya A, Nag A (2019) Functionalized chitosan—carbon dots: a fluorescent probe for detecting trace amount of water in organic solvents. *ACS Omega* 4:11301–11311

34. Yan F, Jiang Y, Sun X, Wei J, Chen L, Zhang Y (2020) Multicolor carbon dots with concentration-tunable fluorescence and solvent-affected aggregation states for white light-emitting diodes. *Nano Res* 13:52–60
35. Yan F, Sun Z, Zhang H, Sun X, Jiang Y, Bai Z (2019) The fluorescence mechanism of carbon dots, and methods for tuning their emission colour: a review. *Microchim Acta* 186:583
36. Boakye-Yiadom KO, Kesse S, Opoku-Damoah Y, Filli MS, Aquib M, Joelle MMB, Farooq MA, Mavlyanova R, Raza F, Bavi R, Wang B (2019) Carbon dots: applications in bioimaging and theranostics. *Int J Pharm* 564:308–317
37. Li H, Yan X, Kong D, Jin R, Sun C, Du D, Lin Y, Lu G (2020) Recent advances in carbon dots for bioimaging applications. *Nanoscale Horiz* 5:218–234
38. Ashrafzadeh M, Mohammadinejad R, Kailasa SK, Ahmadi Z, Afshar EG, Pardakhty A (2020) Carbon dots as versatile nanoarchitectures for the treatment of neurological disorders and their theranostic applications: a review. *Adv Colloid Interface Sci* 278:102123
39. Yang W, Wei B, Yang Z, Sheng L (2019) Facile synthesis of novel carbon-dots/hemin nanoplateforms for synergistic photo-thermal and photo-dynamic therapies. *J Inorg Biochem* 193:166–172
40. Han J, Na K (2019) Transfection of the TRAIL gene into human mesenchymal stem cells using biocompatible polyethyleneimine carbon dots for cancer gene therapy. *J Ind Eng Chem* 80:722–728
41. Ridha AA, Pakravan P, Azandaryani AH, Zhaleh H (2020) Carbon dots; the smallest photoresponsive structure of carbon in advanced drug targeting. *J Drug Deliv Sci Technol* 55:101408
42. He P, Shi Y, Meng T, Yuan T, Li Y, Li X, Zhang Y, Fan L, Yang S (2020) Recent advances in white light-emitting diodes of carbon quantum dots. *Nanoscale* 12:4826–4832
43. Molaei MJ (2020) The optical properties and solar energy conversion applications of carbon quantum dots: a review. *Sol Energy* 196:549–566
44. Liu ML, Chen BB, Li CM, Huang CZ (2019) Carbon dots: synthesis, formation mechanism, fluorescence origin and sensing applications. *Green Chem* 21:449–471
45. Yoo D, Park Y, Cheon B, Park M-H (2019) Carbon dots as an effective fluorescent sensing platform for metal ion detection. *Nanoscale Res Lett* 14:272
46. Han M, Zhu S, Lu S, Song Y, Feng T, Tao S, Liu J, Yang B (2018) Recent progress on the photocatalysis of carbon dots: classification, mechanism and applications. *Nano Today* 19:201–218
47. Wang R, Lu K-Q, Tang Z-R, Xu Y-J (2017) Recent progress in carbon quantum dots: synthesis, properties and applications in photocatalysis. *J Mater Chem A* 5:3717–3734
48. Xiao L, Sun H (2018) Novel properties and applications of carbon nano-dots. *Nanoscale Horiz* 3:565–597
49. Wang X, Feng Y, Dong P, Huang J (2019) A mini review on carbon quantum dots: preparation, properties, and electrocatalytic application. *Front Chem* 7:671
50. Pan D, Zhang J, Li Z, Wu M (2010) Hydrothermal route for cutting graphene sheets into blue-luminescent graphene quantum dots. *Adv Mater* 22:734–738
51. Zhou X, Zhang Y, Wang C, Wu X, Yang Y, Zheng B, Wu H, Guo S, Zhang J (2012) Photofenton reaction of graphene oxide: a new strategy to prepare graphene quantum dots for DNA cleavage. *ACS Nano* 6:6592–6599
52. Tian L, Ghosh D, Chen W, Pradhan S, Chang X, Chen S (2009) Nanosized carbon particles from natural gas soot. *Chem Mater* 21:2803–2809
53. Peng J, Gao W, Gupta BK, Liu Z, Romero-Aburto R, Ge L, Song L, Alemany LB, Zhan X, Gao G, Vithayathil SA, Kaiparettu BA, Marti AA, Hayashi T, Zhu J-J, Ajayan PM (2012) Graphene quantum dots derived from carbon fibers. *Nano Lett* 12:844–849
54. Tao H, Yang K, Ma Z, Wan J, Zhang Y, Kang Z, Liu Z (2012) In vivo NIR fluorescence imaging, biodistribution, and toxicology of photoluminescent carbon dots produced from carbon nanotubes and graphite. *Small* 8:281–290
55. Qiao ZA, Wang Y, Gao Y, Li H, Dai T, Liu Y, Huo Q (2010) Commercially activated carbon as the source for producing multicolor photoluminescent carbon dots by chemical oxidation. *Chem Commun* 46:8812–8814

56. Anilkumar P, Wang X, Cao L, Sahu S, Liu JH, Wang P, Korch K, Tackett KN II, Parenzan A, Sun Y-P (2011) Toward quantitatively fluorescent carbon-based “quantum” dots. *Nanoscale* 3:2023–2027
57. El-Hnayn R, Canabady-Rochelle L, Desmarests C, Balan L, Rinnert H, Joubert O, Medjahdi G, Ouada HB, Schneider R (2020) One-step synthesis of diamine-functionalized graphene quantum dots from graphene oxide and their chelating and antioxidant activities. *Nanomaterials* 10:104
58. Peng H, Sejdic JT (2009) Simple aqueous solution route to luminescent carbogenic dots from carbohydrates. *Chem Mater* 21:5563–5565
59. Zhang Q, Sun X, Ruan H, Yin K, Li H (2017) Production of yellow-emitting carbon quantum dots from fullerene carbon soot. *Sci China Mater* 60:141–150
60. Ye R, Xiang C, Lin J, Peng Z, Huang K, Yan Z, Cook NP, Samuel EL, Hwang C-C, Ruan G (2013) Coal as an abundant source of graphene quantum dots. *Nat Commun* 4:2943
61. Iravani S, Varma RS (2020) Green synthesis, biomedical and biotechnological applications of carbon and graphene quantum dots: a review. *Environ Chem Lett* 18:703–727
62. Sharma A, Das J (2019) Small molecules derived carbon dots: synthesis and applications in sensing, catalysis, imaging, and biomedicine. *J Nanobiotechnology* 17:92
63. Dey S, Govindaraj A, Biswas K, Rao CNR (2014) Luminescence properties of boron and nitrogen doped graphene quantum dots prepared from arc-discharge-generated doped graphene samples. *Chem Phys Lett* 595–596:203–208
64. Yu HW, Li XY, Zeng XY, Lu YF (2016) Preparation of carbon dots by non-focusing pulsed laser irradiation in toluene. *Chem Commun* 52:819–822
65. Nguyen V, Zhao N, Yan L, Zhong P, Nguyen VC, Le PH (2020) Double-pulse femtosecond laser ablation for synthesis of ultrasmall carbon nanodots. *Mater Res Express* 7:015606
66. Liu HP, Ye T, Mao CD (2007) Fluorescent carbon nanoparticles derived from candle soot. *Angew Chem Int Ed* 46:6473–6475
67. Hu C, Yu C, Li M, Wang X, Yang J, Zhao Z, Eychmüller A, Sun Y-P, Qiu J (2014) Chemically tailoring coal to fluorescent carbon dots with tuned size and their capacity for Cu(II) detection. *Small* 10:4926–4933
68. Zhou J, Booker C, Li R, Zhou X, Sham T-K, Sun X, Ding Z (2007) An electrochemical avenue to blue luminescent nanocrystals from multiwalled carbon nanotubes (MWCNTs). *J Am Chem Soc* 129:744–745
69. Li X, Ge F, Li X, Zhou X, Qian J, Fu G, Shi L, Xu Y (2019) Rapid and large-scale production of carbon dots by salt-assisted electrochemical exfoliation of graphite rods. *J Electroanal Chem* 851:113390
70. AHIRWAR S, MALICK S, BAHADUR D (2017) Electrochemical method to prepare graphene quantum dots and graphene oxide quantum dots. *ACS Omega* 2:8343–8353
71. Lee J, Kim K, Park WI, Kim B-H, Park JH, Kim T-H, Bong S, Kim C-H, Chae GS, Jun M, Hwang Y, Jung YS, Jeon S (2012) Uniform graphene quantum dots patterned from self-assembled silica nanodots. *Nano Lett* 12:6078–6083
72. Pan D, Guo L, Zhang J, Xi C, Xue Q, Huang H, Li J, Zhang Z, Yu W, Chen Z, Li Z, Wu M (2012) Cutting sp² clusters in graphene sheets into colloidal graphene quantum dots with strong green fluorescence. *J Mater Chem* 22:3314–3318
73. Liu Q, Guo B, Rao Z, Zhang B, Gong JR (2013) Strong two-photon-induced fluorescence from photostable, biocompatible nitrogen-doped graphene quantum dots for cellular and deep-tissue imaging. *Nano Lett* 13:2436–2441
74. Li L-L, Ji J, Fei R, Wang C-Z, Lu Q, Zhang J-R, Jiang L-P, Zhu J-J (2012) A facile microwave avenue to electrochemiluminescent two-colour graphene quantum dots. *Adv Funct Mater* 22:2971–2979
75. Dang H, Huang LK, Zhang Y, Wang CF, Chen S (2016) Large-scale ultrasonic fabrication of white fluorescent carbon dots. *Ind Eng Chem Res* 55:5335–5341
76. Jiang D, Chen Y, Li N, Li W, Wang Z, Zhu J, Zhang H, Liu B, Xu S (2015) Synthesis of luminescent graphene quantum dots with high quantum yield and their toxicity study. *PLoS ONE* 10:e0144906

77. Yuan F, Li S, Fan Z, Meng X, Fan L, Yang S (2016) Shining carbon dots: synthesis and biomedical and optoelectronic applications. *Nano Today* 11:565–586
78. Baker SN, Baker GA (2010) Luminescent carbon nanodots: emergent nanolights. *Angew Chem Int Ed* 49:6726–6744
79. Tejwan N, Saha SK, Das J (2020) Multifaceted applications of green carbon dots synthesized from renewable sources. *Adv Colloid Interface Sci* 275:102046
80. Zhou Y, Mintz KJ, Sharma SK, Leblanc RM (2019) Carbon dots: diverse preparation, application, and perspective in surface chemistry. *Langmuir* 35:9115–9132
81. Zhang B, Liu CY, Liu Y (2010) A novel one-step approach to synthesize fluorescent carbon nanoparticles. *Eur J Inorg Chem* 28:4411–4414
82. Guo Y, Zhao W (2020) Hydrothermal synthesis of highly fluorescent nitrogen-doped carbon quantum dots with good biocompatibility and the application for sensing ellagic acid. *Spectrochim Acta A* 240:118580
83. Qu K, Wang J, Ren J, Qu X (2013) Carbon dots prepared by hydrothermal treatment of dopamine as an effective fluorescent sensing platform for the label-free detection of iron(III) ions and dopamine. *Chem Eur J* 19:7243–7249
84. Laber CH, Essner JB, Scott TA, Polo-Parada L, Baker GA (2016) Domestic pressure cooker as inexpensive hydrothermal vessel: Demonstrated utility for eco-friendly synthesis of non-toxic carbon dots. *Nano-Struct Nano-Objects* 6:52–58
85. Vandana M, Vijeth H, Ashokkumar SP, Devendrappa H (2020) Hydrothermal synthesis of quantum dots dispersed on conjugated polymer as an efficient electrodes for highly stable hybrid supercapacitors. *Inorg Chem Commun* 117:107941
86. Sarkar S, Banerjee D, Ghorai UK, Das NS, Chattopadhyay KK (2016) Size dependent photoluminescence property of hydrothermally synthesized crystalline carbon quantum dots. *J Lumin* 178:314–323
87. Yuan X, Tu Y, Chen W, Xu Z, Wei Y, Qin K, Zhang Q, Xiang Y, Zhang H, Ji X (2020) Facile synthesis of carbon dots derived from ampicillin sodium for live/dead microbe differentiation, bioimaging and high selectivity detection of 2,4-dinitrophenol and Hg(II). *Dyes Pigm* 175:108187
88. Pei S, Zhang J, Gao M, Wu D, Yang Y, Liu R (2015) A facile hydrothermal approach towards photoluminescent carbon dots from amino acids. *J Colloid Interface Sci* 439:129–133
89. Lee HJ, Jana J, Chung JS, Hur SH (2020) Fabrication of dual emission carbon dots and its use in highly sensitive thioamide detection. *Dyes Pigm* 175:108126
90. Niu W-J, Li Y, Zhu R-H, Shan D, Fan Y-R, Zhang X-J (2015) Ethylenediamine-assisted hydrothermal synthesis of nitrogen-doped carbon quantum dots as fluorescent probes for sensitive biosensing and bioimaging. *Sens Actuators B* 218:229–236
91. Kim Y, Kim J (2020) Bioinspired thiol functionalized carbon dots for rapid detection of lead (II) ions in human serum. *Opt Mater* 99:109514
92. Bakier YM, Ghali M, Sami M, Zahra WK (2020) Highly luminescent un-doped carbon nanodots driven from folic acid and passivated by polyethylene glycol. *Mater Today Proc* 33:1800–1803
93. Prathumsuwan T, Jamnongsong S, Sampattavanich S, Paoprasert P (2018) Preparation of carbon dots from succinic acid and glycerol as ferrous ion and hydrogen peroxide dual-mode sensors and for cell imaging. *Opt Mater* 86:517–529
94. Qin J, Nan Q, Yang J, Yang R (2018) Bright carbon dots via inner filter effect for the sensitive determination of the purine metabolic disorder in human fluids. *Spectrochim Acta A* 203:421–427
95. Hong D, Deng X, Liang J, Li J, Tao Y, Tan K (2019) One-step hydrothermal synthesis of down/up-conversion luminescence F-doped carbon quantum dots for label-free detection of Fe³⁺. *Microchem J* 151:104217
96. Wang S, Wu S-H, Fang W-L, Guo X-F, Wang H (2019) Synthesis of non-doped and non-modified carbon dots with high quantum yield and crystallinity by one-pot hydrothermal method using a single carbon source and used for ClO⁻ detection. *Dyes Pigm* 164:7–13

97. Cui S, Wu Y, Liu Y, Guan Q, Zhang Y, Zhang Y, Luo S, Xu M, Wang J (2020) Synthesis of carbon dots with a tunable photoluminescence and their applications for the detection of acetone and hydrogen peroxide. *Chin Chem Lett* 31:487–493
98. He W, Huo Z, Sun X, Shen J (2020) Facile and green synthesis of N, Cl-dual-doped carbon dots as a label-free fluorescent probe for hematin and temperature sensing. *Microchem J* 153:104528
99. Zhong Y, Li J, Jiao Y, Zuo G, Pan X, Su T, Dong W (2017) One-step synthesis of orange luminescent carbon dots for Ag⁺ sensing and cell imaging. *J Lumin* 190:188–193
100. Fang J, Zhuo S, Zhu C (2019) Fluorescent sensing platform for the detection of p-nitrophenol based on Cu-doped carbon dots. *Opt Mater* 97:109396
101. Wen Q-L, Pu Z-F, Yang Y-J, Wang J, Wu B-C, Hu Y-L, Liu P, Ling J, Cao Q (2020) Hyaluronic acid as a material for the synthesis of fluorescent carbon dots and its application for selective detection of Fe³⁺ ion and folic acid. *Microchem J* 159:105364
102. Tao S, Song Y, Zhua S, Shao J, Yang B (2017) A new type of polymer carbon dots with high quantum yield: from synthesis to investigation on fluorescence mechanism. *Polymer* 116:472–478
103. Rahmani Z, Ghaemy M (2019) One-step hydrothermal-assisted synthesis of highly fluorescent N-doped carbon dots from gum tragacanth: luminescent stability and sensitive probe for Au³⁺ ions. *Opt Mater* 97:109356
104. Sun D, Liu T, Wang C, Yang L, Yang S, Zhuo K (2020) Hydrothermal synthesis of fluorescent carbon dots from gardenia fruit for sensitive on-off-on detection of Hg²⁺ and cysteine. *Spectrochim Acta A* 240:118598
105. Ahmadian-Fard-Fini S, Salavati-Niasari M, Ghanbari D (2018) Hydrothermal green synthesis of magnetic Fe₃O₄-carbon dots by lemon and grape fruit extracts and as a photoluminescence sensor for detecting of *E. coli* bacteria. *Spectrochim Acta A* 203:481–493
106. Senol AM, Bozkurt E (2020) Facile green and one-pot synthesis of Seville orange derived carbon dots as a fluorescent sensor for Fe³⁺ ions. *Microchem J* 159:105357
107. Tu Y, Wang S, Yuan X, Xiang Y, Qin K, Wei Y, Zhang Q, Chen X, Ji X (2021) Facile hydrothermal synthesis of nitrogen, phosphorus-doped fluorescent carbon dots for live/dead bacterial differentiation, cell imaging and two nitrophenols detection. *Dyes Pigm* 184:108761
108. Khan ZM, Rahman RS, Islam S, Zulfequar M (2019) Hydrothermal treatment of red lentils for the synthesis of fluorescent carbon quantum dots and its application for sensing Fe³⁺. *Opt Mater* 91:386–395
109. Dhanush C, Sethuraman MG (2020) Influence of phyto-derived nitrogen doped carbon dots from the seeds of *Azadirachta indica* on the NaBH₄ reduction of Safranin-O dye. *Diam Relat Mater* 108:107984
110. Sharma N, Yun K (2020) Dual sensing of tetracycline and L-lysine using green synthesized carbon dots from *Nigella sativa* seeds. *Dyes Pigm* 182:108640
111. Sabet M, Mahdavi K (2019) Green synthesis of high photoluminescence nitrogen-doped carbon quantum dots from grass via a simple hydrothermal method for removing organic and inorganic water pollutions. *Appl Surf Sci* 463:283–291
112. Li L, Wang X, Fu Z, Cu F (2017) One-step hydrothermal synthesis of nitrogen- and sulfur-codoped carbon dots from ginkgo leaves and application in biology. *Mater Lett* 196:300–303
113. Ramanarayanan R, Swaminathan S (2020) Synthesis and characterisation of green luminescent carbon dots from guava leaf extract. *Mater Today Proc* 33:2223–2227
114. Komalavalli L, Amutha P, Monisha S (2020) A facile approach for the synthesis of carbon dots from *Hibiscus sabdariffa* & its application as bio-imaging agent and Cr(VI) sensor. *Mater Today Proc* 33:2279–2285
115. Yuan M, Zhong R, Gao H, Li W, Yun X, Liu J, Zhao X, Zhao G, Zhang F (2015) One-step, green, and economic synthesis of water-soluble photoluminescent carbon dots by hydrothermal treatment of wheat straw, and their bio-applications in labeling, imaging, and sensing. *Appl Surf Sci* 355:1136–1144
116. Atchudan R, Edison TNJI, Aseer KR, Perumal S, Lee YR (2018) Hydrothermal conversion of *Magnolia liliiflora* into nitrogen-doped carbon dots as an effective turn-off fluorescence sensing, multi-colour cell imaging and fluorescent ink. *Colloids Surf B* 169:321–328

117. Paul A, Kurian M (2020) N-doped photoluminescent carbon dots from water hyacinth for tumour detection. *Mater Today Proc* 25:213–217
118. Ahmed HM, Ghali M, Zahra WK, Ayad M (2020) Optical sensing of pyridine based on green synthesis of passivated carbon dots. *Mater Today Proc* 33:1845–1848
119. Li Y, Liu F, Cai J, Huang X, Lin L, Lin Y, Yang H, Li S (2019) Nitrogen and sulfur co-doped carbon dots synthesis via one step hydrothermal carbonization of green alga and their multifunctional applications. *Microchem J* 147:1038–1047
120. Lu C, Liu J, Gan L, Yang X (2019) Employing *Cryptococcus*-directed carbon dots for differentiating and detecting m-benzenediol and p-benzenediol. *Sens Actuators B* 301:127077
121. Liu Y, Zhou Q, Li J, Lei M, Yan X (2016) Selective and sensitive chemosensor for lead ions using fluorescent carbon dots prepared from chocolate by one-step hydrothermal method. *Sens Actuators B* 237:597–604
122. Wei J, Zhang X, Sheng Y, Shen J, Huang P, Guo S, Pan J, Feng B (2014) Dual functional carbon dots derived from cornflour via a simple one-pot hydrothermal route. *Mater Lett* 123:107–111
123. Mehta VN, Jha S, Basu H, Singhal RK, Kailasa SK (2015) One-step hydrothermal approach to fabricate carbon dots from apple juice for imaging of mycobacterium and fungal cells. *Sens Actuators B* 213:434–443
124. Chen Y, Zhao C, Wang Y, Rao H, Lu Z, Lu C, Shan Z, Ren B, Wu W, Wang X (2020) Green and high-yield synthesis of carbon dots for ratiometric fluorescent determination of pH and enzyme reactions. *Mater Sci Eng C* 117:111264
125. Zhang X-D, Li J, Niu J-N, Bao X-P, Zhao H-D, Tan M (2019) Fluorescent carbon dots derived from urine and their application for bio-imaging. *Methods* 168:84–93
126. Yuan C, Qin X, Xu Y, Li X, Chen Y, Shi R, Wang Y (2020) Carbon quantum dots originated from chicken blood as peroxidase mimics for colorimetric detection of biothiols. *J Photochem Photobiol A* 396:112529
127. Zhang X, Jiang M, Niu N, Chen Z, Li S, Liu S, Li J (2018) Natural-product-derived carbon dots: from natural products to functional materials. *ChemSusChem* 11:11–24
128. Das R, Bandyopadhyay R, Pramanik P (2018) Carbon quantum dots from natural resource: a review. *Mater Today Chem* 8:96–109
129. Zhu H, Wang X, Li Y, Wang Z, Yang F, Yang X (2009) Microwave synthesis of fluorescent carbon nanoparticles with electrochemiluminescence properties. *Chem Commun* 5118–5120
130. Pajewska-Szmyt M, Buszewski B, Gadzała-Kopciuch R (2020) Sulphur and nitrogen doped carbon dots synthesis by microwave assisted method as quantitative analytical nano-tool for mercury ion sensing. *Mater Chem Phys* 242:122484
131. Wang H-J, Hou W-Y, Yu T-T, Chen H-L, Zhang Q-Q (2019) Facile microwave synthesis of carbon dots powder with enhanced solid-state fluorescence and its applications in rapid fingerprints detection and white-light-emitting diodes. *Dyes Pigm* 170:107623
132. Eskalen H, Uruş S, Cömertpay S, Kurt AH, Özgan Ş (2020) Microwave-assisted ultra-fast synthesis of carbon quantum dots from linter: fluorescence cancer imaging and human cell growth inhibition properties. *Ind Crop Prod* 147:112209
133. Zhao C, Li X, Cheng C, Yang Y (2019) Green and microwave-assisted synthesis of carbon dots and application for visual detection of cobalt(II) ions and pH sensing. *Microchem J* 147:183–190
134. Jusuf BN, Sambudi NS, Isnaeni I, Samsuri S (2018) Microwave-assisted synthesis of carbon dots from eggshell membrane ashes by using sodium hydroxide and their usage for degradation of methylene blue. *J Environ Chem Eng* 6:7426–7433
135. Hu Y, Gao Z (2020) Sewage sludge in microwave oven: a sustainable synthetic approach toward carbon dots for fluorescent sensing of para-Nitrophenol. *J Hazard Mater* 382:121048
136. Chatzimitakos T, Kasouni A, Sygellou L, Leonardos I, Troganis A, Stalikas C (2018) Human fingernails as an intriguing precursor for the synthesis of nitrogen and sulfur-doped carbon dots with strong fluorescent properties: analytical and bioimaging applications. *Sens Actuators B* 267:494–501
137. Bourlinos AB, Stassinopoulos A, Anglos D, Zboril R, Karakassides M, Giannelis EP (2008) Surface functionalized carbogenic quantum dots. *Small* 4:455–458

138. Sha R, Jones SS, Badhulika S (2019) Controlled synthesis of platinum nanoflowers supported on carbon quantum dots as a highly effective catalyst for methanol electro-oxidation. *Surf Coat Tech* 360:400–408
139. Rahy A, Zhou C, Zheng J, Park SY, Kim MJ, Jang I, Cho SJ, Yang DJ (2012) Photoluminescent carbon nanoparticles produced by confined combustion of aromatic compounds. *Carbon* 50:1298–1302
140. Li HT, He XD, Liu Y, Huang H, Lian SY, Lee ST, Kang ZH (2011) One-step ultrasonic synthesis of water-soluble carbon nanoparticles with excellent photoluminescent properties. *Carbon* 49:605–609
141. Liu R, Wu D, Liu S, Koynov K, Knoll W, Li Q (2009) An aqueous route to multicolor photoluminescent carbon dots using silica spheres as carriers. *Angew Chem* 121:4668–4671
142. Ma X, Li S, Hessel V, Lin L, Meskers S, Gallucci F (2020) Synthesis of N-doped carbon dots via a microplasma process. *Chem Eng Sci* 220:115648
143. Lu J, Yeo PS, Gan CK, Wu P, Loh KP (2011) Transforming C60 molecules into graphene quantum dots. *Nat Nanotechnol* 6:247–252
144. Yan F, Jiang Y, Sun X, Bai Z, Zhang Y, Zhou X (2018) Surface modification and chemical functionalization of carbon dots: a review. *Microchim Acta* 185:424
145. Li L, Dong T (2018) Photoluminescence tuning in carbon dots: Surface passivation or/and functionalization, heteroatom doping. *J Mater Chem C* 6:7944–7970
146. Yuan N, Chen J, Zhou H, Ali MC, Guan M, Qiu H (2020) Nitrogen-doping to enhance the separation selectivity of glucose-based carbon dots-modified silica stationary phase for hydrophilic interaction chromatography. *Talanta* 218:121140
147. Gao D, Zhang Y, Liu A, Zhu Y, Chen S, Wei D, Sun J, Guo Z, Fan H (2020) Photoluminescence-tunable carbon dots from synergy effect of sulfur doping and water engineering. *Chem Eng J* 388:124199
148. Raju CV, Kalaiyaran G, Paramasivam S, Joseph J, Kumar SS (2020) Phosphorous doped carbon quantum dots as an efficient solid state electrochemiluminescence platform for highly sensitive turn-on detection of Cu²⁺ ions. *Electrochim Acta* 331:135391
149. Desai ML, Basu H, Saha S, Singhal RK, Kailasa SK (2019) Investigation of silicon doping into carbon dots for improved fluorescence properties for selective detection of Fe³⁺ ion. *Opt Mater* 96:109374
150. Zhang X, Ren Y, Ji Z, Fan J (2020) Sensitive detection of amoxicillin in aqueous solution with novel fluorescent probes containing boron-doped carbon quantum dots. *J Mol Liq* 311:113278
151. Luo T-Y, He X, Zhang J, Chen P, Liu Y-H, Wang H-J, Yu X-Q (2018) Photoluminescent F-doped carbon dots prepared by ring-opening reaction for gene delivery and cell imaging. *RSC Adv* 8:6053–6062
152. Wang Y, Man Y, Li S, Wu S, Zhao X, Xie F, Qu Q, Zou W-S (2020) Pesticide-derived bright chlorine-doped carbon dots for selective determination and intracellular imaging of Fe(III). *Spectrochim Acta A* 226:117594
153. Su H, Liao Y, Wu F, Sun X, Liu H, Wang K, Zhu X (2018) Cetuximab-conjugated iodine doped carbon dots as a dual fluorescent/CT probe for targeted imaging of lung cancer cells. *Colloids Surf B* 170:194–200
154. Chen H, Wen K, Chen J, Xing W, Wu X, Shi Q, Peng A, Huang H (2020) Ultra-stable tellurium-doped carbon quantum dots for cell protection and near-infrared photodynamic application. *Sci Bull* 65:1580–1586
155. Man Y, Li Z, Kong W-L, Li W, Dong W, Wang Y, Xie F, Zhao D, Qu Q, Zou W-S (2020) Starch fermentation wastewater as a precursor to prepare S,N-doped carbon dots for selective Fe(III) detection and carbon microspheres for solution decolorization. *Microchem J* 159:105338
156. Zhao D, Zhang Z, Liu X, Zhang R, Xiao X (2020) Rapid and low-temperature synthesis of N, P co-doped yellow emitting carbon dots and their applications as antibacterial agent and detection probe to Sudan Red I. *Mater Sci Eng C* 119:111468
157. Li J, Dong Y, Zhu J, Wang L, Tian W, Zhao J, Lin H, Zhang S, Cao Y, Song H, Jia D, B (2020) N co-doped carbon nanosheets derived from graphene quantum dots: Improving the pseudocapacitive performance by efficient trapping nitrogen. *Appl Surf Sci* 529:147239

158. Wang X, Liu Y, Wang Q, Bu T, Sun X, Jia P, Wang L (2020) Nitrogen, silicon co-doped carbon dots as the fluorescence nanoprobe for trace p-nitrophenol detection based on inner filter effect. *Spectrochim Acta A* 244:118876
159. Nazari F, Tabaraki R (2020) Sensitive fluorescence detection of atorvastatin by doped carbon dots synthesized in deep eutectic media. *Spectrochim Acta A* 236:118341
160. Liu L, Anwar S, Ding H, Xu M, Yin Q, Xiao Y, Yang X, Yan M, Bi H (2019) Electrochemical sensor based on F, N-doped carbon dots decorated laccase for detection of catechol. *J Electroanal Chem* 840:84–92
161. Zhu Z, Yang P, Li X, Luo M, Zhang W, Chen M, Zhou X (2020) Green preparation of palm powder-derived carbon dots co-doped with sulfur/chlorine and their application in visible-light photocatalysis. *Spectrochim Acta A* 227:117659
162. Zhang MM, Ju H, Zhang L, Sun M, Zhou Z, Dai Z, Zhang L, Gong A, Wu C, Du F (2015) Engineering iodine-doped carbon dots as dual-modal probes for fluorescence and X-ray CT imaging. *Int J Nanomed* 10:6943–6953
163. Li D, Yuan X, Li C, Luo Y, Jiang Z (2020) A novel fluorescence aptamer biosensor for trace Pb(II) based on gold-doped carbon dots and DNAzyme synergetic catalytic amplification. *J Lumin* 221:117056
164. Qing W, Chen K, Yang Y, Wang Y, Liu X (2020) Cu²⁺-doped carbon dots as fluorescence probe for specific recognition of Cr(VI) and its antimicrobial activity. *Microchem J* 152:104262
165. Yuan K, Zhang X, Li X, Qin R, Cheng Y, Li L, Yang X, Yu X, Lu Z, Liu H (2020) Great enhancement of red emitting carbon dots with B/Al/Ga doping for dual mode anti-counterfeiting. *Chem Eng J* 397:125487
166. Kumar VB, Kumar R, Gedanken A, Shefi O (2019) Fluorescent metal-doped carbon dots for neuronal manipulations. *Ultrason Sonochem* 52:205–213
167. Li C, Fan P, Liang A, Jiang Z (2019) Using Ca-doped carbon dots as catalyst to amplify signal to determine ultratrace thrombin by free-label aptamer-SERS method. *Mater Sci Eng C* 99:1399–1406
168. Cai T, Zhang Y, Liu D, Tong D, Li S (2019) Nanostructured molybdenum/heteroatom-doped carbon dots nanohybrids for lubrication by direct carbonization route. *Mater Lett* 250:20–24
169. Su Y, Liu S, Guan Y, Xie Z, Zheng M, Jing X (2020) Renal clearable Hafnium-doped carbon dots for CT/fluorescence imaging of orthotopic liver cancer. *Biomaterials* 255:120110
170. Zhao C, Zhang X, Shu X, Liu X, Fang D, Song Y, Wang J (2018) Er-doped carbon dots broadening light absorption range and accelerating electron transport for enhancing photovoltaic performance of CdS quantum dots sensitized cells. *Opt Mater* 84:242–251
171. Cheng J, Wang CF, Zhang Y, Yang SY, Chen S (2016) Zinc ion-doped carbon dots with strong yellow photoluminescence. *RSC Adv* 6:37189–37194
172. Han CP, Xu HT, Wang R, Wang KY, Dai Y, Liu Q, Guo MX, Li JJ, Xu K (2016) Synthesis of a multifunctional manganese(II)-carbon dots hybrid and its application as an efficient magnetic-fluorescent imaging probe for ovarian cancer cell imaging. *J Mater Chem B* 4:5798–5802
173. Zhang HY, Wang Y, Xiao S, Wang H, Wang JH, Feng L (2017) Rapid detection of Cr(VI) ions based on cobalt(II)-doped carbon dots. *Biosens Bioelectron* 87:46–52
174. Qian F, Li X, Tang L, Lai SK, Lu C, Lau SP (2016) Potassium doping: tuning the optical properties of graphene quantum dots. *AIP Adv* 6:075116
175. Lin L, Luo Y, Tsai P, Wang J, Chen X (2018) Metal ions doped carbon quantum dots: synthesis, physicochemical properties, and their applications. *Trends Anal Chem* 103:87–101
176. Liu Y, Wu P, Wu X, Ma C, Luo S, Xu M, Li W, Liu S (2020) Nitrogen and copper (II) co-doped carbon dots for applications in ascorbic acid determination by non-oxidation reduction strategy and cellular imaging. *Talanta* 210:120649
177. Wang L, Liu Y, Yang Z, Wang Y, Rao H, Yue G, Wu C, Lu C, Wang X (2020) A ratiometric fluorescence and colorimetric dual-mode assay for H₂O₂ and xanthine based on Fe, N co-doped carbon dots. *Dyes Pigm* 180:108486
178. Liu T, Li N, Dong JX, Luo HQ, Li NB (2016) Fluorescence detection of mercury ions and cysteine based on magnesium and nitrogen co-doped carbon quantum dots and implication logic gate operation. *Sens Actuators B* 231:147–153

179. Yu C, Xuan T, Chen Y, Zhao Z, Liu X, Lian G, Li H (2016) Gadolinium-doped carbon dots with high quantum yield as an effective fluorescence and magnetic resonance bimodal imaging probe. *J Alloys Compd* 688:611–619
180. Wang Y, Meng H, Jia MY, Zhang Y, Li H, Feng L (2016) Intraparticle FRET of Mn(II)-doped carbon dots and its application in discrimination of volatile organic compounds. *Nanoscale* 8:17190–17195
181. Tammina SK, Yang D, Li X, Koppala S, Yang Y (2019) High photoluminescent nitrogen and zinc doped carbon dots for sensing Fe³⁺ ions and temperature. *Spectrochim Acta A* 222:117141
182. Chen BB, Liu ZX, Zou HY, Huang CZ (2016) Highly selective detection of 2,4,6-trinitrophenol by using newly developed terbium-doped blue carbon dots. *Analyst* 141:2676–2681
183. Gong N, Wang H, Li S, Deng Y, Chen X, Ye L, Gu W (2014) Microwave-assisted polyol synthesis of gadolinium-doped green luminescent carbon dots as a bimodal nanoprobe. *Langmuir* 30:10933–10939
184. Hu Y, Gao Z, Luo J (2021) Fluorescence detection of malachite green in fish tissue using red emissive Se,N,Cl-doped carbon dots. *Food Chem* 335:127677
185. Mu Z, Hua J, Yang Y (2020) N, S, I co-doped carbon dots for folic acid and temperature sensing and applied to cellular imaging. *Spectrochim Acta A* 224:117444
186. Li L-S, Xu L (2020) Highly fluorescent N,S,P tri-doped carbon dots for Cl⁻ detection and their assistance of TiO₂ as the catalyst in the degradation of methylene blue. *J Photochem Photobiol A* 401:112772
187. Wu W, Zhang Q, Wang R, Zhao Y, Li Z, Ning H, Zhao Q, Wiederrecht GP, Qiu J, Wu M (2018) Synergies between unsaturated Zn/Cu doping sites in carbon dots provide new pathways for photocatalytic oxidation. *ACS Catal* 8:747–753
188. Kundu S, Yadav RM, Narayanan TN, Shelke MV, Vajtai R, Ajayan PM, Pillai VK (2015) Synthesis of N F and S co-doped graphene quantum dots. *Nanoscale* 7:11515–11519
189. Liu Y, Duan W, Song W, Liu J, Ren C, Wu J, Liu D, Chen H (2017) Red emission B, N, S-co-doped carbon dots for colorimetric and fluorescent dual mode detection of Fe³⁺ ions in complex biological fluids and living cells. *ACS Appl Mater Interface* 9:12663–12672
190. Bourlinos AB, Rathi AK, Gawande MB, Hola K, Goswami A, Kalytchuk S, Karakasides MA, Kouloumpis A, Gournis D, Deligiannakis Y, Giannelis EP, Zboril R (2017) Fe(III)-functionalized carbon dots—Highly efficient photoluminescence redox catalyst for hydrogenations of olefins and decomposition of hydrogen peroxide. *Appl Mater Today* 7:179–184
191. Vázquez-González M, Liao W-C, Cazelles R, Wang S, Yu X, Gutkin V, Willner I (2017) Mimicking horseradish peroxidase functions using Cu²⁺-modified carbon nitride nanoparticles or Cu²⁺-modified carbon dots as heterogeneous catalysts. *ACS Nano* 11:3247–3253
192. Gogoi J, Chowdhury D (2020) Calcium-modified carbon dots derived from polyethylene glycol: fluorescence-based detection of Trifluralin herbicide. *J Mater Sci* 55:11597–11608
193. Zou F-R, Wang S-N, Wang F-F, Liu D, Li Y (2020) Synthesis of lanthanide-functionalized carbon quantum dots for chemical sensing and photocatalytic application. *Catalysts* 10:833
194. Gong Y, Liang H (2019) Nickel ion detection by imidazole modified carbon dots. *Spectrochim Acta A* 211:342–347
195. Yan F, Jiang Y, Sun X, Ma T, Chen L, Chen L (2020) 4-aminoantipyrine modified carbon dots and their analytical applications through response surface methodology. *Spectrochim Acta A* 227:117543
196. Zhang Z, Zhang D, Shi C, Liu W, Chen L, Miao Y, Diwu J, Li J, Wang S (2019) 3,4-Hydroxypyridinone-modified carbon quantum dot as a highly sensitive and selective fluorescent probe for the rapid detection of uranyl ions. *Environ Sci Nano* 6:1457–1465
197. Copur F, Bekar N, Zor E, Alpaydin S, Bingol H (2019) Nanopaper-based photoluminescent enantioselective sensing of L-Lysine by L-cysteine modified carbon quantum dots. *Sens Actuators B* 279:305–312

198. Lu X, Fan Z (2019) Determination of cholic acid in body fluids by β -cyclodextrin-modified N-doped carbon dot fluorescent probes. *Spectrochim Acta A* 216:342–348
199. Fu Z, He J, Jia F, Wang M, Cui F (2020) Utilizing the interfacial reaction of naphthalenyl thiosemicarbazide-modified carbon dots for the ultrasensitive determination of Fe (III) ions. *Spectrochim Acta A* 225:117485
200. Zhu J, Bai X, Chen X, Xie Z, Zhu Y, Pan G, Zhai Y, Zhang H, Dong B, Song H (2018) Carbon dots with efficient solid-state red-light emission through the step-by-step surface modification towards light-emitting diodes. *Dalton Trans* 47:3811–3818
201. Wu X, Ma L, Sun S, Jiang K, Zhang L, Wang Y, Zeng H, Lin H (2018) A versatile platform for the highly efficient preparation of graphene quantum dots: photoluminescence emission and hydrophilicity–hydrophobicity regulation and organelle imaging. *Nanoscale* 10:1532–1539
202. Liu H, Wang Q, Shen G, Zhang C, Li C, Ji W, Wang C, Cui D (2014) A multifunctional ribonuclease A-conjugated carbon dot cluster nanosystem for synchronous cancer imaging and therapy. *Nanoscale Res Lett* 9:397
203. Guo M, Hou Q, Waterhouse GIN, Hou J, Ai S, Li X (2019) A simple aptamer-based fluorescent aflatoxin B1 sensor using humic acid as quencher. *Talanta* 205:120131
204. Li Z, Wang T, Gu L, Wang H, Zhao Y, Lu S, Zhao W, Sun T (2020) N-doped carbon dots modified with the antibody of Epithelial cell adhesion molecule as HepG2 cells imaging agent by ultra-sensitive response to Al^{3+} . *Nanotechnology* 31:485703
205. Zhou Y, Sharma SK, Peng Z, Leblanc RM (2017) Polymers in carbon dots: a review. *Polymers* 9:67
206. Huang H, Cui Y, Liu M, Chen J, Wan Q, Wen Y, Deng F, Zhou N, Zhang X, Wei Y (2018) A one-step ultrasonic irradiation assisted strategy for the preparation of polymer-functionalized carbon quantum dots and their biological imaging. *J Colloid Interface Sci* 532:767–773
207. Cai T, Zhang H, Chen J, Li Z, Qiu H (2019) Polyethyleneimine-functionalized carbon dots and their precursor co-immobilized on silica for hydrophilic interaction chromatography. *J Chromatogr A* 1597:142–148
208. Hu S, Zhou Y, Xue C, Yang J, Chang Q (2017) A solid reaction towards in situ hybridization of carbon dots and conjugated polymers for enhanced light absorption and conversion. *Chem Commun* 53:9426–9429
209. Liu Y, Li S, Li K, Zheng Y, Zhang M, Cai C, Yu C, Zhou Y, Yan D (2016) A srikaya-like light-harvesting antenna based on graphene quantum dots and porphyrin unimolecular micelles. *Chem Commun* 52:9394–9397
210. Zhu J, Shao H, Bai X, Zhai Y, Zhu Y, Chen X, Pan G, Dong B, Xu L, Zhang H (2018) Modulation of the photoluminescence in carbon dots through surface modification: from mechanism to white light-emitting diodes. *Nanotechnology* 29:245702
211. Zhang X, Wang S, Xu L, Feng L, Ji Y, Tao L, Li S, Wei Y (2012) Biocompatible polydopamine fluorescent organic nanoparticles: facile preparation and cell imaging. *Nanoscale* 4:5581–5584
212. Qian K, Guo H, Chen G, Ma C, Xing B (2018) Distribution of different surface modified carbon dots in pumpkin seedlings. *Sci Rep* 8:7991
213. Ansari S, Masoum S (2020) Recent advances and future trends on molecularly imprinted polymer-based fluorescence sensors with luminescent carbon dots. *Talanta* 223:121411
214. Wulff G, Sarhan A, Zabrocki K (1972) Über die Anwendung von enzymanalog gebauten polymeren zur racemattrennung. *Angew Chem* 84:364–364
215. Arshady R, Mosbach KK (1981) Synthesis of substrate-selective polymers by host-guest polymerization. *Macromol Chem Phys Makromol Chem* 182:687–692
216. Karlsson BCG, O'Mahony J, Karlsson JG, Bengtsson H, Eriksson LA, Nicholls IA (2009) Structure and dynamics of monomer-template complexation: an explanation for molecularly imprinted polymer recognition site heterogeneity. *J Am Chem Soc* 131:13297–13304
217. Szablewski P, Kaczmarek K, Cavazzini A, Chen YB, Sellergren B, Guiochon G (2002) Energetic heterogeneity of the surface of a molecularly imprinted polymer studied by high-performance liquid chromatography. *J Chromatogr A* 964:99–111

218. Kim H, Kaczmarek K, Guiochon G (2005) Mass transfer kinetics on the heterogeneous binding sites of molecularly imprinted polymers. *Chem Eng Sci* 60:5425–5444
219. Kim H, Kaczmarek K, Guiochon G (2006) Intraparticle mass transfer kinetics on molecularly imprinted polymers of structural analogues of a template. *Chem Eng Sci* 61:1122–1137
220. Olsson GD, Karlsson BCG, Shoravi S, Wiklander JG, Nicholls IA (2012) Mechanisms underlying molecularly imprinted polymer molecular memory and the role of crosslinker: resolving debate on the nature of template recognition in phenylalanine anilide imprinted polymers. *J Mol Recognit* 25:69–73
221. Martin PD, Wilson TD, Wilson ID, Jones GR (2001) An unexpected selectivity of a propranolol-derived molecular imprint for tamoxifen. *Analyst* 126:757–759
222. Klejn D, Luliński P, Maciejewska D (2016) Molecularly imprinted solid phase extraction in an efficient analytical protocol for indole-3-methanol determination in artificial gastric juice. *RSC Adv* 6:108801–108809
223. Alvarez-Lorenzo C, Concheiro A (2013) Handbook of molecularly imprinted polymers. Smithers Rapra, Shawbury, United Kingdom
224. Xu X, Xu G, Wei F, Cen Y, Shi M, Cheng X, Chai Y, Sohail M, Hu Q (2018) Carbon dots coated with molecularly imprinted polymers: a facile bioprobe for fluorescent determination of caffeic acid. *J Colloid Interface Sci* 529:568–574
225. Shariati R, Rezaei B, Jamei HR, Ensafi AA (2019) Application of coated green source carbon dots with silica molecularly imprinted polymers as a fluorescence probe for selective and sensitive determination of phenobarbital. *Talanta* 194:143–149
226. Ensafi AA, Nasr-Esfahani P, Rezaei B (2018) Synthesis of molecularly imprinted polymer on carbon quantum dots as an optical sensor for selective fluorescent determination of promethazine hydrochloride. *Sens Actuators B* 257:889–896
227. Bhogal S, Kaur K, Maheshwari S, Malik AK (2019) Surface molecularly imprinted carbon dots based core-shell material for selective fluorescence sensing of ketoprofen. *J Fluoresc* 29:145–154
228. Wang X, Yu S, Wang J, Yu J, Arabi M, Fu L, Li B, Li J, Chen L (2020) Fluorescent nanosensor designing via hybrid of carbon dots and post-imprinted polymers for the detection of ovalbumin. *Talanta* 211:120727
229. Jalili R, Amjadi M (2018) Bio-inspired molecularly imprinted polymer–green emitting carbon dot composite for selective and sensitive detection of 3-nitrotyrosine as a biomarker. *Sens Actuators B* 255:1072–1078
230. Lv P, Xie D, Zhang Z (2018) Magnetic carbon dots based molecularly imprinted polymers for fluorescent detection of bovine hemoglobin. *Talanta* 188:145–151
231. Li S, Pang C, Ma X, Zhao M, Li H, Wang M, Li J, Luo J (2020) Chiral drug fluorometry based on a calix[6]arene/molecularly imprinted polymer double recognition element grafted on nano-C-dots/Ir/Au. *Microchim Acta* 187:394
232. Zhao Y, Chen Y, Fang M, Tian Y, Bai G, Zhuo K (2020) Silanized carbon dot-based thermo-sensitive molecularly imprinted fluorescent sensor for bovine hemoglobin detection. *Anal Bioanal Chem* 412:5811–5817
233. Liu H, Ding J, Zhang K, Ding L (2020) Fabrication of carbon dots@restricted access molecularly imprinted polymers for selective detection of metronidazole in serum. *Talanta* 209:120508
234. Fang M, Zhuo K, Chen Y, Zhao Y, Bai G, Wang J (2019) Fluorescent probe based on carbon dots/silica/molecularly imprinted polymer for lysozyme detection and cell imaging. *Anal Bioanal Chem* 411:5799–5807

Magnetic Polymer Nanocomposites: Manufacturing and Biomedical Applications



Hüsnügül Yılmaz Atay

Abstract Magnetism and magnetic materials have been used in plenty of medical applications for many years. Advances in the synthesis and characterization of magnetic particles, especially nanomagnetic particles, have also helped the use of magnetic biomaterials. The combination of magnetic nanoparticles and a biocompatible material has led to the production of a multifunctional and remotely controlled platform that is useful for a variety of biomedical problems. Biocompatible materials such as magnetite (Fe_3O_4) are among the most widely used biomaterials for different applications, from cell separation and drug delivery to hyperthermia. Apart from that, numerous magnetic materials in bulk as well as nanoparticles have been used for various medical applications. In this section, the current explanation of magnetic nano composites from basic science to the latest innovations is given. Starting with the introduction of magnetism and magnetic materials, characterization of magnetic biomaterials, synthesis techniques, production methods, and application areas were studied. An easy way to understand new techniques emerging in this field is presented to the reader. In addition, more current processes and practices are briefly mentioned.

Keywords Magnetism · Biomaterials · Magnetic nanoparticles · Hyperthermia · Drug delivery · Magnetic bioseparation

1 Introduction

Magnetism is a unique property found in every atom, and it has an important effect on living organisms. If we look at the hemoglobin in our blood, it is seen that it is also an iron complex and is magnetic in nature. Magnetotactic bacteria appear to be perhaps the first living organisms to orient themselves according to the earth's magnetic field. These bacteria contain chains of magnetite particles that are variously aligned. In

H. Yılmaz Atay (✉)

İzmir Katip Çelebi University Department of Materials Science and Engineering Çiğli, İzmir, Turkey

e-mail: husnugul.yilmaz.atay@ikcu.edu.tr

fact, there is substantial evidence that all living organisms contain magnetic particles and act as magnetic receptors, including animals and humans [1, 2].

Magnetism and magnetic materials have been found to play a powerful role in health and biological applications. We first see these practices as the removal of metal objects found in animals and humans' bodies. Recently, a combination of magnetism is used in materials designed as biomaterials. Examples of these are sophisticated biomedical applications such as cell separation, drug delivery, and magnetic intracellular hyperthermia treatment of cancer. Similarly, purification of bone marrow cells from tumor cells using immuno-magnetic beads is an important method used in clinical therapy [1–4].

When we look at the materials that allow the use of magnetism, we come across composite materials. Especially nano composites are at the forefront in this area. More precisely, the inclusion of magnetism in the development of nano technology has opened up new windows of sophisticated biomedical applications [1].

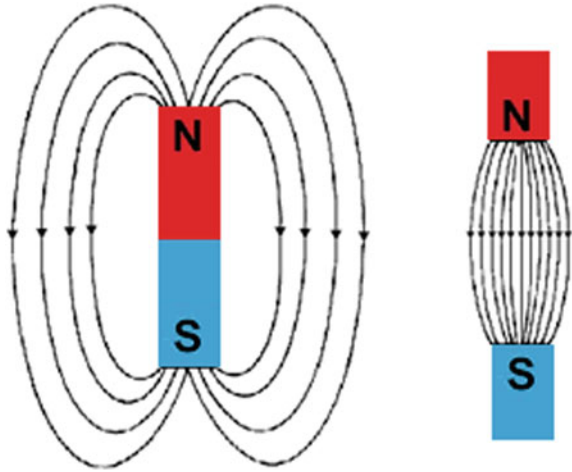
Materials known as nanocomposites are composites where at least one of the phases has dimensions in the nanometer range ($1 \text{ nm} = 10^{-9} \text{ m}$). These materials have emerged as viable alternatives to overcome the limitations encountered in microcomposites and monoliths. These materials are considered twenty-first-century materials because they have a combination of design uniqueness and properties not found in conventional composites [5]. Magnetic nanocomposites, on the other hand, emerge as nanocomposite materials, which are increasingly important and developed due to their potential applications in biomedicine, information technology, magnetic resonance imaging, catalysis, telecommunication and environmental improvement [6].

1.1 Magnetism and Magnetic Materials

We have known magnetism since childhood as the phenomenon in which some material pulls and repels other materials from a distance. Examples of such materials include iron, lodestone, and some steels. In general, it can be said that magnetic forces are generated by moving charged particles and this leads to magnetic fields (Fig. 1) [7].

For example, consider a material placed in an external magnetic field. The atoms in this material have an atomic moment that reacts to this outer field. Magnetic dipoles found in magnetic materials can be thought of as dipoles, small north, and south poles bar magnets. Dipoles have a magnetic dipole moment that can react to the external magnetic field. It can be better understood with some field vectors: external magnetic field strength is denoted by H (units A/m), magnetic induction in the material by B (units of tesla), and magnetization by M (units of A/m). B , H and M associated with (Eq. 1) [7]

$$B = \mu_o(H + M) \quad (1)$$

Fig. 1 Magnetic field lines

where μ_o is the permeability of free space (its magnitude is 1.257×10^{-6} H/m) and M is the magnetic moment m per unit volume of the material. Depending on the type of material and temperature, the value of M may vary. Also, it can be related to the field H through the volumetric magnetic susceptibility χ by the relation (Eq. 2) [7]

$$M = \chi H \quad (2)$$

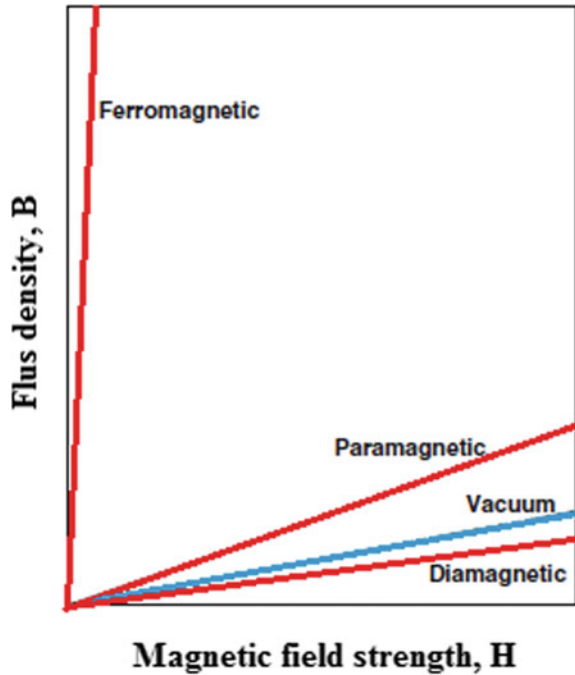
1.2 Categories of Magnetic Materials

There are several types of magnetism that basically depends on the orbital motions of electrons, their rotational motion, and how the electrons interact with each other. The best way to show the different types of magnetism is to describe how materials react to a magnetic field. Although all materials have magnetic properties, the basic distinction between these materials can be explained as follows: Some materials do not have a total atomic magnetic moment interaction, whereas in other materials there is a very strong interaction between their atomic magnetic moments [7].

Accordingly, the magnetic response that occurs in terms of the behavior of atoms causes materials to be classified as diamagnetic, paramagnetic, or ferromagnetic (Fig. 2). Ferromagnetic materials exhibit a long-range magnetic pattern under a certain critical temperature. They are substances such as iron, cobalt, nickel that can be magnetized in the same direction as the magnetic field lines of any magnet while in the magnetic field of that magnet.

Diamagnetic substances are composed of atoms that do not have a net magnetic moment (i.e., orbital shells are all full and no unpaired electrons). Diamagnetism is very weak and not permanent; it continues only as long as there is a magnetic field

Fig. 2 Schematic of the flux density B as a function of H for various materials [7, 8]



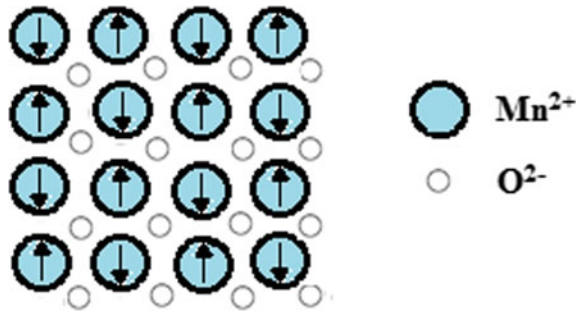
outside. Occurs due to a change in the orbital motion of electrons due to the external field, the direction of the induced magnetic moment is the opposite of the field. In an inhomogeneous area, such materials are attracted towards areas where the area is weak.

Paramagnetic materials have a net magnetic moment due to the unpaired electrons of some of the ions or atoms in the material in their partially filled orbitals. For this reason, every atom has a permanent dipole moment. When a field is applied, these atomic dipoles tend to align with the discrete field, just like a compass needle aligns with the earth's magnetic field [7].

Diamagnetic and paramagnetic materials show magnetization properties only in the presence of an external field. Because the magnetic induction is very weak in these materials, they have low sensitivity values. Typical sensitivity values for diamagnetic copper at room temperature are -0.96×10^{-5} , for paramagnetic aluminum 2.07×10^{-5} , and paramagnetic manganese sulphate 3.7×10^{-3} [8].

The strongest type of magnetism is ferromagnetism. For example, it occurs in many alloy compositions based on iron (b.c.c.), cobalt, nickel. Ferromagnetic materials can exhibit permanent magnetic moments even in the absence of an external field. However, the property is not seen in dia- and para-magnetic materials. Sensitivity values can reach up to 106, which is very high compared to many and diamagnetic materials. Magnetic moments in such materials are mainly due to atomic spin magnetic moments. In these materials, the interactions between atoms cause the spin magnetic moments to align with each other in a cooperative manner. Because of this,

Fig. 3 Schematic of antiparallel alignment of spin magnetic moments in antiferromagnetic MnO [7, 8]

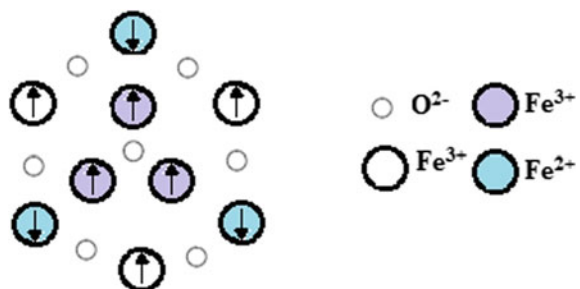


large regions in a crystal can have atoms with rotations aligned with each other. When all magnetic dipoles are aligned, the magnetization reaches its saturation value M_s , for example, the magnitude of M_s for nickel is 5.1×10^5 A/m. [7]

Ferromagnetism results from the cooperatively parallel alignment of the spins. The magnetic moment connection between atoms (or ions) results in the rotational moments of neighboring atoms aligned in opposite directions. Such materials are antiferromagnetic. In the case of MnO, the moments of adjacent Mn^{2+} ions are antiparallel, so the material has no net magnetic moment (Fig. 3).

Hexagonal ferrites and garnet are ceramic materials with ferrimagnetic properties. Cubic ferrites such as magnetite can be represented as MFe_2O_4 where M is a metal. In the Fe_3O_4 state, Fe ions exist in both +2 and +3 valence states. The magnetic moments of the two types of Fe ions are different. In this case, however, there is a net magnetic moment because the rotational moments of the solid material as a whole are not completely canceled. Although the rotation moments of Fe^{3+} ions cancel each other out, magnetization occurs due to the parallel alignment of the moments of Fe^{2+} ions (Fig. 4). By adding other ions such as Ni^{2+} and Co^{2+} to Fe_3O_4 , it is possible to produce ferrite materials with various magnetic properties. This flexibility can be used to adjust magnetic properties for hyperthermia applications by creating a cubic mixed ferrite material [7, 8].

Fig. 4 Schematic depicting the spin magnetic moments for Fe^{3+} and Fe^{2+} in Fe_3O_4 [7, 8]



1.3 Fundamentals of Magnetic Nanoparticles

The large number of electrons in a substance are designed to annihilate each other's magnetic moments. Electrons are therefore combined to form pairs according to the Pauli exclusion principle. In this case, one electron absolutely destroys the magnetic moment of the other electron. In addition, even when electron sequences are made and an unpaired electron is seen, the material is deprived of its magnetic properties due to the contribution of various electrons in the solid to the magnetic moment in different directions [9].

The magnetic moments of the atoms in ferromagnetic materials make these materials behave like small permanent magnets. These moments are interconnected and are in a very smooth or irregular orientation called the magnetic domain or Weiss domain. When a domain contains a large number of molecules, it becomes unstable and splits into two domains oriented in opposite directions. Thus, they are connected to each other in a more stable way.

When exposed to a magnetic field, the domain boundaries act to magnify the magnetic field and dominate the structure. Once the magnetic field is removed, the domains may not revert to their de-magnetized state. This situation causes ferromagnetic materials to turn into permanent magnets.

The domain that is magnetized sufficiently powerfully overcomes all other consequences results in a single domain. This substance is magnetically saturated. When a ferromagnetic substance is heated to the Curie temperature, the molecules begin to vibrate and begin to lose the magnetic domain organization and magnetic properties. If this substance is cooled, the orientation of this domain suddenly returns.

When the particle size shrinks to a single domain and is above the hot blocking temperature, the particle becomes superparamagnetic. If the particle is small enough and the temperature is high enough, the thermal energy overcomes the anisotropy energy and directs the moments randomly.

If we reduce the size of any ferromagnet we will eventually reach a size. The resulting thermal energy at this size ($kBT \sim 25$ meV at 300 K) and anisotropy will make the magnetization direction random. In other words, such materials present no coercion ($H_C = 0$), similar to paramagnets but behave with very large moments and are called superparamagnets. In practice, the randomization of the magnetization direction occurs by excitations on an energy barrier, $B = KV$, given by the product of the anisotropy constant K and the volume, V [9].

Similar to a paramagnet, the magnetization response $M(H)$ of a superparamagnet can also be explained by the Langevin function. The relaxation time, τ , is exponentially dependent on M . With $D = 2R$ where the nanoparticle is split into multiple areas, there is a balance between the additional energy cost of placing the field wall and the reduction-gain in magnetostatic energy.

Considering previous studies, it was seen that the characteristic dimension D in which the single domains are stable was determined by using simple models and mass properties for the domain stability of fine particles found. With $D = 2R$ where

the nanoparticle is split into multiple regions, M is a balance between the additional energy cost of placing the field wall and the reduction in magnetostatic energy-gain. [9–11].

1.4 Role of Magnetism in Biomaterials

When we look at the usage areas of magnetism, we see that some special biological applications come to the fore. For example, in the sorting of cells, interactions occur between biological cells and magnetic nanoparticles leading to separation under the influence of the magnetic field gradient. The properties of hard and soft magnetic materials have been used for different bio applications. Also, particle size dependent properties are also used in this field. As mentioned above, magnetic properties change significantly when particle size falls beyond a critical limit and moves to single area and subfield regions. It was also mentioned above that it shows superparamagnetic (SP) properties when it falls below a critical size [1]. This entity is widely used for magnetic biodiscrimination, MRI contrast agent and drug delivery. From the point of view of biological applications (eg MRI contrast agent, biological separation, etc.), Superparamagnetic particles have been found to be superior to ferro/ferri magnetic particles due to the absence of remanence. Since the material exhibits magnetic properties in the presence of a magnetic field, it can be removed from the suspension by applying a magnetic field in the biological separation process. After this process is completed, it is redistributed in a homogeneous mixture in the absence of magnetic field [12].

In magnetic hyperthermia, it is beneficial to use the ferro, ferri, and superparamagnetic properties of the particles. The losses from magnetization and reorientation of these particles depend on the type of magnetization process, which is determined by its intrinsic properties such as magnetocrystalline anisotropy, and external properties such as particle size and microstructure. Magnetic hysteresis is an important property of the material. Hysteresis loss is the representation of the energy consumed when rotating a material between positive and negative fields. The area within the second quarter of the cycle is used to determine the energy consumed in a cycle. The delayed power loss of an AC device can be obtained by multiplying the frequency by the hysterical loss per cycle. Power loss can be dissipated as heat for hyperthermia applications. When there is a reduction in size, this magnetic nanoparticle behaves superparamagnetically. These SP particles will not exhibit hysteresis losses. However, the Neel relaxation in them will be equally useful in generating and dissipating heat [1].

2 Magnetic Nanoparticles

2.1 Types of Magnetic Nanoparticles

2.1.1 Metal and Metal Oxide Nanoparticles

Transition metals such as iron (Fe), Ni and Co are among the magnetic materials that have been studied in many studies. When we look at these magnetic metals, we see that they exhibit ferromagnetism at low temperatures (and room temperature). Besides, they show paramagnetism features at high temperatures. In the literature, there are studies on the synthesis and magnetic properties of Fe, Ni, and Co nanoparticles, as well as studies investigating the magnetic behavior of the oxides of these metals. Looking at these materials, it is seen that iron oxide nanoparticles stand out due to their biomedical and industrial applications. Iron oxides are compounds consisting of Fe along with O and/or OH. There are 16 iron oxides available in the form of oxides, hydroxides, or oxide-hydroxides. The three main types of iron oxides are hematite, magnetite, and maghemite. Among these, magnetite has the highest saturation magnetization [6, 13].

2.1.2 Ferrites

Ferrites (α -Fe₂O₃) are ferromagnetic materials derived from metal oxides such as magnetite (Fe₃O₄). They do not show conductive properties. These materials have three different structural symmetries: garnet, hexagonal, and cubic or spinel ferrites. The balancing of the charge and relative amounts of oxygen ions is adjusted according to the size and charge of the metal ions. Various studies have been carried out on the diameter and magnetic fields of ferromagnetic particles. When looked specifically at magnetic nanoparticles, it is seen that superparamagnetic iron oxide nanoparticles (SPIONs) are the most exploited. SPIONs have unique magnetic properties thanks to their atomic composition, crystal structure, and size. SPIONs have the ability to generate heat with the loss mechanism obtained from the rotation of magnetic moments in overcoming the energy barrier. The energy is generated by the relaxation of the MNP moment to the equilibrium orientation (ie Neel relaxation). It was said above that the hysteresis is zero for superparamagnetic materials. But in real SPION ensembles, a hysteresis loop with negligible remanence and coercion occurs. This is probably due to some large particles and agglomerates in the community [14, 15].

2.1.3 Dilute Magnetic Semiconductors

Dilute magnetic semiconductors (DMS) appear as a group of materials with both semiconductor properties and magnetic properties. In these materials, some of the cations in the lattice are replaced by magnetic ions. Atomic spin on these magnetic

additives interacts with carriers within the lattice. In this way, a spherical ferromagnetic order is created in the material. Thus, the unusual magnetic properties of these materials are due to the presence of isolated magnetic ions in the semiconductor lattice. Studies on these materials started in the 1980s and still continue. As candidate materials for DMS, we see simple oxides such as SnO_2 , ZnO , TiO_2 or mixed oxides doped with various transition metals (Fe, Co, Ni, Mn) or rare earth metals (Dy, Eu, Er) [16–20].

2.1.4 Polymer Magnets

A polymer magnet or plastic magnet is a nonmetallic magnet made from an organic polymer. This is a new class of magnetic materials which has gained the interest of researchers. Torrance et al. [21] synthesized poly(1,3,5-triaminobenzene) which when oxidized with iodine was reported to show a ferromagnetic phase up to 400 °C. After that, Rajca et al. [22] reported synthesis of organic pi-conjugated polymer with very large magnetic moment and magnetic order at low temperatures below 10 K.

In 2004, Zaidi et al. [23] reported the synthesis of a novel magnetic polymer PANiCNQ produced from polyaniline (PANi) and an acceptor molecule, tetracyanoquinodimethane (TCNQ), the first magnetic polymer to function at room temperature. In the structure of PANiCNQ, the fully conjugated nitrogen-containing backbone is combined with molecular charge transfer side groups. This combination creates a stable structure with high density localized spins. Looking at the magnetic measurements, it is seen that this polymer has a Curie temperature above 350 K and a maximum saturation magnetization of $0.1 \text{ JT}^{-1} \text{ kg}^{-1}$. This indicates that the material is ferri or ferromagnetic. In addition, Crayston et al. [24] have studies examining the synthesis of organic magnets and other developments in the field of organic magnets [6].

2.2 *Synthesis of Magnetic Nanoparticles*

It is possible to encounter the synthesis of magnetic nanoparticles (MNP) in a wide variety of literature. We see different compositions and phases, including iron oxides such as Fe_3O_4 and $\alpha\text{-Fe}_2\text{O}_3$, pure metals such as Fe and Co, and spinel ferrites such as MgFe_2O_4 , MnFe_2O_4 , CoFe_2O_4 and NiFe_2O_4 , ZnFe_2O_4 . In addition, alloys such as CoPt_3 and FePt, dilute magnetic semiconductors and polymer magnets are also among the topics studied in this sense. Various methods have been tried over the past few years in studies that aim to synthesize magnetic nanoparticles with a stable structure and monodisperse shape control. When we look at the methods studied in this sense, it is seen that methods such as hydrothermal techniques, sol-gel processing, surfactant-assisted synthesis, co-precipitation, microemulsion techniques and solution burning come to the fore for the synthesis of high quality magnetic nanoparticles [25–27].

2.2.1 Hydrothermal Technique

It is known that the solvothermal methods mentioned in the literature are also used for the synthesis of ultrafine powders for the synthesis of MNPs. Generally, this technique relies on reactions taking place in reactors or autoclaves in an aqueous environment. The reactions are carried out at high vapor pressure (usually in the range of 0.3–4 MPa) and at high temperature (usually in the range of 130–250 °C). In fact, this process can also be used to grow single-crystal particles that do not contain dislocations. In this way, grains having a better crystallinity than other methods can be obtained. This is why highly crystalline magnetic nanoparticles can be obtained using the hydrothermal technique [28].

Hydrothermal synthesis of magnetic nanoparticles can be carried out with or without specific surfactants. For example, Wang et al. [29] performed one-step hydrothermal synthesis of highly crystalline magnetite nanoparticles (40 nm) without using surfactants. Togashi et al. [30] performed a surfactant-assisted hydrothermal synthesis of superparamagnetic magnetite nanoparticles (20 nm) at 200 °C in the presence of 3,4-dihydroxyhydroxycinnamic acid. Phumying et al. [31] reported a new hydrothermal method for the synthesis of spinel ferrite MFe_2O_4 ($M = Ni, Co, Mn, Mg, Zn$) nanocrystalline powders with different morphologies. On the other hand, hydrothermal synthesis of various other magnetic nanoparticles (such as iron oxide nanoparticles, ferrites and dilute magnetic semiconductors) has also been reported by the researchers [6].

2.2.2 Sol–Gel Method

Sol–Gel is in principle a solution chemistry-based technique used to synthesize pure, stoichiometric, and monodispersed oxide nanoparticles (including iron oxide nanoparticles). In this technique, liquid precursors are primarily hydrolyzed, followed by colloidal sols [6]. Metal precursors, metal or metalloid elements are used as starting materials. These are surrounded by a variety of reactive ligands. They undergo slow hydrolysis and polycondensation reactions to form a colloidal system. The name of this colloidal system is Sol. After sol development, a network is formed that includes a liquid phase called a gel. With this method, which is carried out at low temperatures, large-scale nanoparticles with a relatively narrow size distribution can be produced. There are successful studies in which magnetic nanoparticles are synthesized in this way. Examples include synthesis of Er-doped SnO_2 and Ni-doped ZnODMS nanoparticles [32].

We have used the sol–gel technique many times in the production of magnetic nanoparticles as it is relatively easy, inexpensive, and applicable at low temperatures [33, 34]. In one of our studies, barium hexaferrite nanoparticles were produced by the Sol–Gel method. In another study, we produced magnetic ZnO particles with the same method. In another study where we produced Co-doped ZnO nanoparticles, we examined how the amount of Co-doped affects the magnetic properties.

Figure 5 shows the flow chart of the Co-doped ZnO synthesis using Sol-Gel method. The used precursors are zinc acetate dihydrate ($C_4H_6O_4Zn \cdot 2H_2O$, Aldrich) and cobalt(II) acetate (CH_3CO_2Co , Aldrich), and a complexing agent is citric acid monohydrate ($C_6H_8O_7 \cdot H_2O$, Aldrich). The following compositions of $Zn_{1-x}Co_xO$, with $x=0, 0.03, 0.06, 0.09,$ and 0.12 mol, were prepared. Zinc acetate and cobalt acetate were separately dissolved off in distilled water. The solution was mixed by magnetic stirrer until the transparent solution was obtained. The solution was kept at 80_C in the air until wet gel with high viscosity was obtained. The wet gel was treated at 130_C for 12 h in the oven to prepare dry gel. The dry gel was exposed to the sintering process at 500_C for 3 h to evaporate impurities and in the air in an ash furnace (Fig. 5).

Figure 6 shows XRD patterns of Co-doped ZnO powders ($Zn_{1-x}Co_xO$, with $x=0, 0.03, 0.06, 0.09,$ and 0.12 mol) synthesized by Sol-Gel method. It revealed that all peaks corresponding to (100), (002), (101), (102), (103), (110), and (112) planes related to the hexagonal wurtzite crystal structure the wurtzite structure ZnO with Co-doped concentration up to 12%. There is no sign-related cobalt metal, oxides, or any binary zinc iron phases. All the powders showed peaks similar to pure ZnO, which indicates that no structural deformation occurred in ZnO lattice upon Co-dope. This supports the successful substitutional replacement of Co ions in Zn lattice sites in the ZnO matrix.

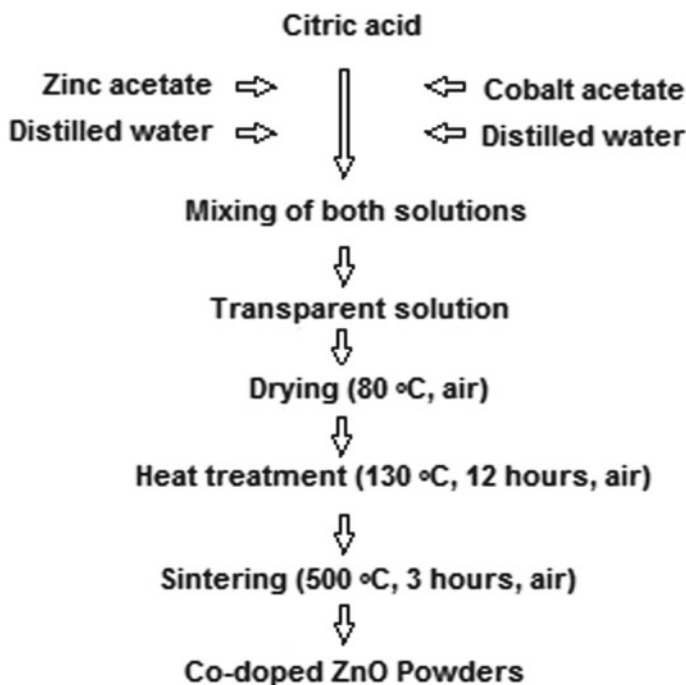
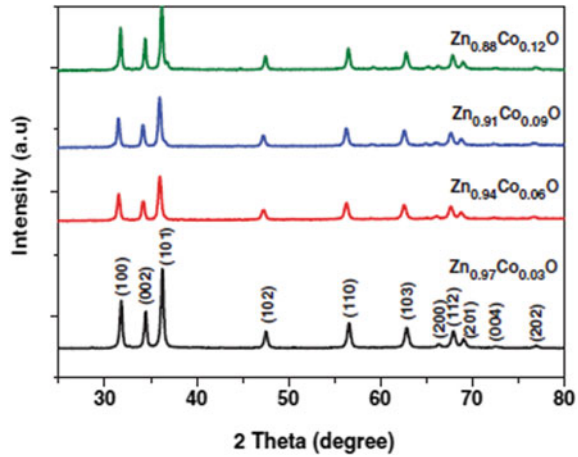


Fig. 5 The flow chart for producing Co-doped ZnO powders [34]

Fig. 6 XRD patterns of Co-doped ZnO powders produced by the Sol-Gel method [34]



The magnetization (M) versus the applied magnetic field (H) for $Zn_{1-x}Co_xO$ ($x=0-12$) powders and different weights of Zn 0.91 Co 0.09 O powders at room temperature are shown in Fig. 7. The magnetic properties of samples were measured by VSM measurements, putting into PTFE Teflon Tape. Room temperature ferromagnetism was observed for all the samples. Co-doped ZnO powders show high saturation magnetization as compared to un-doped ZnO. It is known that pure ZnO shows paramagnetic behavior, Co is the reason for the observed ferromagnetism in the Co-doped ZnO samples. However, in this study, even undoped ZnO powders showed ferromagnetic behavior. This effect comes about owing to the presence of oxygen vacancies that is the critical role in appearance of the ferromagnetic phase has been proved in recent studies. During the calcination process, the presence of carbon ions from precursor substances gives rise to the formation of oxygen vacancies in our samples. In the case of doped diluted magnetic semiconductors, it can be certain that the observed ferromagnetism in the $Zn_{1-x}Co_xO$ powders originate from the Co substitution for Zn in ZnO. Another possible explanation is related to a nanoscale

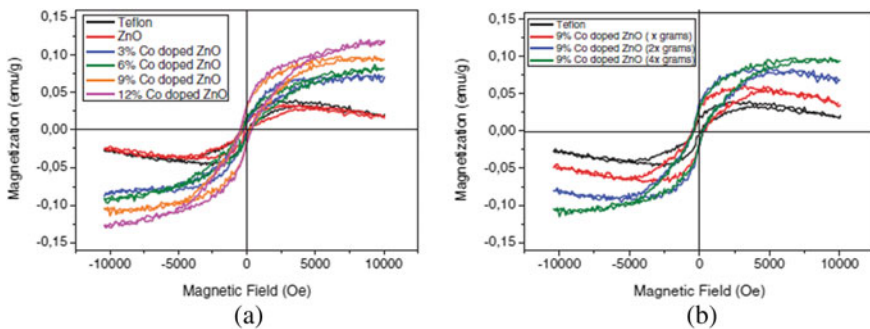


Fig. 7 **a** M–H curves of $Zn_{1-x}Co_xO$ and **b** different weight of Zn0.91Co0.09O [34]

phase separation responsible for the presence of Co-rich magnetic nanoparticles. Figure 7 shows that with increasing Co content from 0 to 0.12, saturation magnetization was increased from 0.035 to 0.12 emu/g, coercivity H_c is 3.4_104 A/m, and loop area is 18.1_103 Oe_emu/g. The effect of the amount of Co-doped ZnO powders in Teflon composite is shown in Fig. 7. The highest Co content ZnO powders (Zn_{0.91}Co_{0.09}O) were used at different weight ratios in composite to compare the amount effects of these powders. With increasing weight ratios of 9% Co-doped ZnO powders in composite, saturation magnetization increased from 0.05 to 0.1.

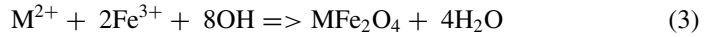
2.2.3 Solution Combustion Method

Solution combustion technique (SCT), in other words self-leveling high-temperature synthesis, is a method used in the production of magnetic materials. This method, which is used in the production of the most advanced materials, is very energy efficient. In this technique, a self-sustaining reaction takes place between an oxidizer (eg, metal nitrate) and a fuel (eg, Glycine, hydrazine). First of all, the substances to be reacted are solved in water. Then the solution obtained is thoroughly mixed in order to achieve molecular level homogenization of the reaction medium. After the water is heated to boiling point and evaporated, the solution can ignite, while the temperature rises rapidly (up to 104 °C/s) to 1500 °C. With these self-sustaining reactions, transformation of the initial mixture into the desired fine crystal powders occurs simultaneously [6].

When we look at the studies in this area, Patil and Sureh [35] are the first scientists to publish the instantaneous synthesis of maghemite (γ -Fe₂O₃) by the combustion process. Deshpande et al. [36] and Erri et al. [37] applied the solution combustion approach using various fuels for the direct synthesis of different iron oxide phases (α - and γ -Fe₂O₃ and Fe₃O₄) for the first time in the literature; such as glycine, hydrazine, and citric acid. After that, many studies were carried out on the synthesis of iron oxide nanomaterials and magnetic nanoparticles used for different purposes by solution burning technique [38, 39].

2.2.4 Co-precipitation

Co-precipitation is one of the easiest and most convenient ways to synthesize MNPs (metal oxides and ferrites). With this technique, MNPs are synthesized from aqueous salt solutions by adding a base at room temperature or under an inert atmosphere at high temperature. The size, shape, and composition of these nanoparticles depend on the type of salts used, e.g., chlorides, sulfates, nitrates. In addition, Fe²⁺ /Fe³⁺ ratio, reaction temperature, pH value, and ionic strength also affect these properties [40]. In the chemical reaction below, the reaction of iron oxide nanoparticles (either Fe₃O₄ or γ -Fe₂O₃) and ferrites prepared in an aqueous environment is shown (Eq. 3) [6].



The symbol M that appears in this reaction can be elements such as Fe^{2+} , Mn^{2+} , Co^{2+} , Cu^{2+} , Mg^{2+} , Zn^{2+} and Ni^{2+} [41]. Iwasaki et al. [42] synthesized Fe_3O_4 nanoparticles by co-precipitation in a new technique he developed. They did not use any additives such as surfactants or oxidizing/reducing agents in this process. They used chilled ball mills as synthesis reaction space. In this way, they both prevented the synthesis reaction and stopped the progress of particle growth due to heat energy. An initial suspension of iron hydroxide and goethite colloids was prepared. The formation of Fe_3O_4 nanoparticles was achieved by grinding this suspension in a ball mill. Simultaneously the crystallization was allowed to proceed without heating.

2.2.5 Microemulsion Technique

In the synthesis process, obtaining particles of similar size is an important parameter. Often times it is a difficult feature to obtain. However, it is possible to synthesize similarly sized MNPs with microemulsion method and it is widely used. Basically, this method uses a thermodynamically stable isotropic dispersion of two immiscible liquids. The process begins with the stabilization of the microdomain of surfactant molecules in one or both liquids by an interfacial film. When the surfactant molecule reduces the interface tension between water and oil, a transparent solution occurs. In this solvent mixture, surfactant molecules self-assemble in various structures. These structures are formed in forms such as micelles, bilayers or vesicles. This process takes place depending on relative concentrations.

When we look at the structures most commonly used in nanoparticle synthesis, we come across micelles in reverse (water in oil) or normal (oil in water) form. In both micelles, the monodisperse droplets forming the dispersed phase range in size from 2–100 nm [6].

Thanks to this dispersed phase, a limited environment for the synthesis and formation of nanoparticles can be provided. Lee et al. [43] carried out the large-scale synthesis of uniform magnetite nanoparticles from reaction salts in microemulsion nanoreactors. In addition, these nanoparticles had a highly crystalline structure. In the presence of iron salts, it was possible to vary the relative concentrations of surfactant and solvent. Thus, the particle size could be controlled between 2 and 10 nm.

Barium ferrite ($BaFe_{12}O_{19}$) nanoparticles were synthesized by Pillai et al. Microemulsion process [44]. In this method, aqueous cores of water-cetyltrimethylammonium bromide-n-butanol-octane microemulsions were used as a microreactor. With these cores, which are typically used in 5–25 nm size, the precursor carbonates (typically 5–15 nm in size) were co-precipitated. The precipitated carbonates were dried and calcined to form barium ferrite nanoparticles.

In addition, nickel-zinc ferrite nanoparticles ($Ni_{0.20}Zn_{0.44}Fe_{2.36}O_4$) were synthesized using reverse micelle process in the study conducted by Morrison et al. In this study, the procedure took place at room temperature without calcination [45]. Liu

et al. Obtained CoFe_2O_4 nanoparticles using sodium dodecyl sulfate (NaDS) as a surfactant to form normal micelles in their microemulsion method [46].

2.2.6 Other Methods of Synthesis

In addition to the above, there are many other methods for the synthesis of magnetic nanoparticles. Among these, methods such as thermal decomposition, sonochemical, electrochemical, bacterial synthesis, polyol method can be counted. Zhao et al. [47] synthesized water-soluble superparamagnetic Fe_3O_4 nanoparticles by thermal decomposition of $\text{Fe}(\text{acac})_3$ in methoxy poly (ethylene glycol) (MPEG). The mean diameter of the particles was around 9.5 ± 1.7 nm. In this study, MPEG functioned as a solvent, reducing agent, and modifying agent. The production of uniform size CoFe_2O_4 ferrite nanoparticles was performed by Mazario et al., who synthesized in one step using an electrochemical technique [48]. In a new study, superparamagnetic ZnFe_2O_4 nanoparticles with a size range of 28–38 nm were synthesized. In this study, polyol process based on the use of varying chain length glycols (diethylene and polyethylene glycol) as solvent was used [49].

3 Fabrication of Hybrid Magnetic Composites

With the development of sophisticated multi-functional composite materials, hybrid structures consisting of magnetic nanoparticles embedded in a polymer matrix have been produced as magnetic nanocomposites. The good mechanical properties of these materials as well as their magnetic field sensitive behavior have led them to attract attention as a new class of smart materials. There are extensive studies in the literature on the development of high performance magnetic polymer composites [9]. These were applied in a variety of applications in structural materials engineering and biosciences. These studies posed some scientific difficulties in understanding the physics behind the magneto-elastic properties of composite materials. These difficulties are generally due to the cumulative effect of various factors such as the chemistry of the material, nanostructure morphology, and interface interactions [50, 51].

When the performance of magnetic composite materials is examined, it is seen that this depends not only on the microstructure but also on the processing techniques. It is even known that the effect of the micro-environment during certain applications has an effect on the material [9]. In this sense, while the examination of structure–property relationships in magnetic nanoparticle reinforced composites continue, this requires high-level characterization tools.

Elastomers, an important class of soft polymeric materials that exhibit low modulus of elasticity, are an important material used as matrix in composites. Magnetic polymer composite is produced by mixing magnetic nanoparticles with an elastomeric matrix such as a poly (vinyl alcohol) based hydrogel or silicone rubber.

As a result of being under the influence of an external magnetic field, it is possible for this material to show controlled stress, contraction, and bending deformations. It can be performed by adjusting the direction and magnitude of the external magnetic field to control the tensile strength of the composite material, deformation movements, and variations in the compression and shear modulus. The materials developed in this way are ideal materials to be used as dampers in the automotive industry, as rotating tools for machines or as mixing pumps in microfluidic devices.

When viewed as a composite, we generally see two types of magnetic nanoparticle loaded elastomers. The first is an isotropic magnetic polymer composite, in which the magnetic nanoparticle fillers have a uniform spatial distribution. The second contains uniaxial in-line filling nanoparticles, which are anisotropic composites [52]. The production of an anisotropic system can be achieved by using elastomer and magnetic nanoparticles under a uniform magnetic field. Increasing the elastic modulus may be possible by parallelizing the direction and compression force of the magnetically aligned nanoparticle chain. This data has been demonstrated by Filipcsei et al. [52], suggesting that strong mechanical anisotropin can be affected by such incorporation of nanoparticle chains. The spatial distribution of magnetic nanoparticles has an important effect on the stress–strain dependence of composites. A deviation from ideal mechanical behavior may occur depending on the direction of the pressure force. Because the effect of the applied force varies according to whether the force is parallel or perpendicular to the magnetic nanoparticle chain structure [9].

In a similar study, ultra-low magnetic fields were used by using superparamagnetic iron oxide coated reinforcement particles. In this way, the position and direction of the reinforcing particles in the polymer matrix can be precisely controlled. It is also possible to lead to numerous properties including out-of-plane global or local increase in composite hardness, strength, wear-resistance, and shape memory effects [52].

The full incorporation of magnetic nanoparticles in the polymer matrix is crucial to the performance of the composite. Several well-known polymerization techniques have been optimized to facilitate this process. These techniques used for grafting various polymer brushes on magnetic nanoparticles consist of click chemistry techniques, ring-opening polymerizations, and grafting-polymerization methods using controlled radical polymerization methods.

It is seen that the production of well-defined and dispersed polymer coated magnetic nanoparticles is possible, especially with controlled radical polymerization approach such as reversible addition-fragmentation chain transfer polymerization (RAFT) and atom-transfer radical polymerization (ATRP) [9]. The grafting of polymer brushes on various nanoparticle types have been successfully achieved using RAFT and ATRP methods. These methods are also methods that facilitate the use of a wide variety of polymers such as poly (methyl acrylate), poly (methyl methacrylate), poly (acrylic acid), and poly (poly (acrylic acid) [53].

A sudden end of the polymer branching or polymerization process is not desirable. Through surface-initiated ring-opening polymerization (ROP), both this was avoided and polymer brushes such as poly- ϵ -caprolactone and poly (lactic acid) were successfully grafted and grown on the surface of magnetic nanoparticles [54].

In addition, in different studies, Cu-catalyzed click chemistry techniques, block copolymers with alkyne termination groups have been used to impregnate magnetic nanoparticles containing azide functionality onto the surface. The creation of higher order hierarchical structures was achieved by coating polymer shells on the surface of magnetic nanoparticles. The seeded emulsion polymerization technique enabled the encapsulation of magnetic nanoparticle clusters in polymer matrices. It is necessary to adjust the concentration of the emulsifier in order to control the size of the emulsion micelle containing monomers and magnetic nanoparticles. Following polymerization of the monomers by the addition of an initiator and a crosslinking agent, crosslinking occurs in a stable polymer shell that locks the magnetic nanoparticle cluster in place. Magnetic nanoclusters produced in this way have been reported to give successful results in optimized MRI contrast enhancement and magnetic hyperthermia applications [55].

On the other hand, magnetic composites made of thermoplastic polymers are also manufactured using various processing methods. Examples include compression molding, melt bonding, solution casting, and melt extrusion. When looking at the manufacture of magnetic thermoplastics, we see that particle agglomeration is a general challenge. To overcome this challenge and prevent aggregation, core-shell magnetic polymer nanoparticles with increased stability have been used [9].

The inclusion of iron oxide nanoparticles in an ultra-high molecular weight polyethylene (UHMWPE) matrix as a platform allowed us to study the effects of inter-particle interaction on the AC magnetic field response of iron oxide nanoparticles. However, the use of UHMWPE as a matrix in composites is extremely difficult due to the difficulties in machining. Because this polymer has an extremely high molecular weight, it is not possible to process it with conventional thermoplastic processing techniques. Also, due to the extremely high viscosity of the polymer, there is a problem in the distribution of magnetic nanoparticle fillers.

It is a known feature that the surface/volume ratio increases with decreasing particle size. This affects the surface properties, interfacial properties, and agglomeration behavior from the perspective of nanoparticles. It is, therefore, necessary to adapt the magnetic nanoparticle surface as well as adjust the interface layer between the particle and the polymer matrix. Because, both the machinability and performance of the composite material depend on these properties.

The use of dispersants in the composite affects the rheology. In this case, the degree of particle agglomeration can also change due to the reduction in inter-particle friction. For example, Bin et al. have used decaline and paraffin as MWCT dispersants in their study where they produced multi-walled carbon nanotube (MWCT) reinforced UHMWPE and achieved high hardness and electrical conductivity in composites [56]. Rong et al. after grafting styrene monomers onto the surface of 7 nm sized SiO₂ nanoparticles, they mixed it with a polypropylene matrix. In their work, they were able to produce cluster-free samples, and the particle-polymer matrix interface interactions were greatly increased [57]. Guoliang et al., in their study, produced composites with better mechanical properties than dry powder direct mechanical dispersion method with liquid-solid mechanical dispersion method [58].

Adapting a liquid–solid mechanical mixing approach, this system was used to produce magnetic UHMWPE composite films with good particle distribution. In this system, blending magnetite nanoparticles with UHMWPE in the presence of an organic solvent dispersant was first achieved by using a high-speed blade mixer. With this method, processing of Al_2O_3 nanoparticle reinforced PEEK polymer and production of carbon nanotube reinforced UHMWPE has been successfully applied. The magnetic composite films were produced by compressing the UHMWPE and iron oxide magnetic powder mixture under 7 metric tons of pressure between PTFE plates and iron steel plates. The mechanical properties of the magnetic polyethylene composite manufactured using the optimized liquid bonding method were compared with the mechanical properties of the composite manufactured using the typical dry mixing method. In this comparison, it was seen that there is a significant increase in elastic modulus with the liquid compounding method. This may be due to improved nanoparticle dispersion in the polyethylene matrix due to the presence of organic solvent during mixing [9].

The study also found that magnetic nanoparticles were superparamagnetic at room temperature even after embedded in the UHMWPE matrix. As a result, it can be said that the morphology and superparamagnetic properties of nanoparticles are preserved in the composite film. This can be stated as an indication that the flexibility of the nanoparticles is subjected to high temperature and pressure conditions during the compression molding stage.

Inclusion of different amounts of magnetic nanoparticles into the UHMWPE matrix is possible by the liquid–solid processing method [59]. Improved heating profile was observed that can be used for magnetic hyperthermia applications. This was accomplished by increasing magnetic nanoparticle loading upon AC field stimulation. However, it was also observed that the elastic modulus and tensile strength of the magnetic polyethylene composite decreased with increasing nanoparticle loading. Overcoming this challenge may be possible by improving polymer-iron oxide nanoparticle interface interactions, for which a hydrothermal carbon coating approach has been applied.

Antiferromagnetic FeO nanoparticles were used as co-reagents in the hydrothermal carbonization of glucose. The reason for this is to create carbon-coated iron oxide nanoparticles. Enhanced magnetic bipolar inter-particle interactions occurred due to the slow oxidation of FeO precursor nanoparticles to ferrimagnetic Fe_3O_4 nanoparticles. This is a situation that facilitates the formation of short iron oxide nanoparticle chain [9]. Finally, after the carbon-coated iron oxide chains were obtained, it was also possible to reveal the improved mechanical properties of the magnetic polymer composite by mixing it into the UHMWPE matrix.

Magnetic polymer composites exhibit superparamagnetic properties at high temperatures. This can be shown to be similar to the behavior of ferrofluids [9]. However, since the positions of the magnetic nanoparticles embedded in the polymer are rigidly fixed, particle movement is also prevented. This is in contrast to magnetic fluids. Therefore, in magnetic polymer composites, Brownian rotation becomes limited as a result of the nanoparticles being held by the polymer network. In this case, the predominant magnetic relaxation mechanism is Néel relaxation. If we assume

that the particles do not interact, the magnetic behavior of the superparamagnetic material can be described by the Langevin function [9]. From this point of view, it would not be wrong to say that the magnetic UHMWPE composite can be used to study magnetic relaxation effects that counteract Brownian motions [60].

4 Biomedical Applications

4.1 *Magnetic Bioseparation*

Bioseparation techniques are becoming more and more important as they are important to the success of many biological processes. Promising among bioseparation techniques, magnetic separation has long been used for applications other than biological separation. Examples of this are separation of magnetic colored impurities from kaolin clay, enrichment of low-grade iron ore, removal of ferromagnetic impurities from boiler water. Although the application of these techniques was limited until 1970, then magnetic separation became useful for some interesting applications in the bioscience and biotechnology fields, especially due to the development of innovative ideas and the improved properties of magnetic materials [61]. So much so that today, we see that the separation technique is regularly used in molecular biology, cell biology, and microbiology. It is also known that the magnetic separation technique has many advantages over other techniques used for the same purpose [1].

Looking at the mechanism of magnetic separation of cells and bio molecules, it appears that it works due to the contrast of magnetic susceptibility between discrete (magnetic) and ambient (other non-magnetic) materials. As mentioned above, some cells or biomolecules have intrinsic magnetic properties. If we classify the magnetic bio-separation method into two modes, in the first case the separator may have sufficient intrinsic magnetic moment, for example, red blood cells and magnetotactic bacteria. In this case, it is possible to separate directly by applying magnetic fields. In the latter case, cells or biomolecules that are not magnetic in nature may be present. In this case, it is possible that these cells and biomolecules can be changed by adding the magnetic-sensitive entity. So it can be manipulated using an external field [1].

Separation of cells or compounds can be accomplished using direct and indirect methods. The process of immobilizing the ligands on magnetic particles and incubating the cells or compounds in the environment for a while is a direct method. The target cells are first bound by these ligands, and then the complex formed can be separated by a magnetic field. On the other hand, we see that in the indirect mode, the target cell initially interacts with the ligand (primary antibody). In the next step, the secondary antibody is immobilized on magnetic particles and added to the medium containing cells. It is suggested that indirect methods work better when antibodies with poor affinity or antigen are less accessible [62]. Finally, separation

of the magnetic complex is achieved using a magnetic separator. Since superparamagnetic materials exhibit magnetic properties only in the presence of a magnetic field, magnetic separation of cells or bio molecules can be done more effectively with these materials.

In addition, ferromagnetic and superparamagnetic particles coated (or encapsulated) with polymers or liposomes can be used for magnetic labeling. It is known that magnetite (Fe_3O_4) or hematite (Fe_2O_3) magnetic minerals are widely used as carriers for this purpose [63].

Another application of magnetic separation is to remove cancer cells from bone marrow. Tumor cell separation from peripheral blood was achieved by immobilization of the antibody on silica-coated with superparamagnetic iron oxide [64, 65]. On the other hand, for biological fluid detoxification methods, there is a study in which ferro-carbon particle is used as magnetic absorber. First, the suspension of absorbent particles is injected into an extracorporeal system, and then it is allowed to absorb low, medium, and high molecular weight toxic substances in the bloodstream during movement. Then the magnetic particles are removed with a high gradient magnetic separator and the purified blood returns to the organism [66].

4.2 Drug Delivery

Magnetic drug delivery technique is performed in such a way that the drug can be encapsulated in a magnetic microsphere or nanosphere. This can also be achieved by conjugating the micro/nanosphere to its surface. If the magnetic carrier is administered intravenously, deposition can occur within the area where the magnetic field is applied. In this case, it increases with magnetic agglomeration. Local delivery of the drug can be achieved by the deposition of the carrier in the target area. The efficiency of magnetic carrier deposition depends on physiological parameters. Examples of this include particle size, surface properties, field strength, and blood flow velocity [67, 68].

Site-directed drug targeting is used in local or regional antitumor therapy. One way to increase the effectiveness of chemotherapy treatment is by magnetic-assisted delivery of the cytotoxic agent to the specific site. Multiple magnetic delivery systems can increase drug concentration efficiency at the tumor site [69]. The therapeutic applications of drug targeting, which are still in the research phase, continue in some clinical trials. Results from these studies show that magnetic drug targeting is a promising area. It signals that new and cost-effective clinical protocols will be developed in the near future. Undoubtedly, together with nano-biotechnology, “magnetic drug distribution” will play an important role in improving human health [1].

4.3 Magnetic Resonance Imaging Contrast Agents

One of the most reliable techniques used in diagnostic, clinical medicine and biomedical research is magnetic resonance imaging (MRI). The acquisition of magnetic resonance images is provided by placing the area of interest in a strong and homogeneous static magnetic field. This static magnetic field allows most of the protons to align with the field because there are abundant hydrogen nuclei (single proton) in the body. These protons then move out of alignment due to the application of an alternating magnetic field generated by the radio frequency coil near the sample. The nuclei move from a low energy state to a higher energy state by absorbing energy from the oscillating magnetic field. If the alternating magnetic field is switched off, the nuclei return to equilibrium. In this case, they emit energy at the same frequency as previously absorbed. On the other hand, this phenomenon induces a signal in the coil, which is the source of the alternating magnetic field. This nuclear magnetization that occurs is converted into diagnostic images by a series of algorithms [70].

MRI can provide information that differs from other imaging modalities. Its major technological advantage is that it can characterize and discriminate among organ using their physical and biochemical properties. The ability of MRI techniques to get images in multiple planes offers special advantages for radiation or surgical treatment. Though MRI can provide definite noninvasive diagnoses, the sensitivity or the specificity of such processes can be improved by the addition of contrasting agents. Difference in proton density as well as in the relaxation process of protons in their physiological environment is the source of T₁ contrast. This can be enhanced with the help of contrasting agents. These may be paramagnetic macromolecular compounds, superparamagnetic iron oxide, or rare earth metal ion (Gd) complexes. Paramagnetic metal ions reduce the T₁ relaxation of water protons and enhance the signal intensity, hence images are brighter. Superparamagnetic iron particles (SPIO) are more effective than monomolecular or macromolecular Gd contrast agents for this purpose [1].

When we look at the most commonly used superparamagnetic materials in this field, we see Fe₃O₄ with different coatings such as dextrans, polymers and silicon. Due to the superparamagnetic iron particles, a significant shortening occurs in T₂ relaxation. This is due to the decrease in signal intensity (SI) that occurs in MR images [71].

4.4 Hyperthermia for Treatment of Cancer

Hyperthermia is basically a form of heat therapy based on the principle that the temperature of the organs is raised to 42–46 C and in this case the viability of cancerous cells is reduced. The basis here is the fact that tumor cells are more sensitive to temperature than normal cells. In hyperthermia, only tumor cells need to be warmed or inactivated, preventing the organs from being affected. For this,

it is important to create a heat distribution system. There are various hyperthermia techniques depending on the heating methods used. However, each has advantages and limitations compared to each other. We can say that the boundary effects limit the microwave, ultrasound and RF hyperthermia. The depth penetration of high-frequency microwave rays is poor. In contrast, low-frequency microwaves are difficult to focus on target areas. In the use of ultrasound, its high penetration and focusing capabilities are good. However, in applications, it is seen that it is limited to high reflection due to strong absorption by the bone and air-filtered spaces (lungs, etc.). Also, it has been observed that it is difficult to heat targets with high perfusion areas to the desired temperature using this technique. The reason for this is that there is continuous heat dissipation [1].

We know that magnetic materials are widely used in the hyperthermia of biological organs. This application is based on the principle that the magnetization process determines the magnetic losses. It is possible to distribute these losses in the form of heat, which raises the temperature of the environment. This can be applied depending on the thermal conductivity and heat capacity of the surrounding environment. The losses can be of different types. These types are determined by intrinsic/extrinsic properties and particle sizes. Besides the hysteresis losses, we see that different losses are exploited for hyperthermia; eddy current losses, and relaxation losses for superparamagnetic particles (Neel relaxation) and friction losses of particles (Brownian motions).

In an external AC magnetic field, heating of magnetic oxides with low electrical conductivity can occur if the particles are able to rotate in a sufficiently low viscosity environment. This is either due to loss processes or friction losses during magnetization redirection [72]. The inductive heating of the magnetic oxides is negligible. Particle size and particle microstructure of the powders used greatly affect their magnetic properties. The magnetic reorientation that causes losses in ferro- or ferri-magnetic particles is dependent on the demagnetization process. This is determined by intrinsic magnetic properties such as magneto crystalline anisotropy and magnetization. At the same time, external properties such as particle size and shape have a great influence.

Induction of magnetic hyperthermia can be applied in different ways. One method is based on the surgical placement of finite-sized magnetic implants into the tumor site. In this way, energy is absorbed from the externally applied AC magnetic field and dissipates in the form of heat. Many glass and glass-ceramic materials have been used for this type of research. These bioactive and biocompatible materials form a bond by forming an apatite layer on the surface. However, due to the difficulty of obtaining homogeneous heat distribution with this method, an increase in temperature should be observed in areas close to the implanted material [1].

Instead of needles or rods as heat mediators, an alternative approach has emerged to use fine particles such that hyperthermia becomes noninvasive. It has been observed that when fluids containing magnetic particles with a size of 1–100 nm are injected, these particles can be easily incorporated into cells since their diameters are in the nanometer range. Heating occurs when these magnetic particles bind the AC magnetic field to the targeted magnetic nanoparticles. This process, in which the

whole tumor can be heated evenly in this way, is called intracellular hyperthermia. Studies have reported that malignant cells occupy nine times more magnetic nanoparticles than normal cells. Consequently, the heat produced in malignant cells is expected to be higher than in normal cells [1].

As for the magnetic fluids used in Hyperthermia processes, these materials can be defined as liquids composed of ultramicroscopic particles. These particles are stabilized using surfactant to prevent their agglomeration, as well as to make a stable colloidal suspension in suitable media such as water or hydrocarbon. These fluids behave like true homogeneous fluids and are highly sensitive to magnetic fields. Ferrofluids, which are among these magnetic fluids, consists of superparamagnetic particles of Fe_3O_4 and other magnetic particles. It is known that those modified or coated with different types of biopolymers or synthetic polymers are used for hyperthermia applications [73].

References

1. Bahadur D, Giri J (2003) Biomaterials and magnetism. *Sadhana* 28(Parts 3 & 4):639–656
2. Häfeli U (1997) In *Scientific and clinical applications of magnetic carriers*. Häfeli U, Schütt W, Teller J, Zborowski M (eds) Plenum, New York, London, p 1
3. Kim DK, Zhang Y, Kehr J, Klason T, Bjelke B, Muhammed M (2001) *J Magn Magn Mater* 225:256–261
4. Liberti PA, Rao CG, Terstappen LWMM (2001) *J Magn Magn Mater* 225:301–307
5. Camargo PHC, Satyanarayana KG, Wypych F (2009) Nanocomposites: synthesis, structure, properties and new application opportunities. *Mater Res* 12(1):1–39
6. Kalia S, Kango S, Kumar A, Haldorai Y, Kumari B, Kumar R (2014) Magnetic polymer nanocomposites for environmental and biomedical applications. *Colloid Polym Sci* 292:2025–2052
7. Ramanujan RV (ed) *Magnetic particles for biomedical applications*. Chapter 17. https://doi.org/10.1007/978-0-387-84872-3_17, C Springer Science+Business Media, LLC 2009, pp 477–491.
8. Callister WD (2003) *Materials science and engineering*. Wiley, New York
9. Bao Y, Wen T, Samia ACS, Khandhar A, Krishnan KM (2016) Magnetic nanoparticles: material engineering and emerging applications in lithography and biomedicine. *J Mater Sci* 51(1):513–553. <https://doi.org/10.1007/s10853-015-9324-2>
10. Ferguson RM, Khandhar AP, Arami H, Hua L, Hovorka O, Krishnan KM (2013) Tailoring the magnetic and pharmacokinetic properties of iron oxide magnetic particle imaging tracers. *Biomed Eng Biomedizinische Technik* 58:493–507
11. Krishnan KM, Pakhomov AB, Bao Y, Blomqvist P, Chun Y, Gonzales M et al (2006) Nanomagnetism and spin electronics: materials, microstructure and novel properties. *J Mater Sci* 41:793–815
12. Lea T, Vartdal T, Nustad K, Funderud S, Berge A, Ellingsen T, Schmid R, Stenstad P, Ugelstad J (1988) *J Mol Recogn* 1:9
13. Maicas M, Sanz M, Cui H, Aroca C, Sanchez P (2010) Magnetic properties and morphology of Ni nanoparticles synthesized in gas phase. *J Magn Magn Mater* 322:3485–3489
14. Krishnan KM (2010) Biomedical nanomagnetism: a spin through possibilities in imaging, diagnostics, and therapy. *IEEE Trans Magn* 46:2523–2558
15. Mahmoudi M, Simchi A, Imani M, Milani AS, Stroeve P (2008) Optimal design and characterization of superparamagnetic iron oxide nanoparticles coated with polyvinyl alcohol for targeted delivery and imaging. *J Phys Chem B* 112:14470–14481

16. Gingasu D, Oprea O, Mindru I, Culita DC, Patron L (2011) Alkali earth metal indates synthesized by precursor method. *Dig J Nanomater Biostruct* 6:1215–1226
17. Vadivel K, Arivazhagan V, Rajesh S (2011) Mn-doped SnO₂ semiconductingmagnetic thin films prepared by spray pyrolysis method. *Int J Sci Eng Res* 2
18. Gan'shina EA, Granovsky AB, Orlov AF, Perov NS, Vashuk MV (2009) Magneto-optical spectroscopy of diluted magnetic oxides TiO₂-δ:Co. *J Magn Magn Mater* 321:723–725
19. Lakshmi YK, Srinivas K, Sreedhar B, Raja MM, Vithal M, Reddy PV (2009) Structural, optical, and magnetic properties of nanocrystalline Zn_{0.9}Co_{0.1}O-based diluted magnetic semiconductors. *Mater Chem Phys* 113:749–755
20. Santi M, Jakkapon S, Chunpen T, Jutharatana K (2006) Magnetic behavior of nanocrystalline powders of Co-doped ZnO diluted magnetic semiconductors synthesized by polymerizable precursor method. *J Magn Magn Mater* 301:422–432
21. Torrance JB, Bagus PS, Johhannsen I, Nazzal AI, Parkin SSP, Batail P (1998) Ferromagnetic interactions in organic-solids—an overview of theory and experiment. *J Appl Phys* 63:2962–2965
22. Rajca A, Wongsriratanakul J, Rajca S (2001) Magnetic ordering in an organic polymer. *Science* 294:1503–1505
23. Zaidi NA, Giblin SR, Terry I, Monkman AP (2004) Room temperature magnetic order in an organicmagnet derived from polyaniline. *Polymer* 45:5683–5689
24. Crayston JA, Devine JN, Walton JC (2000) Conceptual and synthetic strategies for the preparation of organic magnets. *Tetrahedron* 56:7829–7857
25. Kumar P, Singh RK, Rawat N, Barman PR, Katyal SC, Jang H, Lee H-L, Kumar R (2013) A novel method for controlled synthesis of nanosize hematite (α-Fe₂O₃) thin film on liquid-vapor interface. *J Nanoparticle Res* 15:1532(1)–1532(13)
26. Sharma PK, Dutta RK, Pandey AC (2010) Alteration of magnetic and optical properties of ultrafine dilute magnetic semiconductor ZnO:Co²⁺ nanoparticles. *J Colloid Interface Sci* 345:149–153
27. Park J, An K, Hwang Y, Park J-G, Noh H-J, Kim J-Y, Park J-H, Hwang N-M, Hyeon T (2004) Ultra-large-scale syntheses of monodisperse nanocrystals. *Nat Mater* 3:891–895
28. Wu W, He Q, Jiang C (2008) Magnetic iron oxide nanoparticles: synthesis and surface functionalization strategies. *Nanoscale Res Lett* 3:397–415
29. Wang J, Sun J, Sun Q, Chen Q (2003) One-step hydrothermal process to prepare highly crystalline Fe₃O₄ nanoparticles with improved magnetic properties. *Mater Res Bull* 38:1113–1118
30. Togashi T, Naka T, Asahina S, Sato K, Takami S, Adschiri T (2011) Surfactant-assisted one-pot synthesis of superparamagnetic magnetite nanoparticle clusters with tunable cluster size and magnetic field sensitivity. *Dalton Trans* 40:1073–1078
31. Phumying S, Labuayai S, Swatsitang E, Amornkitbamrung V, Maensiri S (2013) Nanocrystalline spinel ferrite (MFe₂O₄, M=Ni Co, Mn, Mg, Zn) powders prepared by a simple aloe vera plantextracted solution hydrothermal route. *Mater Res Bull* 48:2060–2065
32. Sambasivam S, Joseph DP, Jeong JH, Choi BC, Lim KT, Kim SS, Song TK (2011) Antiferromagnetic interactions in Er-doped SnO₂DMS nanoparticles. *J Nanopart Res* 13:4623–4630
33. Yılmaz Atay H, Çelik E (2014) Barium hexaferrite reinforced polymeric dye composite coatings for radar absorbing applications. *Polymer Compos* 35(3):602–610
34. Atay HY, İçin Ö (2020) Manufacturing radar-absorbing composite materials by using magnetic Co-doped zinc oxide particles synthesized by Sol-Gel. *J Compos Mater*
35. Suresh K, Patil K (1993) A combustion process for the instant synthesis of γ-iron oxide. *J Mater Sci Lett* 12:572–574
36. Deshpande K, Mukasyan A, Varma A (2004) Direct synthesis of iron oxide nanopowders by the combustion approach: reaction mechanism and properties. *Chem Mater* 16:4896–4904
37. Erri P, Pranda P, Varma A (2004) Oxidizer–fuel interactions in aqueous combustion synthesis. 1. Iron(III) nitrate–model fuels. *Ind Eng Chem Res* 43:3092–3096
38. Yang J, Li X, Deng X, Huang Z, Zhang Y (2012) Salt-assisted solution combustion synthesis of ZnFe₂O₄ nanoparticles and photocatalytic activity with TiO₂ (P25) as nanocomposite. *J Ceram Soc Jpn* 120:579–583

39. Choodamani C, Nagabhushana GP, Ashoka S, Prasad BD, Rudraswamy B, Chandrappa GT (2013) Structural and magnetic studies of $Mg(1-x)ZnxF_2O_4$ nanoparticles prepared by a solution combustion method. *J Alloys Compd* 578:103–109
40. Reiss G, Huetten A (2005) Magnetic nanoparticles: applications beyond data storage. *Nat Mater* 4:725–726
41. Iida H, Takayanagi K, Nakanishi T, Osaka T (2007) Synthesis of Fe_3O_4 nanoparticles with various sizes and magnetic properties by controlled hydrolysis. *J Colloid Interface Sci* 314:274–280
42. Iwasaki T, Kosaka K, Mizutani N, Watano S, Yanagida T, Tanaka H, Kawai T (2008) Mechanochemical preparation of magnetite nanoparticles by coprecipitation. *Mater Lett* 62:4155–4157
43. Lee BY, Lee J, Bae CJ, Park J-G, Noh H-J, Park J-H, Hyeon T (2005) Large scale synthesis of uniform and crystalline magnetite nanoparticles using reverse micelles as nanoreactors under reflux conditions. *Adv Funct Mater* 15:503–509
44. Pillai V, Kumar P, Multani MS, Shah DO (1993) Structure and magnetic properties of nanoparticles of barium ferrite synthesized using microemulsion processing. *Colloids Surf A Physicochem Eng Asp* 80:69–75
45. Morrison SA, Cahill CL, Carpenter EE, Calvin S, Swaminathan R, McHenry ME, Harris VG (2004) Magnetic and structural properties of nickel zinc ferrite nanoparticles synthesized at room temperature. *J Appl Phys* 95:6392–6395
46. Liu C, Rondinone AJ, Zhang ZJ (2000) Synthesis of magnetic spinel ferrite $CoFe_2O_4$ nanoparticles from ferric salt and characterization of the size-dependent superparamagnetic properties. *Pure Appl Chem* 72:37–45
47. Zhao F, Zhang B, Feng L (2012) Preparation and magnetic properties of magnetite nanoparticles. *Mater Lett* 68:112–114
48. Mazar'io E, Herrasti P, Morales MP, Men'endez N (2012) Synthesis and characterization of $CoFe_2O_4$ ferrite nanoparticles obtained by an electrochemical method. *Nanotechnology* 23:355708
49. Rishikeshi SN, Joshi SS, Temgire MK, Bellare JR (2013) Chain length dependence of polyol synthesis of zinc ferrite nanoparticles: why is diethylene glycol so different. *Dalton Trans* 42:5430–5438
50. Stepanov GV, Borin DY, Raikher YL, Melenev PV, Perov NS (2008) Motion of ferroparticles inside the polymeric matrix in magnetoactive elastomers. *J Phys Cond Matter* 20(204121):6
51. Thévenot J, Oliveira H, Sandre O, Lecommandoux S (2013) Magnetic responsive polymer composite materials. *Chem Soc Rev* 42:7099–7116 [PubMed: 23636413]
52. Filipcsei G, Csetneki I, Szilagyai A, Zrinyi M (2007) Magnetic field-responsive smart polymer composites. In: Abe A, Albertsson A-C, Coates GW, Genzer J, Kobayashi S, Lee K-S, Leibler L, Long TE, Möller M, Okay O, Percec V, Tang BZ, Terentjev EM, Vicent MJ, Voit B, Wiesner U, Zhang X (eds) *Advances in polymer science*, vol 206. Springer, p 137–189
53. Achilleos DS, Vamvakaki M (2010) End-grafted polymer chains onto inorganic nano-objects. *Mater* 3:1981–2026
54. Schmidt AM (2005) The synthesis of magnetic core-shell nanoparticles by surface-initiated ring-opening polymerization of ϵ -caprolactone. *Macromolecul Rapid Comm* 26:93–97
55. Kloust H, Pösel E, Kappen S, Schmidtke C, Kornowski A, Pauer W et al (2012) Ultrasmall biocompatible nanocomposites: a new approach using seeded emulsion polymerization for the encapsulation of nanocrystals. *Langmuir* 28:7276–7281 [PubMed: 22497455]
56. Bin Y, Yamanaka A, Chen QY, Xi Y, Jiang XW, Matsuo M (2007) Morphological, electrical and mechanical properties of ultrahigh molecular weight polyethylene and multi-wall carbon nanotube composites prepared in decalin and paraffin. *Poly J* 39:598–609
57. Rong MZ, Zhang MQ, Zheng YX, Zeng HM, Friedrich K (2001) Improvement of tensile properties of nano- SiO_2 /PP composites in relation to percolation mechanism. *Poly* 42:3301–3304
58. Guoliang PQ, Guo AT, He Z (2008) Mechanical behaviors of Al_2O_3 nanoparticles reinforced polyetheretherketone. *Mater Sci Eng A* 492:383–391

59. Publico-Lansigan MH, Situ SF, Samia ACS (2013) Magnetic particle imaging: advancements and perspectives for real-time in vivo monitoring and image-guided therapy. *Nanoscale* 5:4040–4055 [PubMed: 23538400]
60. Krishnan KM (2016) *Fundamentals and applications of magnetic materials*. Oxford University Press, University of Washington, Seattle
61. Safarik I, Safarikova M (1999) *J. Chromatography B* 722:33–53
62. KarumanchiRSMS, Doddamane S N, Sampangi C, Todd PW (2002) *Trends Biotechnol.* 20: Cell separation and protein purification 1996 Information booklet. Dynal Oslo
63. Akamura N, Matsunaga T (1993) *Anal Chim Acta* 281:585–589
64. Sieben S, Bergemann C, L`ubbe A, Brockmann B, Rescheleit D (2001) *J Magn Magn Mater* 225:175–179
65. Kutushov MV, Kuznetsov AA, Filippov VI, Kuznetsov OA (1997) Scientific and clinical applications of magnetic carriers. In: Häfeli U, Schütt W, J Teller, M Zborowski (eds) Plenum, New York, London, p 391
66. Vladimir P, Torchilin 2000 *Euro. J Pharm Sci* 11:S81–S91
67. Fricker J (2001) *Drug Discovery Today* 6:387–389
68. Widder KJ, Morris RM, Poore GA, Howards DP, Senyei AE (1983) *Eur J Cancer Clin Oncol* 19:135–139
69. Lübbe AS, Alexiou C, Bergemann C (2001) *J Surg Res* 95:200–206
70. Stark DD (1991) *Radiology* 179:333–335
71. Cavaliere R, Ciocatto EC, Heidelburger C, Jonson RO, Margottini M, Mondovi B, Moricca BG, Rossi-Fanelli A (1967) *Cancer* 20:1351–1381
72. Hergt R, Andrä W, d’Ambly CG, Hilger I, Kaiser WA, Richter U, Schmidt H-G (1998) *IEEE Trans Magn* 34:3745–3754
73. Shinkai M, Suzuki M, Yokoi N, Yanase M, Shimizu W, Honda H, Kobayashi T 1998 *Jpn.J. Hyperthermic Oncol. Cancer. Res.* 14: 15–21

Jackfruit Seed Starch-Based Composite Beads for Controlled Drug Release



Amit Kumar Nayak, Saad Alkahtani, and Md Saquib Hasnain

Abstract Jackfruit (*Artocarpus heterophyllus* Lam.; family: Moraceae) seed starch (JSS) is a natural starch candidate, which is already reported as a potential pharmaceutical biopolymeric raw materials/excipients in various pharmaceutical dosage forms, such as binding agent and disintegrants in pharmaceutical tablets, emulsifier in emulsions, suspending agent in suspensions, and mucoadhesive agent in biomucoadhesive dosage forms. Recent years, JSS has been utilized to prepare controlled drug-releasing composite beads, when processed with other biopolymers like sodium alginate, gellan gum, and low methoxy pectin. All these JSS-based composite beads demonstrated *in vitro* controlled releasing of encapsulated drugs over a longer time and significant *in vivo* hypoglycemic actions in the treated alloxan-induced diabetic Albino rats *over prolonged time interval* after administration through oral route. The current chapter presents a comprehensive review of various JSS-based composite beads for controlled sustained releasing of encapsulated drugs.

Keywords Jackfruit seed starch · Composite · Controlled release · Drug delivery

1 Introduction

Development of controlled releasing dosage forms using biocompatible and biodegradable polymeric excipients is a popular trend in the drug delivery research, wherein polymers are being thoughtfully chosen to encapsulate a variety of drugs and also to monitor the releasing of encapsulated drug materials in a controlled manner

A. K. Nayak

Department of Pharmaceutics, Seemanta Institute of Pharmaceutical Sciences, 757086 Mayurbhanj, Odisha, India

S. Alkahtani

Department of Zoology, College of Science, King Saud University, 2455, 11451 Riyadh, Saudi Arabia

M. S. Hasnain (✉)

Department of Pharmacy, Palamau Institute of Pharmacy, Chianki, 822102 Daltonganj, Jharkhand, India

© The Author(s), under exclusive license to Springer Nature Switzerland AG 2022

213

M. S. Hasnain et al. (eds.), *Polymeric and Natural Composites*,

Advances in Material Research and Technology,

https://doi.org/10.1007/978-3-030-70266-3_7

over a longer period [1–3]. In addition, these systems usually exhibited several benefits over the conventional immediate release dosage systems, such as like reduction of drug concentration fluctuations within the therapeutic range, decreased risk of dose-dumping chances, reduced dosing frequencies, more predictable gastric emptying, minimization of side effect incidence, and enhanced patient compliances. [5–7]. Among various controlled drug delivery systems, multiple-unit oral dosage forms have been researched during last few decades [7–9]. The uses of such multiple-unit oral dosage forms are advantageous than the single-unit-controlled releasing oral dosage forms as these (*i.e.*, multiple units) are capable to distribute within a larger area of the gastrointestinal tract, releasing of drugs in a predictable as well as controllable way to bypass the vagaries of gastric emptying and to decrease the possibilities of dose dumping to reduce localized mucosal damage of gastrointestinal tract [10–12]. In recent years, various multiple-unit oral-controlled drug-releasing systems like composite beads and microparticles containing various plant polysaccharides are being investigated by several research groups [13–35].

In recent years, trends toward the exploration and exploitation of plant source originated materials in various important biomedical applications have been recognized as the most emerging field for research and development in the current years [36–39]. These materials are abundantly available from plant resources, and therefore, renewability is the prime advantage for the uses of these materials [40–43]. Plant polysaccharides are currently recognized as a popular biopolymeric material group with a variety of important physicochemical characteristics like high swelling capability in the aqueous environment, degradation into physiological metabolites, excellent stability in the wider pH alterations, etc. [44–47]. Most of the plant polysaccharides are extracted from leaves, pods, fruits, seeds, rhizomes, roots, exudates, etc. [43, 47]. Therefore, these materials are recognized as low cost materials because of very low production cost and larger availability options for the natural resources [48–51]. Moreover, in the biomedical area, the biodegradation of these plant polysaccharides into physiological metabolites support these to be as effectual biopolymeric candidates for various biomedical uses like drug-delivering systems, wound managements, tissue regeneration applications, etc. [51–54]. Recently, a considerable volume of research attempts have been performed in the drug delivery research field for their utilization as various pharmaceutical excipients, such as emulsifier, suspending agents, disintegrating agents, binding agents, granulating agents, matrix formers, release retardants, enteric coats, film formers, and mucoadhesive agents. [43, 47, 55–70]. Among various plant polysaccharides, starches are being widely studied as pharmaceutical excipients in the formulation of several kinds of pharmaceutical dosage forms [71–82]. Even natural starches are being employed to design many controlled release composite beads/microparticles, when processed with other biocompatible polymers [82–87]. Plant-derived starches researched for this purpose are potato starch [88], rice starch [89–91], jackfruit seed starch (JSS) [92–95], tapioca starch [96], etc. In recent years, JSS has been utilized to prepare controlled drug-releasing composite beads, when processed with various anionic polysaccharides, such as like sodium alginate [92, 93], gellan gum [95], and low methoxy pectin [94]. The current chapter presents a useful discussion on already reported JSS-based

composite beads for controlling sustained release of drugs. First part of the current chapter comprises extraction characterization, properties, and pharmaceutical uses of JSS. The final portion includes discussions about various already reported JSS-based composite beads for controlled release of drugs.

2 Jackfruit Seed Starch (JSS)

The jackfruit (*A. heterophyllus* Lam.; family: Moraceae) is a common tropical fruit candidate, generally occurred in India, Malaysia, Bangladesh, China, Vietnam, Indonesia, Philippines, Thailand, and Brazil [97, 98]. By tradition, the *Artocarpus* species is being employed as one of the folk medicinal material in treatment of malarial fevers, worm infections, diarrhea, diabetes, and other disorders [98]. The ripe jackfruit contains mature seeds, which are found to as yellow-colored edible bulbs. Generally, a ripe and mature jackfruit contains 100–500 seeds, which are about 3–5 mm thick. These ripe and mature seeds are separated from horny endocarpus coated within subgelatinous exocarpus—a thin membrane of whitish color. These are of oval and oblong or round shaped [98]. These seeds are consumed in boiled, steamed as well as roasted forms as food materials by the many communities as these contains almost similar compositions as that of food grains [97]. In addition, jackfruit seed flour is being utilized in the preparation of biscuits, breads, sweets, etc. [99]. Jackfruit seeds are nutritious and rich in carbohydrates. It also contains lignans, isoflavones, and some mineral components (like potassium, magnesium, manganese, etc.) [97–100]. The carbohydrates present in the jackfruit seeds mainly possess high amounts of starches [101].

JSS is being extracted from mature and ripe jackfruit seeds and purified. Nayak et al. (2015) reported extraction of JSS from raw jackfruit seeds [45]. In this extraction procedure, 250 g of raw jackfruit seeds were taken. For the removal of superficial cohesive layer, these seeds were cleaned using distilled water. Arils of the superficial coat of these seeds were eliminated by hand, and then, thinner brownish spermodermis were peeled using a solution of 0.6 M potassium hydroxide for a period of 3 h at the room temperature. The pale-white cotyledons were exposed by the alkali treatment and washing of these several times by distilled water to eliminate the alkali traces present on the seed surfaces, completely. Then, these alkali-treated seeds were reduced to small pieces using cutter. These small pieces were wet-grounded by pestle and mortar using distilled water, where seed to water ration was maintained 1:3 to prepare slurry and followed by centrifugation at 3000 rpm for 20 min in room temperature. Centrifuged residue was collected through scraping and resuspended in the solution of 0.5 M sodium thiosulfate maintaining the residue to solution ration of 1:1 for 24 h with a stirring accommodation at regular break for the elimination of protein fractions. Collected filtrated portion was then centrifuged for 5 min with 2000 rpm of centrifugation speed and a brownish layer appeared at the upper portion of the whitish residue, which was scrapped off very cautiously. The whitish residue was made neutralized using 0.1 M hydrochloric acid solution. Subsequently, it is

rinsed using plenty of distilled water. The obtained material was further rinsed for two times using 50% of ethanol. The collected extracted substance was then dried for overnight at a temperature of 40 °C. The dried JSS cakes were grounded and then passed through 0.15 mm mesh-size sieve. The extracted JSS was stored within an airtight desiccator. The extracted JSS was subjected to measure various physico-chemical characteristics: color, odor, taste, aqueous solubility, pH, and viscosity of aqueous JSS solution. The extracted JSS was found whitish colored, odorless, and tasteless powders. The pH of 1% solution of extracted JSS was determined as 6.22 ± 0.15 at 37 °C temperature. Extracted JSS was found to produce more aqueous solubility in hot water. However, it exhibited less aqueous solubility in cold water. The viscosity of 1% solution of extracted JSS at 37 °C temperature and 100 rpm spindle speed was determined as 45.18 ± 1.37 cps. The extracted JSS was subjected to various important phytochemical identification tests, which indicated the presence of carbohydrates. Currently, JSS is recognized as an alternative potential contender material to the conventionally and commercially utilized starches. In recent times, it is being used in various industrial applications including foods and pharmaceuticals [102, 103].

Approximately, 25–35% of amylose content is present in JSS and is also comparable with that of potato starch [104]. JSS displays some important characters relating to physicochemical properties, such as granule size and shape, crystallinity, solubility, viscosity, swellability, and acid resistance, as compared to other conventional starches [103, 104]. Its gelatinization temperature is higher as compared to other conventional starches [105]. Rengsutthi and Charoenrein (2011) studied the morphological structures of extracted JSS granules by using scanning electron microscopy (SEM) [102]. SEM images indicated a range of round-shaped to bell-shaped granules. Average diameter of JSS granules was measured as 10 μm . On the other hand, Bobbio et al., (1978) reported rounded and bell-shaped granules of JSS ranging of average diameter, 7–11 μm [106].

During past few years, JSS is being utilized in the formulations of various pharmaceutical dosage forms as pharmaceutical excipients [105, 107]. Already, it was explored as binding agent in pharmaceutical tablets [108]. Due to highly viscous properties, JSS is also investigated for its suitability as emulsifier and suspending agent in emulsions as well as suspensions, respectively [107]. As mucoadhesive agent, JSS was also utilized to develop biomucoadhesive dosage forms [109]. The cross-linked carboxymethyl JSS was investigated as tablet disintegrants [105]. Recently, it has been utilized as polymer blends with other biocompatible polymers like sodium alginate [92, 93], gellan gum [95], and low methoxy pectin [94] to prepare controlled drug-releasing composite beads.

3 Alginate-JSS Composite Beads for Controlled Drug Release

The usefulness of JSS was tested as polymer blends with alginate to formulate controlled drug-releasing composite beads [92, 93]. Alginates are a group alginic acid salts derived from marine sources, in particular, from few brown marine algae [110, 111]. Alginates are mainly anionic copolymer of α -L-guluronic acid (G) and β -D-mannuronic acid (M) units arranged in the asymmetrical pattern of varying ratios of G-G, M-M, and M-G units linked with 1, 4-glycosidic linkages [112, 113]. Alginates are biocompatible and biodegradable polysaccharide group, which are extensively being utilized in many food applications as emulsifier, stabilizer, thickener, etc. [114–116]. US FDA already has recommended these as one of the GRAS materials [117, 118]. These are also widely employed as biopolymer in several biomedical applications including drug delivery [119–122]. The sodium salt of alginic acid—sodium alginate—has been extensively researched and employed as aqueous soluble biopolymer in numerous formulas of drug delivery dosage forms because of its considerable viscosity in aqueous solutions [123–126]. The important most property of sodium alginate is the ability of ionotropic gelation by the influence of metal cations, such as Ca^{2+} , Ba^{2+} , Zn^{2+} , and Al^{3+} [127–130]. The divalent and/or trivalent metal cations are thought to be incorporated with the electronegative cavities of alginate structure similar to eggs in the so-called “Egg Box model” structuring ionotropically cross-linked alginate hydrogels as a result of the intermolecular interactions in-between- COO^- groups positioned in the alginate structure and metal (divalent and/or trivalent) cations [131–133]. Over the decades, numerous ionotropically cross-linked alginate hydrogels have been explored as carrier matrices for drug-releasing applications [4, 55, 128, 133–135]. Nevertheless, the drug-releasing capability of these ionotropically cross-linked alginate hydrogels is linked with some drawbacks like lower drug encapsulation efficiencies due to longer curing time and burst releasing of the encapsulated drugs as a result of speedy degradation in the alkaline intestinal pH [9, 128, 133, 136]. To manage these potential drawbacks, numerous modifications of ionotropically cross-linked alginate hydrogels have been researched by different research groups [4, 137, 138]. Among these modifications, uses of other biopolymers as blends with sodium alginate are being explored to develop various alginate-based composite hydrogel beads for maximizing encapsulations of drugs and sustained-controlled releasing of encapsulated drugs [3, 4, 9, 18, 139–142].

Recently, alginate-JSS composite beads for controlled release of metformin HCl (an oral hypoglycemic agent, usually given in the management of Type-II or non-insulin-dependent diabetes mellitus) were developed employing polymer-blends solutions of sodium alginate-JSS and calcium chloride (as an ionotropic cross-linking gelation agent) [92]. These alginate-JSS beads of metformin HCl were developed and optimized by using a statistical optimization method based on the 3^2 factorial design (comprising two independent factors with three different levels) and response surface methodology to analyze the influence of sodium alginate-to-JSS ratio in

the bead formula and concentrations of calcium chloride on the drug encapsulations and releases. It was noticed that increased drug encapsulation efficiency of these composite beads and reduced cumulative in vitro releases of metformin HCl after 10 h were found with lowering of sodium alginate-to-JSS ratio (increasing JSS contents in polymer-blends) and increasing calcium chloride (ionotropic cross-linking agent) concentrations. From the numerical optimization analyses, the optimal formulation variable settings were selected as sodium alginate-to-JSS ratio of 1.03 and calcium chloride concentration of 10.39%. Employing these optimal formulation variable settings, optimized alginate-JSS composite beads of metformin HCl were formulated. The optimized composite bead formulation exhibited $97.48 \pm 3.92\%$ of drug encapsulation efficiency and cumulative in vitro release of metformin HCl of $65.70 \pm 2.22\%$ after 10 h of drug-releasing study.

Drug encapsulation efficiencies of alginate-JSS composite beads of metformin HCl were calculated within the range, $69.94 \pm 2.18\%$ to $97.48 \pm 3.92\%$. Average diameter of alginate-JSS composite beads of metformin HCl was calculated within a range of 0.89 ± 0.07 – 1.30 ± 0.11 mm, whereas the optimized composite beads of metformin HCl showed the average diameter of 1.16 ± 0.11 mm. Surface morphology of optimized alginate-JSS composite beads of metformin HCl was examined using scanning electron microscopy (SEM). The photomicrograph of composite beads demonstrated irregular shaped discrete beads (Fig. 1). These beads were free from

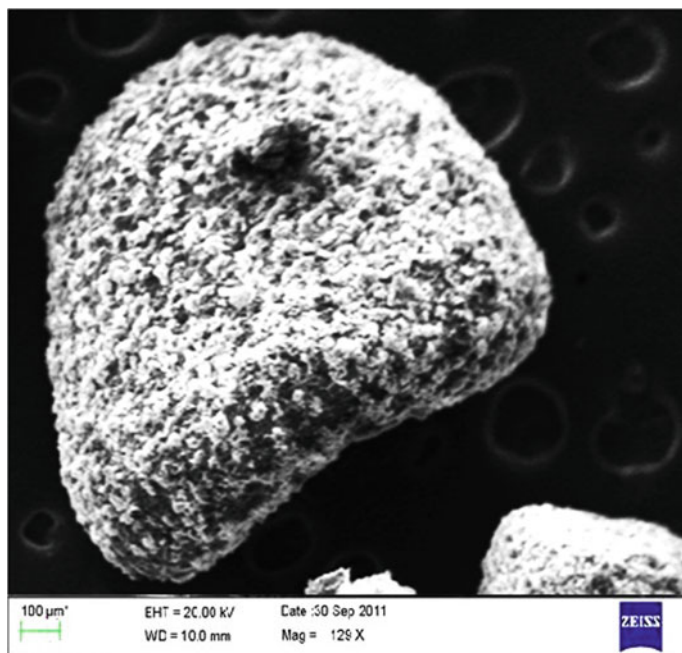


Fig. 1 Photomicrograph of optimized alginate-JSS composite beads of metformin HCl demonstrating irregular shaped discrete beads [92]. (Copyright © 2013 Elsevier B.V.)

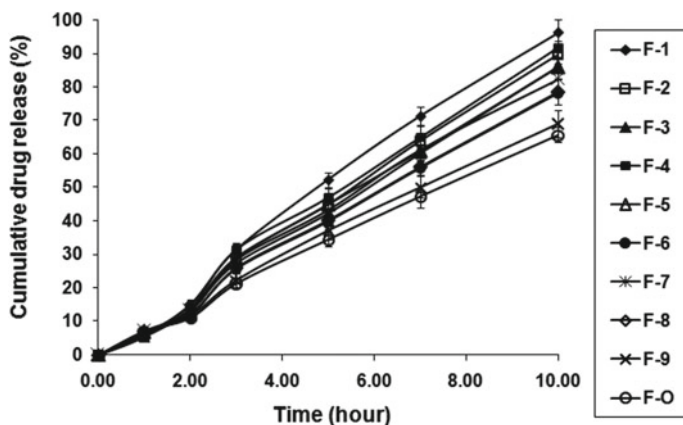


Fig. 2 In vitro releases of metformin HCl from various alginate-JSS composite beads of metformin HCl [Mean \pm S.D., $n = 3$] [92]. (Copyright © 2013 Elsevier B.V.)

agglomeration and possessing a rough surface with typical wrinkles and cracks. These beads exhibited significant characters of metformin HCl after encapsulation without any types of drug-excipients interactions, examined in Fourier transform infrared (FTIR) spectroscopic analyses.

In vitro metformin HCl releasing from various alginate-JSS composite beads in gastric pH (1.2) for initial 2 h and next in intestinal pH (7.4) for the remaining release periods revealed a prolonged sustained metformin HCl releasing pattern over 10 h (Fig. 2). Initial metformin HCl releasing in the gastric pH was found not more than 15% after 2 h. In vitro metformin HCl releasing from these composite beads was followed zero-order kinetics pattern along with super case-II transport mechanism. These results can be attributed by the phenomena of matrix-dissolution through the enlargement or relaxation of the polymeric chains. In vitro swelling index of optimized alginate-JSS composite beads of metformin HCl was found primarily lower in gastric pH (1.2) in comparison with that of intestinal pH (7.4) (Fig. 3). In the intestinal pH, an utmost swelling profile of composite beads was detected at 2–3 h. After which, erosion as well as dissolution of the ionotropically gelled alginate-JSS composite bead matrices occurred.

Ex vivo wash off assessments of optimized alginate-JSS composite beads of metformin HCl using goat intestinal mucosal tissue were revealed comparatively quicker in the intestinal pH (alkaline) than that in the gastric pH (acidic). The percentage of composite beads adhered to the mucosal membrane in the acidic pH (1.2) was observed $62.52 \pm 4.46\%$ over 8 h, whereas this was found $37.60 \pm 3.43\%$ in the intestinal pH (7.4) (Fig. 4). The results of ex vivo wash off of these optimized alginate-JSS composite beads of metformin HCl suggested good mucoadhesivity with the mucosal membrane in the gastric as well as intestinal pHs.

In vivo levels of blood glucose as well as the percentage of average decline of blood glucose after oral administrations of pure metformin HCl and optimized alginate-JSS

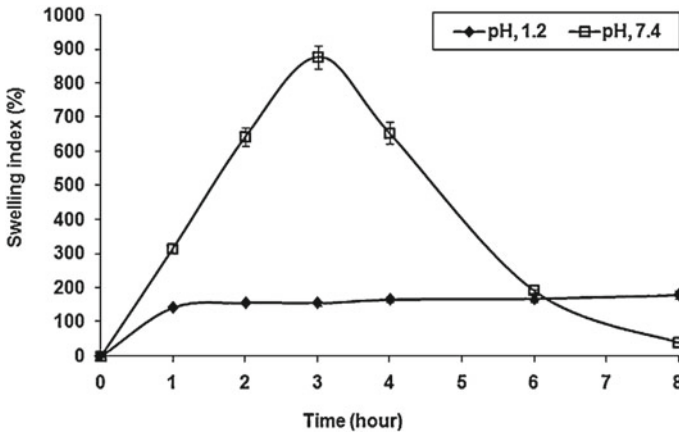


Fig. 3 In vitro swelling behavior of optimized j alginate-JSS composite beads of metformin HCl in gastric pH (1.2) and intestinal pH (7.4) [mean \pm S.D., $n = 3$] [92]. (Copyright © 2013 Elsevier B.V.)

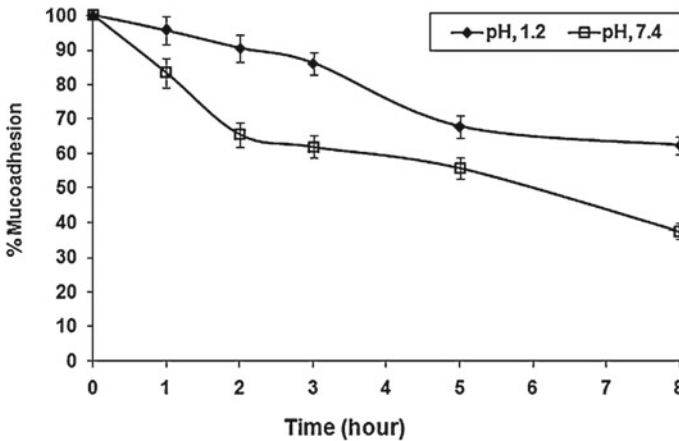


Fig. 4 Results of ex vivo wash-off test to assess mucoadhesive properties of optimized alginate-JSS composite beads of metformin HCl in gastric pH (1.2) and intestinal pH (7.4) [mean \pm S.D., $n = 3$] [92]. (Copyright © 2013 Elsevier B.V.)

composite mucoadhesive beads of metformin HCl to alloxan-induced diabetic Albino rats were measured and analyzed (Fig. 5). The alloxan-induced diabetic rats treated with pure metformin HCl showed a speedy decline in levels of blood glucose within 3 h of oral administration, and after that, it was recovered speedily toward the regular level of blood glucose. On the other hand, alloxan-induced diabetic rats treated with optimized alginate-JSS composite mucoadhesive beads of metformin HCl exhibited a decline in levels of blood glucose, which was comparatively slower than that of pure metformin HCl up to 3 h. However, the decline in the levels of blood glucose was

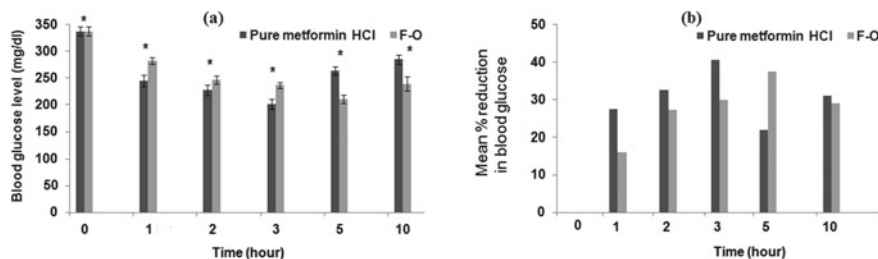


Fig. 5 **a** Comparative in vivo levels of blood glucose and **b** comparative in vivo mean percentage reduction in levels of blood glucose in alloxan-induced diabetic rats after oral administration of pure metformin HCl and optimized alginate-JSS composite beads of metformin HCl (F-O). The data were analyzed for significant differences ($*p < 0.05$) by paired samples t-test [92]. (Copyright © 2013 Elsevier B.V.)

increased progressively with the increment of time and was found to be sustained over a period of 10 h. These in vivo pharmacodynamic results recommended a significant ($p < 0.05$) antidiabetic action by the oral administration of optimized alginate-JSS composite mucoadhesive beads *in the* diabetic rats *over a longer period*.

In another study, alginate-JSS composite beads containing pioglitazone (an oral anti-diabetic drug having short biological half-life of 3–5 h) were developed via ionotropic gelation technique using calcium chloride as ionotropic cross-linking agent and evaluated for the use in the treatment of non-insulin-dependent diabetes mellitus (Type-II) [93]. For the formulation optimization, a computer-aided statistical optimization method based on 3^2 factorial design along with response surface methodology was employed to check and analyze the influences of sodium alginate-to-JSS ratio and concentrations of calcium chloride on the drug encapsulation efficiencies and cumulative percentage drug releases. From the analyses of three-dimensional response surface plots and corresponding two-dimensional contour plots, influences of the tested factors (independent variables, such as sodium alginate-to-JSS ratio and concentrations of calcium chloride) on the responses measured (dependent variables such as drug encapsulation efficiency and cumulative drug release after 10 h) were verified and analyzed. An increased pioglitazone encapsulation efficiency and reduced of cumulative in vitro pioglitazone release after 10 h were found with the decreasing of sodium alginate-to-JSS ratio (increasing JSS contents in the polymer-blends employed) and the increasing concentration of calcium chloride as the ionotropic cross-linking agent. The optimized alginate-JSS composite beads of pioglitazone exhibited $94.07 \pm 3.82\%$ of drug encapsulation efficiency and $64.87 \pm 1.83\%$ of cumulative in vitro drug release after 10 h.

Pioglitazone encapsulation efficiencies of various alginate-JSS composite beads of pioglitazone were ranged between 64.80 ± 1.92 and $94.07 \pm 3.82\%$ [93]. Average bead sizes of these various alginate-JSS composite beads of pioglitazone were ranged between 0.77 ± 0.04 and 1.24 ± 0.09 mm. An average bead size of the optimized composite beads of pioglitazone as 0.85 ± 0.05 mm was calculated by optical microscopy. SEM image of the optimized alginate-JSS composite beads of

pioglitazone demonstrated bead surface morphology of irregular shaping with very rough surface structure, where some typical cracks as well as wrinkles were seen. FTIR spectroscopic analyses suggested the drug-excipients compatibility with the nonexistence of drug-excipient interaction between pioglitazone and sodium alginate-JSS polymer blends employed in the preparation of these composite beads through ionotropic gelation by calcium chloride.

In the gastric pH (acidic) medium, in vitro pioglitazone releases from these composite beads were found very slow (< 16% after 2 h) by reason of pH-sensitive contraction characteristics of the alginate gel in the acidic pH. In intestinal (alkaline) pH, a comparative faster in vitro releasing pattern of encapsulated pioglitazone was noticed as a result of higher swelling of the ionotropically gelled alginate matrices in the alkaline pH medium (7.4). After 10 h of in vitro release study, the cumulative pioglitazone released from these alginate-JSS composite beads was ranged, 64.87 ± 1.83 – $92.66 \pm 4.54\%$. In vitro pioglitazone HCl releasing from these composite beads was followed zero-order kinetics pattern along with super case-II transport mechanism. In vitro swelling performances of various alginate-JSS composite beads of pioglitazone were found to be controlled by pH and the compositions of the swelling mediums. In vitro swelling pattern of these composite beads of pioglitazone was found lower in gastric pH as compared to that of intestinal pH. This reduced swelling was occurred as a result of shrinkage of alginate-based at the acidic pH (1.2). Maximum swelling pattern of these composite beads of pioglitazone was detected at 2–3 h in the intestinal pH, and then, the erosion and dissolution of these composite matrices took place.

In vivo pharmacodynamic efficiencies of optimized alginate-JSS composite beads of pioglitazone were carried out in the alloxan-induced diabetic Albino rats. Comparative levels of blood glucose and the mean percentage reduction of blood-glucose levels in these diabetic rats after oral administration of pure pioglitazone and optimized alginate-JSS composite beads of pioglitazone were measured and compared. These optimized composite beads of pioglitazone demonstrated a significant ($p < 0.05$) hypoglycemic action in the treated alloxan-induced diabetic Albino rats *over prolonged period* of 10 h after administration through oral route.

3.1 Gellan Gum-JSS Composite Beads for Controlled Release Drug Delivery

Gellan gum is an anionic extracellular natural polysaccharide obtained from microbial sources (in particular from *Pseudomonas eloda*) [143, 144]. In recent years, it is extensively utilized in several food and pharmaceutical applications [27, 30]. Gellan gum consists of a tetrasaccharidic structure with a repeating sugar units of glucose, glucuronic acid, and rhamnose (2: 2: 1 of molar ratio) [145]. Deacetylated gellan gum has been investigated for its capacity to produce ionotropically gelled gellan gum-based matrices by the influence of some divalent and trivalent

metal cations (in particular, Ca^{2+} and Al^{3+} ions) [22, 144, 146]. The gelation mechanism of deacetylated gellan gum involves the development of double helical junctional zones subsequently the aggregation of double helical segments to the three-dimensional (3D) network structures through the ionotropic cross-linking interaction with divalent and/or trivalent metal cations and also through the hydrogen bonding [39]. The ionotropic cross-linking gelation of deacetylated gellan gum by divalent and/or trivalent metal cations takes place through the ionotropic cross-linking interaction in-between two carboxylic groups of glucuronic acid residues (present in the gellan gum structural backbone) and divalent and/or trivalent metal cations [144]. On the basis of the ionotropic cross-linking gelation nature of deacetylated gellan gum, different drugs are being encapsulated for the sustained-controlled releases of these [22, 146]. The features of these ionotropically cross-linked gellan gum-based systems were found dependant on various factors, such as gellan gum types, gellan gum concentrations, cross-linker types, cross-linker concentrations, pH of the medium, and curing time. [27, 30, 39]. These ionotropically gelled gellan gum beads are stable enough in lower pH range and unstable in higher pH range because of their rapid swelling rate in higher pH as compared to that of lower pH. This leads more rapidly and premature releasing of encapsulated drugs from a variety of ionotropically gelled gellan gum-based beads in the alkaline intestinal pH [68]. To conquer these inconveniences, various types of modifications of ionotropically gelled gellan gum-based matrices are being researched [22, 27, 95, 145]. Among these modifications, uses of other biopolymers as blends with gellan gum are being explored to develop various ionotropically gelled gellan gum-based composite hydrogel matrices to maximize drug encapsulation efficiency and sustained-controlled drug release [22, 27, 68].

Effectiveness of JSS was evaluated as a sustained drug-releasing matrix formers and mucoadhesive agent in the formulation of gellan gum-JSS composite beads of metformin HCl by means of employing calcium chloride as ionotropic cross-linking agent and gellan gum-JSS composite as polymer blends [95]. To optimize the formula of ionotropically gelled gellan gum-JSS composite beads of metformin HCl, a computer-aided statistical optimization method based on 3^2 factorial design using response surface methodology was employed. From the numerical optimization analyses, the optimal formulation variable settings were selected as gellan gum-to-JSS ratio of 1.38 and calcium chloride concentration of 1.58%. Employing these optimal formulation variable settings, optimized gellan gum-JSS composite beads of metformin HCl were formulated, which exhibited drug encapsulation efficiency of $92.67 \pm 4.46\%$ and cumulative in vitro release of metformin HCl of $61.30 \pm 2.37\%$ after 10 h of drug-releasing study.

Drug encapsulation efficiencies of all these gellan gum-JSS composite beads of metformin HCl were calculated within the range, 67.72 ± 3.20 – $92.98 \pm 4.13\%$. Average bead sizes of all these gellan gum-JSS composite beads of metformin HCl were calculated within the range, 1.21 ± 0.11 – 1.67 ± 0.27 mm. Average diameter of optimized gellan gum-JSS composite beads of metformin HCl was measured as 1.67 ± 0.27 mm. SEM photomicrograph of the composite beads demonstrated a few typical wrinkles as well as cracks on the bead surface with a few pores (Fig. 6). On the basis of FTIR spectroscopy analysis, it was observed that after encapsulation by

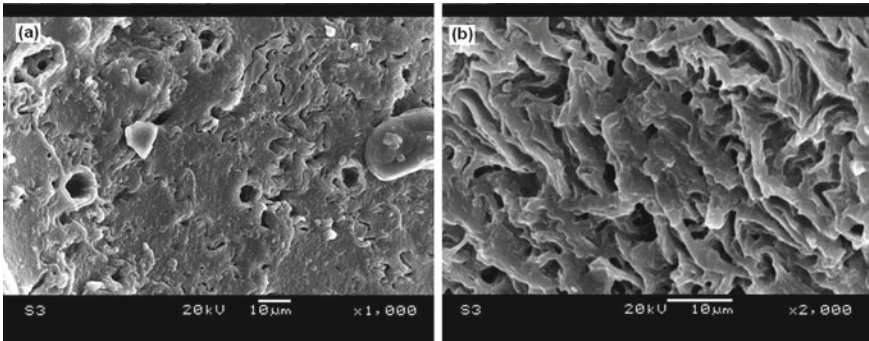


Fig. 6 SEM photograph of optimized gellan gum-JSS composite beads of metformin HCl at **a** $\times 1000$ and **b** $\times 2000$ magnification [95]. (Copyright © 2014 Elsevier B.V.)

ionotropic gelation, the optimized gellan gum-JSS composite beads of metformin HCl contained considerable characters of metformin HCl devoid of any types of interactions between metformin HCl and polymer blends (gellan gum-JSS) used.

In vitro metformin HCl releases from gellan gum-JSS composite beads of metformin HCl in the acidic medium of gastric pH (1.2) was very slow (*i.e.*, $< 15.30\%$ after initial 2 h) (Fig. 7). However, it was found faster in the alkaline medium of intestinal pH (7.4), which might be attributable to the fact of rapid swelling of these composite matrices. The higher and faster swelling power of gellan gum

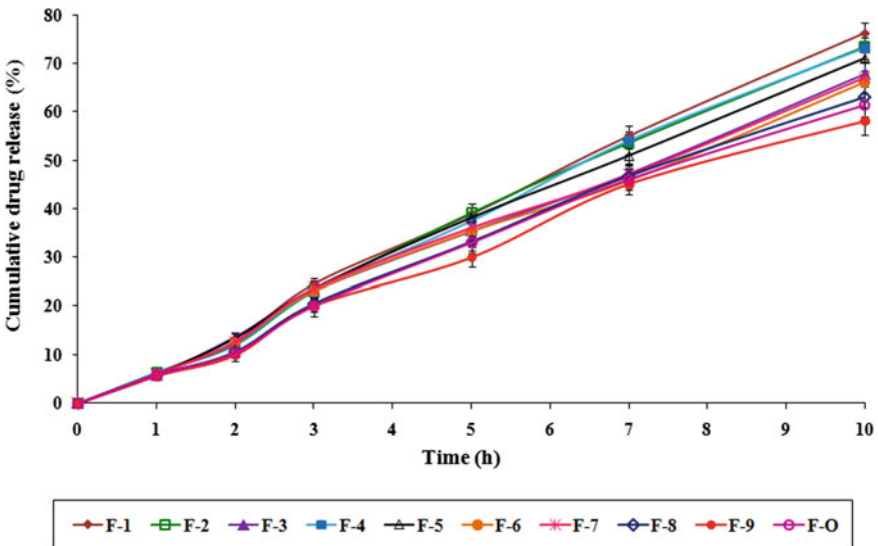


Fig. 7 In vitro drug release from various gellan gum-JSS composite beads of metformin HCl [Mean \pm S.D., $n = 3$] [95]. (Copyright © 2014 Elsevier B.V.)

matrices in the alkaline medium might be caused due to the electrostatic repulsion among the ionized $-\text{COO}^-$ groups of the gellan gum backbone. In vitro cumulative metformin HCl releases from these ionotropically gelled gellan gum-JSS composite beads of metformin HCl were found in the range, 58.19 ± 1.47 – $76.27 \pm 3.20\%$. It was also found that the in vitro releasing of metformin HCl from gellan gum-JSS composite beads followed a controlled releasing pattern (zero-order kinetics) along with super case-II transport mechanism controlled by swelling and relaxation of drug releasing matrices. In vitro swelling of optimized gellan gum-JSS composite beads of metformin HCl was found to be dependent on the pH of the swelling media. Initially, these gellan gum-JSS composite beads demonstrated lower swelling pattern in the acidic media of gastric pH (1.2) with respect to that in the alkaline medium of intestinal pH (7.4) (Fig. 8). These composite beads swelled speedily in the alkaline pH (7.4) within 2–3 h following erosion and dissolution of the swelled matrices.

Ex vivo wash off assessments of optimized gellan gum-JSS composite beads of metformin HCl was tested using goat intestinal mucosal tissue in the intestinal pH (alkaline) and gastric pH (acidic). At the intestinal pH, a comparative quicker ex vivo

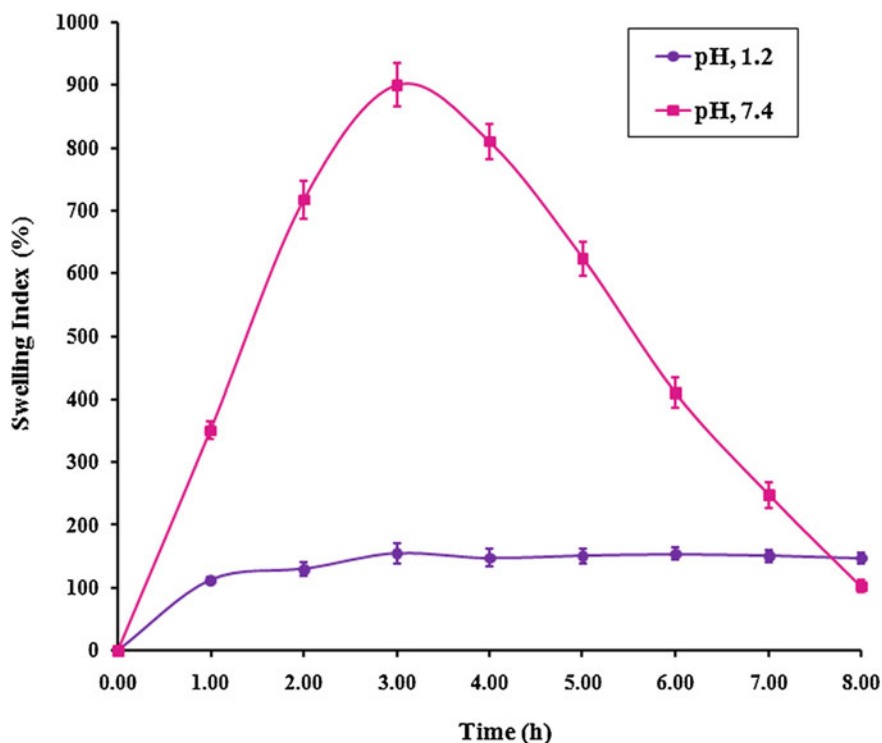


Fig. 8 In vitro swelling behavior of optimized gellan gum-JSS composite beads of metformin HCl in gastric pH (1.2) and intestinal pH (7.4) [Mean \pm S.D., $n = 3$] [95]. (Copyright © 2014 Elsevier B.V.)

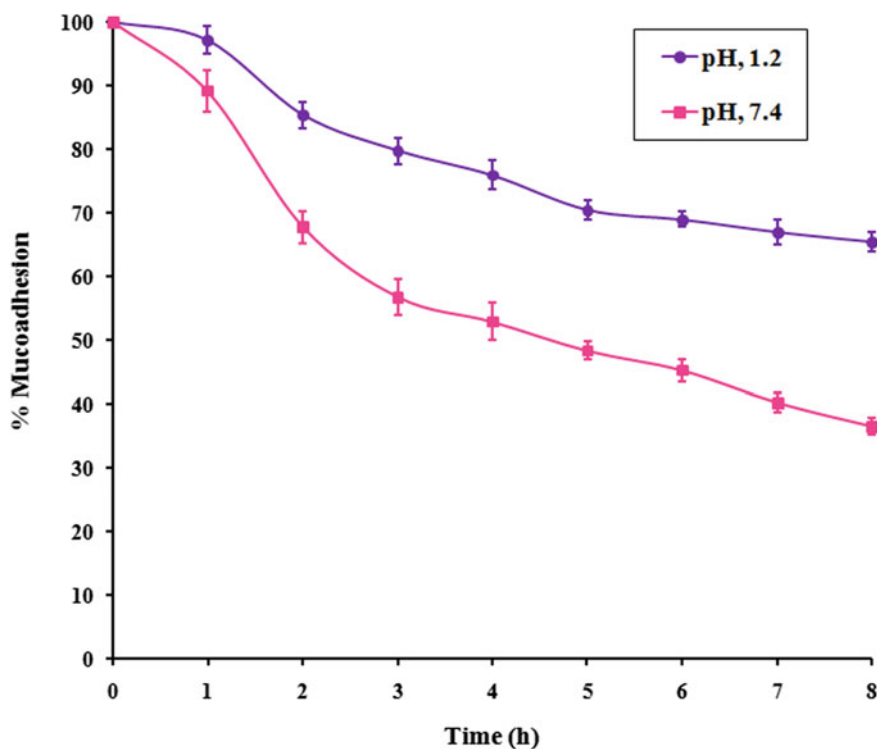


Fig. 9 Ex vivo mucoadhesivity of optimized gellan gum-JSS composite beads of metformin HCl in gastric pH (1.2) and intestinal pH (7.4) [Mean \pm S.D., $n = 3$] [95]. (Copyright © 2014 Elsevier B.V.)

wash off was reported than that in acidic pH (Fig. 9). Thus, the results of ex vivo wash off showed a good mucoadhesive potential of these composite beads for the used in mucoadhesive gastroretentive drug delivery to achieve improved bioavailability of the encapsulated drugs.

The comparative in vivo levels of blood glucose as well as the percentage of average decline in the in vivo levels of blood glucose after administration of pure metformin HCl and optimized gellan gum-JSS composite mucoadhesive beads of metformin HCl through the oral route in the alloxan-induced diabetic Albino rats were measured and analyzed (Fig. 10). The results of the pharmacodynamic evaluation suggested a significant ($p < 0.05$) antidiabetic action over a prolonged period in the treated diabetic rats. Thus, for the attainment of the tight blood-glucose level, the efficacy of these formulated ionotropically gelled optimized gellan gum-JSS composite mucoadhesive beads of metformin HCl was found beneficial, and improved patient compliance in the non-insulin-dependent diabetes mellitus (Type-II) may also be produced via controlling, prolonging as well as enhancing the systemic absorption of metformin HCl.

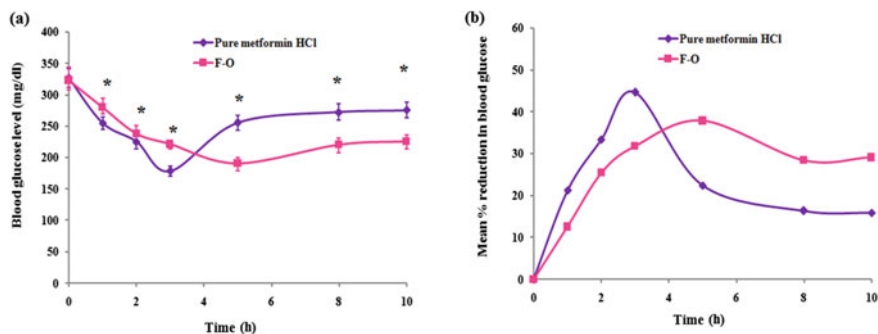


Fig. 10 **a** Comparative in vivo levels of blood glucose and **b** comparative in vivo mean percentage reduction in levels of blood glucose in alloxan-induced diabetic rats after oral administration of pure metformin HCl and optimized gellan gum-JSS composite beads of metformin HCl (F-O). The data were analyzed for significant differences ($*p < 0.05$) by paired samples t-test [95]. (Copyright © 2014 Elsevier B.V.)

3.2 Pectinate-JSS Composite Beads for Controlled Release Drug Delivery

Pectin is a naturally derived water soluble, non-toxic, anionic polysaccharide. Industrially, it is extracted from citrus peels, banana peels, sugar beet roots, apple pomace, pumpkin pulp, etc. [147]. In various pharmaceutical and food applications, it has been utilized as additives, thickeners, emulsifying agents, gelling agents, matrix formers, etc. [2, 24, 39, 147]. Because of its excellent biocompatibility, high biodegradability, appropriate mechanical property, and acid stability, it is extensively utilized as biopolymer in a variety of biomedical applications including drug delivery [26, 28]. The backbone of pectin molecules comprise predominantly a long sequences of partially methyl esterified and linearly linked α -(1-4) D-galacturonic acid residues interrupted with α -(1-2) connected α -L-rhamnopyranose units at regular intervals [39]. According to the degree of methoxylation, pectins are grouped as high methoxyl pectins (50–80% degree of methoxylation) and low methoxyl pectins (25–50% degree of methoxylation) [24]. The degree of methoxylation controls a variety of essential attributes of pectins, such as aqueous solubility and gel-forming potential. In general, low methoxy pectins has shown the potential of ionotropic cross-linking by various divalent metal cations like Ca^{2+} , Zn^{2+} , etc., to produce rigid ionotropically gelled pectinate beads by reason of ionotropic electrostatic interaction in-between $-\text{COO}^-$ groups of pectin-backbone and divalent metal cations [147]. The ionotropic gelation of $-\text{COO}^-$ groups of low methoxy pectin with divalent metal cations as cross-linker stimulates the arrangement of the so-called “Egg Box” structure [2]. This “Egg Box” structure of low methoxy pectin is to some extent unlike than that of the ionotropic gelation of sodium alginate [39]. In recent years, because

of the biodegradability, non-toxicity, acid stable characteristics, economic, and environmental friendly preparation methodology, numerous ionotropically gelled pectinate matrices composed of low methoxy pectin have been exploited as sustained drug-releasing carriers for oral drug delivery [147–150]. The characteristics (such as morphology, drug encapsulation, swelling, and drug release) of these pectinate matrices are generally found dependent on the pectin contents, degree of methylation, formulation methodologies, concentrations of cross-linkers, cross-linking time, pH, etc. [149]. These ionotropically gelled pectinate matrices has been experienced lesser encapsulations of drugs [24, 26, 28]. Moreover, the higher degrees of solubility as well as swellability of these pectinate matrices cause early and premature releases of the encapsulated drugs when exposed to the environment of alkaline pH [2, 149]. To curtail these above-said weaknesses, modifications of ionotropically gelled pectinate matrices have already been researched [40, 148]. Recently, polymer blends of low methoxy pectin with other biocompatible polymers have also been researched to formulate ionotropically gelled pectinate-based composite matrices to improve drug encapsulation, controlled drug-releasing patterns, mucoadhesion, swelling, stability, pharmacodynamic suitability, etc. [24, 26, 28].

In a study, JSS was blended with anionic low methoxy pectin to prepare ionotropically gelled pectinate-JSS composite beads to control the release of metformin HCl by using calcium chloride as an ionotropic cross-linking agent [94]. To optimize the formulations of pectinate-JSS composite beads containing metformin HCl, a 3^2 factorial statistical optimization design based on the response surface methodology was employed, where the influences of low methoxy pectin and JSS contents on the drug encapsulation efficiencies and cumulative percentage drug releases after 10 h were analyzed and optimized. It was noticed that both the efficiency of drug encapsulation was found to be enhanced, and the cumulative percentage drug releases after 10 h was found to be decreased with the increment of low methoxy pectin and JSS contents in the composite bead formula. From the numerical analysis, the selected optimal process variable setting used for the preparation of optimized pectinate-JSS composite beads containing metformin HCl was low methoxy pectin content of 715.38 mg and JSS content of 349.87 mg. The optimized composite beads containing metformin HCl exhibited $94.11 \pm 3.92\%$ of drug encapsulation efficiency and $48.88 \pm 2.02\%$ of cumulative in vitro drug release.

Drug encapsulation efficiencies of these ionotropically gelled pectinate-JSS composite beads of metformin HCl were found within the range, 66.65 ± 2.47 – $94.11 \pm 3.92\%$, and the average bead sizes were found within a range, 1.52 ± 0.15 – 2.06 ± 0.20 mm. The optimized pectinate-JSS composite beads of metformin HCl demonstrated average bead diameters of 2.06 ± 0.20 mm. The morphological analysis of optimized pectinate-JSS composite beads of metformin HCl was done by SEM observation. SEM photograph showed particles of spherical shaped without any kinds of agglomeration (Fig. 11). On the basis of FTIR spectroscopy analyses, it was observed that after encapsulation by ionotropic gelation, the optimized pectinate-JSS composite beads of metformin HCl contain considerable characters of metformin HCl devoid of any types of interactions between these metformin HCl and polymer blends (composed of pectinate-JSS) used.

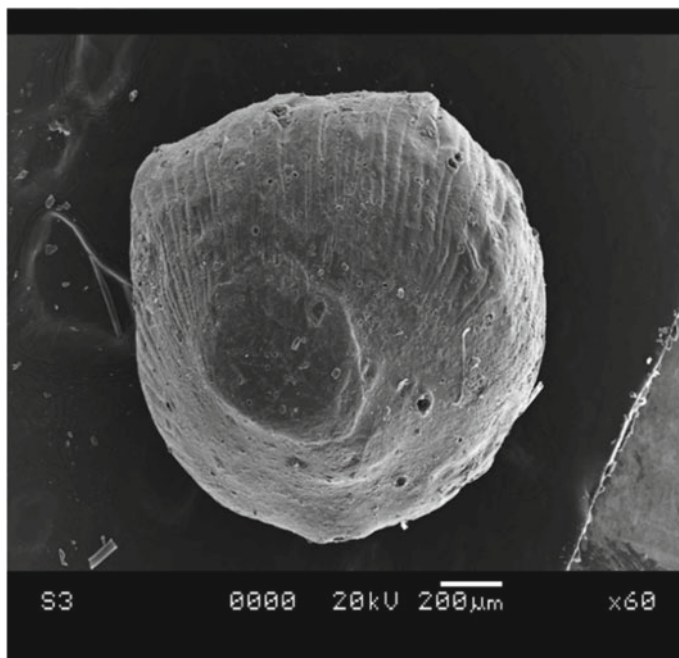


Fig. 11 SEM image of optimized pectinate-JSS composite beads of metformin HCl [94]. (Copyright © 2013 Elsevier B.V.)

In vitro release of metformin HCl from various formulated pectinate-JSS composite beads showed prolonged sustained release over 10 h of drug release study (Fig. 12). The release of metformin HCl in acidic medium (gastric pH, 1.2) was found very slow, which was measured as less than 15% after 2 h due to contraction of ionotropically gelled pectinate-based matrices in acidic pH. Because of higher swelling of the ionotropically gelled pectinate-based matrices in the phosphate buffer (alkaline pH, 7.4), faster in vitro release of metformin HCl from these composite beads were observed. The cumulative drug releases of various formulated pectinate-JSS composite beads of metformin HCl were found in a range, 48.88 ± 2.02 – $89.72 \pm 4.03\%$ after 10 h. In vitro metformin HCl releases from pectinate-JSS composite beads followed controlled releasing pattern (zero-order kinetics was measured in curve fitting) along with super case-II transport mechanism controlled by swelling and relaxation. In vitro swelling of optimized pectinate-JSS composite beads of metformin HCl was found to be controlled by pH and compositions of swelling mediums. The swelling patterns of optimized pectinate-JSS composite beads of metformin HCl were found much lower in acidic gastric pH (1.2) as compared with that in alkaline intestinal pH (7.4) (Fig. 13). Less swelling of these pectinate-JSS composite beads in acidic pH (1.2) was observed. Maximum swelling pattern of these composite beads of metformin HCl was detected at 2–3 h in intestinal pH, and then, erosion and dissolution of these composite matrices took place.

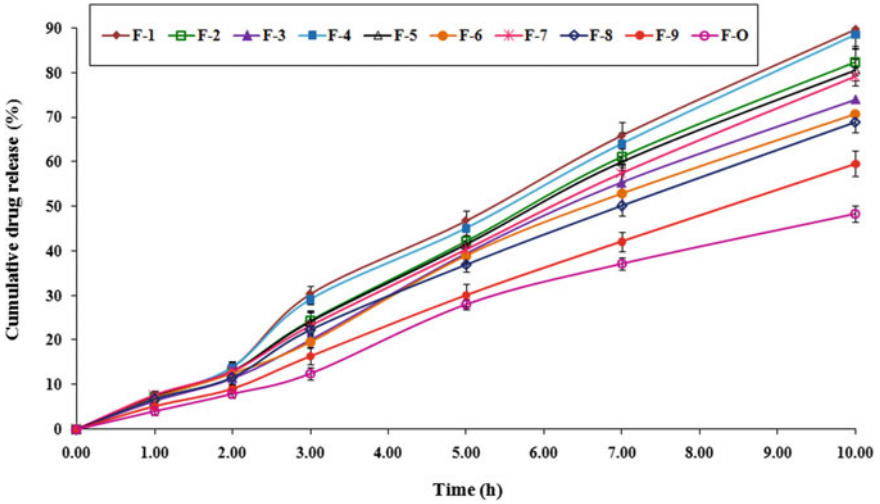


Fig. 12 In vitro drug release from various pectinate-JSS composite beads of metformin HCl [Mean \pm S.D., $n = 3$] [94]. (Copyright © 2013 Elsevier B.V.)

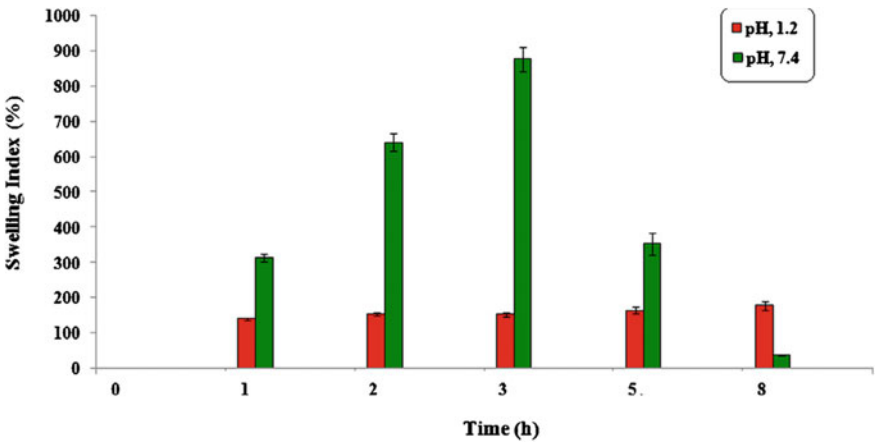


Fig. 13 In vitro swelling behavior of optimized pectinate-JSS composite beads of metformin HCl in gastric pH (1.2) and intestinal pH (7.4) [mean \pm SD, $n = 3$] [94]. (Copyright © 2013 Elsevier B.V.)

Ex vivo wash off study of optimized pectinate-JSS composite beads of metformin HCl was performed using goat intestinal mucosal tissues. Ex vivo wash off of these composite beads in alkaline intestinal pH (7.4) was found faster as compared to that in acidic gastric pH (1.2). The percentage of these beads adhered to the intestinal mucosal tissue in gastric pH (1.2) was reported as $70.05 \pm 4.22\%$ over 8 h of wash off; while in the intestinal pH (7.4), this was found $36.64 \pm 3.45\%$ (Fig. 14).

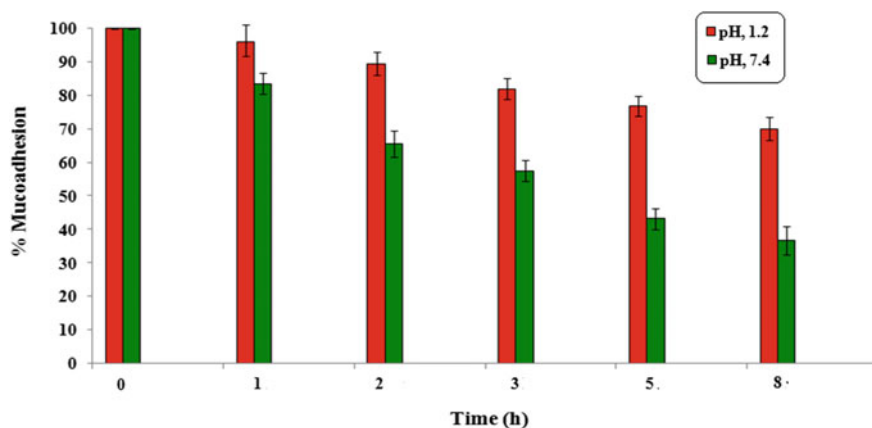


Fig. 14 Ex vivo mucoadhesivity of optimized pectinate-JSS composite beads of metformin HCl in gastric pH (1.2) and intestinal pH (7.4) [mean \pm SD, $n = 3$] [94]. (Copyright © 2013 Elsevier B.V.)

In alloxan-induced diabetic Albino rats, in vivo pharmacodynamic study of optimized pectinate-JSS composite mucoadhesive beads of metformin HCl after oral administration was performed through determining the blood-glucose levels. The relative in vivo blood-glucose level and the average percentage reduction in blood-glucose level demonstrated a significant ($p < 0.05$) antidiabetic action *over a prolonged period in the* alloxan-induced diabetic rats (Fig. 15). These pectinate-JSS composite mucoadhesive beads of metformin HCl *may possibly be lucrative in terms of* prolonged systemic absorption of metformin HCl controlling tight blood-glucose level with higher patient compliances.

4 Conclusion

JSS extracted from jackfruit seeds is one of the natural derived starch materials, which is being used in various industrial applications including foods and pharmaceuticals. JSS is reported as potential pharmaceutical excipients in the formulations of various pharmaceutical dosage forms, such as binding agent and disintegrants in pharmaceutical tablets, emulsifier in emulsions, suspending agent in suspensions, and biomucoadhesive agent in biomucoadhesive dosage forms. Recently, JSS has been utilized as polymer blends with other biocompatible polymers like sodium alginate, gellan gum, and low methoxy pectin to prepare controlled drug-releasing composite beads. All these JSS-based composite beads were prepared through ionotropic-gelation technique. These JSS-based composite beads were found suitable to encapsulate various types of drugs and to release encapsulated drugs in sustained manner

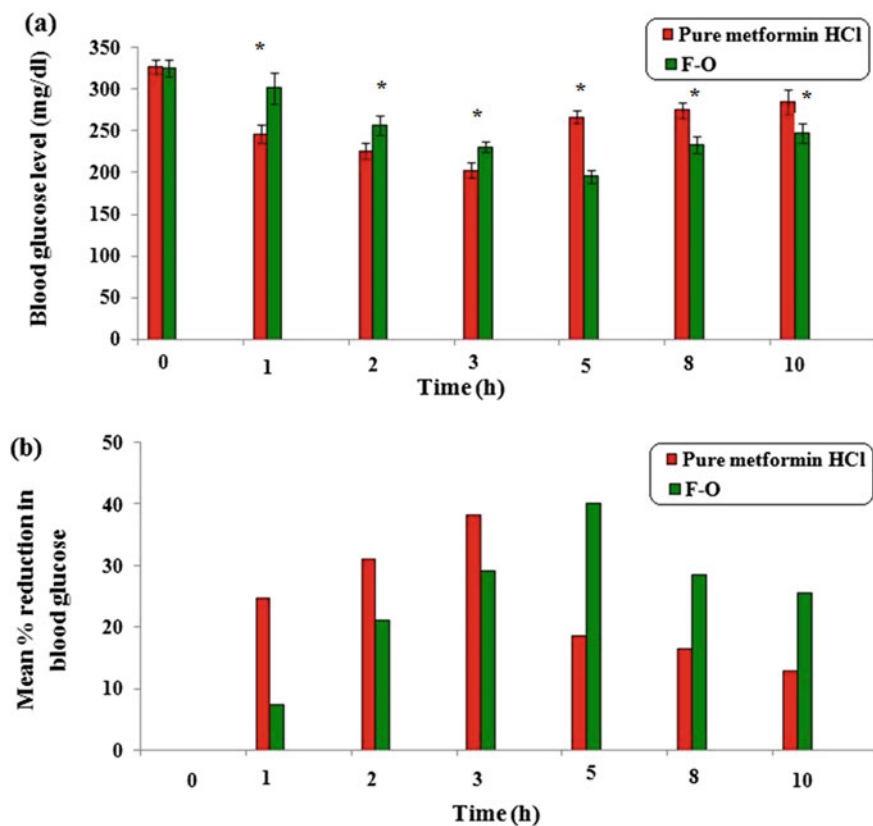


Fig. 15 **a** Comparative in vivo levels of blood glucose and **b** comparative in vivo mean percentage reduction in levels of blood glucose in alloxan-induced diabetic rats after oral administration of pure metformin HCl and pectinate-JSS composite beads of metformin HCl (F-O). The data were analyzed for significant differences ($*p < 0.05$) by paired samples t-test [94]. (Copyright © 2013 Elsevier B.V.)

over prolonged period. All these JSS-based composite beads demonstrated significant hypoglycemic actions in the treated alloxan-induced diabetic Albino rats *over prolonged period* after administration through oral route.

References

1. Nayak AK, Ara TJ, Hasnain MS, Hoda N (2018) Okra gum-alginate composites for controlled releasing drug delivery. In: Inamuddin, Asiri AM, Mohammad A (eds) Applications of nanocomposite materials in drug delivery. Woodhead Publishing Series in Biomaterials, Elsevier Inc., United States, pp 761–785

2. Guru PR, Bera H, Das M, Hasnain MS, Nayak AK (2018) Aceclofenac-loaded *Plantago ovata* F. husk mucilage-Zn²⁺-pectinate controlled-release matrices. *Starch—Stärke* 70:1700136
3. Nayak AK, Pal D, Santra K (2016) Swelling and drug release behavior of metformin HCl-loaded tamarind seed polysaccharide-alginate beads. *Int J Biol Macromol* 82:1023–1027
4. Pal D, Nayak AK (2015) Alginates, blends and microspheres: controlled drug delivery. In: Mishra M (ed) *Encyclopedia of biomedical polymers and polymeric biomaterials*. vol 1. Taylor and Francis, New York, pp 89–98
5. Nayak AK, Ahmad SA, Beg S, Ara TJ, Hasnain MS (2018) Drug delivery: present, past and future of medicine. In: Inamuddin, Asiri AM, Mohammad A (eds) *Applications of nanocomposite materials in drug delivery*. Woodhead Publishing Series in Biomaterials, Elsevier Inc., United States, pp 255–282
6. Nayak AK (2011) Controlled release drug delivery systems. *Sci J UBU* 2:1–10
7. Nayak AK, Hasnain MS (2019) Background: multiple units in oral drug delivery. In: Nayak AK, Hasnain MS (eds) *Plant polysaccharides-based multiple-unit systems for oral drug delivery*. Springer, Singapore, pp 1–17
8. Nayak AK, Hasnain MS, Pal D (2018) Gelled microparticles/beads of sterculia gum and tamarind gum for sustained drug release. In: Thakur VK, Thakur MK (eds) *Handbook of springer on polymeric gel*. Springer Nature, Singapore, pp 361–414
9. Pal D, Nayak AK (2017) Plant polysaccharides-blended ionotropically-gelled alginate multiple-unit systems for sustained drug release. In: Thakur VK, Thakur MK, Kessler MR (eds) *Handbook of composites from renewable materials*, Volume 6, *Polymeric Composites*, WILEY-Scrivener, USA, pp 399–400
10. Nayak AK (2016) Tamarind seed polysaccharide-based multiple-unit systems for sustained drug release. In: Kalia S, Averous L (eds) *Biodegradable and bio-based polymers: environmental and biomedical applications*. USA, Wiley-Scrivener, pp 471–494
11. Malakar J, Nayak AK (2012) Formulation and statistical optimization of multiple-unit ibuprofen-loaded buoyant system using 2³-factorial design. *Chem Eng Res Design* 9:1834–1846
12. Malakar J, Nayak AK, Pal D (2012) Development of cloxacillin loaded multiple-unit alginate-based floating system by emulsion–gelation method. *Int J Biol Macromol* 50(1):138–147
13. Sharma HK, Sarangi B, Pradhan SP (2009) Preparation and in vitro evaluation of mucoadhesive microbeads containing timolol maleate using mucoadhesive substances of *Dellinia india* L. *Arch Pharm Res* 1:181–8
14. Nayak AK, Hasnain MS, Beg S, Alam MI (2010) Mucoadhesive beads of gliclazide: design development and evaluation. *Sci Asia* 36(4):319–325
15. Sharma VK, Bhattacharya A (2008) Release of metformin hydrochloride from ispaghula-sodium alginate beads adhered on cock intestinal mucosa. *Indian J Pharm Edu Res* 42:365–72
16. Nayak AK, Pal D (2011) Development of pH-sensitive tamarind seed polysaccharide-alginate composite beads for controlled diclofenac sodium delivery using response surface methodology. *Int J Biol Macromol* 49:784–793
17. Pal D, Nayak AK (2012) Novel tamarind seed polysaccharide-alginate mucoadhesive microspheres for oral gliclazide delivery. *Drug Deliv* 19:123–131
18. Nayak AK, Das B, Maji R (2012) Calcium alginate/gum Arabic beads containing glibenclamide: development and in vitro characterization. *Int J Biol Macromol* 51:1070–1078
19. Guru PR, Nayak AK, Sahu RK (2013) Oil-entrapped sterculia gum-alginate buoyant systems of aceclofenac: development and in vitro evaluation. *Colloids Surf B: Biointerf* 104:268–275
20. Nayak AK, Pal D (2013) Ionotropically-gelled mucoadhesive beads for oral metformin HCl delivery: formulation optimization and antidiabetic evaluation. *J Sci Indus Res* 72:15–22
21. Nayak AK, Pal D, Pradhan J, Hasnain MS (2013) Fenugreek seed mucilage-alginate mucoadhesive beads of metformin HCl: design optimization and evaluation. *Int J Biol Macromol* 54:144–154
22. Ahuja M, Yadav M, Kumar S (2010) Application of response surface methodology to formulation of ionotropically gelled gum cordia/gellan beads. *Carbohydr Polym* 80:161–7

23. Nayak AK, Pal D, Malakar J (2013) Development, optimization and evaluation of emulsion-gelled floating beads using natural polysaccharide-blend for controlled drug release. *Polym Eng Sci* 53:338–350
24. Nayak AK, Pal D, Das S (2013) Calcium pectinate-fenugreek seed mucilage mucoadhesive beads for controlled delivery of metformin HCl. *Carbohydr Polym* 96:349–357
25. Das B, Dutta S, Nayak AK, Nanda U (2014) Zinc alginate-carboxymethyl cashew gum microbeads for prolonged drug release: development and optimization. *Int J Biol Macromol* 70:505–515
26. Nayak AK, Pal D, Santra K (2014) Development of calcium pectinate-tamarind seed polysaccharide mucoadhesive beads containing metformin HCl. *Carbohydr Polym* 101:220–230
27. Nayak AK, Pal D, Santra K (2014) Tamarind seed polysaccharide-gellan mucoadhesive beads for controlled release of metformin HCl. *Carbohydr Polym* 103:154–163
28. Nayak AK, Pal D, Santra K (2014) Development of pectinate-ispaghula mucilage mucoadhesive beads of metformin HCl by central composite design. *Int J Biol Macromol* 66:203–221
29. Sinha P, Ubaidulla U, Nayak AK (2015) Okra (*Hibiscus esculentus*) gum-alginate blend mucoadhesive beads for controlled glibenclamide release. *Int J Biol Macromol* 72:1069–1075
30. Nayak AK, Pal D, Santra K (2014) Ispaghula mucilage-gellan mucoadhesive beads of metformin HCl: development by response surface methodology. *Carbohydr Polym* 107:41–50
31. Sinha P, Ubaidulla U, Hasnain MS, Nayak AK, Rama B (2015) Alginate-okra gum blend beads of diclofenac sodium from aqueous template using ZnSO₄ as a cross-linker. *Int J Biol Macromol* 79:555–563
32. Hasnain MS, Rishishwar P, Rishishwar S, Ali S, Nayak AK (2018) Isolation and characterization of *Linum usitatissimum* polysaccharide to prepare mucoadhesive beads of diclofenac sodium. *Int J Biol Macromol* 116:162–172
33. Nayak AK, Hasnain MS (2019) Linseed polysaccharide based multiple units for oral drug delivery. In: Nayak AK, Hasnain MS (eds) *Plant polysaccharides-based multiple-unit systems for oral drug delivery*. Springer, Singapore, pp 117–121
34. Nayak AK, Hasnain MS (2019) Some other plant polysaccharide based multiple units for oral drug delivery. In: Nayak AK, Hasnain MS (eds) *Plant polysaccharides-based multiple-unit systems for oral drug delivery*. Springer, Singapore, pp 1123–1128
35. Nayak AK, Pal D (2016) Sterculia gum-based hydrogels for drug delivery applications. In: Kalia S (ed) *Polymeric hydrogels as smart biomaterials*. Springer International Publishing, Switzerland, Springer Series on Polymer and Composite Materials, pp 105–151
36. Hasnain MS, Rishishwar P, Ali S (2017) Use of cashew bark exudate gum in the preparation of 4% lidocaine HCl topical gels. *Int J Pharm Pharm Sci* 9(8):146–150
37. Hasnain MS, Rishishwar P, Ali S (2017) Floating-bioadhesive matrix tablets of hydralazine HCl made of cashew gum and HPMC K4M. *Int J Pharm Pharm Sci* 9(7):124–129
38. Das B, Nayak AK, Nanda U (2013) Topical gels of lidocaine HCl using cashew gum and Carbopol 940: preparation and in vitro skin permeation. *Int J Biol Macromol* 62:514–517
39. Nayak AK, Pal D (2016) Plant-derived polymers: Ionically gelled sustained drug release systems. In: Mishra MM (ed) *Encyclopedia of biomedical polymers and polymeric biomaterials*. vol 8. Taylor and Francis, New York, pp 6002–6017
40. Nayak AK, Pal D, Pany DR, Mohanty B (2010) Evaluation of *Spinacia oleracea* L. leaves mucilage as innovative suspending agent. *J Adv Pharm Technol Res* 1(3):338–341
41. Nayak AK, Pal D (2018) Functionalization of tamarind gum for drug delivery. In: Thakur VK, Thakur MK (eds) *Functional biopolymers*. Springer, Cham, pp 35–56
42. Nayak AK, Bera H, Hasnain MS, Pal D (2018) Synthesis and characterization of graft-copolymers of plant polysaccharides. In: Thakur VK (ed) *Biopolymer grafting, synthesis and properties*. Elsevier Inc., Netherlands, pp 1–62
43. Nayak AK, Hasnain MS (2019) Plant polysaccharides in drug delivery applications. In: Nayak AK, Hasnain MS (eds) *Plant polysaccharides-based multiple-unit systems for oral drug delivery*. Springer, Singapore, pp 19–23
44. Hasnain MS, Rishishwar P, Rishishwar S, Ali S, Nayak AK (2018) Extraction and characterization of cashew tree (*Anacardium occidentale*) gum; use in aceclofenac dental pastes. *Int J Biol Macromol* 116:1074–1081

45. Nayak AK, Pal D, Santra K (2015) Screening of polysaccharides from tamarind, fenugreek and jackfruit seeds as pharmaceutical excipients. *Int J Biol Macromol* 79:756–760
46. Nayak AK, Pal D (2017) Tamarind seed polysaccharide: an emerging excipient for pharmaceutical use. *Indian J Pharm Edu Res* 51:S136–S146
47. Prajapati VD, Jani GK, Moradiya NG, Randeria NP (2013) Pharmaceutical applications of various natural gums, mucilages and their modified forms. *Carbohydr Polym* 92:1685–1699
48. Jena AK, Nayak AK, De A, Mitra D, Samanta A (2018) Development of lamivudine containing multiple emulsions stabilized by gum odina. *Fut J Pharm Sci* 4:71–79
49. Nayak AK, Pal D, Pradhan J, Ghorai T (2012) The potential of *Trigonella foenum-graecum* L. seed mucilage as suspending agent. *Indian J Pharm Edu Res* 46:312–317
50. Nayak AK, Ansari MT, Sami F, Bera H, Hasnain MS. Cashew gum in drug delivery applications. In: Hasnain MS, Nayak AK (eds) *Natural polysaccharides in drug delivery and biomedical applications*. Academic Press, Elsevier Inc., United States, pp 263–283
51. Dey S, Nandy BC, De JN, Hasnain MS, Nayak AK. Tamarind gum in drug delivery applications. In: Hasnain MS, Nayak AK (eds) *Natural polysaccharides in drug delivery and biomedical applications*. Academic Press, Elsevier Inc., United States, pp 285–306
52. Samanta A, De A, Hasnain MS, Bera H, Nayak AK (2019) Gum odina as pharmaceutical excipient. In: Hasnain MS, Nayak AK (eds) *Natural polysaccharides in drug delivery and biomedical applications*. Academic Press, Elsevier Inc., United States, pp 327–337
53. Jana S, Maiti S, Jana S, Sen KK, Nayak AK (2019) Guar gum in drug delivery applications. In: Hasnain MS, Nayak AK (eds) *Natural polysaccharides in drug delivery and biomedical applications*. Academic Press, Elsevier Inc., United States, pp 187–201
54. Nayak AK, Ahmed SA, Tabish M, Hasnain MS (2019) Natural polysaccharides in tissue engineering application. In: Hasnain MS, Nayak AK (eds) *Natural polysaccharides in drug delivery and biomedical applications*. Academic Press, Elsevier Inc., United States, pp 531–548
55. Nayak AK, Hasnain MS, Pal K, Banerjee I, Pal D (2020) Gum-based hydrogels in drug delivery. In: Pal K, Banerjee I, Sarkar P, Kim D, Deng W-P, Dubey NK, Majumder K (eds) *Biopolymer-based formulations, biomedical and food applications*. Elsevier Inc., United States, pp 605–645
56. Hasnain MS, Rishishwar P, Ali S, Alkahtani S, Tabish M, Milivojevic M, Ansari MT, Nayak AK (2020) Formulation and Ex vivo skin permeation of lidocaine HCl topical gels using dillenia (*Dillenia indica* L.) fruit gum. *Rev Mex Ing Quím* 19:1465–1476
57. Hasnain MS, Guru PR, Rishishwar P, Ali S, Ansari MT, Nayak AK (2020) Atenolol-releasing buccal patches made of *Dillenia indica* L. fruit gum: preparation and Ex vivo evaluations. *SN Applied Sci* 2:57
58. Hasnain MS, Rishishwar P, Ali S, Nayak AK (2020) Preparation and evaluation of aceclofenac dental pastes using dillenia fruit gum for periodontitis treatment. *SN Appl Sci* 2(3):1–8
59. Nayak AK, Nanda SS, Yi DK, Hasnain MS, Pal D (2019) Pharmaceutical applications of tamarind gum. In: Nayak AK, Hasnain MS, Pal D (eds) *Natural polymers for pharmaceutical applications, Volume I: plant derived polymers*. Apple Academic Press, USA, pp 1–20
60. Nayak AK, Hasnain MS (2019) Locust bean gum based multiple units for oral drug delivery. In: Nayak AK, Hasnain MS (eds) *Plant polysaccharides-based multiple-unit systems for oral drug delivery*. Springer, Singapore, pp 61–66
61. Hasnain MS, Nayak AK, Ansari MT, Pal D (2019) Pharmaceutical applications of locust bean gum. In: Nayak AK, Hasnain MS, Pal D (eds) *Natural polymers for pharmaceutical applications, Volume I: plant derived polymers*. Apple Academic Press, USA, pp 139–162
62. Hasnain MS, Ahmed SA, Alkahtani S, Milivojevic M, Kandar CC, Dhara AK, Nayak AK (2020) Biopolymers for Drug Delivery. In: Nayak AK, Hasnain MS (eds) *Advanced biopolymeric systems for drug delivery*. Springer, Switzerland, pp 1–29
63. Nayak AK, Hasnain MS (2019) Sterculia gum based multiple units for oral drug delivery. In: Nayak AK, Hasnain MS (eds) *Plant polysaccharides-based multiple-unit systems for oral drug delivery*. Springer, Singapore, pp 67–82

64. Nayak AK, Hasnain MS (2019) Okra gum based multiple units for oral drug delivery. In: Nayak AK, Hasnain MS (eds) Plant polysaccharides-based multiple-unit systems for oral drug delivery. Springer, Singapore, pp 83–92
65. Bera H, Abbasi YF, Hasnain MS, Nayak AK (2019) Sterculia gum in drug delivery applications. In: Hasnain MS, Nayak AK (eds) Natural polysaccharides in drug delivery and biomedical applications. Academic Press, Elsevier Inc., United States, pp 223–247
66. Nayak AK, Hasnain MS (2019) Fenugreek seed mucilage based multiple units for oral drug delivery. In: Nayak AK, Hasnain MS (eds) Plant polysaccharides-based multiple-unit systems for oral drug delivery. Springer, Singapore, pp 93–112
67. Pal D, Chandra P, Sachan N, Hasnain MS, Nayak AK (2019) Pharmaceutical applications of fenugreek seed gum. In: Nayak AK, Hasnain MS, Pal D (eds) Natural polymers for pharmaceutical applications, Vol. I: Plant derived polymers. Apple Academic Press, USA, pp 203–226
68. Nayak AK, Pal D (2014) *Trigonella foenum-graecum* L. seed mucilage-gellan mucoadhesive beads for controlled release of metformin HCl. Carbohydr Polym 107:31–40
69. Nayak AK, Hasnain MS (2019) Gum Arabic based multiple units for oral drug delivery. In: Nayak AK, Hasnain MS (eds) Plant polysaccharides-based multiple-unit systems for oral drug delivery. Springer, Singapore, pp 25–30
70. Nayak AK, Hasnain MS (2019) Tamarind polysaccharide based multiple units for oral drug delivery. In: Nayak AK, Hasnain MS (eds) Plant polysaccharides-based multiple-unit systems for oral drug delivery. Springer, Singapore, pp 31–59
71. Builders PF, Arhewoh MI (2016) Pharmaceutical applications of native starch in conventional drug delivery. Starch/Stärke 68:864–73
72. Vashisht D, Pandey A, Jayaram KK (2015) Physicochemical and release properties of carboxymethylated starches of Dioscorea from Jharkhand. Int J Biol Macromol 74:523–529
73. Misale BV, Gavali HBM, Katare SD, Yadav AV (2008) Sago starch capsule shell: a suitable alternative to gelatin capsule shells. Indian J Pharm Edu Res 42:48–52
74. Deepika V, Kumar KJ, Anima P (2013) Isolation and partial characterization of delayed releasing starches of Colocasia species from Jharkhand India. Carbohydr Polym 96:253–8
75. Manek RV, Builders PF, Kolling WM, Emeje M, Kunle OO (2012) Physicochemical and binder properties of starch obtained from *Cyperus esculentus*. AAPS Pharm Sci Tech 13:379–88
76. Builders PF, Anwunobi AP, Mbah CC, Adikwu MU (2013) New direct compression excipient from tiger nut starch: physicochemical and functional properties. AAPS Pharm Sci Tech 14:818–27
77. Das D, Jha S, Jayram KK (2015) Isolation and release characteristics of starch from the rhizome of Indian Palo. Int J Biol Macromol 72:341–6
78. Okunlola A, Odeku OA (2011) Evaluation of starches obtained from four *Dioscorea* species as binding agent in chloroquine phosphate tablet formulations. Saudi Pharm J 19:95–105
79. Ahmad MZ, Akhter S, Ahmad I, Rahman R, Anwar M, Jain GK, Ahmad FJ, Khar RK (2011) Development of polysaccharide based colon targeted drug delivery system: design and evaluation of Assam Bora rice starch based matrix tablet. Curr Drug Deliv 8:575–581
80. Akin-Ajani OD, Itiola OA, Odeku OA (2005) Effects of plantain and corn starches on the mechanical and disintegration properties of paracetamol tablets. AAPS Pharm Sci Tech 6:E458–E463
81. Casas M, Ferrero C, Jimene-Castellanos MR (2010) Graft tapioca starch copolymers as novel excipients for controlled-release matrix tablets. Carbohydr Polym 80:71–77
82. Nayak AK, Pal D. Natural starches-blended ionotropically-gelled microparticles/beads for sustained drug release. In: Thakur VK, Thakur MK, Kessler MR (eds) Handbook of composites from renewable materials, Nanocomposites: advanced applications, vol 8. Wiley-scrivener, USA, pp 527–560
83. Nayak AK, Hasnain MS (2019) Potato starch based multiple units for oral drug delivery. In: Nayak AK, Hasnain MS (eds) Plant polysaccharides-based multiple-unit systems for oral drug delivery. Springer, Singapore, pp 113–116

84. Nayak AK, Hasnain MS (2020) Ionotropically gelled alginate particles in sustained drug release. In: Nayak AK, Hasnain MS (eds) *Alginates in drug delivery*. Academic Press, Elsevier Inc., United States, pp 203–230
85. Nayak AK, Bera H, Hasnain MS (2020) Particulate matrices of ionotropically gelled alginate- and plant-derived starches for sustained drug release. In: Nayak AK, Hasnain MS (eds) *Alginates in drug delivery*. Academic Press, Elsevier Inc., United States, pp 257–295
86. Nayak AK, Beg S, Hasnain MS, Malakar J, Pal D (2018) Soluble starch-blended Ca²⁺-Zn²⁺-alginate composites-based microparticles of aceclofenac: Formulation development and in vitro characterization. *Fut J Pharm Sci* 4:63–70
87. Malakar J, Nayak AK, Das A (2013) Modified starch (cationized)-alginate beads containing aceclofenac: formulation optimization using central composite design. *Starch—Stärke* 65:603–612
88. Malakar J, Nayak AK, Jana P, Pal D (2013) Potato starch-blended alginate beads for prolonged release of tolbutamide: Development by statistical optimization and in vitro characterization. *Asian J Pharm* 7:43–51
89. Sachan NK, Bhattyacharya A (2009) Feasibility of Assam bora rice based matrix microdevices for controlled release of water insoluble drug. *Int J Pharm Pharm Sci* 1:96–102
90. Sachan NK, Bhattyacharya A (2006) Evaluation of Assam Bora rice starch as a possible natural mucoadhesive polymer in the formulation of microparticulate controlled drug delivery systems. *J Assam Sci Soc* 47:34–47
91. Sachan NK, Bhattacharya A (2009) Modelling and characterization of drug release from glutinous rice starch based hydrogel beads for controlled drug delivery. *Int J Health Res* 2:93–99
92. Nayak AK, Pal D (2013) Formulation optimization of jackfruit seed starch-alginate mucoadhesive beads of metformin HCl. *Int J Biol Macromol* 59:264–272
93. Nayak AK, Pal D, Hasnain MS (2013) Development, optimization and in vitro-in vivo evaluation of pioglitazone-loaded jackfruit seed starch-alginate beads. *Curr Drug Deliv* 10:608–619
94. Nayak AK, Pal D (2013) Blends of jackfruit seed starch-pectin in the development of mucoadhesive beads containing metformin HCl. *Int J Biol Macromol* 62:137–145
95. Nayak AK, Pal D, Santra K (2014) *Artocarpus heterophyllus* L. seed starch-blended gellan gum mucoadhesive beads of metformin HCl. *Int J Biol Macromol* 65:329–339
96. Biswas N, Sahoo RK (2016) Tapioca starch blended alginate mucoadhesive-floating beads for intragastric delivery of metoprolol tartrate. *Int J Biol Macromol* 83:61–70
97. Zhu K, Zhang Y, Nie S, Xu F, He S, Gong D, Wu G, Tan L (2017) Physicochemical properties and in vitro antioxidant activities of polysaccharide from *Artocarpus heterophyllus* Lam. *Pulp Carbohydr Polym* 155:354–361
98. Baliga MS, Shivashankara AR, Haniadka R, Dsouza J, Bhat HP. Phytochemistry, nutritional and pharmacological properties of *Artocarpus heterophyllus* lam. (jackfruit): a review. *Food Res Int* 44:1800–1811
99. Aldana DLM, Gómez BT, Oca MMM, Ayerdi SGS, Meraz FG, Pérez LAB (2011) Isolation and characterization of Mexican jackfruit (*Artocarpus heterophyllus* L) seeds starch in two mature stages. *Starch/Stärke* 63:364–372
100. Madruga MS, de Albuquerque FSM, Silva IFA, do Amaral DS, Magnani M, Neto VQ (2014) Chemical, morphological and functional properties of Brazilian jackfruit (*Artocarpus heterophyllus* L.) seeds starch. *Food Chem* 143:440–445
101. Prakash O, Kumar R, Mishra A, Gupta R (2009) *Artocarpus heterophyllus* (Jackfruit): an overview. *Pharmacog Rev* 3:353–358
102. Rengsuthi K, Charoenrein S (2011) Physicochemical properties of jackfruit seed starch (*Artocarpus heterophyllus*) and its application as a thickener and stabiliser in chilli sauce. *LWT-Food Sci Tech* 44:1309–1313
103. Kavitha K, Kurma SR, Mishra SH (1991) Studies on Jackfruit starch as pharmaceutical adjuvant. *Indian J Nat Prod* 8:20–24

104. Tulyathan V, Tananuwong K, Songjinda P, Jaiboon N (2002) Some physicochemical properties of jackfruit (*Artocarpus heterophyllus* Lam) seed flour and starch. *Sci Asia* 28:37–41
105. Kittipongpatana N, Janta S, Kittipongpatana O (2011) Preparation of cross-linked carboxymethyl jackfruit starch and evaluation as a tablet disintegrant. *Pak J Pharm Sci* 24:415–420
106. Bobbio FO, EI-Dash AA, Bobbio PA, Rodrigues LR (1978) Isolation and characterization of the physio-chemical properties of the starch of jackfruit seeds (*Artocarpus heterophyllus*). *Cer Chem* 55:505–511
107. Khunkitti W, Aromdee C, Vorarat S, Chitropas P (2006) The potential of jackfruit starch for use as suspending agent and emulsifying agent. *Songklan J Sci Technol* 28:145–155
108. Narkhede SB, Bendale AR, Jadhav AG, Patel K, Vidyasagar G (2011) Isolation and evaluation of starch of *Artocarpus heterophyllus* as a tablet binder. *Inter J PharmTech Res* 3:836–840
109. Sabale V, Patel V, Paranjape A (2012) Isolation and characterization of jackfruit mucilage and its comparative evaluation as a mucoadhesive and controlled release component in buccal tablets. *Int J Pharm Investig* 2:61–69
110. Hasnain MS, Jameel E, Mohanta B, Dhara AK, Alkahtani S, Nayak AK (2020) Alginates: sources, structure, and properties. In: Nayak AK, Hasnain MS (eds) *Alginates in drug delivery*. Academic Press, Elsevier Inc., United States, pp 1–17
111. Dey S, Roy S, Hasnain MS, Nayak AK (2020) Grafted alginates in drug delivery. In: Nayak AK, Hasnain MS (eds) *Alginates in drug delivery*. Academic Press, Elsevier Inc., United States, pp 71–100
112. Yang JS, Xie YJ, He W (2011) Research progress on chemical modification of alginate: a review. *Carbohydr Polym* 84:33–39
113. Hasnain MS, Ray P, Nayak AK (2020) Alginate-based interpenetrating polymer networks for sustained drug release. In: Nayak AK, Hasnain MS (eds) *Alginates in drug delivery*. Academic Press, Elsevier Inc., United States, pp 101–128
114. Nayak AK, Ansari MT, Sami F, Balvir Singh HK, Hasnain MS (2020) Alginates as drug delivery excipients. In: Nayak AK, Hasnain MS (eds) *Alginates in drug delivery*. Academic Press, Elsevier Inc., United States, pp 19–39
115. Goh CH, Heng PWS, Chan LW (2012) Alginates as a useful natural polymer for microencapsulation and therapeutic applications. *Carbohydr Polym* 88:1–12
116. Hasnain MS, Nayak AK (2018) Alginate-inorganic composite particles as sustained drug delivery matrices. In: Inamuddin, Asiri AM, Mohammad A (eds) *Applications of nanocomposite materials in drug delivery*. Woodhead Publishing Series in Biomaterials, Elsevier Inc., United States, pp 39–74
117. Nanda SS, Yi DK, Hasnain MS, Nayak AK (2019) Hydroxyapatite-alginate composites in drug delivery. In: Hasnain MS, Nayak AK (eds) *Alginate: versatile polymer in biomedical applications and therapeutics*. Apple Academic Press, USA, pp 483–503
118. Nayak AK, Hasnain MS, Nanda SS, Yi DK (2019) Hydroxyapatite-alginate based matrices for drug delivery. *Current Pharm Design* 25:3406–3416
119. Kurakula M, Rao GSNK, Kiran V, Hasnain MS, Nayak AK (2020) Alginate-based hydrogel systems for drug releasing in wound healing. In: Nayak AK, Hasnain MS (eds) *Alginates in drug delivery*. Academic Press, Elsevier Inc., United States, pp 323–358
120. Nayak AK, Mohanta BC, Hasnain MS, Hoda MN, Tripathi G (2020) Alginate-based scaffolds for drug delivery in tissue engineering. In: Nayak AK, Hasnain MS (eds) *Alginates in drug delivery*. Academic Press, Elsevier Inc., United States, pp 359–386
121. Hasnain MS, Ahmad SA, Chaudhary N, Hoda MN, Nayak AK (2019) Biodegradable polymer matrix nanocomposites for bone tissue engineering. In: Inamuddin, Asiri AM, Mohammad A (eds) *Applications of nanocomposite materials in orthopedics*. Woodhead Publishing Series in Biomaterials, Elsevier Inc., United States, pp 1–37
122. Hasnain MS, Kiran V, Kurakula M, Rao GSNK, Tabish M, Nayak AK (2020) Use of alginates for drug delivery in dentistry. In: Nayak AK, Hasnain MS (eds) *Alginates in drug delivery*. Academic Press, Elsevier Inc., United States, pp 387–404

123. Hasnain MS, Nayak AK, Kurakula M, Hoda MN (2020) Alginate nanoparticles in drug delivery. In: Nayak AK, Hasnain MS (eds) Alginates in drug delivery. Academic Press, Elsevier Inc., United States, pp 129–152
124. Nayak AK, Ghosh Laskar M, Hasnain MS, Pal D (2019) Pharmaceutical applications of alginates. In: Nayak AK, Hasnain MS, Pal D (eds) Natural polymers for pharmaceutical applications, Vol. II: Marine and microbiologically derived polymers. Apple Academic Press, USA, pp 37–70
125. Malakar J, Das K, Nayak AK (2014) *In situ* cross-linked matrix tablets for sustained salbutamol sulfate release—formulation development by statistical optimization. *Polym Med* 44:221–230
126. Malakar J, Dutta P, Purokayastha SD, Dey S, Nayak AK (2014) Floating capsules containing alginate-based beads of salbutamol sulfate: in vitro-in vivo evaluations. *Int J Biol Macromol* 64:181–189
127. Mohanta BC, Javed MN, Hasnain MS, Nayak AK (2020) Polyelectrolyte complexes of alginate for controlling drug release. In: Nayak AK, Hasnain MS (eds) Alginates in drug delivery. Academic Press, Elsevier Inc., United States, pp 297–321
128. Ray P, Maity M, Barik H, Sahoo GS, Hasnain MS, Hoda MN, Nayak AK (2020) Alginate-based hydrogels for drug delivery applications. In: Nayak AK, Hasnain MS (eds) Alginates in drug delivery. Academic Press, Elsevier Inc., United States, pp 41–70
129. Nayak AK, Khatua S, Hasnain MS, Sen KK (2011) Development of alginate-PVP K 30 microbeads for controlled diclofenac sodium delivery using central composite design. *DARU J Pharm Sci* 19(5):356–366
130. Pal D, Nayak AK (2011) Development, optimization and anti-diabetic activity of gliclazide-loaded alginate-methyl cellulose mucoadhesive microcapsules. *AAPS Pharm Sci Tech* 12(4):1431–1441
131. Hasnain MS, Nayak AK, Singh M, Tabish M, Ansari MT, Ara TJ (2016) Alginate-based bipolymeric-nanobioceramic composite matrices for sustained drug release. *Int J Biol Macromol* 83:71–77
132. Das MK, Senapati PC (2008) Furosemide-loaded alginate microspheres prepared by ionic cross-linking technique: Morphology and release characteristics. *Indian J Pharm Sci* 70:77–84
133. Hua S, Ma H, Li X, Yang H, Wang A (2010) pH-sensitive sodium alginate/poly (vinyl alcohol) hydrogel beads prepared by combined cross-linking and freeze-thawing cycles for controlled release of diclofenac sodium. *Int J Biol Macromol* 46:517–523
134. Nayak AK, Das B (2018) Introduction to polymeric gels. In: Pal K, Bannerjee I (eds) Polymeric gels characterization, properties and biomedical applications. Woodhead Publishing Series in Biomaterials, Elsevier Ltd., United States, pp 3–27
135. Morshad MM, Mallick J, Nath AK, Uddin MZ, Dutta M, Hossain MA, Kawsar MH (2012) Effect of barium chloride as a cross-linking agent on the sodium alginate based diclofenac sodium beads. *Bangladesh Pharm J* 15:53–57
136. Chowdhury S, Chakraborty S, Maity M, Hasnain MS, Nayak AK (2020) Biocomposites of alginates in drug delivery. In: Nayak AK, Hasnain MS (eds) Alginates in drug delivery. Academic Press, Elsevier Inc., United States, pp 153–185
137. Das S, Pattanayak D, Nayak AK, Yi DK, Nanda SS, Ansari MT, Hasnain MS (2020) Alginate–montmorillonite composite systems as sustained drug delivery carriers. In: Nayak AK, Hasnain MS (eds) Alginates in drug delivery. Academic Press, Elsevier Inc., United States, pp 187–201
138. Hasnain MS, Ahmed SA, Behera A, Alkahtani S, Nayak AK (2020) Inorganic materials–alginate composites in drug delivery. In: Nayak AK, Hasnain MS (eds) Alginates in drug delivery. Academic Press, Elsevier Inc., United States, pp 231–256
139. Pongjayakul T, Puttipipatkachorn S (2007) Xanthan–alginate composite gel beads: molecular interaction and in vivo characterization. *Int J Pharm* 331:61–71
140. Pal D, Nayak AK. Interpenetrating polymer networks (IPNs): Natural polymeric blends for drug delivery. In: Mishra M (ed) Encyclopedia of biomedical polymers and polymeric biomaterials. vol. 7. Taylor and Francis, New York, pp 4120–4130

141. Singh B, Sharma V, Chauhan D (2010) Gastroretentive floating sterculia-alginate beads for use in antiulcer drug delivery. *Chem Eng Res Des* 88:997–1012
142. Pasparakis G, Bouropoulos N (2006) Swelling studies and in vitro release of verapamil from calcium alginate-chitosan beads. *Int J Pharm* 323:34–42
143. Hamcerencu M, Desbrieres J, Khoukh A, Popa M, Riess G (2008) Synthesis and characterization of new unsaturated esters of gellan gum. *Carbohydr Polym* 71:92–100
144. Milivojevic M, Pajic-Lijakovic I, Bugarski B, Nayak AK, Hasnain MS (2019) Gellan gum in drug delivery applications. In: Hasnain MS, Nayak AK (eds) *Natural polysaccharides in drug delivery and biomedical applications*. Academic Press, Elsevier Inc., United States, pp 145–186
145. Jana S, Das A, Nayak AK, Sen KK, Basu SK (2013) Aceclofenac-loaded unsaturated esterified alginate/gellan gum microspheres: In vitro and in vivo assessment. *Int J Biol Macromol* 57:129–137
146. Babu RJ, Sathigrahi S, Kumar MT, Pandit JK (2010) Formulation of controlled release gellan gum macro beads of amoxicillin. *Curr Drug Deliv* 7:36–43
147. Munarin F, Tanzi MC, Petrini P (2012) Advances in biomedical applications of pectin gels. *Int J Biol Macromol* 51:681–689
148. Nayak AK, Kalia S, Hasnain MS (2013) Optimization of aceclofenac-loaded pectinate-poly (vinyl pyrrolidone) beads by response surface methodology. *Int J Biol Macromol* 62:194–202
149. Das S, Ng K-Y (2010) Resveratrol-loaded calcium pectinate beads: effects of formulation parameters on drug release characteristics. *J Pharm Sci* 99:840–860
150. El-Glibaly I (2001) Oral delayed-release system based on Zn-pectinate gel (ZPG) microparticles as an alternative carrier to calcium pectinate beads for colonic drug delivery. *Int J Pharm* 232:199–221

Polymeric Nanocomposites for Cancer-Targeted Drug Delivery



**Luiza Steffens Reinhardt, Mabilly Cox Holanda de Barros Dias,
Jussania Gnoatto, Anna Wawruszak, Marta Hałasa, Pablo Ricardo Arantes,
Neil J. Rowan, and Dinara Jaqueline Moura**

Abbreviations

α -CD	α -cyclodextrin
ADCs	Antibody-drug conjugates
Ag	Silver
ALK	Anaplastic lymphoma kinase
AuNR	Gold nanorod
BBB	Blood brain barrier
BD	Brownian dynamics
BRAF	V-raf murine sarcoma viral oncogene homolog B1
BRCA	Breast cancer gene
BRD4	Bromodomain containing 4
BTB	Brain tumor barrier
CDK4/6	Cyclin-dependent kinase
CDK7	Cyclin-dependent kinase 7

L. S. Reinhardt (✉) · D. J. Moura

Laboratory of Genetic Toxicology, Federal University of Health Sciences of Porto Alegre, Porto Alegre, Rio Grande do Sul, Brazil

e-mail: luizasteffens@live.com

M. C. H. de Barros Dias · N. J. Rowan

Biosciences Research Institute, Athlone Institute of Technology, Athlone, Co. Westmeath, Ireland

J. Gnoatto

Chemistry Institute, Federal University of Rio Grande do Sul, Porto Alegre, Rio Grande do Sul, Brazil

A. Wawruszak · M. Hałasa

Department of Biochemistry and Molecular Biology, Medical University of Lublin, Lublin, Poland

P. R. Arantes

Department of Bioengineering, University of California, Riverside, USA

© The Author(s), under exclusive license to Springer Nature Switzerland AG 2022

241

M. S. Hasnain et al. (eds.), *Polymeric and Natural Composites*,

Advances in Material Research and Technology,

https://doi.org/10.1007/978-3-030-70266-3_8

CS	Chitosan
CSCs	Cancer stem cells
CT	Chemotherapy
CTS	Chondroitin sulphate
DDFT	Dynamic density functional theory
DOX	Doxorubicin
DPD	Dissipative particle dynamics
EGFR	Epidermal growth factor receptor
FEM	Finite element method
FDM	Finite difference method
FVM	Finite volume method
GO	Graphene-oxide
HATs	Histone acetyltransferases
HDACs	Histone deacetylases
HDI	Histone deacetylase inhibitors
HER2	Human epidermal growth factor receptor 2
IGF-1	Insulin-like growth factor-1
IONPs	Iron oxide NPs
LB	Lattice Boltzmann
LOI	Loss of imprinting
mTOR	Mammalian target of rapamycin
MET	Hepatocyte growth factor receptor
MD	Molecular dynamics
MC	Monte Carlo
MTX-PEG	Methotrexate-PEG
NIR	Near-infrared radiation
NK	Natural killer
NP	Nanoparticle
NSCLC	Non-small cell lung carcinoma
NTRK	Neurotrophic receptor tyrosine kinase
PAA	Poly (acrylic acid)
PARP	Poly (ADP-ribose) polymerase
PCL	Polycaprolactone
PD-1	Programmed cell death protein 1
PD-L1	Programmed cell death protein 1-ligand
PDMS	Poly(N-isopropylacrylamide)-metal NPs
PEG	Poly (ethyleneglycol)
PEI	Poly(ethylene imine)
PGA	Poly (glutamic acid)
PI3K	Phosphatidylinositol 3-kinase
PLGA	Poly (lactic-co-glycolic acid)
PLLA	Poly-L-lactic acid
PMMA	Poly (methyl methacrylate),
pNIPAM	Poly(N-isopropylacrylamide)
PS	Polystyrene

PTT	Photothermal therapy
PTX	Paclitaxel
PU	Polyurethane
PVA	Polyvinyl alcohol
PVDF	Polyvinylidene fluoride
QM	Quantum mechanics
RGD peptide	Arginylglycylaspartic
ROS	Reactive oxygen species
RT	Radiotherapy
SEs	Super-enhancers
SHH	Sonic hedgehog signalling molecule
TDGL	Time-dependent Ginzburg–Landau
VEGF	Vascular endothelial growth factor
WS ₂ -NT-CM-PEI	Tungsten disulphide nanotubes-ceric ammonium nitrate-PEI

1 Introduction

Cancer represents a multifaceted group of diseases that present unregulated cellular death and growth processes. Cancer is developed as a consequence of DNA mutations that can be triggered by the environment or/and DNA replication errors or can be hereditary [1]. This process is comprised by three stages, initiation, promotion and progression, and it is known as the carcinogenesis multistep model [2].

The conventional cancer management involves several different treatment options depending on different parameters and characteristics such as the tumour type and the grade, nevertheless, surgical resection, systemic chemotherapy (CT), radiotherapy (RT) and immunotherapy are the most common therapies. CT drugs are not specific, thus, they can affect healthy cells developing numerous side effects [3]. As an alternative to the CT conventional treatment, nanotechnological approaches that comprise targeted and controlled drug delivery systems can be used to improve the therapy outcomes including patients' quality of life and survival by enhancing drugs distribution, pharmacokinetics and stability [3–5].

Cancer-targeted drug delivery refers, quantitatively and selectively, to drug accumulation within the tumour site [6, 7]. Preferably, for CT formulations to be effective in cancer therapy, they must be biofunctionalized with suitable size and surface charge and must target specific biomolecules.

In the nanosystems field, polymeric nanocomposites have been shown promising features for cancer-targeted drug delivery [8–12], and thus, this chapter will discuss what is known about the use of nanocomposites for cancer management, what has been produced and tested, how these systems can bypass CT drawbacks and how multiscale molecular simulation for nanostructured polymer systems can guide the development of nanocomposites.

2 Cancer Overview

Cancer is currently recognized as a major disease estimating over 18 million of new cases, and resulting over 9,5 million deaths in 2018 worldwide [13]. The most common cancer types for both sexes and all ages in 2018 are lung, breast and colorectal cancer, which account for over 30 percentage of all cancer cases [13]. Taking into account the gender, the top five most common types of cancer are lung, prostate, colorectal, stomach and liver for men, and breast, colorectal, lung, cervix uteri and thyroid for women in 2018 [13].

Cancer is a collective term for diseases characterized by abnormal and uncontrolled cell growth affecting nearby tissues. Cancer cells are able to spread to other body parts (metastasis) using blood and lymph systems [14]. The mechanism of cancer formation is multifactorial and is initiated by environment as well as genetics, highlighting the combination of external factors and internal genetic modifications, which lead to cancer disease [15]. Several risk factors have been identified as crucial in tumorigenesis. These include lifestyle factors such as smoking, alcohol consumption, diet, obesity, cancer-causing substances and other external factors including age, radiation, infectious organisms, environmental pollution and sunlight [16, 17].

Among all risk factors, smoking is well documented [18, 19]. It has to be emphasized that not only regularly smokers belong to the group of increased risk of cancer, but also second-hand smokers are affected [18]. There are growing evidence that obesity is strongly associated with cancer risk and progression [20–22]. The excess of energy resulting from obesity is responsible for changes in insulin, insulin-like growth factor-1 (IGF-1), leptin and steroid hormones levels, what in turn leads to altering nutritional environment, and is able to support tumour initiation and progression [21]. Alcohol consumption is classified as carcinogenic due to its first product of metabolism: acetaldehyde. Acetaldehyde produces free radicals, promoting cancer development [23]. Additionally, ethanol is associated with reduction of inflammatory mediators increasing tumour formation [24]. Lifestyle factors required to be paid attention, as they are potentially changeable, and people are able to reduce or completely eliminate the impact of these factors on their life.

Next to environmental factors, landscape of cancer is created by genetic alterations as well as epigenetic abnormalities. Balance between tumour suppressor genes and oncogenes allows unrestricted cell growth leading to cancer progression. Activation of oncogenes and/or inactivation of tumour suppressors enhances division or inhibits cell apoptosis, as protein products of these genes regulate different cellular pathways that control cell proliferation, migration and apoptosis [25]. The development of malignant tumour occurs as a result of stepwise accumulation of alterations in both proto-oncogenes and tumour suppressor genes, which both are referred to as critical genes [25]. Genetic alteration includes genomic instability as well as genetic mutations affecting changes within nucleotide sequence. In turn, epigenetic modifications do not alter DNA sequence, wherein they are associated with histone modifications, DNA methylation, loss of imprinting (LOI) and regulation by miRNA [25, 26].

The initiation of the carcinogenesis process occurs as a result of either spontaneous mutations or mutations induced by chemical, physical and biological carcinogens.

Tumour suppressor genes encode molecules responsible for the regulation of many pathways and mechanisms involved in programmed cell death, cell division, differentiation and migration, repair of DNA damage, cell cycle checkpoints as well as inhibition of tumour metastasis [27]. Because the main function of tumour suppressors is to suppress the development of tumour, the appearance of mutations within these genes results in the onset of cancer development. By contrast, proto-oncogenes are normal genes that encode proteins involved in cell growth and cell differentiation, nonetheless, as a result of the mutation, the specific protein involved in the regulation is overexpressed and an oncogene is formed. Among the proto-oncogenes it should be distinguished: genes encoding growth factors, transcription factors, receptor and cytoplasmic tyrosine kinases as well as serine/threonine kinases [28, 29].

The traditional cancer treatment strategies include surgery, RT, CT and immunotherapy. Nowadays, innovative cancer therapies such as targeted therapies are being widely studied [30]. CT targets both, rapidly dividing cancer cells as well as normal cells, and is commonly used in combination with surgery or RT depending on type and stage of cancer [31]. The main limitation of CT is high number of serious side effects [32]. CT has short-term and long-term side effects. Short-time side effects are correlated with high toxicity of used drugs and occur during cancer treatment. In turn, long-term side effects include further complications proceeding after adjuvant CT. The side effects depend on the agents' specificity, dosage and duration of treatment [33]. According to The American Cancer Society, the most common CT side effects are: fatigue, loss of hair, infections, anaemia, vomiting, changes in appetite, obstipation, diarrhoea, pain with swallowing, destroying of nerve system as well as skin, nails, urine and bladder changes, and weight and sexual function changes [34]. Additionally, patients treated with CT may develop resistance to chemotherapeutics, leading to cancer recurrence and progression [35].

More accurate and advanced genetic and molecular characterization of cancer landscape significantly contributed to development of efficient immunotherapies. Immunotherapy supports the recognition of cancer cells as foreign to the host immune system and stimulates the immune system [36]. The main goal of this therapy is to improve antitumour response and decrease side effects commonly occurred during CT treatment. The mechanism of action is based on activation (or activation enhancement) of immune system to attack and destroy cancer cells using natural mechanism, which are often avoided in cancer progression [37]. There are growing number of immuno-drugs approved by US Food and Drug Administration [37], and many of immuno-drugs are currently under clinical trials [38]. Although the immunotherapy seems to be burdened with less side effects than CT, the serious adverse effects such as autoimmunity and non-specific inflammation have been observed [37].

Recently, the changes in genetic profile causing mutations and modifications of oncoproteins as well as tumour suppressor proteins have become promising targets in anticancer treatment [39]. These molecular targets are crucial for designing new drugs, which are able to directly affect the targets. In targeted therapy small molecules are used to enter inside the cell, and attack a specific protein or gene [40], as well as

monoclonal antibodies, which in turn are dedicated for targets placed outside the cells [41], and cancer vaccines as well [39]. The main limitation for molecular targeted therapy is its effectiveness only in cells that express a particular target. Moreover, as in CT, development of drug resistance can be expected [39].

Although the growing number of preclinical and clinical studies show satisfactory and promising results for patients at different types and stages of cancers [42–45] leading to decrease of overall cancer morbidity and mortality, the new strategies for cancer treatment are highly needed to reduce side effects and improve patient prognosis. Molecular biology combined with nanotechnology seems to be the key direction in searching for new cancer strategy assuring low-cost, non-invasive and more personalized oncological care [46].

3 Understanding Targeted Therapy

Targeted therapy is one category of cancer treatment that uses CT drugs as well as other compounds to precisely recognize and assault strictly defined types of cancer cells. Targeted therapy has an anticancer effect through numerous mechanisms, including: induction of apoptosis, inhibition of proliferation, suppression of metastasis, regulation of immune function as well as multidrug resistance reversal [47]. Trastuzumab, a recombinant monoclonal antibody, which can recognize the extracellular domain of human epidermal growth factor receptor 2 (HER2) transmembrane protein, was one of the first target-specific drugs that have been registered for clinical use of cancer. Recently, designing targeted drugs and incorporating them into treatment has become the therapeutic standard [48]. Modern targeted therapies include: monoclonal antibodies [48], antibody-drug conjugates [49], nanobodies [50], antiangiogenic agents [51], signal transduction inhibitors [52], immunotherapeutic agents [53], cancer stem cells targeted drugs [54], miRNAs [55] and complexes of super-enhancers targeted agents [56].

3.1 *Antibody–Drug Conjugates (ADCs)*

Antibody–drug conjugates (ADCs) are a category of innovative and promising therapeutic strategy for cancer therapy. ADCs are able to target highly expressed antigens on the surface of carcinoma cells and then selectively deliver cytotoxic active agents. The goal of this therapy is to reduce systemic cytotoxicity in comparison with classic CT drugs and optimizing tumour targeting. Researchers aim to improve the effectiveness of ADCs by using a cleavable linker, which allows the delivery of the toxic payload to surrounding cells that do not expressed the target protein. Thus, ADCs act not only on the heterogeneous tumour, but also on its microenvironment consisting of various cell populations [49].

3.2 *Nanobodies*

The development of targeted therapy significantly expanded the treatment options for oncological patients and sets new directions of research in the field of anti-cancer therapies. Monoclonal antibodies have become a treatment standard in recent years. Despite the popularity of this therapy, traditional monoclonal antibodies have a number of limitations related to their use, such as limited ability to penetrate the tumour, high ability to develop therapeutic resistance and high production costs. Recently discovered nanobodies are an alternative to monoclonal antibodies. By combining the therapeutic advantages of standard antibodies and the targeting potential of nanoscale delivery, nanobodies approach allows high translational potential in preclinical and clinical studies [50].

3.3 *Antiangiogenic Agents*

The vascular endothelial growth factor (VEGF) pathway is the key mediator of angiogenesis in cancer. Creating new blood vessels on the basis of an existing one is the key process for supplying nutrients and oxygen to proliferating cancer cells, which promotes tumour growth and formation of distant metastases. Therefore, many types of therapies, including tyrosine kinase inhibitors or monoclonal antibodies target this axis [51].

3.4 *Immunotherapeutic Agents*

Targeting innate checkpoint molecules on macrophages and natural killer (NK) cells has appeared as a new rational approach against tumours, which are resistant to T cell-mediated immunity. Because different monoclonal antibodies against carcinoma surface proteins have been clinically approved in haematological disorders, innate checkpoint blockade can play a pivotal role in augmenting phagocytosis and antibody-mediated cellular cytotoxicity [57]. Targeting the programmed cell death protein 1 (PD-1) and programmed cell death protein 1 - ligand (PD-L1) interactions is a relatively novel cancer therapeutic strategy. Inhibitors of PD-1/PD-L1 include small-molecule chemical compounds, peptides and antibodies [53].

3.5 *Cancer Stem Cells (CSCs)-Targeted Therapy*

Cancer stem cells (CSCs) are a population of cancer cells, which is responsible for tumour initiation, metastasis and relapse as well as drug and radiation resistance.

Therefore, targeting CSCs is considered a novel potential anticancer-targeted therapeutic strategy. CSCs play a key role in immune evasion, immunomodulation and effector immunity, which changes immune system balance. NOTCH, mammalian target of rapamycin (mTOR), sonic hedgehog signalling molecule (SHH) and Wnt/ β -catenin are associated in CSCs targeted therapies due to the fact that they are involved in regulation the CSCs colonies progression and drug resistance. Understanding the signalling pathways regulating progression of CSCs and drug resistance is crucial in conducting effective targeted therapies [54].

3.6 MiRNAs-Targeted Therapy

MicroRNAs are able to regulate activity both oncogenes and tumour suppressor genes. Therefore, alteration in the expression of microRNAs can lead to tumorigenesis. Expression profiling of microRNAs has increased the possibilities of application of microRNAs as potential biomarkers and targeted therapeutic targets in cancers [55].

3.7 Complexes of Super-Enhancers Targeted Therapy

The overexpression and hyper activation of oncogenes commonly occur in many types of cancers. Latterly, the increased activation of oncogenes by super-enhancers (SEs) has attracted significant attention. Numerous studies indicate that the SEs and their associated complexes play an important role in the development of different types of malignant tumours. Clinical trials have demonstrated that small-molecule inhibitors, like bromodomain containing 4 (BRD4) and cyclin-dependent kinase 7 (CDK7) inhibitors are able to target the SEs resulting in considerable positive effect on cancer treatment [56].

3.8 Nanotechnology-Based Histone Deacetylase Inhibitors

Epigenetic reprogramming, including DNA histone modification and DNA methylation, regulates the expression of genes involved in immune checkpoints, cellular proliferation and the response to antineoplastic drugs [58]. Histone acetylation and deacetylation catalyzed by histone acetyltransferases (HATs) and histone deacetylases (HDACs) are the posttranslational epigenetic mechanisms of gene expression regulation. These epigenetic modifications of DNA structure affect the action of transcription factors, which can repress or induce gene transcription. Mutations and changes of the expression of HDAC genes can cause the aberrant transcription of key genes, which regulate many pivotal cancer pathways, such as cell-cycle regulation,

cell proliferation or apoptosis [59]. Histone deacetylase inhibitors (HDIs) have been accomplished therapeutic success in haematological diseases. Unfortunately, their application in solid tumours is hampered by the low treatment efficacy and confronts big challenges. Medicine with the use of nanotechnology could prolong the circulation half-life, improve drug stability and increase intratumoral drug accumulation. Hence, nanomedicine seems to be a promising approach to enhance HDIs therapy efficacy [60].

Targeted drugs used in the most common types of cancer (breast, colorectal, lung, prostate, skin) are summarized in Table 1.

Hence, since targeted medicine or targeted therapy means precise drug efficiency combine with minor side effects and interaction, at the molecular level, between a biomolecule and a drug, multifunctional drug delivery systems such as polymeric nanocomposites can be designed as biofunctionalized carriers that not only transport drugs but also, when combine to biomolecules such as membrane receptors, nucleic acids, antibodies and enzymes, are able to efficiently target cancerous cells.

4 Nanocomposites

Polymers demonstrate several advantages when it comes to develop drug delivery systems due to their ability to maintain a suitable stability and enhance mechanical and physical properties of compounds, however, depending on the polymer chose, if synthetic or natural, it can present some limitations for specific types of tumours and therefore, restrict its application. Combinations and composites of polymers can bypass these drawbacks and improve the quality of these systems, moreover, by combining nanosized materials while producing nanocomposites the drug delivery system can have multifaceted uses and purposes and it might be able to reach challenging areas such as the brain.

Amid the benefits of a nanocomposite system, this approach can avoid nanoparticle (NP) agglomeration by using a polymeric matrix where the NP can be dispersed [67], besides, the nanocomposite biodegradability increases after producing a composite with nanosized systems [68]. By rule, a nanocomposite is a two-phase system, where, at least one constituent must present a nanosized dimension up to 100 nm [69]. An important characteristic of nanocomposites is a large surface area, which results in higher interaction between its nanocomponents with the polymeric matrix [70].

Likewise, nanocomposite drug delivery systems theoretically are able to achieve requirements to deliver an effective cancer treatment owing to the following features:

- a. Nanocomposites enhance drug pharmacodynamics and pharmacokinetics profiles.
- b. Nanocomposites can selectively eradicate tumour cells without affecting healthy cells.
- c. Nanocomposites prolong and control the release of drugs.

Table 1 Targeted drugs used in the most common types of cancer based on <https://www.cancer.org>

Type of the cancer	Subtype of the cancer	Type of targeted therapy	Drug	Reference
Breast cancer	Targeted therapy for HER2-positive breast cancer	Monoclonal antibodies	Trastuzumab–pertuzumab Hyaluronidase	[61]
		Antibody–drug conjugates	Ado-trastuzumab emtansine Fam-trastuzumab deruxtecan	
		Kinase inhibitors	Lapatinib, Neratinib Tucatinib	
	Targeted therapy for hormone receptor-positive breast cancer	CDK4/6 inhibitors	Palbociclib Ribociclib Abemaciclib	
		mTOR inhibitor	Everolimus	
		PI3K inhibitor	Alpelisib	
	Targeted therapy for women with <i>BRCA</i> mutations	PARP inhibitors	Olaparib Talazoparib	
Targeted therapy for triple-negative breast cancer	Antibody–drug conjugate	Sacituzumab govitecan		
Colorectal cancer	Targeted therapy for colorectal cancer	Drugs that target blood vessel formation (VEGF)	Bevacizumab Ramucirumab Ziv-aflibercept	[62]
		Drugs that target cells with <i>EGFR</i> mutations	Cetuximab Panitumumab	
		Kinase inhibitor	Regorafenib	
Lung cancer	Targeted drug therapy for non-small cell lung cancer	Angiogenesis inhibitors	Bevacizumab Ramucirumab	[63]
		EGFR inhibitors used in NSCLC with <i>EGFR</i> mutations	Erlotinib Afatinib Gefitinib Osimertinib Dacomitinib	
		EGFR inhibitors that target cells with the <i>T790M</i> mutation	Osimertinib	
		EGFR inhibitors used for squamous cell NSCLC	Necitumumab	

(continued)

Table 1 (continued)

Type of the cancer	Subtype of the cancer	Type of targeted therapy	Drug	Reference
		Drugs that target cells with <i>ALK</i> mutations	Crizotinib Ceritinib Alectinib Brigatinib Lorlatinib	
		Drugs that target cells with <i>BRAF</i> changes	Dabrafenib Trametinib	
		RET inhibitors	Selpercatinib	
		MET inhibitors	Capmatinib	
		Drugs that target cells with <i>NTRK</i> mutations	Larotrectinib Entrectinib	
Prostate cancer	Targeted therapy for prostate cancer	PARP inhibitors	Rucaparib Olaparib	[64]
Skin cancer	Targeted therapy for basal and squamous cell skin cancers	Hedgehog pathway inhibitors	Vismodegib Sonidegib	[65]
		EGFR inhibitors	Cetuximab	
	Targeted therapy drugs for melanoma skin cancer	BRAF inhibitors	Vemurafenib Dabrafenib Encorafenib	[66]
		MEK inhibitors	Trametinib Cobimetinib Binimetinib	
		Drugs that target cells with <i>C-KIT</i> changes	Imatinib Nilotinib	

Abbreviations: ALK - anaplastic lymphoma kinase, BRAF—v-raf murine sarcoma viral oncogene homolog B1, BRCA—breast cancer gene, CDK4/6—cyclin-dependent kinase, EGFR—epidermal growth factor receptor, HER-2—human epidermal growth factor receptor 2, MET—hepatocyte growth factor receptor, mTOR—mammalian target of rapamycin, NSCLC—non-small-cell lung carcinoma, NTRK—neurotrophic receptor tyrosine kinase, PARP—poly (ADP-ribose) polymerase, PI3K—phosphatidylinositol 3-kinase, VEGF—vascular endothelial growth factor

- d. Nanocomposites improve the cellular uptake of delivered drugs by a targeted approach.
- e. Nanocomposites can diminish drugs dose decreasing its side effects [8, 11, 12, 71, 72].

5 Polymeric Nanocomposites

Recent advances in the biological, chemical and physical fields combined with the challenges and possibilities in nanomedicine have led to new developments in polymer-based nanocomposites for diverse biological applications.

Polymeric nanocomposites are very attractive structures with a dual assembly: one phase is called reinforcing (strong and low-density materials) and is embedded in the matrix phase (tough or ductile materials) [73] and consists of nanomaterials and polymers (synthetic or natural) that form a multiphase solid material [73, 74]. These complex materials generate an adjustable platform with different properties and functionalities, improving the overall features of the component materials used for their synthesis.

Polymeric nanocomposites present several advantages including the retaining, protecting and releasing of biological compounds such as drugs, genes, enzymes and fluorophores for treatment, imaging and diagnostics [75]. Nanocomposites also present advantages as enhanced chemical, electrical, thermal, magnetic, optical, catalytic and mechanical properties [76]. Therefore, polymeric nanocomposites promote enhanced solubility in aqueous medium, high stability in biological systems and increased biocompatibility [74, 75, 77]. Consequently, this multifaceted matrix has shown great potential in drug and gene delivery as suitable drug carriers due to improved features compared to pure NP and polymers.

NP addition into polymeric matrix changes the characteristics of polymers as drug carriers such as: decreases the burst release leading to slower and sustained release, improves drug stability, allows the encapsulation with two or more compounds and facilitates active targeting by functionalization with specific receptors [78]. The drug delivery behavior by polymeric nanocomposites has been evaluated in several studies due to unique features. Both organic and inorganic particles are silica, gold, carbon nanotubes, quantum dots, graphene, liposomes, dendrimers and with diverse forms are core-shell, tubes, sheets, spherical, cylindrical, bring great potential for polymeric nanocomposites on the biomedical field [79–81]. The NP have many advantages to the drug delivery system because of their adjustable particle size, charges and surface [82].

5.1 *Types of Polymers Used for Nanocomposites Synthesis*

Several polymers can be applied for biological purposes such as natural polymers including polysaccharides or proteins and synthetic polymers. The most common polymers used for nanocomposites synthesis are listed in Table 2.

The natural polymers present advantages as biological recognition, remarkable interactions with cells to promote proliferation, adhesion, non-immune response, and biodegradability [97]. However, they demonstrate poor mechanical strength, high speed of degradation and limited supply [98].

Table 2 Types of polymers (natural and synthetic) used for nanocomposites synthesis

Polymers (synthetic and natural)	Biomedical applications/ characteristics	Source	Reference
Polycaprolactone (PCL)	Drug carrier; implantable material	Synthetic	[83]
Poly (methyl methacrylate) (PMMA)	Drug carrier (high drug permeability); biocompatible	Synthetic	[84]
Poly (L-lactic acid) (PLLA)	Drug carrier; scaffolds for tissue regeneration	Synthetic	[85]
Poly (lactic-co-glycolic) acid (PLGA)	Biocompatible; tailorable degradation rate; ease modifying the surface	Synthetic	[86]
Poly (ethylene glycol) (PEG)	Biocompatible; soluble in water; drug carrier	Synthetic	[87]
Polystyrene (PS)	Biocompatible; drug delivery	Synthetic	[88]
Polyvinylidene fluoride (PVDF)	Thermal stability; stimulus-responsive; tissue regeneration	Synthetic	[89]
Polyvinylalcohol (PVA)	Easy degradable; biocompatible decompose necrotic masses	Synthetic	[90]
Poly (glutamic acid) (PGA)	Biodegradable, biocompatible; water-soluble	Synthetic	[91]
Poly (acrylic acid) (PAA)	Biocide properties; biocompatible	Synthetic	[92]
Polyethyleneimine (PEI)	Drug delivery; attachment promoter	Synthetic	[93]
Alginate	Drug delivery; cell transplantation; biocompatible	Natural	[94]
Collagen	Cell attachment ability; biodegradation	Natural	[95]
Chitosan	Antibacterial activity; hydrophilicity; bone regeneration	Natural	[96]
Cellulose	Hydrophilicity; biofunctionality; biocompatible	Natural	[94]
Hyaluronic acid	Swelling capability; non-immunogenic	Natural	[95]
Starch	Biodegradable; biocompatible	Natural	[94]
Gellan gum	Bioadhesive; biocompatible	Natural	[94]

(continued)

Table 2 (continued)

Polymers (synthetic and natural)	Biomedical applications/ characteristics	Source	Reference
Chondroitin sulphate (CTS)	Biodegradable; water adsorbent	Natural	[95]

Abbreviations: CTS—Chondroitin sulphate, PAA—Poly (acrylic acid), PCL—Polycaprolactone, PEG—Poly (ethylene glycol), PGA—Poly (glutamic acid), PLGA—Poly (lactic-co-glycolic acid), PLLA—Poly (L-lactic acid), PMMA—Poly (methyl methacrylate), PS—Polystyrene, PVA—Polyvinylalcohol, PVDF—Polyvinylidene Fluoride

In contrast, synthetic polymers present good mechanical properties, controllable degradability, adequate supply, and they are cheaper. However, some synthetic polymers can show uncontrollable shrinkage and possible local toxicity [99].

Nanocomposites are very interesting structures to overcome these disadvantages and expand the potential of polymers by the connection between them and NP, improving the overall characteristics of materials.

5.2 *Polymeric Nanocomposites and the Advantages for Cancer-Targeted Therapy*

Material science has been an important tool bringing innovations to the treatment, diagnosis, imaging, contrast agent, photothermal ablation agents and magnetic resonance imaging (MRI) in cancer through the materials composition [100]. Due to their complex structure with NP and specific matrix carriers, polymeric nanocomposites improve a set of factors increasing the drug effectiveness in the biological system [101, 102]. CT drugs can affect the healthy tissues and not just the tumor; therefore, these nanomaterials have shown great potential for target-specificity drugs reducing the side effects and increasing the treatment effectiveness [103, 104].

Polymeric nanocomposites achieve many advantages on their use for cancer treatment, such as:

- a. Increases the lifetime of chemotherapeutics;
- b. Improves the solubility of hydrophobic drugs;
- c. Allows the controlled and sustained drug delivery;
- d. Enhances the bioavailability due to accumulation of nanosystems in the tumor tissues;
- e. Protects the drugs against degradation mechanism of the body;
- f. Avoids immunological recognition by surface functionalization;
- g. Permits site-specific active targeting through the use of ligands as antibodies, peptides, growth factors;
- h. Avoids multiple-drug resistance due to passive targeting;
- i. Allows multimodal system acting, concerning different therapeutic approaches (such as hyperthermia) and diagnosis (such as bioimaging).

These advantages make polymeric nanocomposites a potential system for improved treatment if compared to traditional therapies [93, 105–107]. Different types of nanosystems-based nanocomposites with their formulation techniques are summarized in Table 3.

Polymeric nanocomposites have wide applications in controlled, sustained and targeted drug delivery. As shown in the table above, these systems present a set of advantages for cancer therapy as pH-dependant behavior, infrared-light sensitivity, multitargeting and specific targeting as well. The multifunctional features of nanocomposites bring new alternatives in many fields, such as molecular medicine, mostly cancer diagnostics, therapeutics, theranostics and imaging.

5.3 Localized Treatment of Solid Tumors with Polymeric Nanocomposite Systems

Worldwide, large efforts have been made in order to develop nanocomposites systems for localized treatment of tumors, owing to the systemic side effects associated with CT-based approaches. Another important fact is the major percentage of patients with cancer suffer from metastasis [131, 132]. Moreover, some drugs, biomolecules or nanocarriers cannot penetrate the body barriers including membranes, the brain blood barrier (BBB) and the brain tumor barrier (BTB), which suggests the necessity of targeted drug delivery systems for solid tumors therapy.

5.3.1 Injectable Hydrogels

The use of composite nanosystems also could be beneficial for the treatment of solid tumors prior or after surgical procedures guaranteeing suitable drug concentrations in the tumor site and affected regions. Localized treatment can be achieved mainly by using two platforms: intratumoral injection or direct implantation into the tumor site. Even though surgical resection is the standard procedure to treat solid tumors, the complete resection is often impossible and the tumor recurrence incidence is a still a challenge [133]. Thus, with the benefits that the mechanical properties of polymers provide, polymeric hydrogels can be injected into tumors greatly improving the stability of common used drugs.

Recently, Cacicedo et al. produced a nanocomposite by combining cellulose hydrogel with DOX-loaded lipid nanocarriers. It was observed that its intratumor administration in vivo in an orthotropic breast cancer mouse model significantly reduced tumor size, metastasis incidence and side effects associated with DOX application [134], suggesting that is possible to achieve better responses with lower doses of CT drugs. Another possibility for injectable polymeric nanocomposites is the delivery of photothermal therapeutic agents which provide an in situ thermal effect and the drug release can be controlled by local light-radiation heating. Hence, an

Table 3 Polymeric nanocomposites and their formulation techniques, which have conferred targeting ability and efficacy for anticancer therapeutics

Polymeric nanocomposites	Fabrication technique	Therapy and experimental model used and outcome	Reference
PMMA-Si-Gd NPs functionalized with folic acid	Self-assembly	DOX; MCF-7 (breast cancer cell line); pH-responsive; prevent drug leakage, targeting effect in breast cancer cells	[108]
Tungsten disulphide nanotubes-ceric ammonium nitrate-PEI (WS ₂ -NT-CM-PEI)	Focused ultrasound in an emulsion solvent diffusion	PTT; MCF-7 and HeLa (cervical cancer cell line) cells; improved PTT activity in the functionalized group	[109]
Poly(N-isopropylacrylamide)-metal nanoparticles (PDMS)	Soft lithography	MDA-MB-231 (Breast cancer cell line); device multimodal implantable	[9]
Gold nanorod-attached PEGylated graphene-oxide (AuNR-PEG-GO)	Self-assembly	PTT; A431 (epidermoid carcinoma cell line) and xenograft mice were used for testing; improved PTT activity	[110]
PLGA polymeric vesicles-Quantum dots	Emulsion evaporation	Busulfan; J774A (macrophage) cells and rats were used for testing; enhanced drug delivery and improved imaging	[111]
PLGA-PEG-nanoparticles	Double emulsion method	Curcumin; MCF-7 cells; enhanced cytotoxic effects	[112]
PEG-phospholipids-graphene oxide	Hydration method	Resveratrol; Mice; chemo-PTT; eradicated xenografted tumor	[113]
PEG-PCL micelles functionalized with cyclic RGD peptide	Core-crosslinked; Solvent exchange	DOX; U87-MG (glioblastoma) cells; specific target	[114]
PLGA-Silver (Ag) nanofibres	Electrospinning	Hep-G2 (Liver carcinoma cell line); enhanced antitumor activity	[115]
PVA-graphene oxide-organoclay (PVA-ODA-MMT)	Electrospinning;	Osteocarcinoma cells; enhanced antitumor activity	[116]
PCL-polyurethane-Au nanoparticles (PCL-Diol-PU/Au)	Sol-gel	Temozolomide; U87-MG cells; lower burst release; gold coating enhanced the cytotoxicity	[117]

(continued)

Table 3 (continued)

Polymeric nanocomposites	Fabrication technique	Therapy and experimental model used and outcome	Reference
Polyethylene glycolated methotrexate-PEG-chitosan-iron oxide nanoparticles (MTX-PEG-CS-IONPs)	Electrospinning	Prodrug: MTX-PEG; Cy5.5; HeLa cells and xenograft mice; improved anticancer activity	[118]
Organic frameworks-cyanine-Cis-acetonil-DOX (COF-IR783-CAD)	Non-solvent-aided coacervation followed by a chemical crosslinking	DOX; 4T1 (breast cancer cell line) and xenograft mice; chemo-PTT; significant tumor ablation	[119]
Sodium alginate-Poly dopamine-Polyvinylpyrrolidone (ALG/PDA-PVP)	Reversible condensation	DOX; HT29 (human colon cancer cell line); enhanced therapeutic effect	[120]
Polypyrrole/chitosan shell Ag (AgCl/PPC)	One-step electrostatic spraying	3-amino-2-phenyl-4(3H)-quinazolinone; Ehrlich ascites carcinoma cells (EAC); increased cell death in group treated compared to empty formulation and pH-dependant release	[121]
Iron oxide-polyethylene-glycol NPs (Fe3O4-PEG-NPS)	Magnetic stirring and dialysis	DOX or paclitaxel; A2780 and OVCAR-3 (human epithelial ovarian cancer cell lines); apoptosis activation through NF- κ B and BAX overexpression and Bcl-2/survivin inhibition; DOX-loaded was more efficient than paclitaxel-loaded in vivo	[122]
PMAA-grafted Chitosan NPs with Fe3O4 (DOX@Fe3O4@CS/PMAA)	Coprecipitation	DOX; MDA-MB-231 and MCF-7 (breast cancer cell lines); cell viability reduction and DNA fragmentation; pH-dependant release	[123]
Gold nanorods dopamine and PEG-coated (AuNR-PDA)	Graft-polymerization by crosslinking	DOX or Methylene blue; HeLa cells and xenograft mice; ROS generation under laser irradiation and apoptosis induction; PTT combined therapy led to improved tumor reduction	[124]

(continued)

Table 3 (continued)

Polymeric nanocomposites	Fabrication technique	Therapy and experimental model used and outcome	Reference
N-naphthyl- <i>l</i> -O-dimethylmaleoyl chitosan micelles with nanocrystals of iron(III) and manganese(II) (NCS-DMNPs)	Pegylation and self-polymerization	DOX; NIH3T6.7 (fibroblasts) cells; bioimaging (diagnosis) and drug delivery	[125]
Fe3O4 PLGA-PVP-coated nanoparticles anchored with Herceptin and tamoxifen	Reductive amination and dialysis	Tamoxifen; MCF-7 and HeLa cells; hemocompatible and pH-dependant release; apoptosis induction and selective uptake by MCF-7 (HER2 +); PTT combined therapy with tumor reduction	[126]
N-isopropylacrylamide (NIPAm) and methacrylated β -cyclodextrin-based macromer (M β CD) with incorporated Au-NRs and AD-DOX (NIPAm-M β CD-AuNRs-AD-DOX)	Precipitation and dialysis	DOX and PTT; MCF-7, HeLa cells and S180 (murine sarcoma) cells; slow 1-month release from implant; PTT combined therapy with drug release rate increase; biocompatible and pH-dependant system	[127]
Pluronic F127 system with iron oxide (PF127-Fe3O4-DOX)	Self-crosslinking copolymerization	DOX; BE-2-M17 (neuroblastoma cell line) cells; pH-dependant behavior; effective in vitro	[128]
Lanthanide upconverted NPs co-doped with YB + 3 and TM + 3, mesoporous silica coated with a folate-conjugate and copolymerized MAPEG (MUCNPs@C18@PSMN-FA)	Emulsion/solvent evaporation technique	DOX; Human KB cell lines with folic acid receptor, A549 (human alveolar adenocarcinoma cell line) without folic acid receptor and Beas2B (Human bronchial epithelial cells); NIR mediating release and folate-receptor targeting; bioimaging	[129]
Dopamine loaded poly(N-isopropylacrylamide)-propylacrylamide copolymer (pNIPAm-co-pAm/DP)	Free radical polymerization and self-assembly	PTT and Bortezomib or DOX; MC3T3-E1 (osteoblast precursor cell line) and CT26 (colon cancer cell line) cells; PTT combined therapy with apoptosis and irreversible changes in cell morphology; pH-dependant and NIR-dependant release	[130]

Abbreviations: Ag—Silver; AuNR—Gold nanorod, CS—chitosan, DOX—doxorubicin, DP—dopamine, GO—graphene oxide, UONPs—iron oxide nanoparticles, MAPEG—Poly (ethylene glycol) methacrylate, MTX-PEG—methotrexate-PEG, PCL—Polycaprolactone, pAm: propylacrylamide, pNIPAm—poly(N-isopropylacrylamide), PDNH—poly(DBAM-co-NASco-HEMA), PDMS—Poly(N-isopropylacrylamide), PEG—Poly (ethylene glycol), PLGA—Poly (lactic-co-glycolic) acid, PMAA—Poly(methacrylic acid), PMMA—Poly (methyl methacrylate), PTT—Photothermal therapy, PU—polyurethane, PVA—Polyvinylalcohol, RGD peptide—Arginylglycylaspartic acid, WS2-NT-CM-PEI—Tungsten disulphide nanotubes-ceric ammonium nitrate-PEI, NIPAm—N-isopropylacrylamide, NIR—Near-infrared irradiation, PTT—Photothermal therapy and ROS—reactive oxygen species

ideal system must be multifaceted and biocompatible at the same time, and it should control the release of sufficient CT drugs and other agents such as photothermal agents for extended periods and preferentially target only cancerous cells. In view of this, Liu et al. designed and produced a very elegant injectable nanocomposite hydrogel by using methoxy poly(ethylene glycol)-b-poly(ϵ -caprolactone-co-1,4,8-trioxo[4.6]spiro-9-undecanone) (mPECT) diblock copolymer with gold nanorods (AuNR-PECT) combined with paclitaxel-loaded mPECT NP (PTX/mPECT NP) and α -cyclodextrin (α -CD) for local chemo-photothermal synergetic cancer therapy by applying near-infrared radiation (NIR). The authors tested this system in breast cancer models (in vitro and in vivo) and observed that it was capable of delivering a synergetic treatment and inhibiting tumor growth and recurrence [133]. What makes this system incredibly promising is the fact that it can be applied for different combined and multidrug approaches for targeting different types of tumors by changing the target ligands.

In this context, Xu et al. synthesized a core-shell nanocomposite with PEGylated (polyethylene glycol modified) magnetic Prussian blue (PB) NP for the controlled release of DOX, targeted photothermal ablation and pH-triggered CT of tumor cells. The authors observed a significant growth inhibition in vitro in HeLa cells [135]. However, more experiments are necessary to prove these effects. Similarly, Fan et al. produced cyclo (Arg-Gly-Asp-d-Phe-Cys) [c(RGD)] conjugated DOX-loaded PEG Fe₃O₄@polydopamine (PDA) NP to achieve an integrated tumor diagnosis and treatment [136]. It was shown that this system was able to target tumor cells and it presented a suitable stability, moreover, by using xenograft tumor nude mouse injected with HCT-116 cells it was possible to detect clear contrast signals therefore, this nanocomposite demonstrated effective CT-photothermal therapy under NIR irradiation.

Magnetic NP have been considerably studied to treat cancer cells and more recently, they attracted attention to be used as a multimodal therapy owing to the possibility to deliver drugs and heat locally [137–144]. From this perspective, Hervault et al. developed magnetic nanocomposites by combining a thermo and pH responsive polymeric shell (PEG methyl ether methacrylate—PEGMA, di(ethylene glycol) methyl ether methacrylate—DEGMA, 3-(trimethoxysilyl)propyl methacrylate—TMSPMA and 3-vinylbenzaldehyde) with an iron oxide core [145] for the delivery of DOX. This system demonstrated suitable physical and chemical properties and showed potential for in vitro and in vivo testing. Taken together, these studies provide a in situ strategy for the clinical application of nanocomposites in cancer CT-phototherapy.

6 Future Challenges in Cancer Therapy

One of the biggest challenges related to the applicability of polymeric nanocomposites is the translation of an in vitro study to an in vivo study. It is known that most frequent actions for in vitro release studies embrace: cumulative release that

occurs when a compound is released into the same amount of media volume and non-cumulative release that takes place when there is a continuous replacement of the media mimicking a living organism where the drug concentration drops.

These methods are commonly used in *in vitro* biological experiments where cytotoxic analysis is performed by using cancer cell lines. Although experimental conditions of *in vitro* evaluations mimic those of living organisms, for complex drug delivery system as nanocomposites to be recognized as appropriate and safe for anti-tumor treatment, *in vivo* studies are still indispensable. Unfortunately, only a few studies tested nanocomposites systems *in vivo*, therefore their applicability is still uncertain.

In all assurance, to reach a successful therapy without harming healthy tissues has been the key effort of targeting approaches. It is estimated the enhancement of drug delivery to cancer cells with an improved well-developed nanoparticle [6, 7], however, even with intense research developing in the nanocomposites field, no significant clinical results have been described. It is a challenge to bypass drug delivery issues such as early drug degradation, bloodstream circulation time, tissue membranes and systemic toxicity, therefore, for some cancers, the main promising approach to achieve suitable drug delivery is a biofunctionalized nanocarrier. In fact, several nanocarriers have an initial burst release that can cause acute toxicity or release the total amount of a therapeutic compound before reaching the tumor cells, fortunately, both of these issues can be addressed by using targeted drug delivery with polymeric nanocomposites.

7 Multiscale Molecular Simulation for Nanostructured Polymer Systems

Nanostructured polymer systems present particular features which range from the angstrom level of an individual bond between atoms, to nanometres of the polymer chain, micrometres, millimetres, larger in solutions and polymeric nanostructured (Fig. 1).

The different time scales for each material properties may range from femtoseconds to seconds or even hours. On the literature, there are many examples of multiscale nature of nanostructured polymer systems [147–155]. Because of that, several computational methods were developed in order to address these issues [156–164]. These new methods present novel options to design, optimize and predict polymeric structures and properties.

Until the present moment, no computational method is able to cover different size scales of polymers [165] systems. Therefore, the multiscale simulation framework is considered one of the best choices to deal with this issue. The multiscale approach combines various methods and, in the computational chemistry field, it is considered one of the key topics. In order to perform a multiscale simulation, different theories

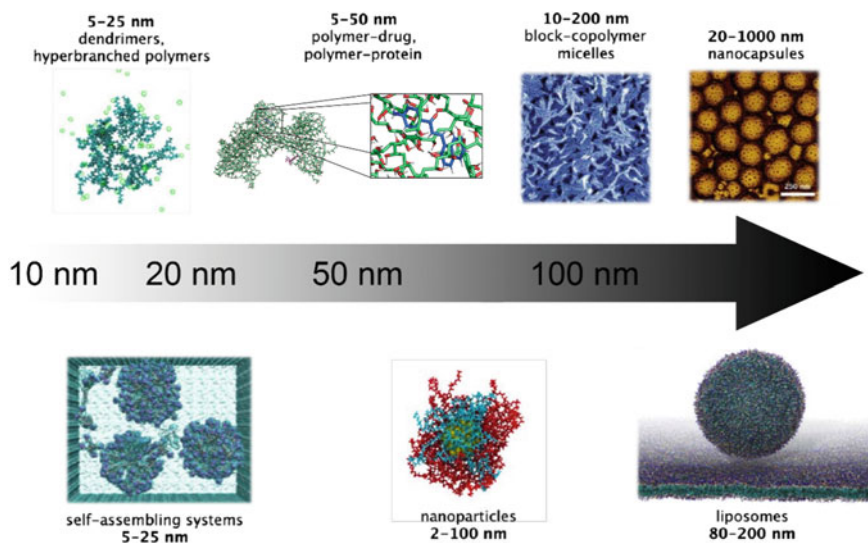


Fig. 1 Nanostructured polymer systems of potential interest for biomedical applications. Increasing structural complexity the dimensions of polymeric systems change from few nanometres to hundreds of nanometres. Adapted from Laurini et al. [146]

and models from four characteristics length and time scales are combined. These features can be divided into the following scales:

- I. The quantum scale: In this method, the nuclei and electrons are part of the calculation, and quantum mechanics (QM) calculations are used to model their state. This approach allows to investigate several phenomena related to chemical reaction, such as rupture and formation of chemical bonds between atoms, the transitions in electrons configurations and other important phenomena on polymers material, that need to be modelled at quantum scale.
- II. The atomistic scale: In the atomistic calculations, all atoms are explicitly represented and treated by a single spheres. The force field, typical interactions in the system, is responsible for the potential energy of the system. These interactions include the bonded interactions that are the bond length, the bond angle and the dihedral angle potentials between atoms. In addition to the bonded interactions, force fields also comprise non-bonded interactions. Non-bonded interactions act between atoms in the same molecule and those in other molecules. Force fields typically distribute non-bonded interactions into two: electrostatic interactions and van der Waals interactions. Molecular dynamics (MD) and Monte Carlo (MC) simulations are examples used at this level to model molecular processes comprising a larger group of atoms, such as proteins, membranes and nucleic acids.
- III. The mesoscopic scale: At this scale, a molecule is defined as a microscopic particle, identified as a bead. In this method, some details of the system are

presented indirectly which offers the opportunity to simulate the phenomena on time scales barely accessible by atomistic simulations. An interesting example is coarse-grained model, where the particles are accumulated in beads. During the calculation, interactions between the beads are used to characterize the system. There are a several methods that were developed to investigate the mesoscopic structures of polymers, including: Brownian dynamics (BD), lattice Boltzmann (LB), dissipative particle dynamics (DPD), dynamic density functional theory (DDFT) and time-dependent Ginzburg–Landau (TDGL).

- IV. The macroscale: In this methodology, the characteristics of atoms and molecules are disregarded, and the system is considered as a continuous. The constitutive laws are responsible for the behaviour of the system. These laws are associated with conservation laws to simulate several phenomena. The main functions, such as velocity and stress components, are continuous. On the other hand, a finite amount of locations which separate continuity regions is considered discontinuous on these calculations. The central supposition at this scale is in substituting a heterogeneous material with a corresponding homogeneous model. To perform molecular simulations at this scale, there are used the following methods: finite volume method (FVM), finite element method (FEM) and finite difference method (FDM).

The development of nanostructured polymer systems requires a comprehensive knowledge of the phenomena at different time and length scales. Because of that, the theoretical and computational methods present great progress, allowing the study of these systems. Finally, given the peculiarities of the polymeric systems, no single method can be used for their simulation. Consequently, it is advantageous to rely on a multiscale molecular modelling approach that has been presented in this chapter. The methodology discussed is an overall design approach for complex nanostructured systems to be effectively interpreted during the experiments and for the design of active nanocomposites and nanosystems.

Final Considerations

Polymeric nanocomposites have been shown suitable mechanical and physicochemical properties to be use as drug delivery systems for cancer therapy. These properties including increased thermal stability, enhanced tensile strength and decreased side effects can be improved by using ligands to target cancer cells. Cancer-drug delivery obtained by targeted approaches has the potential to overcome CT limitations by increasing drug concentrations in the tumor cells and at the same time diminishing the side effects to the normal cells.

Although polymeric nanocomposites are able to provide an efficient drug delivery, it has been observed a lack of in vivo testing, which makes difficult to verify their efficacy. Thus, it is essential, for polymeric nanocomposites research, a collaboration among researchers, regulatory agencies and industry to ensure that these innovative approaches are effective, non-toxic and can be used in the treatment of patients. Further development in nanocomposite technology may prove potent, safe and efficient cancer-targeted drug delivery approaches.

References

1. Tomasetti C, Li L, Vogelstein B (2017) Stem cell divisions, somatic mutations, cancer etiology, and cancer prevention. *Science* 355(6331):1330–1334
2. Siddiqui IA, Sanna V, Ahmad N, Sechi M, Mukhtar H (2015) Resveratrol nanoformulation for cancer prevention and therapy. *Ann N Y Acad Sci* 1348(1):20–31
3. Rita M, Lorena T (2016) Advances on Magnetic Nanocarriers Based on Natural Polymers. *Curr Pharm Des* 22(22):3353–3363
4. Wang M, Thanou M (2010) Targeting nanoparticles to cancer. *Pharmacol Res* 62(2):90–99
5. Zaimy MA, Saffarzadeh N, Mohammadi A, Pourghadamyari H, Izadi P, Sarli A et al (2017) New methods in the diagnosis of cancer and gene therapy of cancer based on nanoparticles. *Cancer Gene Ther* 24(6):233–243
6. Torchilin VP (2010) Passive and active drug targeting: drug delivery to tumors as an example. *Handb Exp Pharmacol* 197:3–53
7. Bae YH, Park K (2011) Targeted drug delivery to tumors: myths, reality and possibility. *J Control Release*. 153(3):198–205
8. Feldman D. Polymers and Polymer Nanocomposites for Cancer Therapy. *Applied Sciences*. 2019;9(18)
9. Kan-Dapaah K, Rahbar N, Soboyejo W (2017) Polymeric composite devices for localized treatment of early-stage breast cancer. *PLoS ONE* 12(2):
10. Mishra DK, Yadav KS, Prabhakar B, Gaud RS. Nanocomposite for cancer targeted drug delivery. *Applications of Nanocomposite Materials in Drug Delivery* 2018, p. 323–37
11. Kaurav H, Manchanda S, Dua K, Kapoor DN (2018) Nanocomposites in Controlled & Targeted Drug Delivery Systems. *Nano Hybrids and Composites*. 20:27–45
12. Senapati S, Mahanta AK, Kumar S, Maiti P (2018) Controlled drug delivery vehicles for cancer treatment and their performance. *Signal Transduct Target Ther*. 3:7
13. Ferlay J, Colombet M, Soerjomataram I, Mathers C, Parkin DM, Piñeros M et al (2019) Estimating the global cancer incidence and mortality in 2018: GLOBOCAN sources and methods. *Int J Cancer* 144(8):1941–1953
14. Institute NC. What is Cancer? 2015 [Available from: <https://www.cancer.gov/publications/dictionaries/cancer-terms/def/cancer>]
15. Parsa N (2012) Environmental factors inducing human cancers. *Iran J Public Health*. 41(11):1–9
16. Wu S, Zhu W, Thompson P, Hannun YA (2018) Evaluating intrinsic and non-intrinsic cancer risk factors. *Nature Communications*. 9(1):3490
17. Anand P, Kunnumakkara AB, Sundaram C, Harikumar KB, Tharakan ST, Lai OS et al (2008) Cancer is a preventable disease that requires major lifestyle changes. *Pharm Res* 25(9):2097–2116
18. García-Esquinas E, Jiménez A, Pastor-Barriuso R, Jones MR, Perez-Gomez B, Navas-Acien A et al (2018) Impact of declining exposure to secondhand tobacco smoke in public places to decreasing smoking-related cancer mortality in the US population. *Environ Int* 117:260–267
19. Lagiou A, Lagiou P (2017) Tobacco smoking and breast cancer: a life course approach. *Eur J Epidemiol* 32(8):631–634
20. Iyengar NM, Gucalp A, Dannenberg AJ, Hudis CA (2016) Obesity and Cancer Mechanisms: Tumor Microenvironment and Inflammation. *J Clin Oncol* 34(35):4270–4276
21. Hopkins BD, Goncalves MD, Cantley LC (2016) Obesity and Cancer Mechanisms: Cancer Metabolism. *J Clin Oncol* 34(35):4277–4283
22. Lennon H, Sperrin M, Badrick E, Renehan AG (2016) The Obesity Paradox in Cancer: a Review. *Curr Oncol Rep*. 18(9):56
23. Seitz HK, Stickel F (2007) Molecular mechanisms of alcohol-mediated carcinogenesis. *Nat Rev Cancer* 7(8):599–612
24. Boffetta P, Hashibe M (2006) Alcohol and cancer. *Lancet Oncol*. 7(2):149–156
25. Wang LH, Wu CF, Rajasekaran N, Shin YK (2018) Loss of Tumor Suppressor Gene Function in Human Cancer: An Overview. *Cell Physiol Biochem* 51(6):2647–2693

26. Peltomäki P (2012) Mutations and epimutations in the origin of cancer. *Exp Cell Res* 318(4):299–310
27. Sherr CJ (2004) Principles of Tumor Suppression. *Cell* 116(2):235–246
28. Cross M, Dexter TM (1991) Growth factors in development, transformation, and tumorigenesis. *Cell* 64(2):271–280
29. Anderson MW, Reynolds SH, You M, Maronpot RM (1992) Role of proto-oncogene activation in carcinogenesis. *Environ Health Perspect* 98:13–24
30. Mun EJ, Babiker HM, Weinberg U, Kirson ED, Von Hoff DD (2018) Tumor-Treating Fields: A Fourth Modality in Cancer Treatment. *Clin Cancer Res* 24(2):266–275
31. Baudino TA (2015) Targeted Cancer Therapy: The Next Generation of Cancer Treatment. *Curr Drug Discov Technol* 12(1):3–20
32. Oun R, Moussa YE, Wheate NJ (2018) The side effects of platinum-based chemotherapy drugs: a review for chemists. *Dalton Trans* 47(19):6645–6653
33. Partridge AH, Burstein HJ, Winer EP (2001) Side Effects of Chemotherapy and Combined Chemohormonal Therapy in Women With Early-Stage Breast Cancer. *JNCI Monographs*. 2001(30):135–142
34. Society AC. Chemotherapy Side Effects 2019 [Available from: <https://www.cancer.org/treatment/treatments-and-side-effects/treatment-types/chemotherapy/chemotherapy-side-effects.html>]
35. Zhang HH, Guo XL (2016) Combinational strategies of metformin and chemotherapy in cancers. *Cancer Chemother Pharmacol* 78(1):13–26
36. Carter BW, Bhosale PR, Yang WT (2018) Immunotherapy and the role of imaging. *Cancer* 124(14):2906–2922
37. Riley RS, June CH, Langer R, Mitchell MJ (2019) Delivery technologies for cancer immunotherapy. *Nat Rev Drug Discov*. 18(3):175–196
38. Sanmamed MF, Chen L (2018) A Paradigm Shift in Cancer Immunotherapy: From Enhancement to Normalization. *Cell* 175(2):313–326
39. Lee YT, Tan YJ, Oon CE (2018) Molecular targeted therapy: Treating cancer with specificity. *Eur J Pharmacol* 834:188–196
40. Nwibo D, Okolo C, Nwibo M (2015) Small Molecule Drugs; Down but Not Out: A Future for Medical Research and Therapeutics. *IOSR Journal of Dental and Medical Sciences*. 14:70–77
41. Joo WD, Visintin I, Mor G (2013) Targeted cancer therapy—are the days of systemic chemotherapy numbered? *Maturitas*. 76(4):308–314
42. Valentino F, Borra G, Allione P, Rossi L (2018) Emerging targets in advanced non-small-cell lung cancer. *Future Oncol*. 14(13s):61–72
43. Tray N, Taff J, Adams S (2019) Therapeutic landscape of metaplastic breast cancer. *Cancer Treat Rev* 79:
44. Das S, Ciombor KK, Haraldsdottir S, Goldberg RM. Promising New Agents for Colorectal Cancer. *Curr Treat Options Oncol*. 2018;19(6):29-
45. Amaria RN, Menzies AM, Burton EM, Scolyer RA, Tetzlaff MT, Antdbacka R et al (2019) Neoadjuvant systemic therapy in melanoma: recommendations of the International Neoadjuvant Melanoma Consortium. *Lancet Oncol*. 20(7):e378–e389
46. de Castro Sant’ Anna C, Junior AGF, Soares P, Tuji F, Paschoal E, Chaves LC, et al. Molecular biology as a tool for the treatment of cancer. *Clin Exp Med*. 2018;18(4):457–64
47. Ke X, Shen L (2017) Molecular targeted therapy of cancer: The progress and future prospect. *Frontiers in Laboratory Medicine*. 1(2):69–75
48. De Laurentiis M, Canello G, Zinno L, Montagna E, Malorni L, Esposito A, et al. Targeting HER2 as a therapeutic strategy for breast cancer: a paradigmatic shift of drug development in oncology. *Annals of Oncology*. 2005;16:iv7-iv13
49. Manzano A, Ocaña A. Antibody-Drug Conjugates: A Promising Novel Therapy for the Treatment of Ovarian Cancer. *Cancers (Basel)*. 2020;12(8)
50. Yang EY, Shah K. Nanobodies: Next Generation of Cancer Diagnostics and Therapeutics. *Front Oncol*. 2020;10:1182-

51. Montemagno C, Pagès G. Resistance to Anti-angiogenic Therapies: A Mechanism Depending on the Time of Exposure to the Drugs. *Front Cell Dev Biol.* 2020;8:584-
52. Huang TT, Lampert EJ, Coots C, Lee JM (2020) Targeting the PI3K pathway and DNA damage response as a therapeutic strategy in ovarian cancer. *Cancer Treat Rev* 86:
53. Guo L, Wei R, Lin Y, Kwok HF. Clinical and Recent Patents Applications of PD-1/PD-L1 Targeting Immunotherapy in Cancer Treatment-Current Progress, Strategy, and Future Perspective. *Front Immunol.* 2020;11:1508-
54. Akbar Samadani A, Keymoradzeh A, Shams S, Soleymannpour A, Elham Norollahi S, Vahidi S, et al. Mechanisms of cancer stem cell therapy. *Clinica Chimica Acta.* 2020
55. Shah V, Shah J. Recent trends in targeting miRNAs for cancer therapy. *Journal of Pharmacy and Pharmacology.*n/a(n/a)
56. Zheng C, Liu M, Fan H (2020) Targeting complexes of super-enhancers is a promising strategy for cancer therapy (Review). *Oncol Lett.* 20(3):2557–2566
57. Alatrash G, Daver N, Mittendorf EA (2016) Targeting Immune Checkpoints in Hematologic Malignancies. *Pharmacol Rev* 68(4):1014–1025
58. Yeon M, Kim Y, Jung HS, Jeoung D. Histone Deacetylase Inhibitors to Overcome Resistance to Targeted and Immuno Therapy in Metastatic Melanoma. *Front Cell Dev Biol.* 2020;8:486-
59. Verza FA, Das U, Fachin AL, Dimmock JR, Marins M (2020) Roles of Histone Deacetylases and Inhibitors in Anticancer Therapy. *Cancers.* 12(6):1664
60. Tu B, Zhang M, Liu T, Huang Y. Nanotechnology-Based Histone Deacetylase Inhibitors for Cancer Therapy. *Front Cell Dev Biol.* 2020;8:400-
61. Society AC. Targeted Therapy for Breast Cancer 2019 [Available from: <https://www.cancer.org/cancer/breast-cancer/treatment/targeted-therapy-for-breast-cancer.html>]
62. Society AC. Targeted Therapy for Colorectal Cancer 2020 [Available from: <https://www.cancer.org/cancer/colon-rectal-cancer/treating/targeted-therapy.html>]
63. Society AC. Targeted Drug Therapy for Non-Small Cell Lung Cancer 2019 Available from: <https://www.cancer.org/cancer/lung-cancer/treating-non-small-cell/targeted-therapies.html>
64. Society AC. Targeted Therapy for Prostate Cancer 2019 [Available from: <https://www.cancer.org/cancer/prostate-cancer/treating/targeted-therapy.html>]
65. Society AC. Targeted Therapy for Basal and Squamous Cell Skin Cancers 2019 Available from: <https://www.cancer.org/cancer/basal-and-squamous-cell-skin-cancer/treating/targeted-therapy.html>
66. Society AC. Targeted Therapy Drugs for Melanoma Skin Cancer 2019 [Available from: <https://www.cancer.org/cancer/melanoma-skin-cancer/treating/targeted-therapy.html>]
67. Chivrac F, Pollet E, Schmutz M, Avérous L (2008) New approach to elaborate exfoliated starch-based nanobiocomposites. *Biomacromol* 9(3):896–900
68. Sothornvit R, Hong S-i, An DJ, Rhim J-W, editors (2010) Effect of clay content on the physical and antimicrobial properties of whey protein isolate/organo-clay composite films
69. Zhang ZL, Le Y, Wang JX, Chen JF (2011) Preparation of stable micron-sized crystalline irbesartan particles for the enhancement of dissolution rate. *Drug Dev Ind Pharm* 37(11):1357–1364
70. Shinde S, Payghan S, D'souza J. Physicochemical assessment of pharmaceutical salt forms: A quality attribute. *Int Res J Invent Pharm Sci.* 2014;2:46–53
71. Yingchoncharoen P, Kalinowski DS, Richardson DR (2016) Lipid-Based Drug Delivery Systems in Cancer Therapy: What Is Available and What Is Yet to Come. *Pharmacol Rev* 68(3):701–787
72. Cho K, Wang X, Nie S, Chen Z, Shin DM (2008) Therapeutic Nanoparticles for Drug Delivery in Cancer. *Clin Cancer Res* 14(5):1310
73. Enisa O-M, Anera K (2020) Nanocomposites: a brief review. *Health and Technology.* 10(1):51–59
74. Mozumder MS, Mairpady A, Mourad AI (2017) Polymeric nanobiocomposites for biomedical applications. *J Biomed Mater Res B Appl Biomater* 105(5):1241–1259
75. Feldman D. Polymer nanocomposites in medicine. 2016. p. 55–62

76. Hussain F, Hojjati M, Okamoto M, Gorga RE (2006) Review article: Polymer-matrix Nanocomposites, Processing, Manufacturing, and Application: An Overview. *J Compos Mater* 40(17):1511–1575
77. Nicole L, Laberty-Robert C, Rozes L, Sanchez C (2014) Hybrid materials science: a promised land for the integrative design of multifunctional materials. *Nanoscale* 6(12):6267–6292
78. Gupta D, Singh D, Kothiyal NC, Saini AK, Singh VP, Pathania D (2015) Synthesis of chitosan-g-poly(acrylamide)/ZnS nanocomposite for controlled drug delivery and antimicrobial activity. *Int J Biol Macromol* 74:547–557
79. Zou Y, Liang J, She Z, Kraatz HB. Gold nanoparticles-based multifunctional nanoconjugates for highly sensitive and enzyme-free detection of E.coli K12. *Talanta*. 2019;193:15–22
80. Li X, Xie C, Xia H, Wang Z (2018) pH and Ultrasound Dual-Responsive Polydopamine-Coated Mesoporous Silica Nanoparticles for Controlled Drug Delivery. *Langmuir* 34(34):9974–9981
81. Luo W, Cheng L, Yuan C, Wu Z, Yuan G, Hou M et al (2019) Preparation, characterization and evaluation of cellulose nanocrystal/poly(lactic acid) in situ nanocomposite scaffolds for tissue engineering. *Int J Biol Macromol* 134:469–479
82. Albanese A, Tang PS, Chan WC (2012) The effect of nanoparticle size, shape, and surface chemistry on biological systems. *Annu Rev Biomed Eng* 14:1–16
83. Kong J, Yu Y, Pei X, Han C, Tan Y, Dong L (2017) Polycaprolactone nanocomposite reinforced by bioresource starch-based nanoparticles. *Int J Biol Macromol* 102:1304–1311
84. Sathya S, Murthy PS, Devi VG, Das A, Anandkumar B, Sathyaseelan VS et al (2019) Antibacterial and cytotoxic assessment of poly (methyl methacrylate) based hybrid nanocomposites. *Mater Sci Eng C Mater Biol Appl*. 100:886–896
85. Lee JH, Park TG, Park HS, Lee DS, Lee YK, Yoon SC et al (2003) Thermal and mechanical characteristics of poly(L-lactic acid) nanocomposite scaffold. *Biomaterials* 24(16):2773–2778
86. Mir M, Ahmed N, Rehman AU (2017) Recent applications of PLGA based nanostructures in drug delivery. *Colloids Surf B Biointerfaces*. 159:217–231
87. Huang H, Xu J, Wei K, Xu YJ, Choi CK, Zhu M et al (2016) Bioactive Nanocomposite Poly (Ethylene Glycol) Hydrogels Crosslinked by Multifunctional Layered Double Hydroxides Nanocrosslinkers. *Macromol Biosci* 16(7):1019–1026
88. Shanmugasundar S, Kannan N, Sundaravadivel E, Zsolt S, Mukunthan KS, Manokaran J et al (2019) Study on the inflammatory response of PMMA/polystyrene/silica nanocomposite membranes for drug delivery and dental applications. *PLoS ONE* 14(3):
89. Arumugam R, Chinnadurai RK, Subramaniam BN, Devaraj B, Subramaniam V, Sekhar SE et al (2018) Scalable novel PVDF based nanocomposite foam for direct blood contact and cardiac patch applications. *J Mech Behav Biomed Mater* 88:270–280
90. Parsa P, Paydayesh A, Davachi SM (2019) Investigating the effect of tetracycline addition on nanocomposite hydrogels based on polyvinyl alcohol and chitosan nanoparticles for specific medical applications. *Int J Biol Macromol* 121:1061–1069
91. Bae HH, Cho MY, Hong JH, Poo H, Sung MH, Lim YT (2012) Bio-derived poly(gamma-glutamic acid) nanogels as controlled anticancer drug delivery carriers. *J Microbiol Biotechnol* 22(12):1782–1789
92. Ahmadvkhani L, Baghban A, Mohammadpoor S, Khalilov R, Akbarzadeh A, Kavetsky T et al (2017) Synthesis and Evaluation of a Triblock Copolymer/ZnO Nanoparticles from Poly(ϵ -caprolactone) and Poly(Acrylic Acid) as a Potential Drug Delivery Carrier. *Drug Res (Stuttg)*. 67(4):228–238
93. Zou Y, Li D, Shen M, Shi X (2019) Polyethylenimine-Based Nanogels for Biomedical Applications. *Macromol Biosci* 19(11):
94. George A, Shah PA, Shrivastav PS (2019) Natural biodegradable polymers based nanoformulations for drug delivery: A review. *Int J Pharm* 561:244–264
95. Finkenstadt VL (2005) Natural polysaccharides as electroactive polymers. *Appl Microbiol Biotechnol* 67(6):735–745
96. Ali A, Ahmed S (2018) A review on chitosan and its nanocomposites in drug delivery. *Int J Biol Macromol* 109:273–286

97. Müllner M (2019) Functional Natural and Synthetic Polymers. *Macromol Rapid Commun* 40(10):
98. Tabasum S, Noreen A, Kanwal A, Zuber M, Anjum MN, Zia KM (2017) Glycoproteins functionalized natural and synthetic polymers for prospective biomedical applications: A review. *Int J Biol Macromol* 98:748–776
99. Mariani E, Lisignoli G, Borzi R, Pulsatelli L. Biomaterials: Foreign Bodies or Tuners for the Immune Response? *International Journal of Molecular Sciences*. 2019;20(3)
100. Feldman D. Polymers and polymer nanocomposites for cancer therapy. *Applied Sciences (Switzerland)*. 2019;9(18): < xocs:firstpage xmlns:xocs = "">
101. Abdelaziz HM, Gaber M, Abd-Elwakil MM, Mabrouk MT, Elgohary MM, Kamel NM et al (2018) Inhalable particulate drug delivery systems for lung cancer therapy: Nanoparticles, microparticles, nanocomposites and nanoaggregates. *J Control Release*. 269:374–392
102. Wang M, Wang D, Chen Q, Li C, Li Z, Lin J (2019) Recent Advances in Glucose-Oxidase-Based Nanocomposites for Tumor Therapy. *Small* 15(51):
103. Bamburowicz-Klimkowska M, Poplawska M, Grudzinski IP (2019) Nanocomposites as biomolecules delivery agents in nanomedicine. *J Nanobiotechnology*. 17(1):48
104. Rahman M, Ahmad MZ, Ahmad J, Firdous J, Ahmad FJ, Mushtaq G et al (2015) Role of Graphene Nano-Composites in Cancer Therapy: Theranostic Applications, Metabolic Fate and Toxicity Issues. *Curr Drug Metab* 16(5):397–409
105. Sivaram AJ, Rajitha P, Maya S, Jayakumar R, Sabitha M (2015) Nanogels for delivery, imaging and therapy. *Wiley Interdiscip Rev Nanomed Nanobiotechnol*. 7(4):509–533
106. Yu X, Wang Z, Su Z, Wei G (2017) Design, fabrication, and biomedical applications of bioinspired peptide-inorganic nanomaterial hybrids. *J Mater Chem B*. 5(6):1130–1142
107. Minelli C, Lowe SB, Stevens MM (2010) Engineering nanocomposite materials for cancer therapy. *Small* 6(21):2336–2357
108. Qin YT, Peng H, He XW, Li WY, Zhang YK (2019) pH-Responsive Polymer-Stabilized ZIF-8 Nanocomposites for Fluorescence and Magnetic Resonance Dual-Modal Imaging-Guided Chemo-/Photodynamic Combinational Cancer Therapy. *ACS Appl Mater Interfaces* 11(37):34268–34281
109. Levin T, Sade H, Binyamini RB, Pour M, Nachman I, Lellouche JP (2019) Tungsten disulfide-based nanocomposites for photothermal therapy. *Beilstein J Nanotechnol*. 10:811–822
110. Demberdorj U, Choi SY, Ganbold EO, Song NW, Kim D, Choo J et al (2014) Gold nanorod-assembled PEGylated graphene-oxide nanocomposites for photothermal cancer therapy. *Photochem Photobiol* 90(3):659–666
111. Ye F, Barrefelt A, Asem H, Abedi-Valuggerdi M, El-Serafi I, Saghaifan M et al (2014) Biodegradable polymeric vesicles containing magnetic nanoparticles, quantum dots and anticancer drugs for drug delivery and imaging. *Biomaterials* 35(12):3885–3894
112. Tabatabaei Mirakabad FS, Akbarzadeh A, Milani M, Zarghami N, Taheri-Anganeh M, Zeighamian V et al (2016) A Comparison between the cytotoxic effects of pure curcumin and curcumin-loaded PLGA-PEG nanoparticles on the MCF-7 human breast cancer cell line. *Artif Cells Nanomed Biotechnol*. 44(1):423–430
113. Hai L, He D, He X, Wang K, Yang X, Liu J et al (2017) Facile fabrication of a resveratrol loaded phospholipid@reduced graphene oxide nanoassembly for targeted and near-infrared laser-triggered chemo/photothermal synergistic therapy of cancer in vivo. *J Mater Chem B*. 5(29):5783–5792
114. Fang Y, Jiang Y, Zou Y, Meng F, Zhang J, Deng C et al (2017) Targeted glioma chemotherapy by cyclic RGD peptide-functionalized reversibly core-crosslinked multifunctional poly(ethylene glycol)-b-poly(ϵ -caprolactone) micelles. *Acta Biomater* 50:396–406
115. Almajhdi FN, Fouad H, Khalil KA, Awad HM, Mohamed SH, Elsarnagawy T et al (2014) In-vitro anticancer and antimicrobial activities of PLGA/silver nanofiber composites prepared by electrospinning. *J Mater Sci Mater Med* 25(4):1045–1053
116. Rzayev ZM, Salimi K, Bunyatova U, Acar S, Salamov B, Turk M (2016) Fabrication and characterization of PVA/ODA-MMT-poly(MA-alt-1-octadecene)-g-graphene oxide e-spun nanofiber electrolytes and their response to bone cancer cells. *Mater Sci Eng C Mater Biol Appl*. 61:257–268

117. Irani M, Sadeghi GMM, Haririan I (2017) The sustained delivery of temozolomide from electrospun PCL-Diol-b-PU/gold nanocomposite nanofibers to treat glioblastoma tumors. *Mater Sci Eng C Mater Biol Appl*. 75:165–174
118. Lin J, Li Y, Wu H, Yu F, Zhou S, Xie L et al (2015) Drug/Dye-Loaded, Multifunctional PEG-Chitosan-Iron Oxide Nanocomposites for Methotrexate Synergistically Self-Targeted Cancer Therapy and Dual Model Imaging. *ACS Appl Mater Interfaces* 7(22):11908–11920
119. Wang K, Zhang Z, Lin L, Hao K, Chen J, Tian H et al (2019) Cyanine-Assisted Exfoliation of Covalent Organic Frameworks in Nanocomposites for Highly Efficient Chemo-Photothermal Tumor Therapy. *ACS Appl Mater Interfaces* 11(43):39503–39512
120. Xu Y, Zhao J, Zhang Z, Zhang J, Huang M, Wang S et al (2020) Preparation of electro-spray ALG/PDA-PVP nanocomposites and their application in cancer therapy. *Soft Matter* 16(1):132–141
121. Salahuddin N, Elbarbary AA, Alkabes HA (2017) Antibacterial and anticancer activity of loaded quinazolinone polypyrrole/chitosan silver chloride nanocomposite. *International Journal of Polymeric Materials and Polymeric Biomaterials*. 66(6):307–316
122. Javid A, Ahmadian S, Saboury AA, Kalantar SM, Rezaei-Zarchi S, Shahzad S (2014) Biocompatible APTES–PEG Modified Magnetite Nanoparticles: Effective Carriers of Antineoplastic Agents to Ovarian Cancer. *Appl Biochem Biotechnol* 173(1):36–54
123. Zarouni M, Salehi R, Akbarzadeh A, Samadi N, Davaran S, Ramezani F et al (2015) Biocompatible Polymer Coated Paramagnetic Nanoparticles for Doxorubicin Delivery: Synthesis and Anticancer Effects Against Human Breast Cancer Cells. *International Journal of Polymeric Materials and Polymeric Biomaterials*. 64(14):718–726
124. Wang S, Zhao X, Wang S, Qian J, He S (2016) Biologically Inspired Polydopamine Capped Gold Nanorods for Drug Delivery and Light-Mediated Cancer Therapy. *ACS Appl Mater Interfaces* 8(37):24368–24384
125. Lim E-K, Sajomsang W, Choi Y, Jang E, Lee H, Kang B et al (2013) Chitosan-based intelligent theragnosis nanocomposites enable pH-sensitive drug release with MR-guided imaging for cancer therapy. *Nanoscale Res Lett* 8:467
126. Vivek R, Thangam R, Kumar SR, Rejeeth C, Sivasubramanian S, Vincent S et al (2016) HER2 Targeted Breast Cancer Therapy with Switchable “Off/On” Multifunctional “Smart” Magnetic Polymer Core-Shell Nanocomposites. *ACS Appl Mater Interfaces* 8(3):2262–2279
127. Xu X, Huang Z, Huang Z, Zhang X, He S, Sun X et al (2017) Injectable, NIR/pH-Responsive Nanocomposite Hydrogel as Long-Acting Implant for Chemophotothermal Synergistic Cancer Therapy. *ACS Appl Mater Interfaces* 9(24):20361–20375
128. Mdlovu NV, Mavuso FA, Lin K-S, Chang T-W, Chen Y, Wang SSS et al (2019) Iron oxide-pluronic F127 polymer nanocomposites as carriers for a doxorubicin drug delivery system. *Colloids Surf, A* 562:361–369
129. Xing Q, Li N, Jiao Y, Chen D, Xu J, Xu Q et al (2015) Near-infrared light-controlled drug release and cancer therapy with polymer-caged upconversion nanoparticles. *RSC Advances*. 5(7):5269–5276
130. GhavamiNejad A, SamariKhalaj M, Aguilar LE, Park CH, Kim CS (2016) pH/NIR Light-Controlled Multidrug Release via a Mussel-Inspired Nanocomposite Hydrogel for Chemo-Photothermal Cancer Therapy. *Scientific Reports*. 6(1):33594
131. Dawson SJ, Tsui DW, Murtaza M, Biggs H, Rueda OM, Chin SF et al (2013) Analysis of circulating tumor DNA to monitor metastatic breast cancer. *N Engl J Med* 368(13):1199–1209
132. Leong SP, Tseng WW (2014) Micrometastatic cancer cells in lymph nodes, bone marrow, and blood: Clinical significance and biologic implications. *CA Cancer J Clin* 64(3):195–206
133. Liu M, Huang P, Wang W, Feng Z, Zhang J, Deng L et al (2019) An injectable nanocomposite hydrogel co-constructed with gold nanorods and paclitaxel-loaded nanoparticles for local chemo-photothermal synergetic cancer therapy. *J Mater Chem B*. 7(16):2667–2677
134. Cacicedo ML, Islan GA, León IE, Álvarez VA, Chourpa I, Allard-Vannier E et al (2018) Bacterial cellulose hydrogel loaded with lipid nanoparticles for localized cancer treatment. *Colloids Surf B Biointerfaces*. 170:596–608

135. Xue P, Sun L, Li Q, Zhang L, Xu Z, Li CM et al (2018) PEGylated magnetic Prussian blue nanoparticles as a multifunctional therapeutic agent for combined targeted photothermal ablation and pH-triggered chemotherapy of tumour cells. *J Colloid Interface Sci* 509:384–394
136. Fan X, Yuan Z, Shou C, Fan G, Wang H, Gao F et al (2019) cRGD-Conjugated Fe(3)O(4)@PDA-DOX Multifunctional Nanocomposites for MRI and Antitumor Chemo-Photothermal Therapy. *Int J Nanomedicine*. 14:9631–9645
137. Huang J, Zhong X, Wang L, Yang L, Mao H (2012) Improving the magnetic resonance imaging contrast and detection methods with engineered magnetic nanoparticles. *Theranostics*. 2(1):86–102
138. Hachani R, Lowdell M, Birchall M, Thanh NTK (2013) Tracking stem cells in tissue-engineered organs using magnetic nanoparticles. *Nanoscale*. 5(23):11362–11373
139. Na HB, Song IC, Hyeon T (2009) Inorganic Nanoparticles for MRI Contrast Agents. *Adv Mater* 21(21):2133–2148
140. Sharifi I, Shokrollahi H, Amiri S (2012) Ferrite-based magnetic nanofluids used in hyperthermia applications. *J Magn Magn Mater* 324(6):903–915
141. Hilger I (2013) In vivo applications of magnetic nanoparticle hyperthermia. *Int J Hyperthermia*. 29(8):828–834
142. Laurent S, Dutz S, Häfeli UO, Mahmoudi M (2011) Magnetic fluid hyperthermia: focus on superparamagnetic iron oxide nanoparticles. *Adv Colloid Interface Sci* 166(1–2):8–23
143. Arruebo M, Fernández-Pacheco R, Ibarra MR, Santamaría J (2007) Magnetic nanoparticles for drug delivery. *Nano Today*. 2(3):22–32
144. Mahmoudi M, Sant S, Wang B, Laurent S, Sen T (2011) Superparamagnetic iron oxide nanoparticles (SPIONs): development, surface modification and applications in chemotherapy. *Adv Drug Deliv Rev* 63(1–2):24–46
145. Hervault A, Dunn AE, Lim M, Boyer C, Mott D, Maenosono S et al (2016) Doxorubicin loaded dual pH- and thermo-responsive magnetic nanocarrier for combined magnetic hyperthermia and targeted controlled drug delivery applications. *Nanoscale*. 8(24):12152–12161
146. Laurini E, Marson D, Fermeglia M, Prici S (2019) In silico design of self-assembly nanostructured polymer systems by multiscale molecular modeling. *Sci, Tech Innov*. 6(3):1–10
147. Steffens L, Morás AM, Arantes PR, Masterson K, Cao Z, Nugent M et al (2020) Electrospun PVA-Dacarbazine nanofibers as a novel nano brain-implant for treatment of glioblastoma: in silico and in vitro characterization. *Eur J Pharm Sci* 143:
148. Chiu C-W, Huang T-K, Wang Y-C, Alamani BG, Lin J-J (2014) Intercalation strategies in clay/polymer hybrids. *Prog Polym Sci* 39(3):443–485
149. Gao D, Li R, Lv B, Ma J, Tian F, Zhang J (2015) Flammability, thermal and physical-mechanical properties of cationic polymer/montmorillonite composite on cotton fabric. *Compos B Eng* 77:329–337
150. Lowe D, Chapman A, Cook S, Busfield J (2011) Micromechanical Models of Young's Modulus of NR/Organoclay Nanocomposites. *J Polym Sci, Part B: Polym Phys* 49:1621–1627
151. Mattausch H, Laske S, Đuretek I, Kreith J, Maier G, Holzer C (2013) Investigation of the influence of processing conditions on the thermal, rheological and mechanical behavior of polypropylene nanocomposites. *Polym Eng Sci* 53(5):1001–1010
152. Decker JJ, Meyers KP, Paul DR, Schiraldi DA, Hiltner A, Nazarenko S (2015) Polyethylene-based nanocomposites containing organoclay: A new approach to enhance gas barrier via multilayer coextrusion and interdiffusion. *Polymer* 61:42–54
153. Gooneie A, Nazockdast H, Shahsavan F (2015) Effect of selective localization of carbon nanotubes in PA6 dispersed phase of PP/PA6 blends on the morphology evolution with time, part 1: Droplet deformation under simple shear flows. *Polym Eng Sci* 55(7):1504–1519
154. Sepahvand R, Adeli M, Astinchap B, Kabiri R (2008) New nanocomposites containing metal nanoparticles, carbon nanotube and polymer. *J Nanopart Res* 10:1309–1318
155. Moniruzzaman M, Winey K. *Polymer Nanocomposites Containing Carbon Nanotubes*. Macromolecules. 2006;39
156. Elliott JA (2011) Novel approaches to multiscale modelling in materials science. *Int Mater Rev* 56(4):207–225

157. Zeng Q, Yu A, Lu M (2008) Multiscale modeling and simulation of polymer nanocomposites. *Progress in Polymer Science - PROG POLYM SCI*. 33:191–269
158. Ayton GS, Noid WG, Voth GA (2007) Multiscale modeling of biomolecular systems: in serial and in parallel. *Curr Opin Struct Biol* 17(2):192–198
159. Ayyaswamy PS, Muzykantov V, Eckmann DM, Radhakrishnan R. Nanocarrier Hydrodynamics and Binding in Targeted Drug Delivery: Challenges in Numerical Modeling and Experimental Validation. *Journal of Nanotechnology in Engineering and Medicine*. 2013;4(1)
160. Raabe D (2002) Challenges in Computational Materials Science. *Adv Mater* 14(9):639–650
161. Kremer K, Müller-Plathe F (2001) Multiscale Problems in Polymer Science: Simulation Approaches. *MRS Bull* 26(3):205–210
162. Murtola T, Bunker A, Vattulainen I, Deserno M, Karttunen M (2009) Multiscale modeling of emergent materials: Biological and soft matter. *Phys Chem Chem Phys* 11:1869–1892
163. Peter C, Kremer K (2009) Multiscale simulation of soft matter systems – from the atomistic to the coarse-grained level and back. *Soft Matter* 5(22):4357–4366
164. Sherwood P, Brooks BR, Sansom MSP (2008) Multiscale methods for macromolecular simulations. *Curr Opin Struct Biol* 18(5):630–640
165. Gooneie A, Schuschnigg S, Holzer C. A Review of Multiscale Computational Methods in Polymeric Materials. *Polymers (Basel)* [Internet]. 2017 2017/01//; 9(1). Available from: <http://europepmc.org/abstract/MED/30970697>, <https://doi.org/10.3390/polym9010016>, <https://europepmc.org/articles/PMC6432151>, <https://europepmc.org/articles/PMC6432151?pdf=render>

Biopolymeric-Inorganic Composites for Drug Delivery Applications



Shaimaa A. Khalid, Ahmed S. Abo Dena, and Ibrahim M. El-Sherbiny

Abstract The everyday progress in the development of new nanomaterials has grasped the attention of drug delivery researchers in recent years. The combination of more than one material to form composites in order to gain new interesting properties and enhance the performance of one another has shown a noticeable progress in the synthesis and applications of drug delivery systems. For instance, biocompatible and biodegradable materials such as biopolymers and inorganic materials are widely used in this aspect. This chapter focuses on the use of biopolymeric–inorganic composites in the preparation of drug delivery systems. The types of biopolymeric and inorganic materials that can be combined into composite materials and their characteristics are summarized herein. The given materials are just examples for the composite materials of interest, and many other composites can be synthesized from different types of inorganic and biopolymeric materials.

1 Introduction

The research of drug delivery and development field regulating the drug sustained release remains a major challenge with advances in technology to overcome the drawbacks of conventional drug therapies attributed to lack of selectivity, unfavorable pharmacodynamics, side effects, short circulating time, and limited drug solubility [1–3]. In addition, translational medicine presents a major obstacle for

S. A. Khalid · A. S. Abo Dena · I. M. El-Sherbiny (✉)
Nanomedicine Laboratory, Center for Materials Science, Zewail City of Science and Technology,
6th of October City 12578, Giza, Egypt
e-mail: ielsherbiny@zewailcity.edu.eg

S. A. Khalid
Food Hygiene Department, Animal Health Research Institute (AHRI), Agricultural Research
Center, Dokki, Giza, Egypt

A. S. Abo Dena
Pharmaceutical Chemistry Department, National Organization for Drug Control and Research
(NODCAR), Giza, Egypt

the use of intelligent materials to control the distribution and release of different agents. The new successful methodologies used for drug delivery are of practical importance to prevent the unnecessary changes in drug stability and properties. In this context, drug delivery aims to (i) decrease the side effects of drugs by targeting the desired organ precisely and (ii) to control the release of the drug in order to avoid the classical overdose or underdose [4]. Furthermore, drug delivery systems (DDSs) protect the drugs of interest from rapid degradation or clearance and increases their concentration in the target tissues [5]. Sustained delivery of drugs poses essential advantages such as reducing the number of doses, limiting the side effects, lowering fluctuations in concentration in the blood stream, reducing dose-dumping risks, enhancing bioavailability, site specificity, and allowing better patient compliance [6, 7]. Numerous formulations for sustained drug release were developed in the form of microparticles [8, 9], nanoparticles [10, 11], tablets [12–14], beads [15–17], buccal patches [18], capsules [19–21], implants [22, 23], etc. These drug releasing systems are commonly formulated using various excipients such as natural/synthetic/semisynthetic biopolymers, inorganic materials (such as metal powders), and bioceramics. Recently, various biopolymers–inorganic composites were developed in the form of nano- or micron-scale particles or fibers to sustain the release of certain drug substances over as long period of time as possible. The synergy of biopolymers and inorganic materials resulted in improved mechanical properties, better drug release sustainability and enhanced encapsulation/loading of many pharmaceutically active substances [24, 25].

Recently, modern science uses materials from natural sources for the treatment of a wide variety of diseases. The use of such natural materials in biomedical and clinical applications is increasing because of their biocompatibility, non-immunogenicity, good mechanical properties, and biodegradability [26]. Natural biopolymers can be obtained from a wide variety of microbes, plants and animals of both land and aquatic inhabitants. In addition, the functional properties of biopolymers such as rheology or gel-forming ability may be used for the chemical modification of pharmaceutical products or for the encapsulation of medicinal products for sustained delivery [27]. Based on their properties, chemically engineered natural biopolymers are the promising biomaterials for drug delivery systems instead of discovering new synthetic polymers due to above-mentioned fascinating characteristics. Functional groups such as hydroxyl, amino, and carboxylic acid groups have broad applicability and strong potential for cross-linking to induce biological inter action with cell-specific agents. Thus, the functionalization of biopolymers through these functional groups can be accomplished to improve their biocompatibility, facilitate the integration of cells, and provide new DDSs. Biopolymer derivatives from plant or animal sources consist of interstitial spaces and stretched cross-linked structures that assist in shape and volume modification depending on different stimuli such as temperature, pH, solvent composition, magnetic and electric fields. They are usually used for their hydrophilic nature and hydrogel-forming ability that may help in the entrapment of interesting bioactive molecules [28, 29]. They also provide softness, low interfacial tension, selective permeability, and super-absorbance [30]. Different shapes such as slab, cubical, and cylindrical can be tailored due to their hydrogel-forming ability.

Generally, composites are material mixtures consisting of two or more physically/chemically interacting materials in which one of them is the reinforcing phase (sheets, particles or fibers) and the other is the matrix phase (ceramics, polymers or metals) within which each constituent retains its distinct characteristics. Indeed, these materials offer new physico-mechanical properties to the composites [31, 32]. Composites are classified based on the composition of matrix reinforcement: inorganic–inorganic composite (e.g., ceramic–ceramic composites, metal–metal composites, ceramic–metal composites, etc.), organic–inorganic composites (e.g., polymer–metal composites, polymer–ceramic composites, etc.) and organic–organic composites [31]. Recently, various composites were developed for different biomedical applications such as the delivery of drugs, antimicrobial agents, cancer therapy, wound dressing, stem cell therapy, and biosensors [33–35].

2 Drug Delivery Systems

Drug delivery is a strategy for the delivery of drugs to specific body areas and the release of them in the desired rate. Locally releasing drugs can help reduce the side effects of systemic therapies while, at the same time, maintaining more optimal concentration of drugs. Also, DDSs could enhance the drug bioavailability [36]. DDSs deal with the encapsulation and loading of drugs through drug carriers such as microparticles, nanoparticles, microcapsules, nanocapsules, hydrogel, implants, films spheroids, gels, dendrimers, beads, biocomposites, and scaffolds [37–39]. Hence, the main objective of using biopolymer carriers is to protect the drug against degradation or damage and to facilitate the delivery of the drug to the site of action precisely [40]. Accordingly, drug delivery may be steady, controlled, or targeted drug delivery. Common DDSs that can be integrated with drugs can be in the form of bulk, micro- or nanoforms.

3 Use of Biopolymers in Drug Delivery

Biopolymers are polymeric biomolecules composed of covalently bonded monomeric units derived from living organisms such as animals, plants, and microorganisms [39, 41]. Recently, a large number of biopolymers were classified as biodegradable biomaterials which can be gradually degraded in the body. Therefore, they are excellent candidates to be used in DDSs [41]. The most common biopolymers that found a wide implementation in DDSs are summarized (Fig. 1).

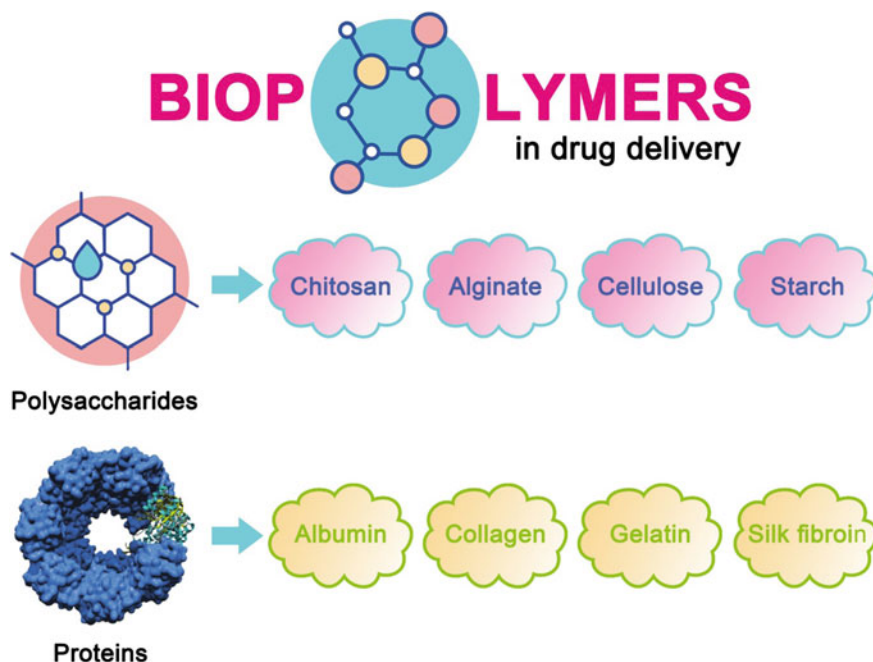


Fig. 1 Some of the common biopolymers used in drug delivery applications

4 Polysaccharides

Polysaccharides are composed of repeating units of monosaccharides. They can be used in DDSs after structural modifications [42]. Chitosan, cellulose, alginate, and starch are the most common polysaccharides used in drug delivery [29]. These common polysaccharides are summarized below.

4.1 Chitosan

Chitosan is a polycationic, non-toxic, highly biodegradable and biocompatible polymer derived from the shells of crustaceans, such as shrimps, prawns and crabs, in the form of chitin. Chitin is then modified by alkaline deacetylation to form chitosan consisting of $\beta(1\rightarrow4)$ glucosamine and N-acetyl glucosamine [29]. Chitosan has many advantages in developing micro/nanoparticles: (i) ability to control the release of active agents, (ii) avoids the use of hazardous organic solvents, and (iii) provides particles soluble in aqueous acid solutions. Chitosan has a great potential for pharmaceutical applications with high charge density, drug loading ability, and mucoadhesion [43]. As a biopolymer, it can be used for enhancing the bioavailability and

release of phytochemicals in DDSs through the interactions of its positive amino groups. For example, polyphenols of strawberry extract were encapsulated in chitosan tripolyphosphate resulting in a sustained release profile of polyphenols at the physiological pH [44]. With the presence of tripolyphosphate (TPP) and polyglutamic acid (γ -PGA), chitosan can form hydrogel structures by ionotropic gelation. It can also form insoluble matrix by polyelectrolyte complexation with polyanions (such as alginate) or by precipitation at pH above its pKa value (i.e. around pH 6.5). In addition, in the presence of glutaraldehyde, it forms hydrogels by covalent cross-linking [45]. The polycationic chitosan was found to enhance intestinal permeation, via the adherence to the anionic intestinal wall, and promote the opening of tight junctions among epithelial cells [46, 47].

Coating of magnetic nanoparticles with chitosan protected them from oxidation reduced their toxicity and aggregation, increase the storage life with increasing in stability. Moreover, chitosan provides suitable functional groups that enable it to bind many drug molecules. In addition, the presence of chelating functional groups enhances the adsorption performance of magnetic chitosan [48]. Chitosan has proven its efficiency to intercalate, exfoliate, and disperse two-dimensional sheets including typically montmorillonite clay and graphene oxide layers. Owing to the presence of ammonium groups in chitosan, stable colloidal chitosan–clay and chitosan–graphene oxide solutions can be obtained [49].

Chitosan has a notable effect on fat metabolism and improves the aqueous solubility of poorly soluble drugs. Chitosan produces gel with molecular counterions such as polyphosphates and sulfates, allowing a wide range of applications including biochemical gel trapping of objects such as plant embryos, whole cells, and algae, pharmaceutical surface coating and food products [50]. Vanillin–chitosan–calcium ferrite hybrid nanoparticles were synthesized by the ionic gelation method, and their release of curcumin was studied at different pH and variable magnetic fields [51].

The chemical properties of chitosan allow its application in various biopolymer–inorganic composites. These composites have attractive characteristics allowing their application in a large number of areas. The good reducing properties of chitosan allowed its use as a capping/reducing agent in the preparation of gold–chitosan hybrid nanoparticles [52]. This chitosan coating enhanced the antimicrobial as well as the physicochemical properties of gold nanoparticles. Other studies reported the use of chitosan for the synthesis of silver nanoparticles [53].

4.2 Alginate

Alginate is a natural anionic polysaccharide with wide biomedical applications due to its low toxicity, low cost, biocompatibility, etc. [54]. Under mild conditions, alginate can form a hydrogel by ionotropic gelation in the presence of cross linkers such as calcium ions, and also by polyelectrolyte complexation with an oppositely charged polymer [28]. The polymeric chain of alginate is composed of (1→4) linked β -D-mannuronic (M) and α -L-guluronic acid (G) residues and is polyanionic in nature

with the presence of carboxyl functional groups in the polymeric chain resulting in mucoadhesive properties with the hydrophobic mucosal layer of the intestinal wall which are enhanced by hydrogen bonding. Such interaction increases the residence time of the polymeric vesicles within the intestinal wall with an improvement in absorption efficiency [45].

Slow and sustained release of anti-HIV drug zidovudine was achieved by the encapsulation of the drug into alginate amide derivative prepared by coupling of glutamic acid. A slow release mechanism was observed in phosphate buffer saline of pH 7.4 [55].

Alginate aerogel was cross-linked with Fe(III) and loaded with ibuprofen with adsorptive deposition from superficial CO₂. Release of ibuprofen from the composite was faster at pH 7.4 than at pH 2.0 due to higher swelling properties and faster dissolution of alginate in PBS [56]. Yin et al. [57] showed the prospective sustain release in gastric fluid (pH 2.1) and intestinal fluid (pH 7.4) of indomethacin from agar–alginate hydrogel with Ca⁺² composite.

4.3 Cellulose

Cellulose-based nanoparticles have many surface properties that help colloidal stability. Moreover, cellulose nanofibers have the ability to enhance the aqueous stability of drugs and increase the sustain release ability [58]. Bacterial cellulose/graphene oxide composite was found to be effective DDSs as a nanocomposite drug carrier [59]. The presence of abundant surface hydroxyl groups makes cellulose an attractive heterogeneous support with transformable oxygenated sites for chemical modification and/or anchoring different types of species (complexes, clusters, nanoparticles, etc.) [60]. Typical examples include the deposition of porous zeolite on various vegetal fibers and the replication of the cellulose surface by titanium dioxide using surface-reactive sol–gel chemistry. Cellulose surface modification allows for introducing more efficient chelating ligands on the surface, e.g., carboxymethyl-cellulose that can be used for controlling the growth of nanoparticles. This chemistry accounts for broadening the versatility of cellulose as a seed for nanoparticle synthesis and stabilization and consequently extends the advanced application range of cellulose-based biopolymeric–inorganic composites. Several excellent review articles summarized the use of cellulose as a support for molecular complexes, metal nanoparticles, metal oxides, and metal sulfides and their applications in catalysis, sensing and separation [61].

4.4 Starch

Starch, a common edible polysaccharide, is isolated from different natural sources such as wheat, corn, rice and potato. Starch has wide biomedical and pharmaceutical

applications as it can be used as a carrier for controlled drug release and in other applications like bone replacement and repair. Morphological, rheological and mechanical properties, enzymatic digestibility, swelling and solubility are key factors behind the selection of starch for these applications [62]. Therefore, starch has been identified as a suitable biopolymer candidate for the synthesis of biopolymeric–inorganic composites for drug delivery applications.

For instance, corn starch with weight of $(162.5)_n$ was combined with multi-walled carbon nanotubes (MWCNTs) by ultrasonic-assisted method for zolpidem delivery [63]. Ampholytic starch excipients [62], acetylated starch nanocrystals [64], and dialdehyde starch derivatives [65] were widely used in DDSs as these materials have core–shell gel structures that display sponge-like viscoelastic attributes when suspended in an aqueous medium. Starch hydrogels were successfully used in oral drug delivery of probiotic bacteria *Lactobacillus plantarum*, and the loaded bacteria was resistant to bile salt solution and abnormal conditions of the gastrointestinal tract in comparison to the non-capsulated bacteria [66].

5 Proteins

Proteins are common biological polymers of amino acids with high molecular weights. Proteins such as collagen, gelatin, albumin, and fibroin were used for the synthesis of many DDSs [67]. Below, the most common types of proteins used for drug delivery are summarized.

5.1 Albumin

Albumin is the most ample protein in human blood plasma (35–50 g/L human serum) [68]. Due to its non-toxicity, biodegradability, and non-immunogenicity, albumin was proven to be appropriate for the drug delivery for many antibiotics and chemopreventive agents [69, 70]. Wunder et al. studied the intake of albumin by synovial fibroblasts of rheumatoid arthritis patients and the potency of methotrexate (MTX) which was covalently coupled to human serum albumin (HSA). The developments showed that inflamed paws in arthritic mice were accumulated with significantly higher amounts of albumin. Liver and kidneys showed significantly lower amounts of albumin. The protein was metabolized by human synovial fibroblasts in vitro and in vivo and the results suggested that MTX-HSA could be more beneficial in the suppression of the onset of arthritis in mice [71].

5.2 Collagen

Collagen is an extracellular fibrous protein that is mainly present in connective tissue of mammals. Collagen has a wide range of applications in wound healing due to its ability to enhance ingrowth of intrinsic tissues [72]. It was used in DDSs in the form of films, fibers, foams, nanoparticles, hydrogels, and minirods [73, 74]. Collagen can be utilized in delivery of platelet-derived growth factors [75], chondrocyte transplantation [76], antibiotics [77], and glucocorticoids [78]. Collagen was coupled with porous titanium dioxide as a drug delivery system for ibuprofen [79].

5.3 Gelatin

Gelatin is a biopolymer resulting from partial hydrolysis of collagen [80]. Gelatin microparticles can be utilized to deliver large molecules as they contain high surface-loading capacity allowing drug molecules to be absorbed into the gelatin hydrogel [81]. Due to its ability to form cross-linked structures, gelatin was used as a tissue adhesive for wound healing and pain management [82]. The introduction of gelatin microspheres into calcium phosphate cement (CPC), a potential material for its biocompatibility and osteoconductivity revealed that the delayed degradation of gelatin microspheres inside the CPC-gelatin scaffolds rendered good handling properties [83].

5.4 Silk Fibroin

Silk fibroin proteins are natural fibers and promising materials for controlled drug delivery because of their biocompatibility, mechanical hardness, self-assembly, and processing malleability [84]. One of the most common uses of silk fibroin is that it can be used in the form of electrospun fibers, films, three-dimensional scaffolds, and hydrogels.

6 Inorganic Materials in Biopolymer Composites

Many inorganic materials show interesting properties such as high antibacterial activity, high electrical and thermal conductivity, excellent magnetic properties, easy surface functionalization chemical inertness, and biocompatibility. The incorporation of inorganic magnetic nanomaterials in biopolymeric matrices provides excellent characteristics resulting from their combined properties that are suitable for a wide range of applications such as drug delivery, therapeutics, diagnostics,



Fig. 2 Examples of inorganic materials that can be combined with biopolymers to form composites with high potentiality in drug delivery applications

and other biomedical applications. The following sections summarize some of the common types of inorganic materials used in biopolymer composites for drug delivery applications (Fig. 2).

7 Metals

Generally speaking, the incorporation of metals into a biopolymeric matrix demonstrated a very wide range of applications. For instance, biopolymeric–metal nanocomposites play a vital role in the regeneration and repair of skin wounds. Moreover, calcium is important for proliferation and differentiation of keratinocytes and for the hemostasis of mammalian skin. Silver nanoparticles (AgNPs) control the proliferation of bacteria which in turn decreases the inflammations. Zinc is also an important factor for protein synthesis, and development of T cells [85].

Silver has unique properties with excellent electrical and thermal conductivity among all metals and silver-based nanocomposites have a wide range of applications in conductive inks, antimicrobials, electronic devices, and catalysis [86, 87]. Silver-based materials exhibit good antimicrobial effects against pathological infections [88]. The development of biopolymer matrices with silver-based materials achieves better treatment strategies. The ability of blood clotting in wound dressing improves

with AgNPs/chitin composites synthesized by Kumar et al. [85]. In addition, biopolymers can be used as stabilizers for nanoparticles suspensions. For example, the biopolymer pectin was used to stabilize polyaniline nanoparticles and form silver–polyaniline (PANi) nanocomposites. Biocompatibility studies of these Ag/PANi NPs in vitro with MTT assay showed an increase in cell viability. In addition, *Escherichia coli* adhesion was increased with the use of higher amounts of pectin [89]. The pectin-stabilized polyaniline nanoparticles were further used for the development of glucose biosensor [90] and for the detection of bacteria [91].

AgNPs were impregnated in collagen-based dressings to be used in wound healing with high antimicrobial activity. The nanocomposites are easy to synthesize via the electrospinning process. AgNPs in the collagen–AgNPs composite are responsible for controlling the deposition of collagen which leads to an improvement of the fibril alignments in wound healing processes [92, 93]. Furthermore, Song et al. [94] developed a new nanocomposite material by covalent cross-linking from AgNPs, histidine, and collagen and the scaffold showed promising antibacterial activity with good mechanical properties. The in vivo study showed regeneration of infected full-thickness burnt skin.

Recently, a wound scaffold was engineered from AgNPs with curcumin and plumbagin. In this study, collagen was used for cross-linking and the resulting fabrications offer higher activity for wound healing [95, 96].

Gelatin-based composites with AgNPs were fabricated for oral wound dressing and the nanocomposites showed antimicrobial properties against bacteria that caused periodontal disease [97]. Moreover, a novel wound dressing of AgNPs with silk fibroin was tested in rabbit model and the results showed that in a short period of time the defects of skin were covered and the wound surface was flattened [98]. Indeed, different nanocomposite materials based on AgNPs were fabricated with various biopolymers such as carboxymethyl chitosan and silk fibroin [99], keratin [100–102], chitosan [103–107], sodium alginate [108–110], and cellulose [111, 112]. Verma et al. [113] revealed accelerated wound healing and antimicrobial activity of sericin and chitosan-capped AgNPs in a rat wound model. The results showed that the combined effect of AgNPs and chitosan in the composite material increased the production of collagen, and re-epithelialization occurred in open wounds which eventually led to rapid wound healing. Anisha et al. [114] reported the use of starch as a stabilizing agent in the preparation of AgNPs-loaded chitosan and hyaluronic acid-based nanocomposite wound dressing sponges. Starch was also used as a reducing agent for the synthesis of colloidal AgNPs [115].

Several diethanolamine-modified olive oil incorporated high methoxyl containing pectin (DMP)-GG hydrogel nanobiocomposites were prepared using zinc acetate crosslinker for the intragastric controlled metformin HCl (MFM) delivery. Upon changing the GG:DMP mass ratios, nanofiller type (neusilin, bentonite, or fluoride) as well as oil addition, the nanocomposites demonstrated different drug encapsulation efficiencies of 50–85% and prolonged drug release of 69–94% in 8 h at pH 4.5 (acetate buffer). The optimal oil-entrapped nanocomposites released the MFM through case-II transport mechanism with the drug release kinetics following the zero-order model. The optimum system established outstanding gastro retentive features and significant

hypoglycemic influence in streptozotocin-induced diabetic rats confirming suitability for the treatment of type-2 diabetes [116].

Polysaccharide-based hydrogel in combination with carbon nanotubes, gold nanowires, and gold nanoparticles (AuNPs) were studied to improve the electrical coupling between adjacent cardiac cells *in vitro*. As with all critically sized constructs, vascularization is paramount to the success of a cardiac construct. One approach is to add proangiogenic growth factors to the matrix to improve host infiltration [117]. Chitosan–AuNPs composites were used for electrochemical study and immobilization of leukemia cells k562 [118]. In addition, an ionic liquid-based enzymatic biosensor was reported by Brondani et al. [119] where AuNPs dispersed in ionic liquid (1-butyl-3-methyl imidazolium hexafluorophosphate) were supported in a chitin matrix cross-linked with glyoxal and epichlorohydrin. Peroxidase enzyme was entrapped in this ionic liquid matrix, and the biosensor electrode was constructed via mixing the resulting mixture with graphite powder and Nujol. The biosensor was successfully applied for the determination of rosmarinic acid content in pharmaceutical samples using square-wave voltammetry. Daneshpour et al. [120] used Fe_3O_4 /trimethyl chitosan/Au nanocomposite as a tag to label DNA probe and polythiophene as an immobilization platform for quantitative evaluation of methylation in tumor suppressor gene RASSF1A. In this case, trimethyl chitosan could form nanocomplex with anionic compounds such as Fe_3O_4 and AuNPs via electrostatic interaction. Differential pulse voltammetry-based studies helped to analyze the methylation in the studied tumor suppressor gene with high specificity and low detection limit.

Calcium silicate is a low-density highly porous material that was proven to be used in tissue engineering and drug delivery [121–123]. Wu et al. [122] synthesized a core–shell composite of alginate and calcium silicate for the delivery of bovine serum albumin by *in situ* one-step method and the entrapment efficiency was found to be 75%. The composite structure exhibited a good sustain release pattern in PBS at pH 3.4 and 7.4. The core–shell structure loaded with bovine serum albumin showed the best performance in apatite-mineralization in simulated body fluids. A composite of calcium silicate–alginate was also developed by reinforcing of calcium silicate into alginate matrix [121]. The entrapment efficiency of metronidazole was found to be 61.70–93.10%. *In vitro* release study of metronidazole from the as-prepared beads proved the pattern of controlled release in the pH of the gastric medium and the beads were floating which is suitable for helicobacter pylori eradication. Nanocomposites of carboxymethyl guar gum (CMG) and different amounts of nanosilica were fabricated and used for the transdermal delivery of diclofenac sodium [124]. It was indicated that the nanocomposite containing 1 wt% of nanosilica was the optimal formulation. The nanocomposite hydrogel with 1wt% of nanosilica had the slowest drug release among all nanocomposites. Hasnain et al. [25] formulated novel kinds of ionotropically gelled calcium alginate–polyvinylpyrrolidone (PVP)–nanohydroxyapatite composite-based bead matrices as carriers for diclofenac sodium. The mean sizing of these composite beads ranged from 0.98 ± 0.07 mm to 1.23 ± 0.15 mm, and the encapsulation efficiency of the beads was from 65.82 ± 1.88 to $94.45 \pm 3.72\%$. The anticancer drug DOX loaded in alginate/ CaCO_3 composite was assessed *in vitro*

with an elevated durability in aqueous solution. The nanoparticles were prepared by carbonate modified co-precipitation technique [125].

Microencapsulation of pancreatic islets in calcium alginate/poly-L-lysine succeeded in producing insulin in response to blood glucose levels when implanted in rats [126]. Chen et al. [127] reported an enzyme-based approach to in situ cell trapping within a biopolymeric hydrogel matrix. They used calcium-independent microbial transglutaminase, known for crosslink proteins, to catalyze gel formation from a pre-gel solution of gelatin and *E. coli* cells.

Hydroxyapatite [$\text{Ca}_{10}(\text{PO}_4)_6(\text{OH})_2$] is a bioceramic material composed of 70% inorganic compounds of apatite calcium phosphate and 30% of organic materials such as collagen and bone marrow cells. It can be extracted from bones of animals or chemically synthesized. It is widely used in the delivery of drugs and other biomedical applications [128]. Owing to its features such as biocompatibility, osteoconductivity and ability to absorb a range of chemicals, it is used in scaffolds of bone tissue regeneration and bone implantable drug release [129]. Moreover, Hydroxyapatite was integrated with biopolymers to improve the osteoconductivity, mechanical behavior, and drug adsorption [130]. Hydroxyapatite–alginate nanocomposite was prepared for controlling the release of ofloxacin encapsulated within the matrix [131]. In another work, hydroxyapatite–alginate nanocomposite beads were designed for the delivery of diclofenac sodium [24] and the release of diclofenac sodium from the nanocomposite showed a pH-responsiveness indicating the compound's sustained release. Recently, core–shell *Gum Acacia*–hydroxyapatite nanocomposite was synthesized with a hydroxyapatite core and *Gum Acacia* shell and naringenin drug was encapsulated into the hydroxyapatite core via pellet press technique [132]. The *Gum Acacia*–hydroxyapatite crystallite size was diminished from 89 to 63 nm by increasing the *Gum Acacia* concentration from 0 to 10%. The pellet samples were dipped into the simulated body fluid in order to examine their bioactivities by scanning electron microscopy. The antimicrobial, hemolytic capacity, and biocompatibility of the drug-containing core–shell composites were also assessed.

Chitosan-based nanogel of CdSe quantum dots was used for drug delivery and imaging of mouse melanoma B16F10 cells. The nanogel showed a good cell viability of the melanoma cells as evident from the in vitro cytotoxicity results [133]. Scaffolds of polymer/ceramic composite have been designed with improved bioactivity, flexibility, good mechanical properties and osteoconductivity that are suitable for use in tissue engineering of bone [134].

Oxidized starch–CuO nanocomposite hydrogels were produced in situ through the synthesis of CuO NPs (with diameters of 39–50 nm) in swollen oxidized starch hydrogels so that the number of CuO NPs was enhanced by increasing the Cu^{2+} concentration. The swelling of the nanocomposite hydrogels examined at two pH values (2.1 and 7.4) proved that they had pH-sensitive swellings relative to the neat oxidized starch hydrogel. Moreover, a controlled drug release was detected for the CuO NPs incorporating oxidized starch [135].

In addition to the above-mentioned metals, titanium (Ti) and its alloys are biocompatible materials with good mechanical properties and a wide range of applications in human bone tissues due to its ability to resist corrosion [136].

8 Metal Oxides and Hydroxides

8.1 Titanium Dioxide (TiO₂)

The recent rise in scientific interest of titanium dioxide (a.k.a. titania or titanium (IV) oxide) is attributed to its photoactivity [137]. UV illumination of TiO₂ in aqueous media results in the formation of an array of reactive oxygen species (ROS) which have the ability to induce cell death in a wide range of diseases ranging from psoriasis to cancer. The incorporation of TiO₂ and other metal oxides in polymeric matrices has found a great interest in the last few years due to their potential use in novel medical therapies.

Hybrid composites of IBU/MC/TiO₂ (titanium tetra *n*-butoxide) have reported a slower release in gastric pH, thus minimizing the side effects of the loaded drug via minimizing the interactions between the drug and the gastric juice [138]. Archana et al. synthesized a nanocomposite formed of TiO₂, chitosan and poly(*N*-vinylpyrrolidone) and used it to prepare antimicrobial dressing [137]. The dressing demonstrated a good biocompatibility and excellent wound healing induction of open excision type wounds in albino rats.

Radmansouri et al. reported the preparation of chitosan/cobalt ferrite/TiO₂ nanofibers for the delivery of doxorubicin hydrochloride [139]. The formulation was used for hyperthermic treatment of tumor cells via controlled drug release. The results proved the possibility of use of the synthesized nanofiber composite in localized cancer therapy via the simultaneous effect of chemotherapy and hyperthermia.

8.2 Zinc Oxide (ZnO)

ZnO composites with biopolymers showed promising medicinal and biomedical activities in recent years. For instance, chitosan/zinc complexes can enhance wound healing and demonstrate good antimicrobial properties [140]. During the preparation of physically cross-linked chitosan hydrogel beads (in the presence of sodium tripolyphosphate crosslinker), ZnO nanoparticles can be synthesized in situ for application as drug delivery platforms. The diameter of the resulting particles lies in the range 10–25 nm [141]. These nanocomposites exhibit high swelling ratio in diverse aqueous solutions, pH sensitivity, and controlled release of ZnO NPs.

Carboxymethyl chitosan (CMCS) and ZnO NPs coated with sodium alginate hydrogel beads were used to control the release of diclofenac sodium and avoid its sensitivity to gastrointestinal environment and minimize their irritating action on the stomach [142]. In another study, pH-sensitive fluorinated CMCS NPs were reported as DDSs using *N*-(3-aminopropyl)-imidazole pre-grafted to the CMCS to fabricate the pH-sensitive NPs whose surface was then modified with perfluorobutyric anhydride to obtain the fluorinated NPs [143]. The cellular uptake tests confirmed that the

surface-fluorinated NPs enhanced the cellular uptake and improved the cytotoxicity in diverse tumor cells without recognition between ligands and host.

Some ZnO-based hydrogel beads were prepared to improve the release of curcumin and to prevent the burst release observed in pure hydrogels. In addition, these hydrogel beads were found to decrease the fast-physiological clearance of curcumin and its sensitivity to ultraviolet light and alkaline solutions [144]. In order to solve the disadvantages of CMCS drug carriers (such as poor mechanical properties and burst drug release), ZnONPs were added to the CMCS beads that were coated with CS via self-assembly to obtain core-shell polyelectrolyte complexes. The 5-fluorouracyl (5-FU) anticancer drug was loaded onto the ZnO/CMC/CS nanobiocomposite hydrogel beads. The *in vitro* 5-FU release and swelling tests were carried out in simulated gastrointestinal condition, and the pH sensitivity of the nanocomposite beads was examined. The beads displayed a sustained drug release profile based on the ratios of CS, CMC, and ZnO NPs [145]. Antibacterial chitosan-GEL/zinc oxide (CS-GEL/*n*ZnO) nanocomposite hydrogels were achieved by *in situ* synthesis of *n*ZnO and employed as naproxen drug carriers [146].

Antibacterial CS-GEL/*n*ZnO nanocomposite hydrogels were prepared by *in situ* synthesis of *n*ZnO and employed as naproxen drug carriers. The scaffolds demonstrated good antibacterial, cytocompatibility, swelling, cell attachment, and biodegradation characteristics. Moreover, the scaffolds exhibited high porosity (pore sizes were in the range 50–400 μm) and *n*ZnO was suitably dispersed into the CS-GEL matrix without agglomeration.

8.3 Magnetic Materials

Magnetic materials (especially metallic ferrous nanoparticles) are of great importance in many applications such as therapeutics, diagnostics, real-time imaging and drug delivery. Superparamagnetic materials include three main iron oxides, namely hematite ($\alpha\text{-Fe}_2\text{O}_3$), maghemite ($\gamma\text{-Fe}_2\text{O}_3$), and magnetite (Fe_3O_4). In addition, transition metals (e.g., Cu, Co, Mn and Ni) demonstrate superparamagnetic properties when mixed with iron oxides. The magnetic properties of these materials rely on their size and crystallinity [147]. One of the disadvantages of applying these magnetic nanoparticles in drug delivery is that they can be easily transported and distributed to the body organs by the blood stream. In some cases, this leads to exerting undesired side effects. This problem can be overcome by adding a capping/coating biomaterial such as natural/synthetic biopolymers that in turn prevent the undesired interactions with the body tissues. Moreover, these biopolymer coatings are usually used to achieve a certain surface functionalization of these magnetic materials, thus allowing their use in the desired specific application.

In one of the previous studies, magnetic Fe_3O_4 nanoparticles were functionalized with (3-amino propyl) triethoxy silane, coated with CS and tragacanth gum (TG), and were used for encapsulation of the curcumin drug [148]. The *in vitro* study of

curcumin release was tested at pH 7.4 and 3.4 and at temperatures of 37 and 40 °C. The results indicated a higher swelling of the nanocomposite at pH 3.4 and 40 °C.

Anti-colon cancer therapy was developed by Fe₃O₄@cellulose nanocrystals (MCNCs) containing curcumin where the entrapment efficiency of curcumin was about 99.35% [149]. The exposure of the nanocomposite to an external field of 0.7 T led to the release of 53.30% of curcumin after 4 days. The proposed composite successfully inhibited the growth of human colon cancer cells by 18%.

A self-healing chitosan–alginate hydrogel was coated with magnetic gelatin microspheres (MGMs) to prepare an anticancer DDS. The hydrogel was formed through crosslinking of carboxyethyl chitosan as well as oxidized alginate by means of Schiff-base reaction [88]. The MGMs incorporated with 5-FU anticancer drug was achieved via emulsion crosslinking process to enhance the biological and mechanical properties of the hydrogel. It was found that adding MGMs with 30 mg/mL concentration to the composite hydrogel caused an appropriate performance and revealed exceptional self-healing capability under physiological conditions [150].

8.4 Aluminosilicates

Silica gels are popular class of bioencapsulation materials owing to their ability to maintain biological activity of the entrapped biomolecules such as enzymes or cells. Silica-based materials have a broad range of dimensions, chemical compositions and forms that can be prepared by sol–gel chemistry. In addition, sol–gel matrices provide chemical inertia, physical rigidity and negligible swelling in aqueous and organic solutions [151]. To achieve long-term stability, hybrids from silica-based materials with biopolymers are often utilized. Kaushik et al. [152] used silica nanoparticles–chitosan composite for the detection of ochratoxin-A by rabbit-immunoglobulin antibodies (IgGs). Through a physical adsorption method, bovine serum albumin and antibodies were integrated into the electrode of chitosan–silica composite.

A composite system of gelatin with mesoporous silica nanoparticles was used as a pH-responsive DDS for the delivery of doxorubicin, allowing its delivery in acidic conditions [81]. Another successful doxorubicin nanocomposite DDS was designed from silk fibroin and sericin with silica and demonstrated a high loading capacity and sustained release of DOX. This complex was very effective in the cancer therapy of human cervical carcinoma (HeLa) cells [153].

9 Carbon Materials–Biopolymers Composites

In the past decade, the development of novel carbonaceous nanomaterials has inspired scientists with new ideas in diagnostics and therapeutics sp² carbonaceous nanomaterials, notably zero-dimensional (0D) carbon dots and fullerenes, one-dimensional (1D) carbon nanotubes (CNTs), and two-dimensional (2D) graphene, have grasped

the attention of the researchers from various fields including drug delivery [154]. The integration of biopolymers with the carbon nanomaterials provides them with more desired properties such as good mechanical stability, active functional groups, and better drug encapsulation ability.

A composite of CNTs and alginate (CNT-ALG) was fabricated by filling CNT in Ca-alginate to increase the mechanical stability. Thus, the CNT-ALG composite microspheres having loose internal structural features were formulated via decreasing the concentration of ALG sol. In addition, a triblock copolymer of PEO137-b-PPO44-b-PEO137 was also introduced within the CNT-ALG composite matrices to enhance the dispersion capability of CNTs in aqueous solution. In this investigation, theophylline was loaded as a model drug candidate within these CNT-ALG composite microspheres [155]. Starch was also used to prepare a nanocomposite with CNTs as a DDS. Hollow efficient nanoparticles and better loading capacity were obtained from core-shell which was used to deliver DOX in liver hepatocellular cells [156].

Single-walled carbon nanotubes (SWNTs) have high electrical and thermal conductivities and high strength; so it represents a potential for polymer matrix composites reinforcement [157]. The nanotubes can enhance the mechanical and electrical characteristics of polymer matrices [158]. SWNTs were integrated into polymer composites to be used after myocardial infarction for repairing of the left ventricles. This device was implanted in rats for in-vivo experimentation resulting in improved ejection fraction and fractional shortening in comparison to untreated hearts due to enhancement of intercellular adhesive junctions and electrochemical junctions [159].

Because of their chemical stability, homogeneity and porosity, carbon nanospheres are another attractive class of carbonaceous nanomaterials. The spherical structure is the result of pairing of pentagonal and heptagonal carbon rings to form waving flakes that follow the sphere's curvature [160]. Different techniques can be used for the preparation of carbon nanospheres such as hydrothermal, pressure carbonization, and thermal/catalytic decomposition but the hydrothermal technique provides a mild, green, and cheap route for the synthesis of homogeneous nanospheres with functional surface groups [161]. When the nanospheres are used for enzyme immobilization, composite the incorporation of a hydrogel-forming biopolymer such as alginate can provide excellent stability. Han et al. [161] reported a highly sensitive amperometric biosensor for the detection of glucose using immobilized glucose oxidase.

Graphene oxide (GO) is a carbon-based material with unique two-dimensional structure which can give extraordinary chemical and physical properties including excellent mechanical properties, large surface area, high carrier mobility, fast electron transportation, good biocompatibility, and good thermal conductivity. GO is composed of a single layer of sp^2 carbon atoms with a two-dimensional honeycomb lattice structure [162, 163]. GO has many applications in drug delivery, biological imaging, tissue engineering, electrochemical biosensors and bioassays [164, 165]. Schauer et al. [166] found that GO sheets increase the proliferation of stem cells and mechanical strength of CS where new functional groups can be introduced by chemical crosslinking to produce composites with good water dispersion, aqueous stability, and biocompatibility and antimicrobial properties. By self-assembly, GO

and CS can be integrated to create a biopolymer composite, in which GO is distributed uniformly in CS. This composite has good mechanical properties and can be used for electrochemical and biomedical applications [167, 168].

DOX as anticancer drug was loaded onto a CMC-GO composite as a pH-responsive DOX DDS which exhibited a higher release rate at pH 5 (i.e., in the tumor microenvironment) than at pH 7.4.

10 Metal–Organic Frameworks (MOFs)

Metal–organic frameworks (MOFs) are inorganic–organic solid structures built of the connection of inorganic subunits to each other through polytopic organic ligands that define cavities of various shapes and sizes [169]. Due to their unique adsorption capacity, large surface area, tunable pores and controlled porosity, MOFs resulted in great progresses in a variety of applications [170]. The highest molecular diversity of MOFs finds its root in the possibility of combining an unlimited number of organic linkers with metallic nodes intimately [7–9]. This gives MOFs the ability to recognize molecular properties through surface functionalization and molecular sieving by regulating pore sizes [171]. Hence, MOFs have many wide applications such as catalysis [172], drug delivery [173], photocatalysis [174], sensing [175], photonics, molecular imaging [176], electronic and optoelectronic devices, energy storage [177], and proton conductivity [178]. The incorporation of biomolecules within MOFs is a step toward more innocuous materials. Thus, the successful achievements in biomimetic and bioinspired functional materials triggered a confrontation between nano-sized MOFs and bio-based building blocks, resulting in a new generation of crystalline materials known as bio-MOFs, metal–biomolecule framework or MOF biocomposites [179, 180].

The performance of polymer@MOF membranes depends massively on the particle size of the MOF crystals and their uniform coating on the material surface. These two parameters need to be balanced to prevent defect when the crystals are bigger and pore clogging of the support if the crystals are too small. The use of CS as an interfacial compatibilizer or a binding agent circumvents some of these drawbacks and accounts for the successful formation of ternary membrane-based composites. Zhu et al. [181] reported the use of CS for enhancing interfacial interactions between hollow ceramic fibers of α -Al₂O₃ and the carboxylic groups of the BTC ligands. The use of CS was pivotal for controlling growth of MOF crystals and serves also as intermediate linker to stretch MOFs to the support. Consequently, MOF crystals of ~300 nm were fabricated, which preclude their inclusion in the pore structure of the hollow ceramic fibers (pore size of around 200 nm) and thus avoid their blockage. The resulting membrane was evaluated for hydrogen separation from a mixture of H₂, CO₂, N₂, and CH₄ [181].

11 Clay Minerals-Biopolymers Composite

Clay minerals are appropriate for modified drug delivery because of their crystalline structures, high surface area-to-volume ratio, high porosity, chemical inertness, swelling properties, good adsorption properties, colloidal particle size, and high exchange capacity of cations [182, 183]. Different types of polymers can be used as carriers for clay minerals in order to sustain their release and control their diffusion [184]. Clays are inexpensive materials, can be modified by impregnation of metal/metal complex, ion exchange, acid, and pillaring treatment to improve the desired catalysis functionality [185]. They develop a colloidal suspension of elementary platelets with negative charges upon delamination with water that can be used to make composites with cationic polymers such as CS [183].

Layered double hydroxides (LDHs), also known as anionic clays, are lamellar ionic solids carrying a layer of positive charges with two types of metallic cations and weakly bound exchangeable anions. They are used for enzyme immobilization in many areas including biosensor applications [186]. However, the inorganic clay matrix based on LDHs tends to develop cracks on dry storage, thereby limiting their reusability. Ding et al. developed a biopolymer composite from negatively charged alginate and positively charged LDH that aggregate together forming a gel resulting in a biocompatible matrix with good adhesion properties [186].

Montmorillonite (MMT) is a natural soft phyllosilicate inorganic clay material formed of aluminum magnesium silicate hydroxide of sodium and calcium with high surface area and ability of exchanging cations [187, 188]. MMT was recognized as safe by USFDA, and it is recommended to be utilized in drug delivery applications [189–191]. Many researchers investigated MMT–alginate composites as the negative charges on the COO^- group of alginate molecules improve the electrostatic interactions with the positive charge of MMT molecules [192]. So, the alginate–MMT composite formed by the reinforcement/incorporation of MMT into alginate matrix can improve the sustainability of drug release due to the enhancement of drug adsorption capacity [190]. Irinotecan, an anticancer drug, was encapsulated into alginate–MMT by the crosslinking gelation method [189]. Kevadiya et al. [189] fabricated alginate–MMT composite for the control of diclofenac sodium release in which Na-alginate and diclofenac sodium were intercalated into MMT by the ionic gelation method. The efficiency of diclofenac sodium encapsulation was increased with the addition of MMT in the bead formulation. Another work by Kaygusuz and Erim [191] reported the fabrication of a pH-responsive alginate–MMT composite with bovine serum albumin as a model protein to investigate the intestinal drug release from the composites. The presence of MMT reinforcement in the composite helps in increasing the loading efficiency of bovine serum albumin to 78% compared to 40% in case of calcium alginate beads.

References

1. Nayak AK (2011) Controlled release drug delivery systems. *Sci J UBU* 2:1–8
2. Pal D, Nayak AK (2015) Alginates, blends and microspheres: controlled drug delivery. In: *Encyclopedia of biomedical polymers and polymeric biomaterials*, 11 volume set. CRC Press, pp 89–98
3. Aw MS, Kurian M, Losic D (2014) Non-eroding drug-releasing implants with ordered nanoporous and nanotubular structures: concepts for controlling drug release. *Biomater Sci* 2(1):10–34
4. Cregg PJ, Murphy K, Mardinoglu A (2012) Inclusion of interactions in mathematical modelling of implant assisted magnetic drug targeting. *Appl Math Model* 36(1):1–34
5. Wilczewska AZ, Niemirowicz K, Markiewicz KH, Car H (2012) Nanoparticles as drug delivery systems. *Pharmacol Rep* 64(5):1020–1037
6. Nayak AK, Pal D (2017) Natural starches blended ionotropically gelled microparticles/beads for sustained drug release. *Handb Compos Renew Mater* 527–59
7. Pal D, Nayak AK (2015) Interpenetrating polymer networks (IPNs): natural polymeric blends for drug delivery. In: *Encyclopedia of biomedical polymers and polymeric biomaterials*, 11 volume set. CRC Press, pp 4120–30
8. Jana S, Saha A, Nayak AK, Sen KK, Basu SK (2013) Aceclofenac-loaded chitosan-tamarind seed polysaccharide interpenetrating polymeric network microparticles. *Colloids Surf B Biointerfaces* 105:303–309
9. Jana S, Das A, Nayak AK, Sen KK, Basu SK (2013) Aceclofenac-loaded unsaturated esterified alginate/gellan gum microspheres: in vitro and in vivo assessment. *Int J Biol Macromol* 57:129–137
10. Kaur H, Ahuja M, Kumar S, Dilbaghi N (2012) Carboxymethyl tamarind kernel polysaccharide nanoparticles for ophthalmic drug delivery. *Int J Biol Macromol* 50(3):833–839
11. Jana S, Gangopadhaya A, Bhowmik BB, Nayak AK, Mukherjee A (2015) Pharmacokinetic evaluation of testosterone-loaded nanocapsules in rats. *Int J Biol Macromol* 72:28–30
12. Beg S, Nayak AK, Kohli K, Swain S, Hasnain MS (2012) Antimicrobial activity assessment of time-dependent release bilayer tablets of amoxicillin trihydrate. *Brazilian J Pharm Sci* 48(2):265–272
13. Malakar J, Nayak AK, Goswami S (2012) Use of response surface methodology in the formulation and optimization of bisoprolol fumarate matrix tablets for sustained drug release. *Int Sch Res Not* 2012
14. Malakar J, Das K, Nayak AK (2014) In situ cross-linked matrix tablets for sustained salbutamol sulfate release-formulation development by statistical optimization. *Polim Med* 44(4):221–230
15. Das B, Dutta S, Nayak AK, Nanda U (2014) Zinc alginate-carboxymethyl cashew gum microbeads for prolonged drug release: development and optimization. *Int J Biol Macromol* 70:506–515
16. Bera H, Kandukuri SG, Nayak AK, Boddupalli S (2015) Alginate sterculia gum gel-coated oil-entrapped alginate beads for gastroretentive risperidone delivery. *Carbohydr Polym* 120:74–84
17. Bera H, Boddupalli S, Nandikonda S, Kumar S, Nayak AK (2015) Alginate gel-coated oil-entrapped alginate-tamarind gum-magnesium stearate buoyant beads of risperidone. *Int J Biol Macromol* 78:102–111
18. Ramkanth S (2017) Fabrication and characterization of transdermal drug delivery using Losartan potassium. *Int Res J Pharm Appl Sci* 7(3):23–30
19. Malakar J, Nayak AK (2012) Theophylline release behavior from hard gelatin capsules containing hydrophilic polymeric matrices. *J Pharm Educ Res* 3(1)
20. Malakar J, Datta PK, Purakayastha S, Das, Dey S, Nayak AK (2014) Floating capsules containing alginate-based beads of salbutamol sulfate: In vitro-in vivo evaluations. *Int J Biol Macromol* 64:181–9
21. Nayak AK, Das B, Maji R (2013) Gastroretentive hydrodynamically balanced systems of ofloxacin: In vitro evaluation. *Saudi Pharm J* 21(1):113–117

22. Nayak AK, Bhattacharya A, Sen KK (2010) Hydroxyapatite-antibiotic implantable minipellets for bacterial bone infections using precipitation technique: preparation, characterization and in-vitro antibiotic release studies. *J Pharm Res* 3(1):53–59
23. Nayak AK, Bhattacharyya A, Sen KK (2011) In Vivo ciprofloxacin release from hydroxyapatite-based bone implants in rabbit tibia: a preliminary study. *ISRN Orthop* 2011
24. Zhang J, Wang Q, Wang A (2010) In situ generation of sodium alginate/hydroxyapatite nanocomposite beads as drug-controlled release matrices. *Acta Biomater* 6(2):445–454
25. Hasnain MS, Nayak AK, Singh M, Tabish M, Ansari MT, Ara TJ (2016) Alginate-based bipolymeric-nanobioceramic composite matrices for sustained drug release. *Int J Biol Macromol* 83:71–77
26. Chandika P, Ko S-C, Jung W-K (2015) Marine-derived biological macromolecule-based biomaterials for wound healing and skin tissue regeneration. *Int J Biol Macromol* 77:24–35
27. Rehm BHA (2010) Bacterial polymers: biosynthesis, modifications and applications. *Nat Rev Microbiol* 8(8):578–592
28. Lim H-P, Tey B-T, Chan E-S (2014) Particle designs for the stabilization and controlled-delivery of protein drugs by biopolymers: a case study on insulin. *J Control Release* 186:11–21
29. Atta S, Khaliq S, Islam A, Javeria I, Jamil T, Athar MM et al (2015) Injectable biopolymer based hydrogels for drug delivery applications. *Int J Biol Macromol* 80:240–245
30. Eskandari S, Guerin T, Toth I, Stephenson RJ (2017) Recent advances in self-assembled peptides: Implications for targeted drug delivery and vaccine engineering. *Adv Drug Deliv Rev* 110:169–187
31. Angadi SC, Manjeshwar LS, Aminabhavi TM (2012) Novel composite blend microbeads of sodium alginate coated with chitosan for controlled release of amoxicillin. *Int J Biol Macromol* 51(1–2):45–55
32. Saxena M, Pappu A, Sharma A, Haque R, Wankhede S (2011) Composite materials from natural resources: recent trends and future potentials. In: *Advances in composite materials-analysis of natural and man-made materials*. IntechOpen
33. Jose JP, Thomas S, Kuruvilla J, Malhotra SK, Goda K, Sreekala MS (2012) Advances in polymer composites: macro- and microcomposites-state of the art, new challenges, and opportunities. *Polym Compos Wiley Weinheim Ger* 1:3–16
34. Grande CJ, Torres FG, Gomez CM, Bañó MC (2009) Nanocomposites of bacterial cellulose/hydroxyapatite for biomedical applications. *Acta Biomater* 5(5):1605–1615
35. Ullah H, Wahid F, Santos HA, Khan T (2016) Advances in biomedical and pharmaceutical applications of functional bacterial cellulose-based nanocomposites. *Carbohydr Polym* 150:330–352
36. Maher S, Mazinani A, Barati MR, Losic D (2018) Engineered titanium implants for localized drug delivery: recent advances and perspectives of Titania nanotubes arrays. *Expert Opin Drug Deliv* 15(10):1021–1037
37. Bedoya DA, Figueroa FN, Macchione MA, Strumia MC (2020) Stimuli-responsive polymeric systems for smart drug delivery. In: *Advanced biopolymeric systems for drug delivery*. Springer, pp 115–34
38. Mazur J, Roy K, Kanwar JR (2018) Recent advances in nanomedicine and survivin targeting in brain cancers. *Nanomedicine* 13(1):105–137
39. Bobo D, Robinson KJ, Islam J, Thurecht KJ, Corrie SR (2016) Nanoparticle-based medicines: a review of FDA-approved materials and clinical trials to date. *Pharm Res* 33(10):2373–2387
40. Hoogenboom R (2019) Temperature-responsive polymers: properties, synthesis, and applications. In: *Smart polymers and their applications*. Elsevier, pp 13–44
41. Zhang Q, Weber C, Schubert US, Hoogenboom R (2017) Thermoresponsive polymers with lower critical solution temperature: from fundamental aspects and measuring techniques to recommended turbidimetry conditions. *Mater Horizons* 4(2):109–116
42. Yang L, Zhang L-M (2009) Chemical structural and chain conformational characterization of some bioactive polysaccharides isolated from natural sources. *Carbohydr Polym* 76(3):349–361

43. Assa F, Jafarizadeh-Malmiri H, Ajamein H, Vaghari H, Anarjan N, Ahmadi O et al (2017) Chitosan magnetic nanoparticles for drug delivery systems. *Crit Rev Biotechnol* 37(4):492–509
44. Pulicharla R, Marques C, Das RK, Rouissi T, Brar SK (2016) Encapsulation and release studies of strawberry polyphenols in biodegradable chitosan nanoformulation. *Int J Biol Macromol*
45. Lehr C-M, Bouwstra JA, Schacht EH, Junginger HE (1992) In vitro evaluation of mucoadhesive properties of chitosan and some other natural polymers. *Int J Pharm* 78(1–3):43–48
46. Maculotti K, Genta I, Perugini P, Imam M, Bernkop-Schnürch A, Pavanetto F (2005) Preparation and in vitro evaluation of thiolated chitosan microparticles. *J Microencapsul* 22(5):459–470
47. Rekha MR, Sharma CP (2009) Synthesis and evaluation of lauryl succinyl chitosan particles towards oral insulin delivery and absorption. *J Control Release* 135(2):144–151
48. Chen J-P, Yang P-C, Ma Y-H, Wu T (2011) Characterization of chitosan magnetic nanoparticles for in situ delivery of tissue plasminogen activator. *Carbohydr Polym* 84(1):364–372
49. Frindy S, Primo A, Bouhfid R, Lahcini M, Garcia H, Bousmina M et al (2016) Insightful understanding of the role of clay topology on the stability of biomimetic hybrid chitosan-clay thin films and CO₂-dried porous aerogel microspheres. *Carbohydr Polym* 146:353–361
50. Sinha VR, Singla AK, Wadhawan S, Kaushik R, Kumria R, Bansal K et al (2004) Chitosan microspheres as a potential carrier for drugs. *Int J Pharm* 274(1–2):1–33
51. Kamaraj S, Palanisamy UM, Mohamed MSBK, Gangasalam A, Maria GA, Kandasamy R (2018) Curcumin drug delivery by vanillin-chitosan coated with calcium ferrite hybrid nanoparticles as carrier. *Eur J Pharm Sci* 116:48–60
52. Mohamady MA, Díaz FG, Grinholm M, Abo Dena AS, El-sherbiny IM, Megahed M (2020) Exploring the physicochemical and antimicrobial properties of gold-chitosan hybrid nanoparticles composed of varying chitosan amounts. *Int J Biol Macromol (Internet)* 162:1760–9. Available from: <https://doi.org/10.1016/j.ijbiomac.2020.08.046>
53. Senthilkumar P, Yaswant G, Kavitha S, Chandramohan E, Kowsalya G, Vijay R, et al (2019) Preparation and characterization of hybrid chitosan-silver nanoparticles (Chi-Ag NPs); a potential antibacterial agent. *Int J Biol Macromol (Internet)* 141:290–8. Available from: <http://www.sciencedirect.com/science/article/pii/S0141813019338978>
54. Lee KY, Mooney DJ (2012) Alginate: properties and biomedical applications. *Prog Polym Sci* 37(1):106–126
55. Joshy KS, Susan MA, Snigdha S, Nandakumar K, Laly AP, Sabu T (2018) Encapsulation of zidovudine in PF-68 coated alginate conjugate nanoparticles for anti-HIV drug delivery. *Int J Biol Macromol* 107:929–937
56. Veres P, Sebők D, Dékány I, Gurikov P, Smirnova I, Fábíán I et al (2018) A redox strategy to tailor the release properties of Fe (III)-alginate aerogels for oral drug delivery. *Carbohydr Polym* 188:159–167
57. Yin Z-C, Wang Y-L, Wang K (2018) A pH-responsive composite hydrogel beads based on agar and alginate for oral drug delivery. *J Drug Deliv Sci Technol* 43:12–18
58. Löbmann K, Svagan AJ (2017) Cellulose nanofibers as excipient for the delivery of poorly soluble drugs. *Int J Pharm* 533(1):285–297
59. Luo H, Ao H, Li G, Li W, Xiong G, Zhu Y et al (2017) Bacterial cellulose/graphene oxide nanocomposite as a novel drug delivery system. *Curr Appl Phys* 17(2):249–254
60. Perelshtein I, Applerot G, Perkas N, Wehrschuetz-Sigl E, Hasmann A, Guebitz G et al (2009) CuO-cotton nanocomposite: formation, morphology, and antibacterial activity. *Surf Coatings Technol* 204(1–2):54–57
61. Foresti ML, Vázquez A, Boury B (2017) Applications of bacterial cellulose as precursor of carbon and composites with metal oxide, metal sulfide and metal nanoparticles: a review of recent advances. *Carbohydr Polym* 157:447–467
62. Sakeer K, Ispas-Szabo P, Benyerbah N, Mateescu MA (2018) Ampholytic starch excipients for high loaded drug formulations: mechanistic insights. *Int J Pharm* 535(1–2):201–216
63. Mallakpour S (2018) Ultrasonic-assisted fabrication of starch/MWCNT-glucose nanocomposites for drug delivery. *Ultrason Sonochem* 40:402–409

64. Xiao H, Yang T, Lin Q, Liu G-Q, Zhang L, Yu F et al (2016) Acetylated starch nanocrystals: preparation and antitumor drug delivery study. *Int J Biol Macromol* 89:456–464
65. Wen N, Gao C, Lü S, Xu X, Bai X, Wu C et al (2017) Novel amphiphilic glucose-responsive modified starch micelles for insulin delivery. *RSC Adv* 7(73):45978–45986
66. Dafe A, Etemadi H, Dilmaghani A, Mahdavinia GR (2017) Investigation of pectin/starch hydrogel as a carrier for oral delivery of probiotic bacteria. *Int J Biol Macromol* 97:536–543
67. Jacob J, Haponiuk JT, Thomas S, Gopi S (2018) Biopolymer based nanomaterials in drug delivery systems: a review. *Mater today Chem* 9:43–55
68. Kratz F (2008) Albumin as a drug carrier: design of prodrugs, drug conjugates and nanoparticles. *J Control Release* 132(3):171–183
69. Tada D, Tanabe T, Tachibana A, Yamauchi K (2005) Drug release from hydrogel containing albumin as crosslinker. *J Biosci Bioeng* 100(5):551–555
70. Ma J, Wang Q, Huang Z, Yang X, Nie Q, Hao W et al (2017) Glycosylated platinum (IV) complexes as substrates for glucose transporters (GLUTs) and organic cation transporters (OCTs) exhibited cancer targeting and human serum albumin binding properties for drug delivery. *J Med Chem* 60(13):5736–5748
71. Wunder A, Muller-Ladner U, Stelzer E, Neumann E, Sinn H, Gay S et al (2003) Albumin-based drug delivery as novel therapeutic approach for rheumatoid arthritis. *Arthritis Res Ther* 5(S3):9
72. Nair LS, Laurencin CT (2007) Biodegradable polymers as biomaterials. *Prog Polym Sci* 32(8–9):762–798
73. Pastorino L, Dellacasa E, Scaglione S, Giulianelli M, Sbrana F, Vassalli M et al (2014) Oriented collagen nanocoatings for tissue engineering. *Colloids Surf B Biointerfaces* 114:372–378
74. MaHam A, Tang Z, Wu H, Wang J, Lin Y (2009) Protein based nanomedicine platforms for drug delivery. *Small* 5(15):1706–1721
75. Yamano S, Lin TY, Dai J, Fabella K, Moursi A (2011) Bioactive collagen membrane as a carrier for controlled-released PDGF. *J Tissue Sci Eng* 2(4)
76. van Susante JLC, Buma P, van Osch GJVM, Versleyen D, van der Kraan PM, van der Berg WB et al (1995) Culture of chondrocytes in alginate and collagen carrier gels. *Acta Orthop Scand* 66(6):549–556
77. Ruszczak Z, Friess W (2003) Collagen as a carrier for on-site delivery of antibacterial drugs. *Adv Drug Deliv Rev* 55(12):1679–1698
78. Berthold A, Cremer K, Kreuter J (1998) Collagen microparticles: carriers for glucocorticosteroids. *Eur J Pharm Biopharm* 45(1):23–29
79. McMaster WA, Wang X, Caruso RA (2012) Collagen-templated bioactive titanium dioxide porous networks for drug delivery. *ACS Appl Mater Interfaces* 4(9):4717–4725
80. Edison TNJI, Lee YR, Sethuraman MG (2016) Green synthesis of silver nanoparticles using *Terminalia cuneata* and its catalytic action in reduction of direct yellow-12 dye. *Spectrochim Acta Part A Mol Biomol Spectrosc* 161:122–129
81. Zou Z, He D, He X, Wang K, Yang X, Qing Z et al (2013) Natural gelatin capped mesoporous silica nanoparticles for intracellular acid-triggered drug delivery. *Langmuir* 29(41):12804–12810
82. Foox M, Zilberman M (2015) Drug delivery from gelatin-based systems. *Expert Opin Drug Deliv* 12(9):1547–1563
83. Habraken W, De Jonge LT, Wolke JGC, Yubao L, Mikos AG, Jansen JA (2008) Introduction of gelatin microspheres into an injectable calcium phosphate cement. *J Biomed Mater Res Part A An Off J Soc Biomater Japanese Soc Biomater Aust Soc Biomater Korean Soc Biomater* 87(3):643–655
84. Numata K, Kaplan DL (2010) Silk-based delivery systems of bioactive molecules. *Adv Drug Deliv Rev* 62(15):1497–1508
85. Kumar PTS, Abhilash S, Manzoor K, Nair SV, Tamura H, Jayakumar R (2010) Preparation and characterization of novel -chitin/nanosilver composite scaffolds for wound dressing applications. *Carbohydr Polym* 80(3):761–767

86. Sun Y, Xia Y (2002) Large scale synthesis of uniform silver nanowires through a soft, self seeding, polyol process. *Adv Mater* 14(11):833–837
87. Firdhouse MJ, Lalitha P (2015) Biosynthesis of silver nanoparticles and its applications. *J Nanotechnol* 2015
88. Konop M, Damps T, Misicka A, Rudnicka L (2016) Certain aspects of silver and silver nanoparticles in wound care: a minireview. *J Nanomater* 2016
89. Amarnath CA, Venkatesan N, Doble M, Sawant SN (2014) Water dispersible Ag@ polyaniline-pectin as supercapacitor electrode for physiological environment. *J Mater Chem B* 2(31):5012–5019
90. Thakur B, Amarnath CA, Sawant SN (2014) Pectin coated polyaniline nanoparticles for an amperometric glucose biosensor. *RSC Adv* 4(77):40917–40923
91. Thakur B, Amarnath CA, Mangoli SH, Sawant SN (2015) Polyaniline nanoparticle based colorimetric sensor for monitoring bacterial growth. *Sensors Actuators B Chem* 207:262–268
92. Kwan KHL, Liu X, To MKT, Yeung KWK, Ho C, Wong KKY (2011) Modulation of collagen alignment by silver nanoparticles results in better mechanical properties in wound healing. *Nanomedicine Nanotechnology, Biol Med* 7(4):497–504
93. Rath G, Hussain T, Chauhan G, Garg T, Goyal AK (2016) Collagen nanofiber containing silver nanoparticles for improved wound-healing applications. *J Drug Target* 24(6):520–529
94. Song J, Zhang P, Cheng L, Liao Y, Xu B, Bao R et al (2015) Nano-silver in situ hybridized collagen scaffolds for regeneration of infected full-thickness burn skin. *J Mater Chem B* 3(20):4231–4241
95. Srivatsan KV, Duraipandy N, Begum S, Lakra R, Ramamurthy U, Korrapati PS et al (2015) Effect of curcumin caged silver nanoparticle on collagen stabilization for biomedical applications. *Int J Biol Macromol* 75:306–315
96. Duraipandy N, Lakra R, Srivatsan KV, Ramamoorthy U, Korrapati PS, Kiran MS (2015) Plumbagin caged silver nanoparticle stabilized collagen scaffold for wound dressing. *J Mater Chem B* 3(7):1415–1425
97. Lee SJ, Heo DN, Lee D, Heo M, Rim H, Zhang LG et al (2016) One-step fabrication of AgNPs embedded hybrid dual nanofibrous oral wound dressings. *J Biomed Nanotechnol* 12(11):2041–2050
98. Min S, Gao X, Han C, Chen Y, Yang M, Zhu L et al (2012) Preparation of a silk fibroin spongy wound dressing and its therapeutic efficiency in skin defects. *J Biomater Sci Polym Ed* 23(1–4):97–110
99. Patil S, George T, Mahadik K (2015) Green synthesized nanosilver loaded silk fibroin gel for enhanced wound healing. *J Drug Deliv Sci Technol* 30:30–36
100. Wang Y, Li P, Xiang P, Lu J, Yuan J, Shen J (2016) Electrospun polyurethane/keratin/AgNP biocomposite mats for biocompatible and antibacterial wound dressings. *J Mater Chem B* 4(4):635–648
101. Wang J, Hao S, Luo T, Cheng Z, Li W, Gao F, et al (2017) Feather keratin hydrogel for wound repair: preparation, healing effect and biocompatibility evaluation. *B Biointerfaces*
102. Tran CD, Proscenc F, Franko M, Benzi G (2016) One-pot synthesis of biocompatible silver nanoparticle composites from cellulose and keratin: characterization and antimicrobial activity. *ACS Appl Mater Interfaces* 8(50):34791–34801
103. Ding L, Shan X, Zhao X, Zha H, Chen X, Wang J et al (2017) Spongy bilayer dressing composed of chitosan-Ag nanoparticles and chitosan-Bletilla striata polysaccharide for wound healing applications. *Carbohydr Polym* 157:1538–1547
104. Ganesh M, Aziz AS, Ubaidulla U, Hemalatha P, Saravanakumar A, Ravikumar R et al (2016) Sulfanilamide and silver nanoparticles-loaded polyvinyl alcohol-chitosan composite electrospun nanofibers: synthesis and evaluation on synergism in wound healing. *J Ind Eng Chem* 39:127–135
105. Phaechamud T, Yodkhum K, Charoenteeraboon J, Tabata Y (2015) Chitosan-aluminum monostearate composite sponge dressing containing asiaticoside for wound healing and angiogenesis promotion in chronic wound. *Mater Sci Eng C* 50:210–225

106. Levi-Polyachenko N, Jacob R, Day C, Kuthirummal N (2016) Chitosan wound dressing with hexagonal silver nanoparticles for hyperthermia and enhanced delivery of small molecules. *Colloids Surf B Biointerfaces* 142:315–324
107. Archana D, Singh BK, Dutta J, Dutta PK (2015) Chitosan-PVP-nano silver oxide wound dressing: in vitro and in vivo evaluation. *Int J Biol Macromol* 73:49–57
108. Acharya C, Panda CR, Bhaskara PK, Sasmal A, Shekhar S, Sen AK (2017) Physicochemical and antimicrobial properties of sodium alginate/gelatin-based silver nanoformulations. *Polym Bull* 74(3):689–706
109. Stojkowska J, Kosti D, Jovanović Ž, Vukašinović-Sekulić M, Mišković-Stanković V, Obradović B (2014) A comprehensive approach to in vitro functional evaluation of Ag/alginate nanocomposite hydrogels. *Carbohydr Polym* 111:305–314
110. Montaser AS, Abdel-Mohsen AM, Ramadan MA, Sleem AA, Sahffie NM, Jancar J et al (2016) Preparation and characterization of alginate/silver/nicotinamide nanocomposites for treating diabetic wounds. *Int J Biol Macromol* 92:739–747
111. Wu J, Zheng Y, Song W, Luan J, Wen X, Wu Z et al (2014) In situ synthesis of silver-nanoparticles/bacterial cellulose composites for slow-released antimicrobial wound dressing. *Carbohydr Polym* 102:762–771
112. Singla R, Soni S, Kulurkar PM, Kumari A, Mahesh S, Patial V et al (2017) In situ functionalized nanobiocomposites dressings of bamboo cellulose nanocrystals and silver nanoparticles for accelerated wound healing. *Carbohydr Polym* 155:152–162
113. Verma J, Kanoujia J, Parashar P, Tripathi CB, Saraf SA (2017) Wound healing applications of sericin/chitosan-capped silver nanoparticles incorporated hydrogel. *Drug Deliv Transl Res.* 7(1):77–88
114. Anisha BS, Biswas R, Chennazhi KP, Jayakumar R (2013) Chitosan-hyaluronic acid/nano silver composite sponges for drug resistant bacteria infected diabetic wounds. *Int J Biol Macromol* 62:310–320
115. Kumar B, Smita K, Cumbal L, Debut A (2014) Green approach for fabrication and applications of zinc oxide nanoparticles. *Bioinorg Chem Appl* 2014
116. Bera H, Kumar S, Maiti S (2018) Facile synthesis and characterization of tailor-made pectin-gellan gum-bionanofiller composites as intragastric drug delivery shuttles. *Int J Biol Macromol* 118:149–159
117. Dvir T, Timko BP, Brigham MD, Naik SR, Karajanagi SS, Levy O et al (2011) Nanowired three-dimensional cardiac patches. *Nat Nanotechnol* 6(11):720–725
118. Ding L, Hao C, Xue Y, Ju H (2007) A bio-inspired support of gold nanoparticles- chitosan nanocomposites gel for immobilization and electrochemical study of K562 Leukemia cells. *Biomacromol* 8(4):1341–1346
119. Brondani D, Zapp E, Vieira IC, Dupont J, Scheeren CW (2011) Gold nanoparticles in an ionic liquid phase supported in a biopolymeric matrix applied in the development of a rosmarinic acid biosensor. *Analyst* 136(12):2495–2505
120. Daneshpour M, Izadi P, Omidfar K (2016) Femtomolar level detection of RASSF1A tumor suppressor gene methylation by electrochemical nano-genosensor based on Fe₃O₄/TMC/Au nanocomposite and PT-modified electrode. *Biosens Bioelectron* 77:1095–1103
121. Javadzadeh Y, Hamedeyazdan S, Adibkia K, Kiafar F, Zarrintan MH, Barzegar-Jalali M (2010) Evaluation of drug release kinetics and physico-chemical characteristics of metronidazole floating beads based on calcium silicate and gas-forming agents. *Pharm Dev Technol* 15(4):329–338
122. Wu C, Fan W, Gelinsky M, Xiao Y, Chang J, Friis T et al (2011) In situ preparation and protein delivery of silicate-alginate composite microspheres with core-shell structure. *J R Soc Interface* 8(65):1804–1814
123. Bera H, Maiti S, Saha S, Nayak AK (2019) Biopolymers-based gastroretentive buoyant systems for therapeutic management of *Helicobacter pylori* infection. In: *Polysaccharide carriers for drug delivery*. Elsevier, pp 713–36
124. Giri A, Ghosh T, Panda AB, Pal S, Bandyopdhyay A (2012) Tailoring carboxymethyl guar gum hydrogel with nanosilica for sustained transdermal release of diclofenac sodium. *Carbohydr Polym* 87(2):1532–1538

125. Zhao D, Zhuo R-X, Cheng S-X (2012) Alginate modified nanostructured calcium carbonate with enhanced delivery efficiency for gene and drug delivery. *Mol BioSyst* 8(3):753–759
126. Lim F, Sun AM (1980) Microencapsulated islets as bioartificial endocrine pancreas. *Science* (80-) 210(4472):908–910
127. Chen T, Small DA, McDermott MK, Bentley WE, Payne GF (2003) Enzymatic methods for in situ cell entrapment and cell release. *Biomacromol* 4(6):1558–1563
128. Kumar Nayak A, Saquib Hasnain M, Malakar J (2013) Development and optimization of hydroxyapatite-ofloxacin implants for possible bone delivery in osteomyelitis treatment. *Curr Drug Deliv* 10(2):241–250
129. Kumar NA, Kumar S (2009) Hydroxyapatite-ciprofloxacin minipellets for bone-implant delivery: preparation, characterization, in-vitro drug adsorption and dissolution studies. *Int J Drug Deliv Res* 1(1):47–59
130. Hasnain MS, Nayak AK (2019) Nanocomposites for improved orthopedic and bone tissue engineering applications. In: *Applications of nanocomposite materials in orthopedics*. Elsevier, pp 145–77
131. Roul J, Mohapatra R, Sahoo SK (2013) Preparation, characterization and drug delivery behaviour of novel biopolymer/hydroxyapatite nanocomposite beads. *Asian J Biomed Pharm Sci* 3(24):33
132. Padmanabhan VP, Kulandaivelu R, Nellaiappan SNTS (2018) New core-shell hydroxyapatite/Gum-Acacia nanocomposites for drug delivery and tissue engineering applications. *Mater Sci Eng C* 92:685–693
133. Wu W, Shen J, Banerjee P, Zhou S (2010) Chitosan-based responsive hybrid nanogels for integration of optical pH-sensing, tumor cell imaging and controlled drug delivery. *Biomaterials* 31(32):8371–8381
134. Zaborowska M, Bodin A, Bäckdahl H, Popp J, Goldstein A, Gatenholm P (2010) Microporous bacterial cellulose as a potential scaffold for bone regeneration. *Acta Biomater* 6(7):2540–2547
135. Gholamali I, Hosseini SN, Alipour E, Yadollahi M (2019) Preparation and characterization of oxidized starch/CuO nanocomposite hydrogels applicable in a drug delivery system. *Starch* 71(3–4):1800118
136. Manam NS, Harun WSW, Shri DNA, Ghani SAC, Kurniawan T, Ismail MH et al (2017) Study of corrosion in biocompatible metals for implants: a review. *J Alloys Compd* 701:698–715
137. Ziental D, Czarczynska-goslinska B, Mlynarczyk DT, Glowacka-sobotta A, Stanisz B, Goslinski T et al (2020) Titanium dioxide nanoparticles: prospects and applications in medicine. *Nanomaterials* 10:387
138. Khalid S, Yu L, Feng M, Meng L, Bai Y, Ali A et al (2018) Development and characterization of biodegradable antimicrobial packaging films based on polycaprolactone, starch and pomegranate rind hybrids. *Food Packag Shelf Life* 18:71–79
139. Radmansouri M, Bahmani E, Sarikhani E, Rahmani K, Sharifianjazi F, Irani M (2018) Doxorubicin hydrochloride—loaded electrospun chitosan/cobalt ferrite/titanium oxide nanofibers for hyperthermic tumor cell treatment and controlled drug release. *Int J Biol Macromol* (Internet) 116:378–84. Available from: <http://www.sciencedirect.com/science/article/pii/S0141813018302319>
140. Patale RL, Patravale VB (2011) O, N-carboxymethyl chitosan-zinc complex: a novel chitosan complex with enhanced antimicrobial activity. *Carbohydr Polym* 85(1):105–110
141. Yadollahi M, Farhoudian S, Barkhordari S, Gholamali I, Farhadnejad H, Motasadzadeh H (2016) Facile synthesis of chitosan/ZnO bio-nanocomposite hydrogel beads as drug delivery systems. *Int J Biol Macromol* 82:273–278
142. Niu B, Jia J, Wang H, Chen S, Cao W, Yan J et al (2019) In vitro and in vivo release of diclofenac sodium-loaded sodium alginate/carboxymethyl chitosan-ZnO hydrogel beads. *Int J Biol Macromol* 141:1191–1198
143. Cheng X, Zeng X, Zheng Y, Wang X, Tang R (2019) Surface-fluorinated and pH-sensitive carboxymethyl chitosan nanoparticles to overcome biological barriers for improved drug delivery in vivo. *Carbohydr Polym* 208:59–69

144. Ghosal K, Das A, Das SK, Mahmood S, Ramadan MAM, Thomas S (2019) Synthesis and characterization of interpenetrating polymeric networks based bio-composite alginate film: a well-designed drug delivery platform. *Int J Biol Macromol* 130:645–654
145. Sun X, Liu C, Omer AM, Lu W, Zhang S, Jiang X et al (2019) pH-sensitive ZnO/carboxymethyl cellulose/chitosan bio-nanocomposite beads for colon-specific release of 5-fluorouracil. *Int J Biol Macromol* 128:468–479
146. Rakhshaei R, Namazi H, Hamishehkar H, Kafil HS, Salehi R (2019) In situ synthesized chitosan-gelatin/ZnO nanocomposite scaffold with drug delivery properties: Higher antibacterial and lower cytotoxicity effects. *J Appl Polym Sci* 136(22):47590
147. Abdel Aziz OA, Arafa K, Abo Dena AS, El-sherbiny IM (2020) Superparamagnetic iron oxide nanoparticles (SPIONs): preparation and recent applications. *J Nanotechnol Adv Mater* 8(1):21–29
148. Shafiee S, Ahangar HA, Saffar A (2019) Taguchi method optimization for synthesis of Fe₃O₄@ chitosan/Tragacanth Gum nanocomposite as a drug delivery system. *Carbohydr Polym* 222:
149. Low LE, Tan LT-H, Goh B-H, Tey BT, Ong BH, Tang SY (2019) Magnetic cellulose nanocrystal stabilized Pickering emulsions for enhanced bioactive release and human colon cancer therapy. *Int J Biol Macromol* 127:76–84
150. Chen X, Fan M, Tan H, Ren B, Yuan G, Jia Y et al (2019) Magnetic and self-healing chitosan-alginate hydrogel encapsulated gelatin microspheres via covalent cross-linking for drug delivery. *Mater Sci Eng, C* 101:619–629
151. Li F, Chen W, Tang C, Zhang S (2009) Development of hydrogen peroxide biosensor based on in situ covalent immobilization of horseradish peroxidase by one-pot polysaccharide-incorporated sol-gel process. *Talanta* 77(4):1304–1308
152. Kaushik A, Solanki PR, Sood KN, Ahmad S, Malhotra BD (2009) Fumed silica nanoparticles-chitosan nanobiocomposite for ochratoxin-A detection. *Electrochem Commun* 11(10):1919–1923
153. Wang J, Yang S, Li C, Miao Y, Zhu L, Mao C et al (2017) Nucleation and assembly of silica into protein-based nanocomposites as effective anticancer drug carriers using self-assembled silk protein nanostructures as biotemplates. *ACS Appl Mater Interfaces* 9(27):22259–22267
154. Liu Z, Robinson JT, Tabakman SM, Yang K, Dai H (2011) Carbon materials for drug delivery & cancer therapy. *Mater Today (Internet)*. 14(7–8):316–23. Available from: [http://dx.doi.org/10.1016/S1369-7021\(11\)70161-4](http://dx.doi.org/10.1016/S1369-7021(11)70161-4)
155. Zhang X, Hui Z, Wan D, Huang H, Huang J, Yuan H et al (2010) Alginate microsphere filled with carbon nanotube as drug carrier. *Int J Biol Macromol* 47(3):389–395
156. Yang J, Li F, Li M, Zhang S, Liu J, Liang C et al (2017) Fabrication and characterization of hollow starch nanoparticles by gelation process for drug delivery application. *Carbohydr Polym* 173:223–232
157. Harrison BS, Atala A (2007) Carbon nanotube applications for tissue engineering. *Biomaterials* 28(2):344–353
158. Pan D, Chen J, Tao W, Nie L, Yao S (2006) Polyoxometalate-modified carbon nanotubes: new catalyst support for methanol electro-oxidation. *Langmuir* 22(13):5872–5876
159. Boccaccini AR, Gerhardt LC (2010) Carbon nanotube composite scaffolds and coatings for tissue engineering applications. In: *Key engineering materials*. Trans Tech Publ; pp 31–52
160. Nieto-Márquez A, Romero R, Romero A, Valverde JL (2011) Carbon nanospheres: synthesis, physicochemical properties and applications. *J Mater Chem* 21(6):1664–1672
161. Han E, Li X, Cai J-R, Cui H-Y, Zhang X-A (2014) Development of highly sensitive amperometric biosensor for glucose using carbon nanosphere/sodium alginate composite matrix for enzyme immobilization. *Anal Sci* 30(9):897–902
162. Guo J, Bian Y-Y, Zhu K-X, Guo X-N, Peng W, Zhou H-M (2015) Reducing phytate content in wheat bran by directly removing the aleurone cell content with teeth roller mill and ultrasonic cleaner. *J Cereal Sci* 64:133–138
163. van Osch DJGP, Zubeir LF, van den Bruinhorst A, Rocha MAA, Kroon MC (2015) Hydrophobic deep eutectic solvents as water-immiscible extractants. *Green Chem* 17(9):4518–4521

164. Bound DJ, Bettadaiah BK, Srinivas P (2014) ZnBr₂-catalyzed and microwave-assisted synthesis of 2, 3-unsaturated glucosides of hindered phenols and alcohols. *Synth Commun* 44(17):2565–2576
165. Sela DA, Mills DA (2010) Nursing our microbiota: molecular linkages between bifidobacteria and milk oligosaccharides. *Trends Microbiol* 18(7):298–307
166. Schauer R, Srinivasan GV, Coddeville B, Zanetta J-P, Guéardel Y (2009) Low incidence of N-glycolylneuraminic acid in birds and reptiles and its absence in the platypus. *Carbohydr Res* 344(12):1494–1500
167. Schwab C, Gänzle M (2011) Lactic acid bacteria fermentation of human milk oligosaccharide components, human milk oligosaccharides and galactooligosaccharides. *FEMS Microbiol Lett* 315(2):141–148
168. Khazaei H, O'Sullivan DM, Jones H, Pitts N, Sillanpää MJ, Pärssinen P et al (2015) Flanking SNP markers for vicine-convicine concentration in faba bean (*Vicia faba* L.). *Mol Breed* 35(1):38
169. Zhou H-C, Long JR, Yaghi OM (2012) Introduction to metal-organic frameworks. ACS Publications
170. Li L, Jiao X, Chen D, Li C (2016) One-step asymmetric growth of continuous metal-organic framework thin films on two-dimensional colloidal crystal arrays: a facile approach toward multifunctional superstructures. *Cryst Growth Des* 16(5):2700–2707
171. Butova VV, Soldatov MA, Guda AA, Lomachenko KA, Lamberti C (2016) Metal-organic frameworks: structure, properties, methods of synthesis and characterization. *Russ Chem Rev* 85(3):280
172. Liu J, Chen L, Cui H, Zhang J, Zhang L, Su C-Y (2014) Applications of metal-organic frameworks in heterogeneous supramolecular catalysis. *Chem Soc Rev* 43(16):6011–6061
173. Sun C-Y, Qin C, Wang X-L, Su Z-M (2013) Metal-organic frameworks as potential drug delivery systems. *Expert Opin Drug Deliv* 10(1):89–101
174. Zeng L, Guo X, He C, Duan C (2016) Metal-organic frameworks: versatile materials for heterogeneous photocatalysis. *ACS Catal* 6(11):7935–7947
175. Hu Z, Deibert BJ, Li J (2014) Luminescent metal-organic frameworks for chemical sensing and explosive detection. *Chem Soc Rev* 43(16):5815–5840
176. Cai W, Chu CC, Liu G, Wang Y-XJ (2015) Metal-organic framework based nanomedicine platforms for drug delivery and molecular imaging. *Small* 11(37):4806–22
177. Zhao Y, Song Z, Li X, Sun Q, Cheng N, Lawes S et al (2016) Metal organic frameworks for energy storage and conversion. *Energy Storage Mater* 2:35–62
178. Ramaswamy P, Wong NE, Shimizu GKH (2014) MOFs as proton conductors—challenges and opportunities. *Chem Soc Rev* 43(16):5913–5932
179. Liang K, Ricco R, Doherty CM, Styles MJ, Bell S, Kirby N et al (2015) Biomimetic mineralization of metal-organic frameworks as protective coatings for biomacromolecules. *Nat Commun* 6(1):1–8
180. Boury B (2017) Biopolymers for biomimetic processing of metal oxides. In: *Extreme biomimetics*. Springer, pp 135–89
181. Zhou S, Zou X, Sun F, Zhang F, Fan S, Zhao H et al (2012) Challenging fabrication of hollow ceramic fiber supported Cu₃(BTC)₂ membrane for hydrogen separation. *J Mater Chem* 22(20):10322–10328
182. Iliescu RI, Andronescu E, Voicu G, Ficai A, Covaliu CI (2011) Hybrid materials based on montmorillonite and citostatic drugs: preparation and characterization. *Appl Clay Sci* 52(1–2):62–68
183. Fan Q, Shan D, Xue H, He Y, Cosnier S (2007) Amperometric phenol biosensor based on laponite clay-chitosan nanocomposite matrix. *Sensens Bioelectron* 22(6):816–821
184. Suresh R, Borkar SN, Sawant VA, Shende VS, Dimple SK (2010) Nanoclay drug delivery system. *Int J Pharm Sci Nanotechnol* 3(2):901–905
185. Giannelis EP (1996) Polymer layered silicate nanocomposites. *Adv Mater* 8(1):29–35
186. Ding S-N, Shan D, Xue H-G, Zhu D-B, Cosnier S (2009) Glucose oxidase immobilized in alginate/layered double hydroxides hybrid membrane and its biosensing application. *Anal Sci* 25(12):1421–1425

187. Rodrigues LA, Figueiras A, Veiga F, de Freitas RM, Nunes LC, da Silva FEC, et al (2013) The systems containing clays and clay minerals from modified drug release: a review
188. Jain S, Datta M (2016) Montmorillonite-alginate microspheres as a delivery vehicle for oral extended release of venlafaxine hydrochloride. *J Drug Deliv Sci Technol* 33:149–156
189. Kevadiya BD, Joshi GV, Patel HA, Ingole PG, Mody HM, Bajaj HC (2010) Montmorillonite-alginate nanocomposites as a drug delivery system: intercalation and in vitro release of vitamin B1 and vitamin B6. *J Biomater Appl* 25(2):161–177
190. Iiescu RI, Andronescu E, Ghitulica CD, Voicu G, Ficai A, Hoteteu M (2014) Montmorillonite-alginate nanocomposite as a drug delivery system-incorporation and in vitro release of irinotecan. *Int J Pharm* 463(2):184–192
191. Kaygusuz H, Erim FB (2013) Alginate/BSA/montmorillonite composites with enhanced protein entrapment and controlled release efficiency. *React Funct Polym* 73(11):1420–1425
192. Kevadiya BD, Joshi GV, Mody HM, Bajaj HC (2011) Biopolymer-clay hydrogel composites as drug carrier: host-guest intercalation and in vitro release study of lidocaine hydrochloride. *Appl Clay Sci* 52(4):364–367

Natural Polymeric-Based Composites for Delivery of Growth Factors



M. D. Figueroa-Pizano and E. Carvajal-Millan

In the complexity of the human body, individual cells need to be connected and communicated continuously between them to realize an ordered and efficient work, regardless of whether or not they are performing the same function within an organ. Around the cells, the extracellular matrix (ECM) creates support and a specific environment where thousands of active molecules are released by the same cells to establish these communication and signalization processes [1, 2]. The active molecules are recognized by specific receptors at the cellular membrane and they can trigger many internal biochemical mechanisms related to cell survival [3]. Thus, cells are stimulated in a synchronic manner to meet with the specific actions that they need and, at the same time, complement the other ones.

In this context, growth factors (GFs) are an extended group of naturally released signaling molecules that have critical roles determining the fate of the cell. They are small and soluble glycoproteins responsible for conveying information from cell to cell to control and regulate their functions, such as proliferation, differentiation, morphogenesis, and migration [4, 5]. They also actively participate in mechanisms as homeostasis, inflammation, wound healing, and antiviral response [6, 7]. Structurally, GFs are formed by polypeptide dimers, which vary in number and type of amino acid residues [8, 9]. GFs are secreted by different kinds of cells (stem, neurons, epithelial, hepatic, muscular, blood, etc.) generally in the same organ or tissue where they go to act [7]. A single GF can be produced in many types of cells in different stages of maturation; however, it can evoke different effects depending on the delivery concentration, the target cell, and the maturation phase of the target cell [7, 10]. All mature forms of GFs reside in the ECM in association with molecules as collagen,

M. D. Figueroa-Pizano (✉) · E. Carvajal-Millan
Biopolymers-CTAOA, Research Center for Food and Development (CIAD), Hermosillo, Sonora,
Mexico

E. Carvajal-Millan
e-mail: ecarvajal@ciad.mx

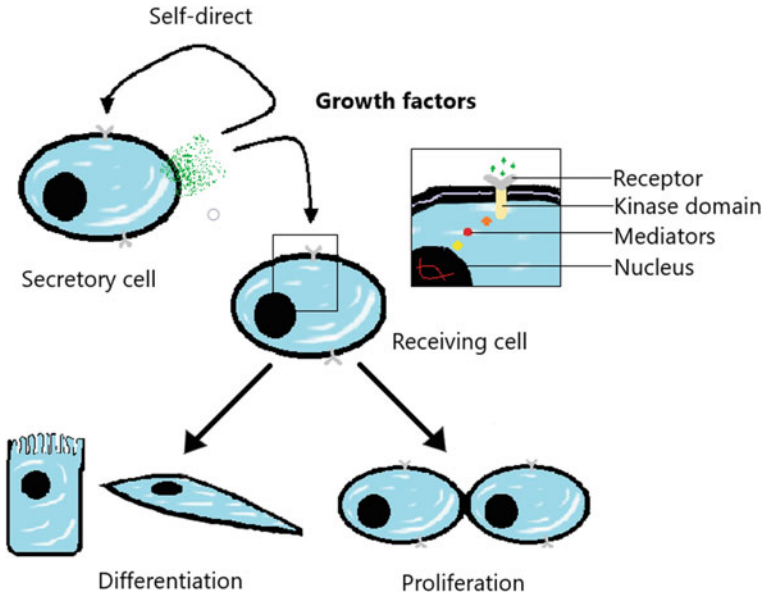


Fig. 1 Schematic representation of different functions regulated by GFs

elastin, glycosaminoglycan, and other components. Those associations protect them from enzymatic degradation and regulate the binding with their receptors, therefore also regulate their activities [11].

GFs can diffuse through the ECM and execute rapid communication between nearby cells, including those from a different population, and act in autocrine or paracrine forms [12, 13]. Some of them also can perform an endocrine action. Besides, the GFs precursors, generally presented as immature protein on the cellular membrane, may be able to stimulate neighboring cells in a juxtacrine way. The carried message by GFs is sending through their binding with a transmembrane receptor, in canonical or non-canonical signaling pathways, into target cells [14, 15]. The receptors are proteins conformed by an extracellular or binding domain, a transmembrane domain, and an intracellular tyrosine kinase domain. After a GF (ligand) binds its receptor by extracellular domain, conformational changes start the transduction process, and the cytoplasmic domain turns into a tyrosine kinase enzyme. In this way, some intrinsic signalization pathways are activated and end in a modification of gene expression, which is translated as the cell behavior [6, 7]. Figure 1 shows a schematic representation of the ways GFs action.

The large number of GFs detected has been grouped into several families considering standard features as their structure, activities, and target cells. The most studied and comprehended families of GFs are presented below:

1. *Fibroblast growth factor (FGF) family* is considered as one of the most varied collections of GFs due to its members are similar in structure, but they can

act in different ways [5]. Around 22 proteins belong to this set of GFs and have been separated into six subfamilies, which are classified into two main classes: paracrine-action FGFs and endocrine-action FGFs [16–18]. In fact, the FGF family encompasses proteins with autocrine, juxtacrine, paracrine, and endocrine action form [19]. Along the embryonic stage, they are produced in all tissues to regulate processes as differentiation, proliferation, apoptosis, and migration of mesenchymal cells [18, 20]. In the mature stage, the paracrine-action FGFs continue these functions to maintain and remodel tissues, while the endocrine-action FGFs regulate some metabolic routes (lipids, carbohydrates, and bile acids) [5, 17]. Generally, paracrine-action of FGFs depends on their union with heparan-sulfate proteoglycan in the ECM. This union gives them stabilization and protection to canonically binding with their receptors [16, 18, 19]. Several members act in blood vessels, skin, bone, nerves, and muscles, and they are considered potent angiogenic factors due to their high regulation of proliferation and migration of endothelial cells.

2. *Platelet-derived growth factor (PDGF) and Vascular endothelial growth factor (VEGF) family* enclosed these two main subfamilies of GFs, which share structural and functional characteristics [21]. Structurally, both PDGF and VEGF present a growth factor core domain, which is distinguished by a conserved cysteine-knot fold with eight residues [22, 23]. These subfamilies play the most important roles during blood vessel formation and they have been recognized as possible regulators of neurogenesis. They also perform essential functions in hematopoietic development and neuroprotection process [24].
 - (a) *Platelet-derived growth factor (PDGF) subfamily* owes its name due to some members are produced and released from platelets in the blood clotting process [25]. The cysteine-knot fold presented in PDGF proteins is composed of eight residues that maintain the 3D structure [22]. PDGFs regulate the proliferation and migration of mesenchymal cells and guide the organogenesis throughout the embryonic stage [26]. The action of these factors depends on the specific receptor which they binding. In the early stage, they seem to influence skin, lungs, kidney, and intestine formation, by linking their alpha-receptor (PDGFR α) [22, 24]. In contrast, PDGFs union with their beta-receptor (PDGFR β) regulates the angiogenesis (creation of blood vessels from already formed) and the formation of the connective tissues. The primary stages of hematopoiesis are also controlled by the union between PDGF and PDGFR β [25]. Besides, they can act as chemotactic factor because they attract and stimulate neutrophil and macrophage cells in injury zones [21, 27]. The PDGFs bio-availability in the ECM is limited by their interactions with α_2 -macroglobulin and PDGF-associated protein (PAP). Also, their binding with glycosaminoglycan and collagen affects their bioactivity [21, 25, 28].
 - (b) *Vascular endothelial growth factor (VEGF) subfamily* encompasses the most specialized and potent GFs able to stimulate the endothelial cells

leading to the production and maintenance of vascular and lymphatic systems [29]. This GFs family actively regulates *de novo* vascularization in all organs (including bone and pulmonary epithelium) during embryonic stage [30–32]. They mainly regulate the angiogenesis process, increase the permeability of blood vessels, and activate the chemotaxis of monocytes [29, 31]. Structurally, they also show a cysteine-knot fold region and high affinity to bind heparan-sulfate proteoglycans, which are necessary for its recognition [23, 29].

3. *Transforming growth factor (TGF- β) family* is very diverse and contains two main groups: TGF- β and bone morphogenetic proteins (BMPs). Both classes mainly regulate osteoblast differentiation in mesenchymal stem cells (MSC). Although each of these GFs has its participation, it is not necessarily in the same proportion [33]. TGF- β plays an essential role in the signalization via for the synthesis of components that form ECM, stimulate monocytes and lymphocytes activity, and participate in the wound healing process [34]. However, TGF- β also can inhibit the proliferation and differentiation of epithelial and adipocytes cells. TGF- β can encourage or interrupt apoptosis [35]. All TGF- β present a distinctive segment of nine cysteine residues in their structure, whereas BMPs only have seven [36]. The BMPs are a large group composed of around 13–20 proteins that are the primary regulators of bone and cartilage formation [37]. They actively stimulate the MSC differentiation to be derived in osteocytes and chondrocytes cells at the embryonic stage [38, 39]. BMPs participate in dorsal-ventral designing and help in the development and conservation of skeletal [39, 40]. They are heparan-sulfate binding proteins in ECM, which gives them stabilization, diffusion, and let them establish signalization with the receptors [40].
4. *Epidermal growth factor (EGF) family* is a significant and profoundly studied group composed of 11–13 proteins (only seven are listed in Table 1) structurally and biologically similar [41–43]. They are engaged to induct differentiation, proliferation, or apoptosis in keratinocytes, oocytes, enterocytes, or lung cells [44, 45]. All GFs that belong to this family present standard glycosylated transmembrane-protein precursors containing six equally and conserved cysteine residues [46]. These protein precursors have an extracellular EGF domain able to stimulate other cells in a juxtacrine manner [42, 44]. Besides, the EGF domain can be cleaved by metalloproteinase to release the mature GFs that present an autocrine or paracrine action [46]. The members of this GFs family have similar affinity by the same receptors, being redundant in function, although each of them can realize a specific role in different tissues or organs (from bone, kidney, and neuron cells) [27].
5. *Neurotrophins (NTs) or Nerve growth factor (NGF) family* is a group of GFs specially devoted to guiding critical processes of neural cells. These factors are part of neurotrophic factors (NF), together with the glial cell line-derived neurotrophic factor (GDNF) family, and some members of the cytokine family [47–49]. All NTs proteins share a very similar structure (about 50%) because

Table 1 Principal members of the GFs families, their receptors, their primary function and their secretory, and target cells

Name family	Subfamily	Growth factor (ligands)	Receptors	Functions that stimulate	Secretory cell	Target cell	
FGF *Heparan-sulfate binding proteins (cofactor) +βK1oto/αK1o1ho (cofactors)	*FGF-1 subfamily	FGF-1 FGF-2	All FGFR FGFR-1	Proliferation Differentiation	Keratinocytes Fibroblasts Endothelial	Fibroblast Epithelial Endothelial	
	*FGF-4 subfamily	FGF-4 FGF-5 FGF-6	FGFR 1-4	Motility Survival Angiogenesis Apoptosis	Muscle Chondrocytes Mast cells Osteoblast Macrophages	Mesenchymal Bone Muscle Neurons	
	*FGF-7 subfamily	FGF-3 FGF-7 (KGF) FGF-10 (KGF-2) FGF-22	FGFR-1,2 FGFR-2 FGFR-1,2 FGFR-2				
	*FGF-8 subfamily	FGF-8 FGF-17 FGF-18	FGFR-3, 2, 1				
	FGF-9 subfamily	FGF-9 FGF-16 FGF-20	FGFR-3, 2, 1				
	FGF-11 subfamily	FGF-11 FGF-12 FGF-13 FGF-14					
	FGF-15/19 subfamily	FGF-15/19 FGF-21 FGF-23	FGFR 1-4 FGFR-1,3 FGFR-1,3,4				

(continued)

Table 1 (continued)

Name family	Subfamily	Growth factor (ligands)	Receptors	Functions that stimulate	Secretory cell	Target cell
PDGF/VEGF <i>*Heparan-sulfate binding proteins</i>	PDGF <i>Subfamily</i>	*PDGF-AA *PDGF-BB *PDGF-AB PDGF-CC PDGF-DD	PDGFR- $\alpha\alpha$ PDGFR- $\alpha\alpha$, - $\beta\beta$, - $\alpha\beta$ PDGFR- $\alpha\alpha$, - $\alpha\beta$ PDGFR- $\alpha\alpha$, - $\alpha\beta$ PDGFR- $\beta\beta$, - $\alpha\beta$	Mitotic: • Proliferation • Survival • Migration Chemotaxis Angiogenesis Production of ECM compounds	Platelets Epithelial Fibroblast Endothelial Macrophages Smooth muscle cell	Mesenchymal Fibroblast Glial cells Muscle Hepatocytes
<i>*Heparan-sulfate binding proteins</i>	VEGF <i>subfamily</i>	*VEGF-A *VEGF-B VEGF-C VEGF-D Placental GF (PlGF)	VEGFR-1, VEGFR-2 VEGFR-1 VEGFR-3 VEGFR-3 VEGFR-1	Angiogenesis: • Proliferation Chemotaxis: • Motility	Endothelial Platelets Fibroblasts Macrophages Keratinocytes Smooth muscle cell Neutrophil	Endothelial Macrophages Smooth muscle cell
TGF- β <i>**Collagen binding proteins</i> <i>*Heparan-sulfate binding proteins</i>	TGF- β <i>subfamily</i>	**TGF- β 1 **TGF- β 2 **TGF- β 3 Nodals ** Activins Some Growth and Differentiation Factors (GDF)	T β R-I, II T β R-II, I TR-I, II T β R-II, ActRII T β RIII (no-binding)	Inhibition of: • Proliferation • Differentiation Promote: • Differentiation Migration Apoptosis Cell adhesion Cytoskeletal organization	Platelets Fibroblasts Macrophages Keratinocytes	Mesenchymal Epithelial Adipocyte Myocytes Osteoblast

(continued)

Table 1 (continued)

Name family	Subfamily	Growth factor (ligands)	Receptors	Functions that stimulate	Secretory cell	Target cell
	*BMPs <i>subfamily</i>	BMP-2 BMP-3 BMP-6 BMP-7 BMP-9 Some GDF	Type I (TβR-I) (all BMPs are more affine for this receptor) Type II (TβR-II)	Bone and cartilage formation: • Proliferation • Differentiation • Morphogenesis • Homeostasis	Fibroblasts Macrophages	Mesenchymal Osteoblast
EGF		EGF TGF alfa Heparin-binding Epidermal growth factor (HB-EGF) Neuregulin 1 Neuregulin 2 Neuregulin 3 Neuregulin 4	ERBB1 ERBB1 ERBB2 (no-binding) ERBB1, ERBB4 ERBB3, ERBB4 ERBB3, ERBB4 ERBB4 ERBB4	Growth Proliferation Migration Differentiation Apoptosis	Epithelial Platelets Macrophages Hepatocytes Keratinocytes	Epithelial Epidermic
Neurotrophins		NGF Brain-derived neurotrophic factor (BDNF) Neurotrophin-3 (NT-3) NT-4/5	TrkA, p75NGFR TrkB, p75NGFR TrkC TrkC	Survival Plasticity Apoptosis Axon growth Dendrite pruning Expression of: Neurotransmitters Ion channels	Schwann cells Fibroblasts Mast cells	Neurons
IGF ***IGF binding proteins		***IGF1 ***IGF2 Insulin (no GF action)	IGFR-1 IGFR-2	Growth Proliferation Differentiation	Hepatocytes Fibroblasts Macrophages Neutrophils Neurons Enterocytes	Hepatocytes Neurons Many types of cells

(continued)

Table 1 (continued)

Name family	Subfamily	Growth factor (ligands)	Receptors	Functions that stimulate	Secretory cell	Target cell
HGF		HGF HGF-like protein (HLP)	c-Met	Proliferation Morphogenesis Motility Angiogenesis	Fibroblast Mesenchymal Stromal Macrophage	Epithelial Endothelial Melanocytes Hepatocytes

The significance of 'asterisk' specifies a characteristic of the FGs depending on the family to which it belongs. The meaning of the asterisk changes for each family and it is specified in the first column on the left below the family name. The GFs marked with an asterisk in the second column have the characteristic of that family

they are produced by common genes with identical sequences [48, 50]. Functionally, they regulate the differentiation, survival, migration, and proliferation of neurons since the development of central and peripheral nervous systems [48, 50–52]. In mature neurons, they also control the establishment of synapses and neuron's plasticity. Besides, they help in the regeneration and remyelination of neurons when the inflammatory process occurs as part of neurodegenerative disease [47, 49, 53].

6. *The insulin-like growth factor (IGF) family* is part of a more complex system of proteins that regulates the cell development throughout the different stages of life and control some physiological aspects [54, 55]. The leading members of this family are positively related to insulin because they share around 50% of structural homology, some receptors, signaling pathways, and in occasions, similar metabolic activities [56–58]. However, IGFs are more focused on the growth-direction, regulating mechanism as proliferation, differentiation, and apoptosis of a great variety of cells [54, 57, 59]. Besides, insulin is produced exclusively in the pancreas and exerts its action freely, while IGFs are secreted mainly by the cells in the liver and other organs, and they bind other specific proteins [60]. IGFs influence the development and restoration of the liver as well as the growth and survival of hepatocyte cells [57, 61]. The production and action of IGFs are in all organs and are stimulated in different grades by growth hormone, as well as depending on the age, lifestyle, and genetic factors [56, 58]. Besides, one of their members (IG-1) acts as a glucose regulator independently of insulin and participates actively in the preparation of injured tissue. While the other (IGF-2) is widely distributed in the brain and central nervous system during the embryonic stage, probably supporting the human development [61]. In adulthood, high levels of IGFs have also found in the nervous system suggesting a necessary action of them [59].

The bioactivity of IGFs is regulated by their association with one group of six proteins closely related to them, named as IGF binding proteins (IGFBPs) [55, 57]. The IGFs present high affinity by IGFBPs, almost the same as they have for their receptors, so most of the time, they are binding to these proteins [56]. The bounding of IGFs with specific IGFBPs mostly inhibit their action because they can limit their union with their receptor [55]. This binding allows to extend the half-life of IGFs in blood-stream or ECM, protect them from proteolytic degradation, storage them in ECM, carry them to target cells, and modulate their interaction with a specific receptor [54, 56–58, 61]. Usually, free-IGFs have a half-life of 10 min, while bounding with IGFBPs it is extended until 30 min, and even they can form a ternary complex with an acid-labile subunit (associated protein, IGFBP-rPs), which extend their life around 10–13 h [57, 61]. The separation of IGFs from IGFBPs is promoted by decreasing their affinity, for example, phosphorylation of IGFBPs or binding them with other molecules in ECM, as well as by proteolytic action [56].

7. *Hepatocyte growth factor (HGF) family* is a small group of GFs formed by at least two proteins with great action on the liver. HGF is the principal member that regulates, in a paracrine fashion, the proliferation, morphogenesis, and

motility of epithelial, endothelial, and melanocyte cells [62–64]. It is considered multi-functional GF because during the embryonic development is essential for many organ formation and maturation. At the same time, in adults, it participates in reparation and regeneration processes of the lacerated liver, lungs, gastrointestinal tract, and kidney [62–65]. Recent studies indicate that HGF also plays an essential role in osteogenesis, bone healing, and restoration of the nervous system [65, 66]. Moreover, it exerts a regulative effect on anti-inflammatory, anti-apoptotic, and anti-fibrotic signal pathways in several organs [62, 66, 67]. Even, HGF has been considered as a modulator in glucose metabolism in several cells since their receptor (c-Met) is similar to the insulin receptor [67]. HGF structure is well characterized as 92 kDa heterodimer, which is bounded to heparin-sulfate in ECM, helping their stabilization and interaction with a specific receptor [8].

Other families no less important, are the Wingless (Wnt) proteins and the hematopoietic growth factor, the latter is recognized to encompass many cytokines with the capacity to regulate the production and activities of blood cells [5, 7]. Indeed, groups of transmembrane receptors as Eph and Notch proteins are considered as GFs because of their juxtacrine signaling that drives cell localization, differentiation, proliferation, and homeostasis in different stages of the cell life [68, 69]. Table 1 presents detailed information about more representative families of GFs: ligands, receptors, functions that regulate, secretory cells, and the target cell.

1 Biomedical Applications of GFs

A wide variety of studies have tried to transfer the essential and natural regenerative functions performed by GFs to different medical applications. Over the years, GFs and their receptors have been thoroughly studied, leading to a very well understanding of their regulatory roles on signalization pathways. Endogenous GFs are considered indispensable orchestrators of molecular and cellular responses to rebuild or regenerate damaged organs and tissues [70]. In that sense, many endogenous GFs have been isolated and produced by genetic engineering, as recombinant proteins, and have been used as exogenous therapeutic agents in regenerative medicine [71]. The employment of these exogenous GFs to treat injuries or chronic disease failures is a good strategic to enhance the natural self-renewal capacity of the cells as well as to improve the overall healing results.

The main therapeutic approaches for GFs have been applied in tissue engineering and in wound healing (Table 2). Regarding tissue engineering, exogenous GFs have been supplemented, as therapeutic protein, for restoration and regeneration of bone, cartilage, tendons, cardiac muscle, peripheral muscle, nervous system, the pulp of the immature tooth, and capillary vessels [70, 72–76]. Usually, transplanted tissue grafts employ stem cells, which are stimulated by exogenous GFs to differentiate them in any specialized cells. Hence, the GFs are becoming in a useful tool for the

Table 2 Main GFs used in tissue engineering and regenerative medicine

Tissue/organ/systems	GFs applied	Result
<i>Blood vessels</i>	VEGF	Vascularization and angiogenesis Migration and proliferation of endothelial cells [71, 78, 85]
	PDGF	Increase size and maturation of vessels [86]
	FGF	Maturation of vessels Stimulates endothelial cell migration Matrix deposition [87]
	TGF- β	Vascular morphogenesis [88, 89]
<i>Muscle (myocardium/skeletal)</i>	bFGF	Promotes myoblast proliferation [90]
	VEGF	Migration cardiac progenitor cells Angiogenesis [91]
	PDGF	Pericyte recruitment [92]
	HGF	Migration of cardiac progenitor cells. Normalization of angiogenesis [91, 93]
<i>Nervous system</i>	NGF	Peripheral nerve regeneration Neurite outgrowth [4]
	NT-3	Neuronal survival [76]
	NT-4	Neuronal survival [76]
	FGF-2 (bFGF)	Nerve regeneration: myelin renewal Stimulates Schwann cell survival [4, 76]
<i>Skin</i>	EGF	Stimulates the proliferation of fibroblasts keratinocytes, and vascular endothelial cell Enhances the production of fibronectin [81, 82]
	VEGF	Re-epithelialization process (migration and proliferation of endothelial cells) Angiogenesis [78]

(continued)

Table 2 (continued)

Tissue/organ/systems	GFs applied	Result
	PDGF	Chemotactic for fibroblasts, neutrophils, monocytes, and smooth muscle cells Activates macrophages to release GFs Promotes fibroblast proliferation Production of extracellular matrix [83]
	FGF	Acts as a mitogen for fibroblasts Induces angiogenesis Stimulates granulation tissue formation Re-epithelialization [83]
	TGF- β -3	Potent chemoattractant for macrophages Stimulates or inhibits proliferation. Granulation tissue formation [83]
	TGF- α	Proliferation of basal cells [71]
	IGF	Promotes re-epithelialization Stimulates fibroblast proliferation [83]
	BMP: BMP-2 and BMP-7	Bone induction: osteoblasts growth and proliferation [13, 73]
<i>Bone</i>	TGF- β	Proliferation periosteal cells Chondrogenic differentiation [73, 74]
	IGF	Osteogenic differentiation [74]
	FGF	Osteogenic differentiation [74] Angiogenesis [13, 74]
	VEGF	Neo-angiogenesis [73] Recruitment of bone-forming cells [13]
	PDGF	Angiogenesis and cell proliferation [74]

*Brain-derived neurotrophic factor

regeneration of tissues or cells with low renewal capacity; for example, HGF has applied to differentiate stem cells into neurons while BMP into tendons [66, 77]. In wound healing management, exogenous GFs have been administrated to treat injuries caused by surgery, trauma, diabetic ulcer, burns, among other types of damages [78–80]. The functional repair of wounds, based on these molecules, is due to the

GFs capacity to generate a microenvironment where proliferation, differentiation and migration processes are stimulating [81, 82]. Besides, GFs can modulate ECM-components production, angiogenesis, inflammatory response, and construction of granulation tissue, which are essential in wound healing [83]. The most recognized GFs involved in wound healing and skin reparation are EGF, KGF, bFGF, PDGF, VEGF, TGF- β , IGF [2, 84].

Beyond the regenerative effects of GFs, they have been harnessed as therapeutic molecules in some diseases or as biomarkers of the disease grade. Because of the pleiotropic effects of HGF, it can serve as treatment of liver, lungs, and kidney diseases [66, 67]. Also, HGF administration improves the management of hepatic insulin resistance because it reduces the fasting blood glucose, triglycerides, and cholesterol levels in mice [94–96]. The IGF-1 level in blood seems to have an association with the development of diabetes, and the recombinant IGF-1 has proved to drop blood glucose concentration and increase blood insulin [58]. Both effects could be used as a biomarker or as a treatment in diabetes. The IGF-1 has shown a protective effect against the development of Parkinson's disease due to their supplementation restored the damage of brain inflammation, the diminished oxidative damage, apoptosis as well as preserved the integrity of blood-brain barrier, and the cognitive capacities [97]. In another study, the NGF presented therapeutic properties for Alzheimer's disease because it had acted as a neuroprotective agent for PC12 cells when they were exposed to a cytotoxic agent, which is present in this disease [98]. Another relatively new emerging therapy based on a cocktail of GFs has been implemented to treat ocular diseases through plasma application (a blood-derived product), which contained a mix of PDGF, TGF- β , VEGF, IGF-1, and HGF [99].

Recently, GFs have been considered as target molecules for new treatment in cancer development. Despite the beneficial actions that GFs promote under physiological conditions for cell growth and survival, many studies have shown their active involvement in several cancers. Among the leading families of GFs and receptors that are found overexpressed in cancer is IGF, VEGF, TGF- β , HGF, EGF, and FGF [100, 101]. They have been identified in the breast, colon, liver, pancreas, prostate, leukemia, brain, lung, kidney, ovary, stomach, and colon cancers. In these types of cancers, the cells are enormously stimulated by GF inducing an accelerated growth, clonal expansion, angiogenesis, metastasis, and cross-talk with neighboring components [101, 102]. However, GFs are genuinely committed to their natural functions binding their receptors indistinguishably in both standard and tumor cells. The excessive action of GFs in cancer cells only helps for disease development because the real cancer origin is the loss of the cellular cycle regulation due to oncogenic mutations. Cancer cells attract macrophages and create the right conditions for unproportioned release of GFs [103]. Additionally, cancer cells present more transmembrane GF's receptors being hypersensitive to the autocrine action of GFs [101, 103]. After elucidation of the critical role that GFs play in cancer development, they have been identified as target molecules to generate molecular antibodies that prevent the action of both ligands and receptors. Indeed, the genes of these molecules have been detected and selectively silenced by short interfering RNAs [104]. Some

GFs-receptors systems highly present in cancers have been considered as an ideal biomarker for the prognosis or diagnosis of these diseases [105].

2 Challenges and Approaches to Develop Devices for GFs Delivery

The promising therapeutic results of GFs showing in several research works and clinical trials have led to the search for adequate administration ways to generate new and improved commercial products. Nowadays, many recombinant humans (rh) GFs proteins, such as rhFGF, rhIGF, rhKGF, and rhEGF, are commercially available, allowing their use in medical products. However, only one product has been approved by the United States Food and Drug Administration (FDA), this is the Regranex[®] gel with becaplermin (rhPDGF) at 0.01%, as a topical treatment for diabetic wounds [11]. Other products based on rhGFs are the INFUSE[®] gel with rhBMP-2 and rhBMP-7, used to treat lumbar spine fusion and open tibial fracture [106]; the Heberprot-P[®], a freeze-dried product, the Regen-D[™] gel, and the Easyef[®] spray contains rhEGF to treat ulcer diabetic wounds; while Fiblast[®] spray contains rhbFGF for being administrated on the skin with burn ulcers [83]. The direct application of GFs using injections, solutions, creams, lotions, gels, sprays, and ointments generally resulted in inefficient delivery due to the gradual deactivation of GFs [79]. In this case, repeated doses of medications are demanded, turning them expensive. However, the constant use of these treatments has several warnings due to adverse effects and consequences they can cause [11, 107]. For that reason, it is imperative to consider the suitable concentrations of GFs to obtain the expected results without inefficient or excessive GFs action. The main concerns about the efficacy of GFs in clinical products are the poor stability and the short-half life that these molecules have [108]. Generally, they are unstable to pH and temperature changes, suffer oxidation of amine groups, and they are very susceptible to enzymatic degradation or inactivation [107]. Many efforts trying to solve these drawbacks are focused on GFs modification to make them stable at physiological conditions, whereas others have concentrated in the development of delivery systems able to preserve GFs the native forms and functions, and carry them to the target cells.

2.1 Approaches for Intrinsic Improvement of Stability and Action of GFs

Many efforts have been made to extend the functional activity of exogenous GF, which are mainly based on structural modification through genetic and protein engineering [11]. Several random, site-direct and combinatorial mutations on GFs genes have been done attempting the production of more stable GFs and with prolonged

half-life [109]. The final GF produced with genetic changes must remain the similarity enough to the natural GFs to be functional. The most effective variations are the creation of relatively small and less complicated GFs and the removal of protease cleavage sites in the structure. Other changes imply an enhanced binding affinity of GFs by their receptors, and the recycling action of the receptors after their internalization to come back to the membrane [106, 109]. Besides, genetic management also envelops the production of recombinant proteins due to all engineering GFs are settled, detected, and isolated from surfaces of bacteria, yeast, or mammalian cells [106].

Other structural modifications have been done in mature GFs with the same purpose of stabilization and increase their half-life. In small GFs, the amino-terminal end is used to cycle the structure and join it with the carboxyl-terminal being less prone to the temperature or protein degradation [106]. Another common modification is grafting polyethylene glycol (PEG) on the GFs chain to expand its half-life. PEGylation of GFs provides them thermal stability and avoids their enzymatic degradation due to the PEG increase of hydrodynamic radius, which masks the cleavage sites [110]. The FDA has approved some of these PEGylated-GFs for their usage in therapeutic products among them are found PEG-IGF-1 and FGF [111, 112]. A possible disadvantage of these modifications are their interferences with the receptor-binding site. Figure 2 shows some of the benefits of the modifications of GFs.

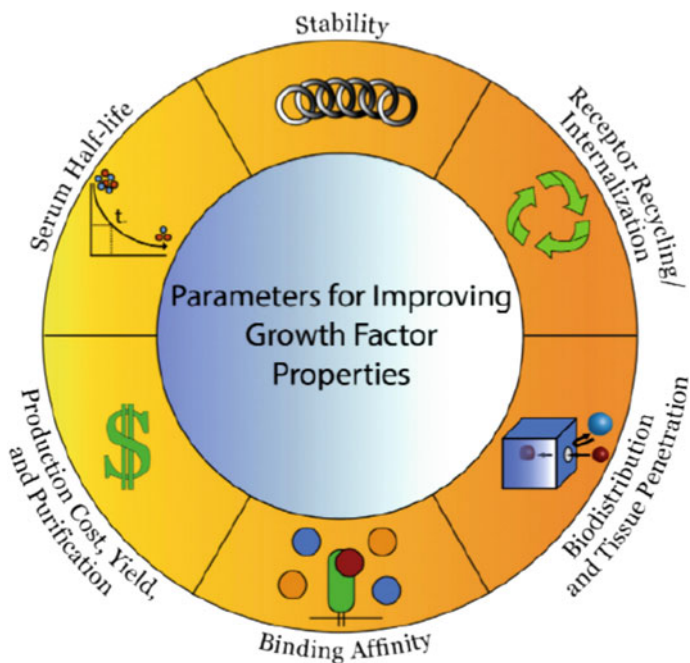


Fig. 2 Main advantages obtained after modification of GFs. *Source* Mitchell et al. [106]

2.2 *Approaches for GFs Delivery Systems*

Another sophisticated strategy, to preserve the intrinsic properties of GFs to use them in the clinical area, is their encapsulation in delivery systems. The incorporation of GFs in matrices of diverse natures has been considered as a practical approach to separate them within a particular microenvironment that conserves their integrity. There is specific interest in lipid particles (mussels and vessels), nanofibrous assemblies, polymeric materials (natural and synthetic), or well, a combination of them [83]. The main advantages of using delivery systems for GFs encapsulation are protection from physical and enzymatic degradation, direction to the target cells, and release in sustained-manner [113]. Additionally, stimulus-responsive delivery system can be fabricated to modulate the GFs release after they sense physiological changes or a disease-specific stimulus [10]. Another advantage of these systems is the possibility of dual or multi GFs encapsulation to obtain a synergistic effect and better therapeutic results [82]. Besides, depending on the nature of the delivery system, similar ECM conditions can be created, pretending to extend the bioactivities of GFs. In this way, the spatial-temporal delivery of GFs can be controlled to reduce the continuous applications and the side-effects as well as to improve their therapeutic and tissue-forming capacities, being them more cost-effective [81, 108]. However, the engineering of these delivery systems is challenging, since mimicking the ECM environment and controlling the release rate of GFs, involves the consideration of several biological and physicochemical aspects.

Notably, three aspects have been recognized as necessary for the correct design process of delivery materials. (1) Biological requirements. The selection of adequate GF before starting is imperative. It is essential to keep in mind their functions, size, structure, and biochemical features because they affect their interaction with the materials [12]. The pretended morphological and histological outcomes also need to have visualized. Additionally, the biological, anatomical, and functional characteristics of the target cell, tissue, or organ should know. (2) Material properties. Depending on the place where the material will be used is essential to select it based on its nature, chemical structure, molecular weight, mechanical properties, compatibility, degradability, and binding/interaction ability with GFs [13, 107, 114]. (3) Delivery strategies. Structure shape and size of the material need to be considered not only for its introduction, direction, or colocation in the place of interest, these features are critical for loading efficiency and release kinetic of GFs [12]. The loading step is vital for GFs activity because it involves the manipulation (vulnerability to denaturalization) and estimation (correct quantity for expected results) of GFs, so the process needs to be simple [13]. The amount of GF loading limits the amount of GFs released and its release kinetic. This latter topic is considered the most important to obtain the desired therapeutic results; its control implies avoiding excessive and insufficient dosages or burst and lag phases. Unbalance in loading and releasing stages could involve inactivation of signal pathways, incomplete or incorrect induction of regenerative effect, or well, a cytotoxic and adverse response causing other clinical complications.

2.2.1 Loading and Releasing Strategies for GFs into Biomaterials

Recently, multiple innovative ways have been proposed to seed the GFs into biomaterials, which later facilitate their release. Some loading methods have been described in detail for polymeric materials and they are presented below. The easiest way is the infusive method because it only requires the GFs in solution, generally in cell culture media, and then, they are directly added and penetrate the material by diffusion. This incorporation can be performed manually or automatically. Recently, the automatic way is based on the use of bioreactors (spinner flasks, rotation wall vessel, and perfusion bioreactor) [115, 116]. Several considerations should be made when this method is used, for example, the materials require a highly porous structure for good penetration, using the manual method there is the risk that GFs solutions are not well distributed while using the automatic method high shear stress could be generated affecting the cell development [12]. Another method is the immobilization of GFs inside the conveyor material through chemical (covalent) or physical (electrostatic, ionic, hydrogen bonds, among others) entrapments [11, 110, 114]. For this, it is essential to consider the functional groups that are contained in the basic chemical structure to establish the chemical or physical link. Besides, during chemical encapsulation, the GFs could be denaturalized.

As mentioned before, the loading step determines the releasing way of the GFs from the carrier. Physically trapped GFs are commonly released by diffusion, erosion, and swelling. In this case, it is also essential to consider the structural characteristic of the carrier (porosity, pore size, hydrophilicity, etc.). Chemically attached GFs are released by cleaving the interaction site between the GF molecule and the carrier matrix [11, 106, 108]. Enzymatic action is frequently employed for that purpose. Most refined release mechanisms are enclosed in the category of programmed delivery. Here, the materials present the capacity to activate and to control the GF releasing based on biological and physical stimuli, such as temperature, pH, light, magnetic field, and enzymatic [10].

A wide variety of regenerative tissue materials have been exhaustively evaluated to detect the best for GFs delivery. Promising results have been obtained for 3D polymeric materials such as hydrogels, scaffolds, several particulate systems (nano, micro, and macro), and for composite materials (Fig. 3) [83]. Most of them are suitable for GFs encapsulation due to its polymeric composition that resembles the ECM where these molecules are found naturally, allowing them to preserve their bioactivity. Specifically, hydrogels are 3D flexible polymeric networks with high water content that display extraordinary smoothness and moisturizing characteristics which help in the injury treatment. This kind of material also presents porous networks, which are ideal for encapsulation of GFs because they can diffuse through them quickly. Besides, some hydrogels are injectable and can be administered in specific sites, adapting their shape to the surrounding environment. Generally, they are prepared with both natural and synthetic polymers. The performance of hydrogels to release GFs have been evaluated in multiple studies for wound healing or tissue engineering, and very satisfactory results have been obtained [12, 107, 117]. However, hydrogels lack of excellent mechanical properties, so their use may be

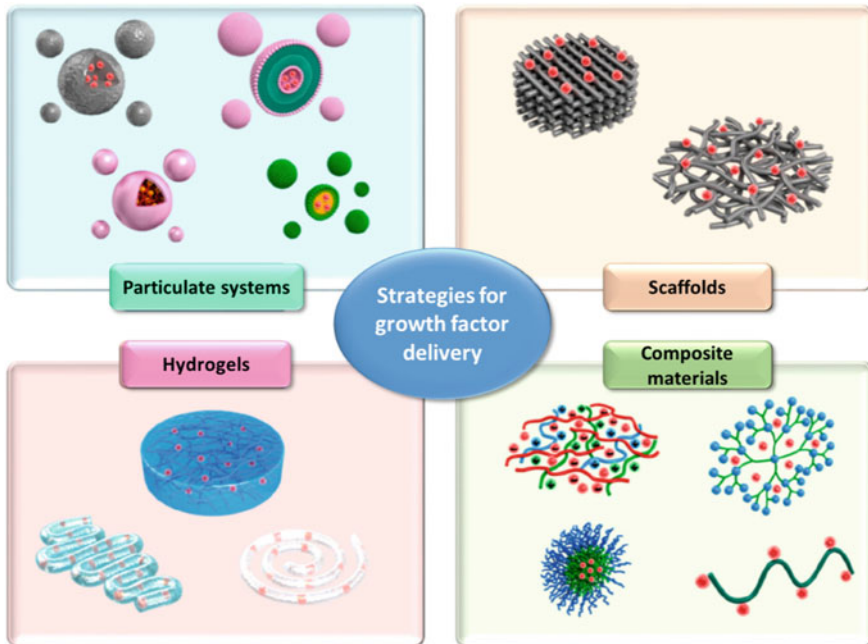


Fig. 3 Classification of the GFs delivery systems according to their matrix structures. *Source* Adapted from Park et al. [81]

limited, avoiding places with a lot of friction or heavy loads. In the case of scaffolds, they are structures designed as 3D culture cells, where differentiation, proliferation, and communication processes are improved [74]. GFs can also be added into scaffolds to enhance the development of cultured cells before implantation as a tissue graft or to be released after grafting to accelerate tissue regeneration. An obstacle to use scaffolds is their complicated implantation in some places inside the human body.

Regarding the GFs release kinetics, both hydrogels and scaffold present burst release effect. The particulate systems may represent a better option to address this undesirable effect. A broad range of particle sizes has been elaborated for the GFs delivery, ranging from 1000 μm (microparticles) to below 1000 nm (nanoparticles) [108]. They have many advantages. For instance, (1) they can be applied in any part of the body; (2) they have shown good releasing patterns of GFs, and (3) they have avoided immunological responses [83]. Their elaboration could be carried out through several efficient methods, although the resulted size distribution sometimes is difficult to control, which makes their commercial production quite problematic. The last class of GFs delivery systems are a combination of the past three; they can even include parts of materials of other nature (non-polymeric). For that reason, they are named composite materials. The desired result of these combinations is a combination of all the benefits, or even improved properties in a single system.

3 Composite Materials for GFs Delivery

Composites have attracted attention in designing drug delivery systems due to the wide variety of material combinations that can be made and result in better capacities. The emergence of these composite materials is based on the drawbacks of isolated materials or systems. For example, liposomal structures serve for the easy incorporation of hydrophobic and hydrophilic drugs and they have low toxicity. However, they are susceptible to be degraded quickly by the action of the reticuloendothelial system, avoiding the sustained drug release. Nevertheless, when they are embedded in polymeric systems, which are stable and do not evoke reticuloendothelial responses, they present prolonged release compared to liposomes alone [118].

Similarly, polymeric systems usually lack of excellent mechanical properties and they are often combined with fibers, metallic, or ceramic particles that reinforce the matrix. Thus, the composite features can be tailored by the types of materials used, their proportion, and distribution in the system [119]. In general, the preparation of composite allows tuning the mechanical properties, to tailor the rate of degradation and adjust the thermal stability problems of the drug delivery systems. As a consequence of these modifications, the release kinetics of drugs, including the GFs kinetics, can be modified. Besides, the adjustable design capacity that composites present allows their use in many places, whether soft and hard tissues [120].

Composites based on the polymeric matrix are widely used in tissue engineering and wound healing care as a strategic delivery system for GFs. Generally, composites are formed by two or more types of materials. One part of them contains a matrix, which is the material that is found in the highest proportion. Based on the nature of this matrix, composites can be classified as polymeric, metallic, or ceramic [119, 121]. The other part is the reinforcements, which are the materials that are found in less quantity and are distributed in the matrix. Depending on the type of reinforcement contained in composites, they can be classified as fiber-reinforced, particle-reinforced, or structural [122–124]. A third part is an intermediate phase (interface) located in the border between the matrix and reinforcement. For tissue engineering and wound healing, the matrix of composite is usually prepared with both natural and synthetic polymers due to their ductility, porous structure, low cost, and secure handling [119]. However, natural polymers have gained attention for the engineering of composite materials due to they are more biocompatible and biodegradables. The main natural polymers employed for composite formation are collagen, alginate, chitosan, hyaluronic acid, heparin, silk fibroin, and PHBV [73].

4 Polysaccharide-Based Composites

4.1 Alginate-Base Composites for GFs Delivery

Sodium alginate is a polysaccharide isolated from seaweed and some bacteria, it is commonly used for tissue engineering or as delivery systems. The high interest to work with this material is due to its excellent biocompatibility and because it is water soluble. It is an anionic polyelectrolyte and its structure is formed by monomeric units of D-mannuronic acid (M) and L-guluronic acid (G) [125]. Alginate-based biomaterials can be assembled quickly and under mild conditions by electrostatic forces using Ca^{++} cations [126]. Frequently, these materials present a high porous structure allowing the incorporation of molecules such as GFs. However, alginate presents several drawbacks, including limited mechanical properties and low degradation rate in mammals (because they do not have the required enzymes) [127]. Many efforts have been focused on the designer of appropriated alginate materials combining it with different ingredients and forming several composites materials.

Alginate-based composites are one of the most used systems for GFs delivery to treat the injuries regeneration or to differentiate stem cells. They have been produced using several methodologies, including a simple drying overnight or more sophisticated electro spinning and 3D bioprinting techniques. By a simple drying overnight method, an EGF-loaded alginate-chitosan composite was created as a potential wound dressing [128]. The membranes were formed by electrostatic interaction between the free amine groups in chitosan chains and the carboxylic groups in alginate. Additionally, they were cross-linked with CaCl_2 . These membranes were composite because of the incorporation of suture threads of linen and cotton in the layers to improve the mechanical properties. The results showed how the threads increase the elongation at the break about 5–8 times when they were cross-linked. Besides, roughness and opacity were also increased, which could be beneficial for cell attachment. However, the extracts of membranes produced with cotton threads were cytotoxic for human fibroblasts. For that, EGF was only incorporated into alginate-chitosan blend containing linen threads before the dried process, and it proved to be useful for fibroblast proliferation. As mentioned before, combination of several materials allows the modulation of different properties in composites. The cellular adaptability of alginate-based composites has been improved by coupled with sequences of cell attachment peptides as RGD (arginine-glycine-aspartic acid) [129]. That is the case of the 3D alginate composite microspheres used for cell encapsulation and for multiple GFs delivery, which was proposed for muscle regeneration [130]. The result of this modification was an increased cell viability of encapsulated mesenchymal cells after two weeks in an *in vitro* evaluation. Besides, the combinatory action of several GFs, including FGF, seems to promote the differentiation of the encapsulated cells because they showed muscle cell-like morphology after four weeks of evaluation.

Naturally, sulfated polymeric components in ECM are crucial in several signaling pathways through their interaction with GFs [131]. Based on that, the alginate backbone has strategically been modified with sulfate groups to provide high affinity and specific binding points for GFs trying to modulate their action like in the original medium [132, 133]. Composites of alginate sulfate with polyvinyl alcohol (PVA) have been fabricated by electrospinning technique for TGF- β delivery [134]. PVA, a biocompatible synthetic polymer with excellent mechanical properties, was employed to provide better electro-spinnability to alginate sulfate and high mechanical strength. The incorporation of TGF- β to the electro-spun composite of alginate-sulfate/PVA was by physical absorption and was improved with the addition of sulfate groups to alginate. Moreover, the release of TGF- β was slower in alginate-sulfate/PVA composites than alginate/PVA composites. Regarding the biocompatibility of these composites, they proved the attachment of mesenchymal stem cells to them, and they maintained excellent cell viability (more than 90%).

As mentioned, alginate-based composites can also be fabricated by the 3D bioprinting technique, although for this, it is necessary to adjust some mechanical properties of alginate. Freeman et al. [135] systematically studied combinations between the molecular weight of alginate and types of cross-linking agents to tuning the bio-ink stiffness. This parameter is essential because it improves the printability for alginate, and it also determines the mesenchymal stem cell differentiation as well as the GFs release rate. They showed that only 45–75% of loaded VEGF remains in the printed composites, and the molecular weight of the alginate faster modulated the GF release. They observed that the combination of different molecular weights of alginate retained more easily the VEGF and released it slowly. Besides, the spatially varying mechanical stiffness in the composite influences the differentiation of mesenchymal cells. In the soft portions, one part of the cells undergo to osteogenesis and another part to adipogenesis, while in the stiffer region, most of the cells underwent to osteogenesis.

The use of alginate-based composites with particle-reinforcement is widely studied for dual release of GFs due to they offer a spatial-temporal behavior. An alginate composite contained FGF-loaded poly(N-isopropylacrylamide) nanogels and diclofenac sodium-loaded poly(N-isopropyl acrylamide-co-acrylic acid) nanogels were created to be used as a step-release dressing. The thermos-sensitive pattern of each embed the nanogel showed that about 92% of loaded diclofenac sodium was released at 37 °C in the first three days, corresponding with the inflammation stage. Whereas 80% of the FGF loaded was released at 25 °C after day 3 to day 8, matching within the tissue formation stage. Finally, the *in vivo* studies indicated that the wound was healing around 96% in 14 days and presented less inflammation and higher angiogenesis than control groups [136]. Another standard version of alginate-based composites used for dual GFs release with particle-reinforcement are the thermosensitive-composites. In these composites, the matrix part, which in this case is alginate, usually presents a sol-gel transition after sensing a temperature change. They are ideal for internal tissue reparation because they can be injected in specific sites to increase the efficacy of GFs, where it is difficult to implant composites in the form of membranes. Several works have been reported the effectiveness

of injectable thermosensitive composites for the stepwise delivery of VEGF and BMPs in bone formation. The strategy consisted of loading VEGF in the alginate matrix of the composite, while BMP-9 and BMP-2 were pre-loaded, by absorption on microspheres of chitosan and modified heparin, respectively [37, 137]. Both VEGF and BMP-2 have presented a high affinity for their corresponding polysaccharide due to they showed an encapsulation efficiency greater than 90% [137]. The release profile obtained in both studies was similar since VEGF showed higher concentrations in each evaluation point compared to the BMPs. However, the subsequent release of these GFs can be changed depending on the loading strategy. The BMP-9 release proved to enhance the proliferation and the osteogenic differentiation of mesenchymal stem cells along the surface of microspheres, which were distributed in the composite matrix [37].

4.2 Chitosan-Based Composites for GFs Delivery

Chitosan is another polysaccharide extensively used in the fabrication of composites for GFs release, especially for those engaged with the bone formation. Chitosan is the only natural cationic polysaccharide composed of β -1,4-D-glucosamine and N-Acetyl-D-glucosamine units, containing free amine groups which are available for chemical modifications [138]. DeWitte et al. [139] joined empty poly(methyl methacrylate-co-methacrylic acid) nanoparticles to the chitosan matrix, via carbodiimide-crosslinker chemistry. Specifically, they used the carboxylic acid found on the surface of the nanoparticles to react with the free amine groups of chitosan chains. This method proved to be useful for the retention of nanoparticles for up to four weeks without negative effects on cell viability or proliferation. The nanoparticle retention effect was proposed as a possible system that could serve to delay the release of GFs. Usually, chitosan-based composites with particle-reinforcement are a promising approach for dual administration of GFs because they have proved spatial-temporal control of their releasing. An attempt to the double release of PDGF and BMP-2 was made from alginate microspheres embedded in a chitosan-based composite [140]. BMP-2 was loaded in core-shell alginate microspheres, while PDGF was separately loaded in another type of microsphere. The release kinetic of both GFs was assessed, and the results showed that only 10% of BMP-2 was released in the first week and 50% until five weeks. In contrast, more than 10% of loaded PDGF was released on the first day and around 55% for day 6. Both GFs showed in vitro bioactivity based on cell effects.

Chitosan-based composites have had a particular use to dual delivery of VEGF and BMP-2 because they can act synergistically and orderly to promote osteogenesis and vascularization [141, 142]. The releasing patterns indicate that osteogenesis is supported by BMP-2 released in a slow and maintained manner over time [143]. While for vascularization, VEGF needs to be released in high concentrations at the beginning and then decreased [144]. Besides, the 2-N-6-O-sulphated chitosan (26SCS) have widely used to mimic the polysaccharides found in the

ECM that regulates the GFs activity and their release. Also, some studies point out a pro-angiogenesis effect [142, 145]. A particle-reinforcement 26SCS composite was formed with poly(lactide-co-glycolide) (PLGA) microspheres for the release of VEGF and BMP-2 [142]. The BMP-2 loaded in PLGA microspheres showed a slow and sustained release without burst effect, while VEGF, charged in the composite matrix, displayed a rapid release profile and burst effect in the two first hours. As mentioned before, this release behavior is desirable in these classes of composite, becoming them in a promising approach for bone reparation treatments.

On the other side, an innovative dual-modular scaffold composite based on 26SCS with VEGF and MBP-2 was used for osteogenesis and vascularization development (Fig. 4). The material was formed with 26SCS and a mesoporous bioactive glass (MBG) with hierarchical porous structures (module 1). Inside of the hollowed channels of module 1, GelMA hydrogels columns were in situ fixed (module 2) [145]. Using this unique building composite was possible to have differentiated spatiotemporal delivery modes of BMP-2, which was in module 1, and VEGF, which was embed in module 2. Also, the arrangement of this chitosan-based composite enhanced the osteogenesis and angiogenesis process at in vitro and in vivo studies. Dual delivery of GFs from chitosan-based composites has also had in other applications. In other work, heparin was bound to the residual amine groups of chitosan-g-polyethylene glycol (PEG) composite to increase the electrostatic binding efficiency and of FGF and VEGF to enhance wound healing [146]. The conjugation of PEG to the chitosan

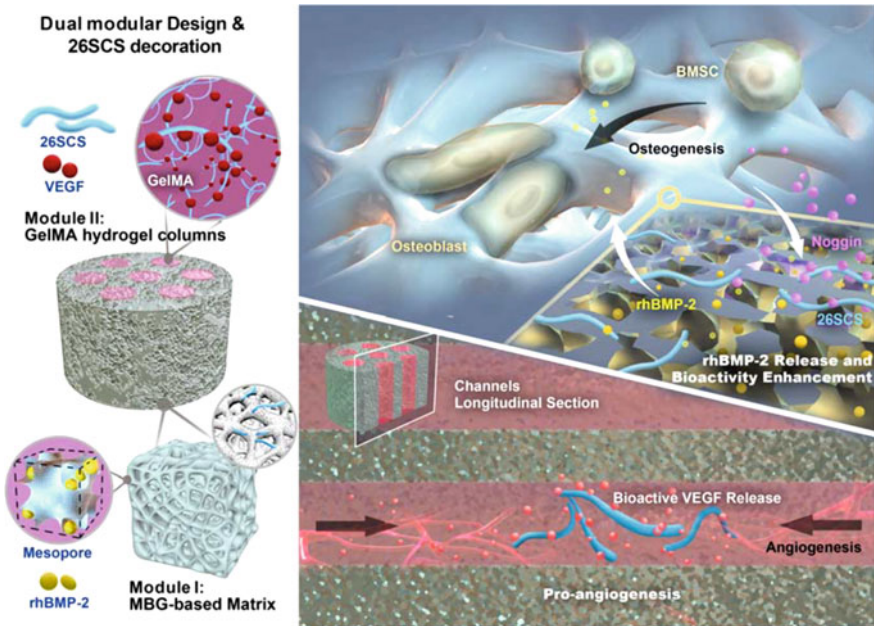


Fig. 4 Schematic representation of dual-modular 26SCS-based composite scaffold for GFs delivery to enhance bone regeneration. *Source* Tang et al. [145]

chains improved the mechanical properties of these composites, which displayed a simultaneous and continuous release profiles of FGF and VEGF to stimulate the proliferation of HaCaT cells. Finally, the dual and simultaneous release of FGF and VEGF increased neovascularization and collagen formation.

Another highly porous structure for BMP-2 delivery was fabricated from chitosan, hydroxyapatite, heparin, and PVA, using glutaraldehyde and cryogelling as cross-linking agents [147]. Incorporation of several components to the mix allowed to have specific functions; for example, the presence of hydroxyapatite in the composite mimics the natural structure for new bone formation. Heparin allowed the electrostatic interaction with BMP-2 to maintain inside the composite. The PVA hindered the formation of polyelectrolyte complexes between chitosan and heparin for more homogeneous matrix assembly, and it improved the mechanical properties. The final composites were biocompatible and released BMP-2 by 30 d to stimulate the differentiation of mesenchymal stem cells into osteocytes.

4.3 Glycosaminoglycan-Based Composites for GFs Delivery

Glycosaminoglycans (GAGs) are a set of structural polysaccharides composed of a random combination of glucuronic acid, glucosamine, iduronic acid, or galactosamine [148]. Some GAGs are found in the ECM of mammals tissues, for example, chondroitin sulfate, heparan sulfate, heparin, dermatan sulfate, keratin sulfate, and hyaluronic acid. In contrast, others, such as carrageenan, fucoidan, and ulvan, are present in seaweeds [149]. Most of them are well-recognized by present highly sulfated chains and to be bonded to several proteins in the ECM (with the exception of the hyaluronic acid). GAGs are considered as regulators of ECM proteins, such as GFs because their unions affect the signalization and functionalization processes that are promoted by these molecules [150]. For that reason, GAGs represent an perfect class of natural polysaccharides to form carrier systems of GFs with particular properties and an enhanced capacity to regulate its delivery in biomedical applications [149].

4.3.1 Heparin/Heparan Sulfate-Based Composites for GFs Delivery

Heparan sulfate or heparin are polysaccharide-origin constituents of ECM, which serve as structural support and have the capacity to join proteins to regulate diverse cellular functions [151]. The primary unbranched chain of heparan sulfate is formed by repeating disaccharide units of D-glucuronic acid (GlcA) and N-acetyl-D-glucosamine (GlcNAc), which are heavily sulfated in a different position [152, 153]. Additionally, the GlcA unit can present 2-O sulfation, changing the disaccharide to L-iduronic acid (IdoA), which is abundant in heparin structure with around 85% [149, 152]. The sulfation patterns that are present in heparan/heparin chains provide negative charge enabling them to bind positively charged amino acids of GFs and moderate their signalization pathways that influence the cell fate [151].

Inspired by the natural function of heparan sulfate or heparin, some composite based on these polysaccharides have been created to protect and deliver GFs in injured tissues. Silva et al. [154] prepared a diblock copolymer with a spontaneous assembly of heparin and polyethylene glycol (Hep-b-PEG) for the protection and delivery of FGF-2. For the engineering of this system, heparin was used without further modifications preserving its biological activity to bind to FGF-2 electrostatically and to form ternary complexes. The composite materials showed in Fig. 5 were microspheres with a particular arrangement of about 400 nm. They were able to encapsulate around 99% of FGF-2 and release more than 80% during 28 d at pH 7.4. The microsphere structure proved to have a protective effect on FGF-2 due to it remains its bioactivity directing the differentiation of MSC onto bone cells. Another polypeptide/heparin-based composite was used to deliver VEGF as a potential treatment in wound healing [155]. In this case, poly(L-lysine) with two shapes (linear and star) were cross-linked with genipin and further ionically complexed with negatively charged heparin, which also bound VEGF. Stronger electrostatic interactions between heparin with VEGF were produced, allowing its stabilization to promote a good healing process.

A novel strategy to create composite materials for sustained delivery of multiple GFs is using the layer-by-layer (LBL) assembly of several polyelectrolytes. Heparin, like other sulfated GAGs, presents a polyanionic character allowing their interaction with polycationic molecules such as GFs or other synthetic polymers. That was the

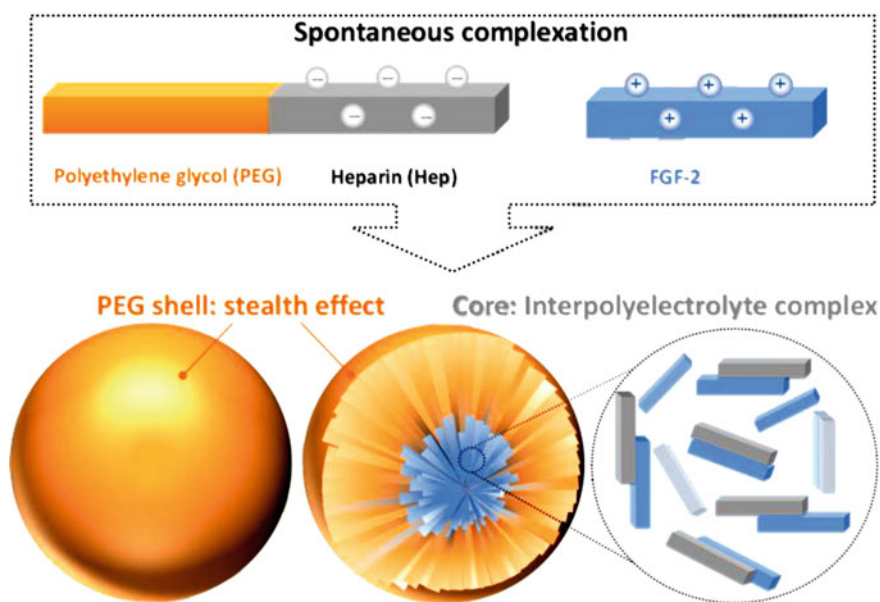


Fig. 5 Representation of self-assembly of polyelectrolyte complexes formed by hep-b-PEG to deliver FGF-2. *Source* Silva et al. [154]

case of a composite based on polymeric implants and subsequent covered with thin polyanionic layers of heparin and dextran sulfate alternated with polycationic layers of several GFs [154]. Specifically, TGF- β , PDGF, and IGF were used. The polymeric implants surfaces were activated by gas plasma (inert argon or reactive oxygen) to provide higher surface area charge for better polyelectrolyte adsorption. Also, the deposition of poly(styrenesulfonate) or poly(ethyleneimine) was performed at the beginning to provide sufficient initial cationic charge. The results showed that the LBL method is an excellent alternative for GFs encapsulation due they can be loaded with around 90% of efficiency, especially in heparin composites. The use of oxygen gas plasma and acidic pH conditions during the engineering process also improves the GFs loading. The LBL composites also exposed an excellent sustain delivery of GFs trough diffusion and erosion processes during 14 days, and they regulated fibroblast proliferation, myofibroblast differentiation, cell morphology, and migration.

4.3.2 Hyaluronic Acid-Based Composites for GFs Delivery

Hyaluronic acid is another GAG that has been used to fabricate composites for GFs delivery. It is a linear polysaccharide composed by repeating disaccharides of D-glucuronic and N-acetyl-D-glucosamine without sulfated units [156]. In this case, the N-acetyl-D-glucosamine units possess carboxyl groups, charging negatively to the hyaluronic acid chains and making them highly hydrophilic. At high molecular weights, hyaluronic acid forms a dense network around the cells, providing mechanical support and interaction with many signal molecules, helping in the regulation of the fate cell [149, 156]. However, hyaluronic acid tends to be degraded fast when it is applied in clinical treatments. In an approach were prepared composites with hyaluronic acid conjugated with sulfate groups, which showed lower degradation by hyaluronidase and improved the retention of TGF. Finally, the new hydrogel composite based on sulfated hyaluronic acid promotes the chondrogenesis being a promising biomaterial for regenerative medicine [157].

5 Protein-Origin Composites

5.1 Collagen-Based Composites for GFs Release

Collagen is a natural polymer considered as the most abundant protein in connective tissue skin, tendon, and cartilage in mammals. In the last years, it has regularly been used as a biomaterial [158]. The collagen presents a distinctive supramolecular structure with many interacting points which allow the design of materials with several applications. However, many times collagen structure requires modifications due to its poor mechanical and thermal stability [159]. To overcome these issues, composite materials based on collagen also represent an alternative, especially for

the tissue engineering area. Collagen-based composite contained hydroxyapatite and NGF, showed the capacity to repair craniofacial injuries [160]. In *in vitro* conditions, the composites presented a burst effect in the first hours of release evaluation, but then they released around 100% during 96 h. The release of NGF from these composites proved to have a stimulation of periosteal and endocortical woven lamellar bone formation, and it improved the remodeling activity in the intracortical region after 30 d of study in Wistar rats. A very similar collagen-based composite with hydroxyapatite was used for the dual release of BMP-2 and VEGF for the effective healing of critical-sized bone defects [161]. In this case, the GFs were soak-loaded onto both sides of the composite. The incorporation of hydroxyapatite in these systems seems to sequester the GFs due to its high affinity with them, causing a longer time of retention inside the composite and a sustained release. These GFs loaded composites demonstrated a complete bridging the gap in the bone defect in a very early time compared with composites without GFs. As in other cases, BMP-2 and VEGF acted synergistically and enhanced the osteogenic and angiogenic processes. One more collagen-hydroxyapatite composite for the release of BMP-2 was presented by Ref. [162]. This composite material was fabricated by the easy and biocompatible methodology of lyophilization and dehydrothermal processes to provoke high porosity and mechanical strength in the material. The obtained results were a successful release of BMP-2, which stimulate osteoblast proliferation and bone repair.

Other types of the collagen-based composite are micro particles combined with porous calcium phosphate and collagen constructed by water in the oil emulsion technique to release BMP-2 [163]. The microspheres of calcium phosphate presented highly interconnected pores where collagen, together with BMP-2, were infiltrated. The *in vitro* release of BMP-2 was in a sustained manner and caused cell differentiation, while *in vivo* evaluation displayed bone regeneration with microspheres. The chemical modification of collagen structure with glutathione and FGF has also been implemented as a strategy to form composites and release, in control manner, the FGF [164]. These composites remain potential therapeutic approaches for myocardial infarction due to their dual function, angiogenesis, and inhibition of cardiac remodeling. The addition of glutathione onto the collagen chain was made by the conjugation of collagen amine groups with the glutathione sulfhydryl groups, with the purpose of increase the binding capacity with the composite. Promising results were obtained with these composites because the modified collagen decreased the degradation of the cardiac matrix and other components as well as the FGF enhanced the vascularization.

5.2 *Gelatin-Based Composites for GFs Release*

Gelatin is a protein-origin polymer obtained from the denaturalization of collagen, which has shown potential as a biomaterial for tissue regeneration due to its similarity with the ECM [165, 166]. However, gelatin biomaterials present some drawbacks

as low mechanical properties and easily enzymatic degradation [166]. An effective way to overcome these issues is using composites, where different materials of several properties can be combined. Also, they represent a manner to improve their therapeutic effectiveness by incorporation of active molecules such as GFs.

Many sophisticated techniques have developed gelatin-based composites with the potential to be used in tissue engineering or wound dressing. A fashionable approach to produce several types of gelatin-based composites that allow the relatively easy incorporation of GFs and preserve their bioactivity is the 3D printing. Especially, FGF has been integrated into 3D-printing gelatin composites used to treat both bone reparation and skin regeneration. Xion et al. [167] produced a gelatin-sulfonated silk composite scaffold with FGF, which proved to trigger the granulation and enhanced the skin regeneration after implantation as well as they encouraged the dermal vascularization. Other 3D printing gelatin-chitosan composite with FGF and magnesium substituted with hydroxyapatite nanocomposites has proved to be biocompatible, presented high cell attachment, and proliferation rate. They also promoted the upregulation of osteogenic-like genes, which evidence their capacities for bone tissue reparation [168]. Another innovative way to prepare gelatin-based composites for GFs delivery was using the modified gelatin methacryloyl (GelMA), which is photocross-linkable with UV light. GelMA-based hydrogel composites reinforced with FGF-loaded chitosan nanoparticles evidenced biocompatibility and fibroblast proliferation during the sustained release of FGF [169].

Other GFs as PDGF, VEGF, and BMPs have also been included in gelatin-based composites with particular characteristics. Specifically, PDGF was absorbed in streptavidin-coated polystyrene microparticles, which were later joined to thermosensitive hydrogels of gelatin using an aptamer [170]. An aptamer is a short sequence of simple-chain nucleic acids able to bind with high affinity to other molecules [171]. The resulted composite showed a gradual dissolution and a slow rate of PDGF release compared with the native gelatin hydrogels. A new injectable nanodiamonds-based composite hydrogel formed by gelatin and chitosan was used to deliver VEGF for wound healing [172]. The nanodiamonds reinforcement improves the mechanical properties of composites, and their complexation with VEGF and subsequent inclusion allowed a sustained release of this GF. On the other hand the electrospinning method has also been employed to produce a gelatin-poly(lactic-co-glycolic acid) composite for dual delivery of VEGF and BMP-2. The composite consisted of randomly-oriented nanofibres that were interconnected in the 3D-reticular structure where cells firmly attached and experienced good morphology and connection [173]. The inclusion of VEGF and BMP-2 and their subsequent and sequential release improved the cell adhesion, proliferation, and differentiation of MSC into osteogenic cells.

Natural-based composites for delivery of growth factors are auspicious materials due to they generally are biocompatible, no toxic, biodegradable, and, don evoke immunogenic responses. In addition, they have great versatility to be combined with materials of serval natures, shapes, and sized to allow their use in any part of the human body. Besides, they can be produced by a wide variety of techniques

under mild conditions. Depending on the set conditions used during their manufacturing, many types of composites based in natural polymers could be created. The most significant benefit of this type of system is their control capacity for sequential delivery of two or even more growth factors to produce appropriate clinical treatments for tissue engineering and wound healing. However, there are different points that are need to solve such as the proper dosage of GFs and an uniformly control of the properties of the natural polymers that are used. Regarding the dosages, the synergistic action of several factors on specific tissue must be studied deeply to achieve the right combination of their release patterns. While the natural polymers suffer from intrinsic variations that affect their properties and limit their use, for that, it is necessary standardized some production procedures.

References

1. Taipale J, Keski-Oja J (1997) Growth factors in the extracellular matrix. *FASEB J* [Internet] 11(1):51–59. Available from: <https://onlinelibrary.wiley.com/doi/abs/10.1096/fasebj.11.1.9034166>
2. Dinh T, Braunagel S, Rosenblum BI (2015) Growth factors in wound healing: the present and the future? *Clin Podiatr Med Surg* 32(1):109–119
3. Brizzi MF, Tarone G, Defilippi P (2012) Extracellular matrix, integrins, and growth factors as tailors of the stem cell niche. *Curr Opin Cell Biol* [Internet] 24(5):645–651. Available from: <http://dx.doi.org/10.1016/j.ceb.2012.07.001>
4. Li R, Li D, Zhang H, Wang J, Li X, Xiao J (2020) Growth factors-based therapeutic strategies and their underlying signaling mechanisms for peripheral nerve regeneration. *Acta Pharmacol Sin* [Internet]. (November 2019):1–12. Available from: <http://www.nature.com/articles/s41401-019-0338-1>
5. Sherbet G (2011) Growth factors and their receptors in cell differentiation, cancer and cancer therapy [Internet] 368. Available from: <https://onlinelibrary.wiley.com/doi/abs/10.1096/fasebj.11.1.9034166>
6. Mina M (2015) Growth factors: biochemical signals for tissue engineering. biochemical signals for tissue engineering. In: *Stem cell biology and tissue engineering in dental sciences* [Internet]. Elsevier Inc, pp 85–97. Available from: <http://dx.doi.org/10.1016/B978-0-12-397157-9.00009-6>
7. Burgess AW (2015) Growth factors and cytokines. In: *Reviews in cell biology and molecular medicine* [Internet]. Wiley-VCH Verlag GmbH & Co. KGaA, Weinheim, Germany, pp 104–126. Available from: <http://doi.wiley.com/10.1002/3527600906.mcb.200300155>
8. Matsumoto K, Nakamura T (1992) Hepatocyte growth factor: molecular structure, roles in liver regeneration, and other biological functions. *Crit Rev Oncog* [Internet]. 3(1–2):27–54. Available from: <http://europepmc.org/abstract/MED/1312869>
9. Sporn MB, Roberts AB (1992) Transforming growth factor- β : recent progress and new challenges. *J Cell Biol* 119(5):1017–1022
10. Qu M, Jiang X, Zhou X, Wang C, Wu Q, Ren L et al (2020) Stimuli-responsive delivery of growth factors for tissue engineering. *Adv Healthc Mater*. 9(7):1–19
11. Niu Y, Li Q, Ding Y, Dong L, Wang C (2019) Engineered delivery strategies for enhanced control of growth factor activities in wound healing. *Adv Drug Deliv Rev* 146:190–208
12. Caballero Aguilar LM, Silva SM, Moulton SE (2019) Growth factor delivery: defining the next generation platforms for tissue engineering. *J Control Release* 306:40–58
13. De Witte TM, Fratila-Apachitei LE, Zadpoor AA, Peppas NA (2018) Bone tissue engineering via growth factor delivery: from scaffolds to complex matrices. *Regen Biomater*. 5(4):197–211

14. Domigan CK, Ziyad S, Iruela-Arispe ML (2015) Canonical and noncanonical vascular endothelial growth factor pathways: New developments in biology and signal transduction. *Arterioscler Thromb Vasc Biol* 35(1):30–39
15. Murakami M, Elfenbein A, Simons M (2008) Non-canonical fibroblast growth factor signalling in angiogenesis. *Cardiovasc Res* 78(2):223–231
16. Charoenlarp P, Rajendran AK, Iseki S (2017) Role of fibroblast growth factors in bone regeneration. *Inflamm Regen* 37(1):1–7
17. Teishima J, Hayashi T, Nagamatsu H, Shoji K, Shikuma H, Yamanaka R et al (2019) Fibroblast growth factor family in the progression of prostate cancer. *J Clin Med* 8(2):183
18. Ornitz DM, Itoh N (2015) The fibroblast growth factor signaling pathway. *Wiley Interdiscip Rev Dev Biol* 4(3):215–266
19. Marseglia G, Lodola A, Mor M, Castelli R (2019) Fibroblast growth factor receptor inhibitors: patent review (2015–2019). *Expert Opin Ther Pat* 29(12):965–977
20. Nunes QM, Li Y, Sun C, Kinnunen TK, Fernig DG (2016) Fibroblast growth factors as tissue repair and regeneration therapeutics. *PeerJ* 2016(1):1–31
21. Borkham-kamphorst E, Weiskirchen R (2015) The PDGF system and its antagonists in liver fibrosis. *Cytokine Growth Factor Rev* 28:53–61
22. Chen P-H, Chen X, He X (2013) Platelet-derived growth factors and their receptors: structural and functional perspectives. *Biochim Biophys Acta* [Internet]. 1834(10):2176–2186. Available from: <https://linkinghub.elsevier.com/retrieve/pii/S1570963912002567>
23. Kong DH, Kim MR, Jang JH, Na HJ, Lee S (2017) A review of anti-angiogenic targets for monoclonal antibody cancer therapy. *Int J Mol Sci* 18(8):1–25
24. Andrae J, Gallini R, Betsholtz C (2008) Role of platelet-derived growth factors in physiology and medicine. *Genes Dev* 22(10):1276–1312
25. Shah P, Keppler L, Rutkowski J (2012) A review of platelet derived growth factor playing pivotal role in bone regeneration. *J Oral Implantol*. 120419070552000
26. Papadopoulos N, Lennartsson J (2018) The PDGF/PDGFR pathway as a drug target. *Mol Aspects Med* [Internet]. 62:75–88. Available from: <https://doi.org/10.1016/j.mam.2017.11.007>
27. Bafico A, Aaronson S (2003) Classification of growth factors and their receptors. In: Holland-Frei cancer medicine, 6th edn [Internet], pp 1–9. Available from: <https://www.ncbi.nlm.nih.gov/books/NBK12423/>
28. Shimomura R, Nezu T, Hosomi N, Aoki S, Sugimoto T, Kinoshita N et al (2018) Alpha-2-macroglobulin as a promising biological marker of endothelial function. *J Atheroscler Thromb* 25(4):350–358
29. Peach CJ, Mignone VW, Arruda MA, Alcobia DC, Hill SJ, Kilpatrick LE et al (2018) Molecular pharmacology of VEGF-A isoforms: binding and signalling at VEGFR2. *Int J Mol Sci* 19(4)
30. Hu K, Olsen BR (2016) The roles of vascular endothelial growth factor in bone repair and regeneration. *Bone* [Internet]. 91(12):30–38. Available from: <http://dx.doi.org/10.1038/s41582-019-0280-3>
31. Hu K, Olsen BR (2017) Vascular endothelial growth factor control mechanisms in skeletal growth and repair. *Dev Dyn* 246(4):227–234
32. Karaman S, Leppänen VM, Alitalo K (2018) Vascular endothelial growth factor signaling in development and disease. *Development* 145(14):1–8
33. Grafe I, Alexander S, Peterson JR, Snider TN, Levi B, Lee B et al (2018) TGF- β family signaling in mesenchymal differentiation. *Cold Spring Harb Perspect Biol* 10(5):1–50
34. Derynck R, Budi EH (2019) Specificity, versatility, and control of TGF- β family signaling. *Sci Signal* 12(570)
35. Zhang Y, Alexander PB, Wang X-F (2017) TGF- β family signaling in the control of cell proliferation and survival. *Cold Spring Harb Perspect Biol* [Internet] 9(4):a022145. Available from: <http://cshperspectives.cshlp.org/lookup/doi/10.1101/cshperspect.a022145>
36. Morikawa M, Derynck R, Miyazono K (2016) Roles in cell and tissue physiology 1–24

37. Gaihre B, Unagolla JM, Liu J, Ebraheim NA, Jayasuriya AC (2019) Thermoresponsive injectable microparticle-gel composites with recombinant BMP-9 and VEGF enhance bone formation in rats. *ACS Biomater Sci Eng.* 5(9):4587–4600
38. Schmidt-Bleek K, Willie BM, Schwabe P, Seemann P, Duda GN (2016) BMPs in bone regeneration: less is more effective, a paradigm-shift. *Cytokine Growth Factor Rev* 27:141–148
39. Kanie K, Kurimoto R, Tian J, Ebisawa K, Narita Y, Honda H et al (2016) Screening of osteogenic-enhancing short peptides from BMPs for biomimetic material applications. *Materials (Basel)* 9(9)
40. Gipson GR, Goebel EJ, Hart KN, Kappes EC, Kattamuri C, McCoy JC et al (2020) Structural perspective of BMP ligands and signaling. *Bone [Internet]*. 140:115549. Available from: <https://doi.org/10.1016/j.bone.2020.115549>
41. Higashiyama S, Iwabuki H, Morimoto C, Hieda M, Inoue H, Matsushita N (2008) Membrane-anchored growth factors, the epidermal growth factor family: beyond receptor ligands. *Cancer Sci* 99(2):214–220
42. Barnard JA, Daniel Beauchamp R, Russell WE, Dubois RN, Coffey RJ (1995) Epidermal growth factor-related peptides and their relevance to gastrointestinal pathophysiology. *Gastroenterology* 108(2):564–580
43. Arienti C, Pignatta S, Tesei A (2019) Epidermal growth factor receptor family and its role in gastric cancer. *Front Oncol* 9:1–11
44. Shirakata Y, Komurasaki T, Toyoda H, Hanakawa Y, Yamasaki K, Tokumaru S et al (2000) Epiregulin, a novel member of the epidermal growth factor family, is an autocrine growth factor in normal human keratinocytes. *J Biol Chem* 275(8):5748–5753
45. Ashkenazi H, Cao X, Motola S, Popliker M, Conti M, Tsafiriri A (2005) Epidermal growth factor family members: endogenous mediators of the ovulatory response. *Endocrinology* 146(1):77–84
46. Mitchell RA, Luwor RB, Burgess AW (2018) Epidermal growth factor receptor: structure-function informing the design of anticancer therapeutics. *Exp Cell Res [Internet]* 371(1):1–19. Available from: <https://doi.org/10.1016/j.yexcr.2018.08.009>
47. Razavi S, Nazem G, Mardani M, Esfandiari E, Esfahani S, Salehi H (2015) Neurotrophic factors and their effects in the treatment of multiple sclerosis. *Adv Biomed Res* 4(1):53
48. Huang EJ, Reichardt LF (2001) Neurotrophins: roles in neuronal development and function. *Annu Rev Neurosci [Internet]*. 24(1):677–736. Available from: <http://www.annualreviews.org/doi/10.1146/annurev.neuro.24.1.677>
49. Sidorova YA, Saarma M (2016) Glial cell line-derived neurotrophic factor family ligands and their therapeutic potential. *Mol Biol* 50(4):521–531
50. Ibáñez CF (1994) Structure–function relationships in the neurotrophin family. *J Neurobiol* 25(11):1349–1361
51. Skaper SD (2012) The neurotrophin family of neurotrophic factors: an overview. In: *Neurotrophic factors [Internet]*, pp 1–12. Available from: <http://link.springer.com/10.1007/978-1-61779-536-7>
52. Skaper SD (2018) Neurotrophic factors: an overview. In: *An automated irrigation system using arduino microcontroller [Internet]*, pp 1–17. Available from: http://link.springer.com/10.1007/978-1-4939-7571-6_1
53. Manti S, Brown P, Perez MK, Piedimonte G (2017) The role of neurotrophins in inflammation and allergy. *Vitam Horm* 104:313–341
54. Rotwein P (2017) Large-scale analysis of variation in the insulin-like growth factor family in humans reveals rare disease links and common polymorphisms. *J Biol Chem* 292(22):9252–9261
55. Li P, Sun XF, Cai GY, Chen XM (2017) Insulin-like growth factor system and aging. *J Aging Sci* 05(01):1–5
56. Fettig LM, Yee D (2020) Advances in insulin-like growth factor biology and -directed cancer therapeutics. *Adv Cancer Res* 147:229–257
57. Adamek A, Kasprzak A (2018) Insulin-like growth factor (IGF) system in liver diseases. *Int J Mol Sci* 19(5):1–24

58. Haywood NJ, Slater TA, Matthews CJ, Wheatcroft SB (2018) The insulin like growth factor and binding protein family: novel therapeutic targets in obesity and diabetes. *Mol Metab* 19:86–96
59. Pardo M, Cheng Y, Sitbon YH, Lowell JA, Grieco SF, Worthen RJ et al (2019) Insulin growth factor 2 (IGF2) as an emergent target in psychiatric and neurological disorders. Review. *Neurosci Res* [Internet]. 149(1):1–13. Available from: <https://linkinghub.elsevier.com/retrieve/pii/S0168010218304358>
60. Kim HS, Rosenfeld RG, Oh Y (1997) Biological roles of insulin-like growth factor binding proteins (IGFBPs). *Exp Mol Med* 29(2):85–96
61. Kasprzak A, Adamek A (2019) Insulin-like growth factor 2 (IGF2) signaling in colorectal cancer—from basic research to potential clinical applications. *Int J Mol Sci* 20(19):1–28
62. Nakamura T, Mizuno S (2010) The discovery of hepatocyte growth factor (HGF) and its significance for cell biology, life sciences and clinical medicine. *Proc Japan Acad Ser B Phys Biol Sci* 86(6):588–610
63. Kato T (2017) Biological roles of hepatocyte growth factor-Met signaling from genetically modified animals (Review). *Biomed Rep* 7(6):495–503
64. Miyagi H, Thomasy SM, Russell P, Murphy CJ (2018) The role of hepatocyte growth factor in corneal wound healing. *Exp Eye Res* [Internet] 166:49–55. Available from: <https://doi.org/10.1016/j.exer.2017.10.006>
65. Fukushima T, Uchiyama S, Tanaka H, Kataoka H (2018) Hepatocyte growth factor activator: a proteinase linking tissue injury with repair. *Int J Mol Sci* 19(11):1–11
66. Yamane K, Misawa H, Takigawa T, Ito Y, Ozaki T, Matsukawa A (2019) Multipotent neurotrophic effects of hepatocyte growth factor in spinal cord injury. *Int J Mol Sci* 20(23)
67. Oliveira AG, Araújo TG, de Carvalho BM, Rocha GZ, Santos A, Saad MJA (2018) The role of hepatocyte growth factor (HGF) in insulin resistance and diabetes. *Front Endocrinol (Lausanne)*. 9:1–10
68. Wilkinson DG (2014) Regulation of cell differentiation by Eph receptor and ephrin signaling. *Cell Adhes Migr* 8(4):339–348
69. Hirsch TZ, Martin-Lannerée S, Reine F, Hernandez-Rapp J, Herzog L, Dron M et al (2019) Epigenetic control of the Notch and Eph signaling pathways by the prion protein: implications for prion diseases. *Mol Neurobiol* 56(3):2159–2173
70. Prabhath A, Vernekar VN, Sanchez E, Laurencin CT (2018) Growth factor delivery strategies for rotator cuff repair and regeneration. *Int J Pharm* [Internet] 544(2):358–371. Available from: <https://linkinghub.elsevier.com/retrieve/pii/S0378517318300061>
71. Lee K, Silva EA, Mooney DJ (2011) Growth factor delivery-based tissue engineering: general approaches and a review of recent developments. *J R Soc Interface* 8(55):153–170
72. Cheraghi M, Namdari M, Negahdari B, Eatemadi A (2017) Recent advances in cardiac regeneration: stem cell, biomaterial and growth factors. *Biomed Pharmacother* [Internet] 87:37–45. Available from: <http://dx.doi.org/10.1016/j.biopha.2016.12.071>
73. Kowalczewski CJ, Saul JM (2018) Biomaterials for the delivery of growth factors and other therapeutic agents in tissue engineering approaches to bone regeneration. *Front Pharmacol* 9:1–15
74. Nyberg E, Holmes C, Witham T, Grayson WL (2016) Growth factor-eluting technologies for bone tissue engineering. *Drug Deliv Transl Res* 6(2):184–194
75. Xu F, Qiao L, Zhao Y, Chen W, Hong S, Pan J et al (2019) The potential application of concentrated growth factor in pulp regeneration: an in vitro and in vivo study. *Stem Cell Res Ther* 10(1):1–16
76. Önger ME, Delibaş B, Türkmen AP, Erener E, Altunkaynak BZ, Kaplan S (2017) The role of growth factors in nerve regeneration. *Drug Discov Ther* 10(6):285–291
77. Rajpar I, Barrett JG (2019) Optimizing growth factor induction of tenogenesis in three-dimensional culture of mesenchymal stem cells. *J Tissue Eng* 10
78. Zarei F, Soleimanejad M (2018) Role of growth factors and biomaterials in wound healing. *Artif Cells, Nanomedicine Biotechnol* 46(sup1):906–911

79. Yamakawa S, Hayashida K (2019) Advances in surgical applications of growth factors for wound healing. *Burn Trauma* 7:1–13
80. Barrientos S, Brem H, Stojadinovic O, Tomic-Canic M (2014) Clinical application of growth factors and cytokines in wound healing. *Wound Repair Regen* [Internet]. 22(5):569–578. Available from: <http://doi.wiley.com/10.1111/wrr.12205>
81. Park JW, Hwang SR, Yoon IS (2017) Advanced growth factor delivery systems in wound management and skin regeneration. *Molecules* 22(8):1–20
82. Park U, Kim K (2017) Multiple growth factor delivery for skin tissue engineering applications. *Biotechnol Bioprocess Eng* 22(6):659–670
83. Gainza G, Villullas S, Pedraz JL, Hernandez RM, Igartua M (2015) Advances in drug delivery systems (DDSs) to release growth factors for wound healing and skin regeneration. *Nanomedicine Nanotechnology Biol Med* 11(6):1551–1573
84. Borena BM, Martens A, Broeckx SY, Meyer E, Chiers K, Duchateau L et al (2015) Regenerative skin wound healing in mammals: state-of-the-art on growth factor and stem cell based treatments. *Cell Physiol Biochem* 36(1):1–23
85. Sarker MD, Naghieh S, Sharma NK, Ning L, Chen X (2019) Bioprinting of vascularized tissue scaffolds: influence of biopolymer, cells, growth factors, and gene delivery. *J Healthc Eng* 2019
86. Chen RR, Silva EA, Yuen WW, Mooney DJ (2007) Spatio-temporal VEGF and PDGF delivery patterns blood vessel formation and maturation. *Pharm Res* 24(2):258–264
87. Nillesen STM, Geutjes PJ, Wismans R, Schalkwijk J, Daamen WF, van Kuppevelt TH (2007) Increased angiogenesis and blood vessel maturation in acellular collagen-heparin scaffolds containing both FGF2 and VEGF. *Biomaterials* 28(6):1123–1131
88. Goumans MJ, Liu Z, Ten Dijke P (2009) TGF- β signaling in vascular biology and dysfunction. *Cell Res* 19(1):116–127
89. Pardali E, Goumans MJ, ten Dijke P (2010) Signaling by members of the TGF- β family in vascular morphogenesis and disease. *Trends Cell Biol* 20(9):556–567
90. Vishal K, Lovato TAL, Bragg C, Chechenova MB, Cripps RM (2020) FGF signaling promotes myoblast proliferation through activation of wingless signaling. *Dev Biol* [Internet] 464(1):1–10. Available from: <http://dx.doi.org/10.1016/j.ydbio.2020.05.009>
91. Salimath AS, Phelps EA, Boopathy AV, Che PL, Brown M, García AJ et al (2012) Dual delivery of hepatocyte and vascular endothelial growth factors via a protease-degradable hydrogel improves cardiac function in rats. *PLoS One* 7(11):1–12
92. Gianni-Barrera R, Burger M, Wolff T, Heberer M, Schaefer DJ, Gürke L et al (2016) Long-term safety and stability of angiogenesis induced by balanced single-vector co-expression of PDGF-BB and VEGF 164 in skeletal muscle. *Sci Rep* 6:1–15
93. Gianni-Barrera R, Butschkau A, Uccelli A, Certelli A, Valente P, Bartolomeo M et al (2018) PDGF-BB regulates splitting angiogenesis in skeletal muscle by limiting VEGF-induced endothelial proliferation. *Angiogenesis* 21(4):883–900
94. Jing Y, Sun Q, Xiong X, Meng R, Tang S, Cao S et al (2019) Hepatocyte growth factor alleviates hepatic insulin resistance and lipid accumulation in high-fat diet-fed mice. *J Diabetes Investig* 10(2):251–260
95. Muratsu J, Iwabayashi M, Sanada F, Taniyama Y, Otsu R, Rakugi H et al (2017) Hepatocyte growth factor prevented high-fat diet-induced obesity and improved insulin resistance in mice. *Sci Rep* [Internet] 7(1):1–7. Available from: <http://dx.doi.org/10.1038/s41598-017-00199-4>
96. Sanchez-Encinales V, Cozar-Castellano I, Garcia-Ocaña A, Perdomo G (2015) Targeted delivery of HGF to the skeletal muscle improves glucose homeostasis in diet-induced obese mice. *J Physiol Biochem* 71(4):795–805
97. Cortázar C, Med JT, Cortázar IC, Aguirre GA, Roldán GF, Estal IM et al (2020) Is insulin-like growth factor-1 involved in Parkinson's disease development? 1–17
98. Zilony-Hanin N, Rosenberg M, Richman M, Yehuda R, Schori H, Motiei M et al (2019) Neuroprotective effect of nerve growth factor loaded in porous silicon nanostructures in an Alzheimer's disease model and potential delivery to the brain. *Small* 15(45):1–13

99. Anitua E, Muruzabal F, de la Fuente M, Merayo J, Durán J, Orive G (2016) Plasma rich in growth factors for the treatment of ocular surface diseases. *Curr Eye Res* 41(7):875–882
100. Shrivastava R, Bhadauria S (2016) Role of growth factor signaling in cancer. *Def Life Sci J* 1(1):34
101. Tiash S, Chowdhury E (2015) Growth factor receptors: promising drug targets in cancer. *J Cancer Metastasis Treat* 1(3):190
102. Presta M, Chiodelli P, Giacomini A, Rusnati M, Ronca R (2017) Fibroblast growth factors (FGFs) in cancer: FGF traps as a new therapeutic approach. *Pharmacol Ther* 179:171–187
103. Witsch E, Sela M, Yarden Y (2010) Roles for growth factors in cancer progression. *Physiology* 25(2):85–101
104. Xie M, Dart DA, Guo T, Xing XF, Cheng XJ, Du H et al (2018) MicroRNA-1 acts as a tumor suppressor microRNA by inhibiting angiogenesis-related growth factors in human gastric cancer. *Gastric Cancer* 21(1):41–54
105. Blondy S, Christou N, David V, Verdier M, Jauberteau MO, Mathonnet M et al (2019) Neurotrophins and their involvement in digestive cancers. *Cell Death Dis* 10(2)
106. Mitchell AC, Briquez PS, Hubbell JA, Cochran JR (2016) Engineering growth factors for regenerative medicine applications. *Acta Biomater* [Internet]. 30:1–12. Available from: <http://dx.doi.org/10.1016/j.actbio.2015.11.007>
107. Subbiah R, Guldberg RE (2019) Materials science and design principles of growth factor delivery systems in tissue engineering and regenerative medicine. *Adv Healthc Mater* 8(1):1–24
108. Wang Z, Wang Z, Lu WW, Zhen W, Yang D, Peng S (2017) Novel biomaterial strategies for controlled growth factor delivery for biomedical applications. *NPG Asia Mater* 9(10)
109. Jones DS, Tsai PC, Cochran JR (2011) Engineering hepatocyte growth factor fragments with high stability and activity as Met receptor agonists and antagonists. *Proc Natl Acad Sci U S A* 108(32):13035–13040
110. Ren X, Zhao M, Lash B, Martino MM, Julier Z (2020) Growth factor engineering strategies for regenerative medicine applications. *Front Bioeng Biotechnol* 7:1–9
111. Braun AC, Gutmann M, Mueller TD, Lühhmann T, Meinel L (2018) Bioresponsive release of insulin-like growth factor-I from its PEGylated conjugate. *J Control Release* [Internet] 279:17–28. Available from: <https://doi.org/10.1016/j.jconrel.2018.04.009>
112. Lühhmann T, Gutmann M, Moscaroli A, Raschig M, Béhé M, Meinel L (2020) Biodistribution of site-specific PEGylated fibroblast growth factor-2. *ACS Biomater Sci Eng* 6(1):425–432
113. Li R, Li D, Zhang H, Wang J, Li X, Xiao J (2020) Growth factors-based therapeutic strategies and their underlying signaling mechanisms for peripheral nerve regeneration. *Acta Pharmacol Sin* (July 2019):1–12
114. Vasita R, Katti DS (2006) Growth factor-delivery systems for tissue engineering: a materials perspective. *Expert Rev Med Devices* 3(1):29–47
115. DiStefano T, Chen HY, Panebianco C, Kaya KD, Brooks MJ, Gieser L et al (2018) Accelerated and improved differentiation of retinal organoids from pluripotent stem cells in rotating-wall vessel bioreactors. *Stem Cell Rep* [Internet] 10(1):300–313. Available from: <https://doi.org/10.1016/j.stemcr.2017.11.009>
116. Kanda Y, Nishimura I, Sato T, Katayama A, Arano T, Ikada Y et al (2016) Dynamic cultivation with radial flow bioreactor enhances proliferation or differentiation of rat bone marrow cells by fibroblast growth factor or osteogenic differentiation factor. *Regen Ther* [Internet] 5:17–24. Available from: <http://dx.doi.org/10.1016/j.reth.2016.06.001>
117. Ham TR, Lee RT, Han S, Haque S, Vodovotz Y, Gu J et al (2016) Tunable keratin hydrogels for controlled erosion and growth factor delivery. *Biomacromolecules* [Internet] 17(1):225–236. Available from: <https://pubs.acs.org/doi/10.1021/acs.biomac.5b01328>
118. Mufamadi MS, Pillay V, Choonara YE, Du Toit LC, Modi G, Naidoo D et al (2011) A review on composite liposomal technologies for specialized drug delivery. *J Drug Deliv* 2011:1–19
119. Zhang G, Lu H, Mamidwar S, Wang MIN, Iii JH, Engineering B (2020) Composites. In: *Biomaterials science: an introduction to materials in medicine*, pp 415–430

120. Scholz MS, Blanchfield JP, Bloom LD, Coburn BH, Elkington M, Fuller JD et al (2011) The use of composite materials in modern orthopaedic medicine and prosthetic devices: a review. *Compos Sci Technol* 71(16):1791–1803
121. Mohan N, Senthil P, Vinodh S, Jayanth N (2017) A review on composite materials and process parameters optimisation for the fused deposition modelling process. *Virtual Phys Prototyp* 12(1):47–59
122. Jiang S, Chen Y, Duan G, Mei C, Greiner A, Agarwal S (2018) Electrospun nanofiber reinforced composites: a review. *Polym Chem* 9(20):2685–2720
123. Rohit K, Dixit S (2016) A review—future aspect of natural fiber reinforced composite. *Polym from Renew Resour* 7(2):43–60
124. Yu L, Dean K, Li L (2006) Polymer blends and composites from renewable resources. *Prog Polym Sci* 31(6):576–602
125. Rinaudo M (2014) Biomaterials based on a natural polysaccharide: alginate. Tip [Internet] 17(1):92–96. Available from: [http://dx.doi.org/10.1016/S1405-888X\(14\)70322-5](http://dx.doi.org/10.1016/S1405-888X(14)70322-5)
126. Lee KY, Mooney DJ (2012) Alginate: properties and biomedical applications. *Prog Polym Sci* 37(1):106–126
127. Pereira L, Cotas J (2012) Introductory chapter: alginates—a general overview. In: Intech [Internet], p 38. Available from: <http://dx.doi.org/10.1039/C7RA00172J%0A> <https://www.intechopen.com/books/advanced-biometric-technologies/liveness-detect-ion-in-biometrics%0A> <http://dx.doi.org/10.1016/j.colsurfa.2011.12.014>
128. Bierhalz ACK, Moraes AM (2017) Composite membranes of alginate and chitosan reinforced with cotton or linen fibers incorporating epidermal growth factor. *Mater Sci Eng, C* 76:287–294
129. Andersen T, Auk-Emblem P, Dornish M (2015) 3D cell culture in alginate hydrogels. *Microarrays* 4(2):133–161
130. Ansari S, Chen C, Xu X, Annabi N, Zadeh HH, Wu BM et al (2016) Muscle tissue engineering using gingival mesenchymal stem cells encapsulated in alginate hydrogels containing multiple growth factors. *Ann Biomed Eng* 44(6):1908–1920
131. Matsuo I, Kimura-Yoshida C (2014) Extracellular distribution of diffusible growth factors controlled by heparan sulfate proteoglycans during mammalian embryogenesis. *Philos Trans R Soc B Biol Sci* 369(1657)
132. Öztürk E, Arlov Ø, Aksel S, Li L, Ornitz DM, Skjåk-Braek G et al (2016) Sulfated hydrogel matrices direct mitogenicity and maintenance of chondrocyte phenotype through activation of FGF signaling. *Adv Funct Mater* [Internet] 26(21):3649–3662. Available from: <http://doi.wiley.com/10.1002/adfm.201600092>
133. Malaeb W, Bahmad HF, Abou-Kheir W, Mhanna R (2019) The sulfation of biomimetic glycosaminoglycan substrates controls binding of growth factors and subsequent neural and glial cell growth. *Biomater Sci* 7(10):4283–4298
134. Mohammadi S, Ramakrishna S, Laurent S, Shokrgozar MA, Semnani D, Sadeghi D et al (2019) Fabrication of nanofibrous PVA/alginate-sulfate substrates for growth factor delivery. *J Biomed Mater Res—Part A* 107(2):403–413
135. Freeman FE, Kelly DJ (2017) Tuning alginate bioink stiffness and composition for controlled growth factor delivery and to spatially direct MSC Fate within bioprinted tissues, vol 7. *Scientific Reports*
136. Lin X, Guan X, Wu Y, Zhuang S, Wu Y, Du L et al (2020) An alginate/poly(N-isopropylacrylamide)-based composite hydrogel dressing with stepwise delivery of drug and growth factor for wound repair. *Mater Sci Eng C* 115(May)
137. Subbiah R, Cheng A, Ruelle MA, Hettiaratchi MH, Bertassoni LE, Gulberg RE (2020) Effects of controlled dual growth factor delivery on bone regeneration following composite bone-muscle injury. *Acta Biomater* [Internet]. Available from: <https://linkinghub.elsevier.com/retrieve/pii/S1742706120304128>
138. Mohebbi S, Nezhad MN, Zarrintaj P, Jafari SH, Gholizadeh SS, Saeb MR et al (2018) Chitosan in biomedical engineering: a critical review. *Curr Stem Cell Res Ther* 14(2):93–116

139. De Witte TM, Wagner AM, Fratila-Apachitei LE, Zadpoor AA, Peppas NA (2020) Immobilization of nanocarriers within a porous chitosan scaffold for the sustained delivery of growth factors in bone tissue engineering applications. *J Biomed Mater Res—Part A* 108(5):1122–1135
140. Min Q, Liu J, Yu X, Zhang Y, Wu J, Wan Y (2019) Sequential delivery of dual growth factors from injectable chitosan-based composite hydrogels. *Mar Drugs* 17(6):10–12
141. Qiao Y, Xu S, Zhu T, Tang N, Bai X, Zheng C (2020) Preparation of printable double-network hydrogels with rapid self-healing and high elasticity based on hyaluronic acid for controlled drug release. *Polymer* (Guildf) [Internet] 186(November):121994. Available from: <https://doi.org/10.1016/j.polymer.2019.121994>
142. Cao L, Kong X, Lin S, Zhang S, Wang J, Liu C et al (2018) Synergistic effects of dual growth factor delivery from composite hydrogels incorporating 2-N,6-O-sulphated chitosan on bone regeneration. *Artif Cells, Nanomedicine Biotechnol* 46(sup3):S1–S17
143. Hunziker EB, Enggist L, Küffer A, Buser D, Liu Y (2012) Osseointegration: the slow delivery of BMP-2 enhances osteoinductivity. *Bone* [Internet] 51(1):98–106. Available from: <http://dx.doi.org/10.1016/j.bone.2012.04.004>
144. Silva EA, Mooney DJ (2010) Effects of VEGF temporal and spatial presentation on angiogenesis. *Biomaterials* 31(6):1235–1241
145. Tang W, Yu Y, Wang J, Liu H, Pan H, Wang G et al (2020) Enhancement and orchestration of osteogenesis and angiogenesis by a dual-modular design of growth factors delivery scaffolds and 26SCS decoration. *Biomaterials* 232
146. Vijayan A, Sabareeswaran A, Kumar GSV (2019) PEG grafted chitosan scaffold for dual growth factor delivery for enhanced wound healing. *Sci Rep* 9(1):1–12
147. Sultankulov B, Berillo D, Kauanova S, Mikhailovsky S, Mikhailovska L, Saparov A (2019) Composite cryogel with polyelectrolyte complexes for growth factor delivery. *Pharmaceutics* 11(12):1–15
148. Pomin VH, Mulloy B (2018) Glycosaminoglycans and proteoglycans. *Pharmaceutics* 11(1):1–9
149. Hachim D, Whittaker TE, Kim H, Stevens MM (2019) Glycosaminoglycan-based biomaterials for growth factor and cytokine delivery: making the right choices. *J Control Release* [Internet] 313:131–147. Available from: <https://linkinghub.elsevier.com/retrieve/pii/S0168365919305656>
150. Köwitsch A, Zhou G, Groth T (2018) Medical application of glycosaminoglycans: a review. *J Tissue Eng Regen Med* 12(1):e23–e41
151. De Pasquale V, Pavone LM (2019) Heparan sulfate proteoglycans: the sweet side of development turns sour in mucopolysaccharidoses. *Biochim Biophys Acta—Mol Basis Dis* [Internet] 1865(11):165539. Available from: <https://doi.org/10.1016/j.bbadis.2019.165539>
152. Sepuru KM, Rajarathnam K (2019) Structural basis of chemokine interactions with heparan sulfate, chondroitin sulfate, and dermatan sulfate. *J Biol Chem* 294(43):15650–15661
153. Nagarajan A, Malvi P, Wajapeyee N (2018) Heparan sulfate and heparan sulfate proteoglycans in cancer initiation and progression. *Front Endocrinol (Lausanne)* 9:1–11
154. Silva C, Carretero A, Soares da Costa D, Reis RL, Novoa-Carballal R, Pashkuleva I (2017) Design of protein delivery systems by mimicking extracellular mechanisms for protection of growth factors. *Acta Biomater* 63:283–293
155. Hsu F-M, Hu M-H, Jiang Y-S, Lin B-Y, Hu J-J, Jan J-S (2020) Antibacterial polypeptide/heparin composite hydrogels carrying growth factor for wound healing. *Mater Sci Eng C* [Internet] 112:110923. Available from: <https://doi.org/10.1016/j.scitotenv.2020.140714>
156. Abatangelo G, Vindigni V, Avruscio G, Pandis L, Brun P (2020) Hyaluronic acid: redefining its role. *Cells* 9(7):1–19
157. Feng Q, Lin S, Zhang K, Dong C, Wu T, Huang H et al (2017) Sulfated hyaluronic acid hydrogels with retarded degradation and enhanced growth factor retention promote hMSC chondrogenesis and articular cartilage integrity with reduced hypertrophy. *Acta Biomater* [Internet] 53:329–342. Available from: <https://linkinghub.elsevier.com/retrieve/pii/S1742706117301186>

158. Liu X, Zheng C, Luo X, Wang X, Jiang H (2018) Recent advances of collagen-based biomaterials: multi-hierarchical structure, modification and biomedical applications. *Mater Sci Eng, C* 2019(99):1509–1522
159. Sheehy EJ, Cunniffe GM, O'Brien FJ (2018) Collagen-based biomaterials for tissue regeneration and repair. *Pept Proteins as Biomater Tissue Regen Repair* 127–150
160. Letic-Gavrilovic A, Piattelli A, Abe K (2003) Nerve growth factor β (NGF β) delivery via a collagen/hydroxyapatite (Col/HAp) composite and its effects on new bone ingrowth. *J Mater Sci Mater Med* 14(2):95–102
161. Walsh DP, Raftery RM, Chen G, Heise A, O'Brien FJ, Cryan SA (2019) Rapid healing of a critical-sized bone defect using a collagen-hydroxyapatite scaffold to facilitate low dose, combinatorial growth factor delivery. *J Tissue Eng Regen Med* 13(10):1843–1853
162. Zhang Z, Ma Z, Zhang Y, Chen F, Zhou Y, An Q (2018) Dehydrothermally crosslinked collagen/hydroxyapatite composite for enhanced in vivo bone repair. *Colloids Surf, B* [Internet] 163:394–401. Available from: <https://linkinghub.elsevier.com/retrieve/pii/S0927776518300110>
163. Seong Y-J, Song E-H, Park C, Lee H, Kang I-G, Kim H-E et al (2020) Porous calcium phosphate–collagen composite microspheres for effective growth factor delivery and bone tissue regeneration. *Mater Sci Eng C* [Internet] 109:110480. Available from: <https://doi.org/10.1016/j.scitotenv.2019.136126>
164. Fan C, Shi J, Zhuang Y, Zhang L, Huang L, Yang W et al (2019) Myocardial-infarction-responsive smart hydrogels targeting matrix metalloproteinase for on-demand growth factor delivery. *Adv Mater* 31(40):1–12
165. Nikkha M, Akbari M, Paul A, Memic A, Dolatshahi-Pirouz A, Khademhosseini A (2016) Gelatin-based biomaterials for tissue engineering and stem cell bioengineering. In: *Biomaterials from nature for advanced devices and therapies* [Internet]. John Wiley & Sons, Inc., Hoboken, New Jersey, pp 37–62. Available from: <http://doi.wiley.com/10.1002/9781119126218.ch3>
166. Afewerki S, Sheikhi A, Kannan S, Ahadian S, Khademhosseini A (2019) Gelatin-polysaccharide composite scaffolds for 3D cell culture and tissue engineering: towards natural therapeutics. *Bioeng Transl Med* 4(1):96–115
167. Xiong S, Zhang X, Lu P, Wu Y, Wang Q, Sun H et al (2017) A gelatin-sulfonated silk composite scaffold based on 3D printing technology enhances skin regeneration by stimulating epidermal growth and dermal neovascularization. *Sci Rep* [Internet] 7(1):4288. Available from: <http://www.nature.com/articles/s41598-017-04149-y>
168. Chen S, Shi Y, Zhang X, Ma J (2019) Biomimetic synthesis of Mg-substituted hydroxyapatite nanocomposites and three-dimensional printing of composite scaffolds for bone regeneration. *J Biomed Mater Res—Part A*. 107(11):2512–2521
169. Modaresifar K, Hadjizadeh A, Niknejad H (2018) Design and fabrication of GelMA/chitosan nanoparticles composite hydrogel for angiogenic growth factor delivery. *Artif Cells, Nanomedicine Biotechnol* 46(8):1799–1808
170. Soontornworajit B, Kerdsiri K, Tungkavet T, Sirivat A (2020) Aptamer–gelatin composite material for prolonging PDGF–BB release 42:180–187
171. Kinghorn AB, Fraser LA, Lang S, Shiu SCC, Tanner JA (2017) Aptamer bioinformatics. *Int J Mol Sci* 18(12)
172. Pacelli S, Acosta F, Chakravarti AR, Samanta SG, Whitlow J, Modaresi S et al (2017) Nanodiamond-based injectable hydrogel for sustained growth factor release: preparation, characterization and in vitro analysis. *Acta Biomater* [Internet] 58:479–491. Available from: <https://linkinghub.elsevier.com/retrieve/pii/S1742706117303070>
173. An G, Zhang WB, Ma DK, Lu B, Wei GJ, Guang Y et al (2017) Influence of VEGF/BMP-2 on the proliferation and osteogenic differentiation of rat bone mesenchymal stem cells on PLGA/gelatin composite scaffold. *Eur Rev Med Pharmacol Sci* 21(10):2316–2328

Biopolymers/Ceramic-Based Nanocomposite Scaffolds for Drug Delivery in Bone Tissue Engineering



K. Lavanya, S. Swetha, and N. Selvamurugan

Abstract Joint repair and reconstructive bone surgeries are growing worldwide. Self-healing of bone is constrained, which entails external stimuli to bolster bone repair and rejuvenation. While conventional approaches (autografts, allografts, or xenografts) have been increasingly utilized to repair bone defects, they all have corresponding drawbacks, thus minimizing their clinical applications. Bone tissue engineering (BTE) is a fascinating approach encompassing bone biology and engineering concepts to combat the flaws associated with grafting, as mentioned above. A variety of biomaterials such as biopolymers (natural and synthetic) and ceramics as scaffolds has been exploited to fabricate the ideal bone constructs using conventional and advanced techniques. Scaffolds loaded with appropriate drugs, including growth factors, bone remodeling molecules, phytochemicals, and other regulatory molecules for sustained and site-targeted delivery, can promote functional bone tissues. Hence, this chapter presents a distinct variety of biopolymer-ceramic-based nanocomposite scaffolds for drug delivery in BTE.

Keywords Bone tissue engineering · Scaffolds · Nanostructure · Drug delivery

Abbreviations

3D	Three dimensional
Alg	Alginate
ALP	Alkaline phosphatase
BG	Bioactive glass/bioglass
BMP	Bone morphogenetic protein
BMSCs	Bone marrow stromal cells
BSA	Bovine serum albumin

K. Lavanya · S. Swetha · N. Selvamurugan (✉)

Department of Biotechnology, School of Bioengineering, College of Engineering and Technology, SRM Institute of Science and Technology, Kattankulathur, Tamil Nadu 603203, India
e-mail: selvamun@srmist.edu.in

BTE	Bone tissue engineering
CaP	Calcium phosphate
CIP	Ciprofloxacin
Col	Collagen
CS	Chitosan
DEX	Dexamethasone
ECM	Extracellular matrix
FGF	Fibroblast growth factor
GDL	Glucono-d-lactone
Gel	Gelatin
GO	Graphene oxide
HA	Hyaluronic acid
HAp	Hydroxyapatite
HGF	Hepatocyte growth factor
HME	Hereditary multiple exostoses
HPCS	Hydroxypropyl chitosan
IGF	Insulin growth factor
MRSA	Methicillin-resistant staphylococcus aureus
MSC	Mesenchymal stem cell
nHAp	Nano-hydroxyapatite
NP	Nanoparticle
OCN	Osteocalcin
OPN	Osteopontin
PCL	Polycaprolactone
PDGF	Platelet derived growth factor
PEUR	Poly(ester urethane)
PHBV	Poly(3-hydroxybutyrate-co-3-hydroxyvalerate)
PLA	Poly(lactic acid)
PLGA	Poly(lactic-co-glycolic acid)
PLLA	Poly-L-Lactic Acid
PTH	Parathyroid hormone
PTMC	Poly(trimethylene carbonate)
PVP	Polyvinyl pyrrolidone
rBMP2	Recombinant bone morphogenetic protein 2
SBF	Simulated body fluid
SDF	Stromal cell-derived Factor
SF	Silk fibroin
TCP	Tricalcium phosphate
TGF- β	Transforming growth factor- β
TiO ₂	Titanium oxide
VEGF	Vascular endothelial growth factor

1 Introduction

The worldwide prevalence of bone diseases and illnesses has been growing. According to comparative statistics, orthopedic grafts' global market value was \$3.3 billion in 2017, which is projected to worsen in 2021, representing a vast expense to the national economy [1, 2]. The bone is a complex tissue that aids in movement and is also given its hard and dense structure, safeguarding our body's vital internal organs [3]. It is primarily made up of two regions, cortical and cancellous/spongy bone. The bone extracellular matrix (ECM) predominantly consists of organic (mainly type I collagen fibers) and inorganic [(hydroxyapatite (HAp) like calcium phosphate)] materials [4–6]. Three crucial cells, namely osteoblasts, osteocytes, and osteoclasts, are accountable for bone remodeling [7–9]. Osteoblasts are major players in osteogenesis and are involved in the formation of mineralized bone matrix. Osteoblasts derived from progenitor cells or mesenchymal stem cells (MSCs) form a protein blend called osteoid, which is composed of polymerized collagen and mineralized with calcium and phosphate in the later bone stages growth [10, 11]. In addition to the abovementioned functions, osteoblasts also secrete regulatory molecules responsible for bone formation [12]. Osteocytes are mature forms of osteoblasts that settle in the ECM, interact with the surrounding osteoblasts, and play a crucial role in mineral homeostasis [13, 14]. Osteoclasts are derived from hematopoietic stem cells and are essentially involved in bone resorption [15, 16]. The synergistic interplay of osteoblasts and osteoclasts sustains the native bone mass and regulates terminal remodeling [17, 18].

Bone defects are categorized into various divisions such as old age, hereditary disorders, fractures, cancer, and infection based on their cause. Among the different defects, the most common ones are bone fractures [19, 20]. Bone fractures can occur in any part of the body. Osteoporosis and bone loss caused due to old age can deteriorate the bone's strength and lead to fractures. Osteomyelitis is a major cause of bone infection, and it leads to pain, redness in the affected area. If it is not treated in time, it may lead to amputation, an irreversible trauma [21]. Bone tumors induce rapid bone remodeling, fractures, and anemic patient conditions that might lead to life-threatening situations. Tumor removal is primarily taken care of through surgery, but sometimes defects occur in this site leading to further complications [22]. Genetic bone diseases such as hereditary bone marrow failure syndromes and hereditary multiple exostoses (HME) require stem cell transplantation or surgical resection as treatment modalities [23]. All the aforementioned bone defects can heal on their own to some extent, but external intervention is required for the proper functional bone regeneration once it exceeds the critical size. These different categories of bone defects have to be looked into individually and must be addressed in a customized manner with new innovative technologies for effective bone treatment. Conventional gold standard procedures, i.e., autografts and allografts, hamper their extensive clinical applications due to the risk of higher non-union occurrences

with host tissues, possible immune infections, donor site morbidity, and implant-related discomfort [24, 25]. Therefore, designing a system to correctly and effectively restore the damaged bone tissue is of great therapeutic importance for patients with bone-related disorders. Bone tissue engineering (BTE) has gained significant interest from researchers as a promising strategy to alleviate bone defects without the limitations and disadvantages of autografts, allografts, or xenografts [26]. BTE is an interdisciplinary technique that uses various biomaterials as scaffolds to recreate the necessary functions of bone tissue [27]. These scaffolds provide a template for cell adhesion in bone tissue formation. Different vital parameters are used to determine the scaffolds' efficiency, i.e., pore size, pore volume, mechanical strength, and chemical properties. BTE focuses on bone structure, bone mechanics, and tissue development for new accessible bone tissues [28]. A variety of biomaterials such as biopolymers (natural and synthetic) and ceramics have been exploited to fabricate the functional ideal bone constructs using conventional (solvent casting particulate leaching, gas foaming, phase separation, electrospinning, freeze-drying) and advanced techniques (3D and 4D bioprinting) [29, 30]. Native bones have a unique hierarchical structure, ranging from nanoscale to macroscale with specifically designed interfaces [3]. Conventional BTE scaffolds exploited the various pore-forming methods to reproduce the microscale and macroscale characteristics of native osseous tissues [31]. However, nanoscale structures are pivotal to regulating cellular activities such as migration, proliferation, differentiation, and ECM development. In view of conventional therapies' significant weakness, nanomaterials have recently emerged as potential candidates for creating ECM-like scaffolds, which effectively substitute faulty tissues [32]. Nanocomposite-based scaffolds offer a closer architectural approximation to the native bone for the aforementioned cellular functions, which lead to the construction of functional tissues [33]. Most importantly, biopolymer-ceramic-based nanocomposites have the potential to effectively release the drug molecules in a sustained and prolonged manner for orthopedic applications [34, 35]. This chapter summarizes recent advances in the synthesis and implementation of different biopolymer-ceramic-derived nanocomposite scaffolds loaded with therapeutic molecules in the field of BTE. A schematic representation of a biopolymer-ceramic-based nanocomposite scaffold in BTE is depicted (Fig. 1).

2 BTE Scaffolds for Drug Delivery

Targeted delivery of drugs to the deformed bone site can significantly augment the rejuvenation of functional bone tissue. Proper bone tissue repair and regeneration involve a complex interaction of cells and growth regulatory cytokines working in congruence with the delivered drug molecules. Bone remodeling drugs can greatly enhance and induce the bone-forming cells' proliferation and differentiation potential by modulating their cellular activities. These delivered drug molecules selectively bind to the cell surface receptors and translocate to the nucleus, thereby determining

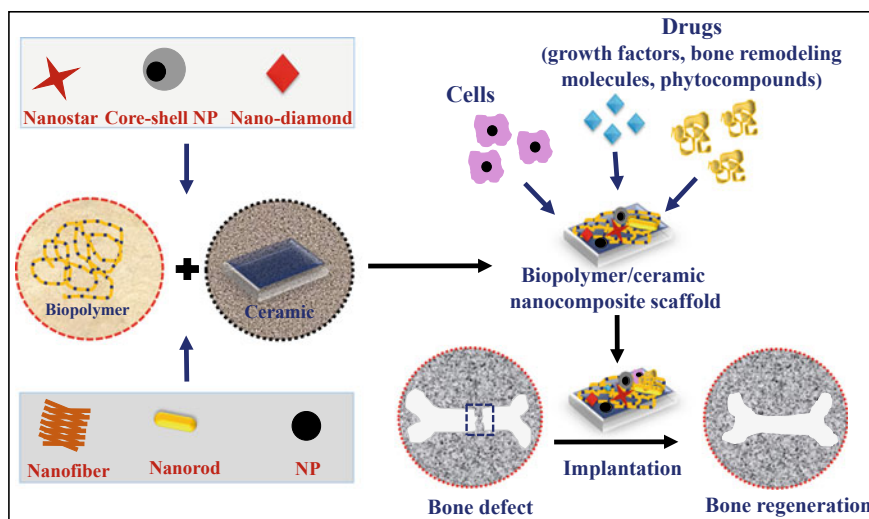


Fig. 1 Schematic representation of biopolymer/ceramic-based nanocomposite scaffolds in BTE applications. Biopolymer/ceramic-based nanocomposites are encapsulated with cells and drug molecules to facilitate bone regeneration effectively

biological responses [36]. In BTE, the multifunctional scaffolds may act as a delivery system for the targeted, sustained delivery of therapeutic drug molecules [37].

2.1 Types of Drug Molecules Used in Bone Regeneration

Several therapeutic molecules have been widely investigated for their potential in osteogenic differentiation ability by regulating the cascade of cellular and molecular signaling pathways in bone regeneration [38]. Growth factors, bone remodeling molecules (anti-bone resorptive and bone-forming), phytocompounds, and other regulatory molecules have been used for drug delivery in bone regeneration. The detailed understanding of the bone healing process and proper utilization of these bioactive molecules greatly aid in significant bone regeneration [39].

2.1.1 Growth Factors

Growth factors are soluble signaling peptides secreted by the vast array of cells to stimulate diverse biological responses like cell survival, proliferation, differentiation, migration, and ECM deposition [40]. Growth factors selectively bind to the cell surface receptor of the targeted cells, resulting in the receptors' conformational change and activate the internal signaling cascades, including the transcription factors

within the cells. This event is followed by nuclear translocation and results in the regulation of gene expression [41]. Since these growth factors are naturally present in the native bone, the healing process naturally takes place. Several growth factors are being employed in the bone repairing process, which include transforming growth factor-beta1 (TGF- β 1), TGF- β 3, bone morphogenetic protein (BMP)-2, BMP-4, BMP-7, fibroblast growth factor (FGF)-2, platelet-derived growth factor (PDGF), vascular endothelial growth factor (VEGF), insulin growth factor (IGF)-1, stromal cell-derived factors (SDF)-1, interleukin (IL)-6, and hepatocyte growth factor (HGF) [42–53]. Though these growth factors have much proved their significance in the number of bone regeneration studies, they are often subjected to proteolytic degradation. Additionally, their short half-life with a rapid clearance rate in vivo is also a major concern [54]. The action of growth factors depends upon cells expressing their receptors, indicating their specificity in biological functions [55]. Also, the diffusion rate of the growth factors through the ECM is very low; thus, it requires highly concentrated doses to reach the therapeutic level. But unfortunately, a higher dosage leads to several side effects, including cytotoxicity, heterotopic bone formation, and cancer. Most importantly, the higher cost of these growth factors restricts their usage in more massive amounts. Therefore, the site-targeted and sustained drug delivery kinetics become crucial to address the pitfalls of the growth factors delivery [56].

2.1.2 Bone Remodeling Drugs

BTE involves using a plethora of drug molecules that aid in the significant regeneration of functional osseous tissue. As mentioned in the introduction, bone remodeling is a coupled process involving bone formation by osteoblasts and bone resorption by osteoclasts. Various osteogenic drugs and small molecular weight compounds are used to treat the defect in bone remodeling. These bone remodeling drugs have been predominantly used with bone tissue-engineered constructs to facilitate osteogenesis. Additionally, several antimicrobial and anti-inflammatory drugs are employed to conquer microbial contaminations, and inflammatory responses occur after incorporating the regenerative scaffolds [57, 58].

Osteogenic Drugs

Sustained osteogenic drugs through engineered bone construct at the site of injury can further intensify bone regeneration and control bone resorption. Here we discuss some of the significant osteogenic drugs widely used in BTE. Bisphosphonate, an interesting drug holds a special place in treating osteoporosis and preventing osteoporotic fractures. Bisphosphonates have mainly been utilized in orthopedic applications because of their high affinity toward osseous tissue [59]. They selectively bind to the apatite crystal matrix by establishing strong bidentate bond by chelating phosphonate groups and calcium ions [60]. Also, it is proven that targeted delivery of bisphosphonates at the site of deformation potentially inhibits osteoclastogenesis

and promotes osteogenesis [61]. Besides, it prevents the wrapping of fibers on the implants by inducing fibroblasts' apoptosis, thereby enhancing their tenacity [62]. Bisphosphonates, including alendronate, risedronate, ibandronate, zoledronic acid, clodronate, etidronate, tiludronate, have been investigated in finding their role on bone regeneration [63–69]. Despite the privileges, bisphosphonates' affinity toward healthy bone may induce certain side effects. Therefore, a sustained and site-targeted delivery of bisphosphonate-related drugs becomes necessary to escape undesirable effects [61]. Sometimes, delayed fracture healing and non-unions occur due to conditions such as osteoporosis, malnutrition, aging, postmenopausal state, or low estrogen. Various bone-building anabolic drugs have been investigated. Parathyroid hormone (PTH) is the primarily approved anabolic drug used to augment the healing process. PTH is an 84 amino acid containing protein secreted by the parathyroid glands. Its predominant role is to regulate the extracellular calcium [70]. Considering PTH's potential biological significances, its derivatives such as teriparatide, abaloparatide, and romosozumab are widely used in bone regeneration therapies [71–73].

The bone regeneration process may also be heightened by administering anti-resorptive drugs to inhibit osteoclast bone resorption. RANKL inhibitors are the selective variant of anti-resorptive drugs, which inhibit osteoclastogenesis by interfering with the binding of RANKL with RANK receptor present on the osteoclast precursors' surface. Denosumab, a monoclonal antibody, is considered as an alternative anti-resorptive drug in the treatment of osteoporosis. It is a RANKL inhibitor, which works by preventing osteoclast cell formation [74].

Low Molecular Weight Drugs

Small molecular drugs and bioactive factors generally have their molecular weight lesser than 900 Daltons. These small compounds are usually stable, display notable osteoinductivity at low doses, and less immunogenic. They are available at an affordable cost [75]. Statins are the most widely used low molecular weight drug in BTE. Statins selectively inhibit 3-hydroxy-3-methyl-glutaryl co A (HMG-CoA) reductase from enhancing BMP-2 secretion of the cells to improve osteogenesis [76]. In bone tissue regeneration, three types of statins, namely simvastatin, lovastatin, and rosuvastatin, are widely utilized. They exhibited fewer adverse effects [77–79]. Other low molecular weight drugs with osteoinductive potential include tilorone, dexamethasone, fingolimod, purnormorphamine, and tetracycline [80–84].

Antimicrobial and Anti-inflammatory Drugs

Microbial contaminations and inflammatory responses are of major setbacks that take place during and after the scaffold implantation. These undesirable reactions at the site of scaffold implantation can lead to the serious issue of implant failure. These difficulties can be overcome by the sustained delivery of the antimicrobial

and anti-inflammatory agents through the engineered construct. As antimicrobial drugs, tetracycline, vancomycin, doxycycline, rifampicin, gentamycin, clindamycin, and moxifloxacin have been widely investigated in BTE [84–90]. The delivery of divalent cations such as gold, silver, zinc, copper, titanium, magnesium, and strontium can display excellent antimicrobial properties and help in bone regeneration as some of them are integral components of the native bone tissue [91–96]. Furthermore, to mitigate the inflammatory responses raised due to the scaffold implantation, several immunosuppressive and anti-inflammatory drugs are being delivered along with the scaffold. Dexamethasone, aspirin, ibuprofen, naproxen, meloxicam, celecoxib, indomethacin, and diclofenac have been administered in treating bone tissue inflammation [81, 97–103]. Impressively, in addition to the antimicrobial and anti-inflammatory properties exhibited by the drugs mentioned above, they are also proved to enhance the bone modulation by improving cell differentiation, alkaline phosphatase activity, and mineralized matrix formation [81, 104]. But unfortunately, the above-discussed drugs, when delivered in high concentration or long-term systemic administration, can cause invariable side effects. This critical issue can be surmounted by designing a proper drug delivery system with targeted and controlled delivery kinetics.

2.1.3 Phytochemicals

Though numerous studies report the delivery of growth factors and drugs for successful osteogenesis, there are also potential side effects like malignancies and cytotoxicity. Furthermore, the sustained and targeted delivery of these compounds and their escalating cost is of major pitfall to be encountered. These necessitate the search for alternative bioactive molecules to bolster the bone regeneration process. Nowadays, researchers are intrigued by phytochemical-incorporated bone regenerative scaffolds [105]. Phytochemicals are non-nutritive secondary metabolites of plants produced during the period stress condition and injury. Interestingly, these plant-derived compounds play a significant role in enhancing and inducing the osteogenesis process [106]. Moreover, its low-cost, high availability, and non-toxic nature makes them a better replacement in the place of growth factors and drugs. Phytocompounds are classified into various groups based on their structural and functional properties. These are alkaloids, phenolics, carotenoids, nitrogen-containing compounds, and organosulfur compounds [107]. To date, a plethora of phytocompounds with osteogenic potential has been explored. It is also reported to enhance osteogenic marker genes such as ALP, OCN, OPN, OSX, OPG, COL1. These phytocompounds bolster bone regeneration by undergoing bone regenerative signaling pathways, viz. BMP signaling pathway, MAPK signaling pathway, and Wnt/ β -catenin signaling pathway [108]. Icariin, silibinin, resveratrol, quercetin, sulforaphane, genistein, sinapic acid, zingerone, chrysin, diosmin, veratric acid, valproic acid, mucic acid are some of the recently investigated phytocompounds with notable osteogenic potential [109–121]. Despite the significances mentioned above of the phytocompounds in bone regeneration, they also express some shortcomings. The hydrophobic nature

of some phytochemicals results in low aqueous solubility and bioavailability. On the other hand, hydrophilic phytochemicals may exhibit low absorption and rapid metabolism. These challenges can be catered by using various drug delivery techniques, and understanding of the biological interaction of phytochemicals with stem cells becomes crucial to improve their therapeutic efficacy [122].

2.2 *Impacts of Scaffolds for Drug Delivery*

Bone regeneration at the deformed site can be promoted by delivering various growth regulatory signaling peptides and drugs [123]. Several techniques have been adopted to deliver the signaling peptides to the site of the fracture. One such traditional approach involves the direct systemic delivery of drugs through oral and intravenous administration [124]. In this strategy, delivered drug molecules are absorbed into the bloodstream and distributed throughout the body with the circulatory system's aid. In this case, a significant quantity of the drug will accumulate in other organs of the body; thus, only a small proportion of the supplied therapeutic dosage range can reach the actual site of the injury [125]. Bone, being a peripheral organ with limited blood supply than other tissues, seriously reduces drug delivery [126]. Additionally, the lack of tissue specificity results in poor penetration of the drug into the targeted tissue, low therapeutic efficacy, systemic cytotoxicity, and several side effects, including liver and renal complications. Moreover, decreased bioavailability, instability, rapid breakdown, and renal clearance rate are major concerns to enhance or maintain the supplied therapeutics [127]. For instance, direct injection of growth peptides at the deformation site is severely prone to degradation as they have a relatively short half-life. When injected intravenously, the half-life of the growth factors such as bFGF, PDGF, VEGF was found to be 3–50 min, 2 min, and 30–45 min, respectively. Additionally, the administered signaling peptides may be susceptible to oxidative damage when the amino acids in them interact with oxygen radicals. Particularly peptides containing tyrosine, tryptophan, histidine, and cysteine residues are more liable to oxidation [128, 129]. These deterrents triggered the need to develop a targeted drug delivery system to facilitate sustained and prolonged drug delivery at the diseased site for a prescribed period. In this regard, site-targeted implantation of the drug encapsulated scaffolds holds an upper hand in overcoming the disincentives mentioned above with systemic drug delivery and providing a comprehensive landscape for successful bone-targeted drug delivery [130].

An ideal scaffold for bone regeneration should (1) be able to biodegrade gradually in congruence with the new bone formation without the release of any toxic by-products; (2) be biocompatible to facilitate cellular attachment, proliferation, and differentiation to fasten bone rejuvenation; (3) be mechanically stable to withstand the load during the amelioration period; (4) possess optimum porosity and pore diameter to facilitate enhanced cellular infiltration, nutrient exchange, and angiogenesis; (5) be able to encapsulate and release drugs in a controlled, sustained manner. Thus, a proper bone tissue-engineered construct should act as a dual function matrix to support new

bone formation and act as a carrier for sustained drug delivery in situ [125, 131, 132]. Different types of scaffolds have been widely utilized for controlled drug release in bone tissue repair. The scaffold architecture has been categorized into different types, including hydrogels, porous scaffolds, electrospun fibers, metallic implants, and 3D bioconstructs. These scaffolds can be fabricated using a variety of conventional fabrication techniques (e.g., electrospinning, gas foaming, freeze-drying, melt molding, solvent casting, phase separation, porogen leaching, sol–gel technique) and modern fabrication techniques (3D printing, 3D bioprinting, and 4D printing) [133, 134]. Scaffolds for drug delivery in BTE are fabricated using several biodegradable polymers (natural/synthetic), bioactive compounds, bio-resorbable inorganic biomaterials including calcium phosphate and its derivatives, bioactive glasses, and mesoporous silica [135]. The selection of suitable biomaterial and the fabrication process for drug delivery solely depends on the type of drugs, their stability, bioactivity, and the desired release kinetics [8]. Therefore, a meticulous selection of biomaterials and their fabrication process concerning the type of drug molecules can aid in controlled and sustained drug delivery.

Various drug delivery strategies are being employed to attain sustained drug delivery based on the nature of signaling molecules to be delivered. Different categories of drug molecules demand distinct delivery strategies to accomplish their desired therapeutic effects. Commonly employed drug delivery strategies for BTE applications involve a surface presentation, controlled sustained drug release, pre-programmed drug release, and stimuli-responsive drug release [136]. Surface presentation of the drug molecule on the bone construct can be done either by physical interaction or chemical conjugation approach. This technique enables the drug molecules' contact with the cells migrating toward the construct and potentially reduces off-target side effects [137]. Another intriguing and promising drug delivery strategy for effective bone regeneration involves controlled sustained drug release, which maintains ideal drug concentration at the site of bone regeneration for the desired period. The drug molecules can be encapsulated directly within the polymeric matrix during the fabrication, or it can also be encapsulated in distinct delivery vehicles such as liposomes, micro/nanoparticles. In this, direct drug encapsulation within the polymeric matrix is considered the most straightforward technique, but it may also affect the bioactivity and the release kinetics of the drug. To mitigate these constraints, drug molecules have been introduced separately using specific delivery vehicles to maintain their bioactivity and controlled release kinetics [138]. Another promising drug delivery strategy is pre-programmed drug delivery, an advanced strategy to achieve sequential release of multiple drug components with diverse release kinetics using multi-compartment scaffolds. Supplying multiple drug components can increase bone regeneration at even low dosage concentrations, thus aids in minimizing the potential risk of cytotoxicity associated with delivering a single drug at a high dose [139]. Following the pre-programmed drug delivery, stimuli-responsive drug release is gaining immense attention to reduce the side effects caused due to increased drug dosing and burst release of drugs in conventional drug delivery. Various stimuli-responsive smart biomaterials release drugs based on demand by different external stimuli such as temperature, pH, magnetic field, electric field, and irradiation. But the

safety concern associated with the intensity of the external stimuli is a major issue. Therefore, safer and less invasive stimuli are more likely to be utilized in clinical treatments [140]. To overcome the challenges associated with the drug delivery strategy, nanotechnology-based research is widely used presently. Especially, nanocomposites are gaining increasing attention in site-targeted and controlled drug delivery [141].

Nanocomposites combine multiple nanomaterials or nanoparticles encapsulated within bulk biomaterial with a nano-range size of 1–100 nm. Nanostructured particles within the composite system can provide exceptional progress in material properties compared to bulk matrix, micro-composites, and macro-composites. The nanocomposite scaffolds' significances include enhanced mechanical properties, controlled drug delivery profile, and molecular permeability [142]. From the scaffold fabrication point of view, these nanocomposites possess thermal stability, chemical resistance, flame retardancy, electrical conductivity, and optical clarity. Nanocomposites' property varies from normal composite materials in terms of having a remarkably higher surface-to-volume ratio [143]. This property facilitates the transport of large quantities of drug molecules within the bone constructs. Considering nanocomposites' paramount privileges in drug delivery, diverse nanocomposite combinations have been widely developed and investigated for BTE applications. Let us discuss the different combinations of nanocomposites and their orthopedic drug delivery applications in the forthcoming topics.

3 Biopolymer/Ceramic Nanocomposite Scaffolds in Bone Regeneration

Nanocomposites scaffolds are an amalgamation of two distinct biomaterials consisting of two phases, a reinforcing phase (nano-range particles, fibers, sheets), embedded in a matrix phase [144]. Various novel nanocomposite systems have been widely investigated to enhance drug solubility, cell-specific targeting of bone, inhibition of rapid drug degradation, and improvement of drug stability to safely reach its site of action without being eliminated in the systemic circulation. The nanocomposite scaffolds can be categorized based on the carrier matrix and filler material utilized [145]. In recent years, natural and synthetic polymers are the most widely used as carrier matrix for the encapsulation of the drug-loaded nanofillers (ceramic materials) due to its tailorable biodegradability. Figure 2 describes a different combination of biopolymer and ceramic-based nanocomposites for orthopedic drug delivery applications.

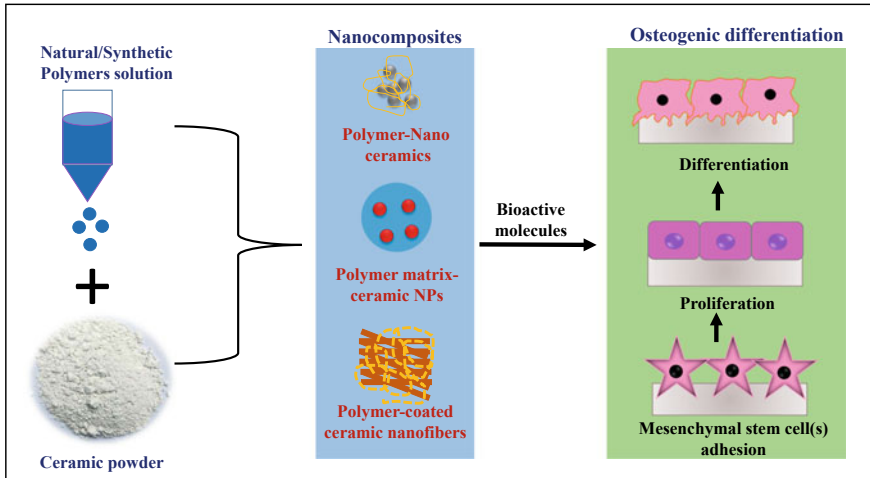


Fig. 2 Different combinations of biopolymers and ceramics are utilized to design biopolymer/ceramic-based nanocomposite bone constructs. Bioactive molecules are included to accelerate the differentiation of mesenchymal stem cells toward osteoblasts

3.1 Biopolymers-Based Nanocomposite Scaffolds

Biomaterials play a predominant role in deciding the scaffolds' characteristics and are categorized into natural and synthetic polymers [146]. The most widely employed natural biopolymer in drug delivery includes chitosan (CS), alginate (Alg), gelatin (Gel), collagen (Col), cellulose, hyaluronic acid (HA), and silk fibroin (SF) [147]. Several biodegradable synthetic polymers like polycaprolactone (PCL), poly(lactic acid) (PLA), polyethylene glycol (PEG), poly(lactic-co-glycolic) acid (PLLA) are increasingly investigated for their drug delivery potential as nanocomposites [148]. These biodegradable polymers can be exploited independently or in combination with one another to achieve controlled drug delivery in various ways, including polymer degradation, polymer disintegration, and drug dispersion within the polymeric network or over a polymer film [149].

3.1.1 Natural Polymers

Natural polymers are increasingly utilized in nanocomposites-based drug delivery for orthopedic applications as they are found to be more biocompatible in nature, biomineralization, and osteogenic potential [150]. Most importantly, natural polymers may contain ligands that facilitate binding with the cell surface receptors to enhance osteogenesis [151]. Here we elucidate the various properties of natural polymers and their current applicability in the fields of orthopedic drug delivery. CS is a biodegradable natural polymer obtained from chitin (shell crusts of crustaceans and

fungal cell walls). It is mainly comprised of β -1, 4-linked N-acetyl-D-glucosamine, and D-glucosamine units [152]. Its intrinsic properties, such as biodegradability, biocompatibility, antibacterial activity, cationic nature, and mucoadhesive properties, make them more attractive in BTE applications. Specifically, the CS's structural resemblance with glycosaminoglycans (GAGs) aids in enhancing the bone regeneration rate [153]. But the mechanical instability of CS restricts its usage in native form; thus, this critical issue can be addressed by formulating CS-based nanocomposites scaffolds with ceramics such as HAp, tricalcium phosphate (TCP), and synthetic polymers [154]. In recent years, CS-based nanocomposites are mostly investigated in orthopedic drug delivery applications due to their increased drug loading efficiency, controlled and prolonged drug release profile [155].

Alg is an anionic polysaccharide made of 1, 4-linked β -D-mannuronic acid (M) with 4C1 ring configuration and α -L-guluronic acid (G) with 4C1 conformation [156]. Alg polymer as a carrier matrix in nanocomposites holds a significant place in orthopedic drug delivery. It exhibited improved biocompatibility, drug encapsulation and release potential, biomineralization capacity, porosity, cell adhesion, proliferation, and osteogenic differentiation [157]. Gel is a proteinaceous biodegradable polymer derived from Col. Gel can mimic the components of the native ECM, and this intriguing property helps to improve cell adhesion and proliferation [158]. The excellent biocompatibility, biodegradability, and porous structure of Gel-based nanocomposites gain immense attention in bone-targeted drug delivery [159]. Unfortunately, the Gel's low stability in various physiological conditions triggered the need for the inclusion of other polymeric or ceramic biomaterials to form a stable nanocomposite for drug delivery [160]. Col is one of the abundantly available natural polymers. Type I Col is the chief composition of ECM, especially in tissues such as bone and tendon, which nourishes the osteogenic cells by facilitating proper nutrients infiltration [161]. As a biomaterial, Col holds a significant place in BTE because of its highly porous nature, simple processing, hydrophilicity, biocompatibility, compatibility with other polymers, absorbability in situ, and low antigenicity [162]. Considering the Col's paramount privileges, it has been extensively utilized as a carrier matrix for nanocomposites in controlled drug delivery applications.

Cellulose is the abundantly available natural polymer obtained from bacterial and plant sources. It is made of long-chain polysaccharides with over 10,000 β -(1-4)-connected D-glucose units [163]. Nanocellulose biomaterial possesses unique properties such as enhanced chemical reactivity, mechanical tenacity, the high specific surface-to-volume ratio, and non-toxicity, making it an exquisite candidate for controlled drug release [164]. Cellulose and its derivatives, such as cellulose ether, cellulose esters, and oxycellulose, have been used widely in drug delivery applications [165]. Hyaluronic acid (HA) is a linear glycosaminoglycan that comprises a repetitive unit of N-acetyl-D-glucosamine and D-glucuronic acid with the monosaccharides coupled together by way of alternating β -1,3 and β -1,4 glycosidic bonds [166]. HA and its derivatives have been extensively utilized as carrier molecules for controlled and sustained drug release [167]. HA's specific binding affinity toward receptor for HA-mediated motility (RHAMM) and CD44 cell surface receptors serves as the foundation for the targeted drug delivery of therapeutic proteins and

drugs [168]. SF is a protein-based natural polymer derived from the domesticated silkworm *Bombyx mori* and spider *Nephila clavipes*. There is a growing desire to develop protein-based nanocomposites in orthopedic drug delivery due to their exceptional functionalities [169]. SF-based drug carriers possess excellent biocompatibility, biodegradability, and non-antigenic nature [170]. SF has been widely investigated as an ideal drug delivery matrix because of active intrinsic amino groups and tyrosine residues, which facilitates the conjugation of various drug molecules [171].

3.1.2 Synthetic Polymers

Synthetic polymers are another class of biodegradable polymers widely used in BTE applications. According to the application site, its major advantages include the ability to customize degradation kinetics and mechanical properties by modifying the functional groups present in them. They can also be synthesized into different forms with desired pore size geometry that is conducive to the growth of blood vessels and neo-bone [172, 173]. On the contrary, they display reduced bioactivity, osteoconductivity, and cell recognition RGD sequences compared to the natural polymers. In this context, several polymers' surface functionalizations can be done to improve their performance in BTE [174–176]. In the following sections, we discuss the characteristics features of some frequently utilized synthetic polymers such as PCL, PLA, and PLGA in nanocomposites-based drug delivery for BTE applications.

Among the various biodegradable polymers investigated, a special focus is made on PCL mainly because of its broad spectrum functionality and compatibility with other polymers. PCL is an aliphatic polymer with semicrystalline nature that displays desirable biocompatibility and mechanical durability [177]. On the other hand, its slow degradation profile may negatively impact new bone formation. Additionally, its hydrophobic surface affects cell adhesion and proliferation and does not allow facile delivery of hydrophobic drug molecules [178]. This hitch can be conquered using a modified form of PCL with several osteogenic, osteoinductive inorganic compounds such as HAp, bioactive glass (BG), and titanium dioxide. Considering the leverage of the modified form of PCL, several PCL-based nanocomposites have been widely exploited in drug delivery application for bone regeneration [179].

PLA is a non-toxic, aliphatic biodegradable polymer obtained from renewable sources like corn, cassava, and sugar cane, which has been extensively researched as a bone substitute material and drug-releasing carrier in BTE [180]. Based on the microstructure, PLA can be classified into three types such as PLLA, poly(D-lactic acid) (PDLA), and their racemic counterpart D,L-PLA (PDLLA). From the above-mentioned PLA categories, PDLLA is frequently utilized in drug delivery systems because of its monophasic assembly [181]. PLGA is a biodegradable linear copolymer of PLLA and glycolic acid (PGA). PLGA holds the upper hand as a promising carrier matrix for drug delivery applications [182]. PLGA has gained extreme importance in drug delivery applications due to its salient features, including biocompatibility, tunable degradation rate, sustained drug release profile, protection of encapsulated drugs from degradation, and target specificity [183]. Nevertheless,

the amorphous nature of the PLGA makes it mechanically unstable and, thus, restricts its usage in load-bearing applications. In this context, PLGA requires the inclusion of nano-sized bioactive ceramics such as HAp, BG, and calcium phosphate (CaP) to create PLGA nanocomposite biomaterials [184].

3.2 Ceramics-Based Nanocomposite Scaffolds

A wide variety of biomaterials have been utilized for orthopedic drug delivery applications. In particular, ceramic-based nanocomposites have gained recognition over the years due to its structural similarity with the native bone tissue's inorganic composition. Ceramics, including HAp, CaP, and BG, have been intensively researched for their drug delivery application [185].

3.2.1 Calcium Phosphate

Among the various biomaterials being utilized to date, CaP has been predominantly scrutinized for its use in the bone regeneration process due to its resemblance to the inorganic mineral segment of native bone, biocompatibility, osteoconductivity, and bio-resorbable nature [186]. CaP is a reservoir of calcium and phosphate ions that persuasively augments stem cells' osteogenic differentiation into the osteoblastic lineage. Depending on the Ca/P ratio and solubility nature, CaP can be classified into different types: HAp, alpha-tricalcium phosphate, and beta-tricalcium phosphate [187]. Considering the preeminent influence of CaP and its derivatives in bone regeneration, CaP has been widely employed as a carrier for various drug molecules and therapeutic cargoes.

3.2.2 Hydroxyapatite

HAp [(Ca)₁₀(PO₄)₆(OH)₂] is the major inorganic composition of the native bone, which holds the potential of regulating the biomineralization process. HAp is increasingly used in bone regeneration applications because of its excellent biocompatibility, osteoconductivity, and tunable physical and chemical properties [188]. Slower degradation kinetics of the HAp much helps control and localizes drug release, thereby minimizing the cytotoxicity [189]. Also, the drug loading capacity, drug release profile, and therapeutic efficacy are depending on the characteristic nature of HAp, i.e., its size, structure, chemical composition, porosity, crystallinity, surface chemistry [190].

3.2.3 Bioactive Glass

BG is an amorphous, silicate-based biomaterial used in BTE applications. The traditional 45S5 bioactive glass comprises 45 SiO₂, 24.5 Na₂O, 24.5 CaO, and 6 P₂O₅ by wt% and has received FDA approval for clinical use as a bone filler in the treatment of deformed bone tissue [191]. The interaction of BG with the physiological fluid results in the release and exchange of soluble ions such as Ca, P, Si, and Na, which binds to the bone to stimulate pertinent intracellular and extracellular signaling cues for enhanced osteogenesis [192]. In recent years, nanocomposites of biopolymers and BGs have been progressively developed for orthopedic drug delivery due to their highly porous structure, large surface area, and bioactive nature biodegradability, and biocompatibility [193].

Each class of the above-discussed biomaterials in drug delivery applications has its advantages and disadvantages. For instance, biopolymers usually serve as an excellent carrier matrix for sustained and prolonged drug delivery due to their native ECM's physicochemical similarities. Nevertheless, some disadvantages, including low mechanical strength, risk of immunogenic reactions, and non-tailorable nature, restrict their native form usage. Similarly, in addition to the ceramics' privileges, it also suffers from certain disadvantages like brittleness, low biodegradability, toxicity, poor drug release profile, and surface morphology. Therefore, to mitigate these catastrophic failures associated with controlled drug release, different biomaterials are being used in combination with one another. In the following sections, we explore the various combinations of the biomaterials mentioned above in orthopedic drug delivery.

4 Biopolymer/Ceramic Nanocomposite Scaffolds for Drug Delivery in Bone Tissue Engineering

Recently, several investigations on biopolymer/ceramic nanocomposite scaffolds have been scrutinized due to their higher mechanical properties, favorable interactions between the material surface and cell membrane, nucleation of the mineralized matrix, and spatially regulated protein binding for cellular adhesion. They offer critical aspects for stem cells' motivation toward specific lineages, compared to either biopolymers or ceramics [194, 195]. As a result, in BTE, this kind of construct can be substituted for innate tissue, as reported in many clinical cases. Single-class materials may not be able to fulfill all the criteria for a given implant application. For this purpose, the composites of multi-scale architectures and the favorable traits for specific applications can be accomplished by combining two or more biomaterials classes. In this section, we address the three-prevailing combination of biopolymer/ceramic nanocomposite scaffolds as follows: natural polymer/ceramic-based nanocomposite scaffolds; synthetic polymer/ceramic-based nanocomposite scaffolds; natural/synthetic polymers/ceramic-based nanocomposite scaffolds.

4.1 *Natural Polymer/Ceramic-Based Nanocomposite Scaffolds*

The utilization of natural polymers in BTE has received substantial recognition due to its desirable biodegradability, secure, and non-immunogenic [196]. Even though hasty degradation and high solubility of natural polymers combined with the increased risk of loss of biological traits during preparation also hinder their utilization as individual scaffold materials. Several experiments showed that the strengthening of natural polymers with ceramic compounds improves their mechanical properties. Natural/ceramic-based nanocomposites boost the mechanical properties and aid to resemble the nano-topography of the native bone [197].

Among the available natural polymers, Alg is typically used in BTE due to its ability to develop hydrogels when multivalent cations interact with its guluronic residues [198]. The feasibility of mixing both Alg and ceramics enables the synergization of these biomaterials' advantages in the production of BTE composite scaffolds. They possessed high mechanical strength, biodegradability, and biocompatibility [199]. Naik et al. reported the production of chemotherapeutic drug methotrexate-loaded nano-TiO₂-HAp-Alg composite scaffolds by freeze-drying technique. Regulated swelling, enhanced biomineralization, limited degradation, and ideal drug release profile have been observed in the recorded nanocomposite scaffold [200]. Another related study includes discovering Ciprofloxacin's (CIP) persistent release from the HAp/Alg nanocomposite matrix. The reported matrix demonstrated a persistent and extended-release of CIP from the nanocomposite matrix [201]. Several findings have suggested that the antibacterial Alg-HAp-dependent nanocomposite scaffolds have been formulated to treat disease associated infections. In this regard, CIP-integrated Alg-nHAp-based scaffolds were fabricated to assess their bioactivity, osseointegration, and bactericidal activity. Bioactivity and antibacterial properties were explicitly reported in the assay results [202]. On the other hand, in orthopedic drug delivery applications, Alg-based photocrosslinked hydrogels have recently gained a more significant role because cells and bioactive factors can be administered in aqueous macromer solutions in a minimally invasive manner. For example, Maji et al. synthesized photocrosslinked Alg/nHAp paste for BTE to deliver BMP-2. The study of immunocytochemistry showed that applying surface-functionalized nHAp and BMP2 to Alg hydrogel improved the prepared paste's osteogenic ability [203].

Gel is another fascinating natural polymer with many benefits, such as biological origin, relatively low-cost commercial production, and non-immunogenicity [204]. A few research pieces utilized the Gel/ceramic nanocomposite scaffolds to combine individual constituents' synergetic properties. By using the foam replication technique, Reiter et al. developed icariin-integrated Gel-coated, 3D sponge-like scaffolds based on 45S5 BG. The data implied that the multiple crosslinking approaches resulted in different icariin release profile [205]. In another analysis, the zoledronic acid (ZA) primed Gel/ β -TCP nanocomposite scaffolds were tested

for its osteogenic potential. Approximately 75% of bone regeneration was accomplished after 4 months in rabbits' cranial fossa [206]. Govindan et al. documented that the phosphate glass (PG) reinforced Gel scaffolds mixed with CIP drugs were developed via the freeze-drying technique for BTE. Composite scaffolds revealed an adequate porosity (~73%) and improved mechanical strength with the compression modulus of 4.89 MPa [207]. Besides, to raise bone progress and to duplicate the role of natural ECM for continuous release of multiple growth factors (BMP-2 and FGF-2), the scaffolds containing the surface-functionalized porous Gel nanofibers coated with HAp using an SBF medium were prepared. As verified by the upregulated expression of bone gene markers (RunX2, COL1 α 1, and OCN), osteogenesis was improved through synergism between multiple growth factor distribution and the nHAp nanofiber coating [208].

CS is one such captivating natural polymer, known to have gained interest over the past two decades as a possible drug and gene delivery carrier because of its unique characteristics. Nonetheless, the loss of uniformity of structure and poor mechanical strength has hampered CS in BTE. To combat these obstacles, CS/ceramic nanocomposites are generally used [209]. Typically, the nanoparticulate composites of HAp and CS were synthesized by ultrasound-assisted sequential precipitation to treat osteomyelitis. There was a controlled release of drug from the matrix, and it also showed antibacterial activity against *Staphylococcus aureus* [210]. Zarghami et al. synthesized similar bactericidal-based nanocomposite scaffolds (CS/BG NPs/vancomycin), and the scaffolds showed a prolonged bactericidal performance [211]. Jolly et al. merged *Phoenix dactylifera* seeds with CS and nHAp and thus prepared the synergistically functionalized nanocomposite scaffolds (PD-CHA) as a bone construct. These nanocomposite scaffolds showed osteoblast cell development and osteogenic differentiation. As early as four weeks in vivo, radiological and histological examination revealed substantial bone regeneration at the deformed site (rat calvarial bone defect) [212]. The use of CS in the production of ceramic-combined organic/inorganic composites for BTE is limited since CS is only soluble in acidic conditions. A semisynthetic CS derivative readily dissolved in water is hydroxypropyl chitosan (HPCS). Due to its antibacterial, antioxidant, biocompatible, and biodegradable substance for cell growth and tissue regeneration, HPCS has recently gained a growing interest in biomedical applications. For instance, Lu et al. developed genipin-crosslinked and fucoidan (FD)-adsorbed nHAp/HPCS composite scaffolds for BTE. These scaffolds accelerated ALP activity and mineralization in osteoblastic cells [213]. We summarize all the reported natural polymer/ceramic-based nanocomposite scaffolds available for BTE in Table 1.

Table 1 Biodegradable natural polymer/ceramic-based nanocomposites for drug delivery in BTE applications

S. No.	Nanocomposites	Fabrication method	Drug	Outcome	Reference
1	nHAp-CS	Nanocrystal-induced biomimetic mineralization method	BMP-2	A sustained delivery of BMP-2 enhanced osteoblast differentiation of BMSCs in vitro	[214]
2	nBG-Gel-Agarose	Freeze gelation	Ciprofloxacin	Controlled drug release reduced the microbial infection and was effective in localized treatment of osteomyelitis	[215]
3	nBG-Alg	Cast molding	Cu ²⁺ , Ca ²⁺	Sustained delivery of bioactive ions stimulated rBMSC differentiation toward the osteogenic lineage	[216]
4	GelMA-ND	Photocrosslinking	Dexamethasone	Promoted osteogenic differentiation of hASCs	[217]
5	Heparin-Col-HAp	Fibrillation and mineralization techniques	VEGF	Stimulated vasculogenesis	[218]
6	HA-CMC	One-pot synthesis	Dexamethasone	Enhanced ALP expression and extracellular mineralization	[219]
7	HA-Dextran-Laponite	Sol-gel	BMP-2	BMP-2 release supported spreading, proliferation and osteogenic differentiation of rBMSCs	[220]
8	Gel-β(TCP)	Solvent casting	Zoledronic acid	Effective against metastatic bone cancer	[206]

(continued)

Table 1 (continued)

S. No.	Nanocomposites	Fabrication method	Drug	Outcome	Reference
9	SF/halloysite nanotubes	Ultrasonication	Vancomycin	Sustained release of vancomycin effectively inhibited bacterial infections	[85]

4.2 Synthetic Polymer/Ceramic-Based Nanocomposite Scaffolds

Synthetic polymers have gained more interest in BTE due to their strong biodegradability and biocompatibility. However, the problem with using these synthetic polymers is their inferiority in mechanical properties, bioactivity, and weak tissue adhesion, which does not result in good osseointegration. To prevent synthetic polymers' pitfalls, the use of a mixture of ceramics and biodegradable synthetic polymers has been reported [221, 222].

Among the existing biodegradable synthetic polymers, PCL polymer-based composites have received increasing importance than another synthetic polymer composite for BTE applications due to its low inflammatory response, elastic characteristics, and sustained biodegradability [223]. Various experiments have focused on the mechanical properties of the PCL/ceramic-based nanocomposite scaffolds as a bone graft substitute. PCL nanofibers containing BG NPs and simvastatin were formed by electrospinning. Incorporation of BG NPs in the nanofibers significantly improved tensile strength and induced bone-like apatite on their surfaces [224]. Nithya et al. fabricated the nanocomposite film (HAp-PCL) through the solvent evaporation method to deliver CIP, a widely used antibiotic agent for bone infections. The film had greater water uptake, extended drug release kinetics, and cytocompatibility against the osteoblast cell line (MG-63) and fibroblast cell line (NIH-3T3) [225]. PCL properties can be customized by crosslinking PCL with different amounts of radical initiators to exhibit a two-mode shape memory effect. Such a technique has been attempted by Liu et al., who have formulated a smart shape-memory porous scaffold (c-PCL/nHAp/BMP-2) to restore a mandibular defect rabbit model. In both conditions (in vitro and in vivo), the scaffold shows robust shape-memory retrieval from the compressed shape. The in vivo micro-CT and histomorphometry findings showed that the porous construct could facilitate neo-bone formation in the rabbit mandibular defect [226].

PLA is a well-known biodegradable polymer with multifunctional advantages, including manufacturing surgical devices and as an ideal scaffold in tissue engineering [227]. PLA/ceramic-based nanocomposites have been documented by Zhou et al., where they prepared the BSA containing amorphous CaP nanospheres/PLA

composite-coated tantalum scaffolds to treat subchondral bone defects in the rabbit model. They found the biomineralization of the scaffolds in their experimental findings [228]. Poly(hydroxybutyrate-co-hydroxyvalerate) (PHBV) is another useful synthetic polymer, which has been studied for the orthopedic drug delivery system [229]. The surface-functionalized CaP/PHBV nanocomposite scaffolds loaded with rhBMP-2 were synthesized to investigate the sustained release of growth factor. These scaffolds showed controlled growth factor delivery, and there were significantly increased ALP activity and the expression of osteogenic differentiation markers in mouse mesenchymal stem cells (C3H10T1/2) [230]. Almeida Neto et al. successfully developed the scaffolds containing PHBV/nanodiamond (nD)/nHAp-loaded with vancomycin. The formulated scaffolds exhibited sustained release of drug up to 22 days, antibacterial activity, and strong cell attachment capacity [231].

Other synthetic polymers such as PLLA, Poly(ester urethane) (PEUR), and polyglutamic acid also played a role in orthopedic drug delivery combined with ceramic materials. Wang et al. combined rhBMP-2 encapsulated CaP NPs with PLLA to build nanocomposite scaffolds. The dual delivery of Ca^{2+} and rhBMP-2 from the hierarchical porous scaffolds demonstrated superior efficacy in guiding the actions of human bone marrow-derived MSCs. They resulted in enhanced biocompatibility and osteogenic differentiation, suggesting their potential activity in BTE [232]. The bone fractures at weight-bearing sites (Tibial Plateau Slot Defects) in sheep were remedied using biphasic ceramic/nHAp-PEUR nanocomposites. The rate of remodeling of the cement was significantly faster, and there was new bone growth formation [233]. In another study, Shu et al. fabricated nano-doped CaP cement delivery systems (nanopoly(g-glutamic acid)/b-TCP-based CaP) loaded with two growth factors, BMP-2 and IGF-1. This hybrid delivery mechanism offered a controlled release of the two growth factors. The introduction of dual growth factors could enhance bone healing and foster bone ingrowth processes at a low-dose [234]. The details of some of the synthetic polymer/ceramic-based nanocomposites in bone fracture repair are listed in Table 2.

4.3 Natural/Synthetic Polymers/Ceramic-Based Nanocomposite Scaffolds

In the preceding parts, we focused on the individual combination of natural and synthetic polymers with ceramic materials to manufacture nanocomposite scaffolds in BTE applications. This section discusses the complex nanocomposite scaffolds constructed with all three forms of biomaterials to build bone and their related heterogeneous tissue structures to understand their effect on osteogenic development. Nazemi et al. fabricated a nanocomposite drug delivery system by incorporating CS/BG scaffolds with DEX-loaded PLGA NPs. The results revealed that the integration of NPs increased the mechanical strength of the scaffolds and achieved a controlled release drug delivery system [237]. Asadian et al. designed the novel

Table 2 Biodegradable synthetic polymer/ceramic-based nanocomposites for drug delivery in BTE applications

S. No.	Nanocomposites	Fabrication method	Drug	Outcome	Reference
1	PCL-HAp	Solvent evaporation	Ciprofloxacin	Effectively controlled bacterial infections	[225]
2	PCL-HAp	Press molding and sugar leaching	BMP-2	Controlled release of BMP-2 significantly promoted bone defect repair	[226]
3	PLGA-PCL-nHAP	–	BMP-2, bFGF	Combined release of BMP-2 and bFGF significantly improved the proliferation and osteogenic differentiation of BMSCs	[235]
4	PHBV-nHA, ND	Injection molding	Vancomycin	Sustained release of vancomycin inhibited the growth of <i>Staphylococcus aureus</i>	[231]
5	PTMC-PLA	Hot pressing method, UV curing	Dexamethasone	Effectively triggered the osteogenic differentiation of MSCs	[236]
6	PHBV-CaP	Selective laser sintering	rhBMP-2	Controlled rhBMP-2 release significantly enhanced the ALP activity and osteogenic differentiation of C3H10T1/2 cells	[230]
7	PLLA-CaP	Cryogenic 3D-printing technique	rhBMP-2	Dual release of Ca ²⁺ and rhBMP-2 improved the cell viability, attachment, proliferation, and osteogenic differentiation of hBMSCs	[232]

(continued)

Table 2 (continued)

S. No.	Nanocomposites	Fabrication method	Drug	Outcome	Reference
8	PCL-nBG	Electrospinning	Simvastatin	Controlled simvastatin release resulted in improved apatite layer formation and bone regeneration	[224]

functional CS-graft-poly(acrylic acid)/nHAp scaffolds loaded with naproxen sodium via the freeze-drying method. The reported scaffolds in the presence of nHAp had a significant effect on suppressing the drug's burst release, and their mechanical properties were found close to the density of trabecular bone [238]. Saber-Samandari et al. devised the bioactive chitosan-graft-poly(acrylic acid-coacrylamide)/HAp nanocomposite scaffolds through a novel multi-step route. The results suggested that the prepared scaffolds displayed a biphasic drug release design with a low primary burst and a sustained release up to 14 days [141]. Apart from scaffolds, the layer-by-layer (LBL) assembly film also has a significant impact in BTE, which provides a larger space for high drug loading efficiency and sustains drug release capacity, which helps significant bone recovery.

For example, the nanocomposite films made up of aspirin-loaded graphene oxide (GO)/CS/HAp were fabricated by the LBL assembly technology. The GO/CS/HAp nanocomposite films had good biocompatibility and could be the ideal platform for the growth of mMSCs [239]. In addition to the significance of nanocomposite films in BTE, cryogels also represent the highly interconnected porous microstructure and enhance the mechanical stability required in BTE scaffolds. Saini et al. prepared the antibacterial cryogels composed of nanosilver HAp-loaded Gel/Alg/PVA. The cryogels exhibited antibacterial and non-cytotoxic properties [58]. However, most nanocomposite scaffolds have not been able to accomplish a dual or multiple drug delivery systems for the loading and continuous release of various types of drugs to achieve the foster bone healing process. To overcome this predicament, the microsphere-incorporated scaffold system was proposed. The microsphere-incorporated scaffold system has a fascinating approach as it can provide site-specific drug delivery and regulates drug releases with distinct release pattern. The drugs may be inserted into the microspheres and the scaffold matrix, respectively, in the microsphere-incorporated scaffold system. Hu et al. have attempted such a strategy. They united the advantages of the porous calcium Alg/HAp scaffolds and PLLA-based microspheres to produce the microsphere/scaffold composites for delivering hydrophilic BSA and hydrophobic ibuprofen (IBU). The hybrid composites demonstrated biocompatible nature. The increasing nHAp concentration or D-gluconic acid δ -lactone (GDL) concentration helped improve the compressive strength and Young's modulus of porous scaffolds [240]. Researchers developed a hybrid scaffold obtained

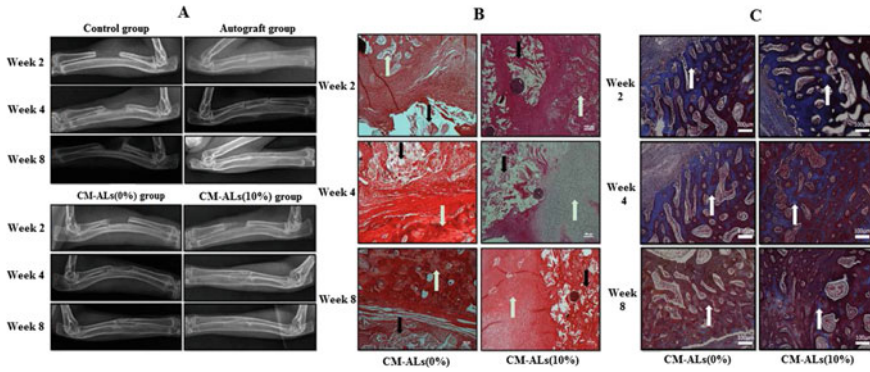


Fig. 3 PLLA/nHAp/CS nanocomposite scaffold-loaded with alendronate was implanted in vivo to treat large-sized bone defects in a rabbit model. **a** X-ray images, **b** HE staining, and **c** Masson staining showed enhanced bone healing and regeneration during 4–8 weeks. Reproduced with permission [241]. Wu et al. 2017, © Copyright 2017, Nature Publishing Groups

from PLLA/nHAp/Alendronate-loaded CS microspheres to repair large-sized bone defects in a similar study. The scaffold showed sustained alendronate release, biocompatible, high mechanical strength, calcium deposition, and ALP activity. Further, in vivo analysis, reported improved hybrid scaffolds' performance with the complete repair of large-sized bone defects within eight weeks in large segmental radius defects of a rabbit model (Fig. 3) [241].

Electrospun-based nanofibrous scaffolds constitute an incredibly attractive subgroup of biomaterials due to special intrinsic features such as high surface-to-volume ratio, which facilitate fundamental cellular roles such as adhesion, proliferation, and differentiation (Fig. 4) [242]. The SF/CaP/PLGA nanocomposite fibrous scaffolds were fabricated by the freeze-drying and electrospinning techniques in one such study. Different kinds of growth factors, namely PDGF and VEGF, were loaded onto scaffolds, and their potential for healing and vascularization were investigated in critical-sized rabbit bone defects in vivo. PDGF and VEGF released from the scaffolds had good bioactivity, facilitating osteoblast attachment, proliferation, and ALP production. Histological analysis revealed the development of a new bone matrix with neovascularization in the angiogenic factors-laden scaffolds after ten weeks of implantation in the rabbit model [243]. In another study, the DEX-loaded mesoporous BG NPs reinforced PCL/Gel osteoinductive fibrous scaffolds were designed to evaluate the long-term therapeutic efficacy in the rat calvarial defect model. Based on in vivo observations, the release of DEX from nanocomposite fibrous scaffolds has been shown to promote bone-forming processes regarding the neo-bone structure's quantity and quality [244].

To facilitate bone regeneration at the deformed site, researchers integrated trace elements into ceramic NPs, which are further strengthened in nanofibers to replicate the natural bone ECM. Kuttappan et al. fabricated nanofibrous scaffolds (silica-coated nHAp/Gel reinforced with electrospun PLLA yarns), encapsulated with FGF2 and

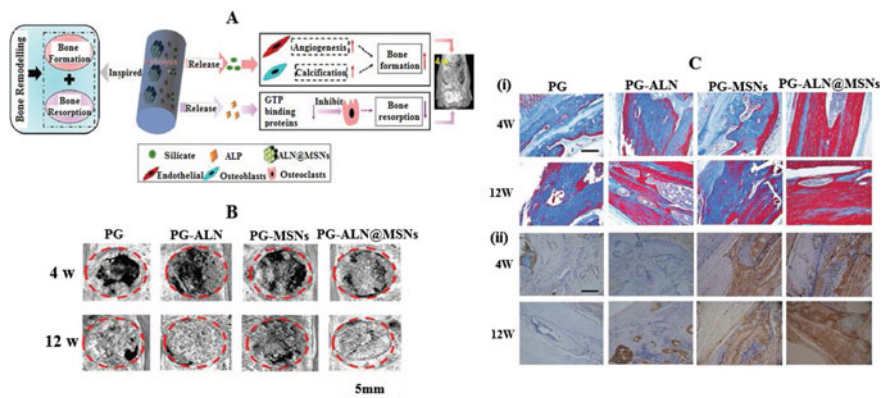


Fig. 4 **a** Schematic representation indicates the dual release of ALN and silicate from the PCL-Gel-Alendronate-Mesoporous silica (PG-ALN@MSN) nanofibers to heighten bone remodeling. **b** From the representative micro-CT images, it was observed that PG-ALN@MSN aids in enhanced bone formation in the 4th week by almost covering 95% of the deformed sites. It became much denser by covering the entire defective sites at the end of the 12th week. **c** Masson staining images of the skull showed a significant increase in new bone regeneration observed at the end of the 12th week in the PG-ALN@MSN complex compared to other reported groups. The images of CD31 immunohistochemistry indicated vascular networks' development during bone remodeling via silicate release from the MSN. Reproduced with permission [242] © Copyright 2018, The Royal Society of Chemistry

BMP2. The scaffold facilitated the delivery of growth factors, improved endothelial and MSCs migration, and proliferation, resulting in angiogenesis and osteogenesis in critical-sized calvarial defects [245]. The therapeutic effectiveness of vancomycin-laden nanocomposite fibrous scaffolds (silica-coated nHAp/Gel reinforced with PLLA yarns) for treating methicillin-resistant *Staphylococcus aureus* (MRSA)-made osteomyelitis in rat femur model was carried out. The scaffolds effectively delivered vancomycin in a sustained mode, which confirmed bactericidal activity against MRSA for 30 days. The implantation of scaffolds into the osteomyelitis rat femur model resulted in substantial bacterial reduction and increased neo-osteogenesis within three months [246]. The descriptions of some nanocomposites-based natural/synthetic polymers/ceramics in BTE are shown in Table 3. Various vital parameters in nanocomposite-based drug delivery are stated in Fig. 5.

5 Conclusions

Effective bone rejuvenation entails a synchronized relationship between therapeutic molecules, cells, and biomaterials. Suitable bone implants should firmly balance the new bone development and resorption across various situations caused by gender,

Table 3 Biodegradable hybrid polymers-based nanocomposites for drug delivery in BTE applications

S. No.	Nanocomposites	Fabrication method	Drug	Outcome	Reference
1	PLLA-nHAp- CS	Particulate leaching method	Alendronate	Sustained release of alendronate resulted in enhanced ALP expression, calcium deposition and osteogenic differentiation of ASCs	[241]
2	SF-CaP-PLGA	Freeze-drying and electrospinning	PDGF, VEGF	Simultaneous release of PDGF, VEGF improved proliferation, ALP production	[243]
3	SF-CaP-PLGA	Freeze-drying and electrospinning	VEGF	Controlled release of VEGF for prolonged time improved angiogenesis, growth and proliferation of osteoblast cells	[247]
4	PCL-Gel-mesoporous nBG	Electrospinning	Dexamethasone	Sustained release of Dexamethasone stimulated the osteogenic differentiation of periodontal stem cells in vitro and in vivo bone regeneration in rat calvarial model	[244]
5	CS-graft- (AA-co-AAm)-nHAp	Freeze-drying	Celecoxib	Model drug anti-inflammatory	[141]
6	Silica-coated nHAp-Gel-PLLA	Aqueous precipitation, electrospinning	Vancomycin	Vancomycin release potentially reduced methicillin-resistant <i>Staphylococcus aureus</i> infection	[246]
7	GO/CS-HAp	Layer-by-layer assembly technology	Aspirin	Sustained release of aspirin reduced the inflammation and facilitated bone formation	[239]
8	PLLA-Gel-nHAp-	Electrospinning	Dexamethasone	Enhanced osteogenesis	[248]

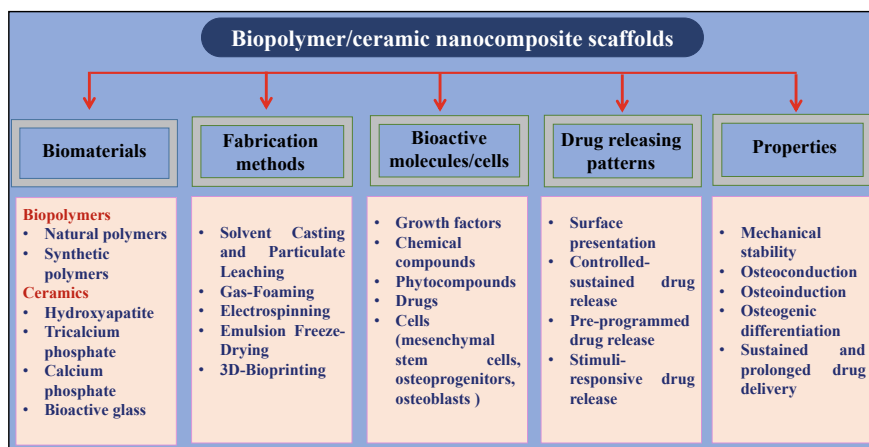


Fig. 5 Biopolymer/ceramic-based nanocomposite scaffolds in BTE applications. Various vital components such as biomaterials, fabrication techniques, bioactive molecules and cells, drug release patterns, and the biopolymer/ceramic-based nanocomposites' properties are illustrated

patient's age, and specific loads at the implantation site. Recent advanced techniques permit great flexibility and more accurate control in the creation of scaffolds. Based on biopolymer/ceramics, nanocomposite scaffolds become an evolving smart approach to balance individual biomaterials' pitfalls and provide effective bone regeneration with sustained/prolonged drug delivery. With a better understanding of biomaterials, bone ECM and cell communication, nanocomposite scaffolds will indisputably become a prevailing tool for the clinical bone defects treatment in the future.

Acknowledgements This study was supported by a fellowship awarded to K.L. (DST/INSPIRE Fellowship/2018/IF180184).

References

1. Agarwal R, García AJ (2015) Biomaterial strategies for engineering implants for enhanced osseointegration and bone repair. *Adv Drug Deliv Rev* 94:53–62
2. Bai X, Gao M, Syed S, Zhuang J, Xu X, Zhang XQ (2018) Bioactive hydrogels for bone regeneration. *Bioact Mater* 3(4):401–417
3. Gong T, Xie J, Liao J, Zhang T, Lin S, Lin Y (2015) Nanomaterials and bone regeneration. *Bone Res* 3:15029
4. Boskey AL, Coleman R (2010) Aging and bone. *J Dent Res* 89(12):1333–1348
5. Clarke B (2008) Normal bone anatomy and physiology. *Clin J Am Soc Nephrol* 3(Supplement 3):S131–S139
6. Chen JH, Liu C, You L, Simmons CA (2010) Boning up on Wolff's Law: mechanical regulation of the cells that make and maintain bone. *J Biomech* 43(1):108–118

7. Bueno EM, Glowacki J (2009) Cell-free and cell-based approaches for bone regeneration. *Nat Rev Rheumatol* 5(12):685
8. Han Y, You X, Xing W, Zhang Z, Zou W (2018) Paracrine and endocrine actions of bone—the functions of secretory proteins from osteoblasts, osteocytes, and osteoclasts. *Bone Res* 6(1):1
9. Mackie EJ (2003) Osteoblasts: novel roles in orchestration of skeletal architecture. *Int J Biochem Cell Biol* 35(9):1301–1305
10. Moreira CA, Dempster DW, Baron R (2019) Anatomy and ultrastructure of bone—histogenesis, growth and remodeling. In *Endotext* [Internet]. MDText. com, Inc
11. Blair HC, Larroure QC, Li Y, Lin H, Beer-Stoltz D, Liu L, Tuan RS, Robinson LJ, Schlesinger PH, Nelson DJ (2017) Osteoblast differentiation and bone matrix formation in vivo and in vitro. *Tissue Eng Part B Rev* 23(3):268–280
12. Su N, Yang J, Xie Y, Du X, Chen H, Zhou H, Chen L (2019) Bone function, dysfunction and its role in diseases including critical illness. *Int J Biol Sci* 15(4):776
13. Schaffler MB, Kennedy OD (2012) Osteocyte signaling in bone. *Curr Osteoporos Rep* 10(2):118–125
14. Franz-Odenaal TA, Hall BK, Witten PE (2006) Buried alive: how osteoblasts become osteocytes. *Dev Dyn Publ Am Assoc Anatomists* 235(1):176–190
15. Kylmaja E, Nakamura M, Tuukkanen J (2016) Osteoclasts and remodeling based bone formation. *Curr Stem Cell Res Ther* 11(8):626–633
16. Teti A (2012) Osteoclasts and hematopoiesis. *BoneKEY reports*. 1
17. Zhao H (2012) Membrane trafficking in osteoblasts and osteoclasts: new avenues for understanding and treating skeletal diseases. *Traffic* 13(10):1307–1314
18. Wang L, Liu S, Zhao Y, Liu D, Liu Y, Chen C, Karray S, Shi S, Jin Y (2015) Osteoblast-induced osteoclast apoptosis by fas ligand/FAS pathway is required for maintenance of bone mass. *Cell Death Differ* 22(10):1654–1664
19. Smith LD, Masood M, Bajaj GS, Couser NL (2018) Genetic abnormalities of the anterior segment, eyelids, and external ocular adnexa. *Ophthalmic Genet Dis* 22:15
20. Smolen JS, Aletaha D, Bijlsma JW, Breedveld FC, Boumpas D, Burmester G, Combe B, Cutolo M, De Wit M, Dougados M, Emery P (2010) Treating rheumatoid arthritis to target: recommendations of an international task force. *Ann Rheum Dis* 69(4):631–637
21. Momodu II, Savaliya V (2019) Osteomyelitis. In *StatPearls* [Internet]. StatPearls Publishing
22. Rajani R, Gibbs CP (2012) Treatment of bone tumors. *Surg Pathol Clin* 5(1):301–318
23. Na K, Park YK (2020) Multiple osteochondromatosis. In: *Tumors and tumor-like lesions of bone*. Springer, Cham, pp 283–292
24. Busch A, Wegner A, Haversath M, Jäger M (2020) Bone substitutes in orthopedic surgery: current status and future perspectives. *Zeitschrift für Orthopädie und Unfallchirurgie*
25. Offner D, de Grado GF, Meisels I, Pijnenburg L, Fioretti F, Benkirane-Jessel N, Musset AM (2019) Bone grafts, bone substitutes and regenerative medicine acceptance for the management of bone defects among French population: issues about ethics, religion or fear? *Cell Med* 11:2155179019857661
26. Koons GL, Diba M, Mikos AG (2020) Materials design for bone-tissue engineering. *Nat Rev Mater* 1–20
27. Amini AR, Laurencin CT, Nukavarapu SP (2012) Bone tissue engineering: recent advances and challenges. *Crit Rev Biomed Eng*. 40(5)
28. Zhu L, Luo D, Liu Y (2020) Effect of the nano/microscale structure of biomaterial scaffolds on bone regeneration. *Int J Oral Sci* 12(1):1–5
29. Pina S, Ribeiro VP, Marques CF, Maia FR, Silva TH, Reis RL, Oliveira JM (2019) Scaffolding strategies for tissue engineering and regenerative medicine applications. *Materials* 12(11):1824
30. Nikolova MP, Chavali MS (2019) Recent advances in biomaterials for 3D scaffolds: a review. *Bioact Mater* 1(4):271–292
31. Hill MJ, Qi B, Bayaniahangar R, Araban V, Bakhtiary Z, Doschak MR, Goh BC, Shokouhimehr M, Vali H, Presley JF, Zadpoor AA (2019) Nanomaterials for bone tissue regeneration: updates and future perspectives. *Nanomedicine* 14(22):2987–3006

32. Li Y, Liu C (2017) Nanomaterial-based bone regeneration. *Nanoscale* 9(15):4862–4874
33. Wang Q, Yan J, Yang J, Li B (2016) Nanomaterials promise better bone repair. *Mater Today* 19(8):451–463
34. Lee JH, Kim HW, Seo SJ (2016) Polymer-ceramic bionanocomposites for dental application. *J Nanomaterials*. 2016
35. Bramhill J, Ross S, Ross G (2017) Bioactive nanocomposites for tissue repair and regeneration: a review. *Int J Environ Res Public Health* 14(1):66
36. Devescovi V, Leonardi E, Ciapetti G, Cenni E (2008) Growth factors in bone repair. *La Chirurgia Degli Organi di Movimento* 92(3):161–168
37. Ekensear AK, Kasper FK, Mikos AG (2013) Perspectives on the interface of drug delivery and tissue engineering. *Adv Drug Deliv Rev* 65(1):89–92
38. Kim YH, Tabata Y (2015) Dual-controlled release system of drugs for bone regeneration. *Adv Drug Deliv Rev* 1(94):28–40
39. Chen FM, Zhang M, Wu ZF (2010) Toward delivery of multiple growth factors in tissue engineering. *Biomaterials* 31(24):6279–6308
40. Tessmar JK, Göpferich AM (2007) Matrices and scaffolds for protein delivery in tissue engineering. *Adv Drug Deliv Rev* 59(4–5):274–291
41. Samorezov JE, Alsborg E (2015) Spatial regulation of controlled bioactive factor delivery for bone tissue engineering. *Adv Drug Deliv Rev* 84:45–67
42. Ye K, Liu D, Kuang H, Cai J, Chen W, Sun B, Xia L, Fang B, Morsi Y, Mo X (2019) Three-dimensional electrospun nanofibrous scaffolds displaying bone morphogenetic protein-2-derived peptides for the promotion of osteogenic differentiation of stem cells and bone regeneration. *J Colloid Interface Sci* 534:625–636
43. Chen L, Shi Y, Zhang X, Hu X, Shao Z, Dai L, Ju X, Ao Y, Wang J (2019) CaAlg hydrogel containing bone morphogenetic protein 4-enhanced adipose-derived stem cells combined with osteochondral mosaicplasty facilitated the repair of large osteochondral defects. *Knee Surg Sports Traumatol Arthrosc* 27(11):3668–3678
44. Sun J, Lyu J, Xing F, Chen R, Duan X, Xiang Z (2020) A biphasic, demineralized, and Decellularized allograft bone-hydrogel scaffold with a cell-based BMP-7 delivery system for osteochondral defect regeneration. *J Biomed Mater Res Part A*
45. Yoon JP, Lee CH, Jung JW, Lee HJ, Lee YS, Kim JY, Park GY, Choi JH, Chung SW (2018) Sustained delivery of transforming growth factor β 1 by use of absorbable alginate scaffold enhances rotator cuff healing in a rabbit model. *Am J Sports Med* 46(6):1441–1450
46. Deng M, Mei T, Hou T, Luo K, Luo F, Yang A, Yu B, Pang H, Dong S, Xu J (2017) TGF β 3 recruits endogenous mesenchymal stem cells to initiate bone regeneration. *Stem cell Res Ther* 8(1):1–2
47. Murahashi Y, Yano F, Nakamoto H, Maenohara Y, Iba K, Yamashita T, Tanaka S, Ishihara K, Okamura Y, Moro T, Saito T (2019) Multi-layered PLLA-nanosheets loaded with FGF-2 induce robust bone regeneration with controlled release in critical-sized mouse femoral defects. *Acta Biomater* 85:172–179
48. Casarrubios L, Gómez-Cerezo N, Sánchez-Salcedo S, Feito MJ, Serrano MC, Saiz-Pardo M, Ortega L, De Pablo D, Díaz-Güemes I, Fernández-Tomé B, Enciso S (2020) Silicon substituted hydroxyapatite/VEGF scaffolds stimulate bone regeneration in osteoporotic sheep. *Acta Biomater* 101:544–553
49. Lee J, Lee S, Ahmad T, Perikamana SK, Lee J, Kim EM, Shin H (2020) Human adipose-derived stem cell spheroids incorporating platelet-derived growth factor (PDGF) and bio-minerals for vascularized bone tissue engineering. *Biomaterials* 12:
50. Qi Z, Xia P, Pan S, Zheng S, Fu C, Chang Y, Ma Y, Wang J, Yang X (2018) Combined treatment with electrical stimulation and insulin-like growth factor-1 promotes bone regeneration in vitro. *PLoS ONE* 13(5):
51. Lauer A, Wolf P, Mehler D, Götz H, Rüzgar M, Baranowski A, Henrich D, Rommens PM, Ritz U (2020) Biofabrication of SDF-1 functionalized 3D-printed cell-free scaffolds for bone tissue regeneration. *Int J Mol Sci* 21(6):2175

52. Witt R, Weigand A, Boos AM, Cai A, Dippold D, Boccaccini AR, Schubert DW, Hardt M, Lange C, Arkudas A, Horch RE (2017) Mesenchymal stem cells and myoblast differentiation under HGF and IGF-1 stimulation for 3D skeletal muscle tissue engineering. *BMC Cell Biol* 18(1):1–6
53. Xie Z, Ye G, Wang P, Li J, Liu W, Li M, Wang S, Wu X, Cen S, Zheng G, Ma M (2018) Interleukin-6/interleukin-6 receptor complex promotes osteogenic differentiation of bone marrow-derived mesenchymal stem cells. *Stem Cell Res Ther* 9(1):1
54. Paidikondala M, Wang S, Yan H, Podiyam O, Hilborn J, Larsson S, Varghese OP rational design of biomaterials for growth factor delivery: impact of hydrogel crosslinking chemistry on the in vitro and in vivo bioactivity of recombinant human bone morphogenetic protein-2
55. Nyberg E, Holmes C, Witham T, Grayson WL (2016) Growth factor-eluting technologies for bone tissue engineering. *Drug Deliv Transl Res* 6(2):184–194
56. Suárez-González D, Lee JS, Diggs A, Lu Y, Nemke B, Markel M, Hollister SJ, Murphy WL (2014) Controlled multiple growth factor delivery from bone tissue engineering scaffolds via designed affinity. *Tissue Eng Part A* 20(15–16):2077–2087
57. Newman MR, Benoit DS (2016) Local and targeted drug delivery for bone regeneration. *Curr Opin Biotechnol* 40:125–132
58. Saini RK, Bagri LP, Bajpai AK (2019) Nano-silver hydroxyapatite based antibacterial 3D scaffolds of gelatin/alginate/poly (vinyl alcohol) for bone tissue engineering applications. *Colloids Surf B* 177:211–218
59. Nadar RA, Margiotta N, Iafisco M, van den Beucken JJ, Boerman OC, Leeuwenburgh SC (2017) Bisphosphonate-functionalized imaging agents, anti-tumor agents and nanocarriers for treatment of bone cancer. *Adv Healthc Mater* 6(8):1601119
60. Iafisco M, Palazzo B, Falini G, Di Foggia M, Bonora S, Nicolis S, Casella L, Roveri N (2008) Adsorption and conformational change of myoglobin on biomimetic hydroxyapatite nanocrystals functionalized with alendronate. *Langmuir* 24(9):4924–4930
61. Cui Y, Zhu T, Li D, Li Z, Leng Y, Ji X, Liu H, Wu D, Ding J (2019) Bisphosphonate-functionalized scaffolds for enhanced bone regeneration. *Adv Healthc Mater* 8(23):1901073
62. Hu X, Neoh KG, Shi Z, Kang ET, Wang W (2013) An in vitro assessment of fibroblast and osteoblast response to alendronate-modified titanium and the potential for decreasing fibrous encapsulation. *Tissue Eng Part A* 19(17–18):1919–1930
63. Hur W, Park M, Lee JY, Kim MH, Lee SH, Park CG, Kim SN, Min HS, Min HJ, Chai JH, Lee SJ (2016) Bioabsorbable bone plates enabled with local, sustained delivery of alendronate for bone regeneration. *J Controlled Release* 222:97–106
64. Cheng X, Zhu Z, Liu Y, Xue Y, Gao X, Wang J, Pei X, Wan Q (2020) Zeolitic imidazolate framework-8 encapsulating risedronate synergistically enhances osteogenic and anti-resorptive properties for bone regeneration. *ACS Biomaterials Sci Eng* 6(4):2186–2197
65. Guo J, Zhang Q, Li J, Liu Y, Hou Z, Chen W, Jin L, Tian Y, Ju L, Liu B, Dong T (2017) Local application of an ibandronate/collagen sponge improves femoral fracture healing in ovariectomized rats. *PLoS ONE* 12(11):
66. Mardas N, Busetti J, de Figueiredo JA, Mezzomo LA, Scarparo RK, Donos N (2017) Guided bone regeneration in osteoporotic conditions following treatment with zoledronic acid. *Clin Oral Implant Res* 28(3):362–371
67. Valenti MT, Mottes M, Biotti A, Perduca M, Pisani A, Bovi M, Deiana M, Cheri S, Dalle Carbonare L (2017) Clodronate as a therapeutic strategy against osteoarthritis. *Int J Mol Sci* 18(12):2696
68. Rangabhatla AS, Tantishaiyakul V, Oungbho K, Boonrat O (2016) Fabrication of pluronic and methylcellulose for etidronate delivery and their application for osteogenesis. *Int J Pharm* 499(1–2):110–118
69. Abass BT, Shekho HA (2009) Effects of tiludronate on healing of femoral fracture in dogs. *Iraqi J Vet Sci* 2:23
70. Ellegaard M, Jørgensen NR, Schwarz P (2010) Parathyroid hormone and bone healing. *Calcif Tissue Int* 87(1):1–3

71. Kim SJ, Park HS, Lee DW, Lee JW (2019) Short-term daily teriparatide improve postoperative functional outcome and fracture healing in unstable intertrochanteric fractures. *Injury* 50(7):1364–1370
72. Bernhardtsson M, Aspenberg P (2018) Abaloparatide versus teriparatide: a head to head comparison of effects on fracture healing in mouse models. *Acta Orthopædica* 89(6):674–677
73. Bhandari M, Schemitsch EH, Karachalios T, Sancheti P, Poolman RW, Caminis J, Daizadeh N, Dent-Acosta RE, Egbuna O, Chines A, Miclau T (2020) Romosozumab in skeletally mature adults with a fresh unilateral tibial diaphyseal fracture: a randomized phase-2 study. *JBJS*
74. Deeks ED (2018) Denosumab: a review in postmenopausal osteoporosis. *Drugs Aging* 35(2):163–173
75. Laurencin CT, Ashe KM, Henry N, Kan HM, Lo KW (2014) Delivery of small molecules for bone regenerative engineering: preclinical studies and potential clinical applications. *Drug Discov Today* 19(6):794–800
76. Izzah Ibrahim N, Mohamed N, Nazrun Shuid A (2013) Update on statins: hope for osteoporotic fracture healing treatment. *Curr Drug Targets* 14(13):1524–1532
77. Yu WL, Sun TW, Qi C, Zhao HK, Ding ZY, Zhang ZW, Sun BB, Shen J, Chen F, Zhu YJ, Chen DY (2017) Enhanced osteogenesis and angiogenesis by mesoporous hydroxyapatite microspheres-derived simvastatin sustained release system for superior bone regeneration. *Sci Rep* 7:44129
78. Kim BB, Tae JY, Ko Y, Park JB (2019) Lovastatin increases the proliferation and osteoblastic differentiation of human gingiva derived stem cells in three dimensional cultures. *Exp Ther Med* 18(5):3425–3430
79. Rezazadeh M, Parandeh M, Akbari V, Ebrahimi Z, Taheri A (2019) Incorporation of rosuvastatin-loaded chitosan/chondroitin sulfate nanoparticles into a thermosensitive hydrogel for bone tissue engineering: preparation, characterization, and cellular behavior. *Pharm Dev Technol* 24(3):357–367
80. Leppäranta O, Tikkanen JM, Bespalov MM, Koli K, Myllärniemi M (2013) Bone morphogenetic protein-inducer tilorone identified by high-throughput screening is antifibrotic in vivo. *Am J Respir Cell Mol Biol* 48(4):448–455
81. Li X, Wang Y, Wang Z, Qi Y, Li L, Zhang P, Chen X, Huang Y (2018) Composite PLA/PEG/nHA/dexamethasone scaffold prepared by 3D printing for bone regeneration. *Macromol Biosci* 18(6):1800068
82. Liu L, Zhao F, Chen X, Luo M, Yang Z, Cao X, Miao G, Chen D (2020) Local delivery of FTY720 in mesoporous bioactive glass improves bone regeneration by synergistically immunomodulating osteogenesis and osteoclastogenesis. *J Mater Chem B* 8(28):6148–6158
83. Gellynck K, Shah R, Parkar M, Young A, Buxton P, Brett P (2013) Small molecule stimulation enhances bone regeneration but not titanium implant osseointegration. *Bone* 57(2):405–412
84. Farzamfar S, Naseri-Nosar M, Sahraeyma H, Ehterami A, Goodarzi A, Rahmati M, Ahmadi Lakalayeh G, Ghorbani S, Vaez A, Salehi M (2019) Tetracycline hydrochloride-containing poly (ϵ -caprolactone)/poly lactic acid scaffold for bone tissue engineering application: in vitro and in vivo study. *Int J Polym Mater Polym Biomater* 68(8):472–479
85. Avani F, Damoogh S, Mottaghtalab F, Karkhaneh A, Farokhi M (2019) Vancomycin loaded halloysite nanotubes embedded in silk fibroin hydrogel applicable for bone tissue engineering. *Int J Polym Mater Polym Biomater*
86. Semyari H, Salehi M, Taleghani F, Ehterami A, Bastami F, Jalayer T, Semyari H, Hamed Nabavi M, Semyari H (2018) Fabrication and characterization of collagen–hydroxyapatite-based composite scaffolds containing doxycycline via freeze-casting method for bone tissue engineering. *J Biomater Appl* 33(4):501–513
87. Praphakar RA, Sumathra M, Ebenezer RS, Vignesh S, Shakila H, Rajan M (2019) Fabrication of bioactive rifampicin loaded κ -Car-MA-INH/Nano hydroxyapatite composite for tuberculosis osteomyelitis infected tissue regeneration. *Int J Pharm* 565:543–556
88. Stevanović M, Djošić M, Janković A, Kojić V, Vukašinović-Sekulić M, Stojanović J, Odović J, Sakač MC, Rhee KY, Mišković-Stanković V (2020) Antibacterial graphene-based hydroxyapatite/chitosan coating with gentamicin for potential applications in bone tissue engineering. *J Biomed Mater Res Part A*

89. Pahlevanzadeh F, Bakhsheshi-Rad HR, Kasiri-Asgarani M, Emadi R, Omidi M, Ismail AF, Afrand M, Berto F (2020) Mechanical property, antibacterial activity and cytocompatibility of a PMMA-based bone cement loaded with clindamycin for orthopedic surgeries. *Mater Technol* 26:1
90. Qiao Z, Yuan Z, Zhang W, Wei D, Hu N (2019) Preparation, in vitro release and antibacterial activity evaluation of rifampicin and moxifloxacin-loaded poly (D, L-lactide-co-glycolide) microspheres. *Artif Cells Nanomed Biotechnol* 47(1):790–798
91. Ribeiro M, Ferraz MP, Monteiro FJ, Fernandes MH, Beppu MM, Mantione D, Sardon H (2017) Antibacterial silk fibroin/nanohydroxyapatite hydrogels with silver and gold nanoparticles for bone regeneration. *Nanomed Nanotechnol Biol Med* 13(1):231–239
92. Felice B, Sánchez MA, Socci MC, Sappia LD, Gómez MI, Cruz MK, Felice CJ, Martí M, Pividori MI, Simonelli G, Rodríguez AP (2018) Controlled degradability of PCL-ZnO nanofibrous scaffolds for bone tissue engineering and their antibacterial activity. *Mater Sci Eng C* 93:724–738
93. Jaidev LR, Kumar S, Chatterjee K (2017) Multi-biofunctional polymer graphene composite for bone tissue regeneration that elutes copper ions to impart angiogenic, osteogenic and bactericidal properties. *Colloids Surf B* 159:293–302
94. Liu W, Su P, Chen S, Wang N, Wang J, Liu Y, Ma Y, Li H, Zhang Z, Webster TJ (2015) Antibacterial and osteogenic stem cell differentiation properties of photoinduced TiO₂ nanoparticle-decorated TiO₂ nanotubes. *Nanomedicine* 10(5):713–723
95. Coelho CC, Araújo R, Quadros PA, Sousa SR, Monteiro FJ (2019) Antibacterial bone substitute of hydroxyapatite and magnesium oxide to prevent dental and orthopedic infections. *Mater Sci Eng C* 97:529–538
96. Wei P, Jing W, Yuan Z, Huang Y, Guan B, Zhang W, Zhang X, Mao J, Cai Q, Chen D, Yang X (2019) Vancomycin- and strontium-loaded microspheres with multifunctional activities against bacteria, in angiogenesis, and in osteogenesis for enhancing infected bone regeneration. *ACS Appl Mater Interfaces* 11(34):30596–30609
97. Li Y, Bai Y, Pan J, Wang H, Li H, Xu X, Fu X, Shi R, Luo Z, Li Y, Li Q (2019) A hybrid 3D-printed aspirin-laden liposome composite scaffold for bone tissue engineering. *J Mater Chem B* 7(4):619–629
98. Kumar P, Dehiya BS, Sindhu A (2019) Ibuprofen-loaded CTS/nHA/nBG scaffolds for the applications of hard tissue engineering. *Iran Biomed J* 23(3):190
99. Karimi S, Ghaee A, Barzin J (2019) Preparation and characterization of a piezoelectric poly (vinylidene fluoride)/nanohydroxyapatite scaffold capable of naproxen delivery. *Eur Polymer J* 112:442–451
100. Yar M, Farooq A, Shahzadi L, Khan AS, Mahmood N, Rauf A, Chaudhry AA, ur Rehman I (2016) Novel meloxicam releasing electrospun polymer/ceramic reinforced biodegradable membranes for periodontal regeneration applications. *Mater Sci Eng* 64:148–156
101. Kordjamshidi A, Saber-Samandari S, Nejad MG, Khandan A (2019) Preparation of novel porous calcium silicate scaffold loaded by celecoxib drug using freeze drying technique: fabrication, characterization and simulation. *Ceram Int* 45(11):14126–14135
102. Mihai IB, Marin MM, Ghica MV, Albu-Kaya M, Dincă LC, Drăgușin D, Dinu-Pîrvu CE (2016) Collagen-indomethacin-hydroxyapatite spongy forms for bone reconstruction treatment. In: International conference on advanced materials and systems (ICAMS), pp 293–298. The National Research and Development Institute for Textiles and Leather-INCOTEX
103. Lin HY, Chang TW, Peng TK (2018) Three-dimensional plotted alginate fibers embedded with diclofenac and bone cells coated with chitosan for bone regeneration during inflammation. *J Biomed Mater Res Part A* 106(6):1511–1521
104. Cheng W, Yue Y, Fan W, Hu Y, Wang X, Pan X, Zhou X, Qin L, Zhang P (2012) Effects of tetracyclines on bones: an ambiguous question needs to be clarified. *Die Pharmazie-An Int J Pharm Sci* 67(5):457–459
105. Raghavan RN, Vignesh G, Kumar BS, Selvaraj R, Dare BJ (2015) Phytochemicals: do they hold the future in stem cell differentiation. *Int J Res Pharma* 6(3):379–381

106. Joseph J, Sundar R, John A, Abraham A (2018) Phytochemical incorporated drug delivery scaffolds for tissue regeneration. *Regenerative Eng Transl Med* 4(3):167–176
107. Roy M, Datta A (2019) Fundamentals of phytochemicals. In: *Cancer genetics and therapeutics*. Springer, Singapore, pp 49–81
108. Xue W, Yu J, Chen W (2018) Plants and their bioactive constituents in mesenchymal stem cell-based periodontal regeneration: a novel prospective. *BioMed Res Int* 2018
109. Xie Y, Sun W, Yan F, Liu H, Deng Z, Cai L (2019) Icaritin-loaded porous scaffolds for bone regeneration through the regulation of the coupling process of osteogenesis and osteoclastic activity. *Int J Nanomed* 14:6019
110. Fernandes CJ, Veiga MR, Peracoli MT, Zambuzzi WF (2019) Modulatory effects of silibinin in cell behavior during osteogenic phenotype. *J Cell Biochem* 120(8):13413–13425
111. Choi Y, Yoon DS, Lee KM, Choi SM, Lee MH, Park KH, Han SH, Lee JW (2019) Enhancement of mesenchymal stem cell-driven bone regeneration by resveratrol-mediated SOX2 regulation. *Aging Dis* 10(4):818
112. Song JE, Tian J, Kook YJ, Thangavelu M, Choi JH, Khang G (2020) A BMSCs-laden quercetin/duck's feet collagen/hydroxyapatite sponge for enhanced bone regeneration. *J Biomed Mater Res Part A* 108(3):784–794
113. Thaler R, Maurizi A, Roschger P, Sturmlechner I, Khani F, Spitzer S, Rumpler M, Zwerina J, Karlic H, Dudakovic A, Klaushofer K (2016) Anabolic and antiresorptive modulation of bone homeostasis by the epigenetic modulator sulforaphane, a naturally occurring isothiocyanate. *J Biol Chem* 291(13):6754–6771
114. Kim M, Lim J, Lee JH, Lee KM, Kim S, Park KW, Nho CW, Cho YS (2018) Understanding the functional role of genistein in the bone differentiation in mouse osteoblastic cell line MC3T3-E1 by RNA-seq analysis. *Sci Rep* 8(1):1–2
115. Balagangadharan K, Trivedi R, Vairamani M, Selvamurugan N (2019) Sinapic acid-loaded chitosan nanoparticles in polycaprolactone electrospun fibers for bone regeneration in vitro and in vivo. *Carbohydr Polym* 216:1–6
116. Srinaath N, Balagangadharan K, Pooja V, Paarkavi U, Trishla A, Selvamurugan N (2019) Osteogenic potential of zingerone, a phenolic compound in mouse mesenchymal stem cells. *BioFactors* 45(4):575–582
117. Menon AH, Soundarya SP, Sanjay V, Chandran SV, Balagangadharan K, Selvamurugan N (2018) Sustained release of chrysin from chitosan-based scaffolds promotes mesenchymal stem cell proliferation and osteoblast differentiation. *Carbohydr Polym* 195:356–367
118. Chandran SV, Vairamani M, Selvamurugan N (2019) Osteostimulatory effect of biocomposite scaffold containing phytochemical diosmin by Integrin/FAK/ERK signaling pathway in mouse mesenchymal stem cells. *Sci Rep* 9(1):1–3
119. Sruthi R, Balagangadharan K, Selvamurugan N (2020) Polycaprolactone/polyvinylpyrrolidone coaxial electrospun fibers containing veratric acid-loaded chitosan nanoparticles for bone regeneration. *Colloids Surf B* 193:
120. Akshaya N, Prasith P, Abinaya B, Ashwin B, Chandran SV, Selvamurugan N (2020) Valproic acid, a potential inducer of osteogenesis in mouse mesenchymal stem cells. *Curr Mol Pharmacol*
121. Ashwin B, Abinaya B, Prasith TP, Chandran SV, Yadav LR, Vairamani M, Patil S, Selvamurugan N (2020) 3D-poly (lactic acid) scaffolds coated with gelatin and mucic acid for bone tissue engineering. *Int J Biol Macromol*
122. Dadashpour M, Pilehvar-Soltanahmadi Y, Zarghami N, Firouzi-Amandi A, Pourhassan-Moghaddam M, Nouri M (2017) Emerging importance of phytochemicals in regulation of stem cells fate via signaling pathways. *Phytotherapy Res* 31(11):1651–1668
123. Mouriño V, Boccaccini AR (2010) Bone tissue engineering therapeutics: controlled drug delivery in three-dimensional scaffolds. *J R Soc Interface* 7(43):209–227
124. Bagherifard S (2017) Mediating bone regeneration by means of drug eluting implants: from passive to smart strategies. *Mater Sci Eng C* 71:1241–1252
125. Santos A, Aw MS, Bariana M, Kumeria T, Wang Y, Losic D (2014) Drug-releasing implants: current progress, challenges and perspectives. *J Mater Chem B* 2(37):6157–6182

126. Sun W, Ge K, Jin Y, Han Y, Zhang H, Zhou G, Yang X, Liu D, Liu H, Liang XJ, Zhang J (2019) Bone-targeted nanoplatform combining zoledronate and photothermal therapy to treat breast cancer bone metastasis. *ACS Nano* 13(7):7556–7567
127. Toussaint ND, Elder GJ, Kerr PG (2009) Bisphosphonates in chronic kidney disease; balancing potential benefits and adverse effects on bone and soft tissue. *Clin J Am Soc Nephrol* 4(1):221–233
128. Aguilar LM, Silva SM, Moulton SE (2019) Growth factor delivery: defining the next generation platforms for tissue engineering. *J Controlled Release* 306:40–58
129. Cottrell JA, Vales FM, Schachter D, Wadsworth S, Gundlapalli R, Kapadia R, O'Connor JP (2010) Osteogenic activity of locally applied small molecule drugs in a rat femur defect model. *J Biomed Biotechnol.* 2010
130. Ferracini R, Martínez Herreros I, Russo A, Casalini T, Rossi F, Perale G (2018) Scaffolds as structural tools for bone-targeted drug delivery. *Pharmaceutics* 10(3):122
131. Dorati R, DeTrizio A, Modena T, Conti B, Benazzo F, Gastaldi G, Genta I (2017) Biodegradable scaffolds for bone regeneration combined with drug-delivery systems in osteomyelitis therapy. *Pharmaceutics* 10(4):96
132. Chen S, Shi Y, Luo Y, Ma J (2019) Layer-by-layer coated porous 3D printed hydroxyapatite composite scaffolds for controlled drug delivery. *Colloids Surf B* 179:121–127
133. Eltom A, Zhong G, Muhammad A (2019) Scaffold techniques and designs in tissue engineering functions and purposes: a review. *Adv Mater Sci Eng* 2019
134. Garg T, Singh O, Arora S, Murthy RS (2012) Scaffold: a novel carrier for cell and drug delivery. *Crit Rev Ther Drug Carrier Syst* 29(1)
135. Sharma B, Varghese S Progress in orthopedic biomaterials and drug delivery
136. Costa PF (2015) Bone tissue engineering drug delivery. *Curr Mol Biol Rep* 1(2):87–93
137. Sofi HS, Ashraf R, Khan AH, Beigh MA, Majeed S, Sheikh FA (2019) Reconstructing nanofibers from natural polymers using surface functionalization approaches for applications in tissue engineering, drug delivery and biosensing devices. *Mater Sci Eng C* 94:1102–1124
138. Jayaraman P, Gandhimathi C, Venugopal JR, Becker DL, Ramakrishna S, Srinivasan DK (2015) Controlled release of drugs in electrosprayed nanoparticles for bone tissue engineering. *Adv Drug Deliv Rev* 94:77–95
139. Liu X, Zhang W, Wang Y, Chen Y, Xie J, Su J, Huang C (2020) One-step treatment of periodontitis based on a core-shell micelle-in-nanofiber membrane with time-programmed drug release. *J Controlled Release* 320:201–213
140. Sood N, Bhardwaj A, Mehta S, Mehta A (2016) Stimuli-responsive hydrogels in drug delivery and tissue engineering. *Drug Delivery* 23(3):748–770
141. Saber-Samandari S, Saber-Samandari S (2017) Biocompatible nanocomposite scaffolds based on copolymer-grafted chitosan for bone tissue engineering with drug delivery capability. *Mater Sci Eng C* 75:721–732
142. Sahoo NG, Pan YZ, Li L, He CB (2013) Nanocomposites for bone tissue regeneration. *Nanomedicine* 8(4):639–653
143. Shen S, Dong YC, Ng WK, Chia L, Tan RB (2010) Nanocomposites for drug delivery. In: *Nanotechnologies for the life sciences*
144. Hasnain MS, Ahmad SA, Chaudhary N, Hoda MN, Nayak AK (2019) Biodegradable polymer matrix nanocomposites for bone tissue engineering. In: *Applications of nanocomposite materials in orthopedics*. Woodhead Publishing, pp 1–37
145. Chen J, Ashames A, Buabeid MA, Faehelebom KM, Ijaz M, Murtaza G (2020) Nanocomposites drug delivery systems for the healing of bone fractures. *Int J Pharm* 585:
146. Armentano I, Puglia D, Luzi F, Arciola CR, Morena F, Martino S, Torre L (2018) Nanocomposites based on biodegradable polymers. *Materials* 11(5):795
147. Pina S, Oliveira JM, Reis RL (2015) Natural-based nanocomposites for bone tissue engineering and regenerative medicine: a review. *Adv Mater* 27(7):1143–1169
148. Bharadwaz A, Jayasuriya AC (2020) Recent trends in the application of widely used natural and synthetic polymer nanocomposites in bone tissue regeneration. *Mater Sci Eng C* 110:

149. Saravanan S, Leena RS, Selvamurugan N (2016) Chitosan based biocomposite scaffolds for bone tissue engineering. *Int J Biol Macromol* 93:1354–1365
150. Kavva KC, Jayakumar R, Nair S, Chennazhi KP (2013) Fabrication and characterization of chitosan/gelatin/nSiO₂ composite scaffold for bone tissue engineering. *Int J Biol Macromol* 59:255–263
151. Ren B, Chen X, Du S, Ma Y, Chen H, Yuan G, Li J, Xiong D, Tan H, Ling Z, Chen Y (2018) Injectable polysaccharide hydrogel embedded with hydroxyapatite and calcium carbonate for drug delivery and bone tissue engineering. *Int J Biol Macromol* 118:1257–1266
152. Keller L, Regiel-Futyr A, Gimeno M, Eap S, Mendoza G, Andreu V, Wagner Q, Kyzioł A, Sebastian V, Stochel G, Arruebo M (2017) Chitosan-based nanocomposites for the repair of bone defects. *Nanomedicine: Nanotechnol Biol Med* 13(7):2231–2240
153. Molaei A, Yousefpour M (2019) Preparation of Chitosan-based nanocomposites and biomedical investigations in bone tissue engineering. *Int J Polym Mater Polym Biomater* 68(12):701–713
154. Ran J, Hu J, Sun G, Chen S, Jiang P, Shen X, Tong H (2016) A novel chitosan-tussah silk fibroin/nano-hydroxyapatite composite bone scaffold platform with tunable mechanical strength in a wide range. *Int J Biol Macromol* 93:87–97
155. Shakir M, Zia I, Rehman A, Ullah R (2018) Fabrication and characterization of nanoengineered biocompatible n-HA/chitosan-tamarind seed polysaccharide: Bio-inspired nanocomposites for bone tissue engineering. *Int J Biol Macromol* 111:903–916
156. Venkatesan J, Bhatnagar I, Manivasagan P, Kang KH, Kim SK (2015) Alginate composites for bone tissue engineering: a review. *Int J Biol Macromol* 72:269–281
157. Bi YG, Lin ZT, Deng ST (2019) Fabrication and characterization of hydroxyapatite/sodium alginate/chitosan composite microspheres for drug delivery and bone tissue engineering. *Mater Sci Eng C* 100:576–583
158. Purohit SD, Bhaskar R, Singh H, Yadav I, Gupta MK, Mishra NC (2019) Development of a nanocomposite scaffold of gelatin–alginate–graphene oxide for bone tissue engineering. *Int J Biol Macromol* 133:592–602
159. Azami M, Tavakol S, Samadikuchaksaraei A, Hashjin MS, Baheiraei N, Kamali M, Nourani MR (2012) A porous hydroxyapatite/gelatin nanocomposite scaffold for bone tissue repair: in vitro and in vivo evaluation. *J Biomater Sci Polym Ed* 23(18):2353–2368
160. Arabi N, Zamanian A, Rashvand SN, Ghorbani F (2018) The tunable porous structure of gelatin–bioglass nanocomposite scaffolds for bone tissue engineering applications: physicochemical, mechanical, and in vitro properties. *Macromol Mater Eng* 303(3):1700539
161. Ferreira AM, Gentile P, Chiono V, Ciardelli G (2012) Collagen for bone tissue regeneration. *Acta Biomater* 8(9):3191–3200
162. Türk S, Altunsoy I, Efe GÇ, İpek M, Özacar M, Bindal C (2018) 3D porous collagen/functionalized multiwalled carbon nanotube/chitosan/hydroxyapatite composite scaffolds for bone tissue engineering. *Mater Sci Eng C* 92:757–768
163. Ao C, Niu Y, Zhang X, He X, Zhang W, Lu C (2017) Fabrication and characterization of electrospun cellulose/nano-hydroxyapatite nanofibers for bone tissue engineering. *Int J Biol Macromol* 97:568–573
164. Sarkar C, Chowdhuri AR, Kumar A, Laha D, Garai S, Chakraborty J, Sahu SK (2018) One pot synthesis of carbon dots decorated carboxymethyl cellulose-hydroxyapatite nanocomposite for drug delivery, tissue engineering and Fe³⁺ ion sensing. *Carbohydr Polym* 181:710–718
165. Abeer MM, Mohd Amin MC, Martin C (2014) A review of bacterial cellulose-based drug delivery systems: their biochemistry, current approaches and future prospects. *J Pharm Pharmacol* 66(8):1047–1061
166. Li H, Qi Z, Zheng S, Chang Y, Kong W, Fu C, Yu Z, Yang X, Pan S (2019) The application of hyaluronic acid-based hydrogels in bone and cartilage tissue engineering. *Adv Mater Sci Eng* 2019
167. Unnithan AR, Sasikala AR, Park CH, Kim CS (2017) A unique scaffold for bone tissue engineering: an osteogenic combination of graphene oxide–hyaluronic acid–chitosan with simvastatin. *J Ind Eng Chem* 46:182–191

168. Trombino S, Servidio C, Curcio F, Cassano R (2019) Strategies for hyaluronic acid-based hydrogel design in drug delivery. *Pharmaceutics* 11(8):407
169. Melke J, Midha S, Ghosh S, Ito K, Hofmann S (2016) Silk fibroin as biomaterial for bone tissue engineering. *Acta Biomater* 31:1–6
170. Mottaghitlab F, Farokhi M, Shokrgozar MA, Atyabi F, Hosseinkhani H (2015) Silk fibroin nanoparticle as a novel drug delivery system. *J Controlled Release* 206:161–176
171. Cilurzo F, Gennari CG, Selmin F, Marotta LA, Minghetti P, Montanari L (2011) An investigation into silk fibroin conformation in composite materials intended for drug delivery. *Int J Pharm* 414(1–2):218–224
172. Cortizo MS, Belluzo MS (2017) Biodegradable polymers for bone tissue engineering. In: *Industrial applications of renewable biomass products*. Springer, Cham, pp 47–74
173. Donnalaja F, Jacchetti E, Soncini M, Raimondi MT (2020) Natural and synthetic polymers for bone scaffolds optimization. *Polymers* 12(4):905
174. Hu C, Ashok D, Nisbet DR, Gautam V (2019) Bioinspired surface modification of orthopedic implants for bone tissue engineering. *Biomaterials* 219:
175. Englert C, Brendel JC, Majdanski TC, Yildirim T, Schubert S, Gottschaldt M, Windhab N, Schubert US (2018) Pharmapolymers in the 21st century: synthetic polymers in drug delivery applications. *Prog Polym Sci* 87:107–164
176. Li Y, Liao C, Tjong SC (2019) Synthetic biodegradable aliphatic polyester nanocomposites reinforced with nanohydroxyapatite and/or graphene oxide for bone tissue engineering applications. *Nanomaterials* 9(4):590
177. Khoshroo K, Kashi TS, Moztarzadeh F, Tahriri M, Jazayeri HE, Tayebi L (2017) Development of 3D PCL microsphere/TiO₂ nanotube composite scaffolds for bone tissue engineering. *Mater Sci Eng C* 70:586–598
178. Wang W, Caetano G, Ambler WS, Blaker JJ, Frade MA, Mandal P, Diver C, Bártolo P (2016) Enhancing the hydrophilicity and cell attachment of 3D printed PCL/graphene scaffolds for bone tissue engineering. *Materials* 9(12):992
179. Rostami F, Tamjid E, Behmanesh M (2020) Drug-eluting PCL/graphene oxide nanocomposite scaffolds for enhanced osteogenic differentiation of mesenchymal stem cells. *Mater Sci Eng C* 115:
180. Liu S, Qin S, He M, Zhou D, Qin Q, Wang H (2020) Current applications of poly (lactic acid) composites in tissue engineering and drug delivery. *Compos B Eng* 199:
181. Sha L, Chen Z, Chen Z, Zhang A, Yang Z (2016) Polylactic acid based nanocomposites: Promising safe and biodegradable materials in biomedical field. *Int J Polym Sci* 2016
182. Mir M, Ahmed N, ur Rehman A (2017) Recent applications of PLGA based nanostructures in drug delivery. *Colloids Surf B: Biointerfaces*. 159:217–231
183. Rasoulianboroujeni M, Fahimipour F, Shah P, Khoshroo K, Tahriri M, Eslami H, Yadegari A, Dashtimoghadam E, Tayebi L (2019) Development of 3D-printed PLGA/TiO₂ nanocomposite scaffolds for bone tissue engineering applications. *Mater Sci Eng C* 96:105–113
184. Elmowafy EM, Tiboni M, Soliman ME (2019) Biocompatibility, biodegradation and biomedical applications of poly (lactic acid)/poly (lactic-co-glycolic acid) micro and nanoparticles. *J Pharm Invest* 1–34
185. Ginebra MP, Espanol M, Maazouz Y, Bergez V, Pastorino D (2018) Bioceramics and bone healing. *EFORT Open Rev* 3(5):173–183
186. Levingstone TJ, Herbaj S, Dunne NJ (2019) Calcium phosphate nanoparticles for therapeutic applications in bone regeneration. *Nanomaterials* 9(11):1570
187. Dorozhkin SV (2015) Calcium orthophosphate bioceramics. *Ceram Int* 41(10):13913–13966
188. Uskoković V, Uskoković DP (2011) Nanosized hydroxyapatite and other calcium phosphates: chemistry of formation and application as drug and gene delivery agents. *J Biomed Mater Res B Appl Biomater* 96(1):152–191
189. Mondal S, Dorozhkin SV, Pal U (2018) Recent progress on fabrication and drug delivery applications of nanostructured hydroxyapatite. *Wiley Interdisc Rev Nanomed Nanobiotechnol* 10(4):

190. Lin K, Chang J (2015) Structure and properties of hydroxyapatite for biomedical applications. In: *Hydroxyapatite (HAp) for biomedical applications*. Woodhead Publishing, pp 3–19
191. Erol-Taygun M, Unalan I, Idris MI, Mano JF, Boccaccini AR (2019) Bioactive glass-polymer nanocomposites for bone tissue regeneration applications: a review. *Adv Eng Mater* 21(8):1900287
192. Jiang S, Zhang Y, Shu Y, Wu Z, Cao W, Huang W (2017) Amino-functionalized mesoporous bioactive glass for drug delivery. *Biomed Mater* 12(2):
193. Madison J, Joy-anne NO, Zhu D (2020) Bioactive glasses in orthopedic applications. In: *Racing for the surface*. Springer, Cham, pp 557–575
194. Iannazzo D, Pistone A, Salamò M, Galvagno S (2017) Hybrid ceramic/polymer composites for bone tissue regeneration. In: *Hybrid polymer composite materials*. Woodhead Publishing, pp 125–155
195. Huang B, Caetano G, Vyas C, Blaker JJ, Diver C, Bártolo P (2018) Polymer-ceramic composite scaffolds: the effect of hydroxyapatite and β -tri-calcium phosphate. *Materials* 11(1):129
196. Filippi M, Born G, Chaaban M, Scherberich A (2020) Natural polymeric scaffolds in bone regeneration. *Front Bioeng Biotechnol* 8:474
197. Swetha M, Sahithi K, Moorthi A, Srinivasan N, Ramasamy K, Selvamurugan N (2010) Biocomposites containing natural polymers and hydroxyapatite for bone tissue engineering. *Int J Biol Macromol* 47(1):1–4
198. Venkatesan J, Nithya R, Sudha PN, Kim SK (2014) Role of alginate in bone tissue engineering. In: *Advances in food and nutrition research*, vol 73. Academic Press, pp 45–57
199. Hatton J, Davis GR, Mourad AH, Cherupurakal N, Hill RG, Mohsin S (2019) Fabrication of porous bone scaffolds using alginate and bioactive glass. *J Funct Biomater* 10(1):15
200. Naik K, Chandran VG, Rajashekar R, Waigaonkar S, Kowshik M (2016) Mechanical properties, biological behaviour and drug release capability of nano TiO_2 -HAp-Alginate composite scaffolds for potential application as bone implant material. *J Biomater Appl* 31(3):387–399
201. Venkatasubbu GD, Ramasamy S, Ramakrishnan V, Kumar J (2011) Hydroxyapatite-alginate nanocomposite as drug delivery matrix for sustained release of ciprofloxacin. *J Biomed Nanotechnol* 7(6):759–767
202. Luciano B, Juan L, Graciela S, Mónica B, Paula M (2020) Antibacterial alginate/nano-hydroxyapatite composites for bone tissue engineering: assessment of their bioactivity, biocompatibility, and antibacterial activity. *Mater Sci Eng C* 115:
203. Maji K, Dasgupta S, Bhaskar R, Gupta MK (2020) Photo-crosslinked alginate nano-hydroxyapatite paste for bone tissue engineering. *Biomed Mater*
204. Hoque ME, Nuge T, Yeow TK, Nordin N, Prasad RG (2015) Gelatin based scaffolds for tissue engineering-a review. *Polym Res J* 9(1):15–32
205. Reiter T, Panick T, Schuhlraden K, Roether JA, Hum J, Boccaccini AR (2019) Bioactive glass based scaffolds coated with gelatin for the sustained release of icariin. *Bioact Mater* 4:1–7
206. Rahmanian M, Dehghan MM, Eini L, Naghib SM, Gholami H, Mohajeri SF, Mamaghani KR, Majidzadeh-A K (2019) Multifunctional gelatin-tricalcium phosphate porous nanocomposite scaffolds for tissue engineering and local drug delivery: in vitro and in vivo studies. *J Taiwan Inst Chem Eng* 101:214–220
207. Govindan R, Gu FL, Karthi S, Girija EK (2020) Effect of phosphate glass reinforcement on the mechanical and biological properties of freeze-dried gelatin composite scaffolds for bone tissue engineering applications. *Mater Today Commun* 22:
208. Udumluck N, Lee H, Hong S, Lee SH, Park H (2020) Surface functionalization of dual growth factor on hydroxyapatite-coated nanofibers for bone tissue engineering. *Appl Surf Sci* 11:
209. Gritsch L, Maqbool M, Mouriño V, Ciraldo FE, Cresswell M, Jackson PR, Lovell C, Boccaccini AR (2019) Chitosan/hydroxyapatite composite bone tissue engineering scaffolds with dual and decoupled therapeutic ion delivery: copper and strontium. *J Mater Chem B* 7(40):6109–6124
210. Uskoković V, Desai TA (2014) In vitro analysis of nanoparticulate hydroxyapatite/chitosan composites as potential drug delivery platforms for the sustained release of antibiotics in the treatment of osteomyelitis. *J Pharm Sci* 103(2):567–579

211. Zarghami V, Ghorbani M, Bagheri KP, Shokrgozar MA (2020) Prolongation of bactericidal efficiency of chitosan—bioactive glass coating by drug controlled release. *Prog Org Coat* 139:
212. Jolly R, Khan AA, Ahmed SS, Alam S, Kazmi S, Owais M, Farooqi MA, Shakir M (2020) Bioactive Phoenix dactylifera seeds incorporated chitosan/hydroxyapatite nanoconjugate for prospective bone tissue engineering applications: a bio-synergistic approach. *Mater Sci Eng C* 109:
213. Lu HT, Lu TW, Chen CH, Mi FL (2019) Development of genipin-crosslinked and fucoidan-adsorbed nano-hydroxyapatite/hydroxypropyl chitosan composite scaffolds for bone tissue engineering. *Int J Biol Macromol* 128:973–984
214. Wang G, Qiu J, Zheng L, Ren N, Li J, Liu H, Miao J (2014) Sustained delivery of BMP-2 enhanced osteoblastic differentiation of BMSCs based on surface hydroxyapatite nanostructure in chitosan–HAp scaffold. *J Biomater Sci Polym Ed* 25(16):1813–1827
215. Ali AF, Ahmed MM, El-Kady AM, Abd El-Hady BM, Ibrahim AM (2020) Synthesis of gelatin-agarose scaffold for controlled antibiotic delivery and its modification by glass nanoparticles addition as a potential osteomyelitis treatment. *Silicon*, pp 1–8
216. Cattalini JP, Hoppe A, Pishbin F, Roether J, Boccaccini AR, Lucangioli S, Mouriño V (2015) Novel nanocomposite biomaterials with controlled copper/calcium release capability for bone tissue engineering multifunctional scaffolds. *J R Soc Interface* 12(110):20150509
217. Pacelli S, Maloney R, Chakravarti AR, Whitlow J, Basu S, Modaresi S, Gehrke S, Paul A (2017) Controlling adult stem cell behavior using nanodiamond-reinforced hydrogel: implication in bone regeneration therapy. *Sci Rep* 7(1):1–5
218. Knaack S, Lode A, Hoyer B, Rösen-Wolff A, Gabrielyan A, Roeder I, Gelinsky M (2014) Heparin modification of a biomimetic bone matrix for controlled release of VEGF. *J Biomed Mater Res Part A* 102(10):3500–3511
219. Sarkar C, Chowdhuri AR, Garai S, Chakraborty J, Sahu SK (2019) Three-dimensional cellulose-hydroxyapatite nanocomposite enriched with dexamethasone loaded metal–organic framework: a local drug delivery system for bone tissue engineering. *Cellulose* 26(12):7253–7269
220. Zhang Y, Chen M, Dai Z, Cao H, Li J, Zhang W (2020) Sustained protein therapeutics enabled by self-healing nanocomposite hydrogels for non-invasive bone regeneration. *Biomater Sci* 8(2):682–693
221. Lei B, Guo B, Rambhia KJ, Ma PX (2019) Hybrid polymer biomaterials for bone tissue regeneration. *Front Med* 13(2):189–201
222. Shi C, Yuan Z, Han F, Zhu C, Li B (2016) Polymeric biomaterials for bone regeneration. *Ann Jt* 1:1
223. Dwivedi R, Kumar S, Pandey R, Mahajan A, Nandana D, Katti DS, Mehrotra D (2020) Polycaprolactone as biomaterial for bone scaffolds: review of literature. *J Oral Biol Craniofac Res* 10(1):381–388
224. Kouhi M, Morshed M, Varshosaz J, Fathi MH (2013) Poly (ϵ -caprolactone) incorporated bioactive glass nanoparticles and simvastatin nanocomposite nanofibers: preparation, characterization and in vitro drug release for bone regeneration applications. *Chem Eng J* 228:1057–1065
225. Nithya R, Sundaram NM (2015) Biodegradation and cytotoxicity of ciprofloxacin-loaded hydroxyapatite-polycaprolactone nanocomposite film for sustainable bone implants. *Int J Nanomed* 10(Suppl 1):119
226. Liu X, Zhao K, Gong T, Song J, Bao C, Luo E, Weng J, Zhou S (2014) Delivery of growth factors using a smart porous nanocomposite scaffold to repair a mandibular bone defect. *Biomacromolecules* 15(3):1019–1030
227. Grémare A, Guduric V, Bareille R, Heroguez V, Latour S, L'heureux N, Fricain JC, Catros S, Le Nihouannen D (2018) Characterization of printed PLA scaffolds for bone tissue engineering. *J Biomed Mater Res Part A* 106(4):887–894
228. Zhou R, Xu W, Chen F, Qi C, Lu BQ, Zhang H, Wu J, Qian QR, Zhu YJ (2014) Amorphous calcium phosphate nanospheres/poly lactide composite coated tantalum scaffold: facile preparation, fast biomineralization and subchondral bone defect repair application. *Colloids Surf B* 123:236–245

229. Köse GT, Korkusuz F, Korkusuz PE, Purali N, Özkul A, Hasırcı V (2003) Bone generation on PHBV matrices: an in vitro study. *Biomaterials* 24(27):4999–5007
230. Duan B, Wang M (2010) Customized Ca–P/PHBV nanocomposite scaffolds for bone tissue engineering: design, fabrication, surface modification and sustained release of growth factor. *J Roy Soc Interface* 7(suppl_5):S615–S629
231. de Almeida Neto GR, Barcelos MV, Ribeiro ME, Folly MM, Rodríguez RJ (2019) Formulation and characterization of a novel PHBV nanocomposite for bone defect filling and infection treatment. *Mater Sci Eng C* 104:
232. Wang C, Zhao Q, Wang M (2017) Cryogenic 3D printing for producing hierarchical porous and rhBMP-2-loaded Ca-P/PLLA nanocomposite scaffolds for bone tissue engineering. *Biofabrication* 9(2):
233. Lu S, McGough MA, Shiels SM, Zienkiewicz KJ, Merkel AR, Vanderburgh JP, Nyman JS, Sterling JA, Tennent DJ, Wenke JC, Guelcher SA (2018) Settable polymer/ceramic composite bone grafts stabilize weight-bearing tibial plateau slot defects and integrate with host bone in an ovine model. *Biomaterials* 179:29–45
234. Shu X, Feng J, Feng J, Huang X, Li L, Shi Q (2017) Combined delivery of bone morphogenetic protein-2 and insulin-like growth factor-1 from nano-poly (γ -glutamic acid)/ β -tricalcium phosphate-based calcium phosphate cement and its effect on bone regeneration in vitro. *J Biomater Appl* 32(5):547–560
235. Su J, Xu H, Sun J, Gong X, Zhao H (2013) Dual delivery of BMP-2 and bFGF from a new nano-composite scaffold, loaded with vascular stents for large-size mandibular defect regeneration. *Int J Mol Sci* 14(6):12714–12728
236. Zhang X, Geven MA, Wang X, Qin L, Grijpma DW, Peijs T, Eglın D, Guillaume O, Gautrot JE (2018) A drug eluting poly (trimethylene carbonate)/poly (lactic acid)-reinforced nanocomposite for the functional delivery of osteogenic molecules. *Int J Nanomed* 13:5701
237. Nazemi K, Azadpour P, Moztafzadeh F, Urbanska AM, Mozafari M (2015) Tissue-engineered chitosan/bioactive glass bone scaffolds integrated with PLGA nanoparticles: a therapeutic design for on-demand drug delivery. *Mater Lett* 138:16–20
238. Asadian-Ardakani V, Saber-Samandari S, Saber-Samandari S (2016) The effect of hydroxyapatite in biopolymer-based scaffolds on release of naproxen sodium. *J Biomed Mater Res Part A* 104(12):2992–3003
239. Ji M, Li H, Guo H, Xie A, Wang S, Huang F, Li S, Shen Y, He J (2016) A novel porous aspirin-loaded (GO/CTS-HA) n nanocomposite films: synthesis and multifunction for bone tissue engineering. *Carbohydr Polym* 153:124–132
240. Hu Y, Ma S, Yang Z, Zhou W, Du Z, Huang J, Yi H, Wang C (2016) Facile fabrication of poly (L-lactic acid) microsphere-incorporated calcium alginate/hydroxyapatite porous scaffolds based on Pickering emulsion templates. *Colloids Surf B* 140:382–391
241. Wu H, Lei P, Liu G, Zhang YS, Yang J, Zhang L, Xie J, Niu W, Liu H, Ruan J, Hu Y (2017) Reconstruction of Large-scale Defects with a Novel Hybrid Scaffold Made from Poly (L-lactic acid)/Nanohydroxyapatite/Alendronate-loaded Chitosan Microsphere: in vitro and in vivo Studies. *Scientific reports* 7(1):1–4
242. Wang Y, Cui W, Zhao X, Wen S, Sun Y, Han J, Zhang H (2019) Bone remodeling-inspired dual delivery electrospun nanofibers for promoting bone regeneration. *Nanoscale* 11(1):60–71
243. Farokhi M, Mottaghtalab F, Ai J, Shokrgozar MA (2013) Sustained release of platelet-derived growth factor and vascular endothelial growth factor from silk/calcium phosphate/PLGA based nanocomposite scaffold. *Int J Pharm* 454(1):216–225
244. El-Fiqi A, Kim JH, Kim HW (2015) Osteoinductive fibrous scaffolds of biopolymer/mesoporous bioactive glass nanocarriers with excellent bioactivity and long-term delivery of osteogenic drug. *ACS Appl Mater Interfaces* 7(2):1140–1152
245. Kuttappan S, Mathew D, Jo JI, Tanaka R, Menon D, Ishimoto T, Nakano T, Nair SV, Nair MB, Tabata Y (2018) Dual release of growth factor from nanocomposite fibrous scaffold promotes vascularisation and bone regeneration in rat critical sized calvarial defect. *Acta Biomater* 78:36–47

246. Krishnan AG, Biswas R, Menon D, Nair MB (2020) Biodegradable nanocomposite fibrous scaffold mediated local delivery of vancomycin for the treatment of MRSA infected experimental osteomyelitis. *Biomater Sci* 8(9):2653–2665
247. Farokhi M, Mottaghitalab F, Shokrgozar MA, Ai J, Hadjati J, Azami M (2014) Bio-hybrid silk fibroin/calcium phosphate/PLGA nanocomposite scaffold to control the delivery of vascular endothelial growth factor. *Mater Sci Eng C* 35:401–410
248. Amjadian S, Seyedjafari E, Zeynali B, Shabani I (2016) The synergistic effect of nano-hydroxyapatite and dexamethasone in the fibrous delivery system of gelatin and poly (l-lactide) on the osteogenesis of mesenchymal stem cells. *Int J Pharm* 507(1–2):1

Biopolymeric Nanocomposites for Orthopedic Applications



Maria Râpă, Raluca Nicoleta Darie-Nita, and Cornelia Vasile

Abstract Among the promising sustainable materials of modern times, biopolymeric nanocomposites have received an increased interest for orthopedic applications due to their excellent mechanical, biocompatibility, bioactivity properties, and special architecture for the cells proliferation, differentiation, and migration in bone tissue regeneration. The aim of this chapter is to summarize the recent research results on the development and applications of various types of biopolymeric nanocomposites utilized in prosthetic devices to bone grafts, for cell delivery, with a special focus on material type, formulations, current design, and performance in bone tissue engineering. Important challenges related to the degradation of biopolymeric nanocomposite scaffolds, wide range of properties, and benefits for bone healing are addressed.

Keywords Bone tissue engineering · Biopolymer · Nanocomposite · Biocompatibility · Orthopedic applications

1 Introduction

Tissue engineering deals with the recuperation, maintenance, or enhancement of tissue functions that are malfunctioning or have been lost due to the different pathological conditions. It is classified into soft tissue (blood vessels, skin, tendons, nerve, and skeletal muscle) and hard tissue (bone) [11]. Bone is the second most transplanted tissue in the world after blood and kidney [46]. The main functions of bones are to assure strength, flexibility and to support the organs in the body. Genetic abnormalities, defects caused by trauma, deficiency in vitamin D, phosphorus, calcium, and hormonal imbalances among other causes are factors that can lead to complications

M. Râpă

University Politehnica of Bucharest, 313 Splaiul Independentei, 060042 Bucharest, Romania

R. N. Darie-Nita · C. Vasile (✉)

Physical Chemistry of Polymers Department, “Petru Poni” Institute of Macromolecular Chemistry, 41A Grigore Ghica Voda Alley, 700487 Iasi, Romania

e-mail: cvasile@icmpp.ro

© The Author(s), under exclusive license to Springer Nature Switzerland AG 2022

377

M. S. Hasnain et al. (eds.), *Polymeric and Natural Composites*,

Advances in Material Research and Technology,

https://doi.org/10.1007/978-3-030-70266-3_12

in the bone structure and function. It is expected that the bone illness to increase in the future due to the growth and aging population. Therefore, it is a huge need for clear approaches leading to bone healing.

Bone tissue engineering (BTE) has emerged in recent years as a new and applicable approach to repair bone defects. Scaffolds are the three-dimensional (3D) structures characterized by the high surface area to promote the cell adhesion, the mechanical ability to support the newly formed tissue, a framework for healing, inducing new tissue formation, and the biocompatibility with the host environment. Materials utilized for the bone scaffold preparation can be classified into metallic biomaterials, polymers (natural and synthetic), ceramics, and glasses.

Metallic biomaterials such as Ti [56], Mg [35], or Ti alloys (e.g., Ti–Nb, Ti–Mo, Ti–Ta, Ti–Nb–Sn) [54] or other metallic alloys (e.g., Mg alloys, Zn–Mn) [9, 30] possess mechanical properties and corrosion resistance properties necessary for the fabrication of scaffolds. Surgical grade stainless steel has been used in orthopedic applications as fixation elements for the stabilization of fractures or as prostheses [4]. These metal biomaterials may cause some deficiencies like high cost of implant processing, loose of osseo-integration and antibacterial effect, bone distortion, and release of metal ions from the implant to the body fluid.

Among the natural polymers most used for the manufacture of scaffolds are extracellular matrix proteins (collagen), as well as some polysaccharides such as poly (hyaluronic acid), chitosan, and alginate. These polymers are considered promising alternative to metallic biomaterials due to the resemblance to natural elements of the cytoskeleton of regenerated tissues. Collagen is the most abundant protein in the human body [13, 33] and represents 90% of the protein content of the bone [34]. Sulfated polysaccharides derived from the extracellular matrix (ECM) of animal tissues (glycosaminoglycans) or plants, such as marine algae (alginate, carrageenan, fucoidan, and ulvan) could be also exploited as promising biomaterials for orthopedic tissue engineering applications due to their high abundance and sustainability together with limited immunogenicity [16, 52]. Improving in the mechanical strength of the natural polymers is a concern for many researchers.

As synthetic polymers, polycaprolactone (PCL), poly (lactic acid) (PLA), poly (glycolic acid) (PGA), and poly (lactic-co-glycolic acid) (PLGA) polymers are usually used as matrices in bionanocomposites used as biomaterials in BTE. These scaffolds provide an acceptable cell support and proliferation, biodegradability, but cannot be used alone for bone regeneration because to the missing of osteo-promotive capacity [5].

Bioactive ceramics, such as hydroxyapatite (HAp) and tricalcium phosphate (TCP), show unique ability to induce osteogenic gene expression in BTE. HAp $[(Ca)_{10}(PO_4)_6(OH)_2]$ is the essential chemical currently used in function of bone, ensuring the release of calcium and phosphorous ions in a similar way to the occurring of natural bone (Ca/P ratio 1.67) [44]. HAp possesses biocompatibility, cell attachment, and osteo-integration. Its major drawbacks are related to brittle nature, a reduced biocompatibility, and biodegradability. Silica-based bioactive materials

have ability to promote osteoblast adhesion, mesenchymal stem cells (MSCs) differentiation, and revascularization leading in a fully functional bone. However, its low degradation rate prevents the formation of new tissue.

Taking into account on the advantages and disadvantages of above-discussed materials for the scaffolds production, one approach to the design of scaffolds for orthopedic applications with improved mechanical strength, biodegradation, bioactivity, and biocompatibility is the combination of ceramics with natural and synthetic polymers.

2 Natural Bone—A Nanostructured Composite

Natural bone is hierarchically structured biomineral with a multiscale arrangement from a macroscopic level (whole bone of various types: long and short bones, flat or tubular), structure of spongy bone tissue, and osteons of compact bone tissue, a microscopic level (cells, matrices, and minerals) to the nanoscale level of single bone apatite crystals and collagen fibers (see Fig. 1) [22, 36].

Bone is a nanomaterial containing 65–70 wt% of inorganic crystals, mainly nano-hydroxyapatite (nHAp), trace amounts of carbonate, magnesium and acid phosphate, and 30–35 wt% organic matrix, mainly collagen [11, 57]. Biological nanocrystalline apatites are the main inorganic components of hard tissues like bones.

In the organic–inorganic nanocomposite structure of bone, calcium phosphate nanoparticles are held within a primarily collagen protein matrix (see Fig. 2a). The nanoparticles contain 50–150 nm thick stacks of very closely packed single crystal platelets, with 2.5–4 nm thickness [10], their large faces being parallel to each other and with their c axes strongly ordered (parallel to collagen fibrils). Figure 2b shows the regions containing the disordered phosphate as the interfaces between the apatite layers and the mineral-bound water. The water is prevented to be excluded due to the citrate anions that connect the mineral platelets in bone and therefore maintains the amorphous mineral ion arrangements on the “surfaces” of the mineral platelets intended to arrange themselves in stacks (Fig. 2c) [18].

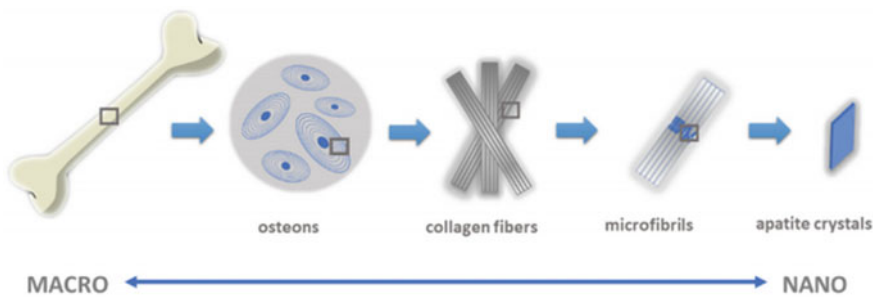


Fig. 1 Multiscale structure of natural bone (open access [36])

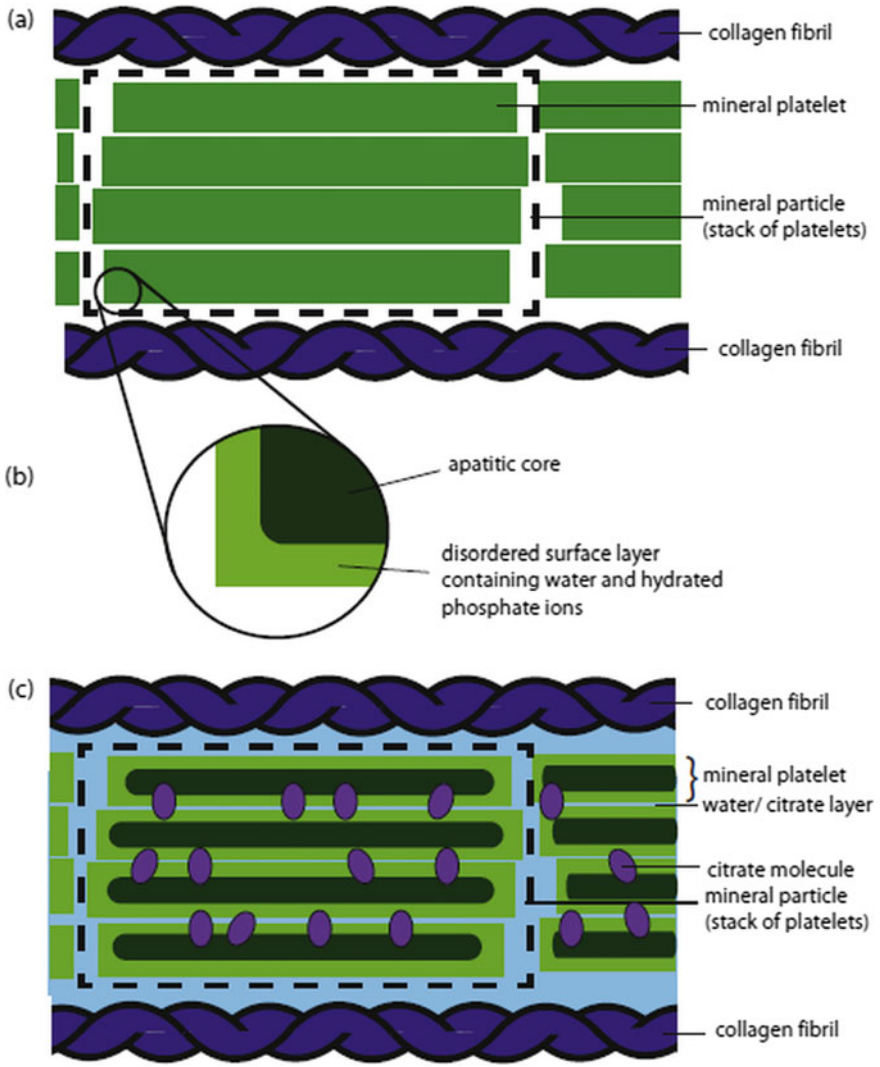


Fig. 2 a Scheme of the bone’s organic–inorganic composite nanostructure. Polycrystalline mineral particles are sandwiched between collagen fibrils. b Schematic view of the structure of a single mineral platelet, with an atomically ordered core resembling the hydroxyapatite surrounded by a surface layer of disordered, hydrated mineral ions. c Schematic view of the detailed structural model of bone mineral where citrate anions and water bind the mineral platelets together (Permission from Elsevier [18])

2.1 Bone Defects

Bone defects differ vary greatly by on size, severity, and location of the defects, these factors enabling accurate planning for treatment and rehabilitation [29].

Congenital or acquired conditions can lead to bone defects. The absence of or wrong development of bones are the common reason for the congenital bone anomalies. Acquired bone defects often occur due to trauma, diseases (osteoporosis and osteosarcoma), infection, or surgeries. Osteoarthritis is an osteo-degenerative disease responsible for bone loss over time [32].

Cavity defects and segmental defects are two general groups for bone defects classification. In cavity defects, the limb biomechanics is not affected by the loss, while for segmental defects, normal biomechanics are impeded and the structural stability of the bone as an organ may be endangered [45].

For orthopedics, the most practical and frequently used is Anderson Orthopaedic Research Institute (AORI) classification which predominantly is based on the size of the bone defect originated from the tibia and femur [51]. AORI classifies bone defects into three types as shown in Fig. 3. The major knee defects are occasionally associated with collateral or patellar ligament detachment; therefore, bone grafting or custom implants are usually required.

Bone defects could be remediated by bone grafting because the natural bone tissue is able to completely regenerate; therefore, it can replace the graft material, resulting in fully integrated region of new bone. Bone morphogenetic proteins, bone growth

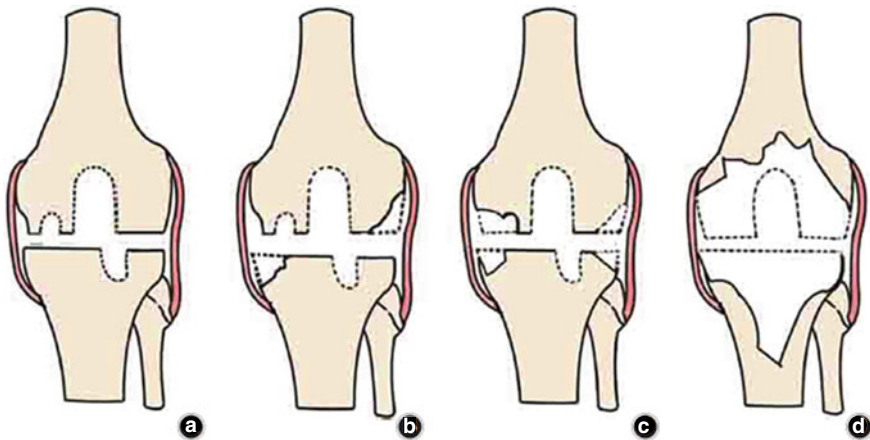


Fig. 3 Bone defects classified according to Anderson Orthopaedic Research Institute: **a** type I (intact metaphyseal bone with minor defects without compromising the stability of a revision component), **b** type IIA (damaged metaphyseal bone with defects in one femoral condyle or tibial plateau), **c** type IIB (damaged metaphyseal bone with more defects in both femoral condyle/tibial plateau), and **d** type III (significant cancellous metaphyseal bone loss with a major portion of the condyle or plateau compromised) (**Open access** [28])

factors, and direct bone anchorage factors strongly influence the biologic mechanisms such as osteo-induction, osteo-conduction, and osseo-integration, powerful interrelated phenomena in bone regeneration[49].

A different classification of bone defects is function of the animal models used to evaluate bone graft substitutes, and the main four types being: the calvarial defect, long bone or segmental defect, partial cortical defect, and cancellous bone defect models [7] (see Fig. 4) (A) Calvarial defects are generally created by introducing a circular burr hole and the subsequent removal of the resulting bone disk. In this case, the underlying dura mater is not damaged by the surgery. (B) The segmental bone defect arises as a large and non-joining wound area (gap) between the bone edges when a segment of the bone is surgically removed. The gap is usually stabilized with a fixation device and/or filled with a tissue-engineered bone substitute to stimulate bone healing and to study bone formation. (C) The burr hole is a partial defect model created when an incomplete hole is drilled into the side of the bone to create a wounded area. The cortical bone is usually penetrated by the burr hole which can extend into the underlying cancellous bone or the bone marrow cavity.

Bone regeneration involves the use of mesenchymal stem cells (MSCs) and bone cells such as osteoblasts, osteoclasts in bone fractures, and defects. Bone grafting techniques are widely used in healing and regenerative therapies of bone defects. Bone grafts are classified based on their source as autograft, allograft (from a donor of the same species), and xenograft (from a donor of a different species) [1]. Autograft for bone repair is the most favorable technique based on the transposition of a patient's bone to the site of the bony defect. Although this graft assures the main characteristics for bone regeneration (osteo-conductive, osteo-inductive signaling molecules, and osteogenic cells properties), it is associated with pain and morbidity at the donor site and the inadequate cellular infiltration and regeneration [53]. Allograft bone refers to the decellularization of bone from human donors. This technique possesses only osteo-conductive properties. Fracture, non-union, infection, and immunogenic response are the possible complications associated to the allograft use. However, the

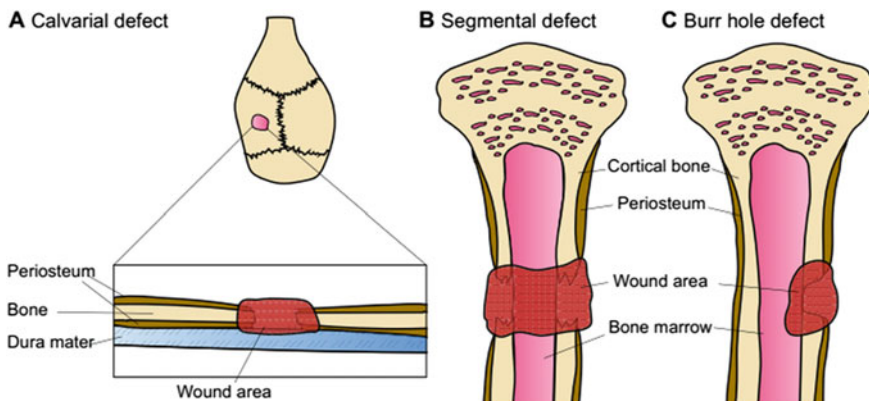


Fig. 4 Bone defect models for evaluation of bone graft substitutes (open access [41])

major hurdles of these grafting techniques are donor site pain, limited availability of donor, inflammation, graft incorporation rejection, concomitant vascularization, and pathogen transmission. To address these problems, the bone tissue engineering (BTE) is an optional therapy of the bone graft solutions.

2.2 Requirements for Bone Scaffolds

Three components are necessary for tissue regeneration: an osteo-conductive scaffold for cell adhesion, osteo-inductive signaling molecules to guide bone formation, and osteogenic cells themselves [53]. In addition, the tridimensional scaffolds should provide the mechanical strength so as to transfer the applied load at the implant site, biocompatibility, to be biodegradable, easy to use clinically, as well as low cost processing. The scaffold should present a suitable elastic modulus to avoid bone resorption—stress shielding. The human femoral cortical bone shows an elastic modulus of $17,900 \pm 3900$ MPa, fracture toughness of 2–6 MPa, and the average strength of 100–230 MPa [1]. Trabecular bone shows an elastic modulus ranging from 0.02 to 2 GPa, while for compact bone, elastic modulus is situated between 3 and 30 GPa [46].

Pereira et al. [46] performed a study about the properties of three scaffolds from $\text{Ti}_6\text{Al}_4\text{V}$ processed by using a commercial selective laser melting equipment, and ZrO_2 and poly-ether-ether-ketone (PEEK) produced by CNC milling. The authors obtained an average pore diameter of 375 μm for $\text{Ti}_6\text{Al}_4\text{V}$ scaffolds and 400 μm in the case of ZrO_2 and PEEK scaffolds. The elastic modulus was of 76.85 ± 1.43 GPa for $\text{Ti}_6\text{Al}_4\text{V}$ scaffolds, and 141.70 ± 1.04 GPa and 2.78 ± 0.06 GPa for ZrO_2 and PEEK scaffolds, respectively. PEEK scaffold exhibited a higher contact angle, leading to a hydrophobic surface and a low cell adhesion and spreading compared to $\text{Ti}_6\text{Al}_4\text{V}$ and ZrO_2 scaffolds. In vitro cytocompatibility and osteogenic ability carried out using SaOS-2 cells showed that the scaffolds were biocompatible and able to host cells for 14 days of the test time [46]. The scaffold's architecture is critical for healing bone process, and pores have an important role to promote cells penetration, tissue ingrowth, vascularization, proliferation, and differentiation [50]. Hydrophobicity of scaffold surfaces influences the cell attachment and absorption of protein by scaffold. It was established that the contact angles values lower than 90° are favorable for cell adhesion [46], while an optimum value for the contact angle was considered of 55° [6].

An ideal biodegradable implant must have low rates of degradation to ensure appropriate mechanical support until the completion of the healing bone process. It was established that 10% loss of total weight is acceptable for bone tissue engineering [3]. Also, the forming of biological bone-like apatite (carbonate-containing HAP crystallites with defective structure) on the surface of scaffold is critical for the connection between the 3D scaffold and the regenerated bone. The influence of vascularized bone niche, stiffness, roughness, pore size, and porosity of biomaterials

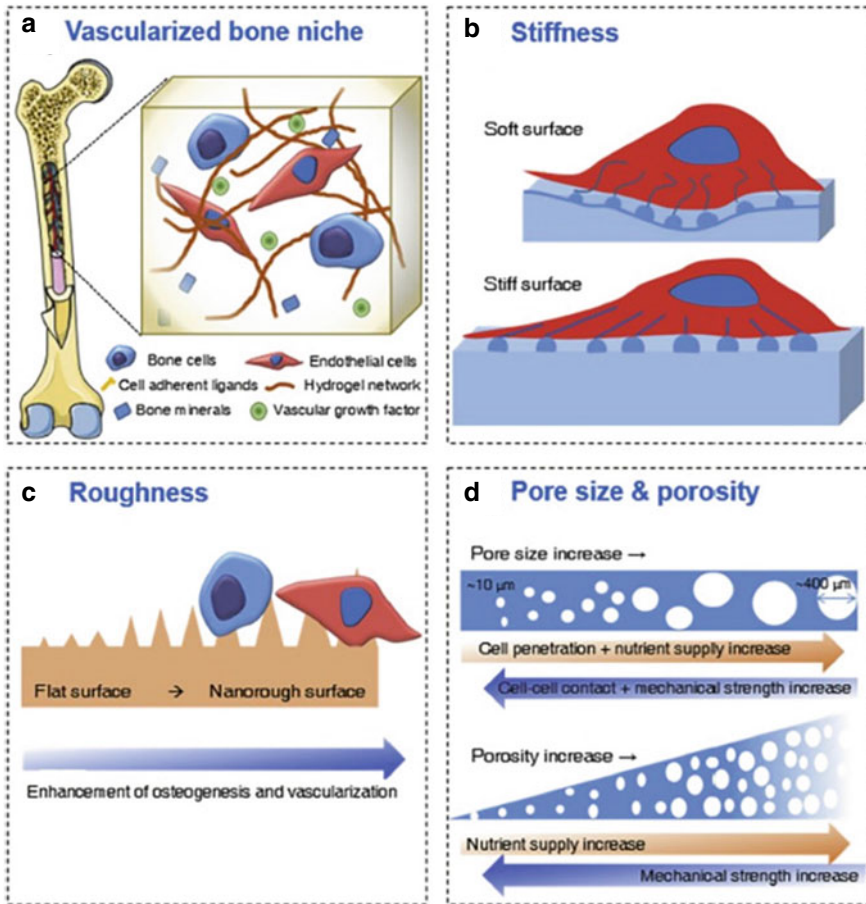


Fig. 5 Vascularized bone niche (a); stiffness (b); roughness (c); and pore size and porosity properties (d) facilitating osteogenic differentiation and vascularization (Reprinted with permission from Afewerki et al. [2])

on the facilitating osteogenic differentiation and vascularization was illustrated by [2] (see Fig. 5).

3 Biopolymeric Nanocomposites for Bone Tissue Regeneration

Combinations of biodegradable synthetic polymers, i.e., PLGA [5], poly (l-lactic acid) (PLLA), poly(3-hydroxybutyrate-co-3-hydroxyvalerate) (PHVB) [17], extra-cellular matrix-based polymers such as collagen, gelatin, chitosan (CS) [40, 42, 50],

or natural biopolymers such as silk fibroin (SF) [31] with nano-sized inorganic materials like HAp, TiO₂, β -tricalcium phosphate (β -TCP), use of polymeric nanosheets [1], or coating of metallic biomaterials with biopolymers [4] and bionanocomposites [20] are widely used for design of bone tissue scaffolds (see Table 1).

The general techniques for scaffold fabrication include solvent casting [57], lyophilization [3, 40], phase separation [31], leaching [14], electrospinning and electrospray [42] extrusion/coextrusion, injection molding [26], 263D printing [48], etc. Different additive manufacturing (AM) [50] approaches such as stereolithography (SLA), selective laser sintering (SLS) [17] (see Fig. 6), and fused deposition modeling (FDM) [5] have been developed in 3D printing. The advances in technology facilitate the use of combinations of methods for obtaining of improved mechanical properties, biocompatibility, and cell migration as polymerization/ copolymerization and cross-linking[43].

The presented formulations in Table 1 show biocompatibility, proved by cell growth and proliferation after direct contact [3, 4, 12, 17, 24, 31, 42].

3.1 Extracellular Matrix Polymeric Scaffolds

As given in Table.1, natural biopolymers such as chitosan (CS), collagen (Col), and gelatin (Gel) are the most used for scaffold preparation due to their similarities with native extra cellular matrix (ECM) [24, 40, 43]. In order to enhance the mechanical strength limiting their applications as the bone to be repaired or substituted, the combination of extracellular matrix with biometallic scaffolds or ceramic nanoparticles has been made. For example, porous composite scaffolds with adequate compression strength and enhanced cell proliferation were fabricated from filling of porous Ti6Al4V part with CS sponge [23]. A content of β -TCP up to 30 wt% into gelatin/CS/nano- β -tricalcium phosphate (β -TCP) (GCT) scaffolds led to obtain pore sizes ranging between 78 and 382 μm ($> 80\%$ porosity), and a good compressive strength which correspond to the spongy bone (see Fig. 7) [39].

The inverse relationship between the inorganic amount of nanoparticles and porosity of the scaffolds was also reported by other authors [31]. Increase in the amount of TiO₂-F up to 15 wt% into silk fibroin (SF)/TiO₂-F scaffolds led to decreasing of pore size (88–78%) and increasing in the mechanical properties of scaffolds. Instead, Di Rienzo et al. [14] showed that the mechanical behavior of the poly(para-phenylene) (PPP) porous scaffolds was not significantly influenced by the small or large pore sizes, i.e., 150 μm to 250 μm and 420 μm to 500 μm , respectively.

An innovative approach to enhance the cell viability, proliferation of osteoblast cell on the scaffold, and increase the bearing load after implantation was provided by Atak et al. [3] that modified nHAp with NH₂ group and incorporated them into chitosan scaffold (CS/Hap-NH₂).

Table 1 Some examples of polymeric compositions with relevant properties for orthopedic applications

Composition	Technique	Recommended applications	Significant results	References
<i>Bio-based polymers/inorganic nanoparticles</i>				
Octadecylamine-functionalized nanodiamond (ND-ODA)/PLLA	Solution casting followed by compression molding	Scaffolds for orthopedic regenerative engineering	280% increase in the strain at failure and 310% increase in fracture energy in tensile tests as compared with the mechanical properties of pure PLLA Ca/P ratio of 1.61	Zhang et al. [57]
Magnesium oxide (MgO) nanoparticles/PLLA/HAp	Casting method	Orthopedic tissue regeneration	MgO nanoparticles reduced bacterial growth of <i>Staphylococcus aureus</i> , increased the adhesion and proliferation of osteoblasts and fibroblasts	Hickey et al. [27]
PLGA/nHAp	Fused deposition modeling	Bone scaffolds	A reduced inflammatory reaction after subcutaneous implantation of the materials in the rat	Babilotte et al. [5]

(continued)

Table 1 (continued)

Composition	Technique	Recommended applications	Significant results	References
PHBV/Ca-P PLLA/CHAp	Selective laser sintering	Bone tissue engineering	High cell viability and normal morphology and phenotype after 3 and 7 days culture on SaOS-2 cells	Duan et al. [17]
<i>Natural biopolymers/inorganic nanoparticles</i>				
HAp/fucoïdan nanocomposites	In situ chemical method	Bone repair/replacement	Slight amount of bone formation by stimulating the osteoblastic activity with rabbit model	Tae Young et al. [52]
Chitosan (CS)/nHAp-NH ₂ bionanocomposite scaffolds	Freeze-drying method	Bone tissue engineering applications	10% of total weight loss Cell viability and proliferation of osteoblast cells on the scaffolds	Atak et al. [3]
SF/TiO ₂ -F	Phase separation method	Bone tissue engineering	Biocompatibility proved by SAOS-2 osteoblast cell line for 1, 3, and 5 days In vitro degradation and bioactivity improved Mechanical properties enhanced by using TiO ₂ -F amount up to 15 wt%	Johari et al. [31]

(continued)

Table 1 (continued)

Composition	Technique	Recommended applications	Significant results	References
AuNPs/CS bionanocomposite film	Electrodeposition method	Modification of implant surface	98% inhibition efficiency of Ti coated film Antibacterial effect	Farghali et al. [20]
nTiO ₂ /gelatin-CS hydrogel		Bone fracture healing	Promote osteoblast Accelerate bone fracture healing	Guo et al. [24]
Gelatin/CS/nano-β-TCP based porous scaffold	Lyophilization method	Nursing bone tissue engineering	> 80% porosity Compressive strength increased from 0.8 to 2.45 MPa Osteogenic potential in vitro without significant inflammatory reaction in vivo	Maji et al. [40]
CS/gelatin/silica-gentamicin	Electrophoretic deposition (EPD) on stainless steel	Coating on removable screws for bone or plate fixation with effective release of antibiotic	Antibacterial activity against <i>Escherichia coli</i> and <i>Staphylococcus aureus</i> at 24 h, ST-2 bone murine stromal cells proliferation (at 7 days culture) was not inhibited	Aydemir et al. [4]

(continued)

Table 1 (continued)

Composition	Technique	Recommended applications	Significant results	References
<i>Hybrid polymers</i>				
CS-g-PMMA/nano-CaO	Emulsion polymerization technique	Bioadhesive bone cement implants	0.35% nano-CaO led to bioactive bone cement with proper tensile strength and compressive strength	Pradhan and Sahoo [47]
P(HEMA) and P(HEMA-co-MMA)/HAp-cartilage powder (CP)/Gel bionanocomposites	Copolymerization	Scaffolds for bone implant	Osteo-conductivity and osteo-inductivity properties; Ca/P ratio of 1.4–1.5 on the surface	Haroun and Migonney [25]
Collagen/PCL-β-TCP scaffold	Additive manufacturing (AM) technology	Bone tissue engineering applications	Improved vascularization	Shanjani et al. [50]
Stimuli-sensitive semi-interpenetrating collagen/poly (N-isopropyl acrylamide) polymeric matrix/Dellite® 67G r Cloisite® 93A nanoclays/HAp	Hydrogel preparation: copolymerization and cross-linking		Suitable swelling characteristics for . In vitro cytocompatibility and cell viability revealed that the hybrid nanocomposites were non-cytotoxic for rat osteoblasts. Controllable enzymatic degradation	Nistor et al. [43]
PHB/BC formulations	Melt-mixing/salt-leaching/pressing technique		Support 3T3-L1 pre-adipocytes proliferation New bone growth at 20 weeks	Codreanu et al. [12]

(continued)

Table 1 (continued)

Composition	Technique	Recommended applications	Significant results	References
Ti6Al4V/CS composite scaffold	Electron beam melting and freeze-drying	Scaffold for orthopedic applications	The ultimate compressive strength was 85.35 ± 8.68 MPa Improved cell attachment, higher proliferation, and well-spread morphology as compared to porous Ti6Al4V part	Guo and Li [23]
<i>Synthetic polymer/inorganic nanoparticles</i>				
Poly(para-phenylene) (PPP)	Powder-sintering/salt-leaching technique	Load-bearing orthopedic biomaterial	Both modulus and strength decreased with increasing porosity from 50 to 90 vol%	Di Rienzo et al. [14]
PAN (7%)/AuNPs (1, 2.5, and 5 w/v% concentrations in water)	Blend electrospinning method Electrosprayed method	Bone tissue engineering	MTT and LDH tests were screened using MG-63 cells and revealed non-cytotoxicity and biocompatibility Improved electrical conductivity	Nekounam et al. [42]
UHMWPE/nHAP	Injection molding	Hip liners	Elastic modulus of 1.65 GPa Yield strength 27.6 MPa	Heidari et al. [26]

(continued)

Table 1 (continued)

Composition	Technique	Recommended applications	Significant results	References
HDPE/nGO nanocomposites	Vacuum compression molding technique	Implants for knee and hip replacement	Efficient fatigue, mechanical, and wear properties	Faisal [19]
PPSU/nTiO ₂	Ultrasonication and solution casting	Orthopedic and trauma implants	Improved storage and Young's moduli, tensile strength and toughness, glass transition and heat distortion temperature, water absorption and thermal stability Antibacterial activity	Diez-Pascual et al. [15]

(continued)

Table 1 (continued)

Composition	Technique	Recommended applications	Significant results	References
Polypropylene (PP)/carbon nanotubes (CNTs) or carbon nanofibers (CNFs)	Melt compounding	Bone replacements	Addition of low CNT/CNF loadings to nHA/PP composites enhanced their mechanical properties due to the large aspect ratio and remarkable high stiffness of carbonaceous nanofillers	Liao et al. [38]
PP/hexagonal boron nitride (hBN) nanoplatelets/nHAp	Extrusion and injection molding	Polymeric nanocomposites for orthopedic applications/bone replacements	Increased elastic modulus of PP composites and decreased tensile elongation with increasing hBN contents; attachment and proliferation of osteoblastic cells on binary PP/hBN and ternary PP/hBN-20%nHA nanocomposites	Chan et al. [8]

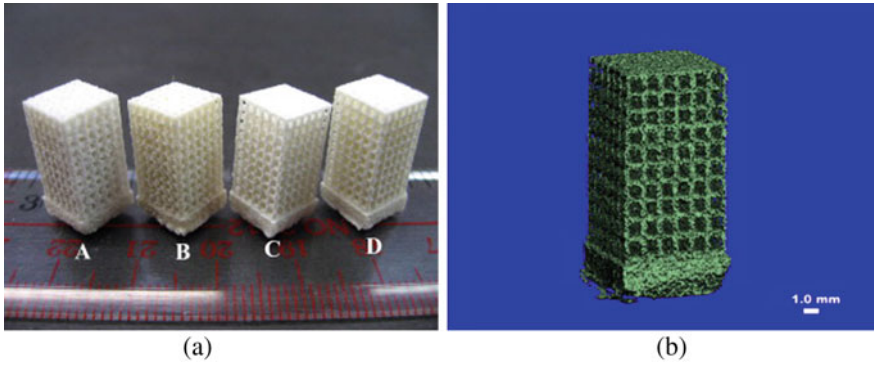


Fig. 6 Scaffolds produced by selective laser sintering **a** (A) PHBV; (B) Ca-P/PHBV; (C) PLLA; (D) CHAp/PLLA; Micro CT image of a Ca-P/PHBV scaffold **b** (Reprinted with permission from Duan et al. [17])

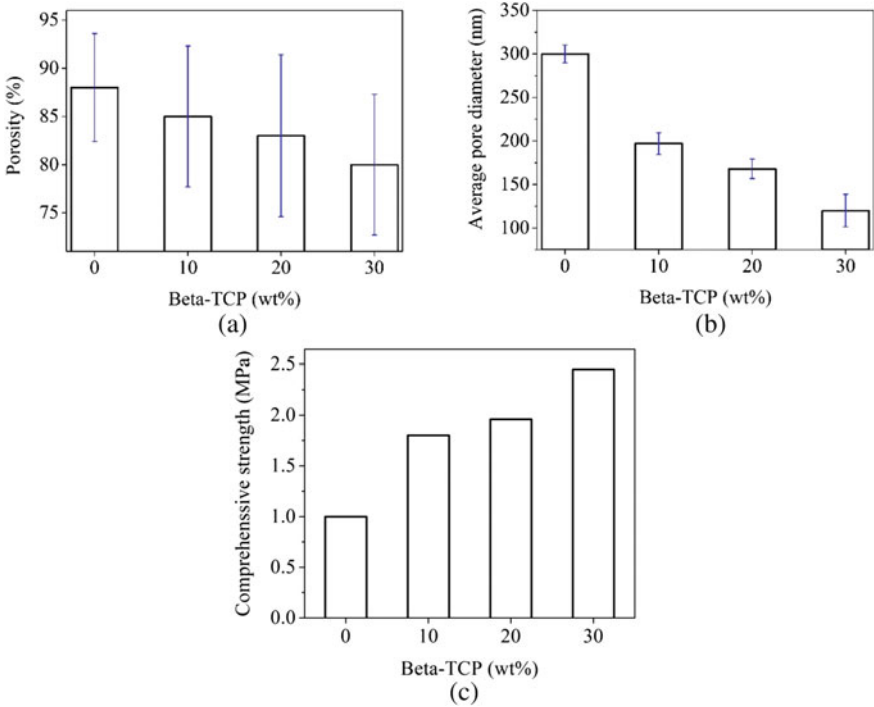


Fig. 7 Influence of β -tricalcium phosphate (β -TCP) bio-filler content on the porosity **(a)** average pore diameter **(b)** and compressive strength of GCT scaffolds ([40] adapted from Maji et al.)

3.2 Synthetic Polymeric Scaffolds

Examples of synthetic polymers used for orthopedic applications are unreinforced thermoplastic polymers (poly(para-phenylene)) (PPP) Di Rienzo et al. [14], poly(hydroxyethylmethacrylate) (P(HEMA)) and poly(hydroxyethylmethacrylate-co-methyl methacrylate) (P(HEMA-co-MMA)) loaded with HAp-cartilage powder (CP) and gelatin [25] (see Table 1).

A comparison between the influence of calcium phosphate (Ca-P) and carbonated hydroxyapatite (CHAp) on the biological properties of poly(hydroxybutyrate-co-hydroxyvalerate) (PHBV)/Ca-P and poly(L-lactic acid) (PLLA)/CHAp nanocomposite microspheres revealed that the improved cell proliferation and alkaline phosphatase activity were achieved only in the case of PHBV/Ca-P scaffold [17].

One current trend among researchers to produce scaffolds for orthopedic applications with adequate mechanic properties is to introduce nanofillers into biopolymeric formulations, such as nHAp [26], nanoparticles of titanium dioxide (nTiO₂) [15], nGO [19], and gold nanoparticles (AuNPs) [42]. Therefore, the effect of 10 wt% nHAp in an ultrahigh molecular weight polyethylene (UHMWPE) matrix was studied using a finite element analysis (FE analysis) and indicated that this bionanocomposite meets the shrinkage, warpage, wear volume, and yield strength properties and could be used for the manufacturing of hip prosthesis [26]. Specimens for further orthopedic implants fabricated by blending of high-density polyethylene (HDPE) with nano-graphene oxide (nGO) in amount ranging of 0.5–2.5 wt% showed good mechanical properties [19].

In another paper, Diez-Pascual et al. [15] reported that the introduction of titanium dioxide (TiO₂) nanoparticles into polyphenylsulfone (PPSU) led to an antibacterial biopolymeric nanocomposite with reduced the water absorption, increased the mechanical and thermal stability of the polymer.

Nekounam et al. [42] exploited the osteogenic and differentiation to bone lineage advantages of gold nanoparticles (AuNPs) to prepare electrical conductive scaffolds based on carbon nanofibers (CNF) obtained by electrospun of polyacrylonitrile (PAN) solution with gold nanoparticles (AuNPs) by two techniques. First is related to the blend electrospinning method, in which PAN solutions and AuNPs are processed by electrospinning, then the carbonization takes place, and the second, electrosprayed method, accordingly, AuNPs solutions were co-electrospun with PAN nanofibers. Both methods led to scaffolds with homogenous gold nanoparticle distribution and adequate biocompatibility demonstrated by MTT and LDH assays.

3.3 Hybrid Polymeric Scaffolds

Pradhan and Sahoo [47] explored the chicken eggshell (nano-CaO) as biofiller to improve the mechanical strength and thermal stability of CS grafted with poly (methyl methacrylate) (PMMA) bionanocomposites.

Another approach to induce the differentiation of mesenchymal stem cells (MSCs) into osteoblast cell is to introduce β -tricalcium phosphate (β -TCP), which is more osteo-conductive than HAp, into collagen/poly (ϵ -caprolactone) (PCL) [50].

Codreanu et al. [12] developed innovative bacterial cellulose-modified polyhydroxyalkanoates (PHB/BC) scaffolds and demonstrated their osteogenic potential in critical-size mouse calvaria defects.

3.4 Multifunctional Biopolymeric Nanocomposites

Current innovations in the materials for orthopedic applications envisage designing of multifunctional biopolymeric nanocomposites with both osteo-inductive and bioactive properties (antimicrobial activity) to protect implants of associated infections, majorly due to bacteria adhesion [2]. In this sense, Ballarre et al. [6] prepared silica-gentamicin (Si-Ge) nanoparticles and incorporated them into a biopolymeric solution containing chitosan and gelatin and coated Ti orthopedic implant with the obtained solution using electrophoretic deposition technique. The new coating of Ti implant showed both occurring of apatite-like deposits after 7 days of immersion in simulated body fluid (SBF) solution and antibacterial activity to *S. aureus* and *E. coli* strains.

Another innovative antimicrobial coating for stainless steel removable screws for bone or plate fixation which could contribute to prevent hospital infections at early implantation times were achieved from chitosan/gelatin/silica-gentamicin [4]. Promising natural bionanocomposites as alternative for regeneration of bone are lignocelulosic materials, which can provide a broad spectrum of antibacterial activity [2, 21].

4 Biomineralization

Controlled biomineralization activity of biomaterials helps avoiding the formation of fibrous capsule, an important issue in bone regeneration and osseo-integration.

An accelerated in bone fracture healing was investigated by Guo et al. [24] that prepared TiO₂/gelatin-chitosan hydrogel sample. The calcium assays in the hydrogel sample was quantified to 4.3 mg highlighting a high mineralization.

Zhang et al. [57] reported for the first time the growth of apatite on the surface specimens with dimension of (4 × 4) mm² prepared from poly(l-lactic acid) (PLLA)/octadecylamine-functionalized nanodiamond (ND-ODA). The biomineralization test was performed by incubation of specimens into SBF at 37 °C, pH 7.4, up to 6 weeks. The incorporation of 10 wt% ND-ODA into polymeric matrix resulted to increase of Ca/P ratio to 1.61 after 6 weeks of incubation. In another paper, the modification of TiO₂ nanoparticles with fluoride ions then its adding into silk fibroin (SF) matrix was evaluated in SBF buffered at 37 °C and pH 7.4 for 28 days [31].

Li et al. [37] realized a bioactive glass (BG)-based hybrid poly (citrate-siloxane) (PCS) elastomer nanocomposite with multifunctional properties for potential bone tissue regeneration, such as elastomeric behavior, bio-imaging tracking, osteogenic cellular response, biomineralization activity, as well as in vivo inflammatory response. Excellent biomineralization activity of PCS-BGN 20% nanocomposites has been proved by characteristic bands of P–O at 563, 603, and 1030 cm^{-1} in FTIR spectra and characteristic crystal plane at 31.8° (XRD) suggesting the formation of biological apatite nanocrystals.

5 Degradation of Biopolymeric Nanocomposites

The degradation of GCT porous scaffolds was studied by Maji et al. [40] using phosphate buffer saline (PBS) at 37 °C for up to 28 days. It was found that the degradation rate of gelatin/chitosan/ β -TCP (GCT) hybrid scaffolds took place by the hydrolysis of gelatin and enzymatic process of chitosan and depended on the ratio between organic/inorganic content, being decreased in the case of high content of in β -TCP. This behavior was explained by the authors by role of β -TCP to act as physical cross-linking sites.

Degradation of CS, CS/n-HAp bionanocomposite scaffolds without and with amine functional group by incubation for six weeks in 500 $\mu\text{g/mL}$ lysozyme in PBS was studied by Atak et al. [3]. The study revealed a weight loss up to 15% in the case of CS and CS/nHAp scaffolds, while CS/nHAp–NH₂ scaffolds reached 10% of total weight loss, due to the cross-linking amino group within the scaffold. In the case of SF/TiO₂–F scaffolds, a weight loss ranging from 2 to 5% was observed after 30 days of incubation in PBS medium [31]. This reduced degradation was explained by a compacted structure of SF/TiO₂–F nanocomposite scaffolds. The low degradation rate is a key indicator about the new bone growth.

Low-generation non-immunogenic and non-toxic poly(amidoamine) (PAMAM) dendrimers have been used as initiators to synthesize star-shaped poly(l-lactic acid (SS-PLLA)), which further act as building blocks to assemble nano- and/or mesoscopic structures, as well as to tune the possible surface functionalities and degradation rate [39]. The nanofibrous hollow SS-PLLA microspheres, excellent injectable cell carrier for cartilage regeneration in knee repair, were prepared using a surfactant-free emulsification process, being composed entirely of nanofibers with an average diameter of 160 ± 67 nm, the same scale as collagen fibers. The degradation rate of the nanofibrous hollow microspheres can be tailored by the molecular weight and molecular architecture of the SS-PLLA.

There are some problems with implants during wearing because of various particles formation [55]. Metallic wear particles are associated with adverse local tissue reactions (ALTR) being a significant clinical problem because they affect implant performance increasing of failure rates, so replacements are necessary to metal-on-metal hip and non-metal-on-metal dual modular neck total hip replacement. Bionanocomposites could be a solution.

6 Conclusions and Future Trends

The most used biopolymeric formulations for preparing of 3D scaffolds are bionanocomposites based on natural biopolymers or synthetic biopolymers and inorganic nanoparticles. The cutting-edge innovations in the scaffolds construction in orthopedic bone regeneration based on biopolymeric nanocomposites are notable when the integration of bone scaffolds and vascular networks takes place. High biocompatibility, proper cell attachment, adequate mechanical strength, together with low fabrication costs, *in vitro* degradation, and biomineralization tests are the most important properties for scaffolds. Tissue engineering should be based on a deep understanding of tissue formation and regeneration, to induce new functional properties of new materials rather than just to implant new spare parts.

Future trends in design of biopolymeric formulations for bone regenerations envisage the use of multifunctional biopolymeric nanocomposites that show both osteo-inductive and bioactive properties (antimicrobial activity) to protect implants of associated infections.

Ongoing research will reveal more details of the inherent qualities of biomaterials and their role in better integration of implants into host tissue or the near-ideal regeneration of host tissue.

References

1. Adithya SP, Sidharthan DS, Abhinandan R et al (2020) Nanosheets-incorporated biocomposites containing natural and synthetic polymers/ceramics for bone tissue engineering. *Int J Biol Macromol*. <https://doi.org/10.1016/j.ijbiomac.2020.08.053>
2. Afewerki S, Bassous N, Harb S et al (2020) Advances in dual functional antimicrobial and osteoinductive biomaterials for orthopedic applications. *Nanomedicine* 24:102143. <https://doi.org/10.1016/j.nano.2019.102143>
3. Atak BH, Buyuk B, Huysal M et al (2017) Preparation and characterization of amine functional nano-hydroxyapatite/chitosan bionanocomposite for bone tissue engineering applications. *Carbohydr Polym* 164:200–213. <https://doi.org/10.1016/j.carbpol.2017.01.100>
4. Aydemir T, Liverani L, Pastore JI et al (2020) Functional behavior of chitosan/gelatin/silica-gentamicin coatings by electrophoretic deposition on surgical grade stainless steel. *Mater Sci Eng C* 115:111062. <https://doi.org/10.1016/j.msec.2020.111062>
5. Babilotte J, Martin B, Guduric V et al (2020) Development and characterization of a PLGA-HA composite material to fabricate 3D-printed scaffolds for bone tissue engineering. *Mater Sci Eng C* 111334. <https://doi.org/10.1016/j.msec.2020.111334>
6. Ballarre J, Aydemir T, Liverani L et al (2020) Versatile bioactive and antibacterial coating system based on silica, gentamicin, and chitosan: improving early stage performance of titanium implants. *Surf Coat Technol* 381:125138. <https://doi.org/10.1016/j.surfcoat.2019.125138>
7. Bigham-Sadegh A, Oryan A (2015) Selection of animal models for pre-clinical strategies in evaluating the fracture healing, bone graft substitutes and bone tissue regeneration and engineering. *Connect Tissue Res* 56(3):175–194. <https://doi.org/10.3109/03008207.2015.1027341>
8. Chan KW, Wong HM, Yeung KWK et al (2015) Polypropylene biocomposites with boron nitride and nanohydroxyapatite reinforcements. *Materials* 8:992–1008. <https://doi.org/10.3390/ma8030992>

9. Chandra G, Pandey A (2020) Preparation strategies for Mg-alloys for biodegradable orthopaedic implants and other biomedical applications: a review. *IRBM*. <https://doi.org/10.1016/j.irbm.2020.06.003>
10. Chen PY, Toroian D, Pa P et al (2011) Minerals form a continuum phase in mature cancellous bone. *Calcif Tissue Int* 88:351–361. <https://doi.org/10.1007/s00223-011-9462-8>
11. Christy PN, Basha SK, Kumari VS et al (2020) Biopolymeric nanocomposite scaffolds for bone tissue engineering applications—a review. *J Drug Deliv Sci Technol* 55:101452. <https://doi.org/10.1016/j.jddst.2019.101452>
12. Codreanu A, Balta C, Herman H et al (2020) Bacterial cellulose-modified polyhydroxyalkanoates scaffolds promotes bone formation in critical size calvarial defects in mice. *Materials* 13(6):1433. <https://doi.org/10.3390/ma13061433>
13. Di Lullo GA, Sweeney SM, Korkko J et al (2002) Mapping the ligand-binding sites and disease-associated mutations on the most abundant protein in the human, type I collagen. *J Biol Chem* 277(6):4223–4231
14. Di Rienzo AL, Yakacki CM, Frensemeier M et al (2014) Porous poly(para-phenylene) scaffolds for load-bearing orthopedic applications. *J Mech Behav Biomed Mater* 30:347–357. <https://doi.org/10.1016/j.jmbbm.2013.10.012>
15. Diez-Pascual AM, Diez-Vicente AL (2014) Effect of TiO₂ nanoparticles on the performance of polyphenylsulfone biomaterial for orthopaedic implants. *J Mater Chem B* 2(43):7502–7514. <https://doi.org/10.1039/c4tb01101e>
16. Dinoro J, Maher M, Talebian S et al (2019) Sulfated polysaccharide-based scaffolds for orthopaedic tissue engineering. *Biomaterials* 214:119214. <https://doi.org/10.1016/j.biomaterials.2019.05.025>
17. Duan B, Wang M, Zhou WY et al (2010) Three-dimensional nanocomposite scaffolds fabricated via selective laser sintering for bone tissue engineering. *Acta Biomater* 6(12):4495–4505. <https://doi.org/10.1016/j.actbio.2010.06.024>
18. Duer MJ (2015) The contribution of solid-state NMR spectroscopy to understanding biomineralization: atomic and molecular structure of bone. *J Magn Reson* 253:98–110. <https://doi.org/10.1016/j.jmr.2014.12.011>
19. Faisal N (2020) Mechanical behavior of nano-scaled graphene oxide reinforced high-density polymer ethylene for orthopedic implant. *Biointerface Res Appl Chem* 10(6):7223–7233. <https://doi.org/10.33263/BRIAC106.72237233>
20. Farghali RA, Fekry AM, Ahmed RA et al (2015) Corrosion resistance of Ti modified by chitosan–gold nanoparticles for orthopedic implantation. *Int J Biol Macromol* 79:787–799. <https://doi.org/10.1016/j.ijbiomac.2015.04.078>
21. Fernandes EM, Pires RA, Mano JF et al (2013) Bionanocomposites from lignocellulosic resources: properties, applications and future trends for their use in the biomedical field. *Prog Polym Sci* 38(10–11):1415–1441. <https://doi.org/10.1016/j.progpolymsci.2013.05.013>
22. Gao C, Peng S, Feng P et al (2017) Bone biomaterials and interactions with stem cells. *Bone Res* 5:17059. <https://doi.org/10.1038/boneres.2017.59>
23. Guo M, Li X (2016) Development of porous Ti6Al4V/chitosan sponge composite scaffold for orthopedic applications. *Mater Sci Eng C* 58:1177–1181. <https://doi.org/10.1016/j.msec.2015.09.061>
24. Guo N, Zhang L, Wang J et al (2020) Novel fabrication of morphology tailored nanostructures with Gelatin/Chitosan co-polymeric bio-composited hydrogel system to accelerate bone fracture healing and hard tissue nursing care management. *Process Biochem* 90:177–183. <https://doi.org/10.1016/j.procbio.2019.11.016>
25. Haroun AA, Migonney V (2010) Synthesis and in vitro evaluation of gelatin/hydroxyapatite graft copolymers to form bionanocomposites. *Int J Biol Macromol* 46(3):310–316. <https://doi.org/10.1016/j.ijbiomac.2010.01.005>
26. Heidari BS, Davachi SM, Moghaddam AH et al (2018) Optimization simulated injection molding process for ultrahigh molecular weight polyethylene nanocomposite hip liner using response surface methodology and simulation of mechanical behavior. *J Mech Behav Biom Mater* 81:95–105. <https://doi.org/10.1016/j.jmbbm.2018.02.025>

27. Hickey DJ, Ercan B, Chung S et al (2014) MgO nanocomposites as new antibacterial materials for orthopedic tissue engineering applications. In: 40th annual northeast bioengineering conference (NEBEC), Boston, MA, pp 1–2. <https://doi.org/10.1109/NEBEC.2014.6972815>
28. Hu YH, Hu RY, Lei PF (2019) Bone defects in revision total knee arthroplasty and management. *Orthop Surg* 11:15–24. <https://doi.org/10.1111/os.12425>
29. Hutten D (2013) Femorotibial bone loss during revision total knee arthroplasty. *Orthop Traumatol Surg Res* 99:S22–S33. <https://doi.org/10.1016/j.otsr.2012.11.009>
30. Jia B, Yang H, Han Y et al (2020) In vitro and in vivo studies of Zn–Mn biodegradable metals designed for orthopedic applications. *Acta Biomater* 108:358–372. <https://doi.org/10.1016/j.actbio.2020.03.009>
31. Johari N, Madaah Hosseini HR, Samadikuchaksaraei A (2018) Novel fluoridated silk fibroin/TiO₂ nanocomposite scaffolds for bone tissue engineering. *Mater Sci Eng C* 82:265–276. <https://doi.org/10.1016/j.msec.2017.09.001>
32. Jovic TH, Jessop JM, Al-Sabah A et al (2018) Chapter 12-The clinical need for 3D printed tissue in reconstructive surgery. In: Thomas DJ, Jessop ZM, Whitaker IS (eds) 3D bioprinting for reconstructive surgery, techniques and applications. Woodhead Publishing. ISBN 978-0-08-101103-4
33. Karsenty G, Park RW (1995) Regulation of type I collagen genes expression. *Int Rev Immunol* 12(2–4):177–185
34. Kern B, Shen J, Starbuck M, Karsenty G (2001) Cbfa1 contributes to the osteoblast-specific expression of type I collagen genes. *J Biol Chem* 276(10):7101–7107. <https://doi.org/10.1074/jbc.M006215200>
35. Khalajabadi SZ, Yajid MAM, Haji Abu AB (2018) In vitro biocorrosion, antibacterial and mechanical properties of silicon-containing coatings on the magnesium-hydroxiapatite nanocomposite for implant applications. *Mater Chem Phys* 214:449–463. <https://doi.org/10.1016/j.matchemphys.2018.04.118>
36. Kołodziejaska B, Kaflak A, Kolmas J (2020) Biologically inspired collagen/apatite composite biomaterials for potential use in bone tissue regeneration-a review. *Materials* 13:1748. <https://doi.org/10.3390/ma13071748>
37. Li Y, Guo Y, Niu W et al (2018) Biodegradable multifunctional bioactive glass-based nanocomposite elastomers with controlled biomineralization activity, real-time bioimaging tracking, and decreased inflammatory response. *ACS Appl Mater Interfaces* 10:17722–17731. <https://doi.org/10.1021/acsami.8b04856>
38. Liao CZ, Wong HM, Yeung KWK et al (2014) The development, fabrication and mechanical characterization of polypropylene composites reinforced with carbon nanofiber and hydroxypapatite nanorod hybrid fillers. *Int J Nanomed* 9:1299–1310. <https://doi.org/10.2147/IJN.S58332>
39. Liu X, Jin X, Ma PX (2011) Nanofibrous hollow microspheres self-assembled from star-shaped polymers as injectable cell carriers for knee repair. *Nat Mater* 10(5):398–406. <https://doi.org/10.1038/nmat2999>
40. Maji K, Dasgupta S, Pramanik K et al (2018) Preparation and characterization of gelatin-chitosan-nano β -TCP based scaffold for orthopaedic application. *Mater Sci Eng C* 86:83–94. <https://doi.org/10.1016/j.msec.2018.02.001>
41. McGovern JA, Griffin M, Hutmacher DW (2018) Animal models for bone tissue engineering and modelling disease. *Dis Models Mech* 11:dmm033084. <https://doi.org/10.1242/dmm.033084>
42. Nekounam H, Allahyari Z, Gholizadeh S et al (2020) Simple and robust fabrication and characterization of conductive carbonized nanofibers loaded with gold nanoparticles for bone tissue engineering applications. *Mater Sci Eng C*:111226. <https://doi.org/10.1016/j.msec.2020.111226>
43. Nistor M-T, Vasile C, Tatia R et al (2018) Hybrid collagen/pNIPAAm hydrogel nanocomposites for tissue engineering application. *Colloid Polym Sci* 296:1555–1571. <https://doi.org/10.1007/s00396-018-4367-y>

44. Pandey A, Midha S, Sharma RK et al (2018) Antioxidant and antibacterial hydroxyapatite-based biocomposite for orthopedic applications. *Mater Sci Eng C* 88:13–24. <https://doi.org/10.1016/j.msec.2018.02.014>
45. Paprosky WG, Perona PG, Lawrence JM (1994) Acetabular defect classification and surgical reconstruction in revision arthroplasty. A 6-year follow-up evaluation. *J Arthroplasty* 9(1):33–44. [https://doi.org/10.1016/0883-5403\(94\)90135-x](https://doi.org/10.1016/0883-5403(94)90135-x)
46. Pereira H, Cengiz IF, Maia FR et al (2020) Physicochemical properties and cytocompatibility assessment of non-degradable scaffolds for bone tissue engineering applications. *J Mech Behav Biomed Mater* 103997. <https://doi.org/10.1016/j.jmbbm.2020.103997>
47. Pradhan AK, Sahoo PK (2017) Synthesis and study of thermal, mechanical and biodegradation properties of chitosan-g-PMMA with chicken egg shell (nano-CaO) as a novel bio-filler. *Mater Sci Eng C* 80:149–155. <https://doi.org/10.1016/j.msec.2017.04.076>
48. Salgado AJ, Coutinho OP, Reis RL (2004) A review. Bone tissue engineering: state of the art and future trends. *Macromol BioSci* 4:743–765. <https://doi.org/10.1002/mabi.200400026>
49. Silvio LDI, Jayakumar P (2009) Chapter 13-Cellular response to osteoinductive materials in orthopaedic surgery. In: Di Silvio L (ed) *Cell response biomaterials*. Woodhead Publishing Series in Biomaterials, pp 313–343
50. Shanjani Y, Kang Y, Zarnescu L et al (2017) Endothelial pattern formation in hybrid constructs of additive manufactured porous rigid scaffolds and cell-laden hydrogels for orthopedic applications. *J Mech Behav Biomed Mater* 65:356–372. <https://doi.org/10.1016/j.jmbbm.2016.08.037>
51. Qiu YY, Yan CH, Chiu KY et al (2011) Review article: bone defect classifications in revision total knee arthroplasty. *J Orthop Surg (Hong Kong)* 19:238–243. <https://doi.org/10.1177/230949901101900223>
52. Tae Young A, Kang JH, Kang DJ et al (2016) Interaction of stem cells with nano hydroxyapatite-fucoidan bionanocomposites for bone tissue regeneration. *Int J Biolog Macromol* 93:1488–1491. <https://doi.org/10.1016/j.ijbiomac.2016.07.027>
53. Valtanen RS, Yang YP, Gurtner GC et al (2020) Synthetic bone tissue engineering graft substitutes: what is the future? *Injury*. <https://doi.org/10.1016/j.injury.2020.07.040>
54. Weng W, Biesiekierski A, Li Y et al (2019) Effects of selected metallic and interstitial elements on the microstructure and mechanical properties of beta titanium alloys for orthopedic applications. *Materialia* 6:100323. <https://doi.org/10.1016/j.mtla.2019.100323>
55. Xia Z, Ricciardi BF, Liu Z et al (2017) Nano-analyses of wear particles from metal-on-metal and non-metal-on-metal dual modular neck hip arthroplasty. *Nanomed Nanotechnol Biol Med* 13(3):1205–1217. <https://doi.org/10.1016/j.nano.2016.11.003>
56. Xu W, Hu W, Li M et al (2006) Sol-gel derived HA/TiO₂ double coatings on Ti scaffolds for orthopaedic applications. *Trans Nonferrous Met Soc China* 16(Supplement 1):s209–s216. [https://doi.org/10.1016/S1003-6326\(06\)60177-5](https://doi.org/10.1016/S1003-6326(06)60177-5)
57. Zhang Q, Mochalin VN, Neitzel I et al (2012) Mechanical properties and biomineralization of multifunctional nanodiamond-PLLA composites for bone tissue engineering. *Biomaterials* 33(20):5067–5075. <https://doi.org/10.1016/j.biomaterials.2012.03.063>

Natural Polymer-Based Composite Wound Dressings



Shreya Sharma, Bhasha Sharma, Shashank Shekhar, and Purnima Jain

Abstract Wound repair is a complicated and firmly synchronized physiological process, entailing the activation of various cell types throughout each succeeding step (homeostasis, inflammation, proliferation, and tissue remodeling). Any impairment within the correct sequence of the healing events could prompt incessant injuries, with probable denouement on the patients' quality of life, and consequential failures on wound care management. Contemporary wound healing treatments like gauzes and bandages primarily are pivoted on passively cushioning the wound and do not proffer properties that escalate the rate of wound healing. Even though these strategies are resilient at safeguarding any infection after application, they are futile at healing a heretofore infected wound or spurring tissue regeneration. The burgeoning of next-generation wound healing treatments aid in enhancing patient care pathways and clinical outcomes. Natural polymers play a significant role in wound care. They deliver a versatile and tunable platform to design the germane extracellular matrix competent to succor tissue regeneration, while contrasting the onset of adverse events. Our goal is to scrutinize the evolution of natural polymers in wound dressing from traditional to modern-day treatment methods. The chief characteristics and properties of a natural polymer, which is widely utilized as biomaterial, are presented. Properties of composite material with peculiar heed on their applications in the skin tissue repair field are discussed. Finally, the unmet needs and developmental perspectives of the new generations of environmentally friendly, naturally derived, smart wound dressings are addressed in light of future research.

Keywords Natural polymer · Biodegradable · Composites · Wound healing · Wound dressing · Sustainability · Biomedical

S. Sharma · B. Sharma (✉) · S. Shekhar · P. Jain
Department of Chemistry, Netaji Subhas University of Technology, Dwarka Sec-3, 110078
Dwarka, India

© The Author(s), under exclusive license to Springer Nature Switzerland AG 2022
M. S. Hasnain et al. (eds.), *Polymeric and Natural Composites*,
Advances in Material Research and Technology,
https://doi.org/10.1007/978-3-030-70266-3_13

401

1 Introduction

The skin, the human body’s largest organ, serves as a protective shield against the strident environment. Perpetuating the virtue of this deterrent to interdict the intrusion of pathogens and toxins is inevitably pre-eminent for survival. To subsist with the wonted traumas of our world, the skin has adapted an astounding proficiency for healing that depends on the joint effort of a number of cellular and tissue types. The wound damages blood vessels underneath the skin, causing them to leak. The leaking blood vessel forms a clot that plugs the wound to bestow an ephemeral shield. Recruitment of immune cells to the wound is essential for clearing debris and limiting infections. Epithelial cells, constituting the outermost or epidermal layer of the skin, proliferate into the wound bed on a scaffold furnished by underlying dermal cells. These coordinated cellular efforts ascertain that the denuded surface is rapidly sealed or re-epithelialized [1]. Figure 1 depicts different phases of wound healing process. Additionally, the dynamic relationship between skin and microbiome is another major contributor to the outcome of the process [2]. The science of wound healing is reported (since 2000 BC) as “three healing gestures”—wound cleaning, applying plaster, and bandaging the wound [3].The majority of the skin lesions heal within a predictable time and are as a result of unexpected accidents or surgical injury. Howbeit, non-healing, chronic wounds and ulcers corollary of burns, or decline in the healing capacity of skin may have a catastrophic influence on individual’s life, spawning pain, diminution of skin function, and in some cases even death.

So as to address all facets of wound care management, suitable materials for wound dressing have been utilized as hydrogels, foams, films, hydrocolloids, or scaffolds. An ideal wound dressing should cohere to the wounded tissue, sustain moist balanced state, permit the exchange of oxygen, and protect from pathogenic intrusion, hence establishing a microenvironment to escalate the healing process. To date, wound

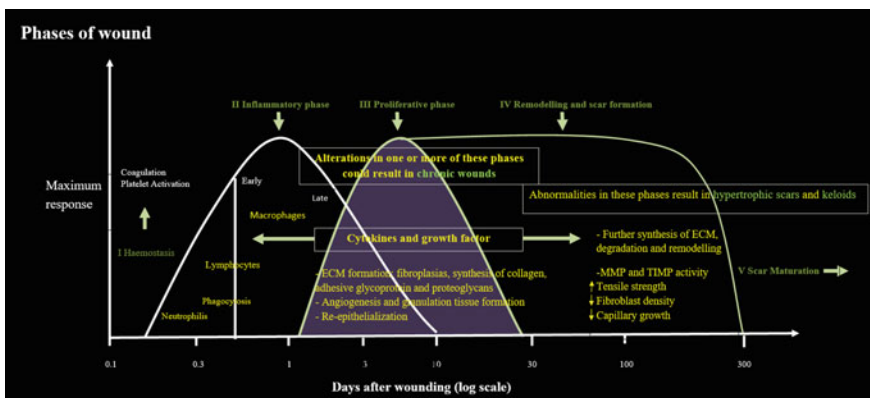


Fig. 1 Phases of wound healing process [ECM: Extracellular matrix, MMP: Metalloproteinases, TIMP: Tissue inhibitors of metalloproteinases]

dressings are categorized as permanent skin substitutes and temporary dressings. The impermanent dressings should extend wound exudate absorption and shielding until wound cessation, while skin substitutes are anticipated to coordinate with the host skin and quicken the recovery cycle [4]. Both synthetic and natural polymers are employed for wound dressing applications. Synthetic polymer, however, are competent only for superficial wounds and abrasions, bestowing paucity of few significant characteristics including; low permeability, absorption, and adherence. Natural polymers including chitosan, cellulose, silk, heparin, keratin, fibrin, alginate, gelatin, fucoidan, etc. similar to macromolecules identified by human body are extensively employed in skin tissue engineering because of their biodegradability, biocompatibility, easy resorption, and capacity for regeneration of the injured tissue [5]. Natural polymers manifest reasonably low mechanical strength in contrast to synthetic polymers and are ordinarily susceptible to microbial contamination. The development and implementation of novel technologies such as cross-linking or blending may enhance the properties of these naturally derived polymers. The composites assist in achieving superior biochemical and mechanical properties over its individual components.

The overarching objective of the chapter is to discuss key aspects of wound healing and to highlight the recent advances in naturally derived polymer composites that contributed to a paradigm shift in wound dressing.

2 Novel Mechanism of Action of Wound Healing

A crucial step during the healing process is the instigation of wound exudate, imitating natural balm that seal wounds from microbes and debris. Exudate production is paramount during the inflammation and proliferation phase of the curing process, but its denouement is not completely perceived. Healing stage wound type, origin, location, and size are the determining factors for variation in the volume of the plasma-derived exudate. Chronic wound *exudate* has a different composition from that of an *acute wound*. *Acute exudates have higher protein content and essential nutrients for epithelial cells in addition to endogenous proteolytic enzymes and their inhibitors* in an exquisite parity, which aid in degradation of arts of extracellular matrix and wound bed readiness before wound closure and remodeling. Chronic wound exudate in contrast, contain copious proteinases that delay or even obstruct the proliferation of key cells embroiled in the wound healing process. Utilization of wound dressings focuses on the expulsion of unreasonable exudate, debris and potential pathogens from the injury bed, while perpetuating the optimal moisture balance indispensable for cell recruitment and wound healing in due time [6].

A noteworthy facet, ordinarily not exploited, is the mechanical stress at the injury site that incredibly impacts the rate and essence of recuperating. Skin mechanical properties assume a radical job in both intact and harmed skin with involvement in the wound healing process. Several paper report that skin wounds were more susceptible to the development of a scar under mechanical stress during the recuperating cycle [7–9]. These observations have affirmed surgeons to reduce tension

post-surgery, at the incision arena [10, 11]. The cells answerable for stress identification in the connective tissue of the injury bed, for example, fibroblasts and myofibroblasts transduce it into a physiological reaction [12]. A few *in vitro* and *in vivo* examinations have indicated that escalated tension aggrandized their multiplication [13], repressed fibroblasts apoptosis [14] activated several signaling pathways that instigate an uneven accumulation of extracellular matrix.

3 Types of Dressings

Wound management is a dynamic skill, and dressing selection is both art and a science. When choosing dressings, the choice should be made on rationalization of medicaments, the timeline for care and how progression and denouement will be computed. Present-day dressings intent to proffer strengthened functionality, for instance, the colossal potential for exudate management, within a nadir contour of product with extended wear time [15]. The most commonly used modern dressings (Table 1) in clinical practice include hydrogel dressings, hydrofiber dressings, hydrocolloid dressings, foam dressings, medicated and non-mediated dressings, composite dressings, superabsorbent dressings, and films [16–18].

4 Advances in Natural Polymeric Biomaterials and Composites

Extracellular matrix plays a pivotal role in wound healing and tissue homeostasis, and therefore designing supportive membranes for cells similar to their native niche is imperative for optimizing cell behaviors. Natural polymers imitate the structural, biomechanical, and biochemical functionalities of extracellular matrix and have an immanent bioactivity and biocompatibility, forming marvelous candidates for the development of matrices for wound dressing applications [19]. Natural polymers bestow extracellular matrix support (gelatin, hyaluronic acid, and collagen), present cell-recognition domains and biomolecules binding sites (keratin and silk fibroin), and may possess immanent anti-inflammatory and antibacterial properties (alginate and chitosan) [20]. The preponderant natural polymers employed in wound healing are collagen, alginate, glucan, dextran, hyaluronic acid, cellulose, chitosan, gelatin, silk fibroin, and keratin. Every aforementioned polymers demonstrate efficacious properties indispensable for wound healing. Natural polymer composites induced wound healing is illustrated in Fig. 2.

Table 1 Selection of suitable wound dressing for various wounds (Type, properties, advantages, drawbacks, and applications)

S. No.	Type	General description and physical properties	Advantages and disadvantages	Indication and method of use	Contraindications and precautions	Suitable conditions
1.	Hydrogels	<ul style="list-style-type: none"> - Composed of three dimensional network of complex hydrophilic polymers with high (90%) water content - Expand in water - Commonly accessible in three forms including sheet hydrogel, impregnated gauze, and amorphous gel - Properties: Clear and transparent, moisturizing, rehydrate eschar, and aid autolytic debridement 	<ul style="list-style-type: none"> - Advantages include; <ol style="list-style-type: none"> (1) Wound monitoring without removal of dressing (2) Removal of necrotic tissue without damage to epithelial cells or granulation (3) Facilitate cell migration and absorption of exudate (4) Allow adjustment of degradation rate which renders them suitable for use as drug carrier and biologically active substance, - Disadvantages include; <ol style="list-style-type: none"> (1) Poor microbial barrier 	<ul style="list-style-type: none"> - Suitable for wounds with minimal-to-moderate exudate - Endure for no longer than three days - Safe on neonatal skin. - Marked cooling and soothing effect on skin - Amorphous gels may be covered with secondary dressings such as films or foams. 	<ul style="list-style-type: none"> - Health professionals to be aware of allergic reactions in older population caused by propylene glycol present in amorphous gels - Irrigation with saline solution for easy removal 	<ul style="list-style-type: none"> Skin tears, surgical wounds, burns, pressure ulcers, radiation dermatitis, etc.

(continued)

Table 1 (continued)

S. No.	Type	General description and physical properties	Advantages and disadvantages	Indication and method of use	Contraindications and precautions	Suitable conditions
2.	Hydrofibers	<ul style="list-style-type: none"> - Composed of nonwoven sodium carboxymethyl cellulose spun into fibers - Variant on hydrocolloid with extra absorbent properties - Form a firm gel in contact with fluid and therefore exhibit properties similar to alginates. -Absorb 25 folds its own weight in fluid 	<ul style="list-style-type: none"> - Advantages include: <ol style="list-style-type: none"> (1) Aids vertical wicking that protects periwound (2) Removal of necrotic tissue without damage to epithelial cells or granulation - Disadvantages include; <ol style="list-style-type: none"> (1) Non-adherence and requirement of secondary dressings to endure 	<ul style="list-style-type: none"> - Suitable for wounds with moderate to excessive exudate - Can be kept in place until dressing is saturated - Should gently rinsed away at time of dressing change 	<ul style="list-style-type: none"> - Should not be used in dry wounds - When used with mild exudates, irrigate with saline solution or sterile water to minimize the bed trauma and associated pain 	<ul style="list-style-type: none"> Postsurgical wounds, leg ulcer debridement, partial thickness burns in pediatrics

(continued)

Table 1 (continued)

S. No.	Type	General description and physical properties	Advantages and disadvantages	Indication and method of use	Contraindications and precautions	Suitable conditions
3.	Hydrocolloids	<ul style="list-style-type: none"> - Composed of absorptive ingredients that form gel(gelatin, pectin, carboxymethylcellulose, etc.) - Occlusive, absorbent and semipermeable to vapor 	<ul style="list-style-type: none"> - Advantages include: <ol style="list-style-type: none"> (1) Aid autolytic debridement (2) Moisture retention and pain free removal. (3) Barrier to entry of oxygen, water, and bacteria and therefore helps in facilitation of angiogenesis and granulation (4) Reduction in wound surface pH that further inhibits bacterial growth - Disadvantages include: <ol style="list-style-type: none"> (1) Potential for anaerobic bacteria to grow in a hypoxic environment (2) Not appropriate for deeper wounds, specially wounds with infection that require oxygen to enhance the healing rate 	<ul style="list-style-type: none"> - Appropriate for partial- and full thickness- acute and chronic wounds with minimal-to-moderate exudate - Adhere well to high friction areas, including sacrum and heels - May produce a distinctive odor in some cases, indicative of product breakdown and not infection 	<ul style="list-style-type: none"> - Should not be used in dry and high exudate content wounds - Regular wound tissue assessment to ascertain the discontinuation of dressing before hypergranulation occurs - Hydrocolloids with waterproof backing are not advised on clinically infected wounds 	Pressure injuries, ulcers (diabetic foot ulcer, chronic venous ulcer), partial- and split- thickness wounds

(continued)

Table 1 (continued)

S. No.	Type	General description and physical properties	Advantages and disadvantages	Indication and method of use	Contraindications and precautions	Suitable conditions
4.	Foam	<ul style="list-style-type: none"> - Semipermeable, either hydrophobic or hydrophilic with a bacterial barrier - Made from polyurethane or are silicone-based 	<ul style="list-style-type: none"> - Advantages include; <ol style="list-style-type: none"> (1) Proffer thermal insulation to the wound, create a moist wound environment, are nonadherent, and allow atraumatic dressing removal. Skin maceration avoided due to excess exudate absorption. (2) Do not need frequent changes due to their properties that conform to wound shape, reduce dead space - Disadvantages include: <ol style="list-style-type: none"> (1) Increased cost due to the need of secondary dressings in cavity foam adhesive (non-adhesive). (2) Ingrowth of newly formed tissue due to infrequent changes that may result in shearing trauma upon removal. (3) Set size of the foam product may be limited by the size of the wound 	<ul style="list-style-type: none"> - Principally employed as primary dressings and secondary dressings with hydrogel or alginate dressing 	<ul style="list-style-type: none"> - Unfit for use in necrotic wounds, dry wounds, hard eschar and wounds requiring frequent review - Tubular retention bandages or light weight cohesive bandages to fix foam dressing in place proffer a safer option in older population 	<p>Chronic wounds, wound-shape cavities, deep ulcers, infected wounds</p>

(continued)

Table 1 (continued)

S. No.	Type	General description and physical properties	Advantages and disadvantages	Indication and method of use	Contraindications and precautions	Suitable conditions
5.	Films	<ul style="list-style-type: none"> - Composed of adhesive, porous, and thin transparent polyurethane. - Properties: transparent, semipermeable, and vary in size and thickness 	<ul style="list-style-type: none"> - Advantages include; <ol style="list-style-type: none"> (1) Wound monitoring without removal of dressing (2) Easily conforms to the body, enable moisture evaporation, reduction in pain, and proffer barrier to external contamination (3) Enable autolytic debridement of necrotic wounds and create a moist healing environment for granulating wounds - Disadvantages include; <ol style="list-style-type: none"> (1) Traumatic on removal (2) Excessive pooling of exudate when used on heavily exuding wounds 	<ul style="list-style-type: none"> - Frequency of dressing change is reliant on wound location, type and size, and may be left unchanged for up to 7 days - Barrier polymer films should be employed for protection of periwound skin 	<ul style="list-style-type: none"> - Clinicians should be cautious in applying and removing films from fragile skin to avoid skin damage 	<ul style="list-style-type: none"> Radiation induced skin wounds, epithelializing wounds, and superficial wounds with limited exudate
6.	Superabsorbents	<ul style="list-style-type: none"> - Reduce PMN elastase (biochemical marker for pathologic granulocyte stimulation) concentration and inhibit microbial growth 	<ul style="list-style-type: none"> - Advantages include; <ol style="list-style-type: none"> (1) Reduction in periwound skin maceration, irritation, and inflammation 			<ul style="list-style-type: none"> Moderate to highly exuding wounds, surgical incisions, lacerations, abrasions, burns, donor or skin graft sites

(continued)

Table 1 (continued)

S. No.	Type	General description and physical properties	Advantages and disadvantages	Indication and method of use	Contraindications and precautions	Suitable conditions
7.	Medicated	<ul style="list-style-type: none"> - Therapeutic agents are incorporated for quick and better recovery of wounds - Antimicrobials are employed for prevention of infections, supplements including minerals and vitamins for removal of dead tissue, growth factors for revitalization of damaged tissues 	<ul style="list-style-type: none"> - Advantages include; <ol style="list-style-type: none"> (1) Microbes at surface of wound are eliminated 	<ul style="list-style-type: none"> - Antimicrobials to be employed only when bioburden is a barrier to healing - Choice must be influenced by the specificity and efficacy of the agent, its cytotoxicity to human cells, its potential to select resistant strains and its allergenicity 	-	Infectious wounds

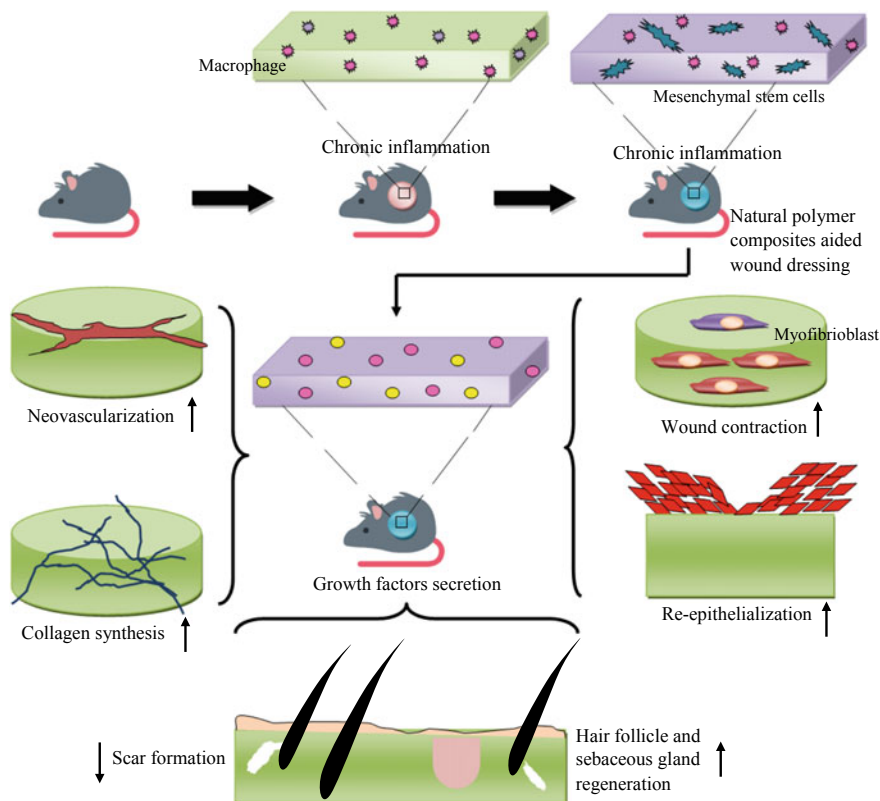


Fig. 2 Natural polymer composites induced wound healing

4.1 Collagen-Based Wound Dressings

Collagen is the most copious extracellular matrix macromolecule and is the chief integrant that delivers structural integrity in human skin. Production of collagen molecules by fibroblasts, at the time of wound healing, stimulates the development of new tissue and wound debridement. Collagen can also bind excess proteases, free radicals, inflammatory cytokines that are widespread in wound bed. As animal derivatives may be liable for allergies and pathogen transmission, an alternative is established by collagen from heterologous expression in insect, and yeast cells [5, 20]. Collage-based wound dressings have been recently recognized in modifying macrophage inflammatory response. Enhanced wound macrophage function and epithelialization deliver a precious archetype addressing significance of collagen based dressings [21]. Collagen based hydrogels have procured considerable admiration in wound healing applications. Howbeit, conventional collagen hydrogel are crippled due to the presence of non-reversible bonds. Self-healing collagen-based hydrogel based on dynamic covalent chemistry are able to repair wounds and

possess superior tissue regeneration ability [22]. Polymer-nanoparticle composites have been extensively used because of unique features endowed as a result of high surface to volume ratio of the particle and versatility and tenability of the materials' physicochemical properties [2, 23]. Silica-collagen encapsulated with drugs—rifampicin and gentamicin demonstrated medicated dressing to prevent bacterial infections in chronic wounds [24]. *Aloe vera* and ZnO nanoparticles incorporated Zein/PCL/Collagennano fiber exhibited enhanced mechanical an antibacterial activity, revealing promising scaffolds for wound healing issues [25].

4.2 Alginate-Based Wound Dressings

Alginate, a polysaccharide with homopolymeric blocks of 1,4-linked β -d-mannuronic and α -l-guluronic residues is mostly abundant in *brown algae* and some bacteria. The characteristic gelation property enables ionic crosslinking upon exposure to divalent ions, giving rise to a biocompatible 3D polymeric cross-linked scaffold [5, 20]. Alginates deliver a highly absorbent, moist environment to the wound to cease blood flow from wounded vasculature. Ion exchange between sodium ions of blood and calcium ions of the polysaccharide causes the fiber to swell and then partly dissolve to form gel. The gel proffers a moist environment and aids the natural healing process in the removal of necrotic tissue. The role of different counter cations for a series of ammonium salts of alginate have revealed the contribution of different features including branching structure, charge density, molecular weight, linearity, hydrophilicity, etc. in anti-hemolytic, antimicrobial efficacy, and cytotoxicity of the dressing [26]. Healing potential of alginate has been recently utilized to deliver moxifloxacin loaded hydrogel for better wound care. The sterile and mucoadhesive nature of the dressings coupled with a controlled and sustained release of antibiotic drug paved path for future research [27].

4.3 Glucan-Based Wound Dressings

β -Glucans isolated from fungi, grain, and yeast manifest the capability of the formation of single and triple-helical resilient gel structures. α -Glucans biosynthesized from starch by the ubiquitous yeast-like fungus *Aureobasidium pullulans*. Both β - and α -Glucans have been employed in wound healing tools because of their non-cytotoxic, quick hemostatic, and antimicrobial characteristics [28–31].

4.4 Dextran-Based Wound Dressings

The non-toxic, hydrophilic polysaccharide composed of linear α -1,6-linked d-glucopyranose residues is resilient to protein adsorption and cell adhesion. Modifications in the polymer backbone tune the discrete properties of biomaterial making them attractive candidates for curing wounds [32–34].

4.5 Cellulose-Based Wound Dressings

Cellulose is utilized as healing matrix for reducing pain and shortening the healing time in chronic wound dressings. The polymers stimulate epithelialization and granulation process for partial and full thickness wounds. Bacterial cellulose, specifically, have been utilized in interesting wound healing tools because of non-toxicity, inability to cause allergies, and prevention of physical rejections. Bacterial cellulose gel films serve as a mechanical barrier, shielding the wound surface from infection and rapid drying. Successful use of bacterial cellulose have been addressed in several publications. However, the polymers require the impregnation of other materials to exhibit antimicrobial activities. Excellent water holding capacity and porosity aids in easy absorption and slow release of the antimicrobial solution. Antimicrobial and wound healing properties of bacterial cellulose gel film and *Bacillus subtilis* has been investigated for delivery of universal wound coating and sanitary hygienic product [35]. Bacterial cellulose impregnated with ϵ -poly-L-Lysine, a non-toxic biopolymer, has been studied for antibacterial wound dressing tools. The potentiality to render antimicrobial characteristics to the polymer without affecting the mechanical and structural properties pave way for future research and development in the arena [36]. Cellulose materials employed in textile wound dressing can cause maceration of wound accompanied with pain, and microbial deposition and growth. Functionalization with hydrogels have reported to enhance the wearability and drug delivery capacity of the matrix. Additionally, new functionalities such as pH and thermo-sensitivity and antimicrobial properties might be introduced for production of novel interactive wound dressings to improve patient's life quality [37].

4.6 Chitosan-Based Wound Dressings

The semi-crystalline, linear polymer has competent biological property including biodegradability, biocompatibility, non-toxicity, mucoadhesion, antimicrobial, and homeostatic activity. The deacetylated chitin-derivative is found in the exoskeleton of fungi and arthropods and is widely exploited in healing of burn and wound treatment. Chitosan has been processed into the hydrogel, nanofiber microsphere, or porous scaffold in tissue engineering [38]. Chitosan impregnated with nanoparticles

such as silver and gold nanoparticles delivers enhanced mechanical properties, well-distributed pores contributing to moisture retention capacity, antimicrobial activity, accelerated re-epithelialization and collagen deposition [39, 40]. Disadvantages of chitosan including poor mechanical properties, fast degradation rate, hardly electro-spinnable is improved by cross-linking and blending with other polymers. Polyvinyl alcohol/Chitosan/Starch nanofibrous mats have been investigated for enhanced water retention, porosity, water absorption coupled with water vapor transmission in wound healing tools. Appropriate wound breathing and efficient handling of exudates accelerated the wound healing process effectively [41]. Chitosan-pectin biopolymeric hydrogel presented sound printability, physical integrity, and flexibility to be utilized as appropriate candidates for personalized wound dressing tools [42].

4.7 Hyaluronic Acid-Based Wound Dressings

The non-immunogenic polysaccharide is composed of N-acetyl-D-glucosamine and glucuronic acid. The hygroscopic nature of hyaluronic acid has been exploited in preparation of hydrogel like constructs, to assist the migration of keratinocytes and angiogenesis, and foster a scar-free wound healing. It interacts with CD44 and RHAMM cell receptors to modulate inflammation, stimulate cell migration, formation of new vasculature in injuries. However, the wound repair mechanism is dependent on the molecular size of the polysaccharides. High molecular weight hyaluronic acids inhibit extracellular proliferation and therefore display anti-inflammatory and immunosuppressive responses along with causing hindrance to the development of new blood vessels. Whereas, short-chain, low molecular weight hyaluronic acid composed of 3–10 disaccharide units, are potent anti-inflammatory molecules that can stimulate extracellular proliferation, migration, and angiogenesis in wounded tissue [5, 20]. Hyaluronic acid-based wound healing tools, either pure or impregnated with other materials have been propounded for the management of both acute and chronic wounds [43–47].

4.8 Gelatin-Based Wound Dressings

The collagen derived natural polymer is procured by incomplete denaturalization of collagen obtained from skin, boiling bones, and connective tissue. Type A gelatin, procured from acid cured tissue are positively charged at a physiological pH and type B gelatin, procured from lime cured tissue are negatively charged at a physiological pH. Ascribable to its biodegradability, biocompatibility, and lower antigenicity in comparison with collagen, gelatin has been employed as drug delivery systems for growth factors, and crosslinking of gelatin has been addressed to modify the degradation and release rate of encapsulated cargos. With a broad molecular weight, under appropriate conditions of pH, temperature, or solvents, gelatin can espouse

different conformations such as microparticles, microspheres, or hydrogels. Gelatin based wound dressings have been engineered with other biomaterials for rendering remarkable next-generation healing properties [48–50].

4.9 Keratin-Based Wound Dressings

Keratin are the most copious group category of filament-forming insoluble proteins produced in epithelial cells of reptiles, birds, mammals including humans. The absence of keratin gene 17 has been reported to delay wound closure whereas down-regulation of keratin gene 16 and keratin gene 6 furnish non-healing phenotypes. Maximum healing was obtained for keratin base dressing on refractory wound (very complicated wounds that are not repairable with conventional dressing alone) population. Integration of antimicrobial products on keratin was also successfully achieved [51]. Keratin extracted from human hair impregnated with carboxymethyl cellulose succeeded in inhibiting growth of bacterial colonies. The effect of keratin addition on fibroblasts revealed better cellular attachment, proliferation, and spreading [52]. Halofuginone-laden keratin dressings proffered novel mechanism for reduction of scarring of severe burn wounds by delivering contracture-inhibiting Halofuginone, a collagen synthesis inhibitor that has been shown to decrease collagen synthesis in fibrosis cases [53].

4.10 Silk Fibroin-Based Wound Dressings

Silk proteins are utilized in wound dressings due to its characteristic properties including flexibility, adherence, absorption of exudates, minimal inflammatory reaction, biodegradability, and biocompatibility. Dressings based on silk fibroin are employed for treatment of a wide variety of chronic and acute wounds. Silk fibroin and its derivatives are prepared as biomaterials are available as sponges, hydrogels, nanofibrous matrices, scaffolds, micro/nanoparticles, and films [54–58].

Table 2 delivers few more instances for better understanding of properties influenced by naturally derived composite matrix.

5 Conclusion

Effective healing of the wound is essential for the personal satisfaction of the patients. This chapter featured several natural polymers and their composites with immuno modulating, bactericidal, and wound healing activities. Both chronic and acute wounds endure disruptions in at least one phase of the recovering cycle, and therefore entail progressed treatment techniques to augment clinical consideration and personal

Table 2 Properties of few naturally derived polymeric composites for wound dressing application

S. No.	Natural polymer	Composite material	Properties	Reference
1.	Silk fibronin	Konjacglucomannan	<ul style="list-style-type: none"> – Enhanced water retention, water absorption capabilities, and compression strength – Similar compressed modulus with native skin – Excellent biocompatibility for cell proliferation and adhesion 	[59]
2.	Chitosan-alginate	Gentamicin	<ul style="list-style-type: none"> – Enhanced drug delivery, skin regeneration, collagen deposition and formation of new blood vessels 	[60]
3.	Vitamin D3 loaded alginate	Calcium carbonate in combination with–glucono- δ -lactone	<ul style="list-style-type: none"> – Enhanced wound closure, re-epithelialization and granular tissue formation 	[61]
4.	Cellulose acetate	Gelatin	<ul style="list-style-type: none"> – Antimicrobial activity with enhanced biological activities – Proper wound for diabetic foot ulcer healing 	[62]
5.	Starch	Polyvinyl alcohol, glycerol, citric acid	<ul style="list-style-type: none"> – Enhanced combinations of water vapor transmission rate and antibacterial activity 	[63]
6.	Hyaluronic acid	Lysozyme	<ul style="list-style-type: none"> – Remarkable adhesion and appropriate viscosity 	[64]
7.	Keratin	Silver nanoparticle	<ul style="list-style-type: none"> – Accelerated wound closure and epithelialization 	[65]
8.	Bovine serum albumin	Polyacrylonitrile	<ul style="list-style-type: none"> – Promising bioactivity Hs68 fibroblasts and HaCat keratinocytes were found to be more viable in the presence of the biomineralized NFs than when they were co-cultured with the neat polyacrylonitrilenanofibres 	[66]

(continued)

Table 2 (continued)

S. No.	Natural polymer	Composite material	Properties	Reference
9.	Silk fibroin-chitosan	Zein nanoparticles with loaded curcumin	– Enhanced stiffness, cell adhesion and proliferation do not have any cytotoxic effect on human gingival fibroblast	[67]
10.	Heparin	Basic fibroblast growth factor	– Diminished inflammation, stabilized basic fibroblast growth factor, upgrade the expressing of vascular endothelial growth factor and transforming growth factor- β in wound site, and better on site cell proliferation	[68]
11.	Bacterial cellulose	Montmorillonite	– Enhanced mechanical and thermal properties of membrane – Decreased the water holding capacity and an improved in the water release rate	[69]
12.	Chitosan	Silicon nanoparticles	– Enhanced the quality of skin regeneration by favorable growth of microvessels, hair follicles and faster formation of epidermis	[70]
13.	Genipin cross-linked gelatin	Cerium oxide	– Cerium oxide act as chemo-attractant to aid in migration of fibroblast cells on the gelatin matrix – Exhibits more infiltration of leukocytes and larger deposition of collagen in contrast to gelatin and control groups	[71]
14.	Sodium alginate	Cellulose nanofibres	– Enhanced structural stability in moist environment and high water/fluid absorption capacity	[72]

(continued)

Table 2 (continued)

S. No.	Natural polymer	Composite material	Properties	Reference
15.	Alginate	Human elastin like polypeptide loaded with the hydrophobic natural antioxidant curcumin	<ul style="list-style-type: none"> – Controlled release of the model compound curcumin leading to a high antioxidant activity of the material and to maintain, and augment the cytocompatibility 	[73]
16.	Collagen and dextran	Zinc oxide	<ul style="list-style-type: none"> – Enhanced pseudoplastic behavior and antimicrobial activity 	[74]
17.	Keratin	Cinnamon	<ul style="list-style-type: none"> – Enhanced the mechanical compliance of the composite and antibacterial properties – Retained its antioxidant properties and reduced expression of pro-inflammatory factors by 5–7 fold 	[75]
18.	Chitosan	Polycaprolactone with nanoclay	<ul style="list-style-type: none"> – Superior controlled-release of curcumin – Enhanced tensile strength – enhanced biocompatibility. 	[76]
19.	Soy protein	Cellulose acetate	<ul style="list-style-type: none"> – Promoted fibroblast proliferation, migration, infiltration, and integrin $\beta 1$ expression – Demonstrated high water retaining capability – Accelerate re-epithelialization and epidermal thinning as well as reduce scar formation and collagen anisotropy 	[77]
20.	Low-methoxy pectin	Zeolite particles	<ul style="list-style-type: none"> – Zeolite particles served as drug loading entities and enhanced hydrogel stability through swelling – Promoted cell viability 	[78]

satisfaction. Contingent on the kind of wound and its location and origin, at least one treatment choices are accessible: effective utilization of antiseptics and antibiotics, innumerable dressing changes every day, and costly medication, for instance, MIST ultrasound therapy and negative weight wound treatment. In spite of the large number of financially accessible items for complex intense and incessant injury therapy, such incurable wounds prevail exigent to manage and require broad clinical intervention. Natural polymers derived wound dressings exhibit intrinsic bioactive properties that can quicken the recuperating process in acute wounds, yet employ a negligible impact in complex acute wounds, for example, severely charred areas or chronic injuries. Combinatorial methodology by fusing engineered or characteristic polymer with remedial bioactive particles like cytokines and development components to advance re-epithelialization, debridement, granulation, and other materials for solid injury healing have proven useful.

The vast majority of these specialists have been utilized forages. Albeit numerous in vivo and in vitro examinations have demonstrated their efficacy in wound healing and recovery, documented clinical trials are as still missing and need to be carried out more often to guarantee the security and adequacy in human application. Contemporary challenge reclines on recognition of dynamic compounds accountable for their injury mending properties and the mechanism followed in question. Management of wound contracture, exudates and bacterial control are still the major challenges in wound healing. Wound contracture is a characteristic method for wound closure; nonetheless, excessive wound contraction prompts functional restrictions, inability, and physical deformity. The majority of wound dressings don't have the ability to retain thick and gooey exudates from wounds. With the emergence of multi-resistant microbes, specialists to improve wound mending and forestall intrusion of microorganisms to the body framework are additionally pertinent. The accrued engrossment of the scientific community in the utilization of either protein-based or polysaccharide-derived dressings is striking, and it reflects the growing perspective of giving back what we borrowed from nature.

Acknowledgements Authors would like to pay gratitude toward the Department of Chemistry and Department of Biological Sciences and Engineering, Netaji Subhas University of Technology, Delhi, India.

References

1. Naik S (2018) Wound, heal thyself. *Nature Med* 24(9):1311–1312
2. Hamdan S, Pastar I, Drakulich S, Dikici E, Tomic-Canic M, Deo S, Daunert S (2017) Nanotechnology-driven therapeutic interventions in wound healing: potential uses and applications. *ACS Central Sci* 3(3):163–175
3. Shah JB (2011) The history of wound care. *J Amer College Certified Wound Specialists* 3(3):65–66

4. Gaspar-Pintilieșcu A, Stanciu AM, Craciunescu O (2019) Natural composite dressings based on collagen, gelatin and plant bioactive compounds for wound healing: a review. *Int J Biolog Macromolecules* 1(138):854–865
5. Mogoșanu GD, Grumezescu AM (2014) Natural and synthetic polymers for wounds and burns dressing. *Int J Pharmaceutics* 463(2):127–136
6. Dabiri G, Damstetter E, Phillips T (2016) Choosing a wound dressing based on common wound characteristics. *Adv Wound Care* 5(1):32–41
7. Evans ND, Oreffo RO, Healy E, Thurner PJ, Man YH (2013) Epithelial mechanobiology, skin wound healing, and the stem cell niche. *J Mech Behav Biomed Mater* 1(28):397–409
8. De Jong LA (1995) Pre-tension and anisotropy in skin: modelling and experiments. Master of Science Thesis, Eindhoven University of Technology. Available on institution repository at (<http://alexandria.tue.nl/repository/books/633250.pdf>, 1995)
9. Diridollou S, Patat F, Gens F, Vaillant L, Black D, Lagarde JM, Gall Y, Berson M (2000) In vivo model of the mechanical properties of the human skin under suction. *Skin Res Technol* 6(4):214–221
10. Atkinson JA, McKenna KT, Barnett AG, McGrath DJ, Rudd M (2005) A randomized, controlled trial to determine the efficacy of paper tape in preventing hypertrophic scar formation in surgical incisions that traverse Langer's skin tension lines. *Plastic Reconstruct Surgery* 116(6):1648–1656
11. Gurtner GC, Dauskardt RH, Wong VW, Bhatt KA, Wu K, Vial IN, Padois K, Korman JM, Longaker MT (2011) Improving cutaneous scar formation by controlling the mechanical environment: large animal and phase I studies. *Annals Surgery* 254(2):217–225
12. Sarrazy V, Billet F, Micaleff L, Coulomb B, Desmoulière A (2011) Mechanisms of pathological scarring: role of myofibroblasts and current developments. *Wound Repair Regen* 19:s10–5
13. Webb K, Hitchcock RW, Smeal RM, Li W, Gray SD, Tresco PA (2006) Cyclic strain increases fibroblast proliferation, matrix accumulation, and elastic modulus of fibroblast-seeded polyurethane constructs. *J Biomech* 39(6):1136–1144
14. Aarabi S, Bhatt KA, Shi Y, Paterno J, Chang EI, Loh SA, Holmes JW, Longaker MT, Yee H, Gurtner GC (2007) Mechanical load initiates hypertrophic scar formation through decreased cellular apoptosis. *The FASEB J* 21(12):3250–3261
15. Vowden K, Vowden P (2017) Wound dressings: principles and practice. *Surgery (Oxford)* 35(9):489–494
16. Weller CD, Team V, Sussman G (2020) First-line interactive wound dressing update: a comprehensive review of the evidence. *Front Pharmacol* 28(11):155
17. Weir D (2020) Wound dressings. In: *Local wound care for dermatologists*, Springer, Cham, pp 25–34
18. Shi C, Wang C, Liu H, Li Q, Li R, Zhang Y, Liu Y, Shao Y, Wang J (2020) Selection of appropriate wound dressing for various wounds. *Front Bioeng Biotechnol* 8
19. Stern D, Cui H (2019) Crafting polymeric and peptidic hydrogels for improved wound healing. *Adv Healthcare Mater* 8(9):1900104
20. Suarato G, Bertorelli R, Athanassiou A (2018) Borrowing from nature: biopolymers and biocomposites as smart wound care materials. *Front Bioeng Biotechnol* 2(6):137
21. Das A, Abas M, Biswas N, Banerjee P, Ghosh N, Rawat A, Khanna S, Roy S, Sen CK (2019) A modified collagen dressing induces transition of inflammatory to reparative phenotype of wound macrophages. *Sci Reports* 9(1):1
22. Ding C, Yang Q, Tian M, Guo C, Deng F, Dang Y, Zhang M (2020) Novel collagen-based hydrogels with injectable, self-healing, wound-healing properties via a dynamic crosslinking interaction. *Polym Int*
23. Xu C, Akakuru OU, Ma X, Zheng J, Zheng J, Wu A (2020) Nanoparticle-based wound dressing: recent progress in the detection and therapy of bacterial infections. *Bioconjugate Chem* 31(7):1708–1723
24. Alvarez GS, Héлары C, Mebert AM, Wang X, Coradin T, Desimone MF (2014) Antibiotic-loaded silica nanoparticle–collagen composite hydrogels with prolonged antimicrobial activity for wound infection prevention. *J Mater Chem B* 2(29):4660–4670

25. Ghorbani M, Nezhad-Mokhtari P, Ramazani S (2020) Aloe vera-loaded nanofibrous scaffold based on Zein/Polycaprolactone/Collagen for wound healing. *Int J Biolog Macromolecules*
26. Zare-Gachi M, Daemi H, Mohammadi J, Baei P, Bazgir F, Hosseini-Salekdeh S, Baharvand H (2020) Improving anti-hemolytic, antibacterial and wound healing properties of alginate fibrous wound dressings by exchanging counter-cation for infected full-thickness skin wounds. *Mater Sci Eng C* 1(107):110321
27. Singh B, Varshney L, Francis S (2017) Designing sterile biocompatible moxifloxacin loaded tragacanth-PVA-alginate wound dressing by radiation crosslinking method. *Wound Med* 1(17):11–17
28. Li H, Yang J, Hu X, Liang J, Fan Y, Zhang X (2011) Superabsorbent polysaccharide hydrogels based on pullulan derivate as antibacterial release wound dressing. *J Biomed Mater Res, Part A* 98(1):31–39
29. Abdel-Mohsen AM, Abdel-Rahman RM, Kubena I, Kobera L, Spatz Z, Zboncak M, Prikrýl R, Brus J, Jancar J (2020) Chitosan-glucan complex hollow fibers reinforced collagen wound dressing embedded with aloe vera. part I: preparation and characterization. *Carbohydrate Polym* 230:115708
30. Lehtovaara BC, Gu FX (2011) Pharmacological, structural, and drug delivery properties and applications of 1, 3- β -glucans. *J Agri Food Chem* 59(13):6813–6828
31. Hosary RE, El-Mancy SM, El Deeb KS, Eid HH, Tantawy ME, Shams MM, Samir R, Assar NH, Sleem AA (2020) Efficient wound healing composite hydrogel using Egyptian *Avena sativa* L. polysaccharide containing β -glucan. *Int J Biolog Macromolecules* 149:1331–1338
32. Gharibi R, Kazemi S, Yeganeh H, Tafakori V (2019) Utilizing dextran to improve hemocompatibility of antimicrobial wound dressings with embedded quaternary ammonium salts. *Int J Biolog Macromolecules* 15(131):1044–1056
33. Mansuroğlu B, Kızılbey K, ŞayanPoyraz F, Yurttaş Z, Fuerkaiti SN, Abaoğlu İY, Başat HN (2020) Chitosan/dextran sulphate sodium hydrogels for wound healing material: preparation, characterisation and in vitro evaluation. *Mater Technol* 4:1–8
34. Turner PR, Murray E, McAdam CJ, McConnell MA, Cabral JD (2020) Peptide chitosan/dextran core/shell vascularized 3D constructs for wound healing. *ACS Appl Mater Interfaces* 12(29):32328–32339
35. Savitskaya IS, Shokatayeva DH, Kistaubayeva AS, Ignatova LV, Digel IE (2019) Antimicrobial and wound healing properties of a bacterial cellulose based material containing *B. subtilis* cells. *Heliyon* 5(10):e02592
36. Fürsatz M, Skog M, Skogl P, Palm E, Aronsson C, Skallberg A, Greczynski G, Khalaf H, Bengtsson T, Aili D (2018) Functionalization of bacterial cellulose wound dressings with the antimicrobial peptide ϵ -poly-L-Lysine. *Biomed Mater* 13(2):025014
37. Pinho E, Soares G (2018) Functionalization of cotton cellulose for improved wound healing. *J Mater Chem B* 6(13):1887–1898
38. Ali Khan Z, Jamil S, Akhtar A, Mustehsan Bashir M, Yar M (2020) Chitosan based hybrid materials used for wound healing applications-a short review. *Int J Polym Mater Polym Biomater* 69(7):419–436
39. Li Q, Lu F, Zhou G, Yu K, Lu B, Xiao Y, Dai F, Wu D, Lan G (2017) Silver inlaid with gold nanoparticle/chitosan wound dressing enhances antibacterial activity and porosity, and promotes wound healing. *Biomacromol* 18(11):3766–3775
40. Liang D, Lu Z, Yang H, Gao J, Chen R (2016) Novel asymmetric wettable AgNPs/chitosan wound dressing: in vitro and in vivo evaluation. *ACS Appl Mater Interfaces* 8(6):3958–3968
41. Adeli H, Khorasani MT, Parvazinia M (2019) Wound dressing based on electrospun PVA/chitosan/starch nanofibrous mats: fabrication, antibacterial and cytocompatibility evaluation and in vitro healing assay. *Int J Biol Macromolecules* 1(122):238–254
42. Long J, Etxeberria AE, Nand AV, Bunt CR, Ray S, Seyfoddin A (2019) A 3D printed chitosan-pectin hydrogel wound dressing for lidocaine hydrochloride delivery. *Mater Sci Eng C* 1(104):109873
43. El-Aassar MR, Ibrahim OM, Fouda MM, El-Beheri NG, Agwa MM (2020) Wound healing of nanofiber comprising Polygalacturonic/Hyaluronic acid embedded silver nanoparticles: In-vitro and in-vivo studies. *Carbohydrate Polym* 15(238):116175

44. Zhang S, Hou J, Yuan Q, Xin P, Cheng H, Gu Z, Wu J (2020) Arginine derivatives assist dopamine-hyaluronic acid hybrid hydrogels to have enhanced antioxidant activity for wound healing. *Chem Eng J* 15(392):123775
45. Duan Y, Li K, Wang H, Wu T, Zhao Y, Li H, Tang H, Yang W (2020) Preparation and evaluation of curcumin grafted hyaluronic acid modified pullulan polymers as a functional wound dressing material. *Carbohydrate Polym* 19:
46. Duan Y, Li K, Wang H, Wu T, Zhao Y, Li H, Tang H, Yang W (2020) Preparation and evaluation of curcumin grafted hyaluronic acid modified pullulan polymers as a functional wound dressing material. *Carbohydrate Polym* 19:116195
47. Graça MF, Miguel SP, Cabral CS, Correia IJ (2020) Hyaluronic acid-based wound dressings: a review. *Carbohydrate Polym* 27:116364
48. Eskandarinia A, Kefayat A, Agheb M, Rafienia M, Baghbadorani MA, Navid S, Ebrahimpour K, Khodabakhshi D, Ghahremani F (2020) A novel bilayer wound dressing composed of a dense polyurethane/propolis membrane and a biodegradable polycaprolactone/gelatin nanofibrous scaffold. *Sci Report* 10(1):1–5
49. Hubner P, Donati N, de MenezesQuines LK, Tessaro IC, Marcilio NR (2020) Gelatin-based films containing clinoptilolite-Ag for application as wound dressing. *Mater Sci Eng C* 1(107):110215
50. ForoutanKoudehi M, Zibaseresht R (2020) Synthesis of molecularly imprinted polymer nanoparticles containing gentamicin drug as wound dressing based polyvinyl alcohol/gelatin nanofiber. *Mater Technol* 35(1):21–30
51. Batzer AT, Marsh C, Kirsner RS (2016) The use of keratin-based wound products on refractory wounds. *Int Wound J* 13(1):110–115
52. Sadeghi S, Nourmohammadi J, Ghaee A, Soleimani N (2020) Carboxymethyl cellulose-human hair keratin hydrogel with controlled clindamycin release as antibacterial wound dressing. *Int J Biol Macromolecules* 15(147):1239–1247
53. Navarro J, Clohessy RM, Holder RC, Gabard AR, Herendeen GJ, Christy RJ, Burnett LR, Fisher JP (2020) In Vivo evaluation of three-dimensional printed, keratin-based hydrogels in a porcine thermal burn model. *Tissue Eng Part A* 26(5–6):265–278
54. Patil PP, Reagan MR, Bohara RA (2020) Silk fibroin and silk-based biomaterial derivatives for ideal wound dressings. *Int J Biol Macromolecules*
55. Nourmohammadi J, Hadidi M, Nazarpak MH, Mansouri M, Hasannasab M (2020) Physico-chemical and antibacterial characterization of nanofibrous wound dressing from silk fibroin-polyvinyl alcohol-*elaegnusangustifolia* extract. *Fibers Polym* 21(3):456–464
56. Zhang Y, Lu L, Chen Y, Wang J, Chen Y, Mao C, Yang M (2019) Polydopamine modification of silk fibroin membranes significantly promotes their wound healing effect. *Biomater Sci* 7(12):5232–5237
57. Hashimoto T, Kojima K, Tamada Y (2020) Gene expression advances skin reconstruction and wound repair better on silk fibroin-based materials than on collagen-based materials. *Materialia* 1(9):100519
58. Hadisi Z, Farokhi M, Bakhsheshi-Rad HR, Jahanshahi M, Hasanpour S, Pagan E, Dolatshahi-Pirouz A, Zhang YS, Kundu SC, Akbari M (2020) Hyaluronic Acid (HA)-Based Silk Fibroin/Zinc Oxide core-shell electrospun dressing for burn wound management. *Macromolecular Biosci* 20(4):1900328
59. Feng Y, Li X, Zhang Q, Yan S, Guo Y, Li M, You R (2019) Mechanically robust and flexible silk protein/polysaccharide composite sponges for wound dressing. *Carbohydrate Polym* 15(216):17–24
60. Bakhsheshi-Rad HR, Hadisi Z, Ismail AF, Aziz M, Akbari M, Berto F, Chen XB (2020) In vitro and in vivo evaluation of chitosan-alginate/gentamicin wound dressing nanofibrous with high antibacterial performance. *Polym Test* 1(82):106298
61. Ehterami A, Salehi M, Farzambar S, Samadian H, Vaez A, Sahrapeyma H, Ghorbani S (2020) A promising wound dressing based on alginate hydrogels containing vitamin D3 cross-linked by calcium carbonate/d-glucono- δ -lactone. *Biomed Eng Lett* 19:1–1

62. Samadian H, Zamiri S, Ehterami A, Farzamfar S, Vaez A, Khastar H, Alam M, Ai A, Derakhshankhah H, Allahyari Z, Goodarzi A (2020) Electrospun cellulose acetate/gelatin nanofibrous wound dressing containing berberine for diabetic foot ulcer healing: in vitro and in vivo studies. *Sci Rep* 10
63. Das A, Uppaluri R, Das C (2019) Feasibility of poly-vinyl alcohol/starch/glycerol/citric acid composite films for wound dressing applications. *Int J Biol Macromolecules* 15(131):998–1007
64. Zhao X, Wang L, Gao J, Chen X, Wang K (2020) Hyaluronic acid/lysozyme self-assembled coacervate to promote cutaneous wound healing. *Biomater Sci* 8(6):1702–1710
65. Konop M, Czuwara J, Kłodzińska E, Laskowska AK, Sulejczak D, Damps T, Zielenkiewicz U, Brzozowska I, Sureda A, Kowalkowski T, Schwartz RA (2020) Evaluation of keratin biomaterial containing silver nanoparticles as a potential wound dressing in full-thickness skin wound model in diabetic mice. *J Tissue Eng Regen Med* 14(2):334–346
66. Homaeigohar S, Tsai TY, Zarie ES, Elbahri M, Young TH, Boccaccini AR (2020) Bovine serum albumin (BSA)/polyacrylonitrile (PAN) biohybridnanofibers coated with a biomineralized calcium deficient hydroxyapatite (HA) shell for wound dressing. *Mater Sci Eng: C*. 111248
67. Akrami M, Tayebi L, Ghorbani M (2020) Curcumin-loaded naturally-based nanofibers as active wound dressing mats: morphology, drug release, cell proliferation and cell adhesion studies. *New J Chem*
68. Peng J, Zhao H, Tu C, Xu Z, Ye L, Zhao L, Gu Z, Zhao D, Zhang J, Feng Z (2020) In situ hydrogel dressing loaded with heparin and basic fibroblast growth factor for accelerating wound healing in rat. *Mater Sci Eng C* 6:111169
69. Hodel KV, Fonseca LM, Santos IM, Cerqueira JC, Santos-Júnior RE, Nunes SB, Barbosa JD, Machado BA (2020) Evaluation of different methods for cultivating gluconacetobacter-hansenii for bacterial cellulose and montmorillonitebiocomposite production: wound-dressing applications. *Polymers* 12(2):267
70. Zhu F, Wang C, Yang S, Wang Q, Liang F, Liu C, Qiu D, Qu X, Hu Z, Yang Z (2017) Injectable tissue adhesive composite hydrogel with fibroblasts for treating skin defects. *J Mater Chem B* 5(13):2416–2424
71. Raja IS, Fathima NN (2018) Gelatin–cerium oxide nanocomposite for enhanced excisional wound healing. *ACS Appl Bio Mater* 1(2):487–495
72. Yadav C, Chhajed M, Choudhury P, Sahu RP, Patel A, Chawla S, Goswami L, Goswami C, Li X, Agrawal AK, Saini A (2020) Bio-extract amalgamated sodium alginate–cellulose nanofibres based 3D-sponges with interpenetrating BioPU coating as potential wound care scaffolds. *Mater Sci Eng C* 11:111348
73. Bergonzi C, d’Ayala GG, Elviri L, Laurienzo P, Bandiera A, Catanzano O (2020) Alginate/human elastin-like polypeptide composite films with antioxidant properties for potential wound healing application. *Int J Biol Macromolecules*
74. Păunica-Panea G, Ficai A, Marin MM, Marin Ş, Albu MG, Constantin VD, Dinu-Pîrvu C, Vuluga Z, Corobea MC, Ghica MV (2016) New collagen-dextran-zinc oxide composites for wound dressing. *J Nanomater* 1
75. Kossyvaki D, Suarato G, Summa M, Gennari A, Francini N, Gounaki I, Venieri D, Tirelli N, Bertorelli R, Athanassiou A, Papadopoulou EL (2020) Keratin–cinnamon essential oil biocomposite fibrous patches for skin burn care. *Mater Adv*
76. Huang Y, Dan N, Dan W, Zhao W (2019) Reinforcement of polycaprolactone/chitosan with nanoclay and controlled release of curcumin for wound dressing. *ACS Omega* 4(27):22292–22301
77. Ahn S, Chantre CO, Gannon AR, Lind JU, Campbell PH, Grevesse T, O’Connor BB, Parker KK (2018) Soy protein/cellulose nanofiber scaffolds mimicking skin extracellular matrix for enhanced wound healing. *Adv Healthcare Mater* 7(9):1701175
78. Kocaaga B, Kurkcuoglu O, Tatlier M, Batirel S, Guner FS (2019) Low-methoxyl pectin–zeolite hydrogels controlling drug release promote in vitro wound healing. *J Appl Polym Sci* 136(24):47640

A View on Polymer-Based Composite Materials for Smart Wound Dressings



S. Baptista-Silva, P. Alves, I. Guimarães, S. Borges, F. Tavaría, P. Granja, M. Pintado, and A. L. Oliveira

Abstract Wound management challenges everyday thousands of health professionals, mainly due to the constant monitoring and difficulties in deciding the correct treatment options. When considering chronic wounds, selecting the ideal dressing defies clinical knowledge, when facing the large amount of different materials, its distinctive properties and the uniqueness of each patient needs. This chapter presents

S. Baptista-Silva (✉) · I. Guimarães · S. Borges · F. Tavaría · M. Pintado · A. L. Oliveira (✉)
Universidade Católica Portuguesa CBQF—Centro de Biotecnologia E Química
Fina—Laboratório Associado, Escola Superior de Biotecnologia, Porto, Portugal
e-mail: sara.baptistadasilva@gmail.com

A. L. Oliveira
e-mail: aloliveira@porto.ucp.pt

I. Guimarães
e-mail: ines.gvguimaraes@gmail.com

S. Borges
e-mail: sandraferreiraborges@gmail.com

F. Tavaría
e-mail: ftavaría@porto.ucp.pt

M. Pintado
e-mail: mmpintado@esb.ucp.pt

P. Alves
Universidade Católica Portuguesa, Instituto de Ciências Da Saúde CIIS—Centro de Investigação Interdisciplinar em Saúde, Porto, Portugal
e-mail: Pjalves@porto.ucp.pt

P. Granja
Instituto de Investigação E Inovação Em Saúde (I3S), Universidade Do Porto, Porto, Portugal
Instituto de Engenharia Biomédica (INEB), Universidade Do Porto, Porto, Portugal
Instituto de Ciências Biomédicas Abel Salazar (ICBAS), Universidade Do Porto, Porto, Portugal
Faculdade de Engenharia Da Universidade Do Porto (FEUP), Porto, Portugal

P. Granja
e-mail: pgranja@i3s.up.pt

an overview on the challenges and complexity of a chronic wound, exploring the event of a wound infection and discussing the large range of polymer-based composite materials and products in use for each specific wound condition, taking into account the key decision aspects defined by the clinicians. Different tissue engineering strategies are also herein addressed with varied reported clinical success, ranging from non-cellularized to considerably sophisticated cellularized products, reproducing the compositional complexity of both dermis and epidermis. Recent advances in smart dressings and sensors are also brought to discussion as sensing the wound can give us new insights about the series of complex biochemical events related to the healing and regeneration process, while contributing for a better wound assessment.

Keywords Polymers · Composite materials · Wound management · Wound dressings

1 Introduction

Wound treatment is based on a complex approach where it is essential to identify the aetiology, make a correct diagnosis, and ensure that the treatment and therapeutic decisions are the most effective for that case. Wounds can be classified as acute or chronic according to their healing process [1, 2]. Acute wounds are associated with a non-complicated process that is generally organized, sequential and able to restore the anatomic and functional integrity of the tissues involved within a reasonable small amount of time. Meanwhile, chronic wounds are associated with difficult or prolonged healing where the reparative process does not follow in a timely or orderly fashion, and thus fails to produce the previous anatomic and functional integrity of the injured site [3]. According to White et al. [4], chronic wounds may be the result of an association between wounds that have an impaired healing process due to the presence of complex underlying pathologies, such as diabetes mellitus, vascular disease or the presence of malignancy. The epidemiological profile of chronic wounds is not fully known, however, it is estimated that there may be more than 20 million chronic wounds worldwide [5], with 1–2% of the population experiencing a chronic wound during their lifetime [6].

Wound care has high associated costs, as studies from Scandinavian countries have reported, they account for 2–4% of the total health care expenses [7], studies from the UK showed that they account for approximately 4.8 billion pounds [8], and studies from the United States showed that they account for an excess of US\$25 billion annually in the treatment of chronic wounds [9]. This burden is expected to grow even more due to aging population and chronic diseases, like diabetes. Aspects such as pain, anxiety and social isolation are aspects that may influence the quality of patient's life besides the wound healing process and cost treatment [10, 11]. Nonetheless these aspects are presently difficult to quantify.

This chapter discusses recent advances in the development of synthetic (including biosynthetic) and biologic (tissue origin) ultimate polymer-based dressing materials

and composites to promote wound care. In specific, this chapter focuses on the current and new solutions that enhance wound healing and tissue regeneration, keeping in mind important aspects such as the improvement of wound care system.

2 Complexity of a Chronic Wound

A chronic wound is related to the complexity and senescence of physiological processes and is associated with stagnation. Chronic wound is described as an interruption in the integrity of skin and underlying tissues progresses through a disorganized and complex shape healing process. These injuries hardly progress through a sequence of normal healing, sequential and timely, and there is a precise balance between production and degradation of molecules [12, 13]; to thereby influence the physiology of healing. Chronic wounds can take several years to heal or even have no cure, causing emotional changes, physical and economic to patients, families and health services.

Healing is an intricate, dynamic and continuous systemic process [14], which requires body activation, production and inhibiting of a large number of molecular and cellular components, the interaction of chemical mediators, and extracellular matrix in an orderly and continuous sequence, conduct the entire process of regeneration/ healing. Its understanding is a critical step towards solving chronic wound problem.

2.1 *Different Stages of Healing*

The healing process is divided into three continuous phases which overlap temporally: inflammatory, proliferative and maturation [15, 16]. Five steps are known during the healing process, including the induction of inflammatory response by injury, reconstitution, migration and proliferation of parenchymal cells and connective tissue; followed by the synthesis of proteins of the extracellular matrix and restructuring of parenchymal elements to restore functionality and finally the connective tissue remodelling [17].

From the moment in which there is tissue loss, platelets come in contact with exposed collagen and other extracellular matrix components, giving the coagulation cascade and the release of vasoactive substances, adhesive proteins, growth factors and proteases [17, 18]. The formation of this provisional matrix is essential for cell migration, in addition to serving as a reservoir for cytokines and growth factors that will be released during the following phases of the healing process [19, 20]. At this stage the Celsius signals are evident as redness, heat, pain, tumor and possible loss of function [21]. The pro-inflammatory cytokines produce proteases that are present in the exudate and break the damaged extracellular matrix proteins [22], a process termed proteolysis. Beyond processes described, there is the phagocytosis of bacteria,

cell debris and foreign bodies, as well as the production of growth factors involved in these inflammatory cells to prepare the wound for the proliferative phase when the endothelial fibroblasts and cells also are incorporated [23]. When the inflammatory process does not lapse, a complex response is triggered that can lead to chronic inflammation [24, 25]. The proliferative phase starts with the granulation tissue formation, connective tissue cell proliferation and migration and re-epithelialization of the wound surface. The epithelial cell proliferation starts with a mitogenic and chemotactic stimulation of keratinocytes, with increased microvascular permeability that allows, through the leakage of proteins, cytokines and cell elements, to the formation of a provisional extracellular matrix which is necessary for the migration and proliferation of endothelial cells [26]. The last stage—Maturation is characterized by deposition of extracellular matrix (ECM) remodelling of tissues and wound contraction [27, 28]. In the course of maturation and remodelling process, most fibroblasts and inflammatory cells disappeared from the wound site, giving rise to apoptosis and cell death processes to scar formation.

2.2 Wound Types and Therapeutic Requirements

From the universe of chronic wounds, the most common are pressure ulcers, venous arterial ulcers, and diabetic ulcers (Fig. 1) [29]. Injuries associated with the lower limbs, venous ulcers are the most common type, accounting for about 80–90% of the wounds, and the remaining arterial and neuropathic [30].

The choice of the most adequate dressing is influenced by the aetiology, specific characteristics of the wound bed, type of tissue present, odour, infection signals and amount of exudation [31, 32]. There is a considerable number of different dressings and techniques available for managing wounds according to its characteristics (Table 1).

Thus, the wound bed, and its tissue type are indicative of the required material, the healing phase, progression and treatment effectiveness:

Necrosis: usually black, indicative of tissue death, hard or soft consistency;

Fibrin: yellowish and can be presented adherent to the wound bed (slough);

Granulation: Reddish colored, slightly damp and firm, it is indicative of good evolution of the healing process;

Epithelialization: pinkish tissue, indicative of wound closure and thus usually arises from their edges.

The first principle of wound bed preparation is the removal of this tissue type and should be performed using debridement; which quantitatively reduces bacterial load, toxins and other substances affecting the immune system [33]. It is clear that healing is systemic, but the choice of the most adequate local treatment technique among the available options or the possibility of an infection event are factors that can contribute to accelerate or delay this process.



Fig. 1 Most common pressure ulcers: **a** Calcaneus pressure injury, **b** Venous Leg ulcer and **c** Diabetic foot—Charcot foot

The evaluation of the risk factors of the patient with wound should be an element guide to all decisions for the prevention and treatment of wounds. Several factors that interfere with the healing process are identified in the literature, and they are consensual that this continuous process may be hampered by systemic and local factors [27, 28]. According Nazarko [34], in addition to these local and systemic risk factors, extrinsic factors must be evaluated (affecting the condition of the person) and assessing the intrinsic (referring to the wound characteristics) that interfere with the healing process (Table 2).

3 The Event of a Wound Infection

When the skin integrity is disrupted becomes prone to infection. As a multi-functional organ, skin possesses particular biochemical and physical properties that influence its microbiology. Some of these properties include a slightly acidic pH, low moisture content, high lipid content (which confers hydrophobic characteristics) and the presence of antimicrobial peptides [35].

Table 1 Wound characteristics and established therapeutic options

Color	Tissues	Exudation	Objectives	Considerations	Therapeutic options
Black	Necrosis Necrotic tissue	Null (dry)	Debride Hydrate	Caution: - Arterial occlusion	Surgical Debridement
		Scarce	Debride Hydrate & Maintain Humidity	- Heel - Malignant lesions - Coagulation Levels	Autolytic or enzymatic debridement
Yellow	Devitalized Fibrin Slough Tissue	Scarce	Removal of necrotic tissue Reduce the bacterial load	Perilesional skin protection	Surgical debridement if necessary Autolytic or enzymatic debridement
		Moderate \ abundant	Removal of necrotic tissue Reduce the bacterial load	Perilesional skin protection	Autolytic or enzymatic debridement Absorbing dressings
Red	Granulation tissue	Scarce	Promote Granulation & Maintain Humidity	Perilesional skin protection Atraumatic treatments	Hydrogels Absorbing dressings
		Moderate \ abundant	Promote Granulation & Management of exudate	Protect new tissues	Absorbing dressings Tissue regeneration material
Pink	Epithelialization	Null	<ul style="list-style-type: none"> • Promote epithelialization • Protection 	<ul style="list-style-type: none"> • Protect new tissues • Decrease Frequency of Treatments 	Silicone films Thin Hydrocolloids

Adapted from WUWHS [31]

Table 2 Risk factors for impaired healing

Intrinsic factors	Extrinsic factors
Age	Aetiologies
Skin condition	Wound site
Associated pathologies	Wound size
Life style	Wound bed tissues—Debris
Nutritional status	Exudation—Maceration
Mobility	Wound edges
Psychological well-being	Surrounding skin
Pain	Pain associated with wound
Immune status	Mechanical stress
	Chemical stress
	Dressing materials
	Medication
	Temperature

The outer surface of adult skin is colonized by a handful of stable inhabitants (resident microorganisms) with rare or transient species contributing to interpersonal variation [36]. Skin physiology determines the pattern of colonization by skin microbes. *Staphylococcus* spp. and *Corynebacterium* spp. are the most abundant in moist sites, while lipophilic microorganisms such as *Propionibacterium* spp. and *Malassezia* spp. dominate in sebaceous areas [37]. The role of transient microorganisms in infection remains largely unknown, although it is likely that they influence the infection life cycle.

Microorganisms are present in all wounds. In acute wounds, the short healing time allows for only a small number of skin contaminants to take residence while in chronic wounds, the continued exposure of devitalized tissue is likely to facilitate the colonization of a wide variety of microorganisms and trigger infection [38]. Bacteria, fungi, viruses or protozoa can cause human infection. However, the presence of microorganisms such as bacteria does not necessarily indicate that an infection exists or that will lead to impair wound healing [39].

The role of bacteria in wound healing has been debated over the years. Some have suggested that bacteria may play a beneficial role in normal wound healing and wounds will heal despite the presence of large numbers of microorganisms [40]. Nonetheless, the detrimental effects of specific pathogens, such as *Clostridium perfringens* and *Streptococcus pyogenes*, have been well recognized. These are typically invasive bacteria that are not normal members of the human skin microbiota. In contrast, some resident microorganisms such as *Staphylococcus aureus*, which are part of the microbiota of many humans, also cause wound infections (Table 3).

Polymicrobial wounds are those containing several potential pathogens. This typically delays wound healing, raising the risk for other complications [42] and is the norm in chronic wounds. The concept of wound bioburden involves the bacterial burden, which is the presence of replication microorganisms within a wound, the bacterial load, the virulence of the microorganism and the host reaction [43]. This leads to increased metabolic load imposed by the multiplying microorganisms in the wound bed, and their ability to spread in tissues and produce toxins [44]. The

Table 3 Bacterial species isolated from chronic wounds

Bacterial genus	Chronic wounds (specimens from 19 wounds)*	
	Swab culture	Tissue PCR
<i>Staphylococcus</i>	28	68
<i>Enterococcus</i>	12	18
<i>Pseudomonas</i>	32	28
<i>Proteus</i>	126	–
<i>Citrobacter</i>	8	28
<i>Corynebacteria</i>	0	68
Anaerobes	0	70

* Frank et al. [41].

interactions of multiple microbial populations in chronic infections are still poorly understood, mainly due to controversies in culturing methods [45]. However, over the past several years, molecular-based methods have been increasingly applied in skin and wound microbiology research. Molecular studies of wound microbiology have revealed very diverse bacterial communities. These studies involved polymerase chain reaction (PCR) amplification of the bacterial gene encoding the small ribosomal subunit RNA (16S). More recent studies have used additional molecular methods including metagenomics for the evaluation of chronic wound microbiota [41]. The results of these studies indicate that chronic wounds contain diverse polymicrobial communities and similar community features, such as the presence of strictly anaerobic bacteria, even though the studies were from diverse geographic regions.

Evidence exists that bacteria colonizing human chronic wounds exist as biofilm communities and not in the planktonic form [35, 46]. Bacteria within a biofilm live in microcolonies encapsulated in a matrix composed of an extracellular polymeric substance. This acts as physical barrier to the permeation and action of antimicrobial agents. Besides this, the biofilm confers a habitat where bacteria can communicate with each other (quorum sensing), which may lead to increased virulence and propensity to cause infection [47]. More than 80% of human infections are caused by biofilms [48]. Chronic wounds have a fertile environment for biofilm formation; necrotic tissues and superficial debris facilitate infection whereas the altered vascularization and subsequent ischemia hinder the immune system to develop an efficient defensive response [49]. It is estimated that 60% of all chronic wounds are colonized by biofilms compared to only 6% of acute wounds [50]. This explains how biofilms can impair the healing process, by being often associated with a persistent inflammatory state, tissue disruption and difficulty in healing. The cascade of events leading to a chronic wound is schematized in Fig. 2. Adding to this, the polymicrobial nature of these infections further complicates diagnosis and treatment. When compared chronic wounds (venous leg ulcers, diabetic foot ulcers and pressure ulcers) with acute, generally are colonized by more anaerobic bacteria and fungi. Diabetic foot ulcers have a high incidence of species of *Bacteroides*, *Peptoniphilus*, *Fingoldia*, *Anaerococcus* and *Peptostreptococcus* [51].

It is tempting for the clinician to start antibiotic treatment, but in case of established mature biofilms, this treatment often has only temporary effect on both inflammation and healing. In addition, the clinician has to rely on the results from a swab or biopsy, which rarely reflects all specimens present in the wound. The bacteria in biofilm are up to 1000 times less susceptible to antibiotics [53], and MIC is not reached in the chronic wound fluid. Even silver as an antimicrobial incorporated in several wound dressings, has limited effect in biofilm *in vitro* [54]. With this in mind, the clinician should exercise restraint in administering antibiotics. This favours biofilm persisting bacteria and promotes resistance. Mechanical removal of wound debris (by ultrasound assisted surgery) and even granulation tissue is an effective way of diminishing the bacterial load and is an important part of treatment protocols. "Biofilm managing strategies" have been implemented, but none have yet proved to be more effective than others [55]. The need for new and more efficient treatment regimens (new biofilm penetrating drugs, new substances to disrupt biofilms) and

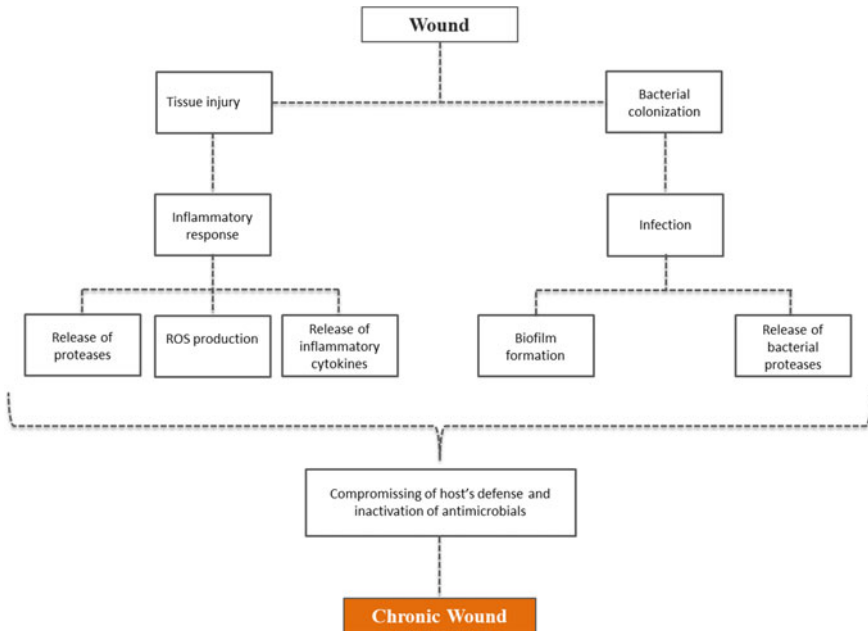


Fig. 2 Cascade of events contribution to a chronic wound. Adapted from McCarty and Percival [52]

research in biofilm (QS manipulation, resistance to antimicrobials) may provide wound care specialists with new, more effective ways to heal wounds.

4 Established Wound Dressing Options

Very few, if any, current wound care products have the capacity to cross the healing process towards tissue restoration [56]. The contexts, realities and needs in wound care around the world are simultaneously equal and different and there are actually a large variety of different dressings for prevention and treatment [57–60] for the most various aetiology’s or wound characteristics. These wound care dressings presently can be divided into two broad categories: synthetic (including biosynthetic) and biologic (tissue origin) polymer-based materials and their composites [56].

Biologic-derived polymers for wound dressings are not recent, they are used since the Egyptian’s [60], however only after the 60’s the first study’s started and more specialized biological-derived dressings have been developed since there [56, 61]. Their effectiveness has increased greatly with recent innovative developments, where various skin substitutes were tested over time, such as human skin allograft, xenograft and amnion, are being used at various wound care centres. The skin substitutes provide faster wound coverage solution that may require less vascularized wound

bed, increase in the dermal component of healed wound, reduce or removed inhibitory factors of wound healing, reduced inflammatory response and subsequent scarring [62]. Nevertheless, these skin substitutes need specific expertise/experience and have a higher cost [63].

4.1 Synthetic/Biosynthetic Dressings in Wound Care

Synthetic/biosynthetic dressings have been designed primarily to promote moist wound healing and function as a barrier against infection, while simultaneously collaborate in the growth of granulation tissue and epithelisation. Currently, chronic wounds are treated with a broad variety of dressings tailored to the requirements of the wound (dry or exuding, clean or infected, superficial or deep) (Table 2). These materials are generically categorized as textiles, polyurethane films, foams, hydrogels, hydrocolloids, and collagen/alginate combination of wound dressings as example in Table 1 [60]. Nonetheless the most common wound dressing are alginates and hydrofibers, well studied, applied and documented in literature. Alginate has relevant properties as a gel-forming [64] and film-forming [65]. Alginate dressings are highly absorbent, being this dressing a good choice for highly exudative wounds. These dressings are described to absorb 15–20 times their weight of fluid, which can be a substantial lifestyle improvement for patients with draining ulcers [66]. Hydrofibers are dressings highly absorbent, they have a similar function of alginates but can absorb three times more. They have been demonstrated to be useful in partial-thickness donor sites and partial thickness burns. All together, these polymer-based materials and their composites can present a wide range of properties resulting in interesting possibilities for the final wound dressing product [67]. The selection of various reinforcements and polymer matrices is very critical in designing a desired product for wound care. Figure 3, shows a schematic illustration of a typical decision tree in wound care.

The wound stage and its characteristics will implicate the best dressing choice. While films will be the ideal solution for superficial wounds; foams will be more adequate for exudative and granulating; hydrogels will be best applied in eschar, deep or tunneling wounds and in wounds with slough; and hydrocolloids will be used in superficial, eschar and granulating wounds and also wounds with slough [68]. It is highlighted the key steps prior dressing application, like wound bed preparation (cleanse, debridement and measurement), the wound evaluation (considering the different levels of exudate) and the consequent ideal solution for each type of wound. Likewise, some common commercial products are listed below.

In this chapter novel and promising polymer-based composite dressings in the different categories, are reported for wound healing.

Foams

Foams are one of the most variable and versatile dressings for chronic wounds, including thin and thick, adhesive and non-adhesive, coated or uncoated [69]. Typically, the most used foams are constituted of polyurethane or a silicone core with a

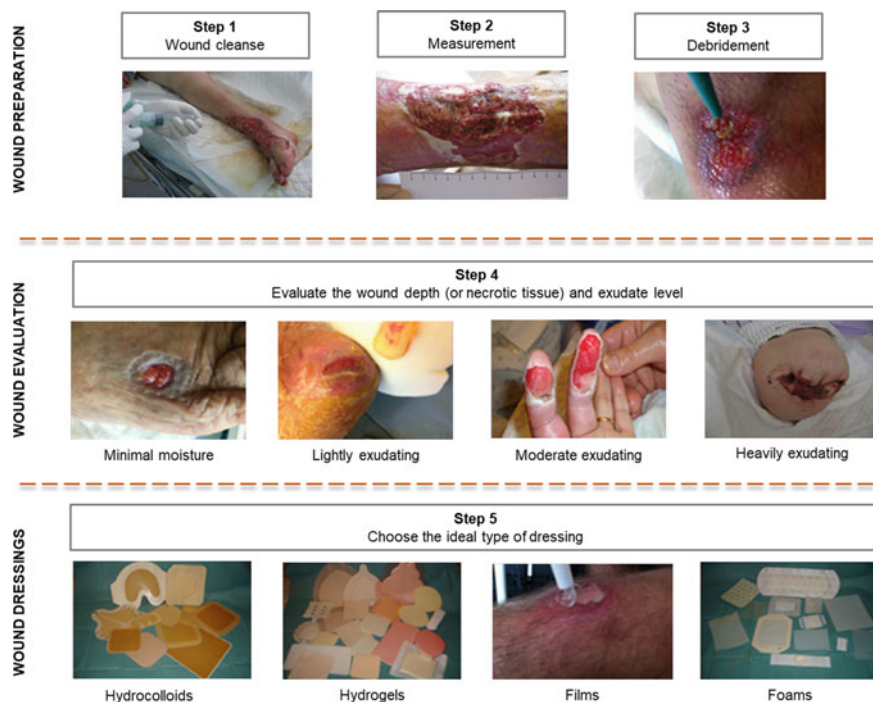


Fig. 3 Schematic illustration of wound care treatment

semi-occlusive out layer. This layer is water vapor permeable and attends to protect against microbial penetration and proliferation, while the polyurethane/silicon serves to give absorptive qualities [66]. Foams are applied in wounds with moderate to high exudate, granulating or necrotic wound, and can be used on infected wounds (Fig. 3). It has been developed foams with antimicrobial activity, as for example silver-containing arabinoxylan foams [70]. There are also available commercial products incorporating silver, such as PolyMem silver[®] (Ferris Cor.) and Mepilex[®] Ag (Mölnlycke Health Care).

Foams afford an atmosphere for autolytic debridement and reduce granulation tissue. Thick foams can be used for venous ulcers to offer an improvement of local compression, which allow to control edema and promote healing [69]. Treatment of wounds using negative pressure therapy uses foams that incorporate tubing to a vacuum source. Generally, two types of foams are used: polyurethane foams, for example, VAC GranuFoam[®] (Kinetic Concepts [KCI], San Antonio, TX); Flexzan[®] (Dow B. Hickam, Inc.), Hydrasorb[®] (Tyco Health Care/The Kendall Co.) or polyvinyl alcohol foams, for example, VAC VersaFoam, (Kinetic Concepts [KCI], San Antonio, TX) [71].

Foams can dry wounds with minimal or mild exudate and may require a saline soak during dressing change to avoid pain and trauma [68]. The absorbent capacity

of wound fluids is dependent on the polymeric material used and the thickness of the foam. They are extremely absorbent, protective and adaptable to body surfaces. Additionally, foams are easily manipulated and can be adjusted to the wound size [72].

Foams are appropriate for deep wounds with exposed bony areas such as the ankle or sacrum or exudative cavities, however they should be frequently changed, since daily to once or twice weekly, because the dressing becomes soaked with exudate. Foams can be adherent or non-adherent, in the latter case it is necessary a secondary dressing to avoid shifting [66]. Nevertheless, they possess some drawbacks, for example they can dehydrate dry wound and also they are opaque and the wound visualization can be compromised. In addition, adhesive foams may be responsible for some cases of contact dermatitis [73].

Recently, several innovative composite foams have been developed. A new foam combining the attributes of volume filling and rapid coagulation of shape memory polymers (SMP) with the ability to swell and fill hydrogels has been developed by Landsman et al. [74]. This SMP polyurethane foam is coated with *n*-vinylpyrrolidone hydrogel (NVP) and polyethylene glycol diacrylate (PEGDA). In a new addition, this composite contains iodine in the form of a complex (PVP-I2 or povidone-iodine), widely used as a surgical antiseptic. The iodine-containing hydrogel gives the composite an antibacterial effect (reducing the viability of common bacteria by 80%) while increasing fluid uptake by 19 times over uncoated SMP foams. In another study by Namviriyachote et al. [75] polyurethane combined (PUC) foam dressings with various biomacromolecules (i.e. carboxymethylcellulose, chitosan, alginate, hydroxypropyl methylcellulose) were fabricated with the adsorption of asiaticoside and silver nanoparticles for traumatic wound treatment. The selected PU-alginate combined foam dressing adsorbed with asiaticoside and silver nanoparticles proved advantages for traumatic dermal wound management. A multilayer dressing consisting of polyvinyl alcohol foam (PVA) and electrospun sodium carboxymethyl cellulose (CMC) surface mesh was developed and characterized by He et al. [76] and co-workers. This composite was further loaded into the PVA foam, with the antimicrobial drug stearyl trimethyl ammonium chloride (STAC) for infection control and the CMC surface mesh offered an effective hemostatic function. Another study shows the potential of alginate-pectin composite foams with different blending ratios using calcium ion cross-linking [77]. In this study, the results suggest that controlling the pectin content in alginate-pectin foams is the key to adjust their mechanical properties, water absorption, and drug-release ability. Alginate-pectin composite foams showed to be promising candidates in different wound-dressing applications. A series of foams composed of PVA)/ alginate (PACFs) were prepared through a crosslinking reaction and lyophilization process [78]. The effect of different alginate content on the physicochemical properties and on the hemostatic function of the PACF was analyzed. The results showed that PACF absorbed plasma, but also stimulated blood cells, further promoting blood clotting, with therefore promising results as wound dressings.

Films

Films are thin, elastic and offer a barrier to microbial colonization [68]. Generally, commercial films are transparent, for example Transeal® (DeRoyal), Bioclusive® (Johnson & Johnson Medical), Mefilm® (Molnlycke Health Care), among others. A suitable wound-dressing film must have crucial properties, including capacity to absorb exudate, to regulate the moisture permeation, to maintain the moisture of the wound and to release the retained bioactive compound [79].

Films can be used in superficial wounds, namely burns, catheter sites and epidermal skin graft harvest sites, being suitable for minimally exudative wounds (Fig. 3) [68]. Films permit an environment for softening dry eschar by autolytic debridement, permit a protection from friction and contribute for pain reduction. A quantity of amorphous hydrogel may be added to the film in order to accelerate the autolytic debridement. These dressings may not be applied on wounds with heavy exudate. Films should be changed when exudate escapes onto intact skin or at a minimum of every 7 days [69].

Films are easy to use in wounds with different shapes, generally allowing for an easy wound visualization and flexibility to use as a primary or as a secondary dressing cover in alginates, foams and hydrogels [66]. Due to their adherence, films are easy to apply and do not need a second dressing [73]. On the other hand, they have non-absorbent characteristics that cause an accumulation of exudate and a maceration of wound edges, being necessary to change them frequently. The adhesive properties of films may potentially injury the skin, mostly in patients with delicate skin, such as elderly people and those with cutaneous atrophy. Therefore, in this case they should reduce the dressing changes to minimum or even avoid the use thereof [68].

Antimicrobial protection has been also addressed over the years and there are already films with this functionality in the market, such as 3 M™ Tegaderm™ CHG Chlorhexidine Gluconate I.V. Securement Dressings (3 M Healthcare) and Acticoat 7 (Smith and Nephew) that contains silver. In this sense Kim and coworkers [80], investigated a nitric oxide-releasing chitosan film. That film demonstrated a stronger antimicrobial activity against *Pseudomonas aeruginosa* and *Staphylococcus aureus* and, simultaneously, the film accelerated wound healing and epithelization in a rat model. Nevertheless, innovative solutions are presently under development. Novel chitosan and cellulose acetate polymer composites were prepared by solvent-casting method [81]. The formed films were loaded with nanosized cerium oxide, and the results revealed to be promising as potential wound covering material. Alginate films containing pyrogenic silica supported silver nanoparticles were prepared via solid state sintering route without the use of any solvent and reducing agent [82]. Films exhibited antimicrobial and antibiofilm activities against *S. aureus* and *P. aeruginosa* and showed no cytotoxicity towards human skin keratinocytes and human fibroblasts HuDe, with promising evidences as wound dressing toward infected tissues. Novel adhesive composite films were prepared for mupirocin dermal delivery. Natural polymers as chitosan, sodium alginate and carbopol were used for films' development to evaluate possible interactions and the impaired drug release properties [83]. Solvent evaporation method was used for the films' preparation. The formulation was found more effective compared to the market product (Bactroban® cream)

for wound healing at Balb-c mice, which highlights the potential for application as a wound care system.

In a different perspective a series of cross-linked films based on the combination of an elastin-derived biomimetic polypeptide (Human elastin-like polypeptide (HELP)) with alginate (ALG) were studied by Bergonzi et al. to obtain a composite with enhanced antioxidant properties [84]. ALG/HELP composite films loaded with the hydrophobic natural antioxidant curcumin were prepared by solvent casting method followed by the cross-linking with calcium chloride. The antioxidant activity correlated to the increase of HELP content, suggested the applicability of these composites as smart biomaterials for different biomedical applications.

Hydrocolloids

Hydrocolloids are moist wound dressings, that usually comprise a backing material (e.g. semi-permeable films, foams or non-woven polyester fibers) and a layer with hydrophilic/colloidal particles that may contain biocompatible gels made of proteins (e.g. collagen, gelatin) or of polysaccharides (e.g. cellulose and its derivatives) [72, 85]. Hydrocolloids are commonly primary dressings, biodegradable, non-breathable, and adherent to the skin, so that no separate taping is required. They are also waterproof, allowing regular water contact with skin.

Hydrocolloid dressings have been carefully addressed by Broussard et al. [66] in are view on wound dressings. The most commonly used are composed of a polyurethane external layer and an internal layer of a hydrophilic polymer such as gelatin e, pectin or carboxymethyl cellulose [86]. In their native stage they are impermeable to water, but once in contact with the wound exudate they are able to absorb it and form a gel, progressively more permeable to water vapour and air, which allows the excess of fluid to be removed without wound desiccation [87]. The moist conditions produced under the dressing and the control of the exudate are intended to promote fibrinolysis, angiogenesis and wound healing, to encourage the production of granulation tissue and to increase the quantity of synthesized collagen, leading to an increase on tissue regeneration, without causing softening and breaking down of the tissue [86]. On the other hand, these dressings also contribute for a better management of pain, due to the hydration enhancement, which will help the autolytic debridement, and will also provide a physical barrier to external microorganisms [86, 88]. Nevertheless, because these products are non-breathable they are not recommended prior to infection control [87].

There are a great variety of commercially available hydrocolloid dressings such as Granuflex®, Aquacel™, Comfeel™, Tegaserb™, Exuderm®, Duoderm®, Ultec™ or Tegaderm™ and these are adequate solutions for both acute and/or chronic wounds, moist or dry, to form a semipermeable thin sheet and to produce a flat, occlusive and adhesive dressing [89]. These dressings are made in sheets that can easily be cut to fit the desired size or shape of ulcers, traumatic injuries, surgical wounds, graft donor sites, superficial wounds, and some burns without the need of separate taping [88]. Due to its diversity and availability at a relatively low cost, to introduce innovation on hydrocolloid dressings, becomes a difficult task. Hydrocolloid drug loading has been attempted by several authors [87, 89, 90] Thu et al. [87] developed a novel bilayer hydrocolloid film based on alginate, which was investigated

as slow-release wound healing vehicle. The bilayer was composed of an upper layer impregnated with model drug (ibuprofen) and a drug-free lower layer, which acted as a rate-controlling membrane [87]. Successful results suggested that they can be exploited as slow-release wound dressings for low exudate wounds. In another study, novel chitosan (Ch) and hyaluronan (HA) wound dressings were developed loaded tiopronin and captopril as antiinflammatory drugs. Composite biomembranes were examined in skin wounds of ischemic rabbits to accelerate the process of healing. Data proved that the biomembranes composed of Ch/HA/tiopronin or Ch/HA/captopril facilitated healing of skin wounds compared to untreated animals and animals treated with Ch/HA membranes [91]. In a different report, a dressing based on PLGA and Aloe vera was developed containing lipid nanoparticles (NLCs). NLCs were added to prevent dressing from adhering to the wound and improve handling. Consequently, the PLGA-AV-NLC membrane promises to be a promising strategy for the treatment of chronic wounds, since it has improved handling compared to formulations without the lipid character of NLCs [92]. To overlap the adhesion loss of hydrocolloid wound dressings which seriously reduces the therapeutic efficiency and patient experience, hydrocolloid dressings were investigated using sodium carboxymethyl cellulose (CMC)-filled hydrocolloid dressings exposing to physiological environment as model. The results promoted the designing of hydrocolloid dressings with both excellent humidity control and sustained self-adhesiveness [93].

Hydrogels

Hydrogels are commonly defined as polymer three-dimensional networks that may be composed of crosslinked natural polymers (e.g. alginate, chitosan, gelatine, silk) or synthetic macromolecules (e.g. polyethylene glycol, polyvinyl alcohol) [94]. Hydrogels have been reviewed by Moura et al. [72] in a wound dressing report about diabetic wound healing and regeneration. Wound dressing hydrogels can be applied either as an amorphous gel or as an elastic film or solid sheet. These dressings usually require a secondary covering such as gauze, that need to be changed frequently, while hydrogel films or sheets may be used as both primary or secondary dressings [95].

Commercially available hydrogels (ActiformCool®, Stimulen™, Regenecare®, Intrasite Gel, Solosite Gel, Kendall™, 2nd skin®, Tegagel™) are flexible, rubbery and soft, nonreactive or irritant, biocompatible, and permeable to metabolites [96]. Typically, hydrogels are non-adherent and cool to the surface of the wound, which may lead to a better management of pain and therefore a better patient acceptability. Commonly they are suitable for cleansing of dry, sloughy or necrotic wounds by rehydrating dead tissues and enhancing autolytic debridement (Fig. 5). Nonetheless hydrogel dressings due to their high content of water (70–90%) are not suitable to be applied in heavily exuding wounds, once fluid accumulation can lead to skin maceration and bacterial proliferation.

The highly-hydrated network of a hydrogel can be held together via physical or chemical crosslinks, can be made biodegradable, and responsive to specific stimuli such as pH and temperature, and can be engineered to deliver therapeutic cells, drugs and soluble factors in a sustained and controlled way [97]. The success of application of hydrogels as a delivery system in wound healing will largely depend

on biomimetic design and engineering, harnessing cell–material interactions in the cell fate and functions [97].

In Table 3 are summarized a few studies on advances in hydrogel formulation for wound healing and regeneration. Shukla et al. [98] studied an apigenin loaded hydrogel using gellan gum—chitosan with polyethylene glycol as a cross linker. Results proven that the prepared hydrogel seems to be highly suitable for wound healing due to adequate properties of biocompatibility, biodegradability, moist nature and antioxidant effectiveness. Agubata et al. [96] developed and evaluated wound healing hydrogels containing hydroxypropyl methylcellulose, ofloxacin and biodegradable microfibrils from surgical sutures. These formulations promoted high collagen deposition after twenty-one days of wounding, with minimal scar formation. Evidences support the promising use of these hydrogels containing for effective wound healing.

Zeng et al. [99], developed injectable gelatin microcryogels which could load cells for enhanced cell delivery and cell therapy for wound healing. In this study, human adipose-derived stem cells (hASCs) laden in gelatine microcryogels, were instigated as primed injectable 3D micro-niches for a new cell delivery methodology for skin wound healing. Results showed wound bed recovery and a direct effect on wound basal layer for healing enhancement. Gong et al. [100] studied a biodegradable *in situ* thermosensitive hydrogel as a controlled drug delivery system composed of curcumin loaded polymeric micelles for successful cutaneous wound repair. Despite advances in the design and development of hydrogels it is still a challenge to develop a hydrogel with good stability and strong mechanical attributes for hemostasis and wound healing. In this sense, a recent study has developed a new polysaccharide hydrogel based of fenugreek gum-cellulose composite. A fenugreek gum was combined with cellulose through hydrogen bonding to form a hydrogel to improve the mechanical properties of the compound hydrogel [101]. Notably, hemostasis and wound healing have been confirmed, which highlights the promising medical potential of the compound hydrogel to promote wound healing [101]. The preparation of hydrogel-based materials with high antibacterial activities and good biosafety at the same time can also be challenging. In order to answer this crucial problem, Yang et al. [102] has developed a physical hydrogel composed of multi-functional chitosan/ carboxymethyl chitosan/ silver polyelectrolyte (CTS/ CMCTS/ AgNPs). A physical hydrogel composed and built by *in situ* photoreduction of silver ions with CMCTS α -hydroxy and acidification sol by semi-dissolving gel transition methods (SD-A-SGT) using natural polymers with no chemical reducer involved. This composite showed desired biosafety and antibacterial activities simultaneously, with great application potentials as wound dressing.

In a different point of view Lin et al., studied the importance of anti-inflammation and angiogenesis in wound healing [103]. Therefore, the team developed a composite hydrogel dressing with stepwise delivery of diclofenac sodium (DS) and basic fibroblast growth factor (bFGF) to be applied in the inflammation stage and new tissue formation stage respectively for wound repair. The *in vivo* wound healing of rats revealed that this composite hydrogel showed a better healing effect with a wound contraction of 96% at 14 d, less inflammation and higher angiogenesis, than all

control groups. This is promising data for hydrogel wound dressings [103]. Hamdi et al developed chitosan and protein isolate composite hydrogels, for carotenoids-controlled delivery and wound healing. The concentration of the protein isolate was increased to turn chitosan hydrogels more elastic, not exceeding 15% (w/w) of protein isolate concentration in the chitosan-protein isolate composite hydrogels revealed low cytotoxicity towards MG-63 osteosarcoma cells. The topical application of adhesives based on this hydrogel compound and enriched with carotenoids, allowed the acceleration of wound healing and complete regeneration being a promising new biomaterial [104].

4.2 Tissue Engineered Skin Substitutes and Advanced Wound Healing

Regenerative medicine is a recent but already widely accepted and expanding field involving the development and/or manipulation of molecules cells, tissues or organs to repair, replace or support injured body parts in order to recover their function [105]. Tissue engineering can be perceived now as among the available regenerative medicine strategies and can be defined as the science of persuading the body to heal itself through the supply of molecular signals, cells and scaffolds, to the adequate anatomic sites [106]. For skin regeneration, it essentially consists in expanding skin or stem cells, cultivating in a biomaterial support structure or scaffold, eventually combining biomolecules of interest such as growth factors, and then implanting the cell-scaffold construct for restoring the barrier function (initial step in burns) or for promoting wound healing (e.g., chronic wounds) [107].

This field has been assuming increasing clinical relevance due to the successful clinical tissue engineering-based products already available, namely for skin regeneration. Its clinically proven potential, associated to the limitation of the previously described technologies, allow tissue engineering, and regenerative medicine in general, to bring hope as solution for several clinical problems presently unsolved.

Tissue engineered skin substitutes, given their potential higher similarity to the natural skin tissue, are capable of overcoming several of the limitations previously described for skin grafts, namely donor shortage, and conventional wound dressings, namely undesirable adhesion to the lesion, impossibility associated to the difficulty in reproducing skin appendages and incapacity to replace the lost tissue, particularly the dermis [85, 108–110].

Tissue engineering has been particularly successful in the field of wound healing, and in particular for the treatment of burns and chronic wounds. This is actually the more mature and only area of application where several different products are already available, recurring to distinct strategies and with varied clinical success, ranging from non-cellularized products, composed of a biodegradable and porous polymeric matrix ready for implantation, to considerably sophisticated cellularized products, reproducing the compositional complexity of both dermis and epidermis

[111–113]. The biomaterial scaffold used can be produced using natural, synthetic or hybrid polymers and serves as a template for cell adhesion, proliferation and differentiation, playing a crucial role in guiding neo tissue morphogenesis [109, 114–116]. Additionally, natural skin healing can be stimulated through the incorporation, into these products, of a myriad of biomolecules such as genes, drugs, cytokines or growth factors [109, 111, 112].

Clinically available skin substitutes can be broadly divided into epidermal, dermal and dermo-epidermal products [109, 111, 117], although other categorization modalities exist. For regenerating superficial wounds, several commercial epidermal substitutes exist, using either autologous or allogeneic keratinocytes, namely MySkin[®] (CellTran, UK), consisting of a silicone layer seeded with autologous keratinocytes, Epicel[®] (Genzyme Biosurgery, USA), made of petrolatum gauze covered by autologous keratinocytes sheets, Epidex[®] (Eurodern, Switzerland), consisting of a silicone membrane cultured with autologous keratinocytes from the outer root sheath, and ReCell[®] (Avita Medical, Australia), where autologous keratinocytes are directly sprayed into the lesion [118–120]. Although generally providing an efficient epidermal coverage epidermal constructs present several limitations, namely long fabrication time due to the obtention and expansion of keratinocytes, difficult handling due to their fragile nature, variable engraftment rates and high cost [109, 120].

For the regeneration of full thickness wounds dermal tissue is required and mechanical stability is important to prevent wound contraction [109, 121]. For wound coverage dermal substitutes are usually associated to a permanent epidermal substitute using autologous split-thickness skin grafts or cultured epithelial autografts [19]. Available products in the market providing effective dermal regeneration include several cell-free products, such as Integra[®] (Integra LifeSciences, USA), a nanofibrous composite bilayer mesh composed of crosslinked collagen and glycosaminoglycan layer and a semi-permeable polysiloxane layer, Hyalomatrix[®] (Anika Therapeutics, USA), a bilayered hyaluronic acid-based scaffold covered with a silicone sheath, Matriderm[®] (MedskinSolutions, Germany), a composite collagen and elastin scaffold, and AlloDerm[®] (Lifecell, USA), a donated human dermis processed to remove cells, as well as cellularized scaffolds containing fibroblasts, such as Dermagraft[®] (Organogenesis, USA), a cryopreserved human fibroblast-derived dermal substitute, generated by the culture of neonatal dermal fibroblasts onto a bioresorbable poly(lactic-co-glycolic acid) (PLGA) mesh scaffold [109, 120, 122, 123].

Dermal-epidermal substitutes are the most advanced tissue engineered currently available in the clinics since they mimic both skin layers (dermis and epidermis) for full skin regeneration. Dermal-epidermal substitutes available in the market include PermaDerm[®] (Regenicin, USA), constituted by a biodegradable collagen scaffold cultured with autologous fibroblasts and keratinocytes, and Apligraf[®] (Organogenesis, USA), a composite bi-layered product composed of two distinct nanofibrous layers, being the lower dermal layer constituted by bovine type I collagen cultured with human allogeneic fibroblasts and the upper epidermal layer constituted by

cultured human allogeneic keratinocytes [109, 111]. Although providing more effective regeneration of full-thickness skin defects than conventional treatments, these products still present several limitations, namely inefficient wound closure due to rejection of allogeneic cells, high production costs [109].

Overall, tissue engineered skin substitutes present several advantages when compared with conventional treatments, including faster regeneration, increased dermal component in the healed wound, lower vascularization requirements, and reduced presence of inhibitory factors [124]. However, they still also present several limitations as previously pointed out, including lack of skin appendages, such as hair follicles, sebaceous glands and sweat glands, poor cell, inefficient vascularization, wound contraction, fibrosis, scarring at graft margins, use of animal-derived serum in cell culture, and high manufacturing costs [109, 112, 120, 124–126].

To overcome these limitations, several advanced skin regeneration strategies are under development in order to address both the fundamental issues underlying the limited understanding of the phenomena involved, as well as the technological barriers inhibiting their implementation. For instance, in order to promote the formation of skin appendages recent studies explore the culture of specific cells, including stem cells, such as Schwann cells, hair follicle cells, or melanocytes into scaffolds [113, 127]. Other strategies explore the used of advanced fabrication technologies, such as electrospinning or 3D printing, to fabricate scaffolds combined with cells and adequate biomolecules with improved complexity in terms of compositional and architectural biomimicry and providing better control over cell seeding [113, 128–132].

5 Sensing the Wound

The management of chronic wounds can greatly benefit from sensing tools able to predict in real time the need for a specific therapeutic intervention and whether the therapy is working or not. Adding diagnostic and theranostic sensors to wound management is an exciting possibility. The immediate benefits for the clinicians and patients are obvious: an increase of the treatment efficiency, the reduction of treatment time, and in extreme cases, lowering the risk of amputation. On the other hand, sensing the wound can give us new insights about the series of complex biochemical events related to the healing and regeneration process, contributing for a better wound assessment.

5.1 Detectable Biomarkers

Research on biomarkers for the assessment of wound status is of extreme relevance. However, this is a slowly progressing field due to the difficulty on isolating specific biochemical and physiological events that could be used to represent each wound

Table 4 Progress on biomarkers for wound healing
Adapted from WUWHs [134]

Main classes of biomarkers (as identified in 2007 consensus meeting)
<ul style="list-style-type: none"> • Bacterial load/specific microbial species/biofilms • Cytokine release in response to specific microbial antigens • DNA—e.g. gene polymorphisms • Enzymes and their substrates—e.g. matrix metalloproteinases and extracellular matrix • Exposed bone • Growth factors and hormones—e.g. platelet-derived growth factor • (PDGF), sex steroids (androgens/oestrogens), thyroid hormones • Immunohistochemical markers—e.g. integrins, chemokine receptors and transforming growth factor beta II receptors • Inflammatory mediators—e.g. cytokines and interleukins • Nitric oxide • Nutritional factors—e.g. zinc, glutamine, vitamins • pH of wound fluid • Reactive oxygen species • Temperature • Transepidermal water loss from periwound skin
Newly identified biomarkers
<ul style="list-style-type: none"> • Uric acid • Glucose • H₂O₂

event [133]. Almost a decade ago Harding et al. [134] have gathered in a consensus meeting for discussing the progress of wound monitorization and have generated a list of potential wound markers, which served as basis to the studies in the following years. More recently other markers have been identified and added to this list, as summarized in Table 4.

Some of these markers have been recently gaining importance while others have led to contradictory results and difficulties upon their detection. Recently, Dragaville et al. [135] reviewed the state-of-the-art on some of the most effective markers, either embedded in dressings or as point-of-care (POC) techniques for wound assessment and monitoring. These include temperature, oxygen, bacteria, pH and biochemical signals.

Among the different wound types, chronic non-healing wounds have been particularly studied for biochemical markers, through several clinical investigations [136, 137]. Proteases, protease inhibitors, and pro-inflammatory cytokines are presently under study either locally at the wound site and/or systemically using high-throughput screening (metabolomic, proteomic, genomic and lipidomic analysis) [138]. Of these, proteases (serine, metalloproteinases, cysteine, aspartic) and specifically matrix metalloproteinases have received the most attention in studies of chronic wounds, showing great potential as targets for wound assessment [137, 139]. In a recent review

by Lindley et al. [138], some steps are proposed for the validation and implementation of these clinically applicable biomarkers, including those measured in tissue (ex. β -catenin), wound fluid (matrix metalloproteinases and interleukins), swabs, wound microbiota, and serum (ex. procalcitonin and matrix metalloproteinases).

The ongoing research on the above mentioned biomarkers or on others certainly discovered in the future gains more relevance when sustained in the idea of developing appropriated sensor tools. Since a wound is a dynamic environment, there is a strong need to develop systems that can diagnose the wound parameters in a minimally invasive way and report continuously on the type of environment inside the wound. Ideally it would consist of individual or combined sensors for pH, temperature, humidity, oxygen, bacteria sensors, etc [135, 140]. To monitor these parameters is not a difficult task, however the generated information needs to be precisely correlated to the events taking place in the wound bed. For instances a pH variation can occur following an inflammatory process or due to an infection [141, 142]. On the other hand, variations in wound pH will influence proteolytic activity and oxygen content and so measurements of enzyme activity may not be relevant unless correlated with pH [142].

5.2 *Multicomponent Biosensor Dressings*

The combination of sensors and dressings with active properties is nowadays considered as the gold standard, although numerous challenges still need to be overcome. A biosensor integrated within the dressing should be able to detect low levels of a certain biomarker (ex: resulting from a bacterial contamination) and consequently emit a recognizable output indicative of infection risk. Ideally this smart sensor should then trigger a material response towards a therapeutic effect, e.g., the controlled release of a pre-loaded drug. This could be achieved by integrating switchable surfaces or stimuli-responsive materials into the dressing to generate smart composites [135, 140, 143, 144]. At the same time the sensor should provide information about different parameters indicative of the status of the wound, in particular pH, temperature, moisture, and exudate production, etc. In doing so, these smart dressings will help shifting the paradigm of chronic wound care from routine management and time-based dressing changes toward cost effective personalized care and knowledge-based treatment [140, 144].

There is a significant effort in the research community to develop near-patient or wearable devices to enable wound care professionals to objectively measure the wound status. There have been advances in monitoring moisture [145–147], pH [145, 146], oxygen, protease [140, 144], and bacterial load [142, 146, 148, 149]; however, only a few of these systems are available for commercial use. At the present time, it is striking how few wound care devices have made it into clinical use. Recent advances on sensor research in wound monitoring have been made mostly on generic physiological status indicators such as, moisture [144, 145], pH [142, 146], oxygen [142, 150], and bacterial load [148, 149] and temperature.

In the case of moisture sensors, only slight advances have been made. A sensor to measure moisture content has been commercialized by Ohmedics Ltd (Glasgow, UK) following research on the moisture status of advanced wound dressings [146]. The WoundSense™ device is a disposable moisture sensor, suitable for use in any dressing and allows moisture monetarization without the need to disturb the dressing. Recently, Milne et al. [140] have reported the first large-scale observational study using this system. The results suggest that a large number of unnecessary dressing changes are being made, with disturbance of the wound bed and impact on healing and costs associated.

Presently, a considerable attention is being paid to wound pH monitoring, as it affects fibroblasts/keratinocytes activity, microbial proliferation and oxygen release to the tissues, altering the immune response of the wound [142]. As reported in the literature [151], the pH of healthy human skin is in the range of 4.0–7.0. In chronic venous leg ulcers and in pressure ulcers, an increase in pH (i.e. alkaline or neutral pH) is a sign of infection, if compared with the normal surrounding skin. Although the ideal pH sensor is yet to be discovered, there have been considerable developments in recent years, mostly in response to the limitations of the traditional glass potentiometric system related to its fragility and inability to measure multiple wound regions simultaneously and continuously [143]. These only provide localized measurements and are not feasible for complex measurements across the surface of a heterogeneous wound surface. Other strategies have been explored over the last years for continuous monitoring of the pH, either through electrochemical [148, 149, 151] or colorimetric methods [152, 153]. Electrochemical sensors measure the concentration of H⁺ ions based on the rate of electrochemical reactions. Recently, Sharp et al. [150] has proposed a version of printed electrodes on flexible acetate sheets that incorporate uric acid for monitoring wound pH. This sensor can detect pH in a broad range, from 4.0 to 10. Guinovart et al. [148] have modified a commercial adhesive bandage to create a pH sensor by screen printing Ag/AgCl and carbon electrodes onto it. This wearable pH sensor has shown to detect variations between 5.5 and 8 of pH values. More recently Rahimi et al. [149] have developed an inexpensive flexible array of pH sensors fabricated on a polymer-coated commercial paper, to be integrated in low-cost dressings as a way to map the pH at various wound sites. Another approach that has attracted noticeable attention is the use of pH sensitive materials and dyes for detection of skin pH [138, 140, 152, 153]. These colorimetric sensors are usually easy-to-read and can be utilized without integrated electronics. However, a key challenge for fabrication and use of these systems is to prevent the dye from leaching out of the dressing onto the skin. In addition, the sensitivity of the dye should cover the entire range of pH variation observed in skin disorders and wounds (pH = 4–9). Recently Tamayol et al. [153], developed a composite hydrogel alginate-based microfibers containing mesoporous particles loaded with a pH-responsive dye. The fabricated pH-responsive microfibers were flexible and able to maintain contact with skin, minimizing the leakage of the dye from the fibers. Non-invasive luminescence imaging is also of great interest for studying biological parameters in wound healing. Schreml et al. [154] have developed the first method for 2D luminescence imaging

of pH *in vivo* on humans. More recently they have described a sprayable luminescent pH sensor able to be applied to very uneven wound tissues [155].

Oxygen is one of the critical factors regulating the wound healing process [156], Acute hypoxia can cause tissue loss in a chronic wound and negatively impact the wound healing process [157]. Thus measuring oxygen concentration in real-time can be an effective tool for monitoring wound status. However, this parameter has only recently gained attention. Mostafalu et al. [158] have created a localized 3D-printed smart wound dressing platform that enables real-time data acquisition of oxygen concentration. The bandage contained a flexible oxygen sensor in a compact package, incorporating a series of off-the-shelf electronic components including a programmable-gain analog front-end, a microcontroller and wireless radio, an integrated electronic system with data readout and wireless transmission capabilities. This flexible platform can allow for a self-operating remote therapy for chronic wounds.

Uric acid (UA) concentration in wound exudate is another key marker which is recently being explored as specific indicator of wound status and infection since it is highly correlated with wound severity [159] and significantly decreases during bacterial infection [160]. Kassal et al. [161] described a new type of smart bandage for determination of uric acid (UA) status, by screen printing an amperometric biosensor directly on a wound dressing. The smart bandage biosensor interfaces with a wearable potentiostat for on-demand wireless data transfer to a computer, tablet, or Smartphone.

As described in this chapter, chronic wounds are extremely susceptible to infection, as the first defense barrier, the skin, is disrupted allowing for bacteria to invade the underlying tissue. Due to the clinical relevance of this problem to diagnose infection on a dressing at early stages and preferably, without its removal is a critical landmark. As herein referred, many of the above described sensors are used in dressings for detecting bacterial infection. But other strategies have been recently proposed, exploring different biochemical markers. For example, in a study by Kristmastuti et al. [162] a porous anodized aluminum oxide (pAAO) based biosensor was developed as a biosensing platform to detect proteinase K, an enzyme which is a readily available model system for the proteinase produced by *P. aeruginosa*. As a proof-of-concept, this platform was successfully tested with human wound fluid, highlighting the potential for detection of bacterial infections in chronic wounds. Hajnsek and coworkers [163] developed an electrochemical sensor for fast detection of wound infection based on the quantification of myeloperoxidase activity as a marker for bacterial infection.

The use of carbon fibre tow as an electrochemical sensing matrix for assessing pyocyanin production, a substance produced by *P. aeruginosa* as a result of quorum sensing during wound colonization, was proposed by Sharp et al. [164]. The proposed small and inexpensive sensor assembly is suggested for use in monitoring *P. aeruginosa* growth. Ciani et al. [165] have reported the design and characterization of an electrochemical biosensor system and impedance detection method capable of the multiparameter detection of TREM-1 (Triggering Receptor-1 Expressed on

Myeloid cells), MMP-9 (Matrix MetalloPeptidase 9) and HSL (N-3-oxo-dodecanoyl-l-HomoSerineLacton), relevant in bacterial quorum sensing. These antigens are used without amplification and with minimal pre-analytical requirements on screen printed electrodes (SPEs), which are cheap, commercially available.

Temperature is an important parameter to assess chronicity, is frequently used for monitoring at-risk patients and anticipate ulceration [166]. However, there is little research using temperature sensors embedded in wound dressings. This can be achieved by incorporating miniaturized wireless sensors within wound dressings, as proposed by Matzeu et al. [167]. They fabricated a sensor using multiwall carbon nanotubes and electrodes produced by electroplating nickel and gold over the copper tracks prepared through a lithography process. Due to the wireless communication ability, this system can be used under a bandage or a wound dressing for minimally invasive, remote monitoring of temperature.

Most of the current methods for incorporating biosensors in dressings to monitoring chronic wounds have been independently developed and therefore are predominantly single-parameter. However due to the complex, multi-stage progression of wound healing the development of wearable integrated systems with sensors and readout teletronics is a major goal in the continuous monitoring of a chronic wound. Some steps are being done in this integrative approach. For instances, Mehmood et al. [167] presented a low-power portable telemetric system for measuring and transmitting real-time information of wound-site temperature, sub-bandage pressure and moisture level from within the wound dressing. Wang et al. [168] reported the use of a sprayable and thermogelating biomaterial (Ploxamer TM; a.k.a. Pluronic) in optical imaging of pH values, local oxygen and temperature. The polymer sensor particles containing molecular probes (such as for sensing O₂, pH or temperature) are incorporated in the host material, and the resulted sensor cocktail was sprayed onto surface of interest at low temperature. On increasing temperature, the sprayed thin film forms a gel and tightly adheres to form a stable sensor film. Two of the most relevant fluctuating wound parameters during the healing process which are pH and glucose concentration. Jankowska et al. [169] presented a fluorescent sensing system to monitor the wound status and to distinguish between an autonomously healing and a chronic wound at an early stage. The system allows monitoring simultaneously pH and Glucose using a fluorescent pH indicator dye, carboxynaphthofluorescein, and a metabolite-sensing enzymatic system, based on glucose oxidase and horseradish peroxidase, immobilized on a biocompatible polysaccharide matrix.

6 Future Perspectives

Chronic wounds have a deep impact in patient's health, social life, and it means an economical general burden, being therefore a current topical interest worldwide. In this chapter, we have focused on the current state of the art in chronic wound healing medicines involving the active treatment of these wounds. The evolution of the different advanced wound dressings, skin substitutes and available commercially

products, have been discussed, highlighting the advantages of combining materials, bioactive compounds and sensors to better face the different stages of the wound. The exact moment of deciding which dressing should be used remains controversial and the existing medical literature is not helpful. Only a few, if any, prospective randomized control trials conclusively prove the superiority of one type of wound dressing over another [170]. Therefore, more wound care research providing level A evidence is needed. Nevertheless, in daily clinics, the decisions need to be taken and all strategies attempt to achieve the same goal: the successful healing.

The chapter covered many advanced wound dressings, including several types of polymeric systems and its composites in the form of foams, films, hydrogels and hydrocolloids for wound healing and tissue-engineered skin substitutes, dressings containing (antibiotics, silver, stem cells, etc). Although there is an enormous diversity of solutions, challenges still remain in tackling the problems associated with chronic wounds, and it is clear that one single advanced dressing does not always address the problems encountered in chronic wounds. Therefore, a combination of the above-mentioned advanced systems will be required, which implies that there is no single perfect dressing for all wounds. Nevertheless, the increasingly advanced biomaterials and their composite systems, creates favourable conditions for: better management and retention of the exudate; better adjustment to certain anatomical sites, not limiting the mobility of its users; better ease of removal of material for visual inspection, exchange of material for suspected infection; possibility to monitor parameters such as the pH or temperature.

The future of dressings points to the “interaction” between the material and user, as well as between the material and the clinician. It is not always easy to achieve or control all the variables involved in the process, because the dressing is optimised to control one or two needs, being optimal for the purpose of its design hence the professional’s assessment of the best material for the priority variable to be controlled at that time. The future will bring possibilities of monitoring, at the wound bed, important events such as: an infection or exudate increase.

As a concluding remark there is no single ideal dressing code for wound healing. In the future it seems crucial to address advanced multi-component dressings that will tackle the problems of chronic wounds such as: pain, inflammation, odour, infection, delayed healing, and associated costs to health systems and populations worldwide. Therefore, a multi-targeted approach seems to be the best way toward wound care, which also should include a more detailed comprehension by the health professional on the use of these advanced dressings and their recommendations.

Acknowledgements This work was supported by National Funds from FCT—Fundação para a Ciência e a Tecnologia through project UIDB/50016/2020. Sara Baptista-Silva gratefully acknowledges FCT for the grants (ref. SFRH/BPD/116024/2016).

References

1. Schultz GS et al (2004) Wound bed preparation and a brief history of TIME. *Int Wound J* 1:19–32
2. Fletcher J (2008) Differences between acute and chronic wounds and the role of wound bed preparation. *Nurs Stand* 22:62–68
3. Lazarus GS et al (1994) Definitions and Guidelines for Assessment of Wounds and Evaluation of Healing. *Arch Dermatol* 130:489–493
4. White RJ, Cutting K, Kingsley A (2006) Topical antimicrobials in the control of wound bioburden. *Ostomy Wound Manag* 52:26–58
5. Boulton AJ, Vileikyte L, Ragnarson-Tennvall G, Apelqvist J (2005) The global burden of diabetic foot disease. *Lancet* 366:1719–1724
6. Gottrup F (2004) A specialized wound-healing center concept: importance of a multidisciplinary department structure and surgical treatment facilities in the treatment of chronic wounds. *Am J Surgery* 187:38–43
7. Gottrup F, Holstein P, Jorgensen B, Lohmann M, Karlsmar T (2001) A new concept of a multidisciplinary wound healing center and a national expert function of wound healing. *Arch Surg* 136:765–772
8. Guest JF et al (2017) Health economic burden that different wound types impose on the UK's national health service. *Int Wound J* 14:322–330
9. Department of Health and Human Services (DHHS). CMS Manual System (2004) Pub. 100–07 State Operations Provider Certification SUBJECT: Revisions to State Operations Manual (SOM), Appendix PP—"Guidance to Surveyors for Long Term Care Facilities. 10:317
10. Bosanquet N, Brown D, Straub J, Harper DR, Ruckley CV (1999) Perceived health in a randomised trial of treatment for chronic venous ulceration. *Eur J Vasc Endovasc Surg* 17:155–159
11. Alves P, Costeira A, Vales L (2009) Reduzir a dor e o trauma no tratamento de feridas. *Rev Nursing* 20–25
12. Edwards J, Howley P, Cohen I (2004) In vitro inhibition of human neutrophil elastase by oleic acid albumin formulations from derivatized cotton wound dressings. *Int J Pharm* 284:1–12
13. Schönfelder U et al (2005) Influence of selected wound dressings on PMN elastase in chronic wound fluid and their antioxidative potential in vitro. *Biomaterials* 26:6664–6673
14. Baranoski S, Ayelo E (2006) O essencial sobre o tratamento de feridas—Princípios práticos
15. Clark RAF, Richard AF (1996). The molecular and cellular biology of wound repair
16. De Mendonça RJ, Coutinho-Netto J (2009) Aspectos celulares da cicatrização. *An Bras Dermatol* 84:257–262
17. Diegelmann RF, Evans MC (2004) Wound healing: an overview of acute, fibrotic and delayed healing. *Front Biosci* 9:283–289
18. Mandelbaum S, Santis É, Mandelbaum M (2003) Cicatrização: conceitos atuais e recursos auxiliares—Parte I. *An Bras Dermatol* 78:393–410
19. Werner S, Grose R (2003) Regulation of wound healing by growth factors and cytokines. *Physiol Rev* 83:835–870
20. Eming SA, Krieg T, Davidson JM (2007) Gene therapy and wound healing. *Clin Dermatol* 25:79–92
21. William M (2015) *Feridas: Conceitos e Atualidades*
22. Schultz GS, Davidson JM, Kirsner RS, Bornstein P, Herman IM (2011) Dynamic reciprocity in the wound microenvironment. *Wound repair Regen. Off. Publ. Wound Heal. Soc. [and] Eur. Tissue Repair Soc* 19:134–148
23. Singer AJ, Clark RAF (1999) Cutaneous wound healing. *N Engl J Med* 341:738–746
24. Robbins S et al (2005) Robbins & Cotran: Patologia—Bases patológicas das doenças
25. Balbino CA, Pereira LM, Curi R (2005) Mechanisms involved in wound healing: a revision. *Rev Bras Ciencias Farm J Pharm Sci* 41:27–51

26. Dvorak H (2002) Vascular permeability factor/vascular endothelial growth factor: a critical cytokine in tumor angiogenesis and a potential target for diagnosis and therapy. *J Clin Oncol* 20:4368–4380
27. Broughton G, Janis J, Attinger C (2006) The basic science of wound healing. *Plast Reconstr Surgery* 117:12–34
28. Gurtner GC, Werner S, Barrandon Y, Longaker MT (2008) Wound repair and regeneration. *Nature* 453:314–321
29. Macdonald JM, Geyer MJ, Organization WH (2010) In: John MM, Mary JG (eds) *Wound and lymphoedema*. vol 7. pp 122
30. Flanagan M (2013) In: *Wound healing and skin integrity: principles and practice*
31. Swanson T, Angel D (2017) Wound infection in clinical practice update. *Aust Nurs midwifery J* 24:33
32. Jones V, Grey JE, Harding KG (2006) Wound dressings. *BMJ* 332:777–780
33. Leaper DJ et al (2012) Extending the TIME concept: what have we learned in the past 10 years?(*). *Int Wound J* 9 Suppl 2:1–19
34. Nazarko L (2005) Part two: carrying out a thorough assessment. *Nurs Resid Care* 7:304–306
35. Percival SL, Emanuel C, Cutting KF, Williams DW (2012) Microbiology of the skin and the role of biofilms in infection. *Int Wound J* 9:14–32
36. Fyhrquist N, Salava A, Auvinen P, Lauerma A (2016) Skin Biomes *Curr Allergy Asthma Rep* 16:40
37. Grice EA, Segre JA (2011) The skin microbiome. *Nat Rev Microbiol* 9:244–253
38. Gethin G (2009) Role of topical antimicrobials in wound management. *J Wound Care* 1–8
39. Dow G, Browne A, Sibbald RG (1999) Infection in chronic wounds: controversies in diagnosis and treatment. *Ostomy Wound Manage* 45(22–29):23–27
40. Edwards R, Harding KG (2004) Bacteria and wound healing. *Curr Opin Infect Dis* 17:91–96
41. Frank DN et al (2009) Microbial diversity in chronic open wounds. *Wound Repair Regen Off Publ Wound Heal Soc [and] Eur Tissue Repair Soc* 17:163–172
42. Bowler PG, Duerden BI, Armstrong DG (2001) Wound microbiology and associated approaches to wound management. *Clin Microbiol Rev* 14:244–269
43. Schultz GS et al (2003) Wound bed preparation: a systematic approach to wound management. *Wound Repair Regen Off Publ Wound Heal Soc [and] Eur Tissue Repair Soc* 11 Suppl 1:S1–28
44. Warriner R, Burrell R (2015) Infection and the chronic wound: a focus on silver. *Adv Skin Wound Care* 18 Suppl 1:2–12
45. Bjarnsholt T, Moser C, Jensen PØ, Høiby N (2011) Chronic wound colonization, infection, and biofilms. *Biofilm Infect* 1–314. <https://doi.org/10.1007/978-1-4419-6084-9>
46. Siddiqui AR, Bernstein JM (2010) Chronic wound infection: facts and controversies. *Clin Dermatol* 28:519–526
47. Scalise A et al (2015) Microenvironment and microbiology of skin wounds: the role of bacterial biofilms and related factors. *Semin Vasc Surg* 28:151–159
48. Davies D (2003) Understanding biofilm resistance to antibacterial agents. *Nat Rev Drug Discov* 2:114–122
49. Zhao G et al (2013) Biofilms and inflammation in chronic wounds. *Adv Wound Care* 2:389–399
50. James GA et al (2008) Biofilms in chronic wounds. *Wound Repair Regen Off Publ Wound Heal Soc [and] Eur Tissue Repair Soc* 16:37–44
51. Percival SL et al (2012) A review of the scientific evidence for biofilms in wounds. *Wound Repair Regen Off Publ Wound Heal Soc [and] Eur Tissue Repair Soc* 20:647–657
52. McCarty SM, Percival SL (2013) Proteases and delayed wound healing. *Adv Wound Care* 2:438–447
53. Bjarnsholt T et al (2007) Silver against *Pseudomonas aeruginosa* biofilms. *APMIS* 115:921–928
54. Falanga V (2000) Classifications for wound bed preparation and stimulation of chronic wounds. *Wound Repair and Regeneration : Official Publication of the Wound Healing Soc [and] the Europ Tissue Repair Soc* 8:347–352

55. Kirketerp-Møller K, Zulkowski K, James G (2010) Chronic wound colonization, infection, and biofilms. *Biofilm Infections* 11–24. https://doi.org/10.1007/978-1-4419-6084-9_2
56. Brown-Etris M, Custshall W, Hiles M (2002) A new biomaterial derived from small intestine submucosa and developed into a wound matrix device. *Wounds* 14:150–166
57. Clark M et al (2014) Systematic review of the use of prophylactic dressings in the prevention of pressure ulcers. *Int Wound J* 11:460–471
58. Black J et al (2015) Use of wound dressings to enhance prevention of pressure ulcers caused by medical devices. *Int. Wound J* 12:322–327
59. Call E et al (2015) Enhancing pressure ulcer prevention using wound dressings: what are the modes of action? *Int. Wound J* 12:408–413
60. Das S, Baker AB (2016) Biomaterials and nanotherapeutics for enhancing skin wound healing. *Front Bioeng Biotechnol* 4:82
61. Eaglstein WH, Falanga V (1998) Tissue engineering and the development of Apligraf, a human skin equivalent. *Cutis* 62:1–8
62. Shores JT, Gabriel A, Gupta S (2007) Skin substitutes and alternatives: a review. *Adv Skin Wound Care* 20:410–493
63. Halim AS, Khoo TL, Mohd Yusoff SJ (2010) Biologic and synthetic skin substitutes: an overview. *Indian J. Plast. Surg. Off Publ Assoc Plast Surg India* 43:S23–8
64. Spasojević D et al (2016) Lignin model compound in alginate hydrogel: a strong antimicrobial agent with high potential in wound treatment. *Int J Antimicrob Agents* 48:732–735
65. Rezvanian M, Amin MCIM, Ng S-F (2016) Development and physicochemical characterization of alginate composite film loaded with simvastatin as a potential wound dressing. *Carbohydr Polym* 137:295–304
66. Broussard KC, Powers JG (2013) Wound dressings: selecting the most appropriate type. *Am J Clin Dermatol* 14:449–459
67. Cherusseri J et al (2017) Polymer-based composite materials: characterizations BT—composite materials: processing, applications, characterizations. In: Kar KK (ed) Springer, Berlin, Heidelberg, pp 37–77. https://doi.org/10.1007/978-3-662-49514-8_2
68. Dabiri G, Damstetter E, Phillips T (2016) Choosing a wound dressing based on common wound characteristics. *Adv Wound Care* 5:32–41
69. Seaman S (2002) Dressing selection in chronic wound management. *J Am Podiatr Med Assoc* 92:24–33
70. Aduba DCJ et al (2016) Fabrication, characterization, and in vitro evaluation of silver-containing arabinoxylan foams as antimicrobial wound dressing. *J Biomed Mater Res A* 104:2456–2465
71. Liu J, Morykwas MJ, Argenta LC, Wagner WD (2011) Development of a biodegradable foam for use in negative pressure wound therapy. *J Biomed Mater Res B Appl Biomater* 98:316–322
72. Moura LIF, Dias AMA, Carvalho E, Sousa, De HC (2013) Recent advances on the development of wound dressings for diabetic foot ulcer treatment —a review. *Acta Biomater* 9:7093–7114
73. Powers JG, Morton LM, Phillips TJ (2013) Dressings for chronic wounds. *Dermatol Ther* 26:197–206
74. Landsman TL et al (2017) A shape memory foam composite with enhanced fluid uptake and bactericidal properties as a hemostatic agent. *Acta Biomater* 47:91–99
75. Namviriyachote N, Muangman P, Chinaronchai K, Chuntrasakul C, Ritthidej GC (2020) Polyurethane-biomacromolecule combined foam dressing containing asiaticoside: fabrication, characterization and clinical efficacy for traumatic dermal wound treatment. *Int J Biol Macromol* 143:510–520
76. He M et al (2020) Smart multi-layer PVA foam/ CMC mesh dressing with integrated multi-functions for wound management and infection monitoring. *Mater Des* 194:108913
77. Oh G-W, Nam SY, Heo S-J, Kang D-H, Jung W-K (2020) Characterization of ionic cross-linked composite foams with different blend ratios of alginate/pectin on the synergistic effects for wound dressing application. *Int J Biol Macromol* 156:1565–1573

78. Wang Y et al (2018) Shape-adaptive composite foams with high expansion and absorption used for massive hemorrhage control and irregular wound treatment. *Appl Mater Today* 13:228–241
79. Bajpai SK, Jyotishi P, Bajpai M (2016) Synthesis of nanosilver loaded chitosan/poly(acrylamide-co-itaconic acid) based inter-polyelectrolyte complex films for antimicrobial applications. *Carbohydr Polym* 154:223–230
80. Kim JO et al (2015) Nitric oxide-releasing chitosan film for enhanced antibacterial and in vivo wound-healing efficacy. *Int J Biol Macromol* 79:217–225
81. Kalaycıoğlu Z et al (2020) Antibacterial nano cerium oxide/chitosan/cellulose acetate composite films as potential wound dressing. *Eur Polym J* 133:109777
82. Ambrogi V et al (2020) Biocompatible alginate silica supported silver nanoparticles composite films for wound dressing with antibiofilm activity. *Mater Sci Eng, C* 112:110863
83. Üstündağ Okur N et al (2019) An alternative approach to wound healing field; new composite films from natural polymers for mupirocin dermal delivery. *Saudi Pharm J* 27:738–752
84. Bergonzi C et al (2020) Alginate/human elastin-like polypeptide composite films with antioxidant properties for potential wound healing application. *Int J Biol Macromol* 164:586–596
85. Boateng JS, Matthews KH, Stevens HNE, Eccleston GM (2008) Wound healing dressings and drug delivery systems: a review. *J Pharm Sci* 97:2892–2923
86. Pott FS, Meier MJ, Stocco JGD, Crozeta K, Ribas JD (2014) The effectiveness of hydrocolloid dressings versus other dressings in the healing of pressure ulcers in adults and older adults: a systematic review and meta-analysis. *Rev Lat Am Enfermagem* 22:511–520
87. Thu H-E, Zulfakar MH, Ng S-F (2012) Alginate based bilayer hydrocolloid films as potential slow-release modern wound dressing. *Int J Pharm* 434:375–383
88. Mazzurco JD, Krach KJ (2012) Use of a hydrocolloid dressing to aid in the closure of surgical wounds in patients with fragile skin. *J Amer Acad Dermatol* 66:335–336
89. Jin SG et al (2015) Mechanical properties and in vivo healing evaluation of a novel Centella asiatica-loaded hydrocolloid wound dressing. *Int J Pharm* 490:240–247
90. Jin SG et al (2016) Influence of hydrophilic polymers on functional properties and wound healing efficacy of hydrocolloid based wound dressings. *Int J Pharm* 501:160–166
91. Valachova K, Svik K, Biro C, Soltes L (2020) Skin wound healing with composite biomembranes loaded by tiopronin or captopril. *J Biotechnol* 310:49–53
92. Garcia-Orue I et al (2019) Composite nanofibrous membranes of PLGA/Aloe vera containing lipid nanoparticles for wound dressing applications. *Int J Pharm* 556:320–329
93. Kong D et al (2020) Adhesion loss mechanism based on carboxymethyl cellulose-filled hydrocolloid dressings in physiological wounds environment. *Carbohydr Polym* 235:115953
94. Marchesan S et al (2013) Self-assembly of ciprofloxacin and a tripeptide into an antimicrobial nanostructured hydrogel. *Biomaterials* 34:3678–3687
95. Dumville JC, O'Meara S, Deshpande S, Speak K (2011) Hydrogel dressings for healing diabetic foot ulcers. *Cochrane Database Syst Rev*. <https://doi.org/10.1002/14651858.CD009101.pub2>
96. Agubata CO, Okereke C, Nzekwe IT, Onoja RI, Obitte NC (2016) Development and evaluation of wound healing hydrogels based on a quinolone, hydroxypropyl methylcellulose and biodegradable microfibrils. *Eur J Pharm Sci Off J Eur Fed Pharm Sci* 89:1–10
97. Toh WS, Loh XJ (2014) Advances in hydrogel delivery systems for tissue regeneration. *Mater Sci Eng C Mater Biol Appl* 45:690–697
98. Shukla R, Kashaw SK, Jain AP, Lodhi S (2016) Fabrication of apigenin loaded gellan gum-chitosan hydrogels (GGCH-HGs) for effective diabetic wound healing. *Int J Biol Macromol* 91:1110–1119
99. Zeng Y et al (2015) Preformed gelatin microcryogels as injectable cell carriers for enhanced skin wound healing. *Acta Biomater* 25:291–303
100. Gong C et al (2013) A biodegradable hydrogel system containing curcumin encapsulated in micelles for cutaneous wound healing. *Biomaterials* 34:6377–6387
101. Deng Y et al (2020) Novel fenugreek gum-cellulose composite hydrogel with wound healing synergism: facile preparation, characterization and wound healing activity evaluation. *Int J Biol Macromol* 160:1242–1251

102. Yang J et al (2020) Preparation of a chitosan/carboxymethyl chitosan/AgNPs polyelectrolyte composite physical hydrogel with self-healing ability, antibacterial properties, and good biosafety simultaneously, and its application as a wound dressing. *Compos Part B Eng* 197:
103. Lin X et al (2020) An alginate/poly(N-isopropylacrylamide)-based composite hydrogel dressing with stepwise delivery of drug and growth factor for wound repair. *Mater Sci Eng, C* 115:111123
104. Hamdi M et al (2020) A novel blue crab chitosan/protein composite hydrogel enriched with carotenoids endowed with distinguished wound healing capability: In vitro characterization and in vivo assessment. *Mater Sci Eng, C* 113:110978
105. Atala A (2009) Foundations of regenerative medicine: clinical and therapeutic applications
106. van Blitterswijk C et al (2008) In: *Tissue engineering*
107. MacNeil S (2007) Progress and opportunities for tissue-engineered skin. *Nature* 445:874–880
108. Jurczak F et al (2007) Randomised clinical trial of Hydrofiber dressing with silver versus povidone-iodine gauze in the management of open surgical and traumatic wounds. *Int Wound J* 4:66–76
109. Groeber F, Holeiter M, Hampel M, Hinderer S, Schenke-Layland K (2011) Skin tissue engineering—in vivo and in vitro applications. *Adv Drug Deliv Rev* 63:352–366
110. Mayet N et al (2014) A comprehensive review of advanced biopolymeric wound healing systems. *J Pharm Sci* 103:2211–2230
111. Shevchenko RV, James SL, James SE (2010) A review of tissue-engineered skin bioconstructs available for skin reconstruction. *J R Soc Interface* 7:229–258
112. Greaves NS, Iqbal SA, Baguneid M, Bayat A (2013) The role of skin substitutes in the management of chronic cutaneous wounds. *Wound repair Regen Off Publ Wound Heal Soc [and] Eur Tissue Repair Soc* 21:194–210
113. Pereira RF, Barrias CC, Granja PL, Bartolo PJ (2013) Advanced biofabrication strategies for skin regeneration and repair. *Nanomedicine (Lond)* 8:603–621
114. Kalyanaraman B, Boyce ST (2009) Wound healing on athymic mice with engineered skin substitutes fabricated with keratinocytes harvested from an automated bioreactor. *J Surg Res* 152:296–302
115. Shevchenko RV et al (2014) The in vitro characterization of a gelatin scaffold, prepared by cryogelation and assessed in vivo as a dermal replacement in wound repair. *Acta Biomater* 10:3156–3166
116. Sharma K, Bullock A, Ralston D, MacNeil S (2014) Development of a one-step approach for the reconstruction of full thickness skin defects using minced split thickness skin grafts and biodegradable synthetic scaffolds as a dermal substitute. *Burns* 40:957–965
117. Yildirim L, Thanh NTK, Seifalian AM (2012) Skin regeneration scaffolds: a multimodal bottom-up approach. *Trends Biotechnol* 30:638–648
118. Gravante G et al (2007) A randomized trial comparing ReCell system of epidermal cells delivery versus classic skin grafts for the treatment of deep partial thickness burns. *Burns* 33:966–972
119. Zweifel CJ et al (2008) Initial experiences using non-cultured autologous keratinocyte suspension for burn wound closure. *J Plast Reconstr Aesthet Surg* 61:1–4
120. Böttcher-Haberzeth S, Biedermann T, Reichmann E (2010) Tissue engineering of skin. *Burns* 36:450–460
121. Philandrianos C et al (2012) Comparison of five dermal substitutes in full-thickness skin wound healing in a porcine model. *Burns* 38:820–829
122. van der Veen VC, Boekema BKHL, Ulrich MMW, Middelkoop E (2011) New dermal substitutes. *Wound Repair Regen* 19:59–65
123. Harding K, Sumner M, Cardinal M (2013) A prospective, multicentre, randomised controlled study of human fibroblast-derived dermal substitute (Dermagraft) in patients with venous leg ulcers. *Int Wound J* 10:132–137
124. Jayarama Reddy V et al (2013) Nanofibrous structured biomimetic strategies for skin tissue regeneration. *Wound Repair Regen Off Publ Wound Heal Soc [and] Eur Tissue Repair Soc* 21:1–16

125. Poinern GEJ et al (2010) Nanoengineering a biocompatible inorganic scaffold for skin wound healing. *J Biomed Nanotechnol* 6:497–510
126. Liu X et al (2012) Antimicrobial electrospun nanofibers of cellulose acetate and polyester urethane composite for wound dressing. *J Biomed Mater Res B Appl Biomater* 100:1556–1565
127. Sriwiriyanont P et al (2012) Morphogenesis of chimeric hair follicles in engineered skin substitutes with human keratinocytes and murine dermal papilla cells. *Experim Dermatol* 21:783–785
128. Nichol JW, Khademhosseini A (2009) Modular tissue engineering: engineering biological tissues from the bottom up. *Soft Matter* 5:1312–1319
129. Zamanian B, Kachouie NN, Nichol JW, Khademhosseini A (2016) Self-assembly of cell-laden hydrogels on the liquid-air interface. 121–131
130. Rustad KC, Sorkin M, Levi B, Longaker MT, Gurtner GC (2010) Strategies for organ level tissue engineering. *Organogenesis* 6:151–157
131. Jakab K et al (2010) Tissue engineering by self-assembly and bio-printing of living cells. *Biofabrication* 2:22001
132. Dias JR, Granja PL, Bártoło PJ (2016) Advances in electrospun skin substitutes progress in materials science advances in electrospun skin substitutes. *Prog Mater Sci* 84:314–334
133. Eming SA, Martin P, Tomic-Canic M (2014) Wound repair and regeneration: mechanisms, signaling, and translation. *Sci Transl Med* 6:265sr6
134. Becker K et al (2009) Diagnostics and wounds: a consensus document. *World Counc Enteros Ther J* 29:18–20 22
135. Dargaville TR et al (2013) Sensors and imaging for wound healing: a review. *Biosens Bioelectron* 41:30–42
136. Eming SA et al (2010) Differential proteomic analysis distinguishes tissue repair biomarker signatures in wound exudates obtained from normal healing and chronic wounds. *J Proteome Res* 9:4758–4766
137. Broadbent J, Walsh T, Upton Z (2010) Proteomics in chronic wound research: potentials in healing and health. *Proteomics Clin Appl* 4:204–214
138. Lindley LE, Stojadinovic O, Pastar I, Tomic-Canic M (2016) Biology and biomarkers for wound healing. *Plast Reconstr Surg* 138:18–28
139. Amato B et al (2015) Role of matrix metalloproteinases in non-healing venous ulcers. *Int Wound J* 12:641–645
140. Mehmood N, Hariz A, Fitridge R, Voelcker NH (2014) Applications of modern sensors and wireless technology in effective wound management. *J Biomed Mater Res B Appl Biomater* 102:885–895
141. Schreml S et al (2010) The impact of the pH value on skin integrity and cutaneous wound healing. *J Eur Acad Dermatol Venereol* 24:373–378
142. Schneider LA, Korber A, Grabbe S, Dissemmond J (2007) Influence of pH on wound-healing: a new perspective for wound-therapy? *Arch Dermatol Res* 298:413–420
143. Salvo P, Dini V, Di Francesco F, Romanelli M (2015) The role of biomedical sensors in wound healing. *Wound Med* 8:15–18
144. McLister A, McHugh J, Cundell J, Davis J (2016) New developments in smart bandage technologies for wound diagnostics. *Adv Mater* 28:5732–5737
145. Milne SD et al (2016) A wearable wound moisture sensor as an indicator for wound dressing change: an observational study of wound moisture and status. *Int Wound J* 13:1309–1314
146. McColl D, Cartlidge B, Connolly P (2007) Real-time monitoring of moisture levels in wound dressings in vitro: an experimental study. *Int J Surg* 5:316–322
147. McColl D, MacDougall M, Watret L, Connolly P (2009) Monitoring moisture without disturbing the wound dressing. *Wounds UK* 5:94–99
148. Guinovart T, Valdés-Ramírez G, Windmiller JR, Andrade FJ, Wang J (2014) Bandage-based wearable potentiometric sensor for monitoring wound pH. *Electroanalysis* 26:1345–1353
149. Rahimi R et al (2016) A low-cost flexible pH sensor array for wound assessment
150. Sharp D (2013) Printed composite electrodes for in-situ wound pH monitoring. *Biosens Bioelectron* 50:399–405

151. Lambers H, Piessens S, Bloem A, Pronk H, Finkel P (2006) Natural skin surface pH is on average below 5, which is beneficial for its resident flora. *Int J Cosmet Sci* 28:359–370
152. Mohr GJ, Müller H (2015) Tailoring colour changes of optical sensor materials by combining indicator and inert dyes and their use in sensor layers, textiles and non-wovens. *Sens Actuators B Chem* 206:788–793
153. Tamayol A et al (2016) Flexible pH-sensing hydrogel fibers for epidermal applications. *Adv Healthc Mater* 5:711–719
154. Schreml S et al (2011) 2D luminescence imaging of pH in vivo. *Proc Natl Acad Sci USA* 108:2432–2437
155. Schreml S et al (2012) A sprayable luminescent pH sensor and its use for wound imaging in vivo. *Experim Dermatol* 21:951–953
156. Schreml S et al (2010) Oxygen in acute and chronic wound healing. *Br J Dermatol* 163:257–268
157. Sen CK (2009) Wound healing essentials: let there be oxygen. *Wound Repair Regen Off Publ Wound Heal Soc [and] Eur Tissue Repair Soc* 17:1–18
158. Mostafalu P et al (2016) A toolkit of thread-based microfluidics, sensors, and electronics for 3D tissue embedding for medical diagnostics. *Microsyst Nanoeng* 2:16039
159. Fernandez ML, Upton Z, Edwards H, Finlayson K, Shooter GK (2012) Elevated uric acid correlates with wound severity. *Int Wound J* 9:139–149
160. Sharp D, Davis J (2008) Integrated urate sensors for detecting wound infection. *Electrochem Commun Electrochem Commun* 10:709–713
161. Kassal P et al (2015) Smart bandage with wireless connectivity for uric acid biosensing as an indicator of wound status. *Electrochem Commun* 56:6–10
162. Krismastuti F, Bayat H, Voelcker N, Schönherr H (2015) Real time monitoring of layer-by-layer polyelectrolyte deposition and bacterial enzyme detection in nanoporous anodized aluminum oxide. *Anal Chem* 87:3856–3863
163. Hajnsek M et al (2015) *Sens Actuators B: Chem An Electrochem Sens Fast Detection of Wound Infection Based on Myeloperoxidase Activity* 209:2014–2016
164. Sharp D, Gladstone P, Smith RB, Forsythe S, Davis J (2010) Approaching intelligent infection diagnostics: carbon fibre sensor for electrochemical pyocyanin detection. *Bioelectrochemistry* 77:114–119
165. Ciani I et al (2012) Development of immunosensors for direct detection of three wound infection biomarkers at point of care using electrochemical impedance spectroscopy. *Biosens Bioelectron* 31:413–418
166. Dini V et al (2015) Correlation between wound temperature obtained with an infrared camera and clinical wound bed score in venous leg ulcers. *Wounds a Compend Clin Res Pract* 27:274–278
167. Mehmood N, Hariz A, Templeton S, Voelcker NH (2015) A flexible and low power telemetric sensing and monitoring system for chronic wound diagnostics. *Biomed Eng Online* 14:17
168. Wang X et al (2015) A water-sprayable, thermogelating and biocompatible polymer host for use in fluorescent chemical sensing and imaging of oxygen, pH values and temperature. *Sens Actuators B Chem* 221:37–44
169. Jankowska DA et al (2017) Simultaneous detection of pH value and glucose concentrations for wound monitoring applications. *Biosens Bioelectron* 87:312–319
170. Buck D, Galiano R (2007) In: *wound care. grabb and smith's plastic surgery*

Index

A

Acetylation, 4, 248
Albumin, 2, 8, 19, 20, 50, 162, 171, 277
Alendronate, 343, 360–362
Alginates, 1, 2, 4–7, 9–11, 48, 50, 51, 65, 68–71, 83, 213, 214, 216–222, 227, 231, 253, 257, 274–276, 280–283, 285, 286, 288, 317–320, 348, 378, 403, 404, 406, 408, 412, 416–418, 434, 436–439, 446
Alkaline phosphatase, 83
Allografts, 337, 339, 340, 382, 433
Aluminosilicates, 285
Anaplastic lymphoma kinase, 251
Antibody-drug conjugates, 246, 250
Anticancer drugs, 2, 5, 133–135, 137, 281, 284, 285, 287, 288
Antimicrobial agents, 273, 432
Apatite nanocrystals, 396
Atom-transfer radical polymerization, 202
Autografts, 99, 337, 339, 340, 382, 442

B

Backing material, 438
Bacterial cellulose, 96, 97, 276, 395, 413, 417
Beads, 10, 69, 152, 188, 213–232, 262, 272, 273, 281–284, 288
Binding agent, 213, 214, 216, 231, 287
Bioactive glass, 321, 346, 350, 352, 396
Bioactive glass ceramic nanoparticles, 75
Bioactive molecules, 1, 272, 341, 344, 348, 363

Biodegradability, 3, 7, 8, 10, 11, 17, 20, 21, 25, 73–75, 79, 85, 89, 94, 95, 99, 169, 227, 228, 249, 252, 272, 277, 347, 349, 350, 352, 353, 356, 378, 403, 413–415, 440
Biodegradable polymers, 2, 5, 7, 21, 25, 136, 346, 348–350, 356
Biofilm, 432, 433, 444
Bioimaging, 125, 154, 254, 258, 396
Biomass, 11, 65, 67, 74
Biomedical, 10, 26, 34, 46, 49, 67, 74, 82, 94, 99, 112, 151–153, 164, 169, 170, 174, 175, 187, 194, 207, 214, 252, 272, 276, 283, 287
Biomedical applications, 1, 11, 14, 16, 20, 26, 48, 49, 51, 52, 65, 94, 109, 110, 112, 125, 136–138, 151, 153, 158, 164, 174, 188, 205, 214, 217, 227, 253, 254, 261, 273, 275, 279, 282, 308, 322, 354, 438
Biomineralization, 75, 348, 349, 351, 353, 357, 395–397
Biomolecules, 1, 82, 159, 172, 205, 243, 249, 255, 273, 285, 287, 404, 441–443
Biomucoadhesive, 213, 216, 231
Bionanocomposite, 3, 86, 93, 378, 385, 387–389, 394–397
Biopolymeric-inorganic composites, 271, 276, 277
Biopolymers, 67, 71, 73, 79, 80, 83, 85, 89, 94, 95, 209, 213, 217, 223, 227, 271–275, 277–280, 282–288, 337, 340, 347, 348, 352, 384, 385, 387, 397, 413

- Biopolymers/ceramic-based nanocomposite, 341, 347, 348, 352, 363
- Bisphosphonate, 342, 343
- Blends, 1, 3, 26, 51, 81–83, 91, 93–95, 112, 119, 123, 125, 216–218, 221–224, 228, 231, 318, 339, 390, 394
- Blood-brain barrier, 13
- Bone, 13, 34, 46, 50, 67, 75, 76, 79, 80, 82, 85, 86, 89, 99, 134, 136, 188, 208, 277, 282, 302, 303, 305, 308, 310, 320–322, 325, 326, 337, 339–351, 353–357, 359–363, 377–386, 389, 392, 394–396, 444
- Bone defects, 325, 337, 339, 340, 354, 358, 360, 363, 378, 381, 382
- Bone diseases, 339
- Bone morphogenetic protein, 302, 342, 381
- Bone regeneration, 20, 253, 321, 325, 339, 341–347, 349–351, 354, 359–363, 378, 382, 395, 397
- Bone remodeling, 337, 339–342, 361
- Bone tissue engineering, 75, 116, 337, 340, 352, 377, 378, 383, 387–390
- Bovine serum albumin, 19, 166, 169, 171, 281, 285, 288, 416
- Breast cancer, 250, 255–257, 259
- Breast cancer gene, 250, 251
- Brownian dynamics, 262
- C**
- Calcium phosphate, 278, 282, 325, 339, 346, 351, 379, 394
- Cancer, 13, 15, 18, 19, 21, 97, 132, 134–136, 175, 188, 206, 207, 243–250, 254, 255, 257–260, 262, 273, 283, 285, 311, 339, 342, 355
- Cancer stem cells, 246, 247
- Cancer-targeted drug delivery, 243, 262
- Cancer treatment, 125, 245, 246, 248, 249, 254
- Carbohydrates, 17
- Carbon dot, 151–153, 155, 164, 175, 285
- Carbon nanodots, 153
- Carbon nanotubes, 9, 12, 65, 91, 92, 94, 109, 111, 114, 119, 122, 132, 133, 135, 153–155, 160, 204, 252, 281, 285, 392, 448
- Carbon polymeric nanodots, 153
- Carbon quantum dots, 153
- Carboxymethylation, 4
- Carboxymethylcellulose, 96
- Carboxymethylcellulose nanowhiskers, 96
- Carboxymethyl chitosan, 283, 440
- Carrageenan, 2, 7, 14, 15, 322, 378
- Casein, 1
- Cellulose, 1, 5, 6, 11, 12, 14, 19, 27–29, 31, 32, 50, 51, 65, 67, 68, 71, 72, 83, 85–89, 95–98, 116, 253, 255, 274, 276, 280, 348, 349, 403, 404, 406, 413, 415–418, 436–440
- Cellulose nanocrystals, 3, 11, 19, 86, 285
- Chemical modification, 4, 29, 40, 45, 71, 85, 99, 272, 276, 320, 325
- Chemotherapy, 125, 137, 206, 243, 283
- Chitin, 1, 8, 274, 280, 281, 348, 413
- Chitosan-based nanogel, 282
- Chlorophenoxy acids, 70
- Chondroitin sulphate, 50
- Chronic wound, 98, 402, 403, 407, 408, 412–414, 425–428, 431–434, 438, 439, 441, 443–445, 447–449
- Ciprofloxacin, 9, 133, 353, 355, 358
- Clay, 14, 109, 205, 275, 288
- Collagen, 2, 4, 7, 13, 18, 19, 48, 50, 75, 136, 253, 277, 278, 280, 299, 301, 304, 317, 322, 324, 325, 338, 339, 348, 378, 379, 384, 385, 389, 395, 396, 404, 411, 412, 414–418, 427, 434, 438, 440, 442
- Conjugates, 5, 151, 153, 164–169, 171, 172, 174, 175, 258
- Controlled release, 7, 8, 13, 83, 134, 214, 215, 217, 222, 223, 227, 259, 281, 283, 346, 354, 357, 358, 362, 418, 445
- Copolymerization, 3, 385, 389
- Co-precipitation, 71, 76, 79, 195, 199, 200, 282
- Core-shell nanocomposite, 259
- Crosslinking, 3, 78, 97, 203, 257, 285, 286, 288, 353, 356, 385, 389, 396, 412, 414, 436
- Crosslinking agent, 70, 78, 80, 203
- Cyanoethylation, 4
- Cyclodextrin, 2, 71, 134, 137, 158, 258, 259
- Cytocompatibility, 49, 78, 284, 356, 383, 389, 418
- D**
- Dexamethasone, 343, 344, 355, 358, 362
- Dextran, 2, 207, 324, 355, 404, 413, 418
- Diamagnetic substances, 189
- Diamagnetism, 189
- Diclofenac sodium, 10, 133, 281–283, 288, 319, 440

- Dilute magnetic semiconductors, 194–196
Disintegrants, 6, 20, 213, 216, 231
Dispersive solid phase extraction, 68, 74
Doxorubicin, 13, 18, 125, 132, 133, 137, 258, 283, 285
Drug carrier, 5, 10, 133, 134, 252, 253, 273, 276, 284, 350, 405
Drug delivery, 1, 2, 4–13, 15, 17–19, 21, 50, 89, 112, 125, 132, 137, 152, 154, 187, 188, 193, 206, 213, 214, 217, 222, 226–228, 243, 252–256, 258, 260, 262, 271–274, 277–279, 281–284, 286–288, 340–342, 345–353, 355, 357–359, 361–363, 413, 416
Drug delivery system, 1, 5, 6, 9, 10, 13–15, 17, 21, 134, 137, 152, 214, 249, 252, 255, 260, 262, 271–273, 278, 317, 344, 345, 350, 357, 359, 414, 440
- E**
Electrospun cellulose, 86
Emulsifier, 6, 203, 213, 214, 216, 217, 231
Energy–dispersive X-ray spectroscopy, 87
Enzyme degradation, 1, 2
Epidermal growth factor receptor, 246, 250, 251
Epithelialization, 411, 413, 416, 428
Esterification, 4
Extracellular matrix, 75, 85, 94, 299, 310, 339, 378, 384, 385, 401–404, 411, 427, 428, 444
- F**
Ferrites, 191, 194–196, 199–201, 283
Ferromagnetism, 190, 191, 194, 198
Ferrous nanoparticles, 284
Fibroblast cells, 12, 18, 94, 356, 417
Fibroblast growth factor, 300, 301, 303, 309–311, 313, 318, 319, 321–323, 325, 326, 342, 417, 440
Fibroblasts, 12, 15, 18, 94, 277, 300, 303–306, 309, 310, 318, 324, 326, 342, 343, 356, 404, 411, 415–418, 428, 437, 440, 442, 446
Fillers, 1, 38–40, 65, 67, 68, 77, 99, 109, 115–117, 119, 123, 124, 138, 202, 203, 347, 352, 393
Film properties, 3, 82
Films, 3, 4, 6, 9, 12, 14, 15, 32, 42, 48–51, 71, 78, 81, 82, 85, 89, 93, 95, 114, 117, 122, 137, 152, 169, 200, 204, 214, 273, 278, 348, 356, 359, 388, 402, 404, 405, 409, 413, 415, 434, 437–439, 449
- Finite difference method, 262
Finite volume method, 262
Fluorescence sensing, 174, 175
Functionalization, 3, 13, 74, 87, 118, 120, 133, 134, 153, 154, 158, 174, 252, 254, 272, 278, 284, 287, 322, 350, 413
- G**
Galactomannan, 6, 15
Gas chromatography–mass spectrometry, 72
Gelatin, 2–5, 7, 18, 80, 277, 278, 280, 282, 285, 325, 326, 348, 384, 385, 388, 394–396, 403, 404, 407, 414–417, 438, 440
Gellan gum, 213, 214, 216, 222–227, 231, 253, 440
Gene delivery, 5, 18, 50, 125, 137, 252, 354
Gentamicin, 388, 395, 412, 416
Glucono-d-lactone, 359
Gold nanorod, 13, 256, 258, 259
Grafting, 3, 78, 120, 126, 136, 202, 203, 313, 316, 337, 381–383
Grapheme oxide, 12, 69
Graphene, 12, 69, 109, 116, 122, 126, 153, 154, 252, 256, 258, 275, 276, 285, 286, 359, 394
Graphene oxide, 69, 122, 256, 258, 275, 276, 286, 359
Graphene quantum dots, 153, 155, 156
Growth factors, 49, 82, 244–246, 251, 254, 278, 281, 299–308, 326, 327, 337, 341, 342, 344, 345, 354, 357, 360, 361, 382, 410, 414, 417, 427, 428, 440–442, 444
Guar gum, 6, 15–17, 281
- H**
Hemicelluloses, 1, 27–29
Heparin, 5, 6, 12, 13, 305, 308, 317, 320–324, 355, 403, 417
Hepatocyte growth factor, 251, 306–311, 342
Hereditary multiple exostoses, 339
Histone acetyltransferases, 248
Histone deacetylase inhibitors, 249
Histone deacetylases, 248
Homeostasis, 299, 305, 308, 339, 401, 404
Human adipose derived stem cells, 98, 99, 355, 440

- Human cervical carcinoma (HeLa) cells, 256–259, 285
- Hyaluronic acid, 2, 7, 13, 14, 19, 48, 50, 89, 156, 253, 280, 317, 322, 324, 348, 349, 378, 404, 414, 416, 442
- Hybrid composites, 34, 40–43, 95, 283, 359
- Hydrocolloids, 402, 404, 406, 407, 434, 438, 439, 449
- Hydrogels, 3, 10, 11, 13, 14, 16, 19, 20, 50, 69–71, 132–134, 137, 201, 217, 223, 255, 259, 272, 273, 275–278, 280–286, 315, 316, 321, 324, 326, 346, 353, 388, 395, 402, 404, 405, 408, 411–415, 418, 434, 436, 437, 439–441, 446, 449
- Hydrophilicity, 4, 86, 87, 89, 96, 253, 315, 349, 412
- Hydrothermal technique, 195, 196, 286
- Hydroxyapatite, 75, 94, 137, 282, 322, 325, 326, 339, 351, 378–380, 394
- Hydroxyethyl cellulose acetate, 85
- Hydroxypropyl chitosan, 354
- Hyperthermia, 187, 188, 191, 193, 203, 204, 207–209, 254
- Hypoglycemic action, 213, 222, 232
- I**
- Immunoglobulin, 71, 285
- Immunotherapy, 243, 245
- Implants, 19, 46, 48, 50, 89, 91, 208, 258, 272, 273, 319, 324, 340, 343, 346, 352, 361, 378, 381, 383, 388, 389, 391, 394–397
- Inflammation, 91, 245, 279, 299, 311, 319, 344, 362, 383, 401, 403, 409, 414, 417, 428, 432, 440, 449
- Injectable polymeric nanocomposites, 255
- Inorganic fibres, 25
- Insulin growth factor, 342
- Iontropic gelation, 221, 222, 224, 227, 228, 275
- J**
- Jackfruit seed starch, 214, 215
- K**
- Keratin, 50, 94, 280, 322, 403, 404, 415, 416, 418
- L**
- Laser ablation method, 114, 155
- Ligands, 1, 13, 21, 70, 158, 196, 205, 247, 254, 259, 262, 276, 284, 287, 300, 303–306, 308, 311, 348
- Lignin, 26, 27, 29, 74
- Lipid nanocarriers, 255
- Locust bean gum, 4
- Low methoxy pectin, 213, 214, 216, 227, 228, 231
- M**
- Macromolecular, 5, 67, 110, 168, 207
- Magnetic bioseparation, 205
- Magnetic materials, 70, 74, 187–190, 192–194, 199, 205, 208, 284
- Magnetic microsphere, 206
- Magnetic nanoparticles, 68, 69, 98, 187, 192–196, 199, 201–204, 208, 209, 275, 284
- Magnetic nanosphere, 206
- Magnetic organic-frameworks, 69
- Magnetic resonance imaging, 188, 207, 254
- Magnetic resonance imaging contrast agents, 207
- Magnetism, 69, 70, 187–190, 193
- Mandibular defect rabbit model, 356
- Mesenchymal stem cells, 13, 19, 79, 86, 302, 319, 320, 322, 348, 357, 379, 382, 395
- Metal organic frameworks, 70
- Metal oxide nanoparticles, 194
- Metformin HCl, 217–221, 223–232, 280
- Methicillin-resistant staphylococcus aureus, 361, 362
- Methotrexate, 97, 133, 257, 258, 277, 353
- Micelles, 5, 167, 200, 201, 203, 256, 258, 440
- Microemulsion technique, 195, 200
- MiRNA, 244, 246, 248
- Molecular imprinting process, 159
- Molecularly imprinted polymer, 151, 175
- Multi-walled carbon nanotubes, 91, 113, 155, 203, 277
- N**
- Nanobodies, 246, 247
- Nanocarriers, 125, 135, 255, 260
- Nanocellulose, 71, 72, 85–87, 89, 117, 124, 349
- Nanoceramics, 75
- Nanoclay, 116, 389, 418
- Nanocomposites, 1, 9–20, 75–77, 79, 86, 90, 91, 93, 99, 109, 110–112, 115, 116,

- 118–126, 136–138, 188, 201, 243, 249, 251–255, 259, 260, 262, 276, 279–286, 326, 337, 340, 341, 347–363, 377, 379, 384, 387, 389, 391, 392, 394–397
- Nanocomposite scaffolds, 136, 337, 340, 341, 347, 348, 351–354, 356, 357, 359, 360, 363, 377, 396
- Nanocrystals, 3, 8, 11, 19, 86, 89, 166, 170, 258, 277, 285, 355, 396
- Nanodiamond, 326, 357, 386, 395
- Nanofibers, 14, 81, 85–87, 94, 97, 98, 116, 122, 276, 283, 354, 356, 360, 361, 392, 394, 413
- Nanofibrous scaffolds, 360
- Nanofillers, 14, 91, 109, 111, 115, 116, 123, 280, 347, 394
- Nanohydroxyapatite, 75–79, 86, 281
- Nanomedicines, 4, 174, 175, 249, 252
- Nanoparticles, 8, 13–21, 32, 51, 65, 68–72, 75, 78–80, 82, 83, 86, 93, 98, 111, 116, 117, 134, 152, 153, 157, 168, 172, 175, 187, 192–196, 199–204, 208, 249, 256–258, 272, 273, 275, 276, 278–286, 316, 320, 326, 346, 347, 379, 385–387, 390, 394, 395, 397, 412–417, 436, 437, 439
- Nanostructured polymer systems, 243, 260–262
- Nanosystems, 243, 254, 255, 262
- Natural fibre, 25–32, 34, 38, 39, 41, 42, 46, 49, 51, 52
- Natural polymer/ceramic-based nanocomposite scaffolds, 352, 353, 357
- Natural polymers, 1–6, 17, 20, 21, 48, 50, 67–70, 74, 75, 99, 252, 317, 324, 327, 348–350, 352, 353, 378, 401, 403, 404, 415, 419, 437, 439, 440
- Natural polysaccharide, 14, 222
- Natural/synthetic polymers/ceramic-based nanocomposite scaffolds, 352, 357
- O**
- Oncogene, 244, 245, 248, 251
- Orthopedic applications, 340, 342, 348, 377–379, 386, 390, 392, 394, 395
- Orthopedic drug delivery, 347–353, 357
- Osseointegration, 353, 356, 378, 382, 395
- Osteoblast cell line, 356, 387
- Osteoblasts, 83, 310, 339, 342, 348, 382, 386, 389
- Osteocalcin, 344, 354
- Osteoclasts, 339, 342, 343, 382
- Osteoconductivity, 75, 278, 282, 350, 351, 389
- Osteocytes, 302, 322, 339
- Osteogenic differentiation, 79, 310, 320, 341, 349, 351, 354, 357, 358, 362, 384
- Osteogenic drugs, 342
- Osteoinductive, 20, 343, 350, 360, 382, 383, 395, 397
- Osteopontin, 13, 344
- Osteosarcoma cells, 441
- P**
- Paramagnetic materials, 190
- Pharmaceutical, 1, 2, 4, 7, 9, 10, 18, 20, 21, 67, 74, 125, 213–216, 227, 231, 272, 275, 281
- Pharmaceutical applications, 1, 5–8, 222, 274, 277
- Pharmaceutical tablets, 213, 216, 231
- Phosphorylation, 4, 307
- Photothermal therapy, 12, 135, 243, 258, 259
- Phthalate esters, 69, 74
- Phytocompounds, 49, 341, 344, 345
- Pioglitazone, 221
- Plant sources, 1, 214, 349
- Polychlorinated biphenyls, 72, 74
- Polydopamine, 72, 159, 169–171, 174
- Polyelectrolyte complexation, 275
- Poly(ϵ -caprolactone), 83, 118, 202, 253, 254, 258, 348, 350, 356, 367, 378, 395
- Poly(ethylene glycol), 50, 82, 157, 159, 201, 253, 254, 258, 259, 313, 323, 348, 439, 440
- Polyhydroxyalkanoates, 1, 89, 395
- Poly(3-hydroxybutyrate), 89, 91, 92
- Poly(3-hydroxybutyrate-co-3-hydroxyvalerate), 317, 338, 357, 384, 393, 394
- Poly(3-hydroxyhexanoate), 89
- Poly(lactic acid), 1, 50, 74, 86, 136, 202, 348, 350, 356, 367, 378
- Poly(lactic-co-glycolic acid), 83, 253, 254, 256, 258, 321, 326, 350, 351, 357, 360, 378, 384, 386, 439, 442
- Poly-l-lactic acid, 253, 254, 350, 357, 359–362, 384, 386
- Polymer blending, 4
- Polymer/carbon nanocomposites, 1
- Polymer composites, 26, 31, 39, 51, 115, 120, 123, 201, 204, 278, 286, 403, 404, 411, 437

- Polymeric matrix, 25, 31, 51, 67, 95, 99, 123, 159, 249, 252, 317, 346, 395, 441
- Polymeric nanocomposites, 121, 243, 249, 252, 254–260, 262
- Polymer magnets, 195
- Poly(*m*-phenylenediamine), 74
- Polypropylene, 30, 32, 34, 46, 48, 70, 73, 117, 203, 392
- Polysaccharides, 2, 6, 7, 9, 48, 50, 65, 79, 214, 252, 274, 320, 322, 323, 349, 378, 414, 438
- Polystyrene, 32, 112, 117–119, 121, 253, 254, 326
- Poly(vinyl alcohol), 3, 4, 81–83, 117, 201, 253, 254, 258, 319, 322, 414, 416, 435, 436, 439
- Proliferation, 75, 79, 80, 83, 86, 94, 98, 99, 136, 244, 246, 248, 249, 252, 279, 286, 299, 301–311, 316, 318, 320, 322, 324–326, 340, 341, 345, 349, 350, 355, 358, 360–362, 377, 378, 383, 385–390, 392, 394, 401, 403, 414–418, 427, 428, 435, 439, 442, 446
- Proteins, 2, 5–8, 17–20, 26, 29, 47, 48, 50, 70, 71, 75, 158, 166, 168–171, 173, 244–247, 252, 261, 277–279, 282, 288, 300–305, 307, 308, 312, 313, 322, 324, 339, 343, 349, 352, 378, 379, 383, 403, 413, 415, 427, 428, 438, 441
- Proto-oncogenes, 244, 245
- R**
- Radiotherapy, 243
- Recombinant bone morphogenetic protein 2, 338
- Regenerative medicine, 26, 48, 50, 135, 308, 309, 441
- Reinforcement, 25, 26, 29–31, 35, 36, 38, 40, 42–44, 75, 95, 96, 115, 116, 125, 135, 136, 202, 288, 317, 321, 326, 434
- Renewable polymers, 67
- Renewable resources, 94, 95
- Reversible addition-fragmentation chain transfer polymerization, 202
- Rhodamine B, 133, 137
- Ring-opening polymerization, 202
- S**
- Silver, 13, 14, 16, 71, 80, 96, 98, 275, 279, 344, 414, 416, 432, 435–437, 440, 449
- Silver nanoparticles, 14, 71, 80, 98, 275, 279, 416, 436, 437
- Simulated body fluid, 76, 87, 88, 281, 282, 354, 395
- Single-walled carbon nanotubes, 112, 153
- Sol-gel method, 16, 167, 196–198
- Solid phase extraction, 68, 70–72, 171
- Solution combustion method, 199
- Soy protein, 1, 418
- Starch, 1, 3, 14, 67, 79, 80, 134, 137, 213–216, 231, 253, 274, 276, 277, 280, 282, 286, 412, 414, 416, 421
- Stromal cell derived factor, 338
- Subchondral bone defects, 357
- Super case-II transport mechanism, 219, 222, 225, 229
- Superparamagnetic iron oxide nanoparticles, 19, 194
- Suspending agent, 213, 214, 216, 231
- Sustained drug release, 2, 272, 284, 317, 346, 349, 350
- Synthetic polymer/ceramic-based nanocomposite scaffolds, 352, 356
- T**
- Tamarind seed polysaccharide, 79, 80
- Targeted delivery, 2, 5, 137, 337, 340, 342–344
- Tensile strength, 3, 7, 14, 29–31, 34, 39, 40, 42, 44, 49, 51, 78, 86, 95, 113, 119, 123, 124, 126–129, 131, 202, 204, 262, 356, 389, 391, 418
- Thermoplastic, 25, 31–33, 44, 74, 89, 91, 95, 117, 118, 203, 394
- Thermoset, 25, 31, 32, 117
- Tissue engineering, 2, 5, 11, 14, 18, 20, 50, 52, 65, 67, 74, 75, 89, 94, 99, 112, 135, 136, 281, 282, 286, 308, 309, 315, 317, 318, 325–327, 352, 356, 377, 378, 389, 397, 403, 413, 426, 441
- Tissue remodeling, 401
- Titanium oxide, 134, 195, 283
- Transforming growth factor- β , 302, 304, 309–311, 319, 324, 342, 417, 444
- Trastuzumab, 246, 250
- Tricalcium phosphate, 13, 80, 349, 351, 378, 385, 389, 393, 395, 396
- Tripolyphosphate, 98, 275, 283

Tumorigenesis, 244, 248

Tumour metastasis, 245

U

Ultra-high molecular weight polyethylene,
203–205, 390, 394

V

Vascular endothelial growth factor, 247, 251,
301, 304, 309–311, 319–323, 325,
326, 342, 345, 355, 360, 362, 417

Vascularization, 281, 302, 309, 320–322,
325, 326, 360, 383, 384, 389, 432,
443

W

Wound dressings, 11, 14, 46, 50, 98, 273,
279, 280, 318, 326, 401–405, 411–
416, 419, 432–434, 436–441, 446–
449

Wound exudates, 403, 438, 447

Wound healing, 2, 5, 49, 50, 75, 278, 280,
283, 299, 302, 308, 310, 311, 315,
317, 321, 323, 326, 327, 401–404,
411–415, 419, 426, 427, 431, 434,
437–441, 444, 446–449

Wound management, 214, 404, 425, 436,
443

Wounds, 37, 279, 280, 283, 310, 312, 319,
382, 401–403, 405–417, 419, 426–
439, 442–449

X

Xanthan gum, 4, 48

Xenografts, 259, 337, 340, 382, 433

X-ray diffraction, 76, 83, 87, 166, 167, 172,
197, 198, 396

Z

Zero-order kinetics, 219, 222, 225, 229

Zinc oxide, 195–199, 283, 284, 412, 418